

UNIVERSITY OF ARIZONA



39001007328019















DIELECTRIC PHENOMENA  
IN  
HIGH-VOLTAGE ENGINEERING





# DIELECTRIC PHENOMENA IN HIGH-VOLTAGE ENGINEERING

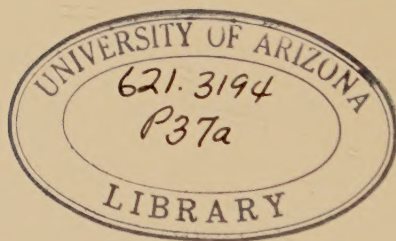
BY  
F. W. PEEK, JR.

THIRD EDITION

McGRAW-HILL BOOK COMPANY, Inc.  
NEW YORK: 370 SEVENTH AVENUE  
LONDON: 6 & 8 BOUVERIE ST., E. C. 4  
1929

COPYRIGHT, 1915, 1920, 1929, BY THE  
MCGRAW-HILL BOOK COMPANY, INC.

PRINTED IN THE UNITED STATES OF AMERICA



THE MAPLE PRESS COMPANY, YORK, PA.



## PREFACE TO THIRD EDITION

Laboratory and field data on high voltage phenomena have been considerably extended and consequently the mechanism of many of the phenomena has become better understood since the second edition of this book. For this reason, it seemed desirable to make a thorough revision at this time and to add the most recent material.

The new material includes the results of recent studies of corona, extensive investigations of the impulse breakdown of gases and insulation, the breakdown of solid and liquid insulation, and the sparkover voltages of different gaps and insulators at very high voltage.

In view of the growing importance of lightning to engineers, a separate chapter has been devoted to that subject, and a vast amount of knowledge, accumulated in the field and laboratory since the previous edition, is included herein.

Care has been taken to present the results of experiment and formulae in such a way they can be directly applied to the design of apparatus, transmission lines, etc.

The valuable assistance of Dr. J. T. Lusignan, Jr. in making this revision is acknowledged.

F. W. PEEK, JR.

PITTSFIELD, MASS.  
*September, 1929.*

## PREFACE TO FIRST EDITION

It is the object of the author to give in this book the properties of gaseous, liquid, and solid insulations, and methods of utilizing these properties to the best advantage in the problems of high-voltage engineering. Such problems require a knowledge, not only of the laws and mechanism of breakdown of dielectrics as determined by experiment, but also a simple working knowledge of the dielectric circuit.

Methods that have proved useful in designing apparatus, transmission lines, insulators, bushings, etc., are discussed and illustrated by practical application. In addition, such subjects as the manner of making extensive engineering investigations and of reducing data, the measurement of high voltages, the effects of impulse and high-frequency voltages, methods of drawing dielectric fields, outline of modern theory, various dielectric phenomena, etc., are considered. In all cases where laws and discussions of dielectric phenomena are given, it has been thought best to accompany these with experimental data.

Much original work is given, as well as reference to other investigations. The author's extensive research was made possible by facilities afforded by the Consulting Engineering Department of the General Electric Company, for which acknowledgment is made. Thanks are due Mr. H. K. Humphrey, and others, who have greatly assisted in the experiments and calculations.

F. W. P., JR.

SCHENECTADY, N. Y.,  
*April, 1915.*

# CONTENTS

PREFACE TO THE THIRD EDITION . . . . .	PAGE V
PREFACE TO THE FIRST EDITION . . . . .	vi
DIELECTRIC UNITS . . . . .	xi
SYMBOLS . . . . .	xiii

## CHAPTER I

INTRODUCTION . . . . .	1
General discussion of energy transfer—Experimental plots of dielectric and magnetic fields—Analogy between magnetic and dielectric fields—Analogy with Hooke's law.	

## CHAPTER II

THE DIELECTRIC FIELD AND DIELECTRIC CIRCUIT. . . . .	9
(Mathematical Consideration)	
General treatment of the dielectric field and dielectric circuit with discussion of principles used—Parallel planes—Field between; permittance, etc.—Concentric cylinders—Permittance or capacity; flux density and gradient—Parallel wires—Principles used in superposition of fields; determination of resultant fields; equation of equipotential surfaces, lines of force and flux density; permittance; gradient and equigradient surfaces—Concentric spheres—Spheres—Two small equal spheres, field of, and permittance; two large equal spheres, gradient, permittance—Conditions for <i>sparkover</i> and local breakdown or <i>corona</i> —Collected formulæ for common electrodes—Combinations of dielectrics of different permittivities—Dielectric flux refraction—Dielectric in series—Dielectric in multiple—Flux control—Imperfect electric elasticity or absorption in dielectrics; dielectric hysteresis.	

## CHAPTER III

ELECTRON THEORY . . . . .	39
Electrons—Ions and atoms—Radioactive materials—Conduction through gases—Ionization by collision—Ionization by photoelectric effect—Thermal ionization—Creation of negative ions—General consideration of ionization—Various stages of breakdown of air.	



## CHAPTER IV

	PAGE
VISUAL CORONA. . . . .	48
<i>General Summary and Discussion</i> —Appearance—Chemical action—Alternating-current and direct-current spacing and size of conductor—Laws of visual corona formation—Theory of corona—Air films at small spacings—Air density—Measuring voltage by corona—Conductor material, cables, oil and water on the conductors, humidity. Ionization—Wave shape, current in wire.	
<i>Experimental Study and Method of Reducing Experimental Data</i> —Tests showing the effects of size and spacing of conductors—Air density—Temperature—Barometric pressure—Strength of air films—Effect of frequency—Conductor material, oil, water, dirt, humidity—Ionization—Current in wire—Stranded conductors—Split conductors.	
<i>Photographic and Stroboscopic Study</i> —Positive and negative corona—Corona at different voltages—Thickness of corona—Oscillograms of corona current, etc.	
<i>Rectifying effect of corona</i> —Lichtenberg figures.	

## CHAPTER V

SPARK-OVER. . . . .	109
Definition—Condition for spark-over or corona—Spark-over between parallel wires, wet and dry—Measurements of and method of calculating—Wires in a cylinder—Needle gap—Sphere gap—Effect of barometric pressure, temperature, humidity, moisture, and rain on spark-over; measurement of voltage by spheres; calculation of curves; precautions in testing—Effect of high pressure, high vacuum, short spacings, and ultra-violet light—Rupturing energy and dielectric spark lag—Law of spark-over, effect of high frequency, oscillatory, and impulse voltages on spark-over, and method of measuring such voltages—Lightning generator—Insulators and bushings—Spark-over of; effect of altitude, etc.—Effect of rain, humidity, smoke and dirt on insulator spark-overs—Three-phase spark-over—Peculiar effects in breakdown.	

## CHAPTER VI

CORONA LOSS . . . . .	169
Method of making a large engineering investigation—Method of reducing data—The quadratic law—Loss on very small conductors—Effect of frequency, size of conductor and spacing; conductor material and surfaces; air density and humidity—The disruptive critical voltage Loss near the disruptive critical voltage; the probability law—Loss during storm—Loss at very high frequency.	

## CHAPTER VII

CORONA AND SPARK-OVER IN OIL AND LIQUID INSULATIONS. . . . .	215
Liquids used for insulating Physical characteristics of transformer	

oil—Spark-over with different electrodes; effect of moisture; temperature—Corona in oil—Law of spark-over and corona in oil—Spark-over of wires, plates, and cylinders—Resistivity of oil—Disruptive energy—Oil films—Transient voltages—Barriers—Comparison of high frequency—60~and impulse arc over.

## CHAPTER VIII

## SOLID INSULATIONS . . . . . 229

Solids used for insulation—Dielectric loss—Insulation resistance and dielectric strength—Rupturing gradient—Methods of testing—Law of strength *vs.* thickness—Cables—Solid *vs.* laminated insulations—Effect of area of electrodes—Impulse voltages and high frequency—Cumulative effect of overvoltages of steep wave front—Law of strength *vs.* time of application—Permittivity of insulating materials—Energy loss in insulations at high and low frequency—Operating temperatures of insulation—Surface leakage—Solid insulating barriers in oil—Impregnation—Mechanical—Direct current—Complete data on permittivity, dielectric strength with time, thickness, etc.

## CHAPTER IX

## LIGHTNING. . . . . 258

Nature of lightning—Lightning characteristics—Voltage and energy of lightning—How induced voltages occur and their values—Traveling waves, their origin and behavior on lines—Where lightning strikes and the chances of being struck—Protection of buildings, oil tanks, magazines, etc.—Explanation of some peculiar effects.

## CHAPTER X

## PRACTICAL CORONA CALCULATIONS FOR TRANSMISSION LINES. . . . . 296

Corona and summary of various factors affecting it—Practical corona formulæ and their application with problems to illustrate—Safe and economical voltages—Methods of increasing size of conductors—Conductors not symmetrically spaced—Voltage change along line—Agreement of calculated losses and measured losses on commercial transmission lines—The corona limit of high-voltage transmission, with working tables and curves.

## CHAPTER XI

## PRACTICAL CONSIDERATION IN THE DESIGN OF APPARATUS WHERE SOLID, LIQUID, AND GASEOUS INSULATIONS ENTER IN COMBINATION. 312

Breakdown caused by addition of stronger insulation—Corona on generator coils—Corona in entrance bushings—Graded cable—Transformer bushing, oil-filled bushings, condenser type bushing—Dielectric field control by metal guard rings, shields etc.—High frequency—Dielectric fields—Methods of plotting, lines of force,

	PAGE
equipotential surfaces, equigradient surfaces—Dielectric fields in three dimensions, experimental determination of dielectric fields—Effect of ground on the dielectric field between wires—Three-phase dielectric fields with flat and triangular spacing of conductors—Occluded air in insulations—Examples of calculations of spark-over between wet wires, of sphere curves, of breakdown of insulation for transient voltages, of strength of porcelain, of energy loss in insulation, etc.	

# CHAPTER XII

DATA APPENDIX . . . . .	356
Measured data on corona loss.	
INDEX. . . . .	397



## DIELECTRIC UNITS

Electromotive force, volts	$e$ volts
Gradient	$g = \frac{e}{x}$ volts/cm.
Permittance or capacitance or capacity	$C = \frac{kKA}{x} = 8.84 \frac{kA}{x} 10^{-14}$ farads
Permittivity or specific capacity	relative $k$ ( $k = 1$ for air)
	absolute (air) $K = \frac{10^9}{4\pi v^2} = 8.84 \times 10^{-14}$ farad cm. <sup>3</sup>
Elastance	$S = \frac{1}{C}$
Elastivity	$\sigma = 1/k$
Flux, displacement	$\Psi = Ce = \frac{e}{S}$ coulombs (or lines of force)
Flux density,	$D = kKg$ flux or displacement per cm. <sup>2</sup>
Intensity	$F$ (unit not used in text)
Stored energy	$w_e = \frac{Ce^2}{2}$ joules
Energy density	$w_o = \frac{gD}{2}$ joules per cm. <sup>3</sup>
Permittance or capacity current	$i_c = \frac{d\psi}{dt} = C \frac{de}{dt}$ amps.
Permittance or capacity current	$i_c = 2\pi fCe$ amps. for sine wave
Permittance in series	$\frac{1}{C} = \frac{1}{C_1} + \frac{1}{C_2} + \frac{1}{C_3}$
Elastance in series	$S = S_1 + S_2 + S_3$
Permittance in multiple	$C = C_1 + C_2 + C_3$
Elastance in multiple	$\frac{1}{S} = \frac{1}{S_1} + \frac{1}{S_2} + \frac{1}{S_3}$
	$v =$ velocity of light $= 3 \times 10^{10}$ cm. per second
	$x =$ spacing cm. $A =$ area in sq. cm.

NOTE.—For non-uniform fields  $e$ ,  $x$ , etc. are measured over very small distances and become  $de$ ,  $dx$ , etc. Then the gradient at any point is  $g = \frac{de}{dx}$ , etc.



## SYMBOLS

The following is a list of the principal symbols used. The use given first is the most general one. The meaning is always given in the text for each individual case.

- $A$  area in square centimeters, constant
- $A'_1 A'_2$  flux foci or flux centers
- $a$  distance, constant
- $b$  barometric pressure in centimeters, constant, distance
- $C$  permittance or capacity
- $C_{r_1 r_2}$  permittance between points  $r_1$   $r_2$
- $C_n$  permittance to neutral
- $c$  constant, distance
- $D$  dielectric flux density
- $d$  distance, constant
- $e$  voltage
- $e_n$  voltage to neutral
- $e_{r_1 r_2}$  voltage between points  $r_1$   $r_2$
- $e_p$  voltage to point  $p$
- $e_v$  visual critical corona voltage
- $e_o$  disruptive critical corona voltage
- $e_d$  disruptive critical corona voltage for small wires
- $e_s$  spark-over voltage
- $f$  frequency
- $f, f_1, f_o$  coefficients used in reducing average gradient to maximum—see page 27
- $F$  constant (sometimes used for dielectric field intensity)
- $g, G$  gradient
- $g$  gradient volts per centimeter or kilovolts per centimeter
- $g$  gradient volts per millimeter for solid insulations
- $g_v$  visual critical gradient
- $g_o$  disruptive critical gradient
- $g_d$  disruptive critical gradient for small wires
- $g_{max}$  maximum gradient—see note below
- $g_s$  spark gradient
- $g_a$  gradient at point  $a$
- $h$  constant, height
- $i$  current amperes
- $K$  dielectric constant for air
- $K = \frac{10^9}{4\pi v^2} = 8.84 \times 10^{-14}$  farads per cm.<sup>3</sup>
- $k$  relative permittivity ( $k = 1$  for air)
- $L$  inductance
- $l$  length, thickness

$M$	constant
$m$	ordinate of center of line of force
$m$	mass
$m_v, m_o$	irregularity factor of conductor surface
$N$	neutral plane
$n$	number
$O$	center point
$P$	point
$p$	power loss
$q$	constant
$r$	radius of wires or cables
$R$	radius of spheres, of outer cylinder
$r$	resistance
$S, s$	spacing between conductor centers
$S'$	distance between flux foci
$S$	elastance—see page 11
$t$	temperature, thickness
$T$	time
$v$	velocity of light in cm./sec. = $3 \times 10^{10}$
$v$	velocity
$w_i$	magnetic stored energy
$w_e$	dielectric stored energy
$w$	weight
$X, x$	centimeter spacing between conductor surfaces, thickness, coordinate of a point
$x_1, x_2$	distance
$y$	coordinate of point
$z$	distance from the center of a conductor or an equipotential circle to flux foci
$\alpha$	constant
$\beta$	constant
$\delta$	relative air density
$\Delta \Sigma$	difference of two sum
$e$	base of natural log
$\Psi$	dielectric displacement or dielectric flux
$\Phi$	magnetic flux
$\phi$	angle, function
$\theta$	angle
$\sigma$	elasticity
$\Sigma$	sum
$\Sigma \Sigma$	sum of two sums
$\omega$	resistance
mm.	millimeter
cm.	centimeter
$\cong$	approximately equal to

Note that voltages in measured data are often given to neutral; in such cases the single-phase line to line voltages are twice (2), and the three-phase (symmetrical)  $\sqrt{3}$  times, these values.

Permittances or capacities are also frequently given to neutral because it is a great convenience in making calculations.

The subscript max. is often used to distinguish between the maximum and root mean square or effective. This is done because insulation breakdown generally depends upon the maximum point of the wave. Such voltages may be reduced to effective sine wave by dividing by  $\sqrt{2}$ . Sometimes when the maximum gradient is referred to it means the gradient at the point in the field where the stress is a maximum. These references are made clear in the text for each individual case.

Tests were made on single-phase lines unless otherwise noted.

Views or theories advanced by the author are always accompanied by sufficient experimental data so that the reader may form conclusions independently.





# DIELECTRIC PHENOMENA

## CHAPTER I

### INTRODUCTION

It is our work as engineers to devise means of transmitting energy electrically, from one point to another point, and of controlling, distributing, and utilizing this energy as useful work. Conductors and insulating materials are necessary. Transmission problems are principally problems of high voltage and, therefore, of dielectrics. In order that energy may flow along a conductor, energy must be stored in the space surrounding the conductor. This energy is stored in two forms, electromagnetic and electrostatic. The electromagnetic energy is evinced by the action of the resulting stresses, for instance, the repulsion between two parallel wires carrying current, the attraction of a suspended piece of iron when brought near the wires, or better yet, if the wires are brought up through a plane of insulating material, and this plane is dusted with iron filings and gently tapped, the filings will tend to form in eccentric circles about the conductors. These circles picture the magnetic lines of force or magnetic field in both magnitude and direction. This field only exists when current is flowing in the conductors. If now potential is applied between the conductors, but with the far ends open circuited, energy is stored electrostatically. The resulting forces in the dielectric are evinced by an attraction between the conductors; a suspended piece of dielectric in the neighborhood is attracted. If the conductors are brought through an insulating plane as before, and this is dusted with a powdered dielectric, as mica dust, the dust will tend to form in arcs of circles beginning on one conductor and ending on the other conductor (see Fig. 1(a) and (b)). The dielectric field is thus made as tangible as the magnetic field. Figure 1(c) is an experimental plot of the magnetic and dielectric fields. Figure 1(d) is the mathematical plot. Figure 1(c) represents the magnetic and dielectric fields in the space surrounding two conductors

which are carrying energy. The power is a function of the product of these two fields and the angle between them. In comparing Figs. 1(c) and (d) only the general direction and relative density of the fields at different points can be considered. The actual number of lines in Fig. 1(c) has no definite meaning. The dielectric lines of force in Fig. 1(d) are drawn so that one-

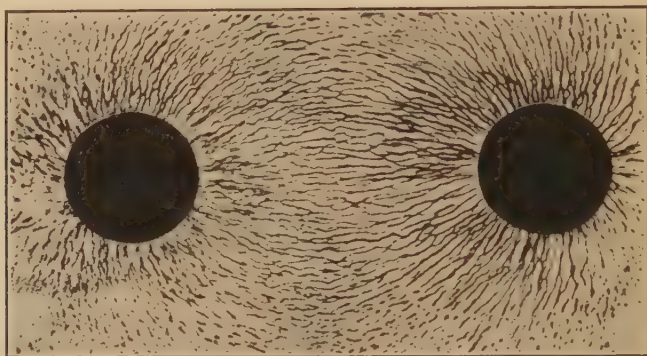


FIG. 1(a).—A photograph of a mica-filing map of the dielectric lines of force between two cylinders.



FIG. 1(b).—A photograph of an iron-filing map of the magnetic lines of force about two cylinders.

twenty-fourth of the total flux is included between any two adjacent lines. Due to the dielectric fields, points in space surrounding the conductors have definite potentials. If points of a given potential are connected together, a cylindrical surface is formed about the conductor; this surface is called an equipotential surface. Thus, in Fig. 1(d), the circles represent

equipotential surfaces. As a matter of fact, the intersection of an equipotential surface by a plane at right angles to a conductor coincides with a magnetic line of force. The circles in Fig. 1(d), then, are the plot of the equipotential surfaces and also of the magnetic lines of force. The equipotential surfaces are drawn so that one-twentieth of the voltage is between any two surfaces.

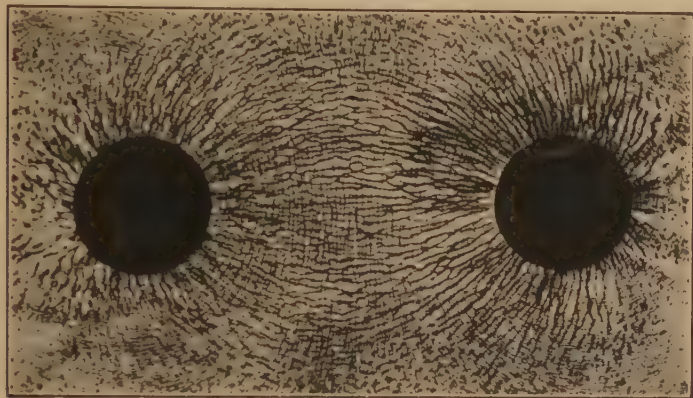


FIG. 1(c).—A photographic superposition of Fig. 1(a) and (b) representing the magnetic and dielectric fields in the space surrounding two conductors which are carrying energy.

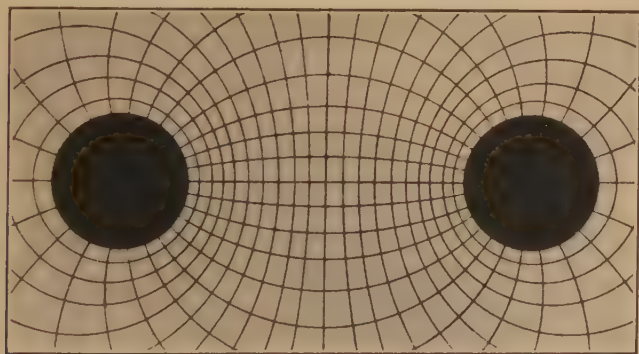


FIG. 1(d).—A mathematical plot of fields shown in Fig. 1(c).

For example: If 10,000 volts are placed between the two conductors, one conductor is at +5000 volts, the other at -5000 volts. The circle ( $\infty$  radius) midway between is at 0. The potentials in space on the different equipotential surfaces, starting at the positive surfaces, are +5000, +4500, +4000, +3500, +3000, +2500, +2000, +1500, +1000, +500, 0, -500,

—1000, —1500, —2000, —2500, —3000, —3500, —4000, —4500, —5000. A very thin insulated metal cylinder may be placed around an equipotential surface without disturbing the field. If this conducting sheet is connected to a source of potential equal to the potential of the surface which it surrounds, the field is still undisturbed. The original conductor may now be removed without disturbing the outer field.<sup>1</sup>

The dielectric lines of force and the equipotential surfaces are at right angles at the points of intersection. The dielectric lines always leave the conductor surfaces at right angles. The equipotential circles have their centers on the line passing through the conductor centers, the dielectric force circles have their centers on the neutral line.

Energy does not flow unless these two fields exist together—for instance, if the dielectric field exists alone it is aptly spoken of as “static.”

The energy stored in the dielectric fields is

$$\frac{e^2 C}{2}$$

where  $e$  is the voltage and  $C$  a constant of the circuit called the permittance (capacity) and the energy stored in the magnetic field is

$$\frac{i^2 L}{2}$$

where  $i$  is the current and  $L$  is a constant of the circuit called the inductance.

The energy stored in the dielectric circuit is thus greater for high voltage, and in the magnetic circuit for high currents.

When energy was first transmitted, low voltages and high currents were used. The magnetic circuit and magnetic field in this way became known to engineers, but as little trouble was had with insulation, the dielectric field was, therefore, not generally considered. If insulation broke down, its thickness was increased without regard to the dielectric circuit.

A magnetic circuit is not built in which the magnetic lines are overcrowded in one place and undercrowded in another place—in other words, badly out of balance. Since voltages have become high it is of great importance to proportion properly the dielectric circuit. Although an unbalanced magnetic field may

<sup>1</sup> Plots made by the author and first published in the *G. E. Rev.*, Vol. XVII, p. 1186, 1914.



mean energy loss, an unbalanced or too highly saturated dielectric field will mean broken down insulation.

The dielectric and magnetic fields may be treated in a very similar way.<sup>1</sup> For instance, to establish a magnetic field a magnetomotive force is necessary; to establish a dielectric field an electromotive force is necessary. If in a magnetic circuit the same flux passes through varying cross-sections, the magnetomotive force will not divide up equally between equal lengths of the circuit. Where the lines are crowded together, the magnetomotive force per unit length of magnetic circuit will be larger than where the lines are not crowded together. The magnetomotive force per unit length of magnetic circuit is called magnetizing force. Likewise for the dielectric circuit where the dielectric flux density is high a greater part of the electromotive force per unit length of circuit is required than at parts where the flux density is low. Electromotive force or voltage per unit length of dielectric circuit is called electrifying force, or voltage gradient. If iron or material of high permeability is placed in a magnetic circuit the flux is increased for a given magnetomotive force. If there is an air gap in the circuit the magnetizing force is much greater in the air than in the iron. If a material of high specific capacity or permittivity, as glass, is placed in the dielectric circuit, the dielectric flux is increased. If there is a gap of low permittivity, as air, in the circuit, the gradient is much greater in the air than in the glass. The electric circuit is also analogous, as will appear later.

A given insulation breaks down at any point when the dielectric flux density at that point exceeds a given value. It is thus important to have uniform density. The flux  $\psi$  depends upon the voltage, the permittivity, or specific capacity of the insulation, and the spacing and shape of the terminal. That is

$$\psi = Ce$$

The flux density  $D$ , at any point, is proportional to the gradient  $g$  or volts per centimeter at that point, and to the permittivity of the dielectric. Thus

$$D = \frac{de}{dx} Kk = gKk$$

also

$$D = \frac{\psi}{A}$$

<sup>1</sup> See KARAPETOFF, "The Magnetic Circuit," and "The Electric Circuit"; STEINMETZ, "Electric Discharges, Waves and Impulses."



As the density is proportional to the gradient, insulations will, therefore, also rupture when the gradient exceeds a given value; hence, if the gradient is measured at the point of rupture, it is a measure of the strength of the insulation. The strength of insulation is generally expressed in terms of the gradient rather than flux density.

By analogy with Hooke's law, the gradient may be thought of as a force or stress, and the flux density as a resulting electrical strain or displacement. Permittivity  $k$ , then, is a measure of the electrical elasticity of the material. Energy is stored in the dielectric with increasing force or voltage and given back with decreasing voltage. Rupture occurs when the unit force or gradient exceeds the elastic limit. Of course, this must not be thought of as a mechanical displacement. In fact, the actual mechanism of displacement is not known.

When two insulators of different permittivities are placed in series with the same flux passing through them, the one with the lower permittivity or less electrical elasticity must take up most of the voltage, that is, the "elastic" one may be thought of as "stretching" electrically and putting the stress on the electrically stiff one. The dielectric circuit is also analogous to the electric circuit when the flux is thought of in place of the current—and the permittance as conductance. The reciprocal of the permittance is sometimes called the elastance  $S$  and corresponds to "resistance" to the dielectric flux. It is convenient when permittances are connected in series, as the total elastance is the sum of the elastances. When permittances are connected in multiple, the total permittance is the direct sum of the permittances. Take two metal plates in air and apply potential between them until the flux density is almost sufficient to cause rupture. Now place a thick sheet of glass between the plates; the permittance and, therefore, the total flux is increased. This increases the stress on the air, which breaks down or glows. The glass does not break down. Thus, by the addition of insulation, the air has actually been broken down.

It is especially important in designing leads and insulators immersed in air to avoid overstress on the air.

It can be seen that a statement of volts and thickness does not determine the stress on the insulation. The stress on insulation does not depend altogether upon the voltage, but also upon the shape of the electrodes; as, for instance, for needle points the flux density at the point must be very great at fairly low voltages,

while for large spheres a very high voltage is required to produce high flux density. For this reason 200 kv. will strike 55 cm. between needle points, while it will strike only about 17 cm. between 12.5-cm. spheres. From the above it can be seen that it is much more important to design the dielectric circuit for proper flux distribution than the magnetic circuit. Local overflux density in the magnetic circuit may cause losses, but local overflux density in the dielectric circuit may cause rupture of the insulation.

Consider now the two conductors of a transmission line with voltage between them. The total dielectric flux begins on one conductor and ends on the other conductor (see Fig. 1(d)). The flux is dense at the conductor surface and less so at a distance from the conductor. Hence, the voltage gradient is greatest at the surface, where the dielectric

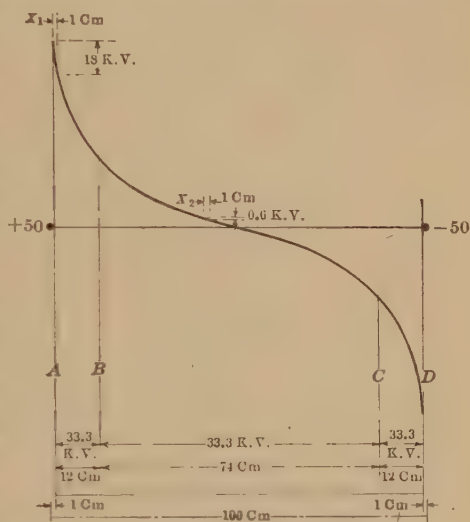


FIG. 2.—Voltage in space between two parallel wires.

cross-section is a minimum, and, therefore, the “flux resistance” or elastance is greatest and breakdown must first occur there. For the particular case shown in Fig. 2, one-third of the voltage is taken up by the space 12 cm. from each conductor, although the total space is 100 cm. The gradient is greatest at the wire surface. That is, if across a small distance  $X_1$ , the voltage is measured near the wire surface and then again across the same space  $X_2$  some distance from the wire, it is found that the voltage is much higher across the small space  $X_1$  near the wire surface than across the one farther out. In actually measuring the gradient, or rather calculating it,  $X$  is taken very small or  $dx$ . The voltage across  $dx$  is  $de$ . The purely mathematical expression for the gradient at the surface of parallel wires is

$$g = \frac{de}{dx} = \frac{e}{2r \log_e \frac{s}{r}}$$

If the conductors are close together, a spark jumps across when the voltage is high enough to produce overflux density at the conductor surface; or corona and spark-over are simultaneous. If far apart, corona forms around the conductor surface and spark-over takes place at some higher voltage.

As voltages or electromotive forces become higher, the proper shaping and spacing of the conductors to prevent dielectric flux concentration becomes of more importance. The dielectric field must now be considered in the design of apparatus as the magnetic field has been considered. Certain phenomena always exist which go unnoticed because of their feeble effect, but which, when conditions are changed, usually in a way to cause a greater energy density, become the controlling features. This is so with the dielectric circuit. The problem first made itself apparent to engineers in the transmission line, which will be taken to illustrate this. When voltages were below about 60,000, the conductors used had sufficient radius or circumference so that the surface flux density or gradient was not sufficient to cause breakdown. As voltages became higher, the sizes of conductors remained about the same and, therefore, the flux density or gradient became greater. The air broke down and caused the so-called corona and resulting loss.

As high voltage engineering problems will be, to a great extent, problems of the dielectric circuit, this will be discussed in the next chapter and calculations made for a few common forms of electrodes. The determination of the dielectric flux density, etc., is purely a mathematical problem. Exact calculations are difficult and often impossible except for simple forms. Exact calculations are not necessary in practical design work, but the general principles must be kept in mind.

## CHAPTER II

### THE DIELECTRIC FIELD AND DIELECTRIC CIRCUIT

If two conductors placed in a dielectric, as, for instance, the two parallel wires of a transmission line in air, are connected together at one end by an electric motor, or resistance and potential is applied across the other end from an alternating-current generator or other source of power supply (see Fig. 3), energy transfers take place. The motor at the far end turns and part of the energy is thus used as useful work—part appears as heat in the motor.

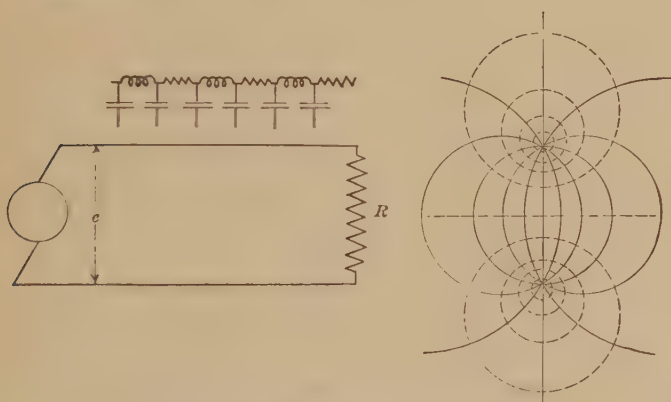


FIG. 3.—Transmission line carrying energy.

As a function of the current in the transmission circuit and a constant called the resistance, energy is absorbed. This energy appears as heat in the conductors; it is proportional to the product of the square of the current and the resistance, and is commonly known as the  $I^2r$  loss. Hence, as it is not returned to the circuit or transferred into useful work, but is dissipated as heat, it is *analogous* to a *friction loss*. During the transmission, energy is stored in the space surrounding the conductors in the electric field in two different forms—magnetic and dielectric.

Energy is stored in the magnetic field, where it is proportional to the square of the current and to a constant of the circuit called the inductance:

$$w_1 = \frac{I^2 L}{2}$$

Magnetic energy is stored with increasing current and delivered back to the circuit with decreasing current. The magnetic energy becomes noticeable or large when the currents are large, or in low-voltage circuits.

Due to the dielectric field, the energy is

$$w_e = \frac{e^2 C}{2}$$

This energy is stored with increasing voltage and delivered back with decreasing voltage. A dielectric may thus by analogy be

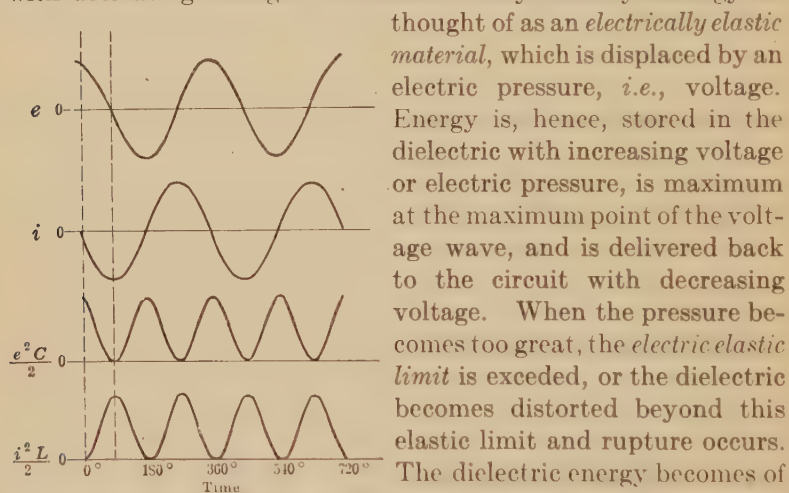


FIG. 4.—Variation of dielectric and magnetic stored energy with voltage and current.

thought of as an *electrically elastic material*, which is displaced by an electric pressure, *i.e.*, voltage. Energy is, hence, stored in the dielectric with increasing voltage or electric pressure, is maximum at the maximum point of the voltage wave, and is delivered back to the circuit with decreasing voltage. When the pressure becomes too great, the *electric elastic limit* is exceeded, or the dielectric becomes distorted beyond this elastic limit and rupture occurs. The dielectric energy becomes of great importance at high voltage and, hence, in the study of insulations, and it only will be con-

sidered here. The electric displacement may be pictured in magnitude and direction by lines of force. The dielectric lines of force for two parallel conductors are shown in Fig. 3, the eccentric circles (dotted) are the magnetic lines of force. The magnetic circles are also equipotential boundary lines for the dielectric field. The dielectric energy is sometimes said to be due to a charge on the conductor. This is often confusing, as the energy is stored not on the conductor but in the surround-



ing space, and may be thought of as due to an electric displacement. The nature of this displacement is not known. It can be seen that in order that a transfer of energy may take place, energy must be stored in the space surrounding the conductors in two forms—magnetic and dielectric. Energy thus flows only in a space in which there is a magnetic and a dielectric field. This energy is proportional to the product of the magnetic and dielectric field intensity and the sine of the included angle. If one field exists alone, there can be no energy flow. The change of stored energy from magnetic to dielectric and back is shown in Fig. 4.

**Dielectric Field between Parallel Planes.**—In the dielectric field the flux or total displacement is

$$\psi = Ce \text{ coulombs (or lines of force)} \quad (1)$$

where  $e$  is the applied electromotive force or voltage, and  $C$  is a constant of the circuit, depending upon its dimensions, and is



FIG. 5.—Dielectric field between parallel planes.

called the capacity, or better, permittance. If  $C$  is measured in farads, and  $e$  in volts,  $\psi$  is expressed in coulombs. Figure 5 shows the simplest form of dielectric circuit. Neglecting the extra displacement at the edges, it is seen that the dielectric lines of force are everywhere parallel and the field is uniform. The dielectric circuit constant, or the permittance, is directly proportional to the area of the cross-section perpendicular to the lines of force, inversely proportional to the spacing along the lines of force, and directly proportional to the dielectric constant or the permittivity.

For large parallel planes without flux concentration at the edges

$$C = \frac{A}{X} k \left( \frac{10^9}{4\pi v^2} \right) = \frac{A}{X} k K \text{ farads} \quad (2)$$



where  $A$  is the area in square centimeters

$X$  is the distance between plates in centimeters

$k$  is the specific inductive capacity, or better, permittivity, and

$v$  is the velocity of light,  $3 \times 10^{10}$  cm., per second

The term in brackets is due to units. The flux density, then, or displacement per unit area, as the flux is uniform, is

$$D = \frac{\psi}{A} = \frac{Ce}{A} = \frac{ek10^9}{4\pi v^2} \text{ coulombs per cm.}^2 \quad (3)$$

To establish this flux or displacement through the distance  $X$  an electromotive force  $e$  is required. The force per unit length of dielectric circuit or *electrifying force* is constant in the uniform field and is then  $\frac{e}{X}$ . The gradient then is

$$g = \frac{e}{X} \text{ volts /cm.}$$

The density may thus be written:

$$D = kg \frac{(10^9)}{4\pi v^2} \quad (4)$$

which is analogous to Hooke's law in Mechanics,

$$\text{strain} = k \text{ times stress}$$

The larger  $k$  is, the greater the displacement is for a given force  $g$ .

Thus  $k$  is the coefficient indicating *electrical elasticity* of the material, or its "conductivity" to the flux. The reciprocal of permittivity is analogous to resistivity and has been termed elasticity  $\sigma$ . The reciprocal of permittance has been termed elastance  $S$ . The dielectric circuit then becomes analogous to the electric circuit

$$\text{Flux} = \frac{\text{volts}}{\text{"flux resistance"}}, \text{ or } \psi = \frac{e}{S}$$

It is often convenient to consider the dielectric circuit in this way, and to use  $\sigma$  and  $S$ , as the total elastance of a number in series is the direct sum. The total permittance of a number in multiple is the direct sum. See two methods, Case 1, page 312, Chap. XI. In studying insulations, it is important to be able to express their relative strengths. Naturally, this is generally done in terms of the force or voltage gradient necessary to cause rupture. It may also be done in terms of the flux density at

rupture; that is, in coulombs per square centimeter. A given insulation breaks down at any point when the flux density exceeds a certain definite value at that point, or when the gradient exceeds a given definite value.

For Fig. 5 where the field is uniform the gradient is

$$g = e/X \text{ kv. per cm.} \quad D = \frac{\psi}{A} = \frac{Ce}{A} = K \text{ kg. coulombs per cm.}^2$$

$$K = \frac{10^9}{4\pi v^2} = 8.84 \times 10^{-14}$$

Hence, if the voltage is increased until rupture occurs and found to be  $e$ , the voltage gradient or the flux density at rupture is known; it would seem that this would be a good form of test piece with which to study insulation. This is not usually the case because of the extra displacement at the edges which is dif-

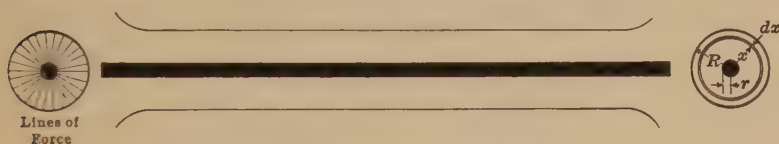


FIG. 6.—Concentric cylinders.

ficult to calculate. This may, however, be made very small at small spacings by proper rounding of the edges. Equations for the voltage gradient, permittance, etc., will now be given for a few of the common electrodes. In general, calculations are made in the same way, except that the field is usually uniform over only very small distances. The total capacity is found by taking the capacities over distances so small that conditions are still uniform and integrating.

**Concentric Cylinders.**—Concentric cylinders make a convenient arrangement for studying dielectric strength, especially that of air and oil. On account of the symmetrical arrangement, the dielectric circuit is readily calculated. For testing, the extra displacement at the ends is eliminated by belling (see Fig. 6).

**Permittance or Capacity.**—In this case the lines of force are radial. The equipotential surfaces are concentric cylinders. The total flux per centimeter length of cylinder is

$$\psi = Ce$$

The permittance may be thought of as made up of a number of permittances in series between  $r$  and  $R$ , each permittance being between two equipotential surfaces  $dx$  centimeters apart.

For a number of permittances in series

$$\frac{1}{C} = \frac{1}{C_1} + \frac{1}{C_2} + \dots$$

The permittance of the condenser of thickness  $dx$ , over which the field is uniform (Fig. 6), per centimeter length of cylinder is

$$dS = d\left(\frac{1}{C}\right) = \frac{dx}{A} \frac{4\pi v^2}{k10^9} = \frac{dx}{2\pi x} \frac{4\pi v^2}{k10^9} = \frac{2v^2}{k10^9} \frac{dx}{x}$$

$$\frac{1}{C} = S = \int_{x=r}^{x=R} d\left(\frac{1}{C}\right) = \int_{x=r}^{x=R} dS = \frac{2v^2}{k10^9} \int_{x=r}^{x=R} \frac{dx}{x} = \frac{2v^2}{k10^9} \log_e \frac{R}{r}$$

$$C = \frac{k10^9}{2v^2 \log_e R/r} = \frac{5.55 \cdot k10^{-13}}{\log_e R/r} \quad \begin{array}{l} \text{farads per centimeter} \\ \text{length of cylinder} \end{array} \quad (5)$$

*Gradient and Flux Density.*—The flux density is greatest at the conductor surface and, hence, the gradient must be greatest there. The flux density at any point  $x$  measured from the center is

$$D = \frac{\psi}{A} = \frac{Ce}{A} = \frac{ek}{A2v^2 \log_e R/r} 10^9$$

$$A = 2\pi x$$

$$\therefore D = \frac{ek}{4\pi x v^2 \log_e R/r} 10^9 = 0.884 \frac{ek}{x \log_e R/r} 10^{-13} \quad \begin{array}{l} \text{coulombs} \\ \text{per cm.}^2 \end{array}$$

$$\therefore g = D \frac{4\pi v^2}{k} 10^{-9} = \frac{e}{x \log_e R/r} \text{ kv. per cm.} \quad (6)$$

$g$  is maximum at the surface of the inner cylinder or where  $x = r$

$$g_{max} = \frac{e}{r \log_e R/r} \text{ kv. /cm.} \quad (6a)$$

**Parallel Wires.**—Parallel wires, one of the most common practical cases, will be considered in detail, in order to illustrate the general method of calculating the dielectric circuit and to show that the expressions for the permittance, flux density, gradient, etc., are quite simple and can be written with the aid of ordinary geometry and calculus.

*Equipotential Surfaces, Lines of Force, and Flux Density.*—All of the equipotential surfaces which arise in this case are cylindrical. Only their intersections with a normal plane need be

considered, therefore, and the problem may be dealt with as affecting only the plane.

The following principles will be used:

1. The resultant field in the space between two conductors is the superposition of the two independent fields. The resultant field due to any number of fields may be found by combining in pairs.

Fluxes may be added directly.

2. The potential at any point is the *algebraic* sum of the potentials due to the independent fields through that point.

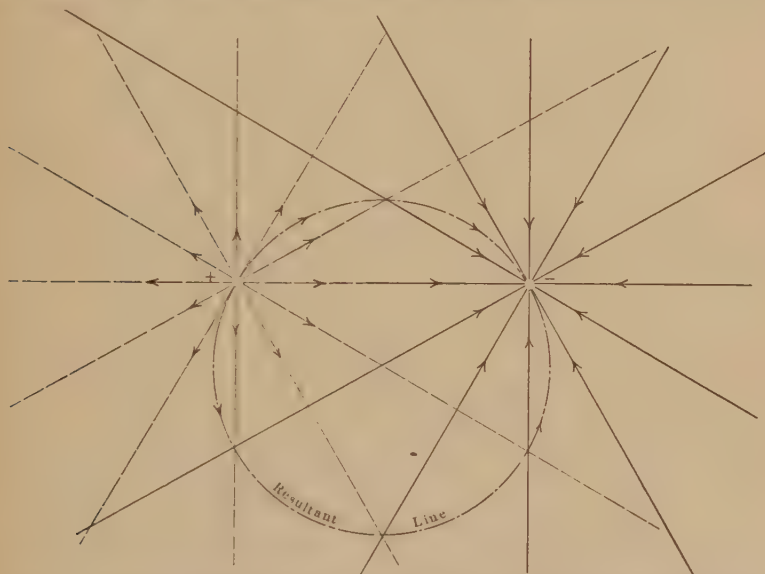


FIG. 7.—Lines of force between parallel wires, by superposition of independent radial fields.

In the same way, the potential difference between two points is the *algebraic* sum of the potential differences due to the independent fields.

3. The density or gradient at a point is the *vector sum* of the densities or gradients due to the independent fields.

When the conductors are infinitely small, the dielectric field may be considered as that resulting from the superposition of the two uniform radial<sup>1</sup> fields from the conductors to an infinite cylinder.

<sup>1</sup> By uniform radial field is meant one in which equal central angles always include equal fluxes.

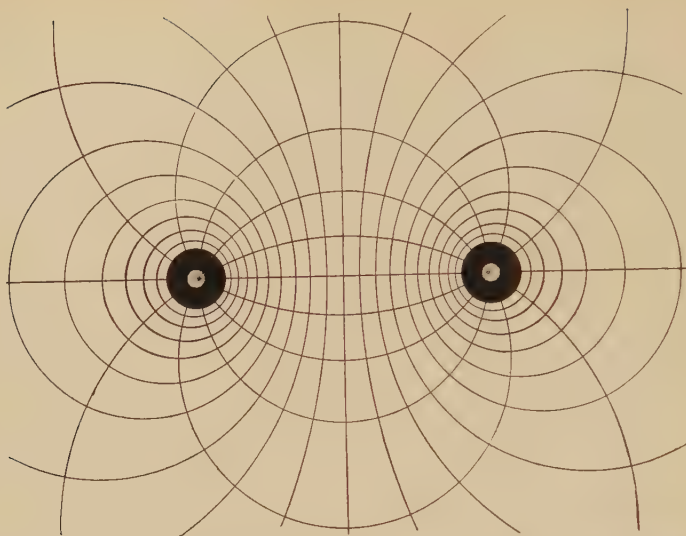


FIG. 8(a).—Lines of force and equipotential surfaces between parallel wires.

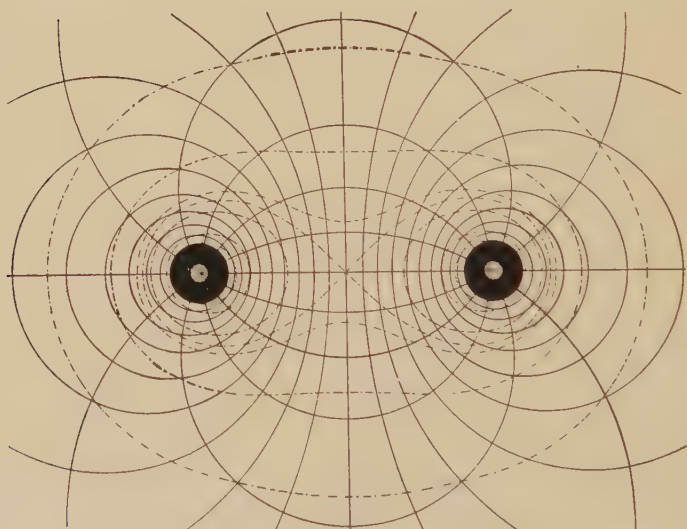


FIG. 8(b).—Lines of force, equipotential surfaces, and equigradient surfaces between parallel wires.

The resultant equipotential surfaces are then cylinders whose right sections are eccentric circles which enclose the wires, and whose centers all lie in the line connecting them; and the lines of force are arcs of circles intersecting in the conductors. The independent radial fields about each conductor are shown in Fig. 7, and the field resulting by superposition is shown in Fig. 8.

The equipotential surfaces will first be considered. It has been shown above that the permittance  $C$  between two equipotential cylinders of radii  $R$  and  $r$  is

$$C = \frac{2\pi kK}{\log_e R/r} \text{ farads per cm.} \quad (5)$$

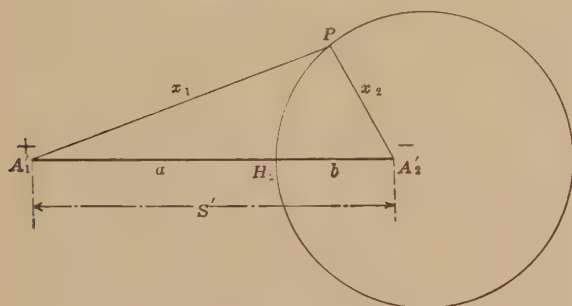


FIG. 9.

This is also the permittance between any two points on these surfaces; therefore, the voltage between points distant  $r_1$  and  $r_2$  cm. from the conductor center is

$$e_{r_1 r_2} = \psi / C_{r_1 r_2} = \frac{\psi \log_e r_1 / r_2}{2\pi kK}$$

Considering now the field resulting from superposition: In Fig. 9, the potential difference between  $H_2$  and  $P$ , due to the radial flux  $\psi$  from  $A'_1$ , is

$$e_{p_1} = \frac{\psi \log_l x_1 / a}{2\pi kK}$$

Similarly, the potential difference between  $H_2$  and  $P$ , due to the radial flux  $-\psi$  from  $A'_2$ , is<sup>1</sup>

$$e_{p_2} = \frac{-\psi \log_e x_2 / b}{2\pi kK}$$

<sup>1</sup> The signs must always be properly placed. It is convenient to give  $\psi$  the sign of the point displacement under consideration. The distances from the displacement points to the points between which potential is sought should always be put in the same order in the log, as,  $x_1/a$ ,  $x_2/b$ , etc. See problems, Case 11 and Case 12, Chap. X.



The total potential difference between  $H_2$  and  $P$  due to the two radial fields, and hence due to the resultant field, is the algebraic sum of the potential difference produced by each field separately:

$$e_p = e_{p_1} + e_{p_2} = \frac{\psi}{2\pi kK} \left( \log_e \frac{x_1}{a} - \log_e \frac{x_2}{b} \right)$$

But, if  $H_2$  and  $P$  are points on the same equipotential surface, the potential difference between them is zero, or

$$e_p = \frac{\psi}{2\pi kK} \left( \log_e \frac{x_1}{a} - \log_e \frac{x_2}{b} \right) = 0$$

Therefore

$$\log_e \frac{x_1}{a} = \log_e \frac{x_2}{b}$$

$$\frac{x_1}{a} = \frac{x_2}{b}$$

$$\frac{x_1}{x_2} = \frac{a}{b} = \text{const.}$$

if  $H_2$  is fixed—that is, for any one equipotential surface.

The equipotential surfaces are cylinders whose sections are circles which surround the infinitely small conductors. These circles have centers on line  $A_1A_2$ , but are not concentric with the conductors. This may be shown as follows:

Assume Cartesian axes through  $A'_2$ , the  $X$  axis containing  $A'_1$ . Let the coordinates of  $P$  be  $x, y$ ,

$$\begin{aligned} x_1 &= \sqrt{(A'_1A'_2 - x)^2 + y^2} = \sqrt{(a + b - x)^2 + y^2} \\ x_2 &= \sqrt{x^2 + y^2} \\ \frac{x_1}{x_2} &= \frac{a}{b} = \sqrt{\frac{(a + b - x)^2 + y^2}{x^2 + y^2}} \\ a^2x^2 + a^2y^2 &= b^2a^2 + b^4 + b^2x^2 + 2ab^3 - 2ab^2x - 2b^3x + b^2y^2 \\ (a^2 - b^2)x^2 + 2b^2(a + b)x + (a^2 - b^2)y^2 &= b^2(a + b)^2 \\ x^2 + \frac{2b^2}{a - b}x + \frac{b^4}{(a - b)^2} + y^2 &= \frac{b^2(a + b)^2}{a^2 - b^2} + \frac{b^4}{(a - b)^2} \\ \left(x + \frac{b^2}{a - b}\right)^2 + y^2 &= \frac{b^2(a + b)}{a - b} + \frac{b^4}{(a - b)^2} \\ \left(x + \frac{b^2}{a - b}\right)^2 + y^2 &= \frac{b^2(a^2 - b^2) + b^4}{(a - b)^2} = \frac{a^2b^2}{(a - b)^2} \\ \left(x + \frac{b^2}{a - b}\right)^2 + y^2 &= \frac{a^2b^2}{(a - b)^2} \end{aligned} \quad (7)$$

This is the equation of a circle whose center has the coordinates  $\frac{b^2}{a-b}, 0$  and whose radius is  $\frac{ab}{a-b}$ . The circle is thus found for any given  $a$  and  $b$ .

The equipotential circle through any point  $P (x_P, y_P)$  is found as follows:

$$a = \frac{a}{a+b} S' = \frac{x_1}{x_1+x_2} S'$$

$$b = \frac{b}{a+b} S' = \frac{x_2}{x_1+x_2} S'$$

Substituting for  $a$  and  $b$  in (7):

$$\left[ x + \frac{\left( \frac{x_2^2}{(x_1+x_2)^2} \right) S'^2}{S' \left( \frac{x_1-x_2}{x_1+x_2} \right)} \right]^2 + y^2 = \frac{\frac{x_1^2}{(x_1+x_2)^2} S'^2 \frac{x_2^2}{(x_1+x_2)^2} S'^2}{S'^2 \left( \frac{x_1-x_2}{x_1+x_2} \right)^2}$$

$$\left( x + \frac{x_2^2 S'}{x_1^2 - x_2^2} \right)^2 + y^2 = \frac{x_1^2 x_2^2 S'^2}{(x_1^2 - x_2^2)^2}$$

$$x_1^2 = (S' - x_P)^2 + y_P^2$$

$$x_2^2 = x_P^2 + y_P^2$$

$$\left( x + \frac{(x_P^2 + y_P^2) S'}{S'^2 - 2x_P S'} \right)^2 + y^2$$

$$= \frac{\{(S' - x_P)^2 + y_P^2\} (x_P^2 + y_P^2) S'^2}{(S'^2 - 2x_P)^2}$$

$$\left( x + \frac{x_P^2 + y_P^2}{(S' - 2x_P)} \right)^2 + y^2 = \frac{\{(S' - x_P)^2 + y_P^2\} (x_P^2 + y_P^2)}{(S' - 2x_P)^2} \quad (7a)$$

The resultant lines of force are arcs of circles with centers on line  $n$  and passing through

the points  $A'_1$  and  $A'_2$ .

This is shown as follows:

Consider Fig. 10. The flux

included in  $PA'_1 A'_2$  per

centimeter length of cylin-

der due to  $A'_1$  is  $\frac{\psi \alpha_1}{2\pi}$ . That

in  $PA'_2 A'_1$  due to  $A'_2$  is

$\frac{\psi \alpha_2}{2\pi}$ .

The total flux between  $P$  and  $A'_1 A'_2$  is the sum of these

$$\psi_P = \frac{\psi}{2\pi} (\alpha_1 + \alpha_2)$$

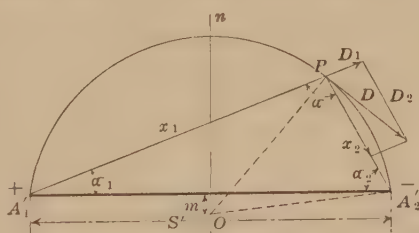


FIG. 10.

The restriction that lines of force cannot cross implies that the flux between any two is constant; hence, if  $P$  move along a flux line,

$$\psi_P = \frac{\psi}{2\pi}(\alpha_1 + \alpha_2) = \text{const.}$$

from which

$$\alpha_1 + \alpha_2 = \text{const.}$$

Hence

$$\alpha = \pi - (\alpha_1 + \alpha_2) = \text{const.}$$

NOTE.—The equation of the line of force may also be found by writing the expression for the flux densities at points and imposing the condition that the component normal to the line of force is zero.

This condition defines a circular arc passing through  $A'_1$  and  $A'_2$ . Choosing, as before, the point  $A'_2$  as the origin of Cartesian coordinates, the equation of these circles is

$$\left(\frac{S'}{2} - x\right)^2 + (y - m)^2 = m^2 + \left(\frac{S'}{2}\right)^2 \quad (8)$$

where  $m$  is the ordinate of the center of any particular circle. The equation of the line of force through  $(x, y)$  is found as follows:

Call the center of circle (lines of force)  $O$

$A'_2'O = PO = \text{radius of circle}$

$$r^2 = (A'_2'O)^2 = \left(\frac{S'}{2}\right)^2 + m^2$$

$$r^2 = (PO)^2 = \left(\frac{S'}{2} - x\right)^2 + (y - m)^2$$

$$\therefore \left(\frac{S'}{2} - x\right)^2 + (y - m)^2 = m^2 + \left(\frac{S'}{2}\right)^2 \quad (8)$$

Through any point  $(x_P, y_P)$ .

Then  $\left(\frac{S'}{2} - x_P\right)^2 + (y_P - m)^2 = \left(\frac{S'}{2}\right)^2 + m^2$

$$m = \frac{x_P^2 + y_P^2 - S'x_P}{2y_P}$$

Substituting this value of  $m$  in (8).

$$\begin{aligned} \left(x - \frac{S'}{2}\right)^2 + \left(y - \frac{x_P^2 + y_P^2 - S'x_P}{2y_P}\right)^2 \\ = \left(-\frac{S'x_P}{2y_P} + y_P\right)^2 + \left(\frac{S'}{2}\right)^2 \end{aligned} \quad (8a)$$

The slope of the equipotential surface at  $(x_P, y_P)$  is found from (7a)

Evaluate  $y$  in terms of  $x$ , differentiate, and put  $x = x_p$ .

NOTE.—Take  $x$  always +.  $m -$  when below  $x$  axis.

$$\frac{dy}{dx_{es}} = - \frac{S'x_p - x_p^2 + y_p^2}{y_p(S' - 2x_p)}$$

The slope of the line of force at  $(x_p, y_p)$  is found in the same way from (8a)

$$\frac{dy}{dx_{lf}} = + \frac{y_p(S' - 2x_p)}{S'x_p - x_p^2 + y_p^2}$$

It will at once be noticed that

$$\frac{dy}{dx_{es}} = - \frac{dy_{lf}}{dx}$$

which shows that the line of force at any point is perpendicular to the equipotential surface at the same point.

The flux density,  $D$ , at any point in the resultant field is the vector sum of the flux densities due to  $A'_1$  and  $A'_2$ , separately. At  $P$  (Fig. 10) the flux density due to  $A'_1$  is

$$D_1 = \frac{\psi}{2\pi x_1}$$

and due to  $A'_2$  is

$$D_2 = \frac{\psi}{2\pi x_2}$$

directed as indicated.

NOTE.—Subscript  $es$  refers to equipotential surface.

Subscript  $lf$  refers to line of force.

The triangles whose sides are  $x_1$ ,  $x_2$ ,  $S'$ , and  $D_2$ ,  $D_1$ ,  $D$  may be shown to be similar, having one angle ( $\alpha$ ) equal, and the including sides proportional.

$$D_2 x_2 = D_1 x_1 = \frac{\psi}{2\pi}$$

Then

$$\frac{D}{S'} = \frac{D_1}{x_2}$$

$$D = S' \frac{D_1}{x_2} = \frac{S'}{x_2} \frac{\psi}{2\pi x_1} = \frac{S'\psi}{2\pi x_1 x_2} \quad (9)$$

The preceding, covering infinitely small wires, is not directly applicable to the ordinary case of large parallel wires. Green's theorem, however, states that if any equipotential surface be kept at its original potential, the flux within it may be removed without any change in the external field. In Fig. 11 the circles

represent equipotential cylinders, surrounding flux centers  $A'_1$  and  $A'_2$ . These cylinders may be maintained at their original potential. The interior may be filled with a conductor. This gives parallel conductors of radius  $r$  and spacing between centers  $S$ . The external field has not been changed, and the preceding discussion still applies.  $A_1$  and  $A_2$  must be located from  $A'_1$  and  $A'_2$ , since  $r$  and  $S$  are the quantities given in any actual case. This is easily done:

$$\begin{aligned} a &= S - r - z \\ b &= r - z \\ z &= \frac{b^2}{a - b} = \frac{r^2 - 2rz + z^2}{S - r - z - r + z} = \frac{r^2 - 2rz + z^2}{S - 2r} \\ zS &= r^2 + z^2 \\ z^2 - Sz + r^2 &= 0 \\ z &= \frac{S - \sqrt{S^2 - 4r^2}}{2} \end{aligned}$$

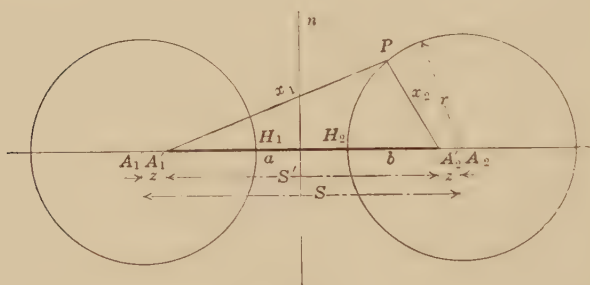


FIG. 11.

Since obviously  $z$  cannot be greater than  $S/2$ , the negative sign is taken for the radical.

$$\begin{aligned} a &= S - r - z \\ &= \frac{2S - 2r - S + \sqrt{S^2 - 4r^2}}{2} \\ &= \frac{S - 2r + \sqrt{S^2 - 4r^2}}{2} \end{aligned}$$

$$\begin{aligned} b &= r - z \\ &= \frac{2r - S + \sqrt{S^2 - 4r^2}}{2} \end{aligned}$$

$$\frac{a}{b} = \frac{S - 2r + \sqrt{S^2 - 4r^2}}{2r - S + \sqrt{S^2 - 4r^2}} \quad (10)$$

$$\begin{aligned}
&= \frac{S - 2r + \sqrt{S^2 - 4r^2}}{2r - S + \sqrt{S^2 - 4r^2}} \times \frac{2r - S - \sqrt{S^2 - 4r^2}}{2r - S - \sqrt{S^2 - 4r^2}} \\
&= \frac{\{ -2S^2 - 4rS + 2(S - 2r) \sqrt{S^2 - 4r^2} \}}{4r^2 - 4rS + 4r^2} \\
&= \frac{(2r - S)(S + \sqrt{S^2 - 4r^2})}{2r(2r - S)} = \frac{S}{2r} + \sqrt{\left(\frac{S}{2r}\right)^2 - 1}
\end{aligned}$$

*Permittance or Capacity.*—In Fig. 11 let  $n$  be a neutral plane. Represent by  $e_n$  the potential between circle  $H_2$  and  $n$  (or  $H_1$  and  $n$ ) and by  $C_n$  the corresponding permittance to neutral per centimeter length of wires. Due to  $A'_1$

$$e_{n1} = \frac{\psi \log_e \frac{x_1}{S'/2}}{2\pi k K}$$

Due to  $A'_2$ .

$$e_{n2} = \frac{-\psi \log_e \frac{x_2}{S'/2}}{2\pi k K}$$

$$e_n = e_{n1} + e_{n2} = \frac{\psi}{2\pi k K} \left( \log_e \frac{x_1}{S'/2} - \log_e \frac{x_2}{S'/2} \right)$$

$$= \frac{\psi}{2\pi k K} \log_e \frac{x_1}{x_2}$$

$$C_n = \frac{\psi}{e_n} = \frac{2\pi k K}{\log_e \frac{x_1}{x_2}} = \frac{2\pi k K}{\log_e \frac{a}{b}}$$

Substituting from (10)

$$\begin{aligned}
C_n &= \frac{2\pi k K}{\log_e \frac{a}{b}} \\
&= \frac{2\pi k K}{\log_e \left[ \frac{S}{2r} + \sqrt{\left(\frac{S}{2r}\right)^2 - 1} \right]} \\
&= \frac{5.55k10^{-13}}{\log_e \left[ \frac{S}{2r} + \sqrt{\left(\frac{S}{2r}\right)^2 - 1} \right]} \text{ farads per cm.}
\end{aligned} \tag{11}$$



If hyperbolic tables are available, a more convenient form is

$$C_n = \frac{2\pi kK}{\cosh^{-1} \frac{S}{2r}} \quad (11a)$$

$$= \frac{5.55k10^{-13}}{\cosh^{-1} \frac{S}{2r}} \text{ farads per cm.}$$

If  $S/r$  be large, then  $\sqrt{\left(\frac{S}{2r}\right)^2 - 1}$  is nearly equal to  $\frac{S}{2r}$ , and approximately

$$C_n = \frac{2\pi kK}{\log_e S/r} \text{ farads per cm.} \quad (11b)$$

The result corresponds exactly to the form (page 23) which would have resulted had the wires been considered very small at the start, or

$$C_n = \frac{2\pi kK}{\log_e a/b}$$

where

$$a = S, b = r$$

*Gradient and Flux Density.*—The flux density at any point on the line joining the centers of the conductors and distant  $x$  from the inner surface of one of them is

$$D = \frac{S'\psi}{2\pi x_1 x_2} \quad \begin{array}{l} x_2 = b + x \\ x_1 = a - x \end{array} \quad (9)$$

$$= \frac{(a+b)\psi}{2\pi(ab + (a-b)x - x^2)}$$

$$= \frac{\psi\sqrt{S^2 - 4r^2}}{2\pi\left\{\frac{4rS - 8r^2}{4} + \left(\frac{2S - 4r}{2}\right)x - x^2\right\}}$$

$$= \frac{\psi\sqrt{S^2 - 4r^2}}{2\pi\{(r+x)(S-2r) - x^2\}}$$

Since

$$\psi = C_n e_n$$

$$D = \frac{\sqrt{S^2 - 4r^2}}{\{2\pi(r+x)(S-2r) - x^2\}} \frac{2\pi kK e_n}{\log_e \left[ \frac{S}{2r} + \sqrt{\left(\frac{S}{2r}\right)^2 - 1} \right]}$$

$$\begin{aligned}
&= \frac{kK e_n \sqrt{S^2 - 4r^2}}{\{(r+x)(S-2r) - x^2\} \log_e \left[ \frac{S}{2r} + \sqrt{\left(\frac{S}{2r}\right)^2 - 1} \right]} \\
&= \frac{0.885 k e_n \sqrt{S^2 - 4r^2} 10^{-13}}{\{(r+x)(S-2r) - x^2\} \log_e \left[ \frac{S}{2r} + \sqrt{\left(\frac{S}{2r}\right)^2 - 1} \right]} \text{ coulombs per cm.}^2
\end{aligned}$$

The gradient along the line of centers is

$$\begin{aligned}
g &= \frac{D}{kK} \\
&= \frac{e_n \sqrt{S^2 - 4r^2}}{\{(r+x)(S-2r) - x^2\} \log_e \left[ \frac{S}{2r} + \sqrt{\left(\frac{S}{2r}\right)^2 - 1} \right]} \text{ kv. per cm.}
\end{aligned} \tag{12}$$

The gradient is greatest at the conductor surface ( $x = 0$ ) and is

$$\begin{aligned}
g_{max} &= \frac{e_n \sqrt{S^2 - 4r^2}}{r(S-2r) \log_e \left[ \frac{S}{2r} + \sqrt{\left(\frac{S}{2r}\right)^2 - 1} \right]} \\
&= \frac{e_n \sqrt{\left(\frac{S}{2r}\right)^2 - 1}}{r \left(\frac{S}{2r} - 1\right) \log_e \left[ \frac{S}{2r} + \sqrt{\left(\frac{S}{2r}\right)^2 - 1} \right]} \text{ kv. per cm.} \\
&= \frac{e_n}{r \sqrt{\frac{S}{2r} - 1} \log_e \left[ \frac{S}{2r} + \sqrt{\left(\frac{S}{2r}\right)^2 - 1} \right]} \text{ kv. per cm.}
\end{aligned} \tag{12a}$$

Where hyperbolic tables are available a more convenient form is

$$g_{max} = \frac{e_n}{r \sqrt{\frac{S}{2r} - 1} \cosh^{-1} \frac{s}{2r}} \text{ kv. per cm.} \tag{12b}$$

$$\text{If } S/r \text{ is large} \quad g_{max} = \frac{e_n}{r \log_e S/r} \tag{12c}$$

As before, this equation would have resulted had the conductors been considered small in the first place. The method of drawing the lines of force, etc., is illustrated in Case 11, page 335, Chap. XI.

**Spheres.**—In studying insulation it is sometimes convenient to use spherical electrodes. The potential between concentric spheres of radii  $R$  and  $r$  may be found as for concentric cylinders

on page 13. The equipotential surfaces are spheres. Between two surfaces at distance  $x$ ,  $dx$  centimeters apart, the permittance is

$$\begin{aligned} dS &= d\left(\frac{1}{C}\right) = \frac{dx}{A} \frac{1}{kK} = \frac{1}{4\pi kK} \frac{dx}{x^2} \\ \frac{1}{C} &= \frac{1}{4\pi kK} \int \frac{dx}{x^2} = \frac{1}{4\pi kK} \left[ \frac{1}{r} - \frac{1}{R} \right] \\ C &= 4\pi kK \frac{Rr}{R-r} \\ e_{rR} &= \frac{\psi}{C} = \frac{\psi}{4\pi kK} \frac{R-r}{Rr} \end{aligned}$$

The potential difference due to  $\psi$  between two points distant  $r_1$  and  $r_2$  from the center of the sphere is

$$e_{r_1 r_2} = \frac{\psi}{4\pi kK} \frac{r_2 - r_1}{r_1 r_2}$$

The equipotential surfaces between two point electrodes or very small equal spheres may be found as follows, using Fig. 11:

The difference of potential between  $H_2$  and  $P$  due to  $A'_1$  is

$$e_{P_1} = \frac{\psi}{4\pi kK} \left( \frac{x_1 - a}{x_1 a} \right)$$

due to  $A'_2$  is

$$e_{P_2} = - \frac{\psi}{4\pi kK} \frac{x_2 - b}{x_2 b}$$

$$e_P = e_{P_1} + e_{P_2} = \frac{\psi}{4\pi kK} \left( \frac{x_1 - a}{x_1 a} - \frac{x_2 - b}{x_2 b} \right)$$

If  $H_2$  and  $P$  are on the same equipotential surface

$$\frac{x_1 - a}{x_1 a} - \frac{x_2 - b}{x_2 b} = 0$$

$$\frac{x_1 x_2}{x_2 - x_1} = \frac{ab}{b - a} = \text{constant}$$

$$\frac{1}{x_1} - \frac{1}{x_2} = \text{constant}$$

is the equation for the equipotential surface.

The fraction of the total flux toward  $P$  through the cone with apex at  $A'_1$  and half angle  $\alpha$  due to  $A'$  is<sup>1</sup>

$$\psi_1 = \frac{\psi}{2} (1 - \cos \alpha_1)$$

<sup>1</sup> The area of a spherical surface is  $4\pi R^2$ . The area of a spherical sector with half angle  $\alpha$  is  $2\pi R^2(1 - \cos \alpha)$ .

Through the cone with apex on  $A'_2$  and half angle  $\alpha_2$  due to  $A'_2$ , it is

$$\psi_2 = \frac{\psi}{2} (1 - \cos \alpha_2)$$

$$\psi_p = \psi_1 + \psi_2$$

If  $P$  follows a line of force  $\psi_p$  must be constant because lines of force cannot cross.

$$\therefore \cos \alpha_1 + \cos \alpha_2 = \text{constant}$$

is the equation of the line force.

The equations for the gradients, etc., of two large spheres of equal radii and spaced apart are given below:

*Spheres of Equal Size in Air (Non-grounded):*<sup>1</sup>

$$g = \frac{e}{X} f \text{ kv. per cm.} \quad (13a)$$

where

$g$  = gradient at surface of sphere in line joining centers

$e$  = volts between spheres

$X$  = distance between nearest surfaces in centimeters

$f$  = a function of  $X/R$  where  $R$  is the radius of either sphere

$f$  may be calculated by the following simple formula:<sup>2</sup>

$$f = \frac{X/R + 1 + \sqrt{(X/R + 1)^2 + 8}}{4}$$

*Spheres of Equal Size in Air (One Sphere Grounded)*

$$g = \frac{e}{X} f_0 \text{ kv. per cm.} \quad (13b)$$

where the letters have the meaning noted above  $f_0$  being a different function of  $X/R$ . For the case of one sphere grounded, the shanks, connecting leads, ground, etc., have a much greater effect than when both are non-grounded and mathematical values of  $f_0$  do not check the measured values. Experimental values for the grounded case are given as  $f_0$  in the following table.

<sup>1</sup> RUSSEL, *Phil. Mag.*, Vol. XI, 1906.

<sup>2</sup> DEAN, *Phys. Rev.*, December, 1912, April, 1913.

DEAN, *G. E. Rev.*, Vol. XVI, p. 148, 1913.

$X/R$	$f$ Non-grounded (calculated and measured)	$f_0$ Grounded (measured) <sup>1</sup>
0.1	1.03	1.03
0.2	1.06	1.06
0.4	1.14	1.14
0.6	1.215	1.22
0.8	1.29	1.31
1.0	1.366	1.41
1.2	1.44	1.51
1.4	1.52	1.62
1.6	1.61	1.73
1.8	1.69	1.85
2.0	1.78	1.97
3.0	2.23	2.59
4.0	2.69	3.21
6.0	3.64	
10.0	5.60	
15.0	8.08	
20.0	10.58	

<sup>1</sup> Distance of grounded sphere to ground in these tests is 4 to 5 diameters

The practical application of this is discussed further on page 124

The gradient at any point in the line joining the centers of the spheres and distance  $y$  from the midpoint of this line is

$$g_y = \left[ \frac{2x^2(x^2(f+1) + 4y^2(f-1))}{[x^2(f+1) - 4y^2(f-1)]^2} \right] \frac{E}{x} \quad (13c)$$

If two equal spheres are never separated a greater distance than twice their radii, appreciable corona can never form, but the first visible evidence of overstress is spark-over. If the separation is greater than  $2R$ , corona forms and it is then necessary to further increase the voltage to cause spark-over. The condition for corona or spark-over will now be given. A wire in a cylinder will be taken, as the calculations are simpler and best illustrate the condition.

**Condition for Spark-over and for Local Breakdown, or Corona.** For a wire in a cylinder the maximum gradient, and, thus, where breakdown will first occur, is at the wire surface

$$g = \frac{e}{r \log_e R/r} \quad (6a)$$

When  $e$  is of such value that  $g$  at the wire surface just exceeds the breakdown strength of air, the air at that point becomes conducting, or corona forms, thus, in effect, increasing the size of the conductor. If this increase lowers the gradient, the breakdown will be local, and it is said that corona is on the wire. If the ratio  $R/r$  is such that the increase in size of the conductor by the conducting air increases the gradient, the broken down area will continue to enlarge, or spark-over will occur. The condition for corona or spark-over may be found thus:

$$g = \frac{e}{r \log_e R/r}$$

For a constant value of  $e$  and  $R$  find the value of  $r$  to make  $g$  a minimum

$$1/g = x = \frac{r \log_e R/r}{e} = \frac{r}{e} (\log_e R - \log_e r)$$

$$\frac{dx}{dr} = \frac{1}{e} (\log_e R - \log_e r - 1)$$

$$= 0 \text{ for extreme of } x$$

$$\frac{1}{e} (\log_e R - \log_e r - 1) = 0$$

$$\log_e R/r = 1$$

$$R/r = e$$

Therefore

$$1/g \text{ is maximum when } R/r = e$$

or

$$g \text{ is minimum when } R/r = e$$

In other words, the stress on the air decreases with increasing  $r$  until  $R/r = e$ . When  $R/r$  is equal to or less than  $e$  an increase in  $r$  increases  $g$ . Thus, if

$R/r \leq e$  and  $g$  is brought up to the

rupturing point,  $g$  progressively increases and spark-over must occur. If  $R/r > e$ , corona forms and the voltage must be still further increased before spark-over occurs.

This is illustrated graphically in Fig. 12. Note that this is plotted between  $r/R$  and  $g$ . Thus, the minimum occurs when  $r/R = 1/e$ . It is interesting to note here that with a given  $R$  a cable has maximum strength when  $r$  is made such that

$$R/r = e$$

This is not the practical ratio, however, as will appear later.

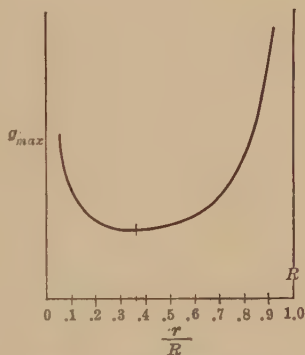


FIG. 12.—Concentric cylinders.—Variation of gradient at surface of inner cylinder as radius is changed—outer cylinder constant.



## COLLECTED FORMULÆ FOR THE COMMON ELECTRODES

## Concentric Cylinders.

$$\text{Capacity} \quad C = \frac{5.55k10^{-13}}{\log_e R/r} \text{ farads per cm.}$$

$$\text{Gradient} \quad g_x = \frac{e}{x \log_e R/r} \text{ kv. per cm.}$$

$$\text{Max. gradient} \quad g = \frac{e}{r \log_e R/r} \text{ kv. per cm.}$$

Corona does not form when

$$R/r < 2.718$$

$x$  = distance from center of cylinder in centimeter

$R$  = centimeter radius of outer cylinder

$r$  = centimeter radius of inner cylinder

## Parallel Wires.

Capacity or permittance to neutral

$$C_n = \frac{5.55k10^{-13}}{\log_e \left[ \frac{S}{2r} + \sqrt{\left(\frac{S}{2r}\right)^2 - 1} \right]} = \frac{5.55k10^{-13}}{\cosh^{-1} \frac{S}{2r}} \text{ farads per cm.}$$

Gradient (at  $x$  cm. distance from wire surface on line through centers)

$$g_x = \frac{e_n \sqrt{S^2 - 4r^2}}{\left\{ (r+x)(S-2r) - x^2 \right\} \log_e \left[ \frac{S}{2r} + \sqrt{\left(\frac{S}{2r}\right)^2 - 1} \right]} \text{ kv. per cm.}$$

Max. gradient (at conductor surface)<sup>1</sup>

$$\begin{aligned} g &= \frac{e_n \sqrt{\left(\frac{S}{2r}\right)^2 - 1}}{r \left(\frac{S}{2r} - 1\right) \log_e \left[ \frac{S}{2r} + \sqrt{\left(\frac{S}{2r}\right)^2 - 1} \right]} \quad \text{or} \\ &= \frac{e_n \sqrt{\left(\frac{S}{2r}\right)^2 - 1}}{r \left(\frac{S}{2r} - 1\right) \cosh^{-1} \frac{S}{2r}} \text{ kv. per cm.} \end{aligned}$$

Corona does not form when

$$S/r < 5.85$$

<sup>1</sup> See same equations in different form, page 25. See formula 12c, page 25.

$S$  = spacing between conductors centers in centimeters

$r$  = conductor radius in centimeters

$e_n$  = kilovolts to neutral

**Equal Spheres in Air.**—Gradient (non-grounded). (At  $a$  centimeters distance from sphere surface on line joining centers.)

$$g_a = \frac{E}{X} \left\{ \frac{2X^2[X^2(f+1) + 4\left(\frac{X}{2} - a\right)^2(f-1)]}{[X^2(f+1) - 4\left(\frac{X}{2} - a\right)^2(f-1)]^2} \right\} \text{ kv. per cm.}$$

Maximum gradient (non-grounded)

$$g = \frac{e}{X} f \text{ kv. per cm.}$$

Maximum gradient (one grounded)

$$g = \frac{e}{X} f_0 \text{ kv. per cm.}$$

$$\text{where } f = \frac{X}{R} + 1 + \sqrt{\frac{(X/R + 1)^2 + 8}{4}}$$

and  $f_0$  = see table, page 28

Corona does not form when  $X/R < 2.04$

$R$  = radius of sphere in centimeters

$X$  = cm. spacing between nearest surfaces

$e$  = kilovolts between spheres

Capacity or permittance

$$C = \frac{X}{36(f-1)} 10^{-11} \text{ farads}$$

**Combination of Dielectrics of Different Permittivities.**—When several dielectrics of different permittivities are combined, as is usually the case in practice, it becomes important to so proportion and shape the electrodes and insulations that one dielectric does not overstress another. This is of especial importance in insulators where dielectrically weak air of low permittivity is necessarily in combination with dielectrically strong insulations of high permittivity.

**Dielectric Flux Refraction.**—When dielectric flux lines pass from a dielectric of permittivity  $k_1$  to another of permittivity of  $k_2$  the lines are bent or refracted. This does not occur, of course,

when the lines strike the surfaces normally, as in a concentric cable, and between parallel plates already considered. The angle of refraction bears a definite relation to the ratio of the two permittivities and can be shown as follows:

Let  $AB$  (Fig. 13) be the common surface of the two insulations.

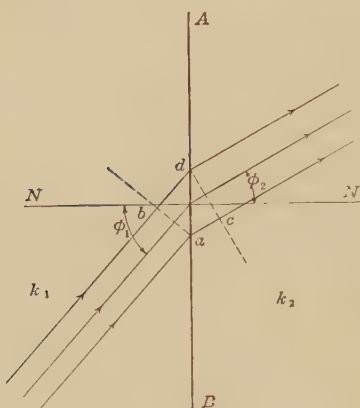


FIG. 13.—Dielectric flux refraction.

The flux  $\psi_1$  makes an angle  $\phi_1$  with the normal  $NN'$  to the surface. The total flux through the equipotential surface  $ab$  is the same as the total flux through the surface  $cd$ . The voltage between  $a$  and  $c$  must be the same as the voltage between  $b$  and  $d$ , because potential at  $a$  = potential at  $b$  and potential at  $c$  = potential at  $d$ .

$$\psi_1 = \psi_2 = \psi$$

Therefore

$$\psi = D_1 ab = D_2 cd \quad (14)$$

In the uniform field

$$g_1 = \frac{e}{bd} \quad g_2 = \frac{e}{ac}$$

where  $e$  is volts,  $a$  to  $c$  = volts  $b$  to  $d$

Therefore

$$g_1 bd = g_2 ac \quad (15)$$

Combining (14) and (15)

$$\frac{D_1}{g_1} \frac{ab}{bd} = \frac{D_2}{g_2} \frac{cd}{ac}$$

But

$$\frac{D_1}{g_1} = K_1 \quad D_2/g_2 = K_2$$

Therefore

$$\frac{K_1}{\tan \phi_1} = \frac{K_2}{\tan \phi_2}$$

Therefore

$$\frac{\tan \phi_1}{\tan \phi_2} = \frac{K_1}{K_2}$$

**Dielectric in Series.**—Take the simple case of two parallel planes with two different dielectrics between them and neglect the flux concentration at the edges (Fig. 14, flux concentration not

shown). As the lines are normal to the electrodes, there is no refraction. The same flux passes from plate to plate.

$$\begin{aligned}
 \psi_1 &= \psi_2 = \psi \\
 C_1 &= \frac{k_1 KA}{x_1} & C_2 &= \frac{k_2 KA}{x_2} \\
 \psi_1 &= C_1 e_1 = \frac{k_1 KA}{x_1} e_1 \\
 \psi_2 &= C_2 e_2 = \frac{k_2 KA}{x_2} e_2 \\
 \frac{k_1 KA}{x_1} e_1 &= \frac{k_2 KA}{x_2} e_2 \\
 e_1 &= \frac{x_1 k_2}{x_2 k_1} e_2 \\
 e &= e_1 + e_2 \\
 e &= e_2 + \frac{x_1 k_2}{x_2 k_1} e_2
 \end{aligned}$$

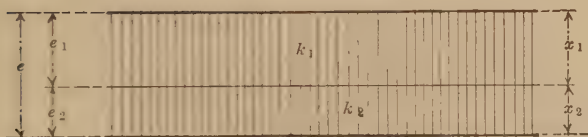


FIG. 14.—Dielectrics of different permittivities in series.

The voltages are, therefore, divided thus

$$\begin{aligned}
 e_2 &= \frac{e}{\left(1 + \frac{x_1 k_2}{x_2 k_1}\right)} \\
 e_1 &= \frac{e}{\left(1 + \frac{x_2 k_1}{x_1 k_2}\right)}
 \end{aligned}$$

The gradients are

$$\begin{aligned}
 g_1 &= \frac{e_1}{x_1} = \frac{e}{x_1 \left(1 + \frac{x_2 k_1}{x_1 k_2}\right)} \\
 g_2 &= \frac{e_2}{x_2} = \frac{e}{x_2 \left(1 + \frac{x_1 k_2}{x_2 k_1}\right)} \quad (16)
 \end{aligned}$$

The voltages and gradients may be found in the same way for any number of insulations in series. The expression for the gradi-

ent at any point  $x$  in a combination of  $n$  insulations in series is

$$g_x = \frac{e}{k_x \left( \frac{x_1}{k_1} + \frac{x_2}{k_2} + \dots + \frac{x_x}{k_x} + \dots + \frac{x_n}{k_n} \right)} \quad (16a)$$

Where the distance between the electrodes is greater than the radius of the edges, the increase in stress at the edges becomes appreciable.

*Concentric Cylinders.*—For concentric cylinders the expression may be found in the same way. The flux lines in this case, also, are normal at every boundary surface and are, hence, not refracted. Consider a wire of radius  $r_1$  surrounded by  $n$  insulations whose inside radii are, respectively,  $r_1, r_2, \dots, r_n$ , and whose permittivities are  $k_1, k_2, \dots, k_n$ .

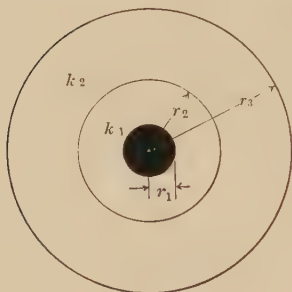


FIG. 15.

At the distance  $x$  from the center of the wire, which falls in the dielectric of inside radius  $r_x$ , outside radius  $r_{x+1}$ , and permittivity  $k_x$ , the expression for

the gradient  $g_x$  is found as follows:

$$\begin{aligned} 1/C &= 1/C_1 + 1/C_2 + \dots + 1/C_x + \dots + 1/C_n \\ &= \frac{1}{2\pi K} \left( \frac{\log_e r_2/r_1}{k_1} + \frac{\log_e r_3/r_2}{k_2} + \dots + \frac{\log_e (r_{x+1}/r_x)}{k_x} + \dots + \frac{\log_e R/r_n}{k_n} \right) \\ C &= 2\pi K \frac{1}{\left( \frac{\log_e r_2/r_1}{k_1} + \frac{\log_e r_3/r_2}{k_2} + \dots + \frac{\log_e r_{x+1}/r_x}{k_x} + \dots + \frac{\log_e R/r_n}{k_n} \right)} \\ D_x &= \frac{\psi}{A} \\ &= \frac{Ce}{A} \\ &= \frac{2\pi K}{2\pi x} \frac{e}{\left( \frac{\log_e r_2/r_1}{k_1} + \frac{\log_e r_3/r_2}{k_2} + \dots + \frac{\log_e r_{x+1}/r_x}{k_x} + \dots + \frac{\log_e R/r_n}{k_n} \right)} \\ g_x &= \frac{D_x}{k_x K} \\ &= \frac{1}{x k_x} \frac{e}{\left( \frac{\log_e r_2/r_1}{k_1} + \frac{\log_e r_3/r_2}{k_2} + \dots + \frac{\log_e r_{x+1}/r_x}{k_x} + \dots + \frac{\log_e R/r_n}{k_n} \right)} \end{aligned} \quad (17)$$

(See Chap. XI for practical application.)

**Dielectrics in Multiple.**—Where dielectrics are combined in multiple, the division between the dielectrics being parallel to

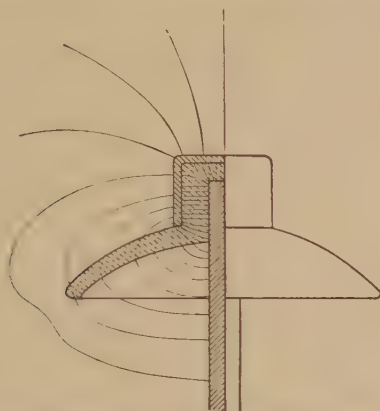


FIG. 16.—The refraction of lines of force passing through a porcelain insulator (permittivity assumed 4).

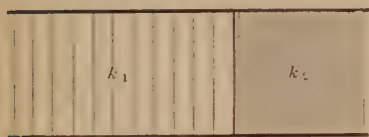


FIG. 17.—Dielectrics in multiple.

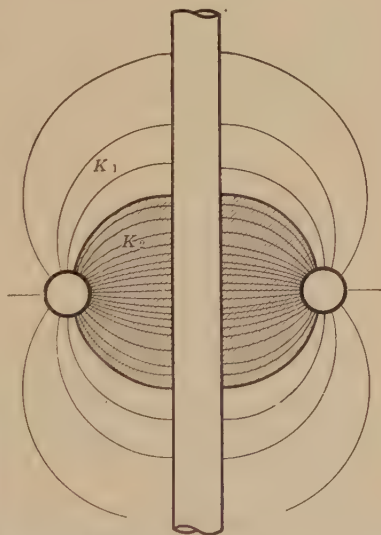


FIG. 18.—Rod and ring with two dielectrics. Boundary of dielectrics along line of force. (Not drawn to scale.)

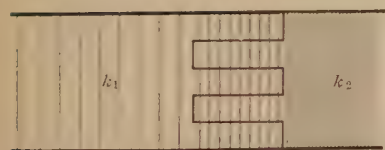


FIG. 19.—Dielectrics in multiple and in series.

the lines of force (Fig. 17), the stress on either is the same as it would be were the other not present. Figure 18 shows a rod



insulated from a ring by a dielectric so shaped as to make use of this fact. Where the division line is not parallel to the lines of force, some lines must pass through both dielectrics (Fig. 19). For these lines the insulators are in series, and the corresponding precautions are necessary, just as in Fig. 14 (see Chap. XI for further discussion).



FIG. 20.—Field not changed by a thin insulated metal plate on an equipotential surface.

**Flux Control.**—In certain electrical apparatus it is very often possible to prevent or reduce dielectric flux concentration by superposing fields upon existing fields. When it is necessary to superpose two fields, as often happens in the course of design, it is important to see that it is properly done. For instance, as a simple case, suppose the two plates *A* and *B* (Fig. 20) are at potentials of 0 and 100 kv., respectively. A thin insulated metal

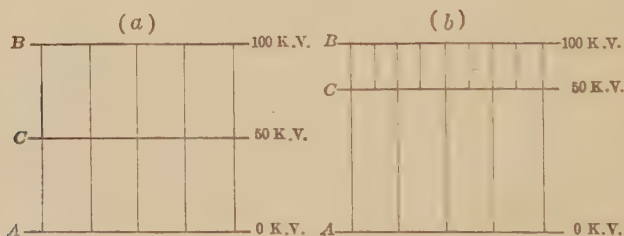


FIG. 21.—(a) Field not changed if the potential of the plate is the same as that of the surface upon which it rests. (b) Field changed by plate at potential different from the surface.

plate *C* may be placed anywhere between *A* and *B* without changing the field as long as it follows an equipotential surface—that is, parallel to *A* and *B*. Unless it follows an equipotential surface flux concentration results. If *C* is insulated and brought to a potential of 50 kv., the field will be disturbed unless *C* follows the 50 kv. equipotential surface, or, in other words, is midway

between the two plates—otherwise the stress in part of the insulation will be greatly increased (see Fig. 21 (a) and (b)).

Figure 21(a) shows the position for no change.

Figure 21(b) shows very great increase of stress on part of the insulation.

A coil of wires in which the turns are at different potentials may be placed in the field with least disturbance if the potential of each coil corresponds to the potential of the equipotential surface upon which it rests, as shown approximately in Fig. 22(a).

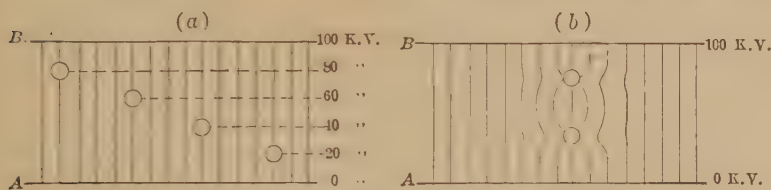


FIG. 22.—Conductors placed in a uniform field.

When insulation is used around small conductors, points, etc., the stress may be very great. This stress may be reduced by superposing a uniform field. For instance, take two small parallel wires with voltage  $e$  between them, the stress is

$$g = \frac{e}{2r \log_e \frac{S}{r}}$$

If a uniform field is superposed, as in Fig. 22(b) of gradient  $g_1 = \frac{e}{S}$ , the stress on the wires becomes

$$g_2 = 2g_1$$

These principles must be used in generator and transformer design, etc., and will be applied later (see Chap. XI).

**Imperfect Electric Elasticity.**—The electric displacement has been shown to follow Hooke's law by analogy, that is

$$\psi = Ce$$

$$D = kg \left( \frac{10^9}{4\pi v^2} \right)$$

or strain = constant  $\times$  stress

The dielectric has so far been assumed to be perfectly elastic. For a perfectly electrically elastic material  $C$  or  $k$  must be constant and independent of the time that the stress  $e$  or  $g$  is applied. This appears to be the case for homogeneous dielectrics as air,

various gases, pure oil, etc., but is not so for non-homogeneous dielectrics. As an example of imperfectly elastic dielectrics, take a cable; when potential is applied between core and case, the displacement immediately reaches very nearly its full value, but gradually increases through an appreciable time slightly above its initial value. It thus *appears* that energy is slowly absorbed and this phenomenon has, therefore, been termed *absorption*. When the above condenser is disconnected from the supply, and then short circuited, the potential difference becomes zero. If the short circuit is removed, a very small potential difference gradually reappears as *residual*. If such a condenser is displaced (charged), and the supply is removed, the displacement gradually disappears by conduction or *leakage*. In measuring the high-voltage direct-current resistance of cable insulation, it is often necessary to allow several minutes to elapse before the current becomes constant. The residual is analogous to residual stretch in an imperfectly elastic metal wire. For instance, if a steel rod is stretched and the stress is removed, it immediately assumes very nearly its initial length, but there is always very small residual stretch which very gradually disappears.

It may be shown theoretically that the phenomenon of absorption should exist for non-homogeneous dielectrics, but not for truly homogeneous dielectrics.

In non-homogeneous dielectrics the effect of this residual is to cause the flux to lag behind the voltage if the voltage change is rapid, as in the case of high frequency. This is analogous to damping. If the change in voltage is slow, however, the effect would not result. A loop may thus be plotted (when the change of voltage is rapid) between voltage and displacement, similar to the hysteresis loop. If the frequency is very low or the dielectric is homogeneous, the loop does not result.

This loop means loss, but it is not analogous to hysteresis loss in iron which is independent of time.

In non-homogeneous dielectrics the absorption may sometimes be due to local conduction in parts of the material (see page 230). The insulation, for instance, may be assumed to be made up of condensers connected together in parts by paths that become very high-resistance conductors at the high voltage. It would take considerable time to charge completely their local condensers through the high resistance. Still greater time would be required to discharge as the voltage decreased.

## CHAPTER III

### THE ELECTRON THEORY

**Electrons.**—If terminals are placed in a vacuum tube and high voltage is applied between them, a visible discharge or beam of rays is shot out from the cathode. These cathode rays proceed in straight lines. A pinhole diaphragm may be placed in their path and a narrow beam obtained (see Fig. 23). This beam may be deflected by a magnetic or dielectric field. J. J. Thomson pointed out that it acts in every way as if it were made up of negatively charged particles traveling at very high velocities.<sup>1</sup> Every test that has been made bears this out. Where the particles strike the glass, it becomes luminescent. These particles of negative electricity or “charged” corpuscles are called electrons. The velocity, charge, and mass of these electrons have been measured.

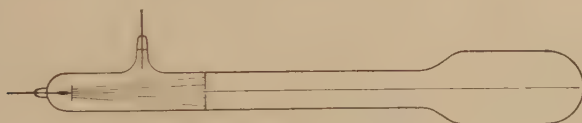


FIG. 23.—Cathode ray tube.

A charged body in motion is deflected by the electric fields in the same way as a wire-carrying current. The deflection depends upon the ratio of the charge  $e$  and the mass  $m$ . By noting the deflection of the cathode rays in the electric field, J. J. Thomson found the value of the ratio  $e/m$ . The most accurate value of the ratio with  $e$  measured in electromagnetic units is  $1.76 \times 10^7$ . Each ion in a gas acts as a nucleus in the condensation of water vapor. The condensation in the presence of the ions may be made to occur by change of pressure. By observing the rate of fall of the cloud, the number of drops or electrons can be calculated. If the total charge is measured,  $e$  can be at once

<sup>1</sup> These rays have been made use of in an oscillograph (see p. 99 Chap. IV). In this instrument the beam acts as a pointer and is made to trace a curve under influence of the fields produced by the current or voltage of the wave which is being measured.

obtained. This was done by C. T. R. Wilson.  $e$  was also later determined by Millikan and found to be  $4.77 \times 10^{-10}$  electrostatic units or  $1.6 \times 10^{-20}$  electromagnetic units. The mass of the electron seems to be about  $\frac{1}{1800}$  of the hydrogen atom, or the same mass as the hydrogen ion in electrolytic conduction. This mass is about  $9.0 \times 10^{-28}$  g. when the velocity is considerably below that of light, but it changes with velocity. It must be considered as that determined by force divided by acceleration. The velocity of the electron usually varies from  $10^7$  to  $10^9$  cm. per second, dependent on the voltage of the electric field.

**Ions and Atoms.**—Although “ion” is a general term often used for positive and negative atoms or molecules, electrons, and positive particles, it is usually meant to signify only the charged atom or molecule. The removal or addition of one or more electrons changes the neutral atom or molecule to a positive or negative ion, respectively.

The atom is supposed to consist of a positive central nucleus surrounded by electrons of sufficient total negative charge to neutralize exactly this positive charge. In the static model of the atom, as developed principally by Lewis and Langmuir, the electrons are supposed to be stationary in shells about the nucleus. This model is usually preferred by the chemists.

The dynamic atom, due principally to its better interpretation of spectral lines, has generally been accepted by the physicists, and will be considered here. This form is largely due to Bohr and Sommerfeld and assumes that the electrons rotate about the nucleus in various orbits, representing different energy levels. It is in reality a miniature solar system, the centrifugal force of the revolving electron just compensating for the electrostatic attraction of the positive nucleus. A new system of wave mechanics has been devised recently by Schrodinger, Heisenberg, Born, etc., to build up an atomic structure to interpret many spectral anomalies which the Bohr atom has so far failed to do.<sup>1</sup> This model is rather vague and highly mathematical, so that the Bohr form is still largely adhered to because of the clearer physical conception which it gives.

It has been determined that the properties of an element are largely due to its atomic structure. Its mass and any possible radioactivity are properties dependent largely on the nucleus,

<sup>1</sup> See articles, *Jour. Frank. Inst.*, Vol. V, p. 205, 1928; p. 323 (SWANN), p. 519 (SWANN); p. 597 (DAVISSON); Vol. V; p. 206, 1928; p. 605 (BRAMLEY).



while its chemical nature and spectra are connected with the distribution of the extra-nuclear electrons, and only indirectly with the nucleus.

The nucleus with its net positive charge is supposed to consist of both electrons and protons, each of the latter being a unit of positive electricity and identical with the hydrogen nucleus. In the neutral atom, the extra-nuclear electrons compensate for the excess positive charge of the nucleus and their number apparently determines the atomic number and the element's place in the periodic table. To change the element, therefore, it is necessary to change the net charge on the nucleus, for example, by the addition or subtraction of a proton or hydrogen nucleus.

If a proton and an electron could both be placed in the nucleus, the resultant charge would be unchanged and, according to the present ideas, the same element would result with unchanged chemical properties but increased atomic weight. Many such elements have been detected, each having different atomic weights but the same chemical properties. They differ only in their nuclei and are called isotopes. For example, tin and xenon have each been found to have at least seven different atomic weights.

The removal of an outer planetary electron of an extra-nuclear orbit apparently merely ionizes the atom and it assumes a positive charge. Its chemical properties and mass are left practically unchanged.

**Radioactive Materials.**—In the disintegration of radioactive substances, alpha, beta, and gamma rays are evolved. The alpha and beta emanations are really charged particles since they may be actuated by electric fields. Gamma rays, like heat, light, and X-rays are electromagnetic waves. Alpha particles are positively charged helium atoms, but possess much greater energies than the ordinary positive particles. Beta particles are identical with cathode particles or electrons but are much more active, having the highest velocities of any material bodies known.

The arrest of rapidly moving electrons when they strike the target produces X-rays. In the same way, gamma rays are produced by the braking effect exerted in the atom on the alpha and beta particles leaving the radioactive nucleus. They possess vastly greater energies than X-rays and would require tube



voltages of at least several million volts. They are surpassed in penetrating power only by the recently discovered cosmic rays, which Millikan has given considerable study. These have approximately fifty times the frequency of gamma rays and are supposed to be due to meteoric changes going on all about the earth, as they seem to enter its surface uniformly from all directions.

Radioactive emanations involving the expulsion of alpha and beta particles are believed to be due to the disintegration of the nuclei of the radioactive materials. This, therefore, involves a transmutation of elements with the consequent change of properties and decreasing mass. Several radioactive substances follow such transmutation series which end in lead of different atomic weights. In that way, therefore, are evolved several of the isotopes of lead.

**Conduction through Gases.**—Take two electrodes in air and apply some low potential between them. Direct ultraviolet

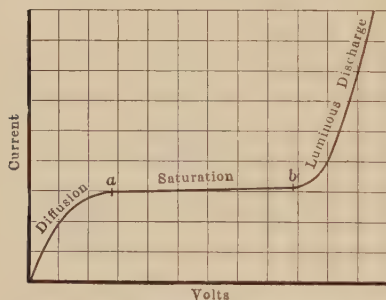


FIG. 24.—Variation of current with voltage through ionized space between parallel plate electrodes.

light upon the negative electrode. If the voltage is gradually increased, the current increases almost directly up to *a* Fig. 24. There is then a considerable range between *a* and *b* where an increase in voltage does not greatly increase the current. At *b* the current suddenly increases very rapidly with increasing voltage. It appears that negative "particles" or elec-

trons are produced or set free at the negative conductor by the ultraviolet light. These particles of electricity are attracted to the positive conductor and, thus, show as current in the galvanometer in the circuit. The number reaching the positive conductor increases with increasing voltage. The current thus increases with increasing voltage. The potential at *a* is sufficient to cause practically all of the negative particles that are produced by the light to reach the positive conductor. An increase of the voltage above the value at *a* can thus cause very little increase in current unless a new source of ionization is applied or the number of ions is increased in some way. When the voltage is

raised above the value at  $b$ , the current increases very rapidly with increasing voltage. A new source of ionization has resulted.

**Ionization.**—As shown above, an ion is merely an atom which has assumed a net positive or negative charge through the loss or gain, respectively, of one or more electrons. By the term "ionization" is usually meant the creation of positive ions by the removal of electrons from neutral atoms.

The electron in the Bohr atom, as stated previously, was assumed to be arranged in certain energy levels, an exchange of energy being evolved in any electronic shift between orbits. Consequently, in the complete removal of an electron from the atom in ionization, an absorption of energy is requisite. This energy may be in mechanical form (ionization by collision); in the form of light (photoelectric ionization); or in the form of heat (thermal ionization).

*Ionization by Collision.*—The theory of ionization by collision, as originally postulated by Townsend and later amended by others, is usually accepted as describing, in a general way, the principal form of electrical breakdown of air. In this process, as the applied field potential is raised, the action is first assumed to start through the imparting of sufficient velocities to the stray ions, believed to be ever present in the atmosphere from radioactive material, ultra-violet light, and other sources, to enable them to dislodge electrons upon colliding with neutral atoms or molecules. At the lower fields, the electrons so created are assumed to be practically the only active agents in the ionizing process, because of their much greater mobilities. Complete breakdown in the form of a spark does not occur until the voltage has been sufficiently increased to enable the less mobile positive ions to assume ionizing velocities. From his measurements between parallel plate electrodes, Townsend originally concluded that the voltage gradient necessary to start this breakdown under normal atmospheric conditions (76 cm. pressure and 25°C. temperature) was 30 kv. per centimeter. In this he assumed that the field, as he measured it between the plates, remained uniform throughout.

Work by physicists since then seems to indicate that a few of the details of the original Townsend theory, particularly in regard to the action of the positive ions, must be modified and extended. From the study of the time lag of spark gaps,<sup>1</sup> it has

<sup>1</sup> ROGOWSKI, W., *Arch. f. Elek.*, Vol. XX, 1928.

been claimed that the movement of the positive ions, as laid down by the above theory, is too slow to allow of their participation in spark-gap breakdowns of extremely brief duration (less than a microsecond). There are also indications that, even at a steady field gradient of 30 kv. per centimeter, the positive ions may not attain sufficient velocities for the ionization attributed to them.<sup>1</sup> To take care of this, Loeb<sup>2</sup> has suggested that, when breakdown occurs between parallel plates at an average gradient of 30 kv. per centimeter, the actual gradient at the cathode surface has been increased to much higher values, due to the formation of a positive space charge there. This, then, provides the positive ions there with sufficient ionizing energies. According to this, we must always look for non-uniform fields just prior to spark-over—even between parallel plate electrodes.

The ionizing energy of a gas or vapor, which is the minimum amount necessary to remove an electron from a neutral atom, is usually expressed as  $Ve$ .  $e$  is the charge of one electron and  $V$  is the ionizing voltage of the gas, or the potential that one electron must fall through unimpeded before assuming a sufficient velocity for dislodging an electron upon collision with the atom. The approximate ionizing potentials of the common gases, oxygen, hydrogen, nitrogen, and helium are, respectively, 13.56, 13.54, 12.2, and 24.48 volts. The ionizing potentials of most metal vapors lie between approximately 4 and 10 volts. The method of determining these potentials is roughly as follows: The gas or vapor in question is placed in a discharge chamber and a slowly increasing voltage applied to the electrodes. At a certain voltage, a sharp rise in current occurs, indicating the start of impact ionization. With this value of voltage, and certain assumptions, the ionizing potential of the gas or vapor may then be calculated.

The breakdown voltage gradient, whether it involves local breakdown by corona or complete failure by sparkover, is usually expressed for conditions of atmospheric pressure. This value necessary for breakdown decreases with the pressure (except for extremely low pressures), due to the improved facilities for ionization. This follows because with decreasing pressure the "mean free path" of the electron increases; that is, the greater

<sup>1</sup> LOEB, L. B., *Jour. Frank. Inst.*, Vol. 205, p. 305, 1928.

<sup>2</sup> Loeb suggests a surface gradient as high as 300 kv. per centimeter.

separation of the gas particles allows the electron to reach greater velocities between collisions for the same field gradient.

In an extremely high vacuum where the gas particles present are too few to take part in any ionization process, excessive gradients are necessary for any breakdowns. In these cases, the charges involved consist of electrons actually pulled from the electrodes. In studies of this nature, Millikan has secured several spark-overs requiring gradients as high as 6,000,000 volts per centimeter.

With very short electrode spacings of a fraction of a millimeter, very high breakdown gradients may also be reached. This is due to the hampering of the ionization process through the actual limiting of the mean free parts of the ionizing bodies.

*Ionization by Photoelectric Effect.*—A condenser or electroscope may be left charged in air a great length of time without considerable loss or leakage. If, however, the surrounding air and the terminals of the condenser or electroscope are subjected to the action of X-rays, ultra-violet light, or radioactive substances, the leakage becomes quite rapid. This is due to the gas becoming conducting because of ionization by photoelectric effect.

This form of ionization is accomplished through the absorption, by the gas molecules and by the metal molecules in the terminal surfaces, of sufficient radiant-light energy to dislodge certain electrons. In gases, radiations of very high frequency are necessary in order to remove electrons completely from the atoms. X-rays and gamma rays produce copious ionization in gases, but ordinary ultra-violet light is effective in but a few gases.

Ultra-violet light is rather active in dislodging electrons from metal surfaces by photoelectric effect, the action varying for different materials. With the alkali metals, such as sodium, potassium, etc., electron emission can be quite copiously created, while for the non-metals, such as carbon, the effect only appears with radiations of much shorter wave lengths.

*Thermal Ionization.*—When extremely high temperatures are reached in a gas or vapor, thermal ionization may take place. From the assumptions of the kinetic theory of gases, this form of ionization really involves impact and radiation transfers of energy. As a rule, physicists doubt the existence of true thermal ionization in the usual laboratory discharges. K. T. Compton<sup>1</sup> says:

<sup>1</sup> COMPTON, K. T., *Trans. A.I.E.E.*, p. 882, 1927.



As regards any direct effect of temperature on the ionizing potential of the gas, this effect will probably be rather small because translating degrees centigrade into volts, about 8000 degrees correspond to only one volt. There are no laboratory experiments that reach a temperature as high as 8000 degrees, so that the average energy imparted to electrons as the result of high temperature or to the molecules by high temperature would in general be only a fraction of a volt.

It would seem that in lightning strokes and in some electric furnaces sufficient temperatures are undoubtedly involved to make thermal ionization a factor.

*The Creation of Negative Ions.*—The ability of negative ions to form depends largely on the nature of the gas or vapor involved. Certain atoms have greater “electron affinities” than others; that is, they have a greater tendency to take hold of stray electrons and thereby change themselves from the state of neutral atoms to negative ions.

*General Consideration of Ionization.*—The whole ionization process involved in any electrical discharge or breakdown is sure to be quite complicated. It will probably involve all the above forms of ionization to some extent.

The light created during any electrical discharge, most of which is often invisible, is supposed to be the energy radiated when electrons and ions recombine, or electrons drop back to inner and more stable orbits within their respective atoms. Such light energy, if of the proper frequency, may be absorbed by neutral atoms in such a way as to cause electrons in them to be displaced to outer orbits. With these excited atoms in such an unstable state through this photoelectric action, the electrons may be then more easily dislodged by collision, and ionization brought about. High temperature may assist in the same manner by creating excited atoms, and dissociating molecules into atoms. Also collisions of insufficient force, in themselves, for complete ionization may, nevertheless, add to this same atomic instability. All these factors tend to lower the ionizing potential of a gas.

*Various Stages of Breakdown of Air.*—The different forms of breakdown of air are generally classified as coronas, glow discharges, sparks, and arcs. It is often difficult to draw sharp lines between these forms with respect to their electrical properties<sup>1</sup> as they share so many characteristics at times.

<sup>1</sup> COMPTON, K. T., *Trans. A.I.E.E.*, p. 868, 1928.

Arcs are usually differentiated from sparks by considering them as involving greater current densities with comparatively lower voltage drops, although there are exceptions to this rule. Physicists generally classify the two by considering the spark to have the greater cathode drop while some add the stipulation that the arc must have a negative volt-ampere characteristic.

The spectroscopist has differentiated between arcs and sparks by means of the spectra produced. In general, the arc would be defined as any discharge involving the excitation of lines or bands in the spectrum indicating excited states of neutral atoms or molecules, or possibly the first stage of ionization, the radiated light energy being emitted by electrons falling back into more stable orbits. Sparks would be characterized as discharges producing spectra indicating higher stages of excitation and ionization, in which greater voltage gradients and higher atomic energies enter.

A few laboratory discharges can be obtained having arc-like characteristics which do not involve thermionic emission or metal vapors. As a rule, most atmospheric arcs encountered by the engineer incur both of these factors, electrons being emitted from the heated negative electrode in the same manner as from the hot filament of a vacuum tube, and metal vapors being boiled off from both the electrodes. Metallic vapors are particularly conducive to low-voltage characteristics, compared to ordinary gases, as, in general, they have lower ionizing potentials; they possess lesser electron affinities, thereby removing fewer electrons from the discharge; and they have more elastic impacts, thus absorbing less energy from colliding electrons and ions.

In ordinary alternating-current flashovers between points, the first visible sign of air breakdown is the corona at the points. The corona brushes increase in length as the voltage is raised, and, if the electrode spacing is not much more than a foot in length and circuit conditions are fairly stable, a faint glow-like discharge appears at intervals completely across the gap when a sufficiently high voltage is reached (see Fig. 74). Soon thereafter complete breakdown of the gap occurs. Recent work with moving films and spectrograms<sup>1</sup> has indicated that this breakdown is first in the form of an extremely brief, condenser-like air spark which cores out a path for the low-voltage arc which immediately follows. It is in this subsequent arc stage that thermionic emission and metal vapors enter to take part in the discharge.

<sup>1</sup> LUSIGNAN, J. T., *Trans. A.I.E.E.*, 1929, p. 246.




## CHAPTER IV

### VISUAL CORONA

#### SUMMARY

**Appearance.**—If potential is applied between the smooth conductors of a transmission line or between concentric cylinders and gradually increased, a voltage is finally reached at which a hissing noise is heard and, if it is dark, a pale violet light can be seen to surround the conductors. This voltage is called the *critical visual corona point*. If a wattmeter is inserted in the line, a loss is noticed. The loss increases very rapidly as the voltage is raised above this point. The glow or breakdown starts first near the conductor surface, as the dielectric flux density or gradient is greatest there. As the broken down air near the surface is conducting, the size of the conductor is, in effect, increased by conducting corona. This increases for the given voltage until the flux density or gradient is below the rupturing gradient, when it cannot spread any more. If the conductors are very close together, a spark strikes between them immediately before visible corona can form. If the conductors are far apart, corona forms first and then, if the voltage is sufficiently increased, a spark strikes across.

Whenever corona is present, there is always the characteristic odor of ozone. Air consists of a mechanical mixture of oxygen ( $O_2$ ) and nitrogen (N). When air is overstressed electrically, the oxygen molecule is split up into O, when it becomes chemically very active. The atoms again combine by the law of probability

into  $O = O$ , ( $O_2$ ), the normal state, and , ( $O_3$ ) or ozone.

Oxygen in the nascent state (O) also combines with metal, organic matter, etc., if such are present. Ozone is also not stable and is, hence, chemically active; it splits up as  $O_2$  and O when the latter combines readily with metals and organic matter. If the electrical stress is very high, the oxygen enters into chemical combination with the nitrogen, forming oxides. The energy loss by

corona is, thus, in a number of forms, as heat, chemical action, light, noise, convection, etc.

**Alternating-current and Direct-current Corona.**—When alternating voltage higher than the critical voltage is applied between two parallel polished wires, the glow is quite even, as shown in Fig. 25. After operation for a short time, reddish beads or tufts form along the wire, while around the surface of the wire there is a bluish-white glow. If the conductors are examined through a

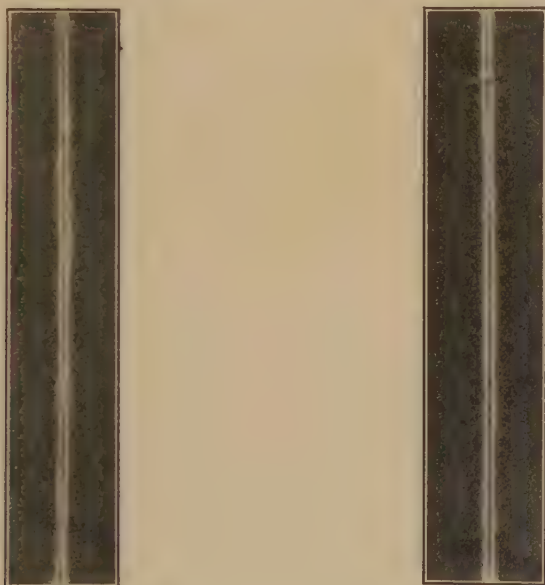


FIG. 25.—Alternating-current corona on polished parallel wires.

stroboscope, so that one wire is always seen when at a given half of the wave, it is noticed that the reddish tufts or beads are formed when the conductor is negative and the smoother bluish-white glow when the conductor is positive (see Fig. 26). Alternating-current corona viewed through the stroboscope has the same appearance as direct-current corona (see Fig. 27, direct-current corona). The direct-current corona on the + wire has exactly the same appearance as the alternating-current corona on the + half of the wave; the same holds for the - wire. Further photographs are shown on pages 85 to 89.

**Influence of Wire Spacing and Diameter.**—For parallel wires the gradient at the wire surface, and, hence, where the

stress is a maximum and the "dielectric elastic limit" is first exceeded, is

$$\frac{d_e}{d_x} = g = \frac{e}{r \log_e s/r} \quad (\text{see (12c) page 25})$$

where  $S$  and  $r$  are the spacing and radius in centimeters, respectively.

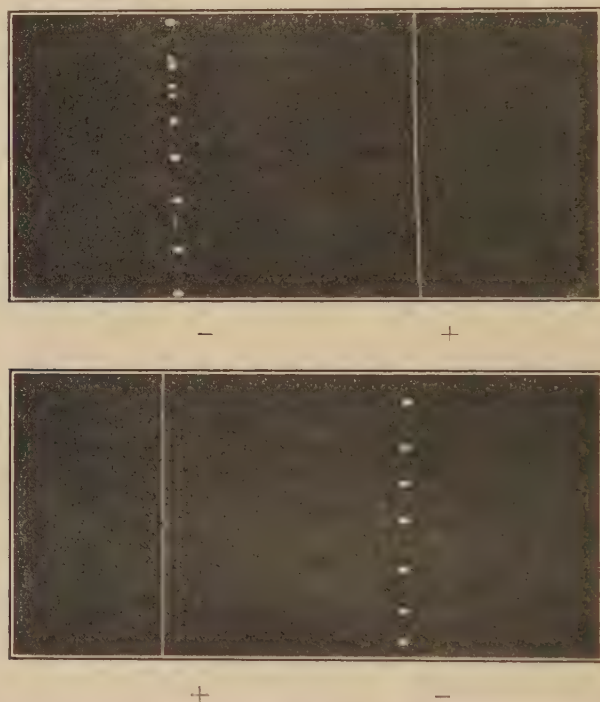
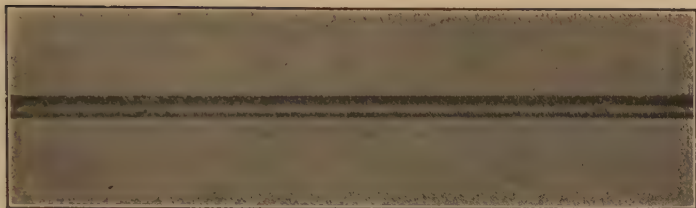


FIG. 26.—Corona on parallel wires. Iron. First polished and then operated at 120 kv. for 2 hours to develop spots. Diameter, 0.168 cm. Spacing, 12.7 cm. Stroboscopic photo., 80 kv. 60 ~. Stroboscope shifted 180 degrees for second photo.

If  $e$  is  $e_v$ , the observed voltage to neutral at which visual corona starts,  $g_v$  is the measure of the stress at breakdown. The expression for this is therefore

$$g_v = \frac{e_v}{r \log_e S/r}$$

If the visual corona voltages are measured for a given conductor at various spacings, it is found that  $g_v$  is a constant, independent of the spacing except for extremely short spacings.



Wire "dead".

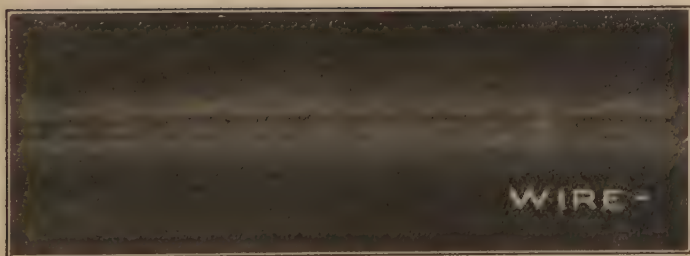
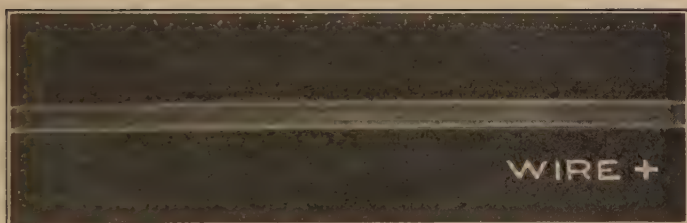


FIG. 27.—Direct-current corona on smooth wires by Watson. (See Fig. 79.)

With regard to size of conductor, it has long been known<sup>1</sup> that air is apparently stronger at the surface of small conductors than larger ones. Of course this does not mean that the voltage required to start corona is greater for small wires than for larger ones (it is, in fact, lower for small conductors at a given spacing), but that the term  $g_v$  or unit stress in the expression

$$e_v = g_v r \log_e S/r$$

is greater for air around small conductors than large ones.

During our first investigations,<sup>2</sup> to be described later, it was found that the relation between the apparent strength of air and the radius of the conductor could be expressed by the simple formula

$$g_v = g_o \left( 1 + \frac{0.301}{\sqrt{r}} \right)$$

where  $g_o$  is a constant equal to about 30 kv. per centimeter. This means that the stress at the conductor surface at breakdown is not the same for all diameters, as already stated, but is always constant at a distance  $a = 0.301 \sqrt{r}$  cm. from the surface (see page 57).

By substitution then

$$e_v = 30 \left( 1 + \frac{0.301}{\sqrt{r}} \right) r \log_e S/r \text{ crest kilovolt to neutral}$$

or for a sine wave

$$e_v = 21.2 \left( 1 + \frac{0.301}{\sqrt{r}} \right) r \log_e S/r \text{ effective kilovolt to neutral}$$

**Very Small Spacings or Films.**—If conductors are placed closer together than this necessary free accelerating or ionizing distance,  $0.301\sqrt{r}$  cm., the rupturing force or gradient must be increased. This will be better illustrated by later experiments, in which at small spacings air has been made to withstand gradients as high as 200 kv. per centimeter.

**Air Density.**—Thus far the discussion has been limited to air at a constant density, or in other words, constant temperature and pressure. All breakdown values have been assumed to be at standard sea level conditions (*i.e.*, 25°C. and 76 cm. barometer), where the air density factor  $\delta$  is taken as equal to unity (1.0).

<sup>1</sup> RYAN, H. J., *Trans. A.I.E.E.*, p. 275, 1904.

<sup>2</sup> PEEK, F. W., "The Law of Corona, I," *Trans. A.I.E.E.*, p. 1889, 1911.



Air at other densities is expressed as a fraction of this, that is, the relative density for any temperature or pressure is

$$\delta = \frac{3.92b}{273 + t}$$

For instance, if the temperature is kept at 25°C. and pressure is reduced to 38 cm.

$$\delta = \frac{3.92 \times 38}{273 + 25} = 0.50 \text{ or } \frac{1}{2} \text{ atmosphere}$$

It has been found, experimentally, that the factor  $a$  referred to in the previous section varies with the air density as follows:

$$a = 0.301 \frac{\sqrt{r}}{\sqrt{\delta}} \text{ cm.}$$

so that

$$g_v = 30\delta \left( 1 + \frac{0.301}{\sqrt{\delta r}} \right)$$

The equation for visual critical corona voltage may now be written

$$e_v = g_v \delta r \log_e S \quad r = g_o \delta \left( 1 + \frac{0.301}{\sqrt{\delta r}} \right) r \log_e S / r \text{ kv.} \quad (20)$$

where  $e_v$  is kilovolt to neutral,  $g_o$  equals 30 for crest values and 21.1 for effective sine wave values.

**Conductor Surface, Cables, Material.**—For rough or weathered conductors, corona starts at lower voltages. This is taken care of by the irregularity factor  $m_v$ . For cables and weathered wires the complete formula becomes

$$e_v = m_v \delta g_v r \log_e S / r$$

For the same surface condition, the starting point is independent of the conductor material.

**Oil and Water, Current in the Conductor, Wave Shape, Etc.**—*Water, sleet, and snow* lower the visual corona voltage.

*Oil* on the conductor surface has very little effect.

*Humidity* has no effect upon the starting point of visual corona.

*Initial ionization* over a considerable range has no appreciable effect at commercial frequencies.

*Current* in the wire has no effect except that due to heating of the conductor and surrounding air.

**Wave Shape.**—The corona point at commercial frequencies depends upon the maximum value of the wave. When results are given in effective volts, a sine wave is assumed. With peaked wave, corona starts at a lower effective voltage than with a



flat-top wave. Direct-current corona starts at a value corresponding to the maximum of the alternating-current wave or 41 per cent. higher than the effective alternating-current critical voltage.<sup>1</sup> See appendix for further data.

*The above summary will now be taken up more in detail and experimental proof given.*

### EXPERIMENTAL STUDY OF VISUAL CORONA

**Effect of Spacing and Size of Conductor.**—The visual critical voltage, or voltage at which visual corona starts on polished

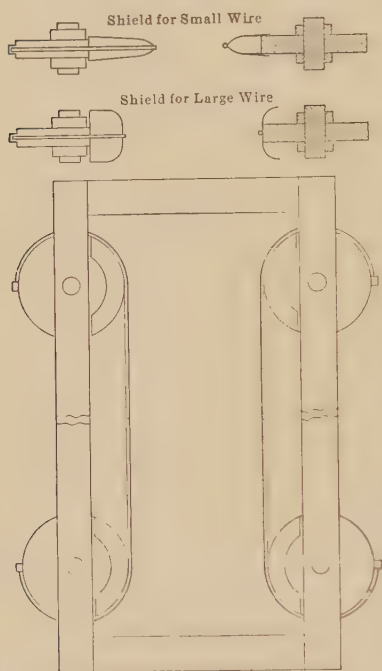


FIG. 28.—Wire support for visual corona tests.

conductors of a given diameter and spacing, at constant air density, can be repeatedly checked within a small percentage. Visual tests were made on two parallel polished conductors supported indoors on wooden wheels in a wooden framework. The wires were not allowed to come directly in contact with the wood but rested on aluminum shields (see Fig. 28). The object of the shields was to prevent the glow at low voltages which would take place if the wires came in contact with the wood. The tests were made in a dark room, and method of procedure was as follows: Conductors of a given size were placed upon a framework; voltage was applied and gradually increased until the visual critical corona

point was reached. Critical points were taken at various spacings and recorded as in Table I. Unless otherwise stated tests were made at 60  $\sim$ .

As the visual critical voltage  $c_v$  is the voltage at breakdown of the air, the surface gradient corresponding to this voltage must be the stress at which air ruptures. This is called the visual

<sup>1</sup> PEEK, "The Effect of High Continuous Voltages on Air, Oil, and Solid Insulation, *Trans. A.I.E.E.*, p. 783, 1916.

critical gradient  $g_r$ . Where the wires are far apart or  $S/r$  is large

$$\frac{de}{dr} = g_v = \frac{e_v}{r \log_e S/r}$$

where

$e_v$  = the (maximum) voltage to neutral

$r$  = radius of the conductor in centimeters

$S$  = distance between centers of conductors in centimeters

Values of gradient calculated for a given conductor at various spacings are given in Table I (see Fig. 29). It is seen that the

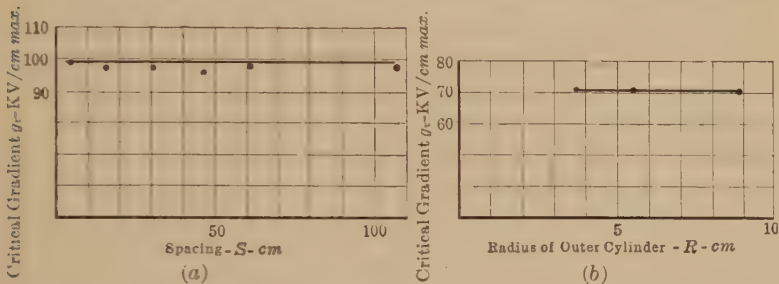


FIG. 29(a).—Variation of visual critical gradient with spacing. (Parallel wires. Diameter constant = 0.034 cm.)

FIG. 29(b).—Variation of visual critical gradient with radius of outer cylinder. (Concentric cylinders. Diameter of inner wire constant = 0.118 cm.)

TABLE I.—VISUAL CRITICAL VOLTAGES AND  $g_v$  WITH VARYING SPACING AND CONSTANT DIAMETER

(Polished Parallel Copper Conductors—Diameter 0.0343 cm.—60 ~)

$s$ cm.	$e_v$ kilovolts between conductors (effective)	$e_v$ kilovolts between conductors (maximum)	$g_v$ kv./cm. (maximum)
2.54	12.1	17.0	99.5
2.93	12.4	17.4	99.0
3.18	12.5	17.7	98.5
3.81	13.0	18.4	99.0
4.45	13.5	19.0	99.5
5.08	13.8	19.4	100.0
5.73	14.0	19.8	99.0
7.62	14.5	20.5	99.0
15.2	16.0	22.6	97.2
30.5	17.7	25.0	97.2
45.6	18.7	26.3	96.1
61.0	19.4	27.4	98.0
106.8	20.6	29.0	97.2
		Average,	99.0

breakdown gradient is constant, or independent of the spacing. This test was repeated for various diameters. The values of the gradients are tabulated in Table II and plotted in Fig. 30.

TABLE II.—VARIATION OF  $g_v$  WITH DIAMETER OF CONDUCTORS  
(Average Values for Polished Parallel Wire. 60 ~. Corrected to 25 deg. C.  
76 cm. Barometric Pressure)

Diameter, cm.	$\frac{de}{dr} = g_v$ kv./cm. (maximum)	Material	Diameter, cm.	$\frac{de}{dr} = g_v$ kv./cm. (maximum)	Material
0.0196	116	Tungsten	0.2043	59.0	Copper
0.0343	99	Copper	0.2560	57.0	Aluminum
0.0351	94	Copper	0.3200	54.0	Copper
0.0508	84	Aluminum	0.3230	50.5	Copper
0.0577	82	Aluminum	0.5130	49.0	Copper
0.0635	81	Tungsten	0.5180	46.0	Copper
0.0780	76	Copper	0.6550	44.0	Copper
0.0813	74	Copper	0.8260	42.5	Copper
0.1637	64	Copper	0.9280	41.0	Copper
0.1660	64	Iron			

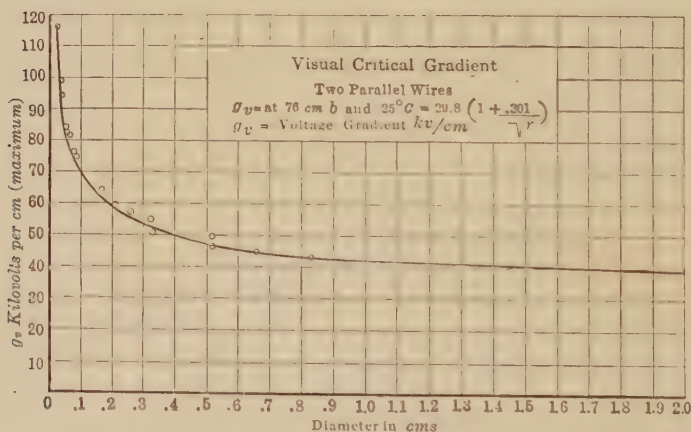


FIG. 30.—Variation of visual critical gradient with size of wire.

The gradient at breakdown at the conductor surface is not constant with varying diameters, but increases with decreasing diameters of conductors—in other words, air is apparently stronger at the surface of small wires than large ones.

The apparent increase in the dielectric strength of air surrounding small conductors was explained years ago as due to a condensed air film at the surface of the conductor. If this were so,

a higher critical gradient would be expected for tungsten than for aluminum. That is, the air film should be denser around the denser metals. These experiments show that the gradient is not affected by the material or density of the conductor.

The explanation first offered in Law of Corona I,<sup>1</sup> before the development of the electron theory to its present state, was that the air at a given density has a constant strength  $g_o$ , but that energy is necessary to cause breakdown or start corona. The air must be stressed over a finite distance at a gradient of  $g_o$  or higher. For a radial field it must, therefore, reach a gradient  $g_r$  to cause a gradient of  $g_o$  a finite distance away. The distance between  $g_r$  and  $g_o$  was called the energy distance. In terms of the electron theory, the reason is probably due to the behavior of the ionization process under the changing electrostatic field conditions with a decreasing conductor radius. The electrons and ions involved have finite sizes and mobilities, so that it is conceivable that below certain conductor sizes the breakdown process, particularly collision ionization, should be sufficiently impaired as to require increasingly higher surface gradients for starting corona. The radial field extending out from a conductor would, of necessity, require that the surface gradient itself be sufficiently greater than the breakdown gradient for a uniform field, in order to allow the field for a certain distance out to assume breakdown proportions. Interesting linear relations for such radial distances at breakdown have been found from the experimental data obtained.

Just before rupture occurs the gradient at the conductor surface is

$$g_r = \frac{e_v}{r \log_e S/r} \quad (21)$$

the gradient  $a$  cm. away from the surface is

$$g_o = \frac{e_v}{(r + a) \log_e S/r} \quad (22)$$

Theoretically, one is also led to believe

$$a = \phi(r)$$

$$\text{or} \quad g_o = \frac{e_v}{(r + \phi(r)) \log_e S/r} \quad (23)$$

It now remains to test this out experimentally and find  $\phi(r)$ .

<sup>1</sup> PEEK, F. W., JR., *Trans. A.I.E.E.*, p. 1889, 1911.

The equation of the experimental curve is found to be

$$g_v = g_o \left( 1 + \alpha / \sqrt{r} \right) = 29.8 \left( 1 + \frac{0.301}{\sqrt{r}} \right) \quad (24)$$

Substituting (24) in (21)

$$g_o \left( 1 + \frac{0.301}{\sqrt{r}} \right) = \frac{e_r}{r \log_e S/r}$$

$$g_o = \frac{e_v}{(r + 0.301\sqrt{r}) \log_e S/r}$$

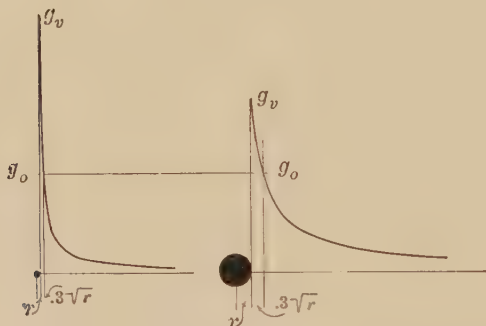


FIG. 31.— $g_v$  and  $g_o$  for small and large wires.

Thus the experimental values bear out the above theory

$$a = \phi(r) = 0.301\sqrt{r}$$

$$g = 29.8 = \text{constant}$$

That is, at rupture the gradient a finite distance away from the conductor surface, which is a definite function of  $r$ , is always constant (see Fig. 31).

$$g_v = 29.8 \left( 1 + \frac{0.301}{\sqrt{r}} \right) \text{ kv. per centimeter}$$



FIG. 32.—Apparatus for determining the visual corona voltage in concentric cylinders.

A similar investigation made on wires in the centers of metal cylinders (see Figs. 29 and 32) shows, as above, that the visual critical gradient  $g_r$  increases with decreasing radius  $r$  of the wire, but is independent of the radius  $R$  of the outer cylinder. The relation between  $r$  and  $g_v$  is given in Table V. For a wire in



the center of a cylinder, the gradient  $g_c$  is slightly higher than for similar parallel wires, apparently due to the fact that the field is everywhere balanced for a wire in the center of a cylinder, which is not the case for parallel wires. The expression for the apparent strength of air for a wire in the center of a cylinder is

$$g_v = 31 \left( 1 + \frac{0.308}{\sqrt{r}} \right) \text{ kv. per centimeter}$$

The method of reducing the results to equations was as follows: Various functions of  $r$  and  $g_r$  were plotted for parallel wires from

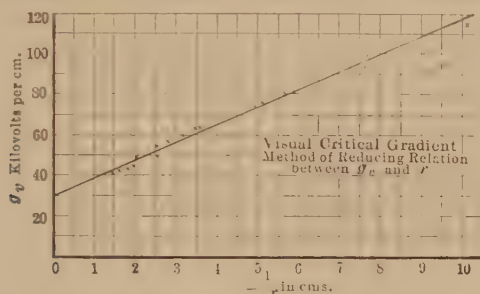


FIG. 33.—Relation between  $g_v$  and  $\frac{1}{\sqrt{r}}$ .

Table II, until it was found that a straight-line law obtained between  $g_c$  and  $1/\sqrt{r}$ . All values of  $g_c$  and  $1/\sqrt{r}$  were then tabulated as in Table III and plotted as in curve (Fig. 33). Points varying widely from the average straight line were then

TABLE III.—RELATION OF VISUAL CRITICAL VOLTAGE GRADIENT TO RADIUS

(Experimental Values Corrected to 76 cm. Barometer and 25 deg. C. Parallel Wires 60 ~)

Diameter, cm.	$g_v$ kv./cm. (max.)	Radius, $r =$ cm.	$\frac{1}{\sqrt{r}}$ cm.	Diameter, cm.	$g_v$ kv./cm. (max.)	Radius, $r =$ cm.	$\frac{1}{\sqrt{r}}$ cm.
0.0196	116.0	0.0098	10.10	0.202	59.1	0.101	3.13
0.0343	99.0	0.0172	7.65	0.257	56.7	0.128	2.76
0.0350	94.0	0.0175	7.58	0.320	54.3	0.160	2.51
0.0508	84.0	0.0254	6.27	0.322	49.6	0.161	2.51
0.0577	81.5	0.0288	5.90	0.513	48.8	0.256	2.01
0.0635	81.0	0.0317	5.64	0.518	44.5	0.259	1.94
0.078	76.0	0.0390	5.08	0.655	43.7	0.327	1.82
0.0813	73.5	0.0406	4.96	0.826	42.2	0.413	1.57
0.1635	63.8	0.0818	3.51	0.928	40.6	0.464	1.44
0.1660	63.4	0.0830	3.45				



discarded as probably in experimental error. The remaining points were then divided into two equal groups and tabulated as in Table IV.

TABLE IV.—RELATION OF  $g_v$  AND  $\frac{1}{\sqrt{r}}$   
(Showing  $\Sigma\Delta$  Reduction)

$g_v$	$\frac{1}{\sqrt{r}}$	$g_v$	$\frac{1}{\sqrt{r}}$
99	7.65	59.0	3.13
82	5.90	54.0	2.51
81	5.64	50.5	2.51
76	5.08	49.0	2.01
74	4.96	41.0	1.44
$\Sigma 412$	$\Sigma 29.23$	$\Sigma 253.5$	$\Sigma 11.60$

$$\Delta \Sigma g_v = 158.5$$

$$\Delta \Sigma \frac{1}{\sqrt{r}} = 17.63$$

$$\Sigma \Sigma g_v = 665.5$$

$$\Sigma \Sigma \frac{1}{\sqrt{r}} = 40.83$$

$$c_1 = \frac{158.5}{17.63} = 9.00$$

$$g = \frac{665.5 - (9 \times 40.8)}{10} = 29.8$$

Therefore 
$$g_v = 29.8 + \frac{9}{\sqrt{r}}$$

$$= 29.8 \left( 1 + \frac{0.301}{\sqrt{r}} \right)$$

In order to give proper weight to the points, the  $\Sigma\Delta$  method was used in the evaluations of the constants for the equation above. This method of reduction, which is self explanatory, is very convenient and especially suitable where a large number of experimental points have been obtained, in which case the results are as reliable as, or more so, than when few points are taken and the unwieldy method of least squares used.

Table V shows the relation of gradient to radius for concentric cylinders.

TABLE V.—RELATION OF VISUAL CRITICAL VOLTAGE GRADIENT TO RADIUS (76 cm. Barometer—25 deg. C.—Concentric Cylinders)

Radius r cm.	a.c. $\rho_v$ kv./cm. (max.)	R cm.	d.c. <sup>1</sup> $\rho_v$ kv./cm.	r cm.	a.c. $\rho_v$ kv./cm. (max.)	R cm.	d.c. $\rho_v$ kv./cm.
0.059	70.4	3.89-5.55-3.65	69.0	0.327	48.1	3.89-5.55-3.65	42.0
0.103	60.7		59.5	0.476	44.9		39.0
0.127	58.4		55.5	0.794	41.9		.....
0.129	56.6		54.5	0.953	41.2		.....
0.190	52.7		49.5	1.113	39.7		.....
0.199	52.7		48.5	1.270	39.2		.....
0.206	51.6		47.5	1.588	38.4		.....
0.254	49.9		44.5	1.905	37.8		.....
0.318	47.1		43.0	2.540	35.0	.....	.....

<sup>1</sup> Direct-current values from WATSON, *Jour. I. E. E.*, Fig. 21, June, 1910

Some investigators have found a maximum difference of 6 per cent between the (+) and (-) corona starting voltages. The difference is generally small and there is usually fair agreement between direct current and maximum alternating current. See additional data in appendix.

**Visual Corona at Very High Voltages.**—Since establishing the above laws of corona, the author has made tests on parallel conductors of over 8 cm. in diameter and at voltages exceeding 1,000,000.<sup>1</sup> Over this large range the calculated and measured voltages check very closely as will be seen by the tabulation of this data in the appendix, page 396 (see Fig. 68).

**Temperature and Barometric Pressure.**—The density of the air varies directly with the pressure, and inversely as the absolute temperature. In these investigations the air density at a temperature of 25°C. and a barometric pressure of 76 cm. has been taken as standard. If the air density at this temperature and pressure is taken as unity, the relative density at other temperatures and pressures may be expressed in terms of it, thus

$$w = \frac{0.00465b}{273 + t}$$

where  $w$  = the weight of air in grams per cubic centimeter  
 $b$  = barometric pressure in centimeters  
 $t$  = temperature in degrees centigrade

<sup>1</sup> PEEK, F. W., JR., "Tests at 1,000,000 Volts," *Electrical World*, Dec. 31, 1921.

At 25 °C and 76 cm. pressure

$$w_{25^\circ - 76\text{cm.}} = \frac{0.00465 \times 76}{273 + 25} = 0.001185 \text{ gram}$$

$w$  at any other temperature and pressure is

$$\begin{aligned} w_t &= \frac{0.00465b}{273 + t} \\ \frac{w_t}{w_{25^\circ - 76\text{cm.}}} &= \frac{0.00465b}{(273 + t)0.001185} = \frac{3.92b}{273 + t} = \delta \\ \delta &= \frac{3.92b}{(273 + t)} \end{aligned}$$

$g_o$  should vary directly with the air density factor  $\delta$ ;  $g_r$ , however, should not vary directly with  $\delta$ , as the thickness of the ionizing film should also be a function of  $\delta$ . The equation for  $g_v$  should take the form

$$g_v = g_o \left( 1 + \frac{\alpha}{\phi(\delta)\sqrt{r}} \right) \quad (25)$$

Whether  $\delta$  is varied by change of temperature or air pressure, the effect should be the same as long as the temperature is not so high that the air is changed or affected by the heat, as ionization, etc.

**Temperature.**—A series of experiments on visual corona was carried on over a temperature range of 20 to 140°C. The apparatus is shown in Fig. 32. It consists of a polished wire in the center of a brass cylinder. The cylinder was placed horizontally in a large asbestos lined "hot box," heated by grids at the bottom. In order to get uniform temperature, the cylinder was shielded, and time was allowed to elapse after each reading. Temperature was observed by a number of thermometers distributed in the hot box.

After the heating became uniform, voltage was applied and gradually increased until the glow appeared. The central conductor was observed through a window placed in the front part of the box so that the whole length of the conductor could be seen. It was found that it made no appreciable difference in the starting voltage whether or not the box and tube were "aired out" after each test.

Three sizes of brass cylinders were used having inside radii of 8.89, 5.55, and 3.65 cm., respectively. The central conductors ranged in size from 0.059 to 0.953 cm. radii. Tables VI and VII are typical data tables.

TABLE VI.—VARIATION OF STRENGTH OF AIR WITH TEMPERATURE  
For Polished Copper Tube Inside of Brass Cylinder  
 $r = 0.953$   $R = 5.55$  cm. Tests at 60 ~

Observed values					Calculated from equation
Kv. effective	Temp. C°	$\delta$ cm.	$\delta$	$g_s(\text{max.})$	$g'_s(\text{max.})$
48.5	18	75.4	1.016	40.7	41.4
46.5	37	75.4	0.954	39.1	39.1
45.2	50	75.4	0.915	38.0	37.7
43.4	66	75.4	0.873	36.5	36.2
41.0	85	75.4	0.826	34.5	34.5
39.6	100	75.4	0.793	33.3	33.3
37.6	119	75.4	0.754	31.6	31.9

TABLE VII.—VARIATION OF STRENGTH OF AIR WITH TEMPERATURE  
For Polished Copper Tube Inside of Brass Cylinder  
 $r = 0.476$  cm.  $R = 5.55$  cm. Tests at 60 ~

Observed values					Calculated from equation
Kv. effective	$t$	$\delta$	$\delta$	$g_s(\text{max.})$	$g'_s(\text{max.})$
41.0	-13	75.5	1.139	49.6	50.0
40.0	0	75.5	1.084	48.3	48.0
37.0	20	74.9	1.001	44.8	44.9
35.7	41	75.5	0.942	43.2	42.7
33.2	70	75.5	0.863	40.1	39.7
31.5	87	75.5	0.823	38.1	38.1
29.5	121	75.5	0.753	35.7	35.4
28.7	130	75.5	0.734	34.7	34.7

Columns 1, 2, and 3 give observed values. The gradient at the surface of the inner cylinder is

$$g = \frac{e}{r \log_e R/r}$$

Column 5 gives the surface gradient for the voltage  $e_s$  calculated directly from observed values. It can be seen, from the data, that  $g_s$  for a given  $r$  varies with  $\delta$  but is independent of  $R$  or  $S$ .

By  $\Sigma\Delta$  reduction of all of the data, the following equations connecting  $g_s$  with  $r$  and  $\delta$  were obtained:

*For Concentric Cylinders.*

$$g_v = 31\delta \left(1 + \frac{0.308}{\sqrt{\delta r}}\right) \text{ kv. per centimeter maximum} \quad (25a)$$

*For Parallel Wires.*

$$g_v = 29.8\delta \left(1 + \frac{0.301}{\sqrt{\delta r}}\right) \text{ kv. per centimeter maximum} \quad (25b)$$

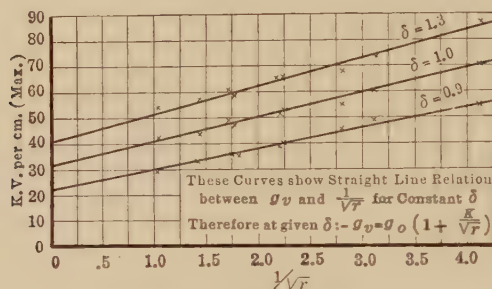


FIG. 34.—Effect of temperature on the strength of air. × measured values.

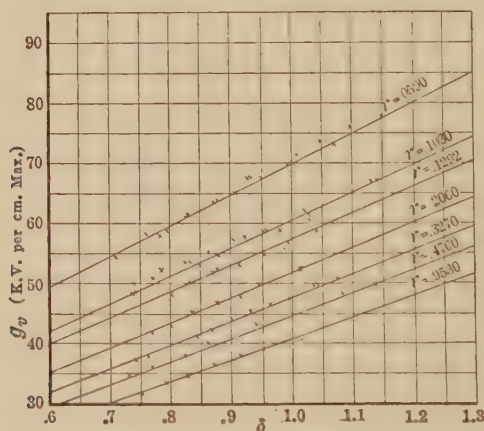


FIG. 35—Effect of temperature on the strength of air. ( $r$  = radius of wire in cm. × measured values. Drawn curves calculated.)

Referring to the tables, column 6 gives values of  $g_v$  calculated from equation (25a). By comparing with the experimental values in column 5 it is seen that the difference is generally less than 1 per cent.

$g_o$  has a slightly higher value for wires in a concentric cylinder than for parallel wires. This does not mean that the strength of air differs in the two cases. For a wire in a cylinder, the field is balanced all around and should give more nearly the true value.

In Figs. 34, 35, and 36 the drawn lines are the calculated values, while the crosses are the observed values.

**Barometric Pressure.**—It will be noted in Fig. 36 that while the calculated curve is almost a straight line down to  $\delta = 0.5$ , below this point there is a decided bend to zero. The lower part of this

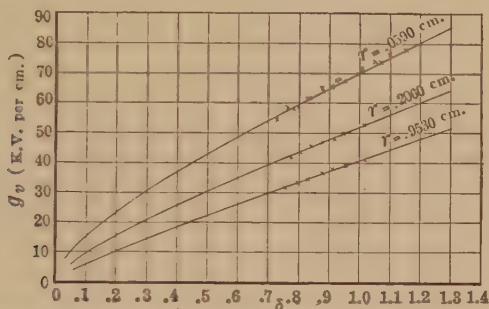


FIG. 36.—Effect of temperature on the strength of air. (× measured values. Drawn curves calculated.)

curve was drawn from calculations. In order to check experimentally the above law over a wide range of  $\delta$ , and also to show that the effect was the same whether the change was made by varying temperature or pressure, tests were made over a large pressure range. A glass cylinder lined with tin foil 7.36 cm. in

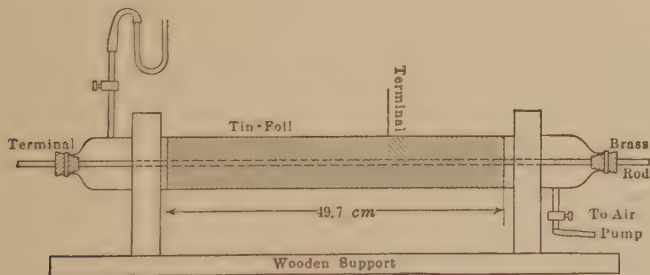


FIG. 37.—Apparatus for determining the effect of pressure on strength of air.

diameter with a small slit window in the center was used for this purpose (see Fig. 37). Tests were made on wires 0.508 to 0.157 cm. in diameter, and a pressure range of 1.7 to 76 cm. Table VIII is typical of observed and calculated values. Fig. 38 shows how these follow the previously predicted curve. A



$\Sigma\Delta$  reduction of the values also confirms the above formulæ.  
For concentric cylinders

$$g_v = 31\delta \left( 1 + \frac{0.308}{\sqrt{\delta r}} \right) \text{ max. kv. per centimeter}$$

For parallel wires

$$g_v = 30\delta \left( 1 + \frac{0.301}{\sqrt{\delta r}} \right) \text{ max. kv. per centimeter}$$

TABLE VIII.—VARIATION OF STRENGTH OF AIR WITH PRESSURE  
Diameter of Brass Rod = 0.381 cm. in 7.36-cm. Diameter Glass  
Tube Covered with Tin Foil—60 ~

Pres. abs. cm. Hg	Volts read (eff.)	Temp. deg. C.	$\delta =$ $\frac{3.92b}{273 + t}$	$g_v =$ $\frac{e_v}{r(\log_e R/r)}$ kv./cm. (eff.)	$\frac{1.414}{\delta} g_v$ $g_v$ max., measured kv./cm.	$g_v$ max., calculated $31\delta \left( 1 + \frac{0.301}{\sqrt{\delta r}} \right)$ kv./cm.
5.3	2,880	27.0	0.069	5.08	7.19	7.80
10.7	4,580	24.0	0.141	8.09	11.45	12.40
11.2	4,920	27.0	0.146	8.68	12.28	12.15
19.3	7,400	27.0	0.252	13.06	18.47	18.58
27.7	9,550	27.0	0.362	16.87	23.85	24.06
36.6	12,000	27.0	0.478	21.20	30.00	29.60
46.4	14,450	25.0	0.612	25.50	36.07	35.70
47.0	14,600	27.0	0.614	25.80	36.50	35.80
55.7	16,300	27.0	0.728	28.80	40.75	40.75
60.0	17,760	25.5	0.792	31.35	44.30	43.50
66.0	18,400	27.0	0.867	32.50	46.00	46.75
75.0	21,100	25.0	0.997	37.25	52.70	52.25

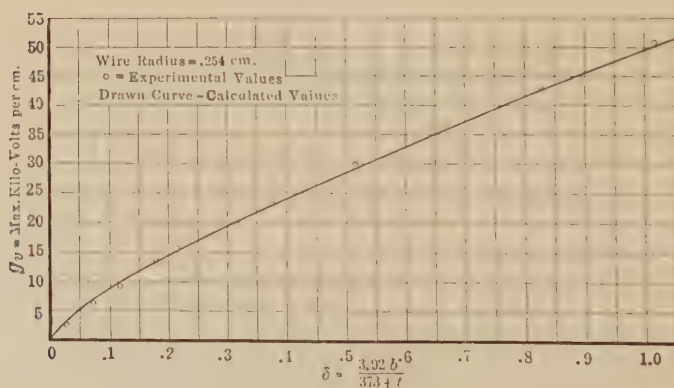


FIG. 38. Effect of pressure on the strength of air.

The above equation was afterwards verified by other research workers<sup>1</sup> and found to hold down to a few centimeters pressure. S. Whitehead has plotted the results of several of these observers<sup>1</sup> (see Fig. 39) to show this relation between the surface gradient of a wire in a cylinder and pressure with various gases. The rate of increase of the dielectric strength with pressure is seen to vary for the different gases which would thereby introduce different constants into the above equation. The effect of polarity will be discussed later (see page 166) as well as the apparent anomalies existing in the breakdown of gases (see page 167).

**Electric Strength of Air Films.**—It is interesting to speculate what will happen at very small spacings or when the distance between conductor surfaces is in the order of  $a$  (see Fig. 40).

As the free "accelerating" or "ionizing" distance is then somewhat limited, a greater force or gradient should be required when the distance

between the conductors approaches  $a$ . Experiments were made to determine this, using spheres as electrodes. The ideal electrodes for this purpose would be concentric cylinders, but the use

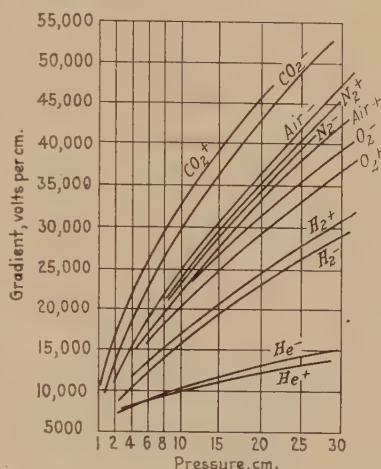


FIG. 39.—Relation between d.c. surface breakdown gradient of wire in cylinder and pressure, for various gases and polarities.

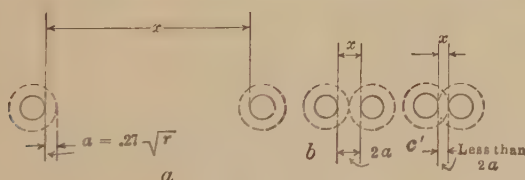


FIG. 40.

of these, as well as parallel wires at small spacing, seemed impracticable. Spark-over and corona curves were made on spheres

<sup>1</sup> WHITEHEAD, S., "Dielectric Phenomena, Electrical Discharges in Gases," p. 99, Ernest Benn, Ltd., London.

ranging in diameter from 0.3 to 50 cm. and spacings from 0.0025 to 50 cm. This discussion applies only to spacings up to  $2R$  where corona cannot form.

In these tests a 60-cycle sine wave voltage was used. For the small spacing the spheres were placed in a very rigid stand. One shank was threaded with a fine thread, the other was non-adjustable. In making a setting the adjustable shank was screwed in until the sphere surfaces just touched, as indicated by completing the circuit of an electric bell and single cell of a dry battery. A pointer at the end of the shank was then locked in place, after which the shank was screwed out any given number of turns or fraction of turns, as indicated on the stationary dial. For larger spacings other stands were used.

A typical spark-over spacing curve and corona spacing curve is shown in Fig. 41. Theoretically, up to a spacing of  $2R$ , corona cannot form, but spark-over must be the first evidence of stress.

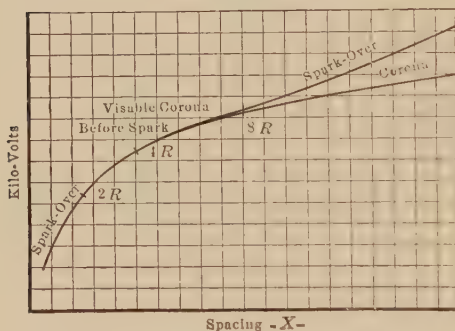


FIG. 41.—Variation of corona and spark-over voltages with spacing for spheres.

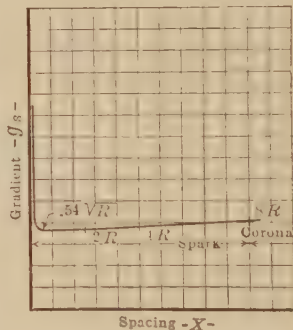


FIG. 42.—Variation of strength of air with spacing for spheres.

Practically, corona cannot be detected at 60~ until a spacing of  $8R$  is reached. This is because, up to this point, the difference between the corona starting points and the spark point is very small. Above  $8R$  the spark-over curve approaches a straight line, as in the case of the needle gap curve. The corona curve above  $2R$  and the spark curve below  $2R$  are apparently continuous. The gradient curve (Fig. 42), is calculated from the voltage curve (Fig. 41). Where the spacing is less than  $0.54\sqrt{R}$ , the gradient increases first slowly and then very rapidly with decreasing spacing. Between  $X = 0.54\sqrt{R}$  and  $2R$  the gradient is very

nearly constant. Above about  $3R$  spacing the gradient apparently increases. This apparent increase is probably due to the effect of the shanks, etc., which become greater as  $X$  is increased. The effect of the shanks is to distribute better the flux on the sphere surface and cannot be taken account of in the equation for gradient. This was shown experimentally by using different sizes of shanks at the larger spacing. Thus, when the spacing is greater than  $3R$ , the sphere is not suitable for studying the strength of air, as the gradient cannot be conveniently calculated. It is, hence, not a suitable electrode for studying corona, as corona does not form until the spacing is greater than  $2R$ . The maximum gradient at the surface of a sphere (non-grounded) may be calculated from the equation.<sup>1</sup>

$$g = \frac{E}{X} f \quad (13a)$$

where  $X$  is the spacing

$E$  the voltage

$$f = 1/4 \left( \frac{X}{R} + 1 + \sqrt{\left( \frac{X}{R} + 1 \right)^2 + 8} \right)$$

The gradient for the non-grounded case may be conveniently calculated by use of the table on page 28. The gradient on the line connecting the sphere centers at any distance  $a$  from the sphere surface may be calculated from the complicated equation<sup>2</sup>

$$g_a = \frac{E}{X} \left[ \frac{2X^2 \left[ X^2(f+1) + 4 \left( \frac{X}{2} - a \right)^2 (f-1) \right]}{\left[ X^2(f+1) - 4 \left( \frac{X}{2} - a \right)^2 (f-1) \right]^2} \right] \quad (26)$$

Some of the experimental values are given in Tables IX and X. Typical voltage gradient curves are shown in Figs. 43, 44, and 45.

<sup>1</sup> DEAN, G. R., *G. E. Rev.*, Vol. XVI, p. 148, 1913.

<sup>2</sup> DEAN, G. R., also *Phys. Rev.*, December, 1912, April, 1913.

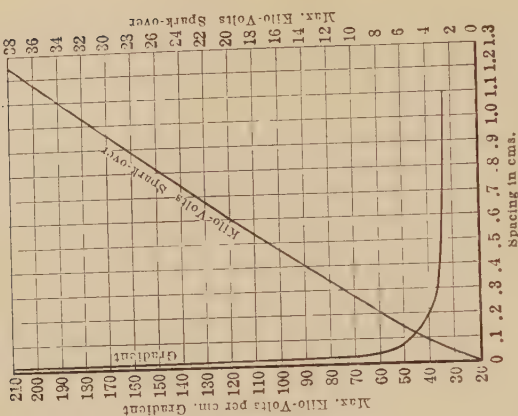


Fig. 43.

Fig. 43.—Radius of sphere,  $R = 0.238$  cm.

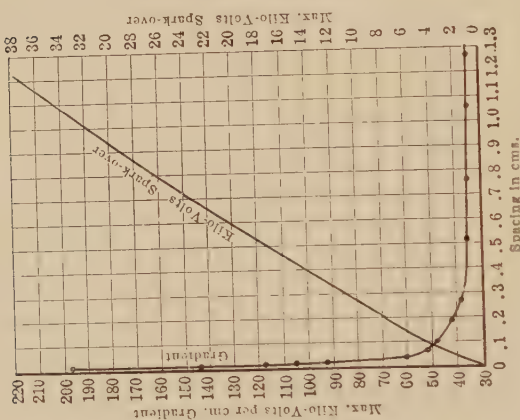


Fig. 44.

Fig. 44.— $R = 3.33$  cm.

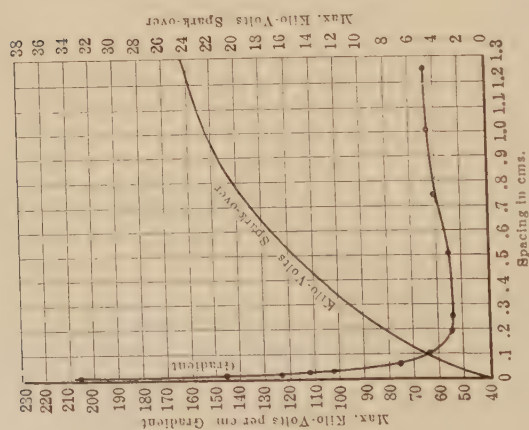


Fig. 45.

Fig. 45.—Variation of strength of air and spark-over voltages with spacing.



TABLE IX.—SPARK-OVER OF SPHERES AT SMALL SPACINGS  
Brass Spheres  $R = 3.33$  cm., Diameter = 2-5/8 in.—60 ~

$X$	Spacing	$e_{eff.}$	$\delta$	$e_{max.}$	$g_{max.}$	$X/R$
In.	Cm.	Kv.	$\frac{3.92b}{273+t}$	$= \frac{\sqrt{2}(e_{eff.})}{\delta}$ (corrected)	$= \frac{e_{max.}}{X} f$ kv./cm.	
0.001	0.00254	0.363	1.028	0.497	196.0	0.00076
0.002	0.00508	0.531	1.030	0.729	143.6	0.00152
0.003	0.00762	0.654	1.027	0.899	118.1	0.00228
0.004	0.01016	0.775	1.026	1.07	105.2	0.00305
0.005	0.0127	0.845	1.016	1.17	92.3	0.00382
0.010	0.0254	1.07	1.000	1.52	60.0	0.00764
0.020	0.0508	1.86	1.002	2.62	51.8	0.01528
0.040	0.1016	3.27	1.002	4.62	45.9	0.03056
0.075	0.1905	5.43	1.002	7.66	41.0	0.05730
0.100	0.254	6.92	1.002	9.77	39.5	0.0764
0.200	0.508	12.40	1.002	17.50	33.3	0.1528
0.300	0.762	17.70	1.002	25.00	35.4	0.2292
0.400	1.016	22.70	1.002	32.00	34.8	0.3056
0.500	1.270	27.75	1.002	39.20	34.9	0.382

TABLE X.—SPARK-OVER OF SPHERES AT SMALL SPACINGS  
Brass Spheres  $R = 12.5$  cm., Diameter = 9.84 in.—60 ~

$X$	Spacing	$e_{eff.}$	$\delta$	$e_{max.}$	$g_{max.}$	$X/R$
In.	Cm.	Kv. (read)	$= \frac{3.92b}{273+t}$	$= \frac{\sqrt{2}(e_{eff.})}{\delta}$ (corrected)	$= \frac{e_{max.}}{X} f$ kv./cm.	
0.005	0.0127	0.807	1.023	1.116	87.9	0.00101
0.010	0.0254	1.220	1.021	1.689	66.5	0.00203
0.020	0.0508	2.050	1.031	2.849	55.9	0.00406
0.040	0.1016	3.38	1.022	4.68	46.2	0.00813
0.100	0.254	7.03	1.020	9.75	38.6	0.0203
0.200	0.508	12.54	1.012	17.44	34.8	0.0406
0.300	0.762	17.91	1.016	24.92	33.5	0.0609
0.400	1.016	22.82	1.010	31.76	32.0	0.0812
0.500	1.27	27.63	1.010	38.67	31.5	0.1016
1.000	2.54	53.0	1.000	74.90	31.6	0.2032
1.500	3.81	75.3	1.000	106.30	30.9	0.3048
2.000	5.08	96.4	1.000	136.20	30.5	0.4064
2.500	6.35	117.4	1.000	166.00	30.7	0.5080
3.000	7.62	139.2	1.000	196.90	31.2	0.6096
3.500	8.89	158.0	1.000	223.40	31.3	0.7112
4.000	10.16	174.9	1.000	247.10	31.0	0.8128
4.500	11.43	190.8	1.000	269.50	31.0	0.9144
5.000	12.70	203.6	1.000	287.20	30.8	1.0160



In Table XI are tabulated, for different sizes of spheres, the spark-over gradient at the constant part of the curve, the average gradient between  $X = 0.54\sqrt{R}$  and  $X = 3R$ , and the approximate minimum spacing at which the gradient begins to increase

TABLE XI.—MAXIMUM RUPTURING GRADIENTS FOR SPHERES  
(Average for Constant Part of the Curve)

$R$ Radius in cm.	Spacing $X$ , where $g_s$ begins to increase (cm.)	$g_s$ max. kv./cm. for constant part of curve
0.159	0.18	63.8
0.238	0.25	55.6
0.356	0.26	51.4
0.555	0.40	46.9
1.270	0.51	40.0
2.540	0.85	36.8
3.120	.....	35.8
3.330	0.95	34.8
6.25	1.30	32.5
12.50	2.0	31.3
25.00	.....	30.0

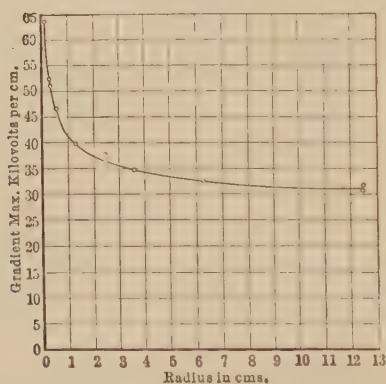


FIG. 46.—Variation of the apparent strength of air with sphere radius. Points measured gradient from constant part of curve. Drawn curve, calculated from equation (27).

in value. The gradient-radius curve is plotted in Fig. 46. This curve is very closely given by the equation

$$g_s = g_0 \left( 1 + \frac{\alpha}{\sqrt{R}} \right) \quad (27)$$

which has exactly the same form as the similar curve for cylinders. The value of  $g_o$  is, however, lower than for the balanced field of a wire in a cylinder.

$$\text{For a wire in a cylinder } g_o = 31 \quad g_v = 31 \left( 1 + \frac{0.308}{\sqrt{r}} \right) \quad (25a)$$

$$\text{For parallel wires } g_o = 30 \quad g_v = 30 \left( 1 + \frac{0.301}{\sqrt{r}} \right) \quad (25b)$$

$$\text{For spheres } g_o = 27.2 \quad g_v = 27.2 \left( 1 + \frac{0.54}{\sqrt{R}} \right) \quad (28)$$

It is probable that the average breakdown gradient of air is 31 kv. per centimeter, as represented by the balanced field. It is apparently less for parallel wires due to the unbalanced field and still less for spheres where the field is unbalanced to a greater extent.

The curve between the sphere radius and the approximate minimum spacing below which the gradient begins to increase appreciably is plotted in Fig. 47 from Table XI. The curve is represented by the equation

$$X = 0.54\sqrt{R} \quad (29)$$

which means that when the spacing is less than  $0.54\sqrt{R}$  the gradient increases in value, at first slowly, then very rapidly.

It is now interesting to investigate the meaning of equation (27). In Fig. 48 the exact gradient is plotted from equation (26) for different distances from the sphere surface on the line connecting the centers and at given spacings as indicated by the small diagram in the upper corner of the figure. It is seen that for small distances from the sphere surface, the curves for the different spacings fall together. Over the small range the gradient  $g_a$  at any point  $a$  centimeters from the sphere surface on the center line may be found approximately from

$$g_a \cong \frac{E}{(R + 2a)} \left( \frac{R}{X} \right) f \quad (30)$$

The only reason for giving this approximation, which holds only for very small values of  $a$  and is only true when  $a = 0$ , is

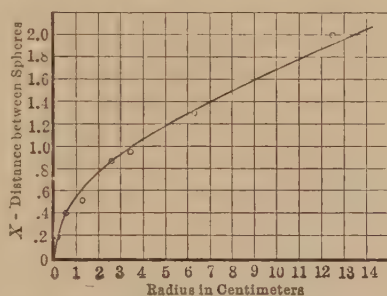


FIG. 47.—Sphere spacing below which apparent strength begins to increase.

that (26) is too complicated to handle. The error due to this approximation is shown in Table XII.

TABLE XII

$R = 1.27$ cm. Energy distance, $a = 0.27\sqrt{R} = 0.3$ cm.				$R = 12.5$ cm. Energy distance, $a = 0.95$ cm.			
$a$	$g_a$ , Exact	$g_a$ , Approx.	$X$	$a$	$g_a$ , Exact	$g_a$ , Approx.	$X$
0.0	39.9	39.9	0.76	0.0	31.3	31.3	4
0.1	34.6	34.0	0.76	0.2	30.3	30.3	4
0.2	31.9	30.0	0.76	0.4	29.5	29.4	4
0.4	29.7	24.1	0.76	0.6	28.6	28.5	4
				0.8	28.3	27.7	4
				1.0	27.5	26.9	4
0.0	39.9	39.9	1.21	0.0	31.3	31.3	10
0.1	34.2	33.4	1.21	0.2	30.3	30.3	10
0.2	30.5	29.5	1.21	0.4	29.5	29.4	10
0.4	26.5	23.7	1.21	0.6	28.6	28.7	10
				0.8	28.0	27.7	10
				1.0	27.5	26.9	10

Then

$$g_s = \frac{(E_s)}{(X)} f = \frac{E_s}{R} \left( \frac{R}{X} f \right) \text{ exact mathematical} \quad (13a)$$

$$g_s = g_o \left( 1 + \frac{\infty}{\sqrt{R}} \right) \text{ experimental for approximately constant part of curve} \quad (27)$$

$$g_a \cong \frac{E}{(R + 2a)} \left( \frac{R}{X} f \right) \text{ approximate mathematical} \quad (30)$$

Equating (13a) and (27)

$$\frac{E_s}{R} \left( \frac{R}{X} f \right) = g_o \left( 1 + \frac{\infty}{\sqrt{R}} \right)$$

$$g_o = \frac{E_s}{(R + \infty \sqrt{R})} \left( \frac{R}{X} f \right)$$

which is the same form as (30) and means that at a distance

$$\propto \frac{\sqrt{R}}{2} = \frac{0.54\sqrt{R}}{2} = 0.27\sqrt{R} \text{ cm.}$$

from the sphere surface, the gradient at rupture is always approximately constant and is  $g_o$ . As breakdown must take place at approximately  $a = 0.27\sqrt{R}$  cm. from the sphere surface, the

gradient should begin to increase at the spacing  $2a = 0.54\sqrt{R}$ . This is approximately so, as shown in Fig. 47 and equation (30). The increase is at first slow at  $X = 2a$  and very rapid at  $X = a$ . Figure 48 shows that, at  $a = 0.27\sqrt{R}$ , the gradient is not exactly constant for different spacings or the curves do not fall together.

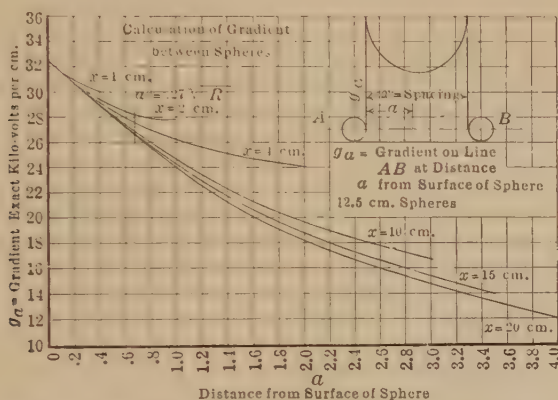


FIG. 48.—Gradient at different points on line through centers of spheres. Calculated from (26).

This means that  $g_a$  and  $\alpha$  in equation (27) cannot be exactly constant for a given radius but must also be a function of  $X$ . This is experimentally shown to be the case, as there is a slight variation over the range  $X = 0.54\sqrt{R}$  and  $X = 2R$ .

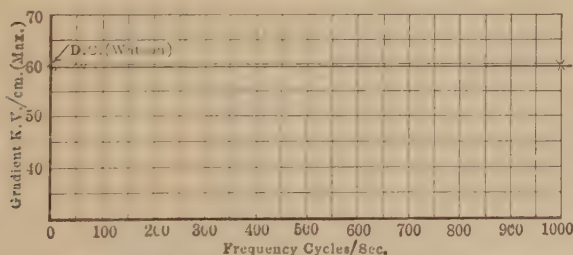


FIG. 49.—Variation of the apparent strength of air with frequency.

**Influence of Frequency on the Visual Gradient.**—The effect of frequency on  $g_r$  for the practical range of 25 to 60 cycles, if any, is very small and can be neglected. A few measurements are shown in Fig. 49. For the test range it is difficult to tell whether the slight variations are due to changes in wave shape or to fre-

quency. There is a possibility of frequency entering this as a function

$$g_v = g_o \left( 1 + \frac{\alpha}{\phi(f) \sqrt{\delta r}} \right)$$

Investigations up to 1000 cycles show very little if any change. In this investigation the sine wave voltage was measured with a static voltmeter calibrated at 60 cycles. Measurement at 30,000 cycles (sine wave from a generator) made by the static voltmeter showed a slightly lower voltage than at 60 cycles.<sup>1</sup> Direct current points by Watson are given in Fig. 49. See appendix. Over the commercial range of frequency, however, there is no appreciable effect of frequency. For transient corona see appendix.

**Corona Caused by Lightning and Impulse Voltages of Short Duration.**—An extensive investigation has shown that lightning and impulse voltages, lasting less than a millionth of a second, cause corona which has most of the characteristics of that caused by continuously applied voltage.<sup>2</sup>

For large conductors at atmospheric pressure, the impulse critical corona voltage is approximately the same as for direct current, while for smaller conductors and at reduced air pressures, the impulse critical voltage is relatively higher. The appearance of the discharge for a (+) and (−) conductor is the same as for the corresponding direct current.

**Effect of Oil, Water, or Dirt on the Visual Corona Point.**—These tests were made in a manner exactly similar to the dry tests. In the oil tests, the surface of the wire was coated with a thin, even film by means of an oiled cloth. For the wet tests water was sprayed on the conductor surface before each reading by means of an atomizer. Figs. 50 and 51 are dry, wet, and oil curves for two different sizes of wire.

For spark-over, both water and oil have approximately the same effect, that is, give very nearly the same spark-over voltage for all sizes of conductor. The curves very closely follow the needle-gap curve.

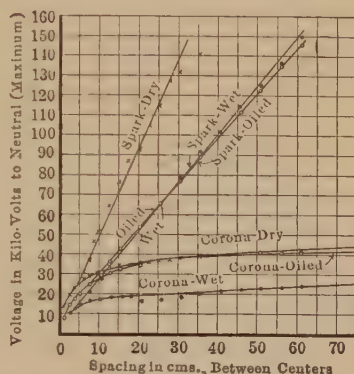
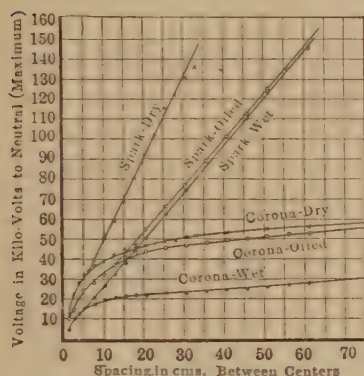
<sup>1</sup> See pp. 106, 107.

<sup>2</sup> PEEK, F. W., JR., "The Effect of Transient Voltages on Dielectrics I," *Trans. A.I.E.E.*, Vol. XXXLV, p. 857, 1915.

"The Effect of Transient Voltages on Dielectrics III," *Trans. A.I.E.E.*, p. 940, 1923.



For corona, water very greatly lowers  $g_v$ . Oil lowers  $g_v$  but to a much less extent than water. When the conductor is very small, the percentage increase in diameter, due to oil, more than compensates for the lowering effect. The *approximate* apparent visual corona gradient for oil- and water-coated conductors may be found.



FIGS. 50 and 51.—Spark-over and corona voltages for parallel wires. (Wire surfaces dry, wet, and oiled. Max. kv. to neutral.  $\delta = 1$ . Fig. 50.—Wire radius 0.205 cm. Fig. 51.—Wire radius 0.129 cm.)

Water surfaces by fine spray or fog

$$g_v \cong 9 \left( 1 + \frac{0.815}{\sqrt{r}} \right) \text{ max. kv. per centimeter}$$

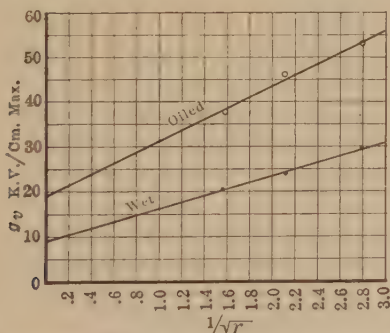


FIG. 52.—Apparent strength of air around wires with wet and oiled surfaces.

Oil film surfaces

$$g_v \cong 19 \left( 1 + \frac{0.65}{\sqrt{r}} \right) \text{ max. kv. per centimeter}$$

See Fig. 52.



If a water-coated wire above the visual corona point is examined in the dark, it has the appearance of an illuminated atomizer. The surface quickly becomes dry.

Dirt on the surface of the conductor, by increasing the gradient, causes local brush discharges, and if the surface is rough, corona starts at a lower voltage. This is taken care of in the formulæ by an irregularity factor  $m_r$  (see pages 81 and 191). Thus, for a weathered or oxidized wire

$$g_v = g_o m_v \delta \left( 1 + \frac{0.301}{\sqrt{\delta r}} \right)$$

The corona starting voltage for wet or oiled wires may be found by calculating  $g_v$  in the above equations and substituting in equation (20).

**Conductor Material.**—With the same surface condition the visual corona point is independent of the material. This is shown in Table II.

**Humidity.**—Tests made over a very wide humidity range show that humidity has no appreciable affect upon the starting point of visual corona provided the conductor surface is dry. After corona is present humidity has an affect on the spark-over voltage. This is discussed in Chap. IV.

**Ionization.**—Change of initial ionization of the air even to a considerable extent has no appreciable affect on the starting point of corona. This was found by test by increasing the voltage on the wire in the cylinder until considerably above the corona voltage, and then, while the cylinder was full of ionized air, lowering the voltage below the corona point and again raising it until glow appeared. The starting point was not appreciably changed.

Flooding a conductor with ultra-violet light from a mercury arc or similar source has also been found not to affect greatly the corona starting voltage. Initial ionization has been found to reduce the time lag of breakdowns, however, and introduce a steadying effect on the values of rupturing voltage read. This results because of the continued presence of ions for starting ionization the instant breakdown field stresses are reached.

**Current in Wire.**—A test was made to see if heavy currents flowing in the wire would change the starting point of visual corona. The test arrangement was as shown in Fig. 53.

Tests were made with both alternating-current in phase and out of phase, and direct-current in the wire. The results are

given in Tables XIII, XIV, and XV. The temperature of the wire was measured by the resistance method. The values in the last column are all corrected from the wire temperature to  $\delta = 1$ .

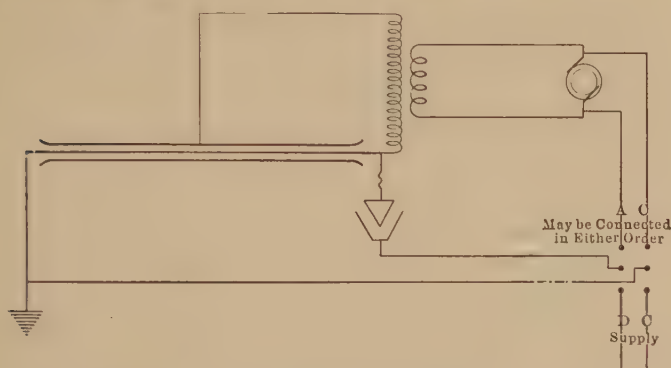


FIG. 53.—Apparatus for measuring corona starting point with current in the wires.

If the current has no appreciable effect, as appears to be the case, these should all be equal. The variation is probably due to

TABLE XIII.—CORONA STARTING POINT WITH CURRENT FLOWING THROUGH WIRE  
Concentric Cylinders

Radius of wire.....0.129 cm.  
Radius of cylinder.....5.46 cm.

Kv. eff.	Amp. d.c.	Average temperature		Barom. cm.	$\delta$ (using wire temp.)	$\sigma_v$	$\sigma_v$ reduced to $\delta = 1$
		Air	Wire				
20.0	0.0	26	26	75.6	0.991	58.4	58.9
19.7	15.2	26	32	.....	0.970	57.5	59.2
19.4	31.4	26	48	.....	0.922	56.7	61.4
18.5	39.0	26	64	.....	0.878	54.1	61.6
17.8	49.2	26	82	.....	0.824	52.0	63.1
16.9	75.0	26	120	.....	0.753	49.4	65.6
20.4	0.0	23	23	.....	1.000	59.6	59.6
20.3	18.0	23	27	.....	0.987	59.3	59.9
19.4	33.0	23	50	.....	0.917	56.7	61.8
17.9	50.8	24	91	.....	0.813	52.2	64.2
12.9	99.6	24	320	.....	0.500	37.6	75.2
16.4	67.6	26	102	.....	0.790	47.9	60.6
13.9	78.6	26	212	.....	0.610	40.8	67.0
16.1	61.6	26	144	.....	0.710	47.0	66.2

TABLE XIV.—CORONA STARTING POINT WITH CURRENT FLOWING THROUGH WIRE

## Concentric Cylinders

Radius of wire.....0.205 cm.  
 Radius of cylinder.....5.46 cm.

Kv. eff.	Amp.	Average temperature		Barom. cm.	$\delta$ (using wire temp.)	$\theta_v$	$\theta_r$ reduced to $\delta = 1$
		Air	Wire				
25.3	14 (d.c.)	23	23	76.2	1.01	53.15	52.6
25.2	0	23	23	76.2	1.01	53.0	52.5
25.2	14 (a.c. in phase)	23	23	75.8	1.005	52.8	52.6
25.1	14 (a.c. out of phase)	23	23	75.8	1.005	52.6	52.3
25.1	0	23	23	75.8	1.005	52.6	52.3
25.2	0	24	24	75.25	0.994	52.8	53.2
25.2	14 (d.c.)	24	30	75.25	0.974	52.8	54.3
25.2	34 (d.c.)	25	60	75.25	0.886	52.4	59.1
23.8	56 (d.c.)	29	60	75.25	0.886	50.0	56.3
23.3	70 (d.c.)	30	73	75.25	0.853	48.8	57.3
21.8	114 (d.c.)	.....	110	75.25	0.771	45.7	59.2
25.0	60 (d.c.)	31	31	75.25	0.971	52.4	53.9
25.0	0	31	31	75.25	0.971	52.4	53.9
24.8	23 (a.c.)	31	44	75.25	0.931	52.0	55.8

difficulty in getting the exact temperature of the air. The air immediately surrounding the wire is assumed to be at the same temperature as the wire. This causes a correction that is too large. Current flowing in a wire thus, probably, does not appreciably effect the corona point unless the temperature of the wire is increased.

TABLE XV.—CORONA STARTING POINT WITH CURRENT FLOWING THROUGH WIRE

## Concentric Cylinders

Radius of wire.....0.476 cm.  
 Radius of cylinder.....5.465 cm.

Kv. eff.	Amp. d.c.	Average temperature		Barom. cm.	$\delta$ (using wire temp.)	$\theta_r$	$\theta_r$ reduced to $\delta = 1$
		Air	Wire				
36.5	0	27	27	75.5	0.985	44.3	45
36.5	80	27	27	75.5	0.985	44.3	45

**Stranded Conductors or Cables.**—While the visual critical corona point is quite sharp and definite for wires, it is not so for cables or standard conductors. Corona, after it first appears, increases gradually for a considerable range of voltage until a certain definite voltage is reached, where the increase is very rapid. The first point has been called the local corona point and the second point the decided corona point. The curve (Fig. 54) for these corona points is compared with the curve for a smooth

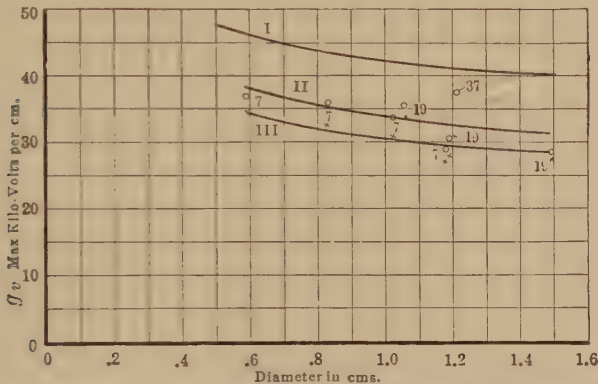


FIG. 54.—Apparent visual critical corona voltages for parallel cables. Numerals denote number of strands: I, polished copper wire; II, decided corona on cable, o; III, local corona all along cable, x.

conductor. The starting point for cables may be found by the use of an irregularity factor  $m_v$ .

$$g_v = g_o m_v \left( 1 + \frac{0.301}{\sqrt{r}} \right) \text{ kv. per centimeter}$$

where  $m_v = 0.82$  for decided corona

$m_v = 0.72$  for local corona

$r$  = overall radius of cable

This applies to cables of six strands or over.

It is interesting to note that, for the decided corona point, the visual critical voltage of a cable is about 3 per cent. lower than that of a wire with the same cross-section, or, more exactly "the diameter of a solid wire with the same critical voltage is about 97 per cent. that of the wire having the same cross-section as the cable."<sup>1</sup> This is shown in Table XVI. This irregularity factor is further discussed on page 191.

<sup>1</sup> WHITEHEAD, J. B., *Trans. A.I.E.E.*, p. 1857, 1911.

TABLE XVI.—EFFECT OF STRANDING  
Whitehead, A.I.E.E., June, 1911, Table III

Cables, strands outer layer	Diameter over all (A)	Diameter solid of equal section (B)	Diameter solid of equal crit- ical volts (C)	C/B	C/A	Pitch of spiral	
						Cm.	Diameters
3	0.349	0.272	0.247	0.907	0.708	3.81	10.9
4	0.404	0.332	0.320	0.965	0.792	3.49	8.6
5	0.45	0.381	0.370	0.971	0.822	4.44	9.9
6	0.49	0.430	0.420	0.975	0.857	6.02	12.3
7	0.541	0.480	0.465	0.969	0.868	6.66	12.3
8	0.589	0.530	0.516	0.975	0.877	6.35	10.8
9	0.64	0.581	0.567	0.977	0.886	6.98	10.9
3	0.336	0.27	0.307	0.767	0.616	None	None
4	0.378	0.312	0.25	0.802	0.665	None	None

**Conductors of the Same Potential Close Together.**—When conductors of the same potential are arranged close together, the

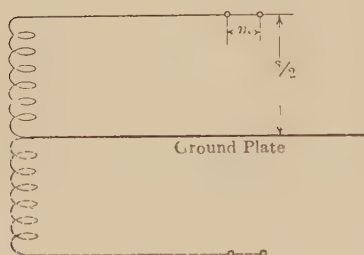


FIG. 55.—Arrangement for two conductors at same potential, and plate.

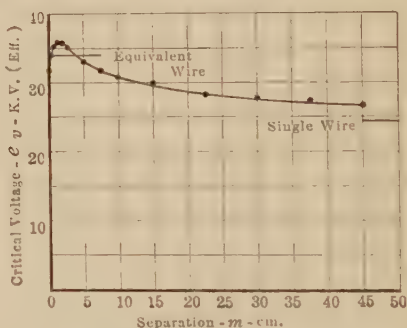


FIG. 56.—Critical voltage on two conductors at the same potential and various separations (see Fig. 55).

critical breakdown voltage is much greater than that of a single conductor or when they are far apart. The simplest case, that of two, is shown in Fig. 55. The two conductors for a given test were kept at a constant distance  $S/2$  from the ground plate. Potential was applied between the conductors and plate. The separation  $m$  was then varied and critical voltages read at different spacings. Refer to Fig. 56 (0.163-cm. wire 30 cm. from neutral plane). When  $m = 0$ ,  $e_v = 31.5$  eff. As the spacing  $m$  was increased,  $e_v$  increased to a maximum of 35.8 kv. With increasing  $m$ ,  $e_v$  then gradually decreases to a constant value which is the



same as that for a single wire. The maximum voltage is about 5 per cent. greater than the critical voltage of a single conductor of the same cross-section.

With the same amount of conductor material, much higher voltages can be used without corona loss when the conductor is

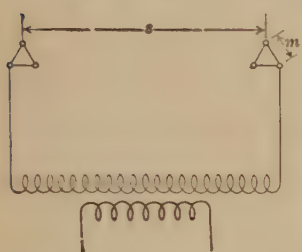


FIG. 57.—Conductors of the same potential arranged in a triangle.

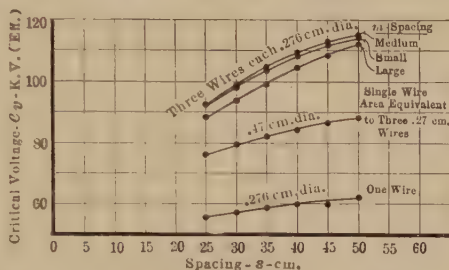


FIG. 58.—Critical voltages for conductors arranged as in Fig. 57.

split up into three or more small conductors, properly arranged, than with a single conductor. The results of tests made on a single-phase line with split conductors arranged in a triangle, as in Fig. 57, are given in Fig. 58. Figure 58 shows curves for a single split wire and also for a single wire of a cross-section equal

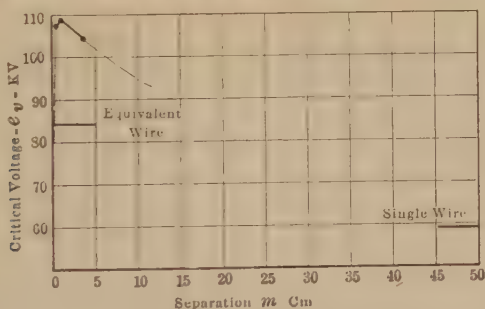


FIG. 59.—Critical voltage of conductors arranged as in Fig. 57. ( $S = \text{constant} = 40 \text{ cm.}$ ,  $m$  varying.)

to that of the three split conductors. Figure 59 shows how the voltage varies with varying  $m$ .

With the split conductor arrangement, in the special case given, the critical voltage is from 20 to 30 per cent. greater than that of a single wire containing the same amount of material.

Whitehead has made similar tests on three wires in a triangle and also four wires placed on a square in the center of a cylinder.



He finds 16 per cent. increase for three wires and 20 per cent. for four over the critical voltage of a single conductor of the same total material.

### STROBOSCOPIC AND PHOTOGRAPHIC STUDY

**Photographic Study.**—A photographic study of corona on wires and cables was made as follows: Two parallel conductors were spaced 122 cm. between centers. The camera was focused on one conductor only. The distance to the lens was such as to show the conductors at approximately actual size. An exposure was made for a given time at a given voltage. The plate was then shifted slightly, the voltage increased, and a second exposure was made for the same time. That is, a given series shows that same part of the same single wire at different voltages. This operation was repeated until the series for a given wire was complete. A glass lens was used unless otherwise stated. These photographs are shown in Figs. 60 to 67.

Photographs 66 and 67 were made to show the effects of moisture. In Fig. 66 the stranded cable was brought up to the critical point. Water was then thrown on the cable. The result is shown in Fig. 67. What was a glow at the surface of the dry cable became at the wet spots, a discharge extending from 5 to 8 cm. from the conductor surface. The discharge has the appearance of an illuminated atomizer. Figure 68 shows corona photographs taken at voltages close to 1,000,000 volts.

**Diameter of Corona.**—On a smooth wire the boundary line of corona appears to be fairly definite. The apparent visual diameter may be measured by viewing through a slit. The apparent diameter may be recorded photographically. If the photograph is made through a quartz lens, the ultra-violet rays will not be cut off from the plates as when a glass lens is used.

Whitehead has made some measurements on the *apparent* diameter, comparing the visual method and the photographic method with both quartz and glass lenses. He finds that the apparent diameters are, respectively, by the visual, glass lens, and quartz lens methods in the ratios of 1 : 1.6 : 1.9.<sup>1</sup> It therefore appears that there is a considerable content of the corona in the ultra-violet which is not visible to the eye. As soon as corona appears it seems to have a definite finite thickness.

<sup>1</sup> WHITEHEAD, J. B., *Trans. A.I.E.E.*, p. 1093, 1912.

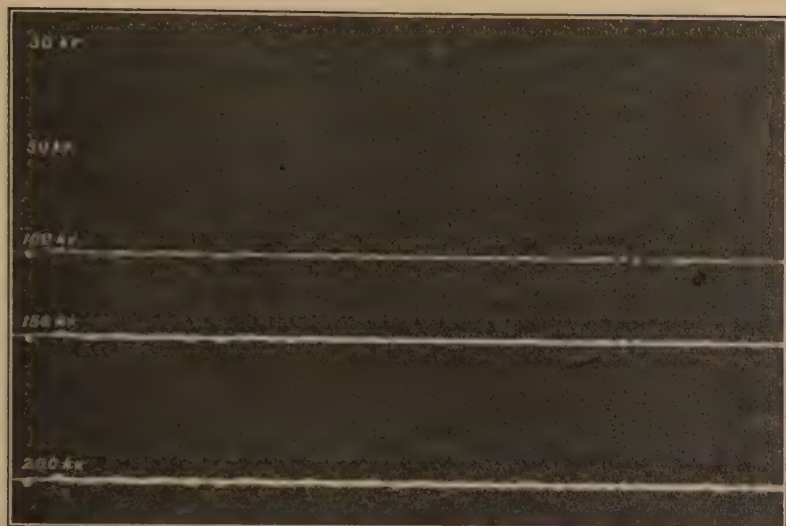


FIG. 60.—Corona on bright tinned phosphor-bronze wire. Diameter, 0.051 cm.

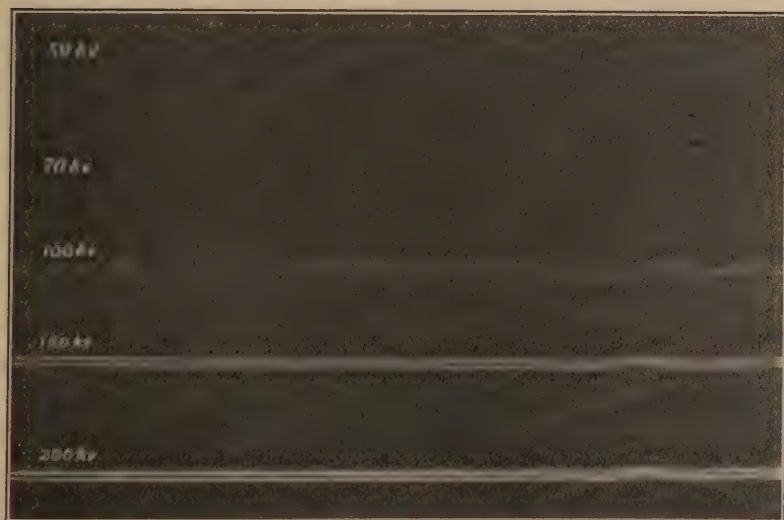


FIG. 61.—Corona on copper wire polished after each exposure. Diameter, 0.186 cm.

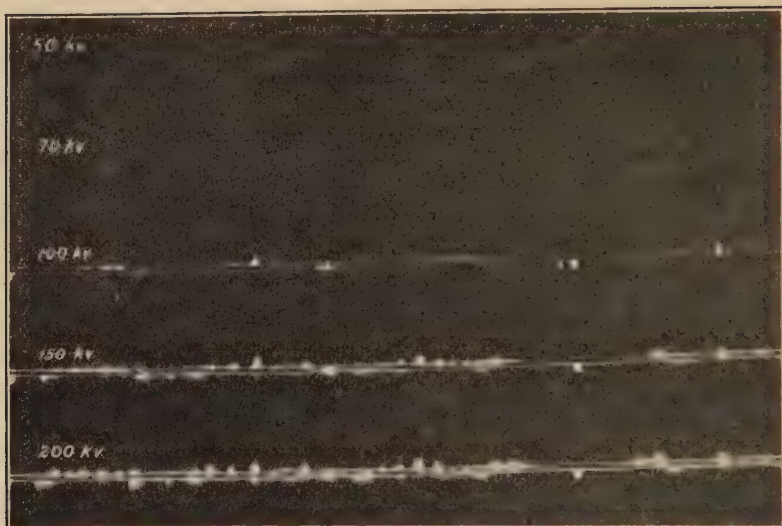


FIG. 62.—Corona on a polished copper wire. Diameter, 0.186 cm. Operated at 200 kv., then allowed to stand idle. (This shows effect of oxidation.)

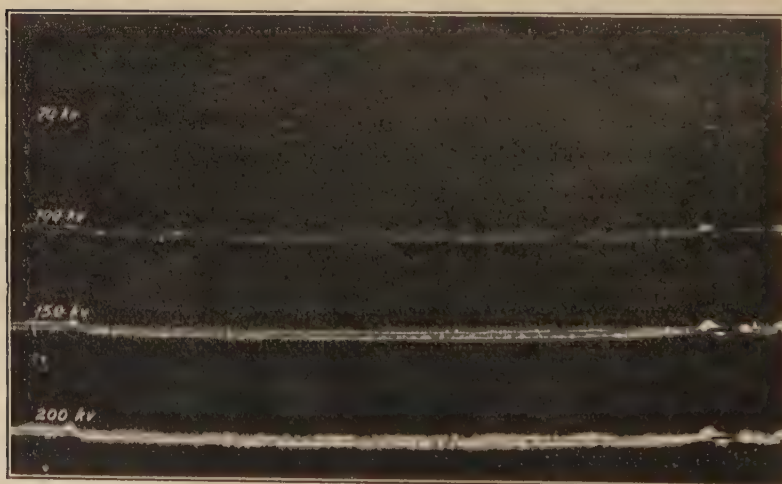


FIG. 63.—Corona on a weathered galvanized iron wire. Diameter, 168 cm.

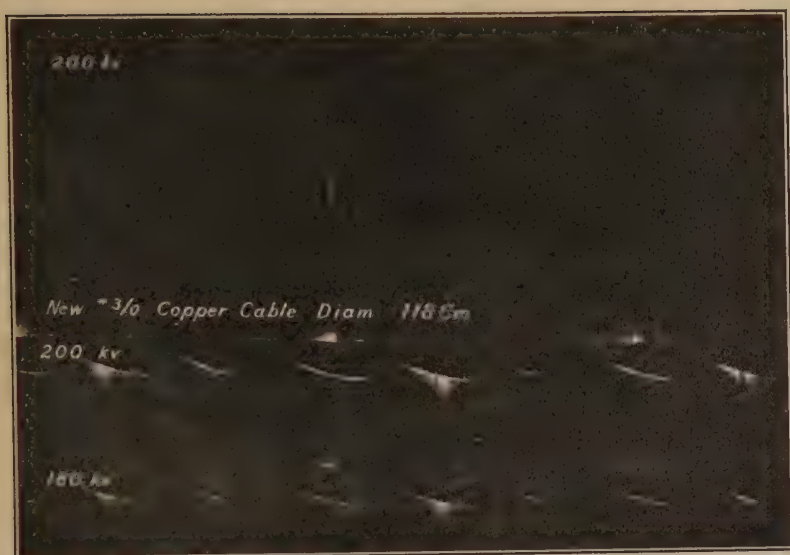


FIG. 64.—Corona on a 1.25 cm. polished brass rod and unpolished copper cable.



FIG. 65.—Corona on a No. 3/0 weathered cable.



FIG. 66.—Corona on a No. 3/0 line cable. Dry.

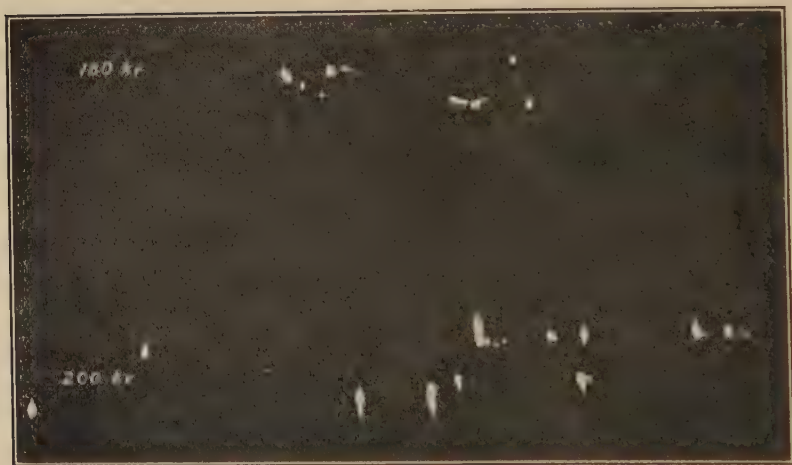


FIG. 67.—Corona on a No. 3/0 line cable. Wet.



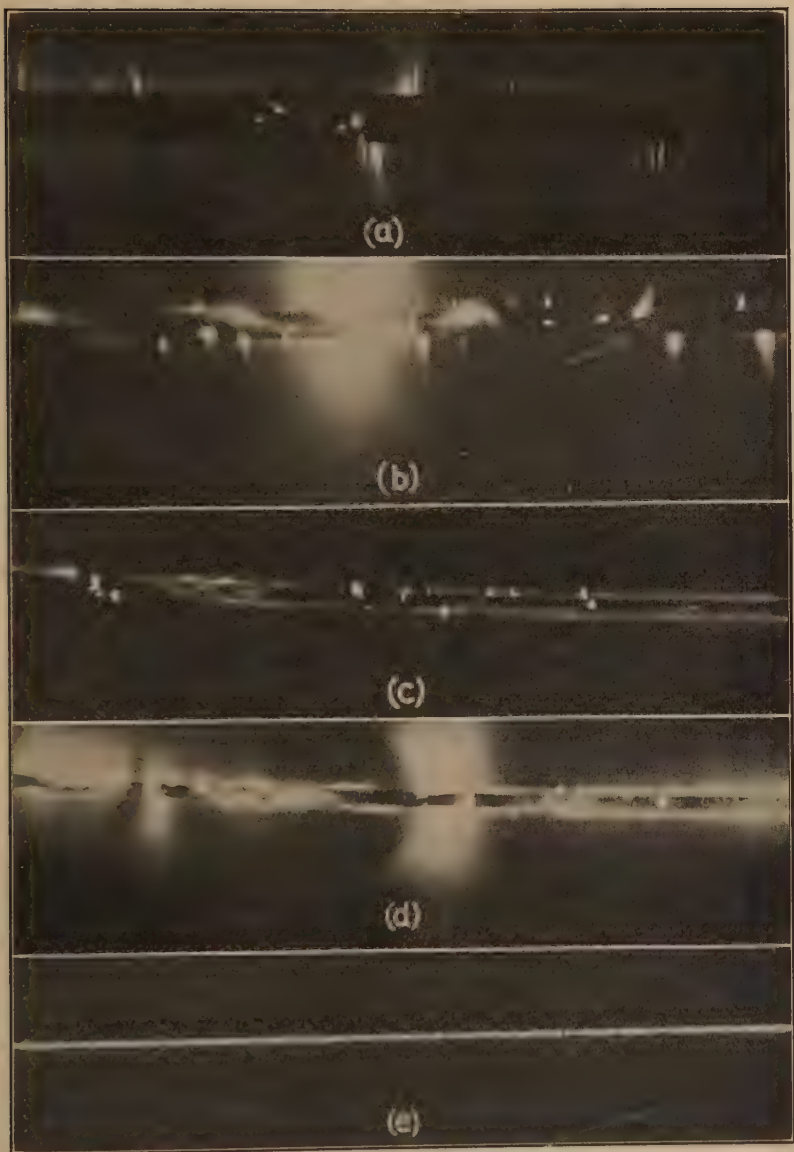
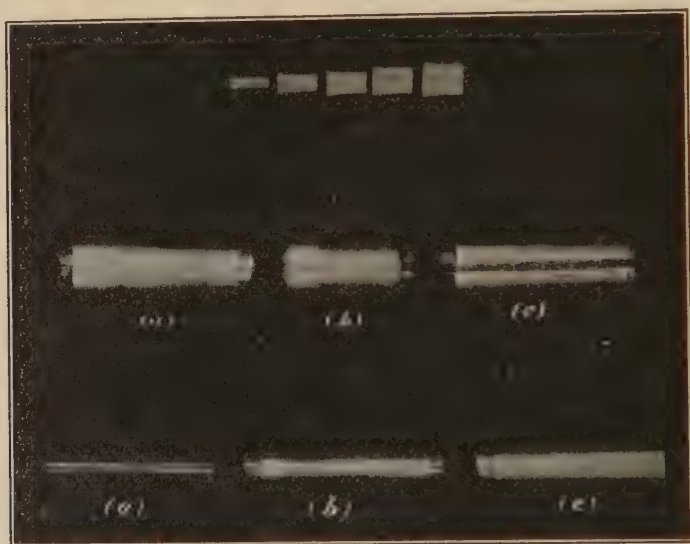


FIG. 68.—Corona on conductors at very high 60-cycle voltages.

(a) 3.5 inch tube at 900,000 volts, (b) 1.75 inch tube at 800,000 volts, (c) 1.0 inch tube at 500,000 volts, (d) 1.0 inch tube at 780,000 volts, (e) 0.04 inch tube at 800,000 volts.



Figures 69, 70, and 71 taken from Whitehead are self-explanatory. Figure 72 shows the apparent diameter of corona on a given wire. In Fig. 73 is a curve through the same points. Throughout this curve the correction of 1.18 has been used to include the ultra-violet. Near the starting voltage, however, the corona seems to be very largely ultra-violet. This explains



DIAMETER OF CORONA.

FIG. 69 (Upper).—Diameter of corona on 0.233-cm. wire in 18.6-cm. cylinder.  $e_s = 21.5$  kv. Glass lens kilovolts 22.5, 25, 27.5, 30, 32.5, respectively. (Whitehead.)

FIG. 70 (Middle).—Diameter of corona showing effect of ultra-violet. (a) 0.232 cm. (b) 0.316 cm. (c) 0.399 cm. Left side of (a)(b)(c) quartz lens. Right side of (a)(b)(c) glass lens. (Whitehead.)

FIG. 71 (Lower).—Corona on 0.233 cm. wire at 22.5, 27.5, 32.5 kv.  $e_s = 20.75$  kv. Glass lens. (Whitehead.)

the low point at 22.5 kv. At the start the corona appears to take, immediately, a definite finite thickness; the rate of increase is then quite rapid but gradually assumes a linear relation.

In the hope of throwing further light on the discharge and loss mechanism, an investigation of corona and spark was made with the help of the stroboscope.

A needle gap was first arranged across the transformer with a high steadying resistance. The impressed voltage was adjusted until corona appeared all the way between the conductors as in Fig. 74. In this case it seemed possible that the corona on the

positive wire extended out farther than the corona on the negative wire and that the positive discharges overlapped, giving the effect of a single discharge completely across between the conductors.

Examination of this was then made through the stroboscope which was so set that the right needle, Fig. 74(2), was seen when positive, and the left when negative. To the eye, the discharge from the positive needle has a bluish-white color and extends out a considerable distance, the negative appears as a red and hot point. The photograph shows more of the negative than is seen by the eye. Figure 74(1) is the discharge as it appears without stroboscope. 74(2) with the right needle as positive.

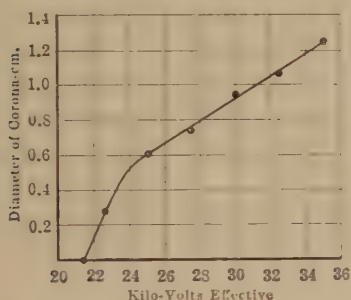


FIG. 72.

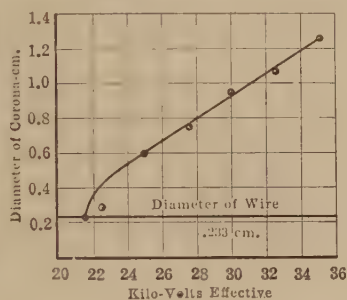
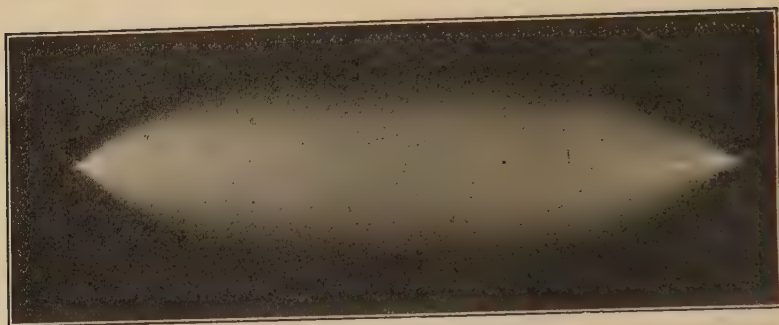


FIG. 73.

FIGS. 72 and 73.—Diameter of corona (0.233-cm. wire in 18.6-cm. cylinder).

74(3) with stroboscope shifted 180 degrees to show left needle as positive. In 74(4) the stroboscope has the same position as 74(3), but the voltage is higher, and many fine static sparks can be seen.

If voltage above the visual corona point is impressed on two parallel polished wires, a more or less even glow appears around the wires. After a time the wires have a beaded appearance. On closer examination the beads appear as reddish tufts, while in between them appears a fine bluish-white needle-like fringe. On examination through the stroboscope it can be seen that the more or less evenly spaced beads are on the negative wire, while the positive wire has the appearance, if not roughened by points, of a smooth bluish-white glow. At "points" the positive discharge extends out at a great distance in the form of needles; it is possible that it always extends out but is not always visible except as surface glow. Thus, the appearance of beads and fringe to the unaided eye is really a combination of positive and negative



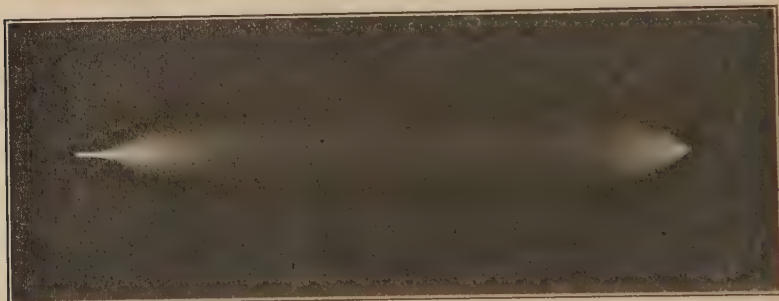
(1) Without stroboscope, 72,000 volts.



Left (-)

(2) With stroboscope, 72,000 volts.

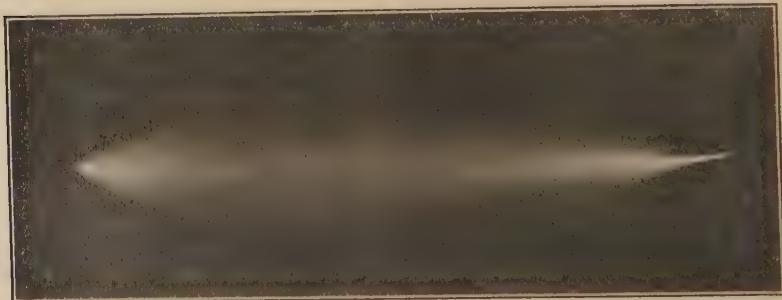
Right (+)



Left (+)

(3) Same as (2), stroboscope rotated 180°.

Right (-)



Left (+)

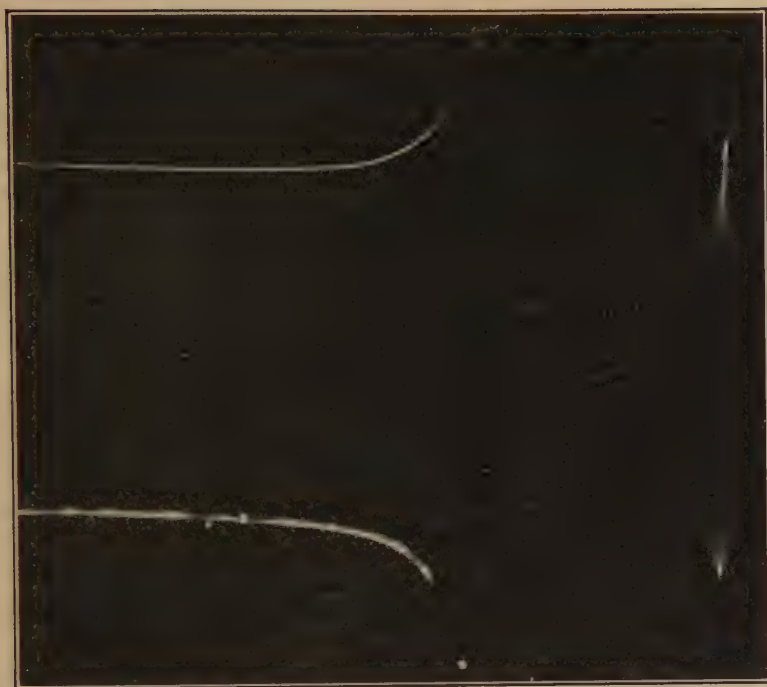
(4) Same as (3), voltage increased to 84,000.

Right (-)

FIG. 74.—Corona between copper needle points. 20.5-cm. gap.



FIG. 75.—Comparison of corona on wires and needles. Phosphor-bronze wire, 14.5 cm. spacing, needles 18 cm. spacing. Volts, 71,000. Without stroboscope.



+

FIG. 76.—Comparison of — and + A. C. corona on wire and points. (Same as Fig. 75 with stroboscope.)

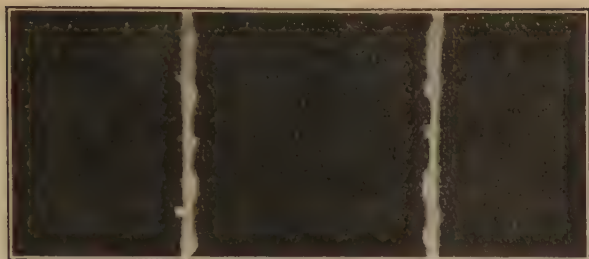
corona. In Figs. 75 and 76 two wires are placed close together at the top. The bottom is bent out and needles are fastened on. Figure 75 is without a stroboscope. Figure 76 is taken with a stroboscope set to show positive right and negative left. Thus, positive and negative coronas for points and wires are directly compared. Figure 77(1) is taken without the stroboscope, (2) with right negative, (3) with stroboscope shifted 180 electrical degrees to show the right positive. These wires were, at the start, highly polished. At first corona appeared quite uniform, but, after a time, under voltage, the reddish negative tufts separated, more or less evenly spaced as shown. Figure 26 shows similar photographs taken on a slightly different conductor set-up. Figure 78 shows a section without voltage. The bright spots are still polished and correspond in position to the negative tufts. The space in between is tarnished. The polishing of the surface at the negative spots is probably due to the bombardment at the surface there by the heavier positive ions. This takes place with either copper or iron wire.

Figure 79 shows positive and negative corona on wires widely spaced to get uniform field distribution. A close examination of the negative shows beads about to form. Figure 80 shows a similar pair of conductors. The negative in this case has formed a spiral, apparently following the grain twist of the conductor.

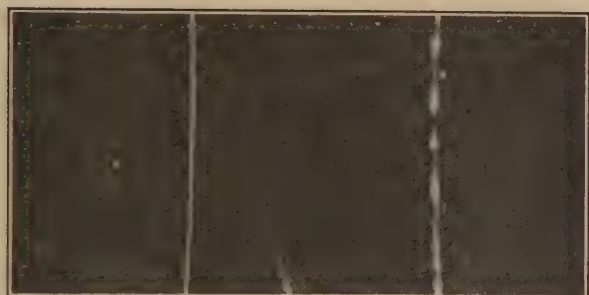
A large fan-like bluish discharge is often observed extending several inches from the ends of transformer bushings, points on wires, etc. This discharge has the appearance of a bluish spray, reddish at the point. The stroboscope shows that the bluish spray is positive, while the red point at the base of the spray is negative. Figure 81 shows one of two parallel polished rods (120 cm. spacing) supported at the top and brought to sharp points at the bottom; 81(1) shows how each wire appears without stroboscope; 81(2) is the wire when positive, 81(3) the wire when negative. Note the dark space on 81(3) between the point and negative corona spiral of tufts. 81(1) shows this space to have only the positive glow.

Water was placed on a pair of parallel conductors. At the wet places the positive corona extended out in long fine bluish-white streamers (see Fig. 82 without stroboscope). With certain forms of dirt on the wires the negative corona appears as red spots, the positive always as streamers. It is also interesting to note that, if a uniformly rough wire is taken, as a galvanized wire or





(1) Without stroboscope.



Left (+)

(2) With stroboscope.

Right (-)



Left (-)

(3) With stroboscope  
rotated 180°.

Right (+)

FIG. 77.—Corona on parallel wires. No. 13 B. and S. copper wire. Spacing, 12.7 cm. Volts, 82,000.



FIG. 78.—Section of wire (Fig. 77). "Dead." Bright spots position of negative "beads."

FIG. 80.—Copper wire. Diameter 0.26 cm. Spacing, 120 cm. Volts, 200,000. Polished at start. Note negative corona apparently following spiral "grain" of wire.



Left (-)

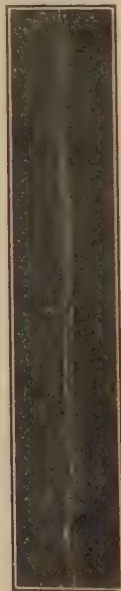


Right (+)

FIG. 79.—Polished brass rod. Diameter, 0.475 cm. Spacing, 120 cm., Volts, 150,000. Note that negative "beads" are just starting to form.



Left (-)



Right (+)

FIG. 80.

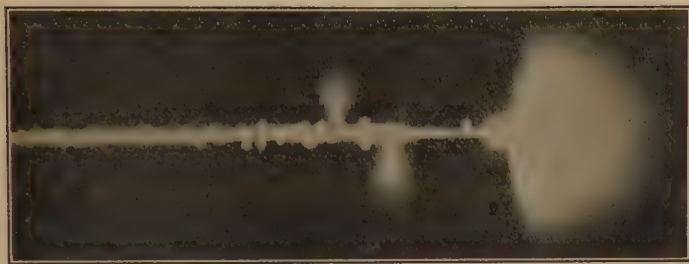
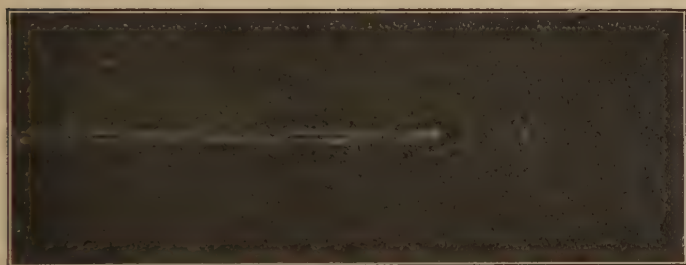


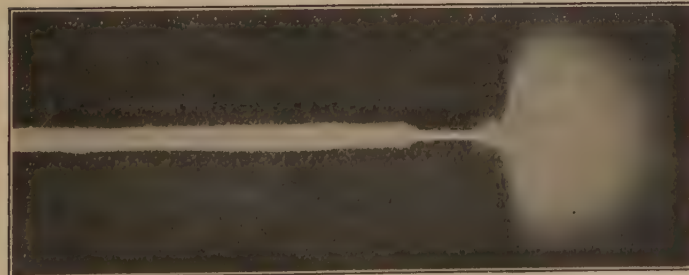
Fig. 81.—Same as Fig. 81 (1).  
Surface dirty.



(3) With stroboscope —.  
Diameter, 0.325 cm. Spacing,



(2) With stroboscope +.  
One of two parallel polished steel rods pointed at ends.  
ing, 120 cm. Volts, 180,000.



(1) Without stroboscope ±.

Fig. 81.—One of two parallel polished steel rods pointed at ends.

"weathered" wire, the positive appears as bluish needles, while the reddish negative is more uniform than on the "corona-spotted" polished wire, in which case the negative corona appears as concentrated at the untarnished spots.

**Mechanical Vibration of Conductors.**—Years ago a pair of 20-mil steel conductors, 500 ft. long, were strung at about 10-ft.



FIG. 83.—Mechanical vibration of parallel wires in corona, due to electrostatic forces.

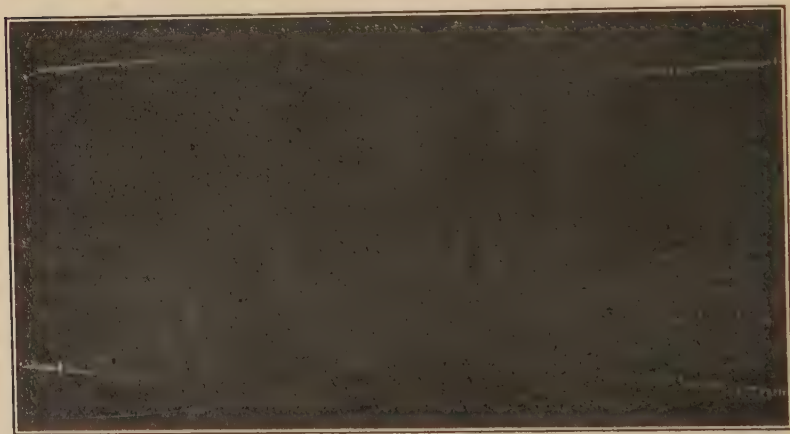


FIG. 84.—Mechanical vibration of parallel wires in corona, due to electrostatic forces.

spacing, for power loss measurements. It was noticed at high voltage that the conductors vibrated, starting with a hardly perceptible movement which, in a few minutes, had an amplitude of several feet at the center of the span. Generally, one wire

vibrated as fundamental, the other as third harmonic. The period of the fundamental in this case was about one per second.

Figures 83 and 84 show this condition repeated in the laboratory on short lengths of conductor. In Fig. 83 one wire is vibrating as the fundamental, the other as the second harmonic. The motion is rotary. For the wire with a node in the center (Fig. 83), it is extremely interesting to note that for about one-half of the rotation the wire appears very bright, for the other half rotation the wire is much less bright. This seems to mean that each part of the wire is rotating at the power supply frequency—60 cycles per second. Hence, it has the effect of the stroboscope, and for part of the rotation there is always negative corona and for the other part always positive corona.

**Corona Current Oscillograms.**—Oscillograms showing instantaneous values of corona current were obtained with the low-voltage hot filament cathode ray oscillograph.<sup>1</sup> The cathode ray oscillograph, which was referred to on page 39 depends on the control by the phenomena studied of the path of the electron stream striking the fluorescent screen on the end of the cathode-ray tube. On the outside of this may be placed a photographic film. With periodic phenomena, the figure is usually allowed to retrace itself a number of times in order to secure a discernible figure on the film. Accordingly, it ordinarily appears in polar coordinates and is known as a cyclogram. (See page 202, Chap. VI for additional discussion.)

Figure 85 gives examples of such cyclograms taken during corona current studies, the vertical deflections or components of the figures being proportional to currents and the horizontal ones proportional to impressed voltages. This figure shows the cyclogram records together with some of the waves translated to rectangular coordinates. The current waves include both corona and capacity current components.

This oscillographic study of corona<sup>1</sup> brought out several new interesting features of its mechanism. One of these was the manner in which the starting point of corona with respect to the voltage wave appears earlier as the voltage is raised; that is, as the applied voltage is increased above the visual critical

<sup>1</sup> PEEK, F. W., JR., "Law of Corona and the Dielectric Strength of Air IV," *Trans. A.I.E.E.*, p. 1009, 1927.

LLOYD and STARR, "Corona Loss Measurements by Means of the Cathode Ray Oscillograph," *Trans. A.I.E.E.*, p. 997, 1927.





Instantaneous voltages,  $e_i$ , when plotted with applied voltages show that  $e_i$  is zero at approximately  $2e_v$ .

If the above rule held over a wide range of voltage, it would be found that

$$e + e_i = 2e_v = \text{constant}$$

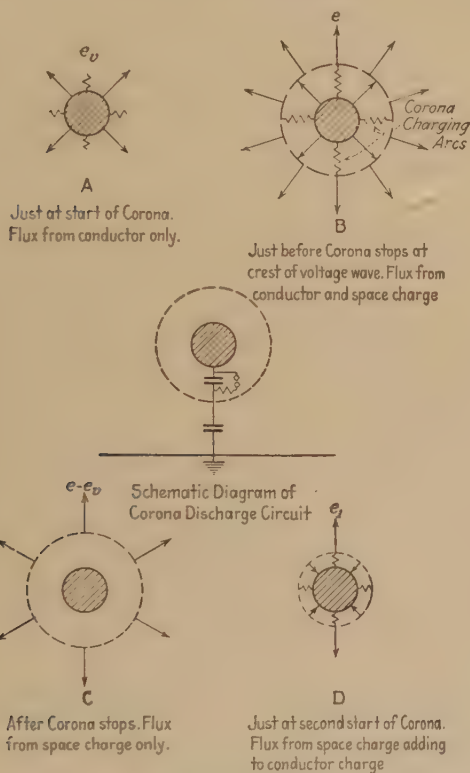


FIG. 86.—Mechanism of corona.

As a matter of fact, as would be expected, the tests show that  $e + e_i$  is not constant, but approximately so, near the critical voltage. Actually, the effect is as if the total space charge were not effective in reducing the critical voltage, but that

$$e_i = e_v - (e - e_v)a$$

where  $a$  is a leakage factor and is less than unity.

The reason for the above is quite evident, as shown in Fig. 86. After corona starts, a tube of corona surrounds the conductor and is charged through the "corona arcs" up to the maximum

of the wave when the arcs go out or corona stops. This corona tube or "space" charge increases quite suddenly to a finite diameter at the start and then more gradually as the maximum of the wave is approached. This charge caused by the excess voltage returns towards the conductor with the falling wave and adds to the charge caused by the applied voltage on the next half cycle. When the sum of these charges is sufficient to cause the breakdown gradient, corona starts at an instantaneous voltage less than the normal visual critical voltage. With the start of corona there is a sudden rush of current. When twice the visual

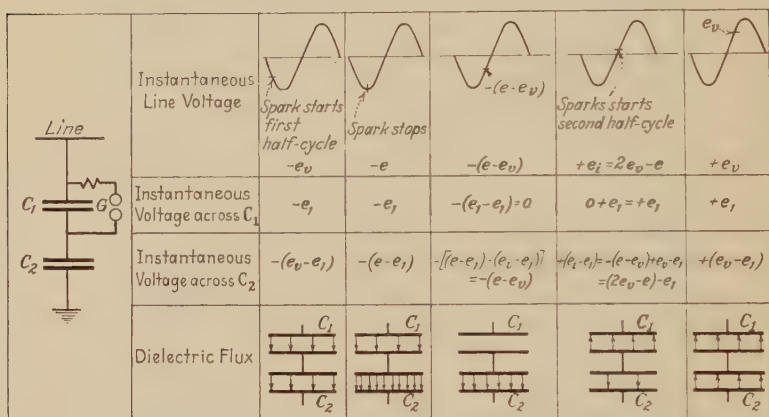


FIG. 87.—Artificial corona circuit-operation of single gap, fixed capacitance.

critical voltage is applied, the excess voltage is equal to the critical voltage. The charge due to this excess voltage is then sufficient to cause corona without any additional charge. Corona thus starts on the following half cycles on the zero of the wave, as shown above. If the applied voltage is further increased, corona starts below the zero of the wave or on the falling voltage.

Corona characteristics can be produced artificially by means of condensers. For example, take two condensers and place a gap, in series with a resistance, across one of them. If voltage is applied and gradually increased, capacity current flows until the gap breaks down. There is a sudden rush of current. The spark, which represents the corona, continues to the maximum of the voltage wave when it stops. This leaves an excess charge on one condenser which adds to the charge caused by the line voltage on the next half cycle. The gap breaks down at lower

and lower instantaneous voltage as the applied voltage is increased and becomes zero when the applied voltage is twice the initial starting voltage, as discussed in the case of actual corona above. This is all illustrated diagrammatically in Fig. 87.

Bennett has made some very interesting oscillograms of corona current.<sup>1</sup> Figures 88(a)(b)(c) show the voltage wave applied between a cylinder and a concentric wire, and the resulting current. The current wave includes both capacity and corona current components. The part of the wave above the zero line occurs when the wire is (−) and that below when the wire is (+); 88(a) is for a voltage very slightly above the critical voltage and shows a very sudden sharp hump in the current wave when the wire is (+) and a spread-out hump when the wire is (−). This gives the appearance of corona starting at a slightly lower voltage on the (+) wire; (b) and (c) show the positive and negative humps at higher voltage. The oscillation is caused largely by the sudden "corona spark" discharging through the reactance and capacity of the circuit.

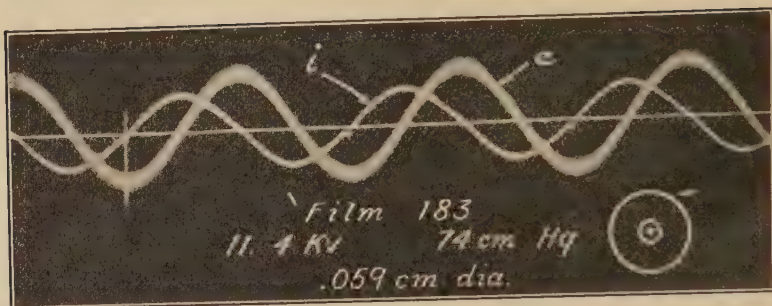
Figure 89 shows an oscillogram of corona current and the corresponding impressed voltage wave taken at Stanford University.<sup>2</sup> The current wave represents the discharge from a point at a potential above ground of approximately 1,000,000 volts, the capacity current being negligible.

**The Rectifying Effect of Corona.** —Due to the difference in size and mobility of the positive and negative ions, there is a marked contrast in the discharges from positive and negative points. Figures 74 and 75, page 92, illustrate this. If a grounded metal plane is placed sufficiently close to a point in corona, a certain amount of charge will reach the plane. A sensitive ammeter inserted in the ground circuit of the plane will measure this corona current, which will be found to depend not only upon the voltage and spacing, but also on the polarity of the point: that is, there will be a different amount of charge moving across to the grounded plane when the point is negative than when it is positive. If an alternating voltage is applied to the point, more charge will reach the plane on one half than on the opposite half cycle, so that rectification takes place. Similar results can be

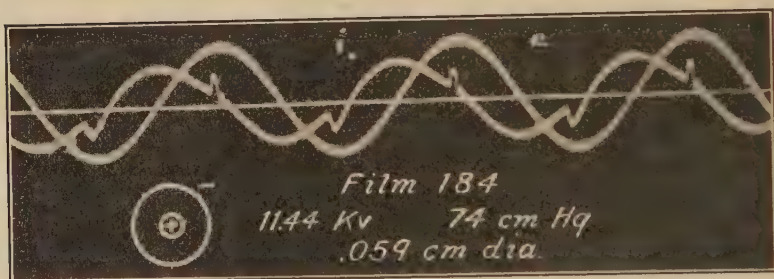
<sup>1</sup> BENNETT, E., *Trans. A.I.E.E.*, p. 571, 1914.

<sup>2</sup> CARROLL and COZZENS, *Trans. A.I.E.E.*, 1929.

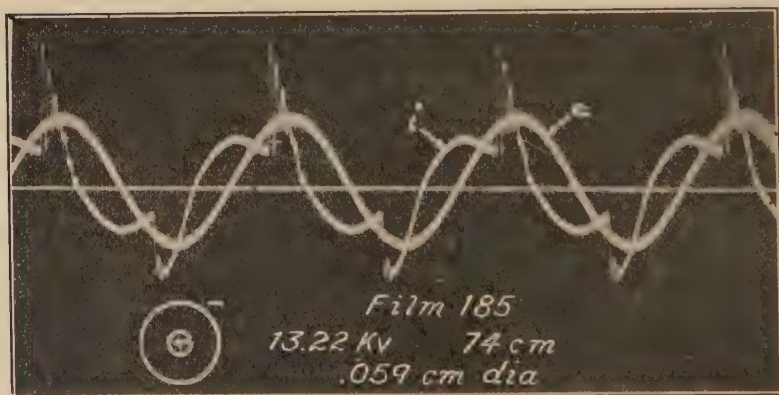




(a)



(b)



(c)

FIG. 88.—Oscillograms of corona current. (E. Bennett, Trans. A.I.E.E., p. 571, 1914.)



obtained with a wire in corona inside of a cylinder. The unsymmetrical shape of the corona current waves of Figs. 88 and 89 shows this rectifying effect. The sign of this net unidirectional flow with alternating voltages depends on the spacing, shape of the electrodes, and voltage. In most cases, more charge will be found to pass across to the plane or larger electrode when the smaller electrode involving the greater corona discharge is positive. As a rule this means of rectifying alternating currents involves too low a flow of unidirectional current to render it



Fig. 89.—Corona current from needle point at one million volts. (*Carroll & Cozzens, Stanford Univ.*)

practical for ordinary use. The amount and sign of the rectification by corona also will vary, dependent upon the particular gas and pressure used.

If measurements are made of the field about an electrode in corona having an applied alternating voltage, the same rectifying effect can be detected, since the space will be found to be charged up to a unidirectional potential above ground. Field measurements made between transmission conductors<sup>1</sup> indicate that the space at the theoretical neutral is built up to a negative potential above ground at the start of corona, and changes to positive at higher voltages.

**Lichtenberg Figures.**—Interesting electrostatic field conditions have been recorded by corona discharges on certain dielectric

<sup>1</sup> CARROLL and LUSIGNAN, *Trans. A.I.E.E.*, p. 50, 1928.

surfaces. In 1777 Dr. G. C. Lichtenberg with sulphur dust secured discharge figures radiating out from a charged electrode. In 1888 Trouvelet<sup>1</sup> and Brown<sup>2</sup> produced the same figures on photographic plates. Interesting gap discharge figures were also obtained on photographic plates by F. E. Nipher.<sup>3</sup>

Recently, considerable work has been done in the use of such photographic figures for securing voltage records.<sup>4,5</sup>

J. F. Peters<sup>4</sup> was the first to develop an instrument making use of Lichtenberg figures for recording, photographically, voltages on transmission lines. This instrument was called a klydonograph.

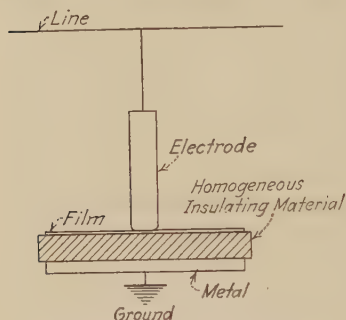


FIG. 90.—Elementary diagram of method for producing photographic Lichtenberg figures.

The most suitable arrangement for producing the figures for voltage measurements is illustrated in Fig. 90. Figure 91 shows some typical figures secured. The action is probably similar to that occurring in ordinary photography, the light from the corona discharge of the electrode over the surface merely affecting the chemical properties of the silver particles in the film through a form of photoelectric effect. In that way

a larger figure is probably recorded than can be seen with the eye, as the discharge may involve a certain amount of light beyond the visible range which could still affect the film.

Because of the distinct difference in visual appearance that we have seen to exist with positive and negative corona discharges, it is to be expected that such should also be true with positive and negative Lichtenberg figures. Figure 91 shows this to be the case, the two polarities differing in both size and shape for the same applied voltage. The form of the figure has also been found to vary somewhat for different wave shapes, so that it is possible to identify with fair accuracy the wave front of a surge as well as the voltage magnitude. In general the size of figure for a given wave shape varies approximately linearly with

<sup>1</sup> *Lumière elec.*, Vol. XXX, 1888.

<sup>2</sup> *Phil. Mag.*, Vol. XXVI, 1888.

<sup>3</sup> *Trans. Acad. Sci. St. Louis*, Vol. XIX, June, 1910.

<sup>4</sup> PETERS, J. F., *Elec. World*, Vol. CLXXXIII, 1924.

<sup>5</sup> McEACHRON, K. B., *Trans. A.I.E.E.*, 1926.

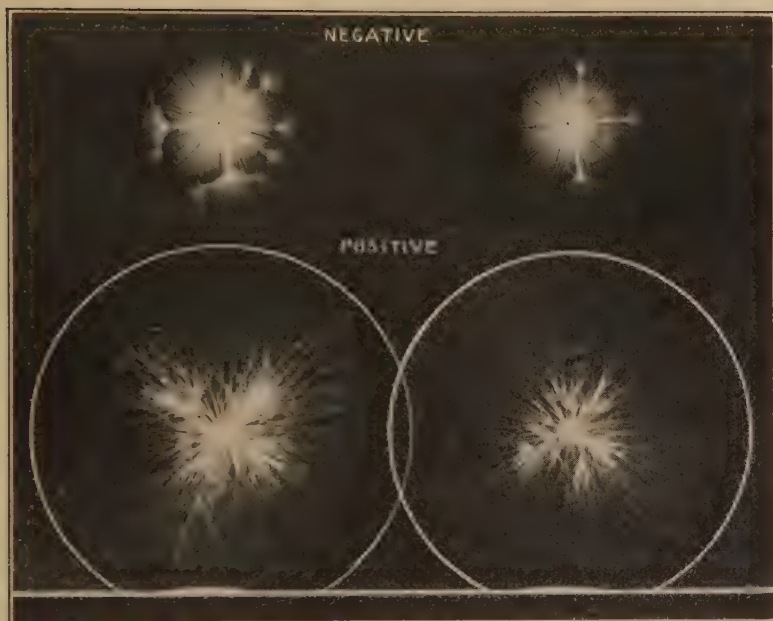


FIG. 91.—Lichtenberg figures of 5,000,000 volt lightning generator surges, taken with surge voltage recorder.

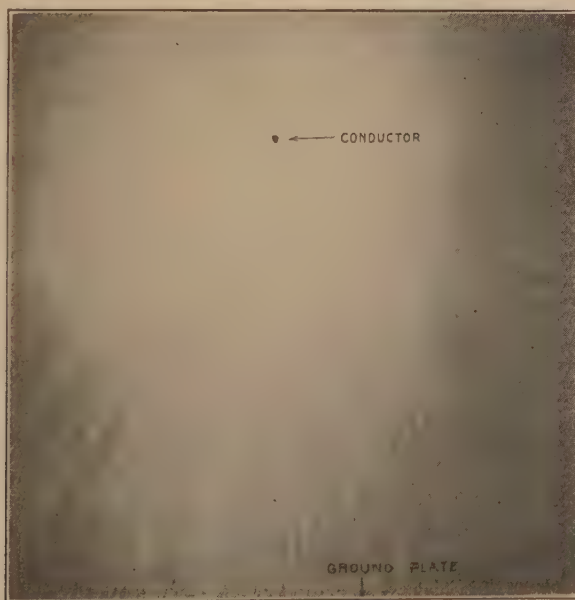


FIG. 92.—Lichtenberg figure showing electrostatic field between wire and ground plane.

the applied voltage up to a certain point when the figure breaks to form "slips" which then allow no accurate analysis. The direct range of reliable voltage records, with the ordinary klydonograph or surge voltage recorder, is approximately between 1500 and 30,000 volts. This range may be extended indefinitely by means of a potentiometer.

Using this same method of recording discharge figures, it is possible to obtain pictures of electrostatic fields under various conditions. Figure 92 shows an example of the field between a conductor and a ground plane, the film being so placed as to secure a cross-section of the field normal to the conductor axis. On this record the discharge paths are seen to follow the electrostatic flux lines from the conductor surface to the plane.

## CHAPTER V

### SPARK-OVER

By spark-over is generally meant the disruption of a gaseous dielectric from one conductor to another conductor. Strictly speaking it is the name applied to the initial discharge and not the arc that follows, as was discussed earlier (see page 47, Chap. III). In this chapter it is only the factors affecting the initial complete breakdown that will be discussed, so that the term spark-over only will be used.

**Parallel Wires.**—If impressed voltage is gradually increased on two parallel wires placed a considerable distance apart in air, so that the ratio  $S/r$  is above a certain critical value, the first evidence of stress in the air is visual corona. If the voltage is still further increased, the wires become brighter and the corona has the appearance of extending farther out from the surface. Finally, when the voltage has been sufficiently increased, at some chance place a spark will bridge between the conductors. When the spacing is small, so that  $S/r$  has a critical ratio, spark and corona may occur simultaneously, or the spark may bridge across before corona appears. If the spacing is still further reduced so that  $S/r$  is below the critical ratio, the first evidence of stress is complete spark-over and visible corona never appears (see page 28).

Extensive tests have been made.<sup>1</sup> The method of conducting tests was to start at the smaller spacings with a given value of  $r$  and measure the spark-over voltage. Unless otherwise stated the frequency used was 60  $\sim$ . When the spacings were above the critical ratio of  $S/r$ , and corona formed before spark-over, the corona voltage was noted first. The voltage was then increased until spark-over occurred. The spark-over point is not as constant or consistent as the corona point and is susceptible to change with the slightest dirt spot on the conductor surface, any unsteady condition in the circuit, humidity, etc. At the beginning of the tests it was found necessary, in order to get consistent results, to put water tube resistances in series with the

<sup>1</sup> See "Law of Corona II," *Trans. A.I.E.E.*, p. 1051, 1912.



conductors to eliminate resonance phenomena. These resistances were high, but not sufficiently so to cause an appreciable drop in voltage before arc-over.

Table XVII is a typical data table. Each point is the average of a number of readings.

TABLE XVII.—CORONA AND SPARK-OVER FOR PARALLEL WIRES  
Temperature 17 deg. C., bar. 75.3 cm.  
Wire No. 0, diameter 0.825 cm.

Test No. 166 values read 60 ~			No. 0 wire, corrected to 25° C., 76 bar.			
Spacing	Effective kv. to neutral		Maximum values to neutral		Maximum	
Cm. S	Corona $e_s$	Spark $e_s$	Corona $e_s$	Spark $e_s$	Corona $g_s$	Spark $g_s$
2.54	None	15.8	.....	21.9	.....	41.4
3.81	None	22.5	.....	31.2	.....	42.5
5.08	None	27.3	.....	37.9	.....	43.2
6.35	None	31.05	.....	43.2	.....	43.8
7.62	None	35.0	.....	48.5	.....	44.9
8.89	None	37.35	.....	51.8	.....	45.0
10.16	40.4	40.9	56.0	56.7	44.0	44.6
12.70	41.8	42.1	58.0	58.1	44.0	44.1
13.97	43.7	46.0	60.7	60.5	44.2	46.7
15.24	45.9	48.1	63.6	67.0	45.1	48.9
15.78	46.6	54.1	64.8	75.0	43.8	50.8
20.32	48.9	59.6	67.7	82.8	44.0	53.7
22.86	50.1	66.2	69.7	91.7	43.7	56.8
25.40	51.1	71.5	70.7	99.2	43.1	60.4
27.94	52.1	79.0	72.4	109.7	42.9	65.1
30.48	53.1	84.5	74.0	117.0	42.9	67.9
33.02	54.1	89.6	74.8	124.0	42.4	70.2
35.56	55.1	95.5	76.5	132.5	42.6	73.9
38.10	56.1	102.3	77.8	141.9	42.7	77.8
40.64	57.1	106.5	79.4	149.0	42.9	80.5
60.96	63.3	.....	87.0	.....	42.9	.....

In columns 4 and 5 are voltages reduced to the maximum value to neutral and corrected to standard  $\delta$ . Column 6 gives the surface gradient for corona. Column 7 gives the surface gradient for spark, up to the spacing where corona starts first; above this critical spacing it gives the apparent surface gradient as the conductor above this point must be larger on account of corona. As the field around the conductors at the small spacings is very

much distorted, it is necessary to use formula 12(a) or 12(b) to calculate the surface gradient.

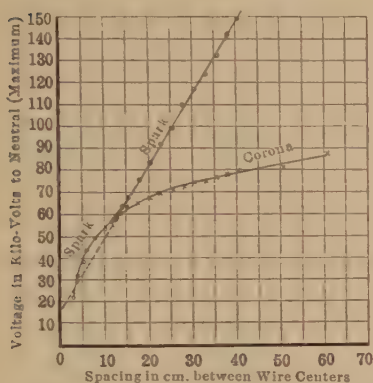


FIG. 93.—Spark-over and visual corona voltages.

(Parallel polished copper wires, 0.825 cm. diameter.  $\delta = 1$ .)

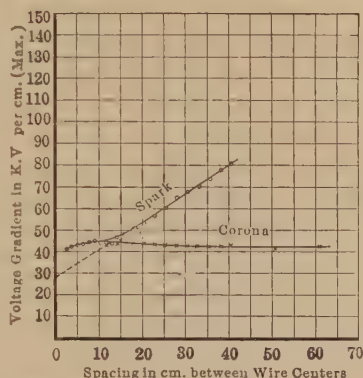


FIG. 94.—Corona gradient and apparent spark gradient.

Figure 93 is a typical curve. Voltage is plotted with spacing for spark and corona. Up to spacing 12.4 cm. there is spark-over

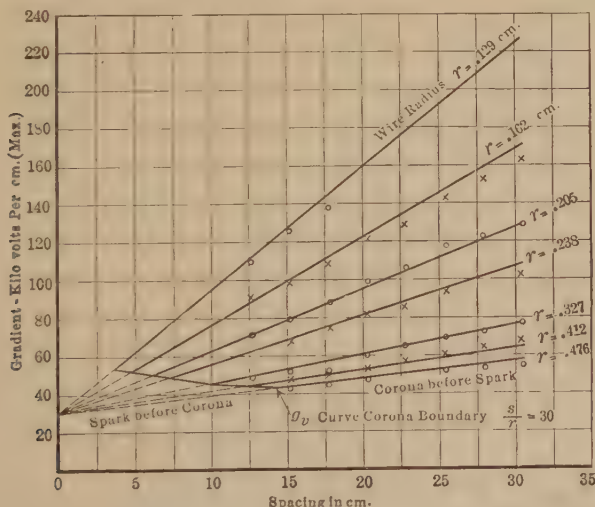


FIG. 95.—Apparent spark-over gradients for parallel wires. (Points measured, curves calculated.)

before corona. This curve seems to be continuous with the corona curve which starts at this point. The spark curve here branches and is very close to a straight line within the voltage

range. In Fig. 94 the surface gradient curves are plotted. The corona gradient is a straight line parallel to the  $X$  axis with a slight hump at the critical ratio of  $S/r$ . The *apparent* spark gradient is also a straight line, within the test range. It intersects the corona line at the critical ratio point, or at what may be termed the triangular point, and extended it cuts the  $g$  axis at  $g = 30$ . These are characteristic curves (see also Figs. 50 and 51). For a given spacing the spark-over voltage increases as the size of the conductor decreases.

It is important to note that, for all sizes of wire, the spark gradient curve extended as a straight line cuts the gradient axis at approximately  $g = 30$ . Spark curves extended as straight lines through the critical ratio point and intersecting the gradient axis at  $g = 30$  are shown in Fig. 95. The triangular point or critical ratio of  $S/r$  is tabulated in Table XVIII. Its average

TABLE XVIII.—CRITICAL RATIOS  $S/r$ —EXPERIMENTAL VALUES  
Intersection point of  $g_v$  and  $g_s$

Size, B. & S.	Radius cond., cm.	$S$ , cm.	$S/r$	Size, B. & S.	Radius cond., cm.	$S$ , cm.	$S/r$
0	0.461	13.5	29.3	6	0.205	6.2	30.2
0	0.412	11.7	28.4	8	0.162	4.8	29.6
2	0.327	10.2	31.2	10	0.129	4.0	31.0
4	0.260	7.9	30.4	12	0.103	3.0	29.1
5	0.230	7.3	31.7			Average	30.1

value is  $S/r = 30$ . If it is assumed that the spark-gradient curve is a straight line the conditions are, that it must cut the corona gradient line at  $S/r = 30$  and extended must cut the  $g$  axis at  $g_o = 30$ .

The gradient for  $g_r$ , or the gradient at the triangular point or below it, is

$$g_o = g_o \left( 1 + \frac{0.301}{\sqrt{r}} \right) \quad (18)$$

therefore, the approximate apparent gradient at or above the triangular point is

$$\begin{aligned} g_s &= g_o \left( 1 + \frac{0.301}{\sqrt{r}} \frac{S}{r} \frac{1}{30} \right) \\ &= 30 \left( 1 + \frac{0.01}{\sqrt{r}} \frac{S}{r} \right) \text{ kv. per centimeter maximum} \end{aligned}$$

This follows because of the assumption of a straight line through two fixed points.

The approximate spark-over voltage above the triangular point is

$$e_s = g_s r \log_e R/r \text{ kv. to neutral maximum.}$$

Below the triangular point it may be found by substituting  $g_v$  for  $g_s$ .

In Fig. 95 each drawn curve is for  $g_s$  values calculated for varying spacing at constant radius. The points are measured values. The corona boundary line is the  $g_v$  curve; it intersects the  $g_s$  curves at  $S/r = 30$ . Corona does not form below this line, but it sparks across immediately. This is greater than the theoretical ratio, as explained below (see also pages 28 and 29).

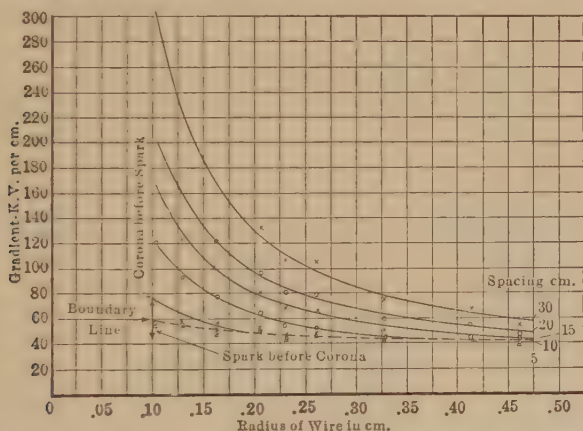


FIG. 96.—Apparent spark-over gradients for parallel wires. (Points measured, curves calculated.)

In Fig. 96 each curve is drawn for a constant spacing and varying radius. The broken line is the critical ratio line. It also corresponds to the  $g_v$  curve. For spacings below this line, spark-over takes place immediately before visible corona forms, and the  $g_s$  values fall pretty well on the  $g_v$  line, as shown by triangles.

Figure 97 is voltage plotted in the same way. Below the corona boundary, where spark occurs before corona, the  $e_s$  curve does not hold. The broken lines are calculated from  $g_v$  and  $e_v$ . The points are observed values. Thus, corona gradient and spark-over gradient and, hence, spark voltage and corona voltage below  $S/r = 30$ , are the same.

No great accuracy is claimed for this formula. It may, however, be useful in approximately determining the arc-over between conductors in practice. Dirt or water, however, will greatly modify the results, as will appear below.

The reason that spark takes place before visual corona can form at small spacings or below  $S/r = \infty$  is discussed on page 18 for concentric cylinders, in which case  $g$  was taken as constant.

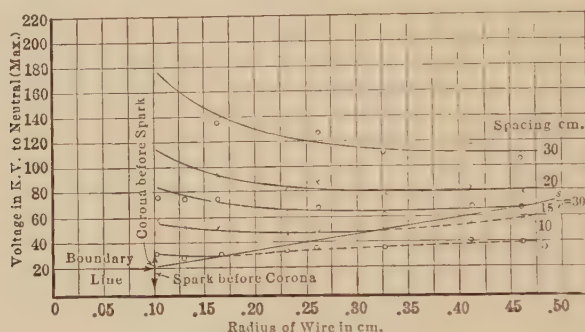


FIG. 97.—Spark-over voltages between parallel wires. (Maximum values to neutral given. Points measured, curves calculated.)

We know, however, that  $g_v$  is a function of  $r$ , and for air

$$g_v = g_o \left( 1 + \frac{0.301}{\sqrt{r}} \right)$$

$$e_v = g_o \left( 1 + \frac{0.301}{\sqrt{r}} \right) r \log_e R/r$$

- Differentiating for maximum

$$\frac{de}{dr} = g_o \left( 1 + \frac{0.301}{2\sqrt{r}} \right) \left( \log_e R/r - 1 - \frac{0.301}{\sqrt{r}} \right)$$

or,  $e_v$  is maximum when

$$\left( 1 + \frac{0.301}{2\sqrt{r}} \right) \left( \log_e R/r - 1 - \frac{0.301}{\sqrt{r}} \right) = 0 \quad (31)$$

This gives a ratio of  $R/r$  greater than  $e$ . The experimental ratio in Fig. 98 is 3 and checks with the above.

If a very small value of  $r$  is taken, corona forms and then, after the voltage is sufficiently increased, spark-over occurs. It might be supposed that with increasing voltage the center wire would



become larger and larger in effect due to conducting corona and, finally, when  $\frac{R}{\text{radius} + \text{corona}} = \text{critical ratio}$ , spark-over would occur. This is not the case. It takes a much higher voltage for the small wire corona than for metallic cylinders with  $R/r$  at maximum ratio. Hence, corona seems to be either in *effect* a

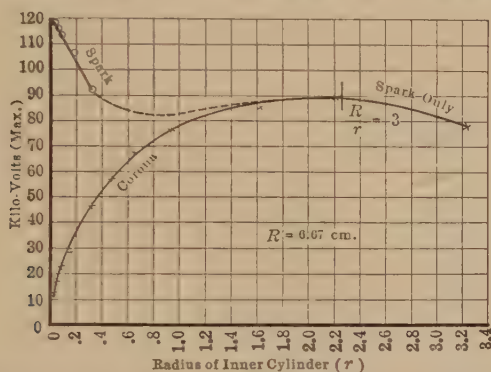


FIG. 98.—Spark-over and corona voltages for concentric cylinders with varying diameter of inner cylinder.

series resistance or it grades or distributes the flux density (see Fig. 98). Taking the exact equation for parallel wires

$$g_v = \frac{e_r}{r \left[ \frac{\sqrt{\frac{S}{2r} - 1}}{\sqrt{\frac{S}{2r} + 1}} \cosh^{-1} \frac{S}{2r} \right]} \quad (12b)$$

$$e_v = g_o \left( 1 + \frac{0.301}{\sqrt{r}} \right) r \left[ \frac{\sqrt{\frac{S}{2r} - 1}}{\sqrt{\frac{S}{2r} + 1}} \cosh^{-1} \frac{S}{2r} \right]$$

Varying  $r$  for constant  $S = 10$  it is found that  $e_v$  is maximum when  $S/r = 6.67$ . Experiments show this ratio to be 30. This is probably because, at the small spacing, the corona acts as a flexible conductor which collapses and forms a point.

The visual corona voltages, or the spark-over voltages *below* the critical ratio of  $S/r$  or  $R/r$ , should be of possible value for voltage measurement on account of the accuracy at which they may be determined or calculated for different temperatures, barometric pressures, etc.

**Influence on Spark-over of Water and Oil on the Conductor Surface.**—Tests with oil and water on the conductor surface were made in a manner exactly similar to the dry spark-over and corona tests. In the oil tests, the surface of the wire was coated with a thin even film by means of an oiled cloth. For the wet tests, water was sprayed on the conductor surface by means of an atomizer, before each reading. Figures 50, 51, and 99 are dry, wet, and oil curves for three different sizes of wire.

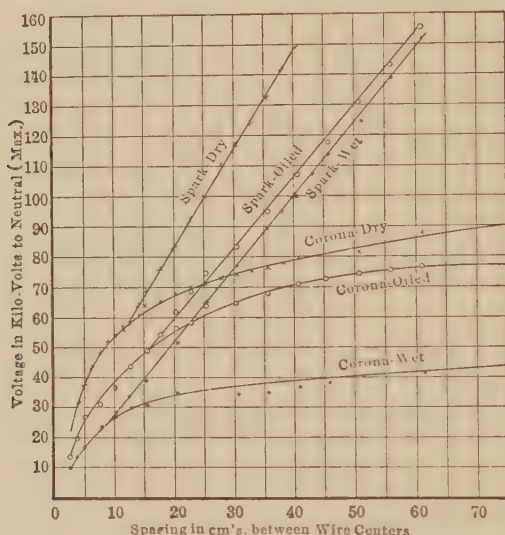


FIG. 99.—Spark-over and visual corona for parallel wires. (Diameter, 0.825 cm. Polished copper. Surfaces dry, wet, and oiled. Maximum volts to neutral given.)

For spark-over both water and oil have approximately the same effect. This curve tends to approach the needle-gap curve.

For corona, water very greatly lowers  $g_v$ . Oil lowers  $g_v$  but to a much less extent than water. Where the conductor is very small, the percentage increase in diameter, due to oil, more than compensates for the lowering effect.

The spark gaps which have been useful in measuring high voltages will now be considered.

**The Gap as a Means of Measuring High Voltages.**—A gap method of measuring high voltages is often desirable in certain commercial and experimental tests. A gap will measure the maximum point of practically all voltage waves and is, therefore, used in many insulation tests where breakdown also depends upon

the maximum voltage. In most commercial tests an accuracy of 2 or 3 per cent. is sufficient. A greater accuracy can be obtained with the sphere gap for special work where extra precautions are taken.

**The Needle Gap.**—The needle gap is somewhat erratic at high voltages because, due to the corona brushes and broken-down air that precede the spark-over, variations are introduced by humidity, oscillations, etc.<sup>1</sup>

The needle gap is also inconvenient at short spacings because needles must be replaced after each discharge, as the calibration varies somewhat with the sharpness of the points. This condition of the points requires less attention at spacings over several feet in length.

The effect of humidity is shown in Fig. 100, where it can be seen that a higher voltage is required to spark over a given needle gap when the humidity is high than when it is low. (Curves, Fig. 100, are intended only to illustrate this effect.) It is probable that the corona streamers in humid

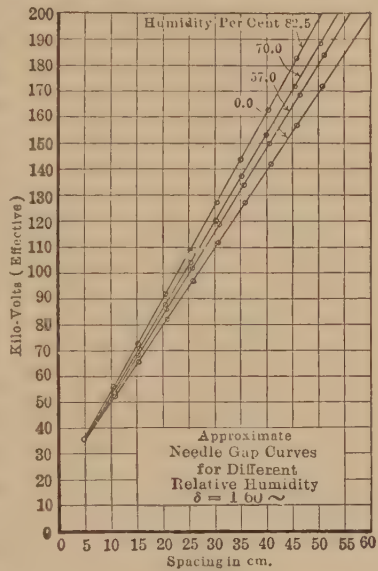


FIG. 100.

TABLE XIX.—AVERAGE NEEDLE SPARK-OVER VOLTAGES

No. 00 Needle,  $\delta = 1$ 

A.I.E.E.

Kv. eff.	Spacing (cm.)	Kv. eff.	Spacing (cm.)
10	1.19	40	6.10
15	1.84	45	7.50
20	2.54	50	9.00
25	3.30	60	11.80
30	4.10	70	14.90
35	5.10	80	18.00

<sup>1</sup> PEEK, F. W., JR., "Discussion," *Trans. A.I.E.E.*, p. 812, 1913.PEEK, F. W., JR., *G.E. Rev.*, Vol. XVI, p. 486, 1913.

air cause a "fog," and then agglomerate the water particles, which, in effect, increase the size of the electrodes.

There is the added possibility that the water particles may arrange themselves throughout the field under the electrostatic

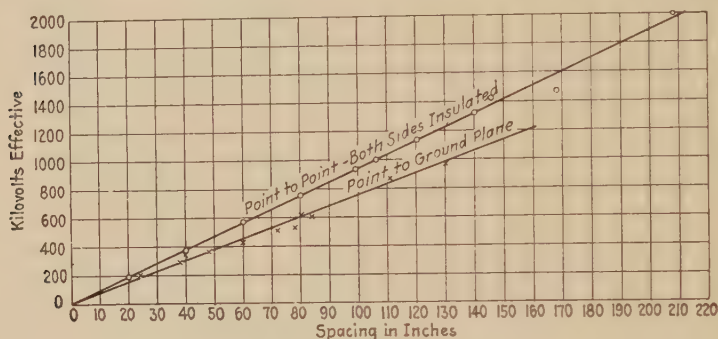


FIG. 101.—60-cycle spark-over voltage of needle point gap and point-to-plane gap.

forces in such a way as to redistribute the stresses. This might then tend to lessen any localized gradients, thereby increasing the strength of the air. The above reasons have also been given for the increase of the strength of oil by moisture under certain conditions (see Chap. VII, page 218).

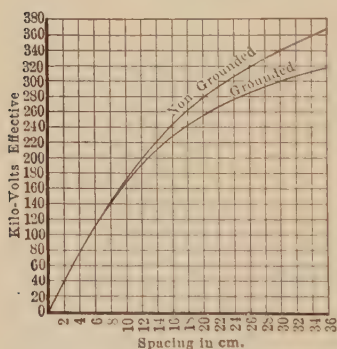


FIG. 102.—Spark-over voltages of 25-cm. spheres.

All spark-gap curves of whatever form of gap must be corrected for air density—that is, altitude and temperature. The spark-over of the needle gap decreases with decreasing air density but the correction is erratic and unreliable.

Table XIX shows the needle-gap spark-over values for the lower voltages. Figure 101 gives the complete spark-over curve up to 2,000,000 volts.

**The Sphere Gap.**<sup>1</sup>—The voltage required to spark over a given gap between spheres increases with the diameter of the spheres. For accurate work it is preferable to use spacings less than the

<sup>1</sup> CHUBB and FORTESCUE, *Trans. A.I.E.E.*, p. 739, 1913.

PEEK, F. W., JR., *Trans. A.I.E.E.*, p. 923, 1914.

PEEK, F. W., JR., *G. E. Rev.*, Vol. XVI, p. 286, 1913.

diameter of the sphere. This is especially so where one sphere is grounded. A larger sphere should then be used. With this spacing limit the first evidence of stress is complete spark-over and all of the undesirable effects and variables due to prolonged brush discharge and broken-down air, as with points, are eliminated. Humidity has no measurable effect, if the sphere surfaces remain dry.

The space factor is relatively small. Several thousand measurements may be made without repolishing. The curve may be calculated. The only correction is the air-density correction. This has been investigated and the results are given below. The correction is quite simple. Figure 102 gives typical

TABLE XX.—SPHERE GAP SPARK-OVER VOLTAGES  
2.0-cm. Spheres

Spacing		Kilovolts effective	
Cm.	In.	Non-grounded	Grounded
0.2	0.508	5.6	5.6
0.3	0.762	8.0	8.0
0.4	1.016	10.3	10.3
0.5	1.27	12.5	12.5
0.6	1.52	14.8	14.6
0.7	1.78	17.0	16.7
0.8	2.03	18.9	18.6
0.9	2.28	20.8	20.2
1.0	2.54	22.6	21.7
1.2	3.05	25.9	24.4
1.4	3.56	28.9	26.4
1.6	4.06	.....	28.2
1.8	4.57	.....	30.0



TABLE XXI.—SPHERE GAP SPARK-OVER VOLTAGES  
6.25-cm. Spheres

Spacing		Kilovolts effective	
Cm.	In.	Non-grounded	Grounded
0.5	0.197	12.0	12.0
1.0	0.394	22.5	22.5
1.5	0.591	31.5	31.5
2.0	0.787	41.0	41.0
3.0	1.181	57.5	56.0
4.0	1.575	70.5	66.0
5.0	1.969	81.0	73.0
6.0	2.362	89.0	79.0
7.0	2.756	96.0	83.0
8.0	3.150	102.0	88.0
9.0	3.543	107.0	90.5
10.0	3.937	110.0	93.0

Each point is the average of five readings. The average variation between maximum and minimum for a given setting is less than 0.5 per cent. For the grounded case, the curves were made with the grounded sphere 4 to 5 diameters above ground. See Table XXXIV.

TABLE XXII.—SPHERE GAP SPARK-OVER VOLTAGES  
12.5-cm. Spheres

Spacing		Kilovolts effective	
Cm.	In.	Non-grounded	Grounded
0.25	0.098	6.5	6.5
0.50	0.197	12.0	12.0
1.0	0.394	22.0	22.0
1.5	0.591	31.5	31.5
2.0	0.787	41.0	41.0
3.0	1.181	59.0	59.0
4.0	1.575	76.0	75.0
5.0	1.969	91.0	89.0
6.0	2.362	105.0	102.0
7.0	2.756	118.0	112.0
8.0	3.150	130.0	120.0
9.0	3.543	141.0	128.0
10.0	3.937	151.0	135.0
12.0	4.72	167.0	147.0
15.0	5.91	188.0	160.0
17.5	6.88	201.0	168.0
20.0	7.87	213.0	174.0

sphere-gap curves for both spheres insulated and for one sphere grounded. Tables XX to XXVI give spark-over curves for 2.0, 6.25, 12.5, 25, 50, 75, and 100-cm. spheres at sea level (25°C., 76 cm. barometer).  $\delta = 1$ .

TABLE XXIII.—SPHERE GAP SPARK-OVER VOLTAGES  
25-cm. Spheres

Spacing		Kilovolts effective	
Cm.	In.	Non-grounded	Grounded
0.5	0.197	11	11
1.0	0.394	22	22
1.5	0.591	32	32
2.0	0.787	42	42
2.5	0.983	52	52
3.0	1.181	61	61
4.0	1.575	78	78
5.0	1.969	96	94
6.0	2.362	112	110
7.5	2.953	135	132
10.0	3.937	171	166
12.5	4.92	203	196
15.0	5.91	230	220
17.5	6.88	255	238
20.0	7.87	278	254
22.5	8.85	297	268
25.0	9.83	314	280
30.0	11.81	339	300
40.0	15.75	385	325

*Calculation of Curves.*—The gradient or stress on the air at the sphere surface, where it is greatest, is found mathematically

$$g = \frac{e}{X} f \text{ kilovolt/centimeter} \quad (13)$$

Where  $e$  is the applied voltage in kilovolts,  $X$  is the spacing in centimeters,  $f$  is a function of  $X/R$ , and  $R$  is the radius of the sphere in centimeters.

TABLE XXIV.—SPHERE GAP SPARK-OVER VOLTAGES  
50-cm. Spheres

Spacing		Kilovolts effective	
Cm.	In.	Non-grounded	Grounded
2	0.787	40.0 <sup>1</sup>	40
4	1.575	76.5	76
6	2.362	115.5	112
8	3.150	149.0	145
10	3.937	189.0	185
12	4.72	224.3	220
14	5.51	255.5	250
16	6.30	285.0	275 <sup>2</sup>
20	7.87	335.0	320
25	9.83	393.0	377
30	11.81	445.0	420
35	13.80	493.0	456
40	15.75	537.0	489
45	17.72	573.0	516
50	19.19	605.0	541
55	21.65	633.0	561
60	23.62	660.0	579
65	25.60	684.0	594
70	27.56	705.0	608
75	29.55	725.0	619

<sup>1</sup> These values are calculated.<sup>2</sup> Spacings above 16 cm. are calculated.

Then

$$g_s = \frac{e_s}{X} f \text{ kv./centimeter}$$

where  $e_s$  is the spark-over voltage and  $g_s$  is the apparent strength of air.

$f$  is found mathematically and tabulated on page 28, for the non-grounded and grounded cases. For the non-grounded case, we have found, experimentally, that  $g_s$ , the apparent surface gradient at spark-over, increases with decreasing radius of sphere, as  $g_v$  for corona on wires increases for decreasing radius of wire.

TABLE XXV.—SPHERE GAP SPARK-OVER VOLTAGES (75-CM. SPHERES)

Spacing		Kilovolts effective	
Cm.	In.	Non-grounded	Grounded
20	7.87	360	360
30	11.81	490	490
40	15.75	615	595
50	19.69	715	665
60	23.62	795	725
70	27.56	870	775
80	31.50	920	.....
90	35.43	970	.....
100	39.37	1010	.....

TABLE XXVI.—SPHERE GAP SPARK-OVER VOLTAGES (100-CM. SPHERES)  
These values are calculated

Spacing		Kilovolts effective	
Cm.	In.	Non-grounded	Grounded
1.0	0.394	20	20
3.0	1.181	60	60
5.0	1.969	100	100
10.0	3.937	195	195
15.0	5.91	283	280
20.0	7.87	364	360
30.0	11.81	520	505
40.0	15.75	650	615
50.0	19.69	770	730
60.0	23.62	870	810
70.0	27.56	956	895
80.0	31.50	1044	956
90.0	35.43	1107	1010
100.0	39.37	1182	1057
110.0	43.35	1238	1090
120.0	47.20	1290	1133
130.0	51.20	1335	1160
140.0	55.70	1378	1189
150.0	59.10	1412	1212

For a given size of sphere,  $g_s$  is practically constant, independent of spacing, between the limits of  $X = 0.54\sqrt{R}$  and  $X = 2R$ .

The *average* gradient between these limits of separation is

$$g_s = 27.2 \left( 1 + \frac{0.54}{\sqrt{R}} \right) \text{ kv./centimeter maximum} \quad (a)$$

$$g_s = 19.3 \left( 1 + \frac{0.54}{\sqrt{R}} \right) \text{ kv./centimeter effective sine wave.}^1 \quad (b)$$

The maximum variation from the average between the limits may be 2 per cent. When  $X$  is less than  $0.54\sqrt{R}$ ,  $g_s$  increases very rapidly because the spacing is then comparable with the "ionizing distance"<sup>1</sup> (see page 67, Chap. IV). Above  $X = 3R$ ,  $g_s$  apparently gradually increases. This increase seems only apparent and due to the shanks, surrounding objects, etc., better distributing the flux or lessening the flux density. When both spheres are insulated and of practical size, the change is not great within the prescribed limits. In this case the neutral of the transformer should be grounded so that spheres are at equal and opposite potential. When one sphere is grounded, however, this apparent increase of gradient is very great if the mathematical  $f$ , which does not take account of the effect of surrounding objects, is used. For this reason  $f$  was found experimentally, assuming  $g_s$  constant within the limits, as it is in the non-grounded case, and finding values of  $f_o$  corresponding to the different values of  $X/R$ . Any given value of the ratio  $X/R$  should require a constant  $f_o$  to keep  $g_s$  constant independent of  $R$ . This was found to check.<sup>2</sup>

The curves may be approximately calculated thus

$$e_s = g_s \frac{x}{\bar{f}} \begin{array}{l} \text{(non-grounded)} \\ \text{effective sine wave} \end{array} \quad (13a)$$

$$e_s = g_s \frac{x}{\bar{f}_o} \begin{array}{l} \text{(grounded)} \\ \text{effective sine wave} \end{array} \quad (13b)$$

where  $g_s$  is calculated from the equation (b), and  $f$  or  $f_o$  are found from the table on page 28 for the given  $X/R$ . These equations have been given for theoretical rather than practical reasons. *Curves should be calculated only when standard measured curves*

<sup>1</sup> PEEK, F. W., JR., "Law of Corona III," *Trans. A.I.E.E.*, p. 1767, 1913.

<sup>2</sup>  $f_o$  was determined with the grounded sphere 4 to 5 diameters above ground. In practice, this may vary from 4 to 10 diameters without great error (see Table XXXIV). Voltage values in tables correspond to 4 to 5 diameters above the ground for this case.



cannot be obtained. Measured curves are given here. The average error, however, for curves calculated from the above equations, for 2-cm. diameter spheres and over, should not be greater than 2 per cent. The accuracy of calculations is not as great as in the case of the starting point of corona on wires.

*The Effect of Air Density or Altitude and Temperature: Correction Factor. Practical Application.*—We have found that the average gradient for various air densities may be expressed

$$g_s = 27.2\delta \left( 1 + \frac{0.54}{\sqrt{\delta R}} \right) \text{kv./centimeter maximum}$$

$$g_s = 19.3\delta \left( 1 + \frac{0.54}{\sqrt{\delta R}} \right) \text{kv./centimeter effective.}$$

where  $\delta$  is the relative air density (see page 62). This correction does not apply for small spacings at low air density.

The standard curve may be made to apply to any given altitude by multiplying the standard curve voltage at different spacings by the correction factor thus

$$e_1 = e \left\{ \frac{19.3\delta \left( 1 + \frac{0.54}{\sqrt{\delta R}} \right)}{19.3 \left( 1 + \frac{0.54}{\sqrt{R}} \right)} \right\}$$

$$= e \sqrt{\delta} \left\{ \frac{\sqrt{\delta R} + 0.54}{\sqrt{R} + 0.54} \right\} = ea$$

In order to avoid the trouble of calculating in practice, the factor is tabulated in Tables XXVII and XXVIII. This correction is very accurate. Table XXVII gives the correction factor for different sizes of spheres at different barometric pressures and at constant temperature. When the voltage strikes across a given gap the voltage  $e$  corresponding to the gap is found from the standard curve and multiplied by the correction factor  $a$ , or a curve may be plotted corresponding to a given barometric pressure.

Thus

$$e_1 = ea$$

Table XXVIII gives the correction factor for various values of  $\delta$ .  $\delta$  may be calculated for the given temperature and barometric pressure and correction factor then found from the table. Figure

TABLE XXVII

Approximate corresponding altitude	Barometer		Values of $a$ at 25 deg. C. for standard spheres of the following diameter, cm.							
	Cm., Hg	In., Hg								
Ft.			6.25	12.5	25.0	37.5	50.0	75.0	100.0	
0	76.00	29.92	1.000	1.000	1.000	1.000	1.000	1.000	1.000	
500	74.58	29.36	0.981	0.980	0.980	0.979	0.979	0.979	0.979	
1,000	73.14	28.79	0.964	0.963	0.962	0.961	0.960	0.960	0.960	
1,500	71.77	28.25	0.948	0.946	0.945	0.944	0.943	0.942	0.942	
2,000	70.42	27.72	0.932	0.929	0.927	0.926	0.925	0.924	0.924	
2,500	69.09	27.20	0.916	0.913	0.911	0.909	0.908	0.907	0.907	
3,000	67.74	26.67	0.902	0.899	0.897	0.895	0.893	0.892	0.891	
3,500	66.51	26.18	0.887	0.884	0.882	0.880	0.878	0.876	0.875	
4,000	65.25	25.69	0.873	0.870	0.867	0.865	0.863	0.861	0.860	
4,500	64.01	25.23	0.859	0.855	0.852	0.850	0.848	0.846	0.845	
5,000	62.79	24.72	0.845	0.841	0.838	0.835	0.833	0.831	0.830	
6,000	60.45	23.80	0.817	0.812	0.808	0.805	0.803	0.801	0.800	
7,000	58.22	22.93	0.791	0.786	0.782	0.779	0.776	0.774	0.772	
8,000	56.03	22.05	0.765	0.759	0.754	0.750	0.748	0.746	0.744	
9,000	53.84	21.20	0.739	0.733	0.728	0.724	0.721	0.719	0.717	
10,000	51.85	20.41	0.716	0.709	0.703	0.698	0.694	0.692	0.690	
12,000	48.09	18.93	0.669	0.661	0.656	0.651	0.647	0.644	0.642	
15,000	42.88	16.88	0.606	0.596	0.589	0.585	0.580	0.577	0.575	

103 gives the standard curve for the 25-cm. sphere (non-grounded) (25°C., 76 cm. barometric pressure) and curves calculated therefrom for 25°C. and various barometric pressures.

*Experimental Determination of the Effect of Air Density.*—The equation for the air density correction factor was determined by an extensive investigation of the spark-over of spheres in a large wooden cask arranged for exhaustion of air. This cask was built of paraffined wood and was 2.1 meters high by 1.8 meters in diameter inside (see Fig. 104).

Tests were made by setting a given size of sphere at a given spacing, gradually exhausting the cask, and reading spark-over voltage at intervals as the air pressure was changed. (Temperature was always read, but varied only between 16 and 21°C.) This was repeated for various spacings on spheres ranging in diameter from 2 cm. to 25 cm. At the start, the possible

TABLE XXVIII.—CALCULATED VALUES OF  $a$  FOR DIFFERENT VALUES OF  $\delta$ 

$$a = \sqrt{\delta} \left\{ \frac{\sqrt{\delta R + 0.54}}{\sqrt{R + 0.54}} \right\}$$

Relative air density	Values of $a$ Diameter of standard spheres in cm.						
$\phi$	6.25	12.5	25.0	37.5	50.0	75.0	100.0
0.50	0.547	0.535	0.527	0.522	0.519	0.517	0.516
0.55	0.594	0.583	0.575	0.570	0.567	0.565	0.564
0.60	0.640	0.630	0.623	0.618	0.615	0.613	0.612
0.65	0.686	0.677	0.670	0.665	0.663	0.661	0.660
0.70	0.732	0.724	0.718	0.714	0.711	0.709	0.708
0.75	0.777	0.771	0.766	0.762	0.759	0.757	0.756
0.80	0.821	0.816	0.812	0.809	0.807	0.805	0.804
0.85	0.866	0.862	0.859	0.857	0.855	0.854	0.853
0.90	0.910	0.908	0.906	0.905	0.904	0.903	0.902
0.95	0.956	0.955	0.954	0.953	0.952	0.951	0.951
1.00	1.000	1.000	1.000	1.000	1.000	1.000	1.000
1.05	1.044	1.045	1.046	1.047	1.048	1.049	1.049
1.10	1.092	1.092	1.094	1.095	1.096	1.097	1.098

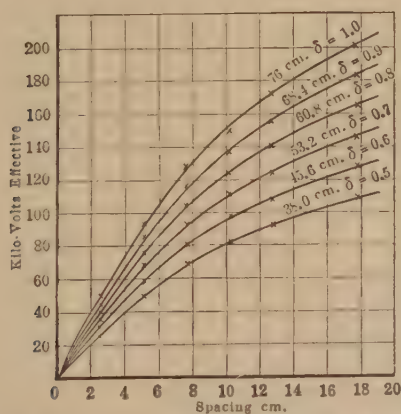


FIG. 103.—Sphere gap spark-over voltages at various air pressures. (12.5-cm. spheres. Non-grounded. Curves calculated. Points measured.)

effect of spark-overs on the succeeding ones in the cask was investigated and found to be nil or negligible. A resistance of 1 to 4 ohms per volt was used in series with the spheres. Wave shape was measured and corrected for. Voltage was read on a



FIG. 104.—Cask for the study of the variation of spark-over and corona voltages with air pressure.

voltmeter coil, by step-down transformer and by ratio. Precautions were taken as noted elsewhere.

In order to illustrate the method of recording data, etc., a small part of the data for various spheres and spacings is given in Tables XXIX to XXXII. Considerable data are plotted in curves, Figs. 105 to 107. The points are measured values. The drawn lines are calculated by multiplying the voltage values from the standard curves at  $\delta = 1$ , by the correction factor.

TABLE XXIX.—SPHERE GAP SPARK-OVER VOLTAGES AND GRADIENTS  
5.08-cm. Spheres. Non-grounded

Spacing		Relative air density	Kv.		$g_s$ measured	
Cm.	In.		Effective	Maximum	Effective	Maximum
5.08	2	1.018	78.4	111.0	27.4	38.9
5.08	2	0.980	75.6	107.0	26.5	37.6
5.08	2	0.944	73.1	103.5	25.6	36.2
5.08	2	0.903	70.7	100.0	24.8	35.0
5.08	2	0.872	68.7	97.2	24.0	34.0
5.08	2	0.836	64.0	90.5	22.4	31.7
5.08	2	0.798	63.6	90.0	22.3	31.5
5.08	2	0.764	61.1	86.4	21.4	30.2
5.08	2	0.726	58.9	83.3	20.6	29.2
5.08	2	0.682	56.1	80.5	19.6	28.2
5.08	2	0.654	54.0	76.4	18.9	26.8
5.08	2	0.618	51.5	73.0	18.0	25.6
5.08	2	0.578	49.0	69.3	17.2	24.3
5.08	2	0.544	45.8	64.7	16.0	22.6
5.08	2	0.510	43.3	61.2	15.2	21.4

TABLE XXX.—SPHERE GAP SPARK-OVER VOLTAGES AND GRADIENTS  
12.5-cm. Spheres. Non-grounded

Spacing		Relative air density	Kv.		$g_s$ measured	
Cm.	In.		Effective	Maximum	Effective	Maximum
12.7	5	0.982	163.0	230.0	23.1	32.7
12.7	5	0.951	156.0	221.0	22.2	31.4
12.7	5	0.917	150.0	212.5	21.3	30.2
12.7	5	0.880	147.0	208.0	20.9	29.5
12.7	5	0.846	143.5	203.0	20.4	29.8
12.7	5	0.807	139.5	197.5	19.8	28.0
12.7	5	0.780	134.5	190.0	19.1	27.0
12.7	5	0.736	131.0	185.5	18.6	26.3
12.7	5	0.699	125.0	177.0	17.7	25.1
12.7	5	0.666	120.5	170.0	17.1	24.2
12.7	5	0.637	115.5	163.0	16.4	23.1
12.7	5	0.598	109.5	155.0	15.5	22.0
12.7	5	0.561	104.5	147.5	14.8	21.0
12.7	5	0.541	101.0	142.5	14.3	20.2



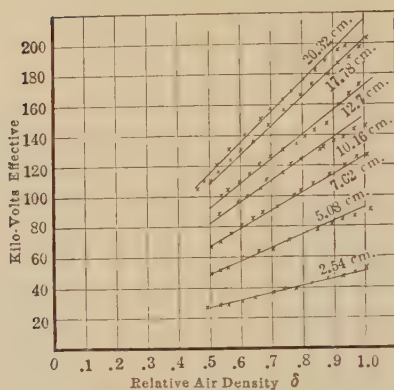


FIG. 105.—Spark-over voltages at different air densities. (12.5-cm. spheres non-grounded. Figures on curves denote spacing.)

TABLE XXXI.—SPHERE GAP SPARK-OVER VOLTAGES AND GRADIENTS

12.5-cm. Spheres. Grounded

Spacing		Relative air density	Kv.		$\epsilon_s$ measured	
Cm.	In.		Effective	Maximum	Effective	Maximum
6.35	2.5	0.908	95.5	135.0	21.2	30.0
6.35	2.5	0.869	92.5	130.5	20.5	29.0
6.35	2.5	0.828	88.6	125.0	19.7	27.8
6.35	2.5	0.796	85.8	121.0	19.0	26.9
6.35	2.5	0.758	81.1	114.5	18.0	25.4
6.35	2.5	0.723	78.2	110.5	17.3	24.5
6.35	2.5	0.690	73.2	103.5	16.2	23.0
6.35	2.5	0.653	71.5	101.0	15.9	22.4
6.35	2.5	0.620	68.2	96.3	15.1	21.4
6.35	2.5	0.582	64.3	90.9	14.2	20.2
6.35	2.5	0.539	60.7	85.8	13.5	19.0
6.35	2.5	0.439	55.6	78.5	12.3	17.4

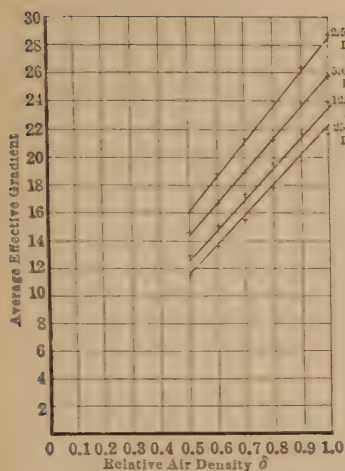


FIG. 106.

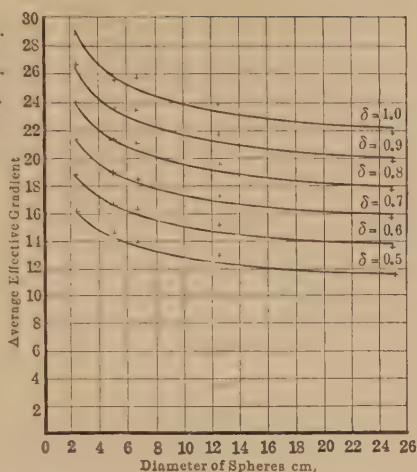


FIG. 107.

Spark-over gradients at different air densities for several sizes of spheres.

(Points measured. Curves calculated from  $g_s = 19.3\delta \left(1 + \frac{0.54}{\sqrt{\delta R}}\right)$ .)

TABLE XXXII.—SPHERE GAP SPARK-OVER VOLTAGES AND GRADIENTS  
25-cm. Spheres. Non-grounded

Spacing		Relative air density	Kv.		$g_s$ measured	
Cm.	In.		Effective	Maximum	Effective	Maximum
7.62	3	1.018	139.0	196.5	22.2	31.5
7.62	3	0.978	133.5	189.0	21.4	30.3
7.62	3	0.942	129.5	183.0	20.8	29.3
7.62	3	0.906	126.0	178.0	20.2	28.5
7.62	3	0.888	121.5	172.0	19.5	27.6
7.62	3	0.839	115.0	163.0	18.4	26.1
7.62	3	0.796	111.0	157.0	17.8	25.2
7.62	3	0.752	105.5	149.0	16.9	23.9
7.62	3	0.718	101.5	142.0	16.3	22.7
7.62	3	0.685	96.2	136.0	15.4	21.8
7.62	3	0.646	91.5	129.5	14.6	20.7
7.62	3	0.608	87.0	123.0	13.9	19.7
7.62	3	0.570	81.3	115.0	13.0	18.4
7.62	3	0.527	74.7	105.5	12.0	16.9
7.62	3	0.491	70.8	100.0	11.3	16.0

The calculated values check the measured values closely.

The equation for the correction factor was deduced from measured values as follows:

From a former investigation it was found that at  $\delta = 1$  the average gradient

$$g_s = g_o \left( 1 + \frac{0.54}{\sqrt{R}} \right)^1$$

From this investigation it was found that the average gradient at various values of  $\delta$  is

$$g_s = g_o \delta \left( 1 + \frac{0.54}{\sqrt{\delta R}} \right)$$

TABLE XXXIII.—AVERAGE EFFECTIVE RUPTURING GRADIENT FOR SPHERES OF SEVERAL DIAMETERS AND VARYING AIR DENSITIES

Diameter of Spheres, cm. Surface Gradients

Columns marked "Calc." are from,  $g_s = 19.3\delta \left( 1 + \frac{0.54}{\sqrt{\delta R}} \right)$

$\delta$	2.54		5.08		12.5		25	
	Meas.	Calc.	Meas.	Calc.	Meas.	Calc.	Meas.	Calc.
1.00	28.7	28.5	25.8	25.8	24.0	23.4	21.9	22.2
0.90	26.2	26.1	23.7	23.3	21.8	21.2	19.9	20.1
0.80	24.0	23.7	21.3	21.3	19.6	19.1	17.9	18.0
0.70	21.3	21.2	19.0	19.0	17.4	16.9	15.7	15.9
0.60	18.7	18.7	16.7	16.6	15.2	14.7	13.6	13.8
0.50	16.1	16.1	14.6	14.3	13.0	12.5	11.6	11.7

The average measured gradients for various values of  $\delta$  are given in Table XXXIII, the calculated values from the equation are also given. The check is quite close. It should be remembered, however, that these are average values over this range of spacing and that there is a small variation at different spacings as already explained (see Figs. 106 and 107).

**Effect of High Pressure, High Vacuum, Short Spacings, Etc., on Dielectric Strength of Gases.**—Since ionization by collision is the essential factor in the ordinary breakdown of gases, any effect that will hamper its action will tend to increase the breakdown voltage necessary (see page 45, Chap. III). Accordingly,

<sup>1</sup> PEEK, F. W., JR., "Law of Corona III," *Trans. A.I.E.E.*, p. 1767, 1913.

PEEK, F. W., JR., "Discussion," *Trans. A.I.E.E.*, p. 812, 1913.

as the data just given on air density has shown, the spark-over voltage rises with increased pressure.

The reason for this is that the decreased spacing of the gas particles has lowered the mean free paths of the ions and electrons so that greater gradients are necessary for accelerating them to ionizing speeds between collisions. At extremely high pressures some investigators working at comparatively short spacings<sup>1</sup> have found that there is a certain pressure above which the dielectric strength no longer increases (see Fig. 108). This has been explained on the assumption that the gas particles have become so closely packed that collision ionization has

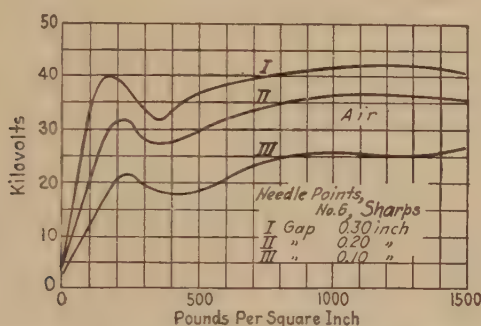


FIG. 108.—Breakdown strength of air between needle points under high pressures. (Ryan-Ekern.)

practically ceased, when some other form of breakdown begins to predominate which is not affected by gas pressure. This form may involve actual pulling of electrons from the electrodes by electro-mechanical forces set up by high field gradients there.

Inversely, collision ionization may also be seriously hampered in extremely high vacuums, as previously discussed (see page 45, Chap. III), due to the scarcity of gas particles for taking part in the ionization process. Millikan and his fellow workers have given this aspect considerable study<sup>2</sup> and have obtained breakdowns requiring gradients as high as 6,000,000 volts per centimeter which, undoubtedly involve electrons pulled from the metal also

Another instance of an apparent increase of dielectric strength of a gas caused by hampering collision ionization (and preventing normal space charge formation) is that occurring in the break-

<sup>1</sup> RYAN, H. J., *Trans. A.I.E.E.*, p. 1, 1911.

<sup>2</sup> MILLIKAN and SHACKELFORD, *Phys. Rev.*, Vol. XV, 1920.

down of very small gaps. Breakdown tests at short spacings, and the results obtained therefrom, were described in Chap. IV, page 67.

**Effect of Ultra-violet Light, Etc., on Spark-over Voltages.**—Ultra-violet light and similar short-wave radiations have been shown to cause some electron emission by photoelectric effect from metal surfaces, but to create inappreciable ionization in air and most gases (see Chap. III, page 45). Accordingly, when an ultra-violet light source is directed towards a gap, the only effect is a small electron emission from the electrodes. In very short gaps of a few millimeters spacing, and in a vacuum, where there is less chance of sufficient stray ions being present for starting collision ionization as soon as the applied field reached breakdown proportions, the time lag and, consequently, the breakdown voltage value may be lessened somewhat by the presence of electrons created by ultra-violet light. With larger spacings at atmospheric pressure, however, there is an ample number of stray ions present for initiating the ionization process so that the relatively few electrons added by the ultra-violet light have a negligible effect.

In most atmospheric spark-overs, in practice, ultra-violet light has been found to cause no measurable reduction in the average breakdown voltage. The only apparent effect has been to decrease the variation of the breakdown voltage values at the small gap spacings. This is particularly true for rapidly applied voltages and impulses.

With X-rays, however, the photoelectric effect is sufficiently intense to cause appreciable reductions of time lag and spark-over voltage, especially with impulses.

**Precautions against Oscillations in Testing.**—A non-inductive resistance of 1 or 4 ohms per volt should always be placed directly in series with the gap. For the non-grounded gap, one-half should be placed on each side. When one gap is grounded, all of the resistance should be placed on the insulated side. One object of the resistance is to prevent oscillations from the test piece, as a partial arc-over on a line insulator, reaching the gap. Another object is to limit the current discharge. This resistance is of special importance when tests are being made on apparatus containing inductance and capacity. If there is no resistance, when the gap sparks over, oscillations will be pro-



duced which will cause a very high local voltage rise over parts of the winding. If sufficient resistance is used, these oscillations will be dampened out. This is illustrated in Fig. 109 which shows results of a test on a high-voltage transformer.

Referring to Fig. 109, the high-voltage winding of the transformer under test is short circuited and connected to one terminal of the testing transformer. The other side of the testing trans-

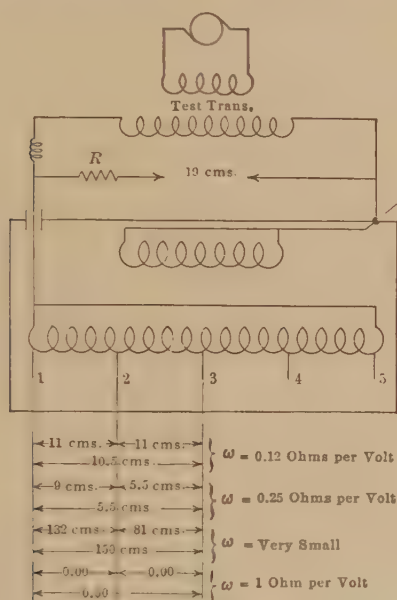


FIG. 109.

former is grounded. The low-voltage winding of the transformer under test is short circuited, connected to the case and ground. Voltage is gradually applied to the transformer under test until the "measuring gap" sparks over. Insulated taps, 1, 2, 3, 4, 5, are brought out at equally spaced points on the high-tension winding of the transformer under test. Auxiliary needle gaps are placed between 1 and 2, 2 and 3, and 1 and 3 to measure the voltage which appears across these sections of the winding when the main measuring gap discharges. The numbers between 1 and 2, 2 and 3, and 1 and 3 represent the sparking distances of the local voltages caused by a discharge of the measuring gap. Four cases are given with different values of resistance  $\omega$  in the

main gap. When  $\omega = 1$  ohm per volt, the local oscillations are completely damped out.

With small resistance in the gap, a 19-cm. spark-over causes a voltage to build up between coils 1 and 3 (which sparks over a 150-cm. gap), although the total applied voltage across the transformer is only equivalent to a 19-cm. gap. The apparatus may thus be subjected to strains far beyond reason, and either broken down or very much weakened. Water-tube resistance is the most reliable. A metallic resistance, if non-inductive and small capacity, may be used. Carbon or graphite rods, although rather erratic in their resistance values, are often used because of their cheapness and simplicity.

When the tested apparatus is such that there is considerable incipient arcing before spark-over, it is better to use the sphere to determine the equivalent ratio of the transformer at a point in voltage below the voltage at which this arcing occurs. The sphere gap should then be widened out, the spark-over voltage measured on the low-voltage side of the transformer or in the voltmeter coil, and multiplied by this equivalent ratio. It must also be remembered that resistances do not dampen out low frequency surges resulting from a short circuit, etc.

*Miscellaneous Precautions.*—In making tests it is desirable to observe the following precautions:

The shanks should not be greater in diameter than one-fifth the sphere diameter. Metal collars, etc., through which the shanks extend should be as small as practicable, and not come closer to the sphere than the gap distance at maximum opening. The effect of a large plate or plates on the shanks is given in Table XXXIV. The sphere diameter should not vary more than 0.1 per cent. and the curvature, measured by a spherometer, should not vary more than 1 per cent. from that of a true sphere of the required diameter. The spheres should be at least twice the gap setting from surroundings. This is especially important if the objects are large conducting, or semi-conducting masses, walls, floor, etc. Care must also be taken to place the spheres so that external fields are not superposed upon the sphere gap. This is likely to result, especially in the non-grounded case, from a large mass of resistance units or connecting leads, etc., in back of and in electrical connection with either sphere. The error may be plus or minus as indicated for the small plates in Table XXXIV. Great precautions are necessary at very high voltages

to prevent leakage over stands, supports, etc., and to prevent corona and brush discharges. Unless such precautions are taken errors will result.

TABLE XXXIV.—EFFECT OF METAL PLATES ON THE SHANKS. DISTANCE TO GROUND ON ARC-OVER—OF 6.25-CM. SPHERES  
Per Cent. Change of Voltage

Sphere gap, cm.	Non-grounded 5 cm. diameter plates. 6.25 cm. back of		Grounded 5 cm. diameter plates. 6.25 cm. back of	
	Both spheres	One sphere	Insulated sphere	Grounded sphere
1.5	0.0	0.0	+ 0.7	-0.7
3.0	+1.0	-1.0	+ 1.5	-1.5
6.0	+2.0	-2.0	+ 3.0	-2.0

APPROXIMATE EFFECT OF DISTANCE ABOVE GROUND WHEN ONE SPHERE IS GROUNDED

Diameters of grounded sphere above ground	Percentage variation from standard curves for different spacings		
	$x = 2R$	$x = R$	$x = \frac{R}{2}$
0	- 10.0	- 5.5	0.0
1	- 4.5	- 3.0	0.0
2	- 2.0	- 1.0	0.0
3	- 1.0	- 0.5	0.0
4	- 0.0	- 0.0	0.0
5	+ 0.5	+ 0.3	0.0
6	+ 1.0	+ 0.5	0.0
10	+ 2.5	+ 1.0	0.0
20	+ 2.5	+ 1.0	0.0

NOTE: The spacing,  $X$ , is given in terms of radius,  $R$ , to make the correction applicable to any size of sphere. The distance of the grounded sphere above ground is, for the same reason, given in terms of the sphere diameter. The (+) sign means that a higher voltage is required to arc over the gap than that given by the standard curve; the (-) sign indicates that a lower voltage is required. The standard curves are made with the grounded spheres from 4 to 5 diameters above ground. In practice it is desirable to work between 4 and 10 diameters, never under 3. Above 10 the variations in per cent. error remain about the same.

When both spheres are insulated, with the transformer neutral at the mid point, there is practically no variation in voltage for different distances above ground.

In making voltage measurements with spheres, even though they have been thoroughly cleaned and polished beforehand, it generally happens that the first few spark-overs occur at abnormally low voltages. It is only after a number of spark-overs have been taken that the breakdown voltage approaches a higher constant value. The larger the diameter of sphere used,

the lower the initial spark-over voltage. The effect is probably attributable to microscopic irregularities due to particles in the surface that must be ejected by several voltage applications before steady measuring properties exist. In general, this initial voltage reduction is not more than 10 per cent., and it disappears after a few spark-overs.

**Sixty-cycle Spark-over of Suspension Insulators.**—The spark-over voltage of suspension insulators varies with the number of units, spacing and type of units. Figure 110 shows a 60-cycle spark-over curve for one standard type of cap and pin unit of  $5\frac{3}{4}$ -in. spacing and 10-in. diameter. The breakdown voltage is

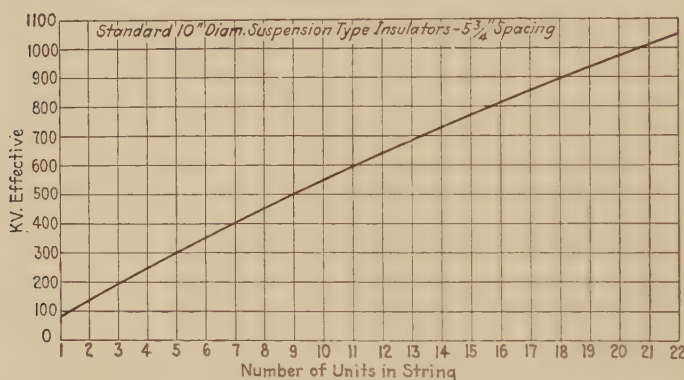


FIG. 110.—60-cycle flashover voltages of cap and pin suspension insulator strings.

roughly proportional to the spacing of the units for similar types, so that the above curve is not restricted to use with the  $5\frac{3}{4}$ -in. insulator only. This applies when the spacing is not large compared to the diameter. For the 10 in. diameter unit it holds between the 4 in. and 6 in. spacing.

**Rain and Water on Sphere Surface.**—Figures 111 and 112 show the effect of rain and water on points and spheres. The ratio of dry to rain (0.2 in. per minute) spark-over voltage for a given spacing will average about 2.5 for 6.25 to 50-cm. spheres.

**High Frequency, Oscillations, Impulses.**—A great deal of confusion often results in discussing the effects of high frequency on insulation without differentiating between continuous sine wave high frequency, oscillations, and steep wave front impulses. This is so because the effects may be quite different, and are all attributed to the same cause.

High frequency from an alternator, or a series of oscillations, may cause high-insulation loss, heating, and the resulting weakening of the insulation. Single trains of oscillations, or single

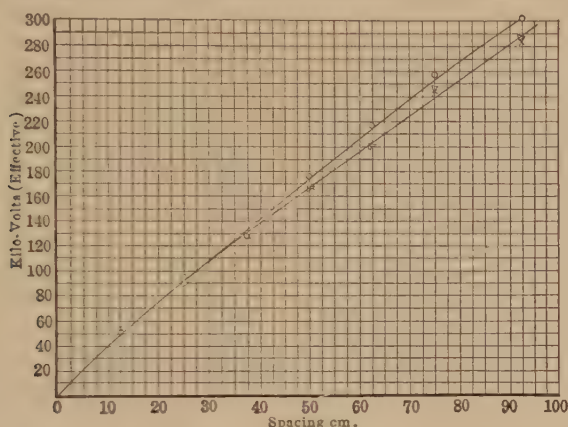


FIG. 111.—Spark-over voltages between points. o, dry;  $\Delta$ , wet; x, rain. 0.25' per minute.  $60^\circ$  points on 1.25 cm. rods.

impulses, may not produce heating. Energy, and therefore definite finite time, is required to rupture insulation. For a single impulse, or oscillation, where the time is limited, a greater

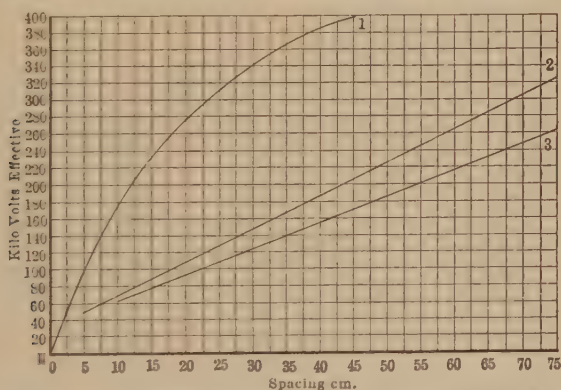


FIG. 112.—Spark-over voltages between 25 cm. spheres. 1, dry; 2, wet surface; 3, rain (0.25" per min.).

voltage should be required to break down a given insulation than for continuous high frequency or for low frequency. Experiments bear this out.<sup>1</sup> High local voltages may result from high

<sup>1</sup> PEEK, F. W., JR., "The Effect of Transient Voltages on Dielectrics," *Trans. A.I.E.E.*, Vol. XXXIV, p. 1857, 1915. (See Appendix.)



frequency, oscillations, etc. The flux may lag behind the voltage in non-homogeneous insulations. (This does not apply to air.) For a given thickness of a homogeneous insulation, and when heating does not result, a greater oscillatory or impulse voltage of short duration is generally necessary to cause puncture than at 60 cycles.

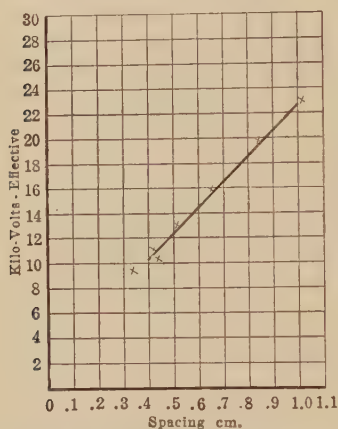


FIG. 113.—Sphere-gap spark-over voltages at 60 cycles and 1000 cycles. 5.08 cm. spheres.

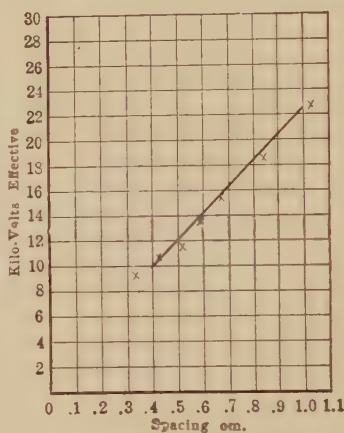


FIG. 114.—Sphere-gap spark-over voltages at 60 cycles and 1000 cycles. 12.5 cm. spheres.

(Drawn curves 60 cycles. Points 1000 cycles.)

Some of the effects will now be discussed:

*Frequency.*—Over the commercial range there is no variation in sphere-gap voltages due to frequency. Figures 113 and 114 show spark-over curves up to 25 kv. at 1000-cycle sine wave from an alternator. The voltage was measured by a static voltmeter calibrated at 60 cycle. The drawn curve is the 60-cycle curve, the points are measured values. The direct-current spark-over voltage is generally equal to the maximum of the 60 ~ spark-over voltage.<sup>1</sup> Figure 115 gives a 60-cycle curve, and also a 40,000-cycle curve from a sine wave alternator. The voltage in this case was measured by a static voltmeter. No special care was taken to polish the sphere surfaces. At low frequencies, at rough places on the electrode surface, there is local overstress; but even if the air is broken down, the loss at these places is very small and the streamers inappreciable. At continuous high frequency, 40,000 cycles, for example, a local

<sup>1</sup> PEEK, F. W., JR., "The Effect of High Continuous Voltages on Air, Oil and Solid Insulation," *Trans. A.I.E.E.*, p. 783, 1916. (See Appendix.)

breakdown at a rough point probably takes place at very nearly the same gradient as at 60 cycles, but the energy loss after the breakdown at this point occurs may be one thousand times as great. This forms a needle-like streamer which increases the stress and local loss. Spark-over then takes place from the "electric needle" at a lower voltage than the true sphere-gap voltage; thus, it seems that the air at high frequency of the above order is only apparently of less strength. These electric needles, when once formed, may be blown to different parts of the sphere surface. The corona starting point appears to take place at a lower voltage at high frequency, because the local loss at rough points, which occurs before the true critical voltage is reached, is very high at high frequency and distorts the field and masks the true starting voltage. The loss at rough points starts at the same voltage at low frequency but is inappreciable and cannot change conditions. If the sphere surfaces are very highly polished, it seems that the high-frequency spark-over voltage should check closely with the 60-cycle voltage.

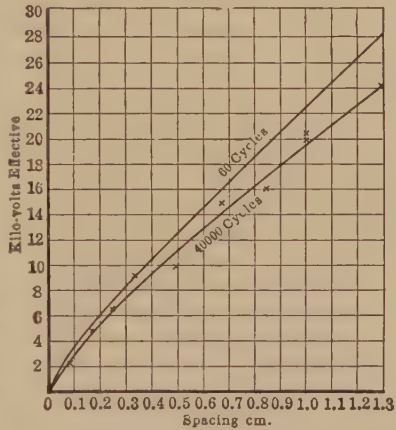


FIG. 115.—Sphere gap spark-over voltages at 60 cycles and 40,000 cycles.

This should also apply for corona on polished wires. The following limitation, however, applies to both cases. At continuous high frequency when the rate of energy or power is great, frequency may enter into the gradient equation thus

$$A\sqrt{\frac{r}{\delta}} \phi(f)$$

and spark-overs take place at lower voltages at very high frequency. This is more fully discussed in Chap. VIII.

Destruction of insulation by high frequency, when heating does not result, is due to local overvoltage. For instance, low high-frequency voltage may be applied to a piece of apparatus containing inductance and capacity, as a transformer. On account of the capacity and inductance, very high overvoltage

may be built up and breakdown result due to overvoltage. The petticoat of an insulator may be broken down by an electric needle, formed as described above, bringing the total stress on the thin petticoat. The sphere curves check very closely for oscillatory voltage of short duration and voltages of *steep wave front*, even under ordinary conditions of surface. With needle gaps the results are quite different at high and low frequency. At continuous high frequency the needle point and the surrounding space become hot, due to the loss, and spark-over takes place at low voltage. For impulses, the opposite is true. The sphere gap is, thus, the most reliable means of measuring oscillatory voltages and voltages of steep wave front. When used for continuous high frequency, the surfaces must be kept highly polished.

*Dielectric Spark Lag with Steep Wave Front.*—A fixed minimum voltage is required to spark over a given gap when the time of application is not limited. Energy is necessary to rupture gaseous, liquid, and solid insulation; this introduces a time element.

This effect may be shown roughly by Fig. 116. The spark-over voltage of a given needle gap is  $e_1$ , and always practically constant, if the time of application is not limited. Spark-over may take place after the continuously applied voltage  $e_1$  has been on for some time  $t_1$ . If a voltage increasing at a rapid rate, as represented by *A* in Fig. 116, is applied, spark-over will not take place when the continuously applied spark-over voltage  $e_1$  is reached, because the time  $t_1$  is required to produce the spark-over at this voltage. The spark will probably begin to form when the voltage reaches the value  $e_1$ , however. The voltage will, therefore, rise above  $e_1$ , and spark-over will take place after the time  $t_2$  has elapsed and the voltage has risen to  $e_2$ . When the voltage is applied at a more rapid rate along wave *B*, the spark, as before, will begin to form approximately when voltage  $e_1$  is reached. The voltage will continue to rise and reach the value  $e_3$  during the time  $t_3$ , before the spark-over occurs. Thus, on account of the time lag, when voltage is applied at a very rapid rate, as by an impulse, spark-over does not occur when the continuously applied breakdown voltage is reached. The voltage "overshoots" this value during the time that rupture is taking place. The excess in voltage is greater, the greater the rate of application. The time lag for any given gap or insulation has,

thus, not a fixed value but depends on the wave shape of the impulse or rate of application of the voltage. In making a study of such phenomena, it is necessary to use certain definite wave shapes. The continuously applied (60-cycle or direct-current) spark-over voltage is the lowest voltage at which spark-over can take place.

The time required to spark over a gap varies with the spacing and shape of the electrodes. For a given 60-cycle voltage setting, the time required to form a spark is greatest for gaps between points and least for gaps between well-rounded surfaces. For spheres, the time lag is so small that discharge usually takes

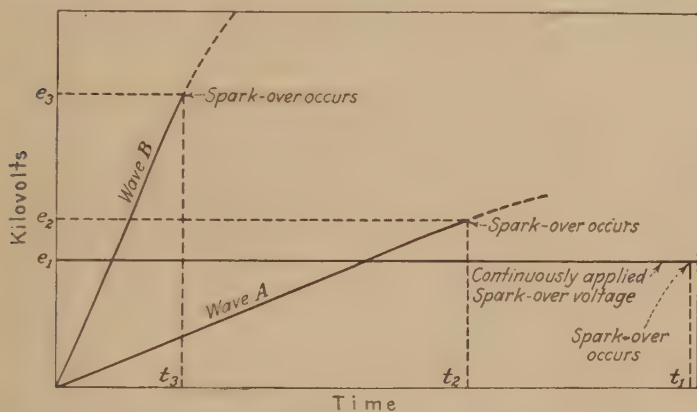


FIG. 116.—Diagrammatic illustration of why the lightning or impulse spark over voltage is higher than the continuously applied.

place before the impulse voltage can rise appreciably above the continuously applied or 60-cycle spark-over voltage.

The needle gap requires the maximum time of any gap, as considerable air must be ionized before spark-over can result. Another way of considering it is that the corona increases the capacity and places resistance in series with it as it forms. It requires time to charge a condenser through resistance. With a sphere gap the field is practically uniform throughout, so that the gradients reach breakdown proportions everywhere along the path between electrodes at approximately the same instant. Consequently, the time lag of the sphere gap is very small.

*Impulse Ratio.*—The term "impulse ratio" was first used<sup>1</sup> to express roughly the overvoltage characteristic of a given wave

<sup>1</sup> PEEK, F. W., JR., *Trans. A.I.E.E.*, Vol. XXXIV, p. 1857, 1915.



with respect to a given gap. It is equal to the ratio of the spark-over voltage of the applied wave to the 60-cycle crest spark-over voltage, for the same gap.

Sphere gaps, if used at spacings less than one diameter, will breakdown at values practically equal to the continuously applied or 60-cycle crest spark-over voltage, even for steep impulse waves which reach this value in time intervals as short as  $\frac{1}{10}$  microsecond. Due to this negligible time lag, as previously discussed, sphere gaps usually have an impulse ratio of approximately unity. Table XXXVI gives test results secured from early work with the original laboratory lightning generator (see Fig. 117) which show the spheres to have impulse ratios close to unity even at abnormally long spacings.

TABLE XXXV.—IMPULSE RATIO OF NEEDLE GAP

Spacing of needles (cm.)	Voltage required to cause needle gap to spark over		Ratio impulse to 60 cycles, voltage
	60 cycles (max.)	Impulse measured by 25-cm. spheres (dia.) (max.)	
4.3	43.1	62.0	1.45
8.0	64.8	96.1	1.49
12.0	85.0	140.0	1.65
25.0	134.0	260.0	1.94

NOTE: Above impulse wave has 5 microsecond effective duration.

TABLE XXXVI.—IMPULSE RATIO OF 6.25-CM. SPHERE  
(Compared to 25-cm. Sphere)

6.25-cm. diameter sphere gap, cm.	Voltage required to cause 6.25-cm. sphere to spark over at gaps greater than the diameter		Ratio impulse to 60 cycles, voltage
	60 cycles (max.)	Impulse measured by 25-cm. sphere (dia.) (max.)	
6	127	134	1.05
8	144	152	1.05
9	154	160	1.04
10	156	168	1.06
12	168	180	1.08
15	180	198	1.10

NOTE: Above impulse wave has 5 microsecond effective duration.



Table XXXV gives the impulse ratios for needle gaps taken at the same time. The analysis of this high overvoltage characteristic of needle gaps was given in the previous section. In this it was apparent that the steeper the wave front the greater the impulse ratio. From the results of Table XXXV it can be seen that with the same wave shape the impulse ratio also increases with increased spacing and, therefore, increased breakdown voltage. Recent impulse spark-over tests, which will be described later, have indicated impulse ratios as high as 3.5.

*Impulse or Lightning Generator.*—A lightning generator giving single impulses of known wave shape and voltage was devised by the author in 1913 to study the effects of impulse voltages on air, oil, and solid insulation as well as to make a study of lightning protection.<sup>1</sup>

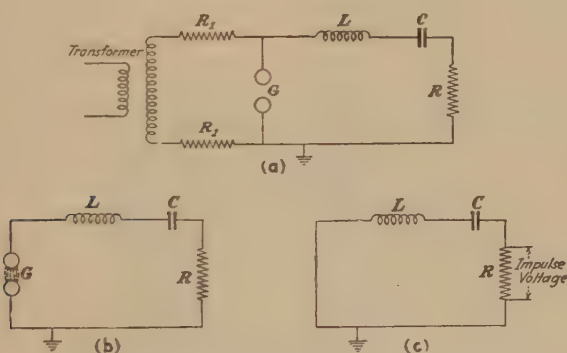


FIG. 117.—Original laboratory lightning generator circuit.

The circuit is shown in Fig. 117(a). The gap is set at some desired voltage. The transformer voltage is increased until discharge occurs. At that instant, the condenser  $C$  is charged up to a voltage corresponding to the gap setting. There is very little drop in the resistance  $R$ , since the 60-cycle charging current is relatively small. A dynamic arc forms at  $G$  and holds. This acts as a switch and the condenser discharges through the known inductance and resistance  $R$  and the arc.  $R$  is a very small fraction of  $R_1$ . For the large impulse current  $R_1$  is practically equivalent to infinity. The circuit producing the impulse is shown in Fig. 117(b) or is, in effect, that shown in 117(c). The

<sup>1</sup> PEEK, "The Effect of Lightning Voltages on Dielectrics," *Trans. A.I.E.E.*, p. 1857, 1915.

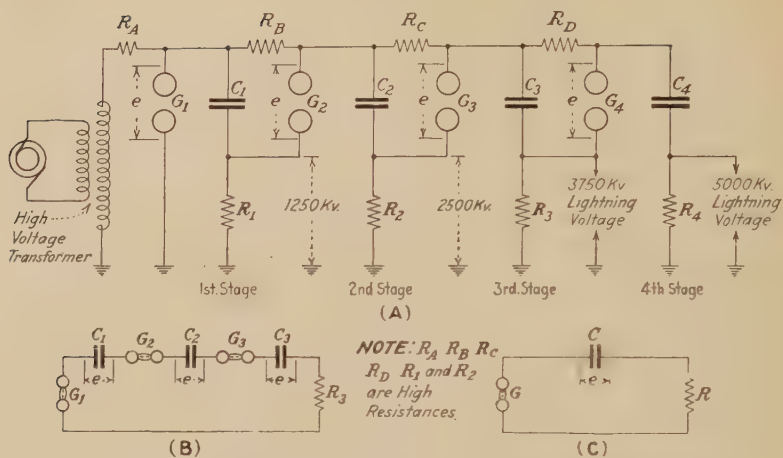


FIG. 118.—Circuit diagram of 5,000,000 laboratory lightning generator.



FIG. 119A.—5,000,000 volt laboratory lightning stroke.

condenser discharging through the known resistance and inductance causes a transient current that can be calculated readily. The current produces an impulse voltage drop across  $R$ . This is the impulse voltage used in testing.

The original generator which gave 200,000 volts was added to from time to time by the author and in 1923 was increased up to 2,000,000 volts to ground.<sup>1</sup>

Up to the early part of 1927, the laboratory lightning work had progressed so far that it seemed important to double the 2,000,000 volts available at that time. This high voltage was desirable so that full size apparatus could be tested and results obtained without extrapolation. Accordingly, a 3,600,000-volt generator was built and placed in operation. At the beginning of 1928, the generator was extended to give 5,000,000 volts and laboratory lightning studies were begun at this voltage. Double the directly generated voltages due to reflection have been measured at the ends of transmission lines.

A radically new method was developed to obtain these last very high voltages.<sup>2</sup> The effect is of adding two, three, four, or more of the original



FIG. 119B.—Lightning sparkover of suspension insulator string of 27 standard cap and pin units by 5,000,000 volt generator.

<sup>1</sup> PEEK, "Electrical World," p. 1135, 1923.

<sup>2</sup> PEEK, "Lightning—Progress in Lightning Research in the Field and in the Laboratory," *Trans. A.I.E.E.*, p. 436, 1929.

generators in series at the proper instant so that all of the respective impulse voltages add together. No rectifiers are used. The alternating-current voltage is applied directly to each unit generator. At that instant on the crest of the wave, that each unit is fully charged, gap spark-overs take place that connect the generators in series and the impulse occurs. The connections are shown in Fig. 118A. The condensers of the four generators  $C_1$ ,  $C_2$ ,  $C_3$  and  $C_4$  are charged from the trans-

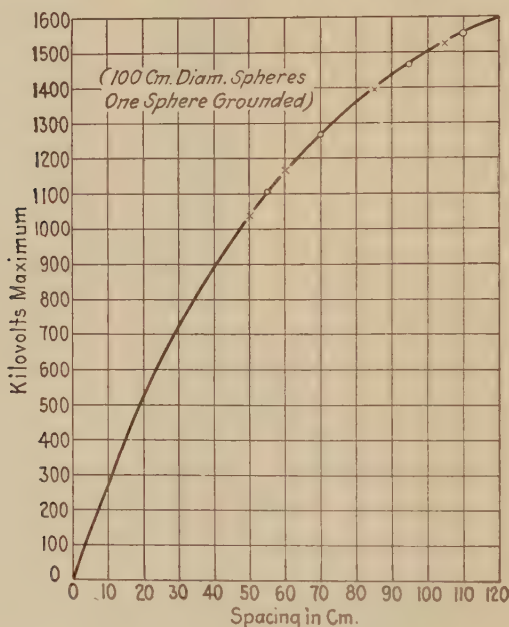


FIG. 120.—Impulse sparkover curve of 100 cm. sphere gap.

former to a crest voltage corresponding, approximately, to the  $G_1$  gap setting. Sparkover occurs on  $G_1$  followed immediately by sparks on  $G_2$ ,  $G_3$  and  $G_4$ . Resistance  $R_A$ ,  $R_B$ ,  $R_C$ ,  $R_D$ ,  $R_1$ ,  $R_2$ , and  $R_3$  permit the small 60-cycle charging current to flow but are, in effect, infinite to the very high impulse current. The result is as shown in Fig. 118B. Three gaps are in series on 3,600,000 kv. and four on 5,000,000 kv. One, two, three, four, or more steps can be used. The wave shape is determined by  $R$ ,  $L$ , and  $C$ . Waves varying in duration from a few microseconds to 1000 microseconds have been experimented with. A capacity of at least 0.0034 microfarad is usually used per unit. The maximum energy is about 14,000 watt-seconds.

Figure 119A and B show 5,000,000 volt spark-overs of a needle gap and insulator string by the lightning generator. The maximum sparking distance possible with such a voltage depends upon what wave shape of surge the lightning generator is adjusted to give. With a surge of a very short duration, a spark-over of



FIG. 121.—Impulse sparkover between 100 cm. spheres.

only 13 ft. can be secured at 5,000,000-volts crest. Longer distances can be broken down with long waves, as will be explained later, as much as 28 ft. being possible with 1000-microsecond front.

The appearance of the discharge and the destructive effects of the laboratory lightning generator are similar to those of natural lightning; wood may be blown apart, fires may be set, metal conductors can be vaporized and made to disappear,



discharges in water and oil produce explosive results, etc. (see Appendix, Table X, page 319).

*Impulse Spark-over of Gaps and Insulators.*—Extensive spark-over tests have been made under the author's direction with both the old and the new laboratory lightning generators. Figure 120 shows an impulse spark-over curve of a 100-cm. sphere gap.

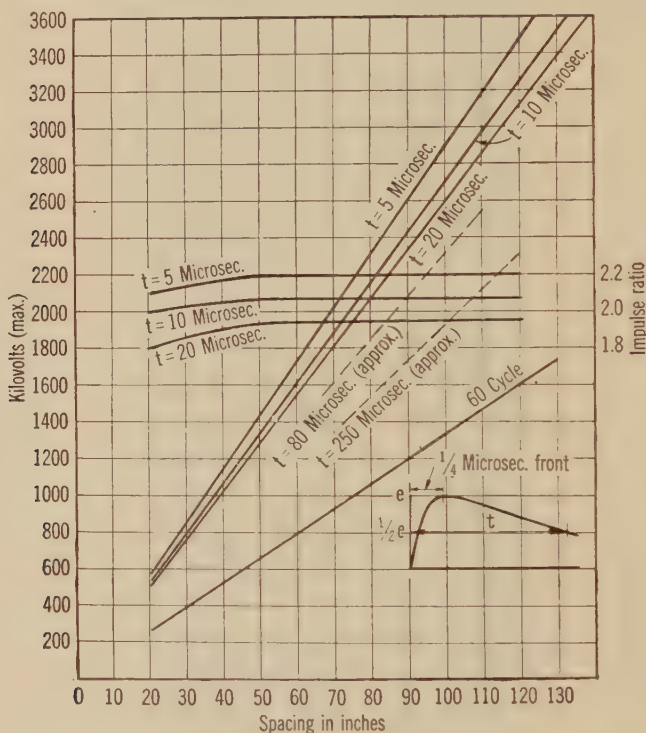


FIG. 122.—Impulse sparkover voltages of point gap for different wave shapes. Above voltages are crest values of waves sparking over 50 per cent. of time, breakdowns occurring along tails.

Due to the negligible time lag of spheres and, consequently, their unity impulse ratio characteristic, the above curve is practically identical with the 60-cycle calibration curve when the latter is plotted in crest values of voltage.

As was discussed previously (see Electron Theory, Chap. III, page 43), theoretical analysis indicates that there is probably some local breakdown at the sphere surfaces just prior to complete flashover even with the spheres perfectly smooth. Figure 121 shows a 1500-kv. impulse flashover of a meter sphere gap in

which the brief surface brushes are seen extending out along the lines of flux, particularly from the upper ungrounded sphere where the field intensities are greatest. It is only possible to observe this effect when steep impulse waves are applied to the spheres. It is not visible with more slowly applied voltages, such as 60-cycles. The probable reason for this is that breakdown has a tendency to start simultaneously along many electrostatic flux paths, but one of them eventually attains a greater conductivity than the others, so that the voltage gradient along

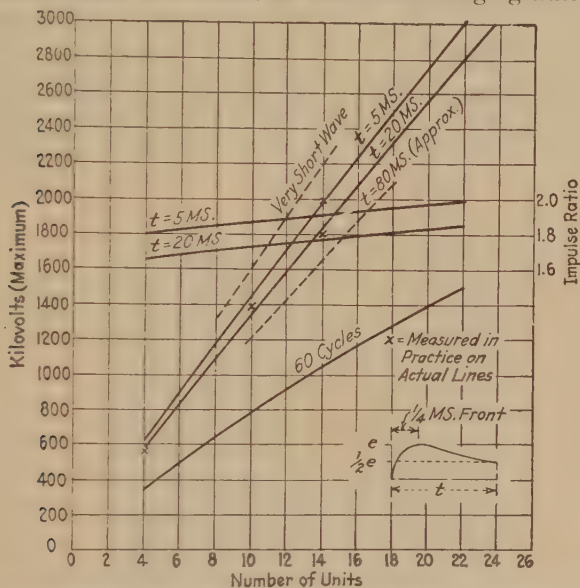


FIG. 123.—Impulse sparkover voltages of suspension insulator strings for different wave shapes. Above voltages are crest values of waves sparking over 50 per cent. of time, breakdowns occurring along tails.

it drops to a lower value than is necessary to sustain the remaining breakdown paths. The latter then disappear and the one favored path proceeds across the gap as long as the field terminating at its outer end is above the breakdown gradient of the air. With a rapidly applied impulse wave, the time involved is so short that many breakdown paths have a chance to extend out appreciably from the sphere surface before one of their number has a chance to assume low voltage characteristics. With a slowly applied voltage, however, such as 60-cycles, the favored breakdown path develops from the start, and “short-circuits” the field about it so that no other streamers have a chance to appear.

Figure 116 shows a curve indicating the overvoltage characteristics of a needle gap. It is seen that the shorter the time for spark-over, the higher the impulse ratio, or the steeper the wave front, the greater must be the voltage, providing breakdown occurs on the front of the wave. As will be indicated later (see page 155), whether the point of breakdown occurs on the front or tail of the wave depends upon the wave shape and the crest voltage. Figure 122 gives impulse flashover curves of a needle gap at various spacings and with different shapes of applied waves. The time factor  $t$ , indicated on the curves, characterizes the waves by the time intervals that they persist above the half-voltage values.

Figure 123 gives curves of impulse flashover voltages on standard 10-in. diameter,  $5\frac{3}{4}$ -in. spacing, suspension insulator units. This spark-over voltage is proportional to the overall distance from line to ground so that for use with other insulator spacings the curve voltages should be varied proportionally. While the operating frequency spark-over voltage of an insulator is reduced when the surfaces become wet or during rain, tests have shown that the lightning spark-over voltage is unchanged when the duration of the lightning impulse is short.

The impulse ratio of a sphere gap is practically unity and it will indicate the voltage at the crest of the wave. It is generally desirable to know the effective duration of the wave, however, as well as its crest, so that a "time gap" is necessary. The suspension insulator is a very good gap for this purpose. An example will best illustrate the use of such a gap. Assume that it is desired to compare the lightning spark-over voltage of two entirely different types of bushings, but that it is not possible to do this in the same laboratory with exactly the same waves. A sphere-gap measurement would give the crest of the wave, but equal spark-over voltages would not indicate equivalent bushings unless the shapes of the waves were known. A very good comparison can be obtained, however, by the insulator time gap even if the waves differ considerably. This can be done by placing an insulator string in parallel with the bushing and applying impulses and adding or removing units from the string until 50 per cent. of the sparks occur on each. The equivalent breakdown strength of the bushing is thus obtained in terms of line insulators. Since the impulse ratio of bushings and insulators varies up and down together over a wide range with varying

wave shape, the effect of variations due to such differences is eliminated, and a good comparison is obtained. The lightning spark-over voltage of the bushing for any particular wave can

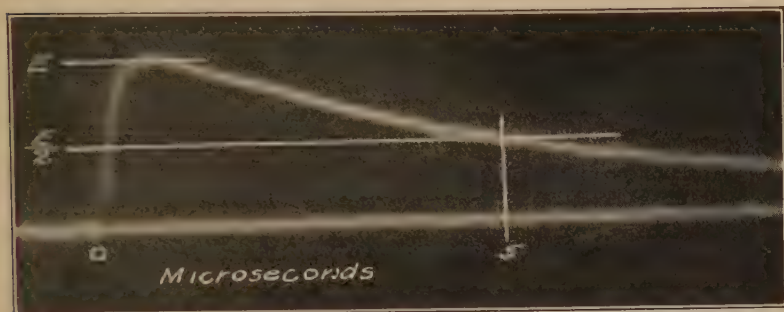


FIG. 124.—Cathode-ray oscillogram of typical impulse wave of lightning generator.

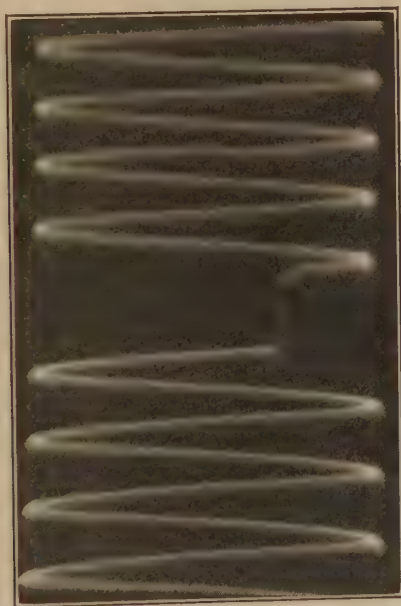


FIG. 125.—Impulse wave recorded on cathode-ray oscillograph using oscillatory sweep for timing axis.

then be determined from the lightning spark-over curve of the insulator string. The insulator time gap also offers a convenient method for comparing the lightning strength of solid insulation.



The impulse ratios of actual surges imposed on lines by lightning have been determined in the field. This has been done by measuring the crest voltage of a surge, actually causing a flash-over, by means of a surge voltage recorder or klydonograph and comparing it with the normal 60-cycle flashover voltage of the insulator. Such voltage values measured on transmission lines are indicated by crosses on Fig. 123. Impulse ratios of natural lightning obtained in this way vary from 1.8 to 2.0. In a few cases, values as high as 2.7 were obtained, indicating either very steep wave fronts, or high-voltage waves of extremely brief

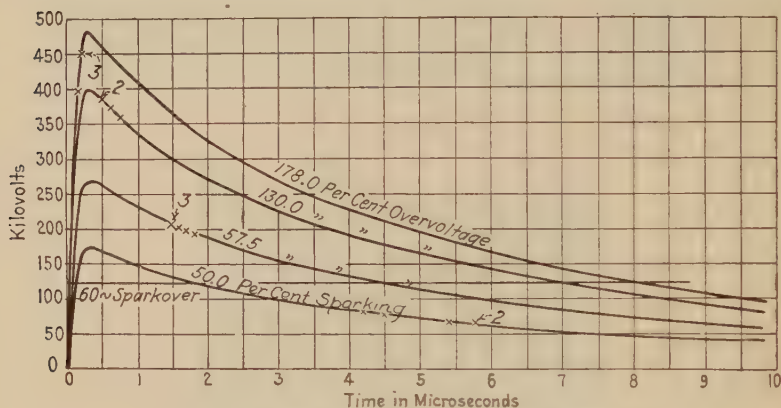


Fig. 126.—Impulse sparkover of 19.9 cm. needle gap.

duration, probably the former. The impulse ratios obtained as a whole seem to indicate an effective duration from 1 to 20 microseconds, this effective duration being the time that the wave is above the 60-cycle spark-over voltage of the insulators. Laboratory impulse work on insulation has been carried out with applied waves having the above characteristics, so as to simulate field conditions as closely as possible. The nature of lightning surges themselves is discussed further in a later chapter (see Chap. IX, page 258). (See Fig. 205, and pages 281–282.)

The use of shields and arcing devices on insulator strings, particularly for protection from flashovers under lightning impulses is described in detail in Chap. XI, page 324.

*Oscillographic Study of Impulse Flashovers.*—In the first studies of transients, wave shapes could not be pictured directly; it was necessary to calculate them. The cathode-ray oscillograph (see Chap. III, page 39) now affords a means by which oscillo-



grams can be taken readily. It is interesting that these oscillograms, measuring time in microseconds (millionths of a second), check the early work.<sup>1</sup> Figure 124 shows a typical oscillogram of an impulse wave of the new laboratory lightning generator. This particular wave reaches its crest in a fraction of a microsecond and then decays to half value in 5 microseconds. Surges

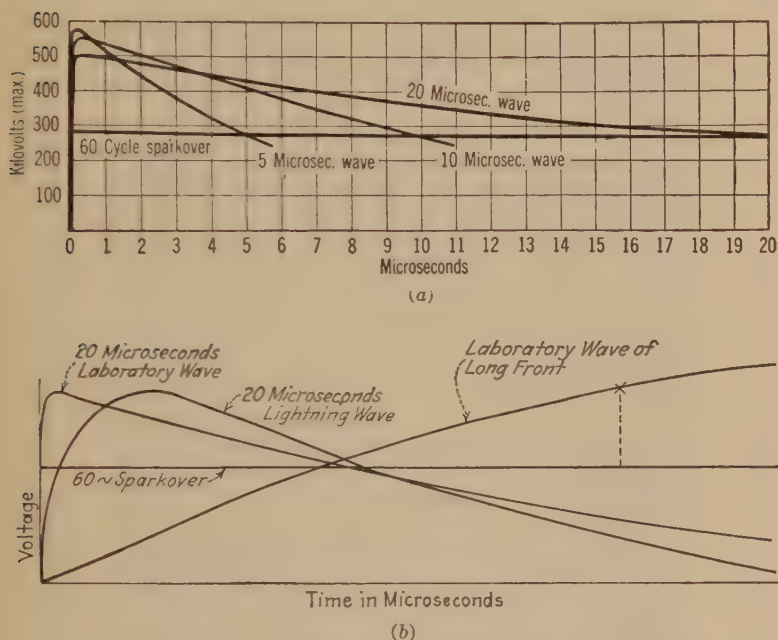


FIG. 127.—Effect of wave shape on impulse sparkover.

(a)—Impulse waves with same front showing change of sparkover voltage with wave length (sparking on 50 per cent of applied impulses)—50 cm. needle gap.

(b)—Impulse waves of same impulse ratio and approximately same effective duration.

are frequently measured along a high-frequency timing wave, as in Fig. 125.

This oscillographic method has afforded a definite means of analyzing the breakdown characteristics of a given wave on a given gap. Whether the front or the tail of the wave is the controlling factor in determining the lightning spark-over depends upon the voltage. This is well illustrated in the oscillo-

<sup>1</sup> PEEK, F. W., JR., *Trans. A.I.E.E.*, Vol. XXXIV, p. 1857, 1915.

grams of Fig. 126, representing actual test records on a 19.9-cm. point gap. The same wave shape was used throughout these tests. In the first tests, the voltage was increased until

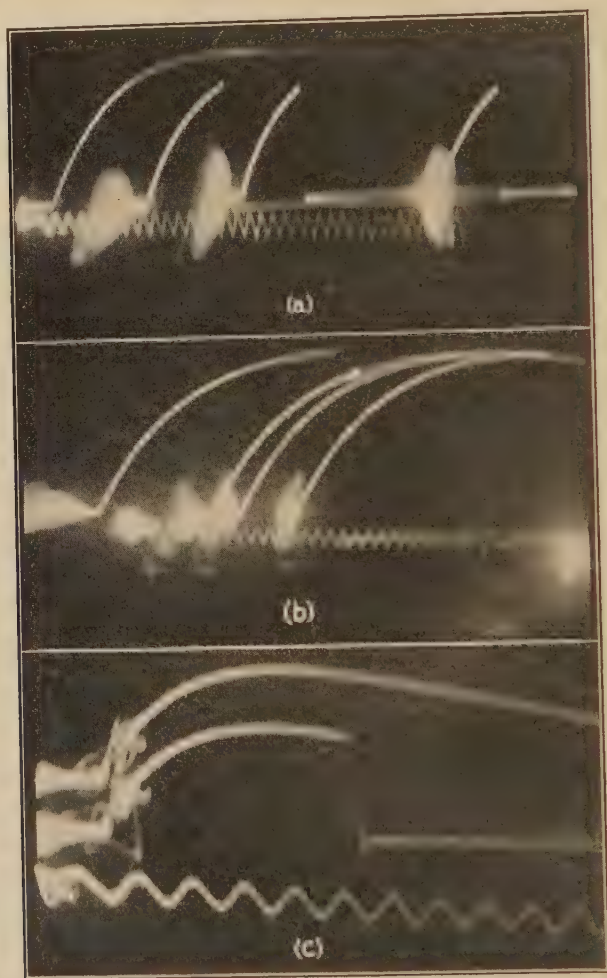


FIG. 128.—Typical cathode ray oscillograms of impulse breakdowns of air gaps.

- a*—Impulse breakdown of 13 cm. needle gap on front of wave.
- b*—Impulse breakdown of 12.5 cm. spheres, spaced 9.5 cm. on crest of wave.
- c*—Impulse breakdown of 13 cm. needle gap on tail of wave.

spark-over occurred at 50 per cent. of the applied impulses. An impulse wave with a crest voltage of 175 kv. was required for breakdown while the 60-cycle crest spark-over value for the same

distance was 125 kv. The impulse ratio was accordingly 1.40. The actual sparking points on the wave are indicated by the crosses. An interesting fact was found here—probably for the first time—namely, that spark-over actually took place after the tail of the wave had decreased below the 60-cycle value. Apparently the breakdown effect, once started by the over-voltage, continues, so that the spark actually forms after the wave has fallen below the minimum 60-cycle crest spark-over voltage. This is of great theoretical interest. A wave 57.5 per cent. in excess of the minimum impulse spark-over voltage was next applied to the gap. As can be seen from Fig. 126, spark-over still took place on the tail but at a higher value. Breakdown of the gap occurred on every applied impulse. With 130 per cent. excess voltage, spark-over took place practically on the crest of the wave, while at 178 per cent. overvoltage, it occurred on the front of the wave. The corresponding impulse ratios for this short gap cover a range from 1.4 to 3.50. Figure 127(a) shows the variation in spark-over voltage with waves of the same front but with 5, 10, and 20 microseconds duration above the 60-cycle spark-over voltage. In Fig. 127(b) are shown waves of various fronts but of the same impulse ratio, so that the effective durations or time intervals prior to spark-over above the 60-cycle value are the same. In general, such waves manifest the same breakdown properties. In Fig. 128 are given actual oscillograms of impulse spark-overs of gaps in air. These oscillograms show cases of breakdowns occurring on the front, crest, and tail of typical waves.

**Precautions in Testing and Design Work.**—The line insulator is generally designed so that at commercial frequencies the spark-over voltage is lower than the puncture voltage. For lightning or impulse, both the spark-over voltage and the puncture voltage should be much higher. By applying a sufficient number of impulses at voltages higher than the 60-cycle puncture voltage, an improperly designed insulator may be punctured. During the time that the air is breaking down, this overstress produces small cracks in the porcelain. The effect is cumulative. The cracks gradually extend and puncture results. This subject is, hence, of great importance.

It is necessary in making operating frequency spark-over measurements on certain apparatus to guard against superposed oscillations. For instance, on line insulators at operating fre-

quency there is generally considerable corona discharge long before spark-over. This discharge may cause oscillations which will affect the measuring gap and cause it to indicate higher normal frequency voltages than really exist. This is largely eliminated in practice by the use of high resistance in the measuring gap.

Resistance should not be used in series with a gap for measuring transient impulse voltages, however, since the extremely high-transient current will cause most of the voltages to appear across the resistance (see Appendix page 390).

The author has used the impulse ratio to study the change in the voltage and wave front of a wave as it travels on a transmission line.<sup>1</sup> The impulse ratio decreases as the wave front.

The lightning spark-over voltage of line insulators may be several times the operating frequency spark-over voltage. While the normal frequency spark-over voltage of an insulator is reduced when the surfaces become wet or during rain, the lightning spark-over voltage is unchanged.

Some of the peculiar effects observed in researches with impulse voltages are as follows:

Much higher impulse voltages are usually required to spark-over a given distance than voltages at operating frequencies; conductors at normal frequency voltages are often good insulators for lightning voltages, *i.e.*, water may be punctured like oil (see Table X, Appendix, page 391); the wet and dry spark-over voltages of insulators are equal; etc.

**Effect of Altitude on the Spark-over Voltages of Bushings and Insulators.**—For non-uniform fields, as those around wires, spheres, insulators, etc., the spark-over voltage decreases at a lesser rate than the air density. The theoretical reasons for this have been given, as well as the laws for regular symmetrical electrodes for cylinders and spheres. (See pages 62 and 125.)

It is, however, not possible to give an exact law covering all types of leads, insulators, etc., as every part of the surface has its effect. The following curves and tables give the actual test results on insulators and bushings of the standard types. The correction factor for any other bushings or insulator of the same type may be estimated with sufficient accuracy. When there is

<sup>1</sup> PEEK, "High Voltage Phenomena," *Jour. Frank. Inst.*, January, 1924.



doubt  $\delta$  may be taken as the maximum correction. It will generally be advisable to take  $\delta$  because the local corona point on leads and insulators will vary directly with  $\delta$ . This is so because the corona must always start on an insulator in a field which is locally more or less uniform.

The tests were made by placing the leads or insulators in the large wooden cask, already referred to, exhausting the air to approximately  $\delta = 0.5$ , gradually admitting air and taking the 60 cycle spark-over voltage at various densities as the air pressure increased. The temperature was always read and varied between 16 and 25°C.

At the start a number of tests were made to see if a spark-over in the cask had any effect upon the following spark-overs by ionization or otherwise. It was found that a number of spark-overs could be made in the cask with no appreciable effect. During the test, the air was always dry and the surfaces of the insulators were kept clean.

TABLE XXXVII.—SUSPENSION INSULATORS—FOUR UNITS

Bar. cm.	Vac. cm.	Pressure	Temp. cent.	$\delta$	Kilovolts arc-over 60 cycles (eff.)
75.4	37.4	38.0	22.0	0.50	121.0
75.4	34.3	41.1	22.0	0.54	131.0
75.4	30.0	45.4	22.0	0.60	144.0
75.4	26.4	49.0	22.0	0.65	158.5
75.4	23.0	52.4	22.0	0.70	165.0
75.4	19.3	56.0	22.0	0.74	177.5
75.4	17.5	57.9	22.0	0.87	183.2
75.4	15.0	60.4	22.0	0.80	195.0

TABLE XXXVIII.—TERMINALS  
Correction Factor for Leads Shown in Fig. 129

$\delta$	(a)	(b)	(c)	(d)
1.00	1.00	1.00	1.00	1.00
0.90	0.92	0.91	0.92	0.92
0.80	0.83	0.82	0.83	0.85
0.70	0.74	0.72	0.75	0.77
0.60	0.70	0.65	0.64	0.66
0.50	0.61	0.56	0.54	0.57



TABLE XXXIX.—POST AND PIN INSULATORS  
Correction Factor for Insulators Shown in Fig. 130

$\delta$	(a)	(b)	(c)
	Post	Pin	
1.00	1.00	1.00	1.00
0.90	0.93	0.91	0.94
0.80	0.84	0.81	0.86
0.70	0.76	0.72	0.75
0.60	0.68	0.62	0.65
0.50	0.60	0.52	0.53

TABLE XL.—SUSPENSION INSULATOR  
Fig. 131  
Correction Factor for Units in String as Follows

$\delta$	Number of units				
	1	2	3	4	5
1.00	1.00	1.00	1.00	1.00	1.00
0.90	0.96	0.93	0.90	.....	.....
0.80	0.91	0.84	0.80	.....	.....
0.70	0.86	0.76	0.70	.....	.....
0.60	0.80	0.66	0.60	.....	.....
0.50	0.72	0.55	0.50	.....	.....

TABLE XLI.—SUSPENSION INSULATOR  
Fig. 132  
Correction Factor for Units in String as Follows

$\delta$	Number of units				
	1	2	3	4	5
1.00	1.00	1.00	1.00	1.00	1.00
0.90	0.94	0.92	0.90	0.90	.....
0.80	0.87	0.84	0.80	0.80	.....
0.70	0.81	0.73	0.70	0.70	.....
0.60	0.72	0.63	0.60	0.60	.....
0.50	0.62	0.52	0.50	0.50	.....

Table XXXVII is a typical data sheet. Tables XXXVIII–XLI give even values of  $\delta$  and the corresponding measured cor-

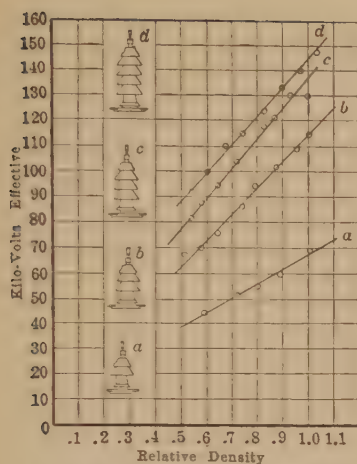


FIG. 129.—Variation of spark-over voltage of transformer leads with air density.

- (a) 15.2 cm. high by 17.8 cm. dia.  
 (b) 21.6 cm. high by 17.8 cm. dia.  
 (c) 28 cm. high by 17.8 cm. dia.  
 (d) 38.1 cm. high by 17.8 cm. dia.

Height measured from case to metal cap on top.

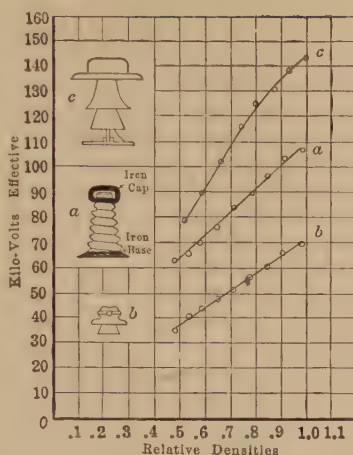


FIG. 130.—Variation of spark-over voltage insulators with air density.

- (a) 30.2 cm. high.  
 (b) 13.5 cm. high by 16.8 cm. dia.  
 (c) 28.6 cm. high by 36 cm. dia.

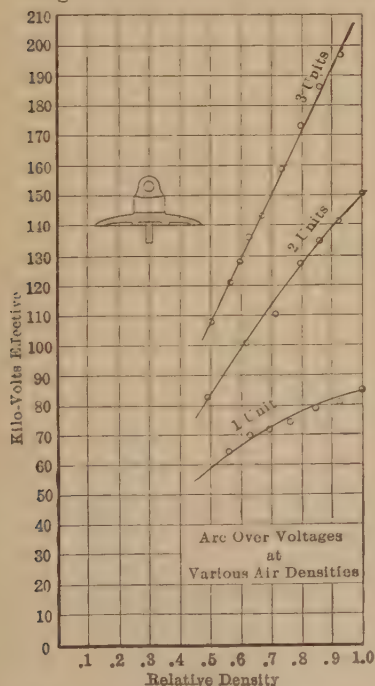


FIG. 131.—Suspension insulator. (Dia., 30 cm. Spacing 16.5 cm.)

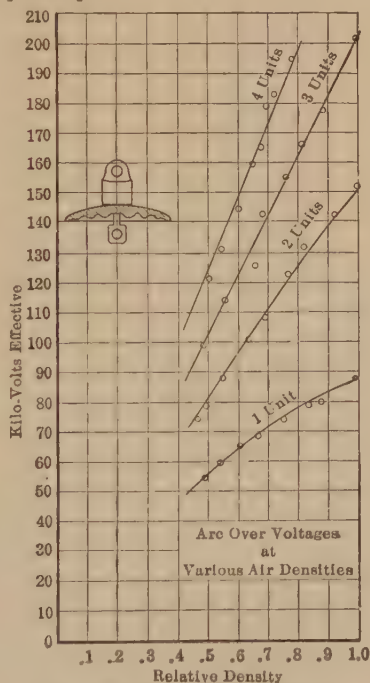


FIG. 132.—Suspension insulator. (Dia., 27 cm. Spacing 17 cm.)

rection factors. If the spark-over voltage is known at sea level or  $\delta = 1$  (76 cm. barometer, temperature  $25^{\circ}\text{C}.$ ), the spark-over at any other value of  $\delta$  may be found by multiplying by the corresponding correction factor. It will be noted that in most cases the correction factors are very nearly equal to  $\delta$ .  $\delta$  would be the correction factor in a uniform field and should be, as already stated, taken as such in most cases, especially where dirt and

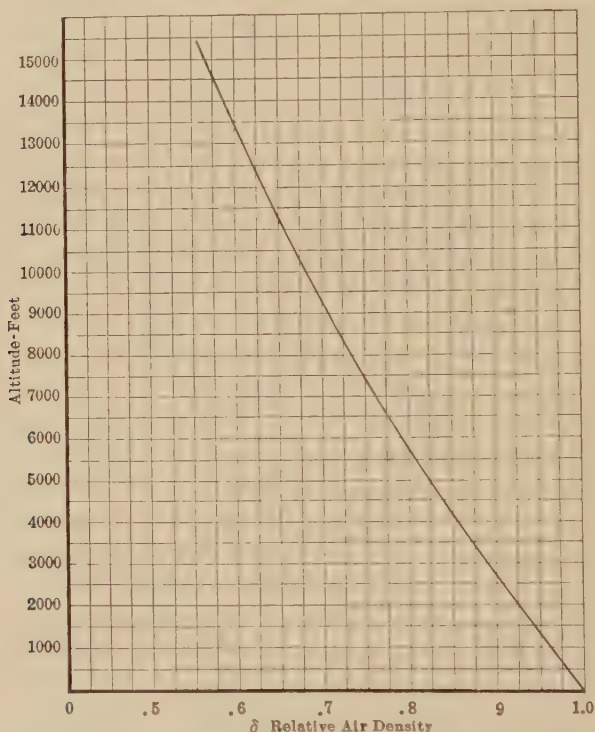


FIG. 133.—Approximate variation of air density with altitude.

moisture enter, as in practice. Furthermore, it should be taken as it is the actual correction factor for the starting point of local corona on insulators.

Figure 133 is a curve giving different altitudes and corresponding  $\delta$  at  $25^{\circ}\text{C}.$  If the spark-over voltage is known at sea level at  $25^{\circ}\text{C}.$ , the spark-over voltage at any other altitude may be estimated by multiplying by the corresponding  $\delta$ , or more closely if the design is the same as any in the tables, by the correction factor corresponding to  $\delta$ . If the local corona starting point is

known at sea level, it may be found for any altitude by multiplying the corresponding  $\delta$ . If the barometric pressure and temperature are known,  $\delta$  may be calculated.

As an example of the method of making corrections: Assume a suspension insulator string of three units with a spark-over voltage of 205 kv. (at sea level 25°C. temperature).  $\delta = 1$ . What is the spark-over voltage at 9000 ft. elevation and 25°C.?

From Fig. 133, the  $\delta$  corresponding to 9000 ft.

$$\delta = 0.71$$

Then the approximate spark-over voltage at 9000 ft., 25°C. is

$$e_1 = 0.71 \times 205 = 145 \text{ kv.}$$

If this happens to be the insulator of Fig. 132, the correction factor corresponding to  $\delta = 0.71$  is found in Table XLI, by interpolation, to be 0.71. The actual spark-over voltage for the special case happens to check exactly with that given by  $\delta$ . For practical work, a correction may generally be made directly by use of Fig. 133.

The spark-over voltage of an insulator is 100 kv. at 70 cm. barometer and 20°C. What is the approximate spark-over voltage at 50 cm. barometer and 10°C.?

$$\delta_1 = \frac{3.92 \times 70}{273 + 30} = 0.94$$

$$\delta_2 = \frac{3.92 \times 50}{273 + 10} = 0.61$$

$$e_1 = 100 \times \frac{0.61}{0.94} = 65 \text{ kv.}$$

If the local corona starting point is known at sea level, it may be found very closely for any other altitude by multiplying by the correction  $\delta$ . Figure 231, p. 310 gives an alignment chart from which any value of  $\delta$  may be obtained readily for given values of temperature and pressure.

**Effect of Rain and Humidity on the Spark-over of Insulators and Bushings.**—The wet or rain spark-over voltage is generally lowered from 30 to 90 per cent. of the dry spark-over voltage dependent upon the type of insulator and the rainfall. The reduction is much less for heavily corrugated and skirted insulators and bushings than for those with smoother surfaces. It also depends upon the rate of rainfall and the resistance of the water. Figure 134 shows curves of the flashover voltages of suspension string of 3, 5, and 8 units with different resistances of rain water

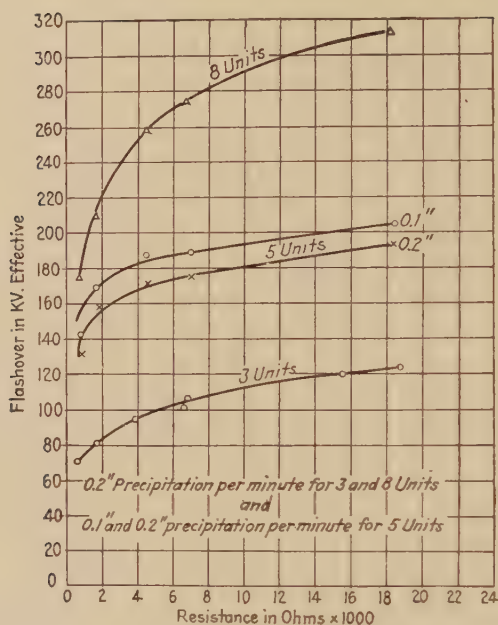


Fig. 134.—Curves showing effect of water resistance on wet 60-cycle sparkover voltages of suspension insulator strings.

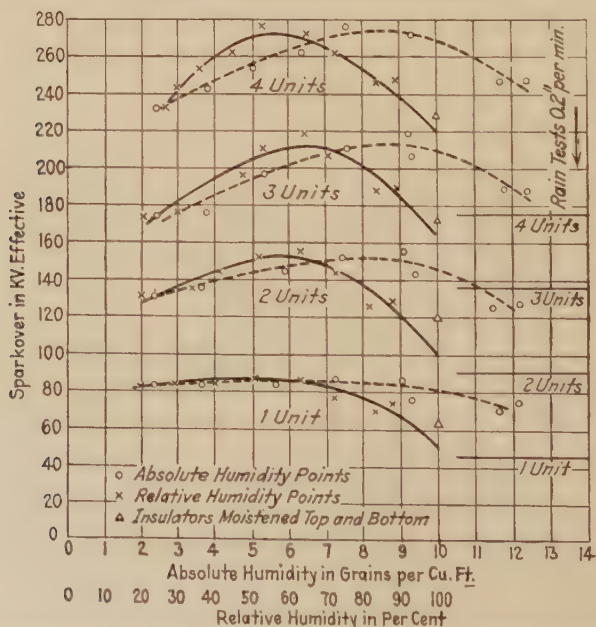


Fig. 135.—Curves showing effect of humidity on sparkover voltages of suspension insulator strings. (Relative Humid. at 25° Cent.)



and rates of rainfall. The insulators are the same as those used in the dry spark-over curve of Fig. 110, page 138, so that a direct comparison of typical wet and dry spark-over values may be made.

The lightning or impulse spark-over voltage is generally not lowered by rain<sup>1</sup> (see Appendix, Table XI, page 392).

Figure 135 shows the effect of humidity on the spark-over voltage of various strings of suspension insulators, the particular type of unit used in these curves being the same as in Figs. 110 and 134. The rise in voltage with humidity up to a certain point on each of the curves may be attributed to the same cause as that given previously in this chapter for needle gaps (see page 117).

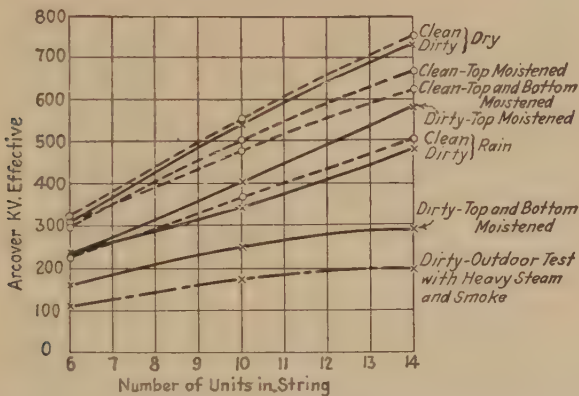


FIG. 136.—Curves showing effects of smoke, dirt, moisture, etc., on 60-cycle sparkover voltages of suspension insulator strings.

**The Effect of Smoke and Dirt Deposits on Insulator Flashovers.**—Dirt, soot, salt, etc., on the surface of insulators do not, as a rule, lower the flashover voltages appreciably, provided they are perfectly dry. When moist, however, the spark-over voltage may be reduced to a third of the dry sparkover value. Figure 136 shows the effect of different surface conditions on the flashover voltage values of various lengths of insulator strings. The worst condition depicted in Fig. 136, as shown by the lowest curve, is encountered with an atmosphere heavy with smoke and steam, and the insulator surfaces dirty and moist.

Many operating companies find it absolutely necessary to clean periodically all insulator surfaces in order to maintain

<sup>1</sup> PEEK, G. E. *Rev.*, Vol. XIX, p. 567, 1916.

operation in sections particularly exposed to atmospheres of dirt, smoke, salt, fogs, and the like.

**Effect of Polarity on Spark-over.**—On p. 103, Chap. IV was discussed the difference in the corona starting voltages and the intensity of corona on an unsymmetrical gap with a positive and a negative impressed unidirectional voltage. A similar difference is found in the spark-over voltages of such gaps, breakdown in air at atmospheric pressure always taking place at a lower voltage when the electrode having the more intense field is positive.<sup>1</sup> This difference is greatest in the direct-current spark-over between a point and a plane, the breakdown voltage with the point positive always being less than half of the voltage with a negative point for spacings up to several feet, at least. This polarity factor also occurs with impulse voltages, the same applied wave being capable of breaking down a longer gap when the electrode in the more intense field is positive than when it is negative. This difference in the effect of polarity is less with impulse than with a continuously applied direct-current voltage, and decreases the shorter the length of the impulse wave (see Table V, Appendix, page 388).

This same effect of electrode shape on polarity has been found in the puncture of liquid and solid insulations.<sup>2</sup> In the flashover of insulators there will be a similar difference in the positive and negative breakdown values provided there is an appreciable difference in the electrostatic fields at the opposing electrodes (see Appendix, Table V, page 388, and Table VII, page 389). With usual suspension insulator string set-ups, however, the difference in flashover voltage values is generally not very great.

**Three-phase Spark-over.**—If three wires are placed at the corners of an equilateral triangle and three-phase voltage applied, the maximum voltage gradient or stress at the conductor surface is  $\frac{2}{\sqrt{3}}$  ( $= 1.155$ ) times the stress that occurs when single-phase voltage is applied between any two of the wires. The maximum three-phase stress on any conductor thus does not occur at the instant of maximum voltage between conductors but at the instant of maximum voltage between that conductor and neutral. Corona on the various conductors thus rotates and starts at a 15.5 per cent. lower line to line voltage than at single phase.

<sup>1</sup> PEEK, *Trans. A.I.E.E.*, p. 783, 1916.

<sup>2</sup> MARX, E., *Archiv für Elektrotechnik*, Vol. XX, p. 589, 5/6, 1928.

When conductors are close together, corona and spark-over are coincident for reasons explained elsewhere. Therefore, with many conductor arrangements and three-phase voltages the spark-over occurs at a 15.5 per cent. lower voltage than single phase. This is not at the instant of maximum voltage between conductors.

Even at large spacings the three-phase spark-over occurs at a lower voltage than single phase. Three-phase spark-over between points is shown in Fig. 137. Under symmetrical conditions the sparks always form a *Y*.

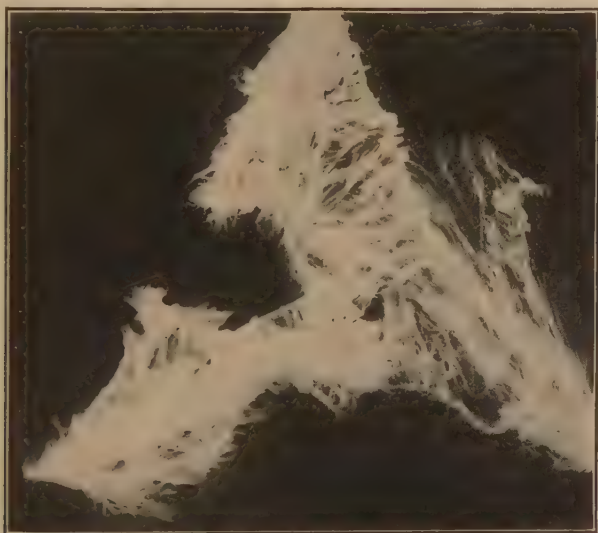


FIG. 137.—Three-phase 60-cycle flashover between three needle points (distance between points—120 in.).

**Some Peculiar Effects in the Breakdown of Gases.**—Apparent anomalies frequently occur in the behavior of gases under breakdown conditions. Examples of some of these may be found in Fig. 39, p. 67. Here it is seen that the question of whether the breakdown gradient at the surface of a wire is lower for positive or negative potentials, depends on the gas to be ruptured. It is also apparent that air has a higher corona breakdown gradient than either of its components, oxygen or nitrogen. Several investigators have found by spectral analysis that although oxygen by itself has a lower corona starting gradient than nitrogen, yet the corona spectrum of air shows no signs of

oxygen participating in the ionization process, nitrogen radiations being the only effects discernible in the spectrum. In Fig. 39 it is also evident that although helium shows the lowest corona rupture voltage, it has the highest ionizing potential (see page 44, Chap. III) of any of the other gases involved.

Such peculiar effects in the breakdown of gases have been noted and commented on in the past by various investigators. As yet no clear and tangible explanation has been given for these apparent anomalies so that they will not be discussed further here.

## CHAPTER VI

### CORONA LOSS

The starting voltage of corona and the various factors affecting it were discussed in Chap. IV. In the present chapter, the power loss resulting from corona is taken up, and the investigation, from which the laws of corona were developed is described.<sup>1</sup> The method of determining the various relations from the data for these laws is shown, and the many laboratory and field tests which have checked the laws since are included. In particular,

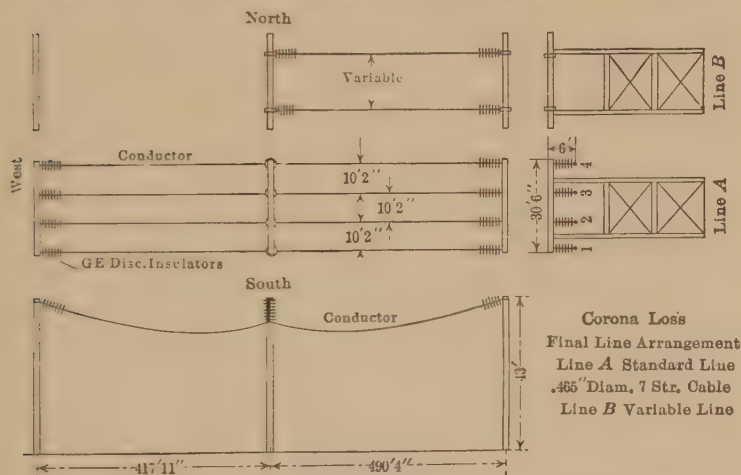


FIG. 138.—Experimental outdoor line.

there are given descriptions of more exacting laboratory measurements recently made with the cathode ray oscillograph, which also serve to substantiate the earlier work.

**Lines, Apparatus, and Method of Test.**—The Lines. The first investigation was made out of doors. The conductors used in this investigation were supported by metal towers arranged in two parallel lines of two spans each. The length of each span was approximately 0.150 km. (500 ft.). These tower lines will be

<sup>1</sup> "Law of Corona I," *Trans. A.I.E.E.*, p. 1889, 1911.



designated by *A* and *B*, respectively. The conductors were strung in a horizontal plane with seven disk suspension insulators at each point of support. For preliminary tests four No. 3.0 B. & S. (1.18 cm. diameter) seven-strand, hard-drawn copper cables were put in place on each line. A seven-strand steel ground cable was also strung. After a number of tests had been made the ground cables were removed from line *A*. The conductors on line *A*, however, were kept in place as a standard throughout all the investigations. The conductors were removed from *B*, and the first span of this line was used to support various sizes of conductors at various spaces (see Fig. 138).

These lines were erected in a large field. The prevailing winds were from the west over open country, that is, free from smoke from the city and the factory on the east.

*Test Apparatus.*—A railroad track was run directly under the line, and the testing apparatus was housed in three box cars. This proved a very convenient arrangement, as the cars could be quickly run back to the factory when changes or repairs were necessary.

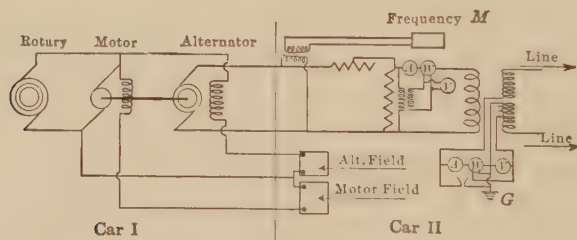


Fig. 139.—Circuit connections in corona loss measurements.

The high-voltage transformer and the testing apparatus were placed in car No. 2. The portion of the car roof over the transformer was made of heavy canvas. This could be quickly rolled back, and the leads from the line were dropped directly to the transformer terminal. By means of a framework and canvas cover, the transformer could be protected from the weather and investigations carried on during rain and snow storms. The power supply, speed, and voltage, were all controlled from car No. 2. In fact all of the adjustments could be made from this car (see Fig. 139). The transformer was rated at 100 kw., 200,000 volts, and 60 cycles. On the low side were four 500-volt coils. These coils could be connected in multiple or series for change of

ratio. The high-tension winding was opened at the neutral and taps were brought out for the ammeter and current coil of the wattmeter. Three taps were also brought out here from the main winding for voltage measurement (see Fig. 139).

Car No. 3 served as a dark room for making photographs and visual tests on short wires and cables.

*Methods of Test.*—Accurate power measurements of corona are difficult to make, because of the nature of the load, low power factor, and high voltage. It is not desirable to make the measurements on the low side because of the difficulty in separating the transformer iron and load losses, and these may be sometimes as large as the corona losses. In these tests, the current coil of the wattmeter and the ammeter were put in the high-tension winding of the transformer at the neutral point and the neutral was grounded. The voltage coil of the wattmeter was connected to a few turns of the high-tension winding at the neutral.<sup>1</sup> All of the loss measurements were also duplicated on the low side as a check. Frequency was held at the test table by means of the motor field and a vibrating reed type of frequency meter.

Voltage was controlled in two ways—by the potentiometer method and by rheostats in the alternator field. The potentiometer method operates by a resistance in series with the supply on the low side of the transformer for voltage control and a multiple resistance across the transformer, taking about three times the exciting current, to prevent wave distortion. When the leading current was very high a reactance was arranged to shunt the generator and approximately unity power factor could be held. This prevented overloading the generator and reduced wave shape distortion. For a set of tests at a given frequency the ratio of the main transformer was kept the same. Where losses at several frequencies were to be compared, the main transformer ratio also was changed to keep the flux on the generator as nearly constant as possible—for instance, at 45 cycles a ratio of 500/200,000 would be used, while at 90 cycles a ratio of 1000/200,000 would be used. Wattmeters especially adapted to the tests were constructed. These were of the dynamometer type; each was provided with a 75-volt and 150-volt tap. The voltmeter coil ratio on the transformer and the wattmeter tap were always changed to give the best reading. Four wattmeters were used

<sup>1</sup> HENDRICKS, A. B., JR., *Trans. A.I.E.E.*, p. 167, 1911.

TABLE XLII.—EXPERIMENTAL LINE—A. CORONA LOSS—10-6-10. 4 P.M.

Low side total readings			High side total readings		
Volts	Amperes	Kilowatts	Kilovolts	Amperes	Kilowatts
Line on					
395	16.5	0.40	80.5	0.077	0.10
435	17.9	0.60	90.5	0.087	0.13
490	20.5	0.70	101.6	0.101	0.17
535	22.6	0.80	111.1	0.112	0.22
590	24.7	1.00	120.4	0.119	0.28
635	27.1	1.10	130.2	0.135	0.35
680	29.2	1.40	139.2	0.145	0.45
735	31.6	1.80	150.0	0.158	0.68
780	33.4	2.40	159.0	0.169	1.10
812	35.3	3.30	165.8	0.178	1.80
830	36.3	3.60	169.0	0.181	2.40
862	37.5	5.12	176.6	0.190	3.60
893	39.2	6.35	183.2	0.199	4.70
914	40.5	7.50	187.0	0.207	6.00
975	43.9	11.40	200.0	0.227	9.30
1020	47.8	14.50	209.0	0.243	12.60
1050	49.3	17.00	214.2	0.253	14.60
1080	52.7	19.50	220.2	0.267	17.60
1125	55.5	22.80	223.4	0.283	20.30
Line off					
400	1.14	0.40	80.0	0.005	0.05
500	1.37	0.62	100.5	0.007	0.10
600	1.63	0.82	121.5	0.008	0.15
718	1.87	1.18	143.5	0.010	0.21
812	2.05	1.45	161.0	0.011	0.28
905	2.29	1.80	181.0	0.013	0.35
1015	2.69	2.20	202.2	0.015	0.44
1095	3.25	3.64	217.0	0.017	0.54

## Weather

Cloudy—rain in morning. Barometer 75 cm. Temperature: wet 10°C., dry 12°C.

## Line and connections

(1 and 3) (2 and 4) ground wires in place.

Total conductor length..... 109,500 cm.

Spacing..... 310 cm.

No. 3/0 seven-strand cable diameter..... 1.18 cm.

Transformer ratio .....1000/200,000

Frequency..... 60 cycles.

in these tests. The meters were all carefully calibrated in the laboratory at unity power factor and at 0.10 leading power factor, at both 25 and 60 cycles.

Humidity, temperature, and barometric pressures, as well as general weather observations, were taken during each test.

**Indoor Line.**—Later, an extensive investigation was made in a large laboratory room, 17 meters (57 ft.) wide by 21 meters (70 ft.) long. The lines were strung diagonally between movable wooden towers. Strips of treated wood 1.25 cm. square by 80 cm. long were used as insulators. The total length of conductor possible with four wires was 80 meters. By this arrangement it was possible to make a more complete study on the smaller sizes of conductors, and also to extend the investigation over a greater frequency range. The apparatus used was otherwise the same as in the outdoor tests.

**The Quadratic Law.**—Table XLII is a typical data sheet for Line A. Figure 140 and Fig. 143 show the characteristic corona curves. The corrected values for Table XLII are recorded in Table XLIII.

TABLE XLIII.—CORONA LOSS, OBSERVED VALUES CORRECTED FROM TABLE XLII

Kilovolts between lines $e^1$	Line ampere	Kilovolts to neutral $e$	Kilowatts line loss $p$	K.v.a.	Power factor
80.5	0.072	40.2	.....	5.80	.....
90.5	0.081	45.2	.....	7.33	.....
101.6	0.094	50.8	.....	9.55	.....
111.1	0.104	55.5	.....	11.55	.....
120.4	0.111	60.2	0.11	13.40	0.008
130.2	0.126	65.1	0.15	16.40	0.009
139.2	0.135	69.6	0.22	18.80	0.012
150.0	0.147	75.0	0.40	22.10	0.018
159.0	0.157	79.5	0.79	25.00	0.032
165.8	0.166	82.9	1.42	27.60	0.051
169.0	0.168	84.5	2.04	28.40	0.072
176.6	0.177	88.3	3.21	31.20	0.103
183.2	0.185	91.6	4.28	33.90	0.126
187.0	0.193	93.5	5.55	36.10	0.154
200.0	0.212	100.0	8.78	42.40	0.207
209.0	0.227	104.5	12.02	47.50	0.253
214.2	0.237	107.1	13.99	50.70	0.276
220.2	0.250	110.1	16.94	55.10	0.307

The shape of the curve between kilovolts and kilowatts suggests a parabola. After trial it was found that the losses above the knee of the curve follow a quadratic law. Below the knee it was found that the curve deviates from the quadratic law. This variation near the critical voltage is due to dirt spots, irregularities, and other causes, as discussed later. The main part of the curve may be expressed by<sup>1</sup>

$$p = c^2(e - e_o)^2 \quad (32)$$

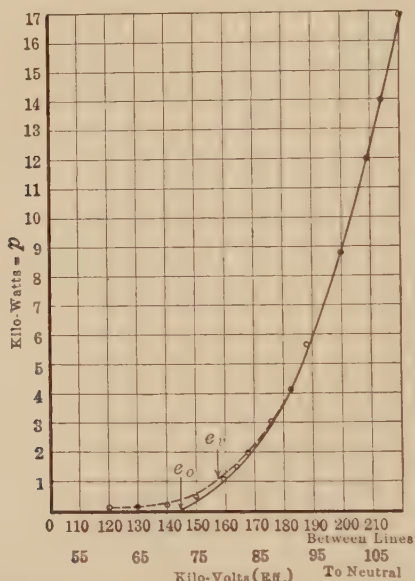


FIG. 140.—Characteristic corona loss curve for large stranded conductor.

Line A conductors 1-2-3-4. 3/0, 7-strand cable, diameter, 1.18 cm. Total conductor length, 109,500 cm. Spacing, 310 cm. Points, measured values. Curve calculated from  $p = 0.0117 (e - 72.2)^2$ .  $e_o$  = Disruptive critical voltage.  $e_v$  = Visual critical voltage. Test table XLIII

where

$p$  = the line loss

$e$  = kilovolts to neutral

$e_o$  is called the disruptive critical voltage, measured in kilovolts to neutral

The meaning of  $e_o$  and  $c^2$  will be considered later. The best mechanism of evaluation of constants for a given set of tests may now be considered. Equation (32) may be written

$$\sqrt{p} = c(e - e_o)$$

<sup>1</sup> PEEK, F. W., JR., "Law of Corona I," *Trans. A.I.E.E.*, p. 1889, 1911.



then, if the quadratic law holds, the curve between  $\sqrt{p}$  and  $e$  will be a straight line.  $e_o$  will be the point where the line cuts the  $e$  axis, and  $c$  will be the slope of the line (see Fig. 141);  $e_o$  and  $c$  may be evaluated graphically in this way. It is difficult to know how to draw the line accurately and give each point the proper weight. To do this the  $\Sigma\Delta$  method is used, as follows:<sup>1</sup>

The values of  $e$  and  $p$  for the set of readings to be investigated are first tabulated and a curve plotted (Fig. 141). All points that

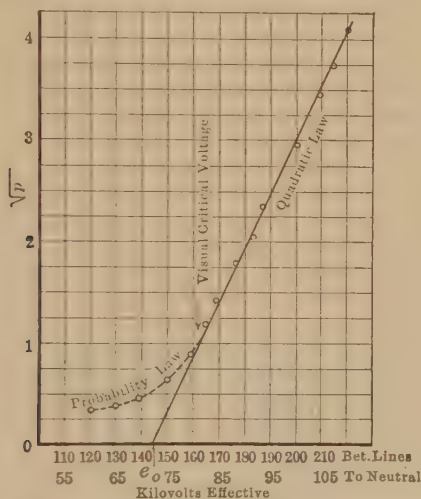


FIG. 141.—Corona loss curve plotted between  $\sqrt{p}$  and  $e$ . (Large conductor. Data same as Fig. 140.)

differ greatly from the straight line are eliminated as probably in error, or, as at the lower part of the curve, following a different law. The remaining readings are taken and formed into two groups, each of an equal number of readings.

$$\text{Group 1. } \Sigma_1 e \quad \Sigma_1 \sqrt{p}$$

$$\text{Group 2. } \Sigma_2 e \quad \Sigma_2 \sqrt{p}$$

$$\text{Then } \Delta \Sigma e = \Sigma_1 e - \Sigma_2 e \quad \Delta \Sigma \sqrt{p} = \Sigma_1 \sqrt{p} - \Sigma_2 \sqrt{p}$$

$$\Sigma \Sigma e = \Sigma_1 e + \Sigma_2 e \quad \Sigma \Sigma \sqrt{p} = \Sigma_1 \sqrt{p} + \Sigma_2 \sqrt{p}$$

$$c = \frac{\Delta \Sigma \sqrt{p}}{\Delta \Sigma e}$$

$$e_o = \frac{\Sigma \Sigma e - \Sigma \Sigma \sqrt{p} \cdot c}{n}$$

where  $n$  is the number of points used.

<sup>1</sup> STEINMETZ, "Engineering Mathematics," p. 232.

Thus  $e_o$  and  $c$  are determined.

TABLE XLIV.—CORONA LOSS, CALCULATED VALUES FOR FIG. 140

$$p = c^2(e - e_o)^2$$

$$p = 0.0117 (e - 72.2)^2$$

Kilovolts between lines $e'$	Kilovolts to neutral $e$	Kilowatts $p = c^2(e - e_o)^2$	Kilovolts between lines $e'$	Kilovolts to neutral $e$	Kilowatts $p = c^2(e - e_o)^2$
144.4	72.2	0.0	183.2	91.6	4.41
150.0	75.0	0.10	187.0	93.5	5.32
159.0	79.5	0.63	200.0	100.0	9.03
165.8	82.9	1.34	209.0	104.5	12.25
169.0	84.5	1.77	214.2	107.1	14.25
176.6	88.3	3.04	220.2	110.1	16.80

TABLE XLV.—CORONA LOSS  
Method of Reducing (Data from Table XLIII)

Kilovolts between line $e'$	Kilovolts to neutral $e$	Kw., $p$	$\sqrt{p}$
120.4	60.2	0.11	0.332
130.2	65.1	0.15	0.388
139.2	69.6	0.22	0.470
150.0	75.0	0.40	0.632
159.0	79.5	0.79	0.889
165.8	82.9	1.42	1.192
169.0	84.5	2.04	1.428
176.6	88.3	3.21	1.792
183.2	91.6	4.28	2.069
187.0	93.5	5.55	2.356
200.0	100.0	8.78	2.963
209.0	104.5	12.02	3.467
214.2	107.1	13.99	3.740
220.2	110.1	16.94	4.116

Total conductor length.....109,500 cm.  
 Spacing..... 310 cm.  
 No. 3/0 seven-strand cable diameter ..... 1.18 cm.

$e$	$\sqrt{p}$	$\Delta \Sigma e = 36.6$	$\Delta \Sigma \sqrt{p} = 3.935$
91.6	2.069	$\Sigma \Sigma e = 606.8$	$\Sigma \Sigma \sqrt{p} = 18.711$
93.5	2.356		
100.0	2.963		
104.2	3.467		
107.1	3.740		
110.1	4.116		
$c = \frac{\Delta \Sigma \sqrt{p}}{\Delta \Sigma e} = 0.108$			
$c^2 = 0.0115$			
$\Sigma_2 e = 285.1$	$\Sigma_2 \sqrt{p} = 7.388$	$\Sigma \Sigma e - \frac{\Sigma \Sigma \sqrt{p}}{c}$	
$\Sigma_1 e = 321.4$	$\Sigma_1 \sqrt{p} = 11.323$	$e_o = \frac{\quad}{n}$	
	$e_o = 72.1$		
	$e_o' = 144.2$		

Table XLV shows the method of reducing. The curve (Fig 140) is drawn from the equation  $p = 0.0117 (e - 72.2)^2$ . The circles show the experimental values, and indicate where the losses deviate from the quadratic law.

Table XLVI gives a similar set of data for a small wire. The results are plotted in Figs. 142 and 143.

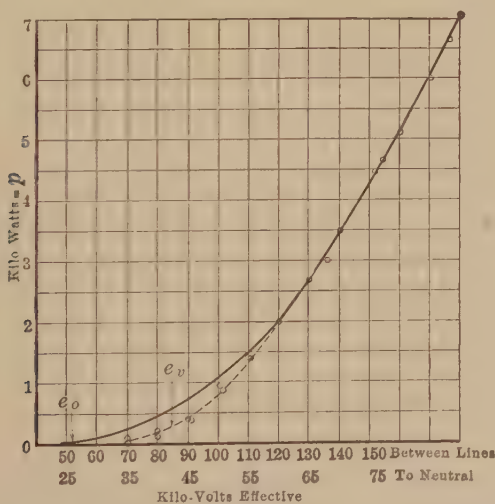


FIG. 142.—Characteristic corona loss curve for small wire.

No. 8 copper wire. Diameter, 0.328 cm. Total length, 29,050 cm. Spacing, 0.328 cm. Table XLVI, Line B.

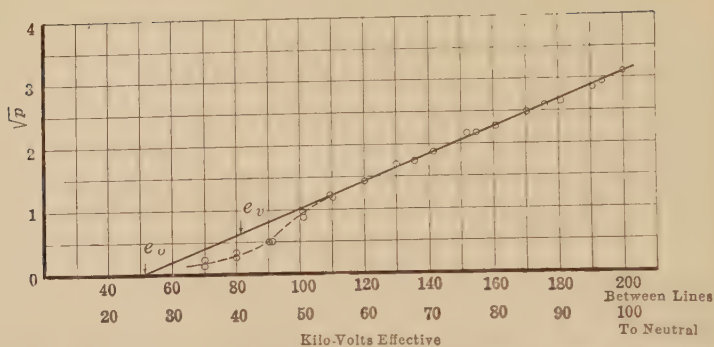


FIG. 143.—Corona loss curve plotted between  $\sqrt{p}$  and  $e$ . (Small conductor. Data same as Fig. 142.)

TABLE XLVI.—CORONA LOSS  
 $\Sigma\Delta$  Method of Reducing

Kilovolts between line $e'$	Kilovolts to neutral $e$	Kilowatt line loss $p$	$\sqrt{p}$
70.0	35.0	0.02	0.14
80.0	40.0	0.07	0.26
91.2	45.6	0.26	0.51
101.3	50.6	0.85	0.92
110.0	55.0	1.42	1.19
120.0	60.0	2.02	1.42
130.0	65.0	2.71	1.65
141.5	70.7	3.51	1.87
70.0	35.0	0.06	0.24
80.0	40.0	0.10	0.32
90.5	45.2	0.26	0.51
101.3	50.6	0.96	0.98
109.9	54.9	1.43	1.20
152.0	76.0	4.45	2.11
160.4	80.2	5.17	2.27
170.0	85.0	6.06	2.46
180.6	90.3	7.04	2.65
190.6	95.3	8.26	2.87
200.0	100.0	9.52	3.08
193.6	96.8	8.60	2.93
176.0	88.0	6.65	2.58
155.0	77.5	4.66	2.16
136.0	68.0	3.01	1.73

Total conductor length.....	29,050 cm.
Spacing .....	183 cm.
No. 8 H. D. copper wire—diameter .....	0.328 cm.
Temperature .....	1.5
Barometer .....	76.6

$e$	$\sqrt{p}$	$e$	$\sqrt{p}$	$\Sigma \Sigma e = 841.1$	$\Delta \Sigma e = 93.7$
				$\Sigma \Sigma \sqrt{p} = 24.15$	$\Delta \Sigma \sqrt{p} = 3.80$
100.0	3.08	80.2	2.27		
96.8	2.93	77.5	2.15		
95.3	2.87	68.0	1.73		
90.3	2.65	60.0	1.42		
85.0	2.46	88.0	2.58		
				$e_o = \frac{841.1 - 24.15}{10}$	
					$c = \frac{3.80}{93.7} = 0.0410$
					$c^2 = 0.00168$
					$p = 0.00168(e - 25.2)^2$
467.4	13.99	373.7	10.15		

To investigate the law further it is now necessary to determine the various factors affecting  $e_o$  and  $e^2$ . These will be taken up

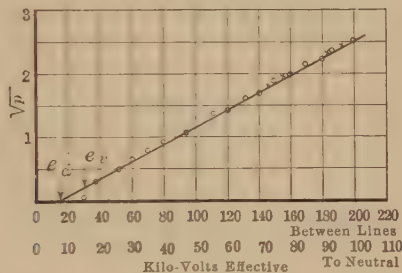


FIG. 144.—Corona loss plotted between  $\sqrt{p}$  and  $e$  to illustrate the quadratic law. Phosphor-bronze conductor. Diameter, 0.051 cm. Spacing, 366 cm. Total length, 29,050 cm. Temp.,  $-6.5^\circ \text{C}$ . Bar., 77.3 cm. Line B.

under separate headings. The loss near the critical point will then be discussed.

In Fig. 144,  $\sqrt{p}$  and  $e$  are plotted. This is an especially interesting curve on account of its range. The measurements are taken up to twenty times the disruptive critical voltage, and show how well the quadratic law holds. Figures 145 and 146 are plotted in the same way to illustrate the quadratic law.

**Frequency.**—To determine the way that frequency enters into the power equation

$$p = c^2(e - e_o)^2$$

a series of loss curves were taken on line A at various frequencies.

These tests indicated that the loss varied almost directly with the frequency over the range investigated. The data are given in Tables XLVII and XLVIII. Thus when the frequency does



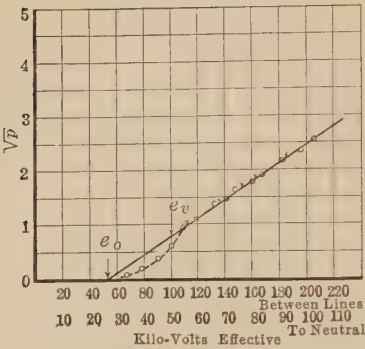


FIG. 145.

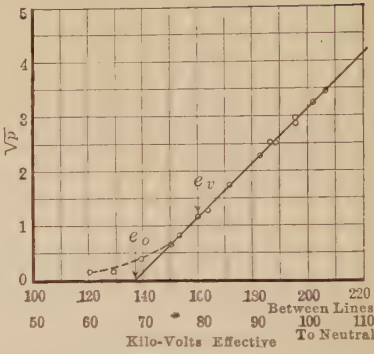


FIG. 146.

Corona loss plotted between  $\sqrt{p}$  and  $e$  to illustrate the quadratic law.

FIG. 145.—No. 8 copper wire. Diameter, 0.328 cm. Total length, 29,050 cm. Spacing, 244 cm. Temp. 1.5. Bar., 76.6. Line B.

FIG. 146.—3/0, 7-strand weathered cable. Diameter, 1.18 cm. Spacing, 310 cm. Total length, 109,500 cm. Temp., 16. Bar., 75.3. Line A.

TABLE XLVII.—LINE A. CONDUCTOR 2-3. TOTAL LENGTH 54,750 CM.

Kilovolts between lines	210	200	190	180
<i>f</i>	Kilowatts loss			
47	4.9	3.2	2.0	1.3
60	5.1	3.7	2.6	1.6
70	6.1	4.3	2.8	1.7
80	6.9	5.0	3.4	1.9
.....	.....	.....	3.6	2.1
90	7.5	5.6	3.8	2.6
100	8.0	5.6	3.7	2.4
115	9.3	7.1	5.0	3.4

TABLE XLVIII.—LINE A. CONDUCTORS 1-2-3-4. TOTAL LENGTH 109,500 CM.

Kilovolts between lines	210	200	190	180
<i>f</i>	Kilowatts loss			
50	9.24	6.30	3.80	2.20
60	10.50	7.30	4.65	2.65
70	12.1	8.60	5.50	3.20
80	14.0	10.20	6.80	3.95

not vary greatly from 60 cycles the equation may be written

$$p = af(e - e_o)^2$$

It was then decided to make the investigation over a greater range of frequency, and on shorter lines to prevent wave distortion due to load, etc. These measurements were made on the indoor line. Table XLIX gives data for a 0.333-cm. radius wire. Care was taken to keep the wave shape as nearly constant as possible. The results are plotted in Fig. 147.  $e_0$  is the same for

TABLE XLIX.—CORONA LOSS AT DIFFERENT FREQUENCIES  
New Galvanized Cable

Radius = 0.334 cm. Total length = 0.0815 km.  
Spacing = 61 cm.  $\delta = 1.00$   
Effective kv. Indoor line

Kilovolts to neutral $e_n$	Kilowatts per km. (p)	$\sqrt{p}$	Kilovolts to neutral $e_n$	Kilowatts per km. (p)	$\sqrt{p}$	Kilovolts to neutral $e_n$	Kilowatts per km. (p)	$\sqrt{p}$	Kilovolts to neutral $e_n$	Kilowatts per km. (p)	$\sqrt{p}$
Test 50B, 40 cycles			Test 51B, 60 cycles			Test 52B, 90 cycles			Test 53B, 120 cycles		
50.5	1.10	1.05	54.0	3.31	1.82	89.5	61.5	7.84	45.0	0.67	0.82
53.5	2.57	1.59	62.5	9.15	3.02	85.8	54.0	7.35	50.7	2.88	1.69
56.2	4.15	2.04	68.0	14.55	3.88	87.0	56.0	7.48	53.7	6.73	2.59
59.2	5.84	2.42	72.0	20.10	4.48	82.8	48.2	6.93	56.2	10.30	3.21
64.0	9.10	3.02	78.0	28.45	5.20	77.5	37.50	6.13	60.2	15.60	3.94
66.8	11.55	3.40	87.3	40.20	6.32	74.0	31.60	5.64	69.0	30.00	5.46
71.5	15.95	3.99	91.5	49.70	7.02	66.0	18.90	4.35	72.7	37.40	6.10
73.7	18.44	4.30	82.0	34.60	5.83	60.4	12.75	3.75	71.0	32.00	5.65
70.7	15.23	3.95	72.8	21.10	4.67	50.3	4.90	1.40	75.5	41.30	6.42
67.5	12.30	3.50	52.7	5.23	2.90	54.3	5.02	2.24	81.0	53.50	7.30
65.0	10.20	3.36	56.0	5.65	2.32	58.4	9.45	3.08	87.5	69.80	8.35
60.2	6.64	2.58	61.5	10.20	3.20	.....	.....	.....	95.0	90.00	9.50
58.2	5.28	2.29	67.2	15.75	3.90	.....	.....	.....	80.0	51.20	7.15
46.7	0.80	0.89	70.2	19.30	4.38	.....	.....	.....	75.5	41.50	6.42
.....	.....	.....	.....	.....	.....	.....	.....	.....	70.5	29.70	5.42
.....	.....	.....	.....	.....	.....	.....	.....	.....	66.5	25.60	5.06
.....	.....	.....	.....	.....	.....	.....	.....	.....	59.5	13.65	3.69

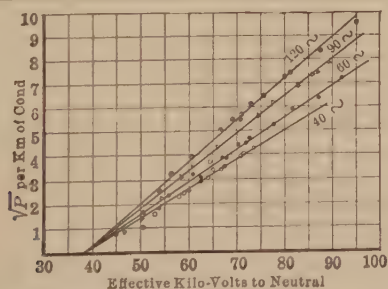


Fig. 147.—Corona loss curves at different frequencies. (Plotted from Table XLIX.)

all frequencies but the slope  $c$  varies with the frequency. Values of  $c^2$  for various frequencies from 30 to 120 cycles and three different sizes of conductor are given in Table L, and plotted in Fig.

TABLE L.—VARIATION OF  $c^2$  WITH FREQUENCY  
(Indoor Line)

Frequency	Tests 1-6B $r = 0.032$ cm. $s = 61$ cm. Length = 0.0815 km. $\delta = 1.00$		Tests 37-40B $r = 0.105$ cm. $s = 61$ cm. Length = 0.0815 $\delta = 1.00$		Tests 50-53B $r = 0.334$ cm. $s = 61$ cm. Length = 0.0815	
	$c^2$ per km.	$e_o$	$c^2$ per km.	$e_o$	$c^2$ per km.	$e_o$
30	0.0052	9.5	0.0071	21.5	.....	.....
40	0.0061	9.5	0.0092	21.5	0.0139	38.0
60	0.0078	9.5	0.0119	20.5	0.0173	38.0
75	0.0092	9.5	0.0144	20.5	.....	38.0
90	0.0107	9.5	0.0157	20.5	0.0240	38.0
120	0.0134	9.5	0.0203	19.0	0.0297	38.0

148. The points over this measured range lie on a straight line, and this line extended cuts the frequency axis at  $-25$ . This

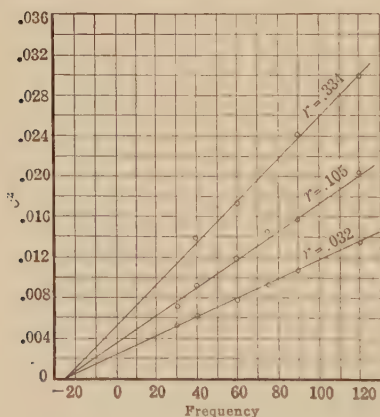


FIG. 148.—Variation of  $c^2$  with frequency. (Data from Table L.)

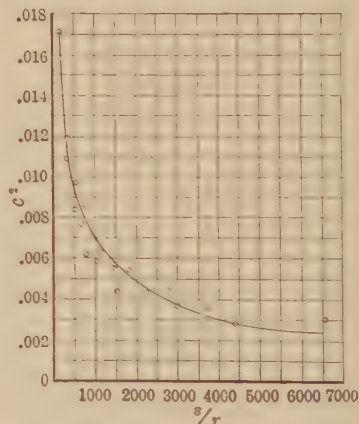


FIG. 149.—Variation of  $c^2$  with  $s/r$ .

seems to mean for a given wire and spacing a constant loss plus a loss which varies directly as the frequency.

The equation may be written

$$p = a(f + 25)(e - e_o)^2$$

At zero frequency the equation reduces to

$$p = 25a(e - e_o)^2$$

This is not necessarily the direct-current loss. Watson has made laboratory measurements of direct-current loss, using an influence machine as the source of power.<sup>1</sup> Some of these measurements are compared with the alternating-current loss in Table LI, for the same maximum voltages; the difference between the direct-current loss and the alternating-current loss for the same effective voltages is of course *much* greater.

TABLE LI.—COMPARISON OF D.C. CORONA LOSS WITH LOSS AT 60 CYCLES FOR SAME MAXIMUM VOLTAGE

Voltage gradient <i>g</i>	D.c. amps. <i>i</i>	D.c. kilovolts <i>e</i>	D.c. loss <i>p</i> kw./km.	Corresponding a.c. effective kilovolts <i>e</i> <sub>1</sub>	Measured 60-cycle loss <i>p</i> <sub>1</sub> kw./km.	Ratio 60 cycles d. c. loss $\frac{p_1}{p}$
61	0.003	55	0.16	39.8	0.25	1.52
66	0.004	59	0.24	42.0	0.37	1.58
69	0.005	62	0.31	44.0	0.50	1.61
75	0.007	67	0.47	48.0	0.80	1.67

$$s = 100 \text{ cm.}$$

$$\tau = 0.0597 \text{ cm.}$$

D.c. measurements from Watson, Institute of Electrical Engineers.

**Relation between  $c^2$  and  $s/r$ .**—The power equation may be written over the commercial range of frequency

$$p = c^2(e - e_o)^2 = a(f + 25)(e - e_o)^2$$

where the relation between  $c^2$  and  $s/r$  has not to this point been investigated. The relation will first be determined for the practical sizes of conductors at practical spacings of the outdoor line, and later over greater range from the indoor data. Only 60-cycle values will be used, as the data at this frequency are very complete. In Table LII are values of  $c^2$  for various sizes of wire and cable at various spacings.  $c^2$  varies greatly with the radius of the conductor  $r$  and the spacing  $s$ . Plotting  $s/r$  and  $c^2$  a curve is obtained that suggests a hyperbola. The curve between  $\log c^2$  and  $\log s/r$  is a straight line. Therefore the following relation between  $c^2$  and  $s/r$  is established.

$$c^2 = A (s/r)^d \quad (33)$$

The fair weather value of  $c^2$  for standard line A 1-2-3-4 may now be examined in Table LIII.

<sup>1</sup> WATSON, *Jour. Inst. Elec. Eng.*, June, 1910.

TABLE LII.—EXPERIMENTAL VALUES—LINES A AND B

Relation between $c^2$ and $s/r$						
Test No.	Diameter, cm.	$\frac{s}{r}$	$\delta$	$c^2 \times 10^6$ per km.	Style of conductor	Material
95	0.168	6550	1.07	280	Wire	Gal. iron
92	0.168	4880	1.07	256	Wire	Gal. iron
86	0.168	3700	1.08	326	Wire	Gal. iron
138	0.328	2980	1.10	331	Wire	Copper
94	0.168	2730	1.07	410	Wire	Gal. iron
137	0.328	2230	1.10	391	Wire	Copper
91	0.168	1820	1.07	506	Wire	Gal. iron
128	0.518	1530	1.05	412	Wire	Copper
136	0.328	1490	1.10	513	Wire	Copper
82	0.585	1480	1.07	513	Cable	Gal. iron
135	0.328	1120	1.10	570	Wire	Copper
94a	0.168	1090	1.07	633	Wire	Gal. iron
77	0.585	1060	1.07	543	Cable	Gal. iron
79	0.585	770	1.08	571	Cable	Gal. iron
134	0.328	740	1.10	772	Wire	Copper
126	0.518	700	1.11	687	Wire	Copper
18	1.181	525	1.02	950	Cable	Copper
80	0.585	520	1.07	784	Cable	Gal. iron
125	0.518	350	1.11	1070	Wire	Copper
73	0.585	310	1.07	1018	Cable	Gal. iron
100	0.953	193	1.08	1584	Cable	Gal. iron

TABLE LIII.—RELATION OF  $c^2$  TO  $\frac{1}{\delta}$  FOR MAIN EXPERIMENTAL LINES  
 Line A 1-2-3-4  
 (Standard Line A)

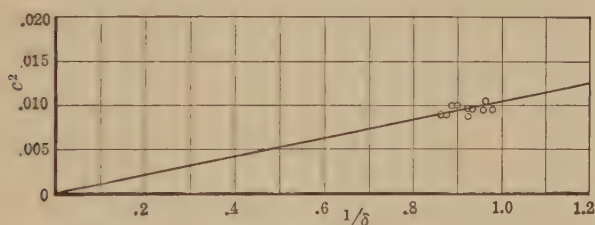
Test No.	$c^2 \times 10^6$ per km.	$\frac{1}{\delta}$	$\delta$	Test No.	$c^2 \times 10^6$ per km.	$\frac{1}{\delta}$	$\delta$
18	945	0.982	1.020	103	980	0.901	1.112
36	1050	0.966	1.037	104	892	0.878	1.138
37	945	0.959	1.043	105	890	0.866	1.158
84	945	0.933	1.074	109	869	0.928	1.078
101	955	0.925	1.081	119	991	0.888	1.127

It is seen that these values are not exactly constant but apparently vary with the temperature and barometric pressure.  $c^2$  and  $1/\delta$  in curve (Fig. 150) suggest that  $c^2$  varies as  $1/\delta$ . Multiplying by  $\delta$  then, reduces  $c^2$  to the standard temperature of 25°C.



TABLE LIV  
(Corrected  $c^2$  and  $s/r$ )

Test No.	Diameter, cm.	$s/r$	$c^2 \times 10^5$ read per km.	$c^2 10^5$ corrected to 25° C., 76 cm. bar.	Corr. factor $\delta$	$\log(c^2 10^5)$ corrected to 25° C., 76 cm. bar.	$\log \frac{s}{r}$	Style of conductor
95	0.168	6550	280	300	1.07	5.704	8.787	Wire
92	0.168	4880	256	275	1.07	5.620	8.492	Wire
86	0.168	3700	326	347	1.08	5.852	8.215	Wire
138	0.328	2980	331	364	1.09	5.892	8.000	Wire
137	0.328	2230	391	429	1.09	6.062	7.709	Wire
77	0.585	1060	543	582	1.07	6.372	6.966	Cable
126	0.518	700	687	755	1.10	6.637	6.551	Wire
18	1.181	525	950	965	1.02	6.821	6.263	Cable
80	0.585	520	784	840	1.07	6.733	6.254	Cable
125	0.518	350	1070	1190	1.11	7.083	5.858	Wire
73	0.585	310	1018	1090	1.07	6.995	5.763	Cable
100	0.953	193	1584	1710	1.08	7.405	5.263	Cable

FIG. 150.—Relation between  $c^2$  and  $1/\delta$ .TABLE LV.—ΣΔ REDUCTION OF RELATION OF  $c^2$  TO  $\frac{s}{r}$   
( $c^2$  Corrected to 25 deg. C.—76 cm. Barometric Pressure)

Test No.	$\log_e(c^2 10^5)$	$\log_e \frac{s}{r}$	Test No.	$\log_e(c^2 10^5)$	$\log_e \frac{s}{r}$
95	5.704	8.787	126	6.637	6.551
92	5.620	8.492	18	6.871	6.263
86	5.852	8.215	80	6.733	6.254
138	5.892	8.000	125	7.083	5.858
137	6.062	7.709	73	6.995	5.736
77	6.372	6.966	100	7.444	5.263
		35.502			41.763
		48.169			35.925

$$\Sigma_1 \log \epsilon (c^2 10^5) = 35.50 \quad \Sigma_1 \log \epsilon \frac{s}{r} = 48.17$$

$$\Sigma_2 \log \epsilon (c^2 10^5) = 41.76 \quad \Sigma_2 \log \epsilon \frac{s}{r} = 35.92$$

$$\Delta \Sigma \log \epsilon (c^2 10^5) = -6.26 \quad \Delta \Sigma \log \epsilon \frac{s}{r} = 12.25$$

$$\Sigma \Sigma \log \epsilon (c^2 10^5) = 77.26 \quad \Sigma \Sigma \log \epsilon \frac{s}{r} = 84.09$$

$$d = \frac{\Delta \Sigma \log \epsilon c^2 \times 10^5}{\Delta \Sigma \log \epsilon \frac{s}{r}} = \frac{-6.26}{12.25} = -0.51 \approx -0.50$$

$$c^1 = \frac{\log (c^2 10^5) - d \Sigma \Sigma \log \epsilon \frac{s}{r}}{n} = 9.92$$

$$\log (c^2 10^5) = -0.5 \log \epsilon \frac{s}{r} + 9.92$$

$$c^2 = 20,500 \sqrt{\frac{r}{s}} 10^{-5}$$

and 76 cm. barometric pressure. This particular correction is not satisfactory as the range of  $\delta$  is small. It seems the best until more complete data are obtained. In Table LIV all values of  $c$  are corrected to 25°C. and 76 cm. barometer, and the constants calculated by the  $\Sigma\Delta$  method in Table LV. This gives:  $c^2 = 20,500 \sqrt{r/s} \times 10^{-5}$  per kilometer of total conductor at 25°C., 76 cm. barometer and 60 cycles.

Curve 149 is plotted from the points calculated in Table LVI, while the circles show the actual experimental points.

TABLE LVI.—CALCULATION OF CURVE NO. 149 FROM

$$\left( c^2 \times 10^5 = 20,500 \sqrt{\frac{r}{s}} \right)$$

$\frac{s}{r}$	$\sqrt{\frac{r}{s}}$	$c^2 \times 10^5$	$\frac{s}{r}$	$\sqrt{\frac{r}{s}}$	$c^2 \times 10^5$
250	0.0633	129	2000	0.0224	460
500	0.0447	915	3000	0.0183	376
1000	0.0316	648	4000	0.0158	324
1500	0.0258	530	6000	0.0128	262

Curve 151 shows a straight-line relation between  $\log s/r$  and  $\log c^2$ . The equation for the power loss at 25°C. and 76 cm. barometric pressure and any frequency may now be written

$$p = 241(f + 25) \sqrt{r/s} (e - e_0)^2 10^{-5} \quad (34)$$

where  $p$  = the energy loss per kilometer of conductor in kilowatts

$e$  = kilovolts to neutral

$e_o$  = disruptive critical kilovolts to neutral at 25°C. and 76 cm. barometric pressure

$f$  = the frequency in cycles per second

$r$  = the radius of the conductor in cm.

$s$  = the distance between conductor centers in cm.

The value of  $e_o$  varies with the radius of the conductor  $r$ , and the spacing  $s$ , and will be discussed later.

**Relation between  $c^2$ ,  $r$ , and  $s$  for Small Conductors and Small Spacings. (Indoor Line.)**—The loss was investigated for very small conductors at large and small spacings, and for large conductors at small spacings, on the indoor line. The conductors ranged from 0.025 to 0.046 cm. in radius, and the spacings from

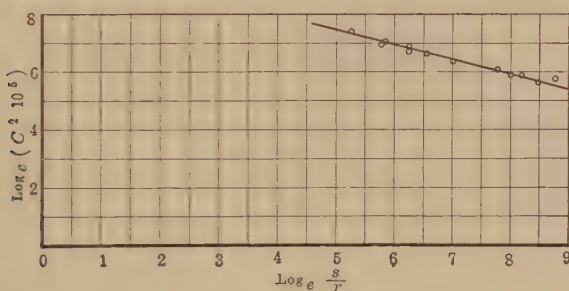


FIG. 151.—Determination of equation between  $c^2$  and  $s/r$ .

12.5 to 275 cm. The quadratic law still holds—the relation between  $c^2$ ,  $r$ , and  $s$ , however, becomes more complicated. This is also true of the disruptive critical voltage. Below a spacing of about 15 cm. it is difficult to express the loss in terms of a law, as the results are erratic, probably due to the great distortion of the field, which is augmented when the corona starts, greatly increasing the loss above the quadratic.

For conductors 0.025 cm. in radius and above, and 15 cm. spacing and above, this data shows that

$$c^2 = 20,500 \sqrt{\frac{r + \frac{6}{s} + 0.04}{s}} 10^{-5} \text{ per km. of conductor} \quad (33a)$$

The more complete equation is, therefore,

$$p = 241(f + 25) \sqrt{\frac{r + \frac{6}{s} + 0.04}{s}} (e - e_d)^2 10^{-5} \text{ kw. per km. of conductor.}^1 \quad (34a)$$

In Fig. 152 the points are measured corona loss values, while the curve is calculated from equation (34a) ( $r = 0.032$ , spacings 46 and 275 cm.). Data are given in the appendix.

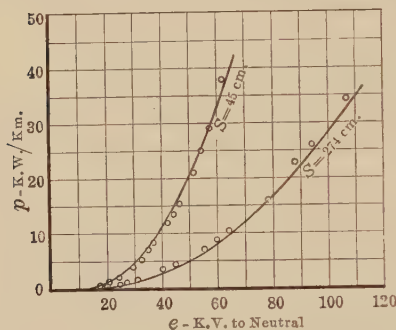


FIG. 152.—Comparison of calculated and measured corona loss for small conductors at small and large spacings.

(Points measured. Curves calculated from equation (34a) Conductor radius, 0.032 cm. Spacings, 46 cm. and 275 cm.  $\delta = 1.01$ .)

$s$  = distance between conductor centers

$r$  = the radius

Where  $r$  and  $s$  are in centimeters and  $e$  is in kilovolts,  $g$  is expressed in kilovolts per centimeter. If  $e_o$ , which has been called the *disruptive critical voltage*, is taken for  $e$ ,

$$g_o = \frac{e_o}{r \log_e s/r}$$

$g_o$  then is the stress at the conductor surface corresponding to  $e_o$ , and will be called the *disruptive gradient*, to distinguish it from the visual gradient  $g_v$  (see top of page 175 for determination of  $e_o$  values). Values of  $g_o$  for wires and cables taken under a variety of conditions on the outdoor line are given in Tables LVII and LVIII. These values are corrected to standard temperature and pressure by dividing by  $\delta$ .

<sup>1</sup> PEEK, F. W., JR., "High Voltage Engineering," *Jour. Frank. Inst.*, December, 1913.

**The Disruptive Critical Voltage.**—As discussed in Chap. IV, page 50, the point of greatest stress around a cylindrical conductor is at its surface. When  $s/r$  is large, the gradient at the surface of the conductor may be expressed

$$g = \frac{de}{dx} = \frac{e}{r \log_e s/r} \quad (12c)$$

where  $e$  = the voltage to neutral

TABLE LVII.—DISRUPTIVE CRITICAL VOLTAGE GRADIENT FOR WIRES  
(Values Corrected to 76 cm. Barometer and 25 deg. C., Outdoor Line)

Test No.	Spacing, cm.	Radius, cm.	$g$ , kv. cm. max.	Per cent. variation from mean	Per cent. variation max. to min.
91	152.0	0.084	31.3		
94	229.0		31.6		
92	410.0		29.1		
95	550.0		36.5		
			Avg. = 30.9	5.8	7.9
134	122.0	0.164	28.8		
135	183.0		27.1		
136	244.0		29.0		
137	366.0		25.7		
138	488.0		25.3		
			Avg. = 27.2	7.0	12.7
125	91.4	0.259	28.7		
126	183.0		26.5		
127	275.0		26.0		
128	397.0		26.2		
			Avg. = 26.9	6.7	9.4
122	91.4	0.463	28.7		
123	183.0		30.4		
120	214.0		30.5		
124	275.0		31.0		
			Avg. = 30.1	4.8	7.6

Total Avg. 29.0

If the values of  $e_o$  for standard line A (1.8-cm. seven-strand cable) are examined it is found that the average value of  $g_o$  is 25.8 kv. per centimeter maximum. For cables between 0.583 cm. and 1.18 cm. in diameter and various spacings, the average value of  $g_o$  is 25.7 kv. per centimeter maximum, or, in other words,  $g_o$  is constant for *commercial* sizes of cables, at practical spacings, and is 25.7 kv. per centimeter maximum. In determining the value  $g_o$  for seven-strand cables,  $r$  was taken for convenience as the outside radius. Hence, the above  $g_o$  is not the actual  $g_o$  as obtained for wires, but is an apparent  $g_o$ . The actual  $g_o$  may be



obtained by taking some mean radius  $r_2$  between the outside radius  $r$  and the radius to the point of contact of the outside strands  $r_1$ .  $r_2$  approaches  $r$  in value as the number of strands is increased.

TABLE LVIII.—DISRUPTIVE CRITICAL VOLTAGE GRADIENT FOR CABLES  
(Values Corrected to 76 cm. Bar. and 25 deg. C., Outdoor Line)

Test No.	Spacing, cm.	Radius, cm.	$g$ , kv./cm. max.	Per cent. variation from mean	Per cent. variation max. to min.
73	91.4	0.292	26.5	.....	.....
80	152.0	.....	24.0	.....	.....
79	244.0	.....	23.9	.....	.....
77	310.0	.....	23.9	.....	.....
82	432.0	.....	25.0	.....	.....
			Avg. = 24.7	7.3	9.8
100	91.4	0.476	25.5	.....	.....
115	91.4	.....	26.2	.....	.....
116	183.0	.....	26.0	.....	.....
117	275.0	.....	26.4	.....	.....
118	366.0	.....	28.1	.....	.....
			Avg. = 26.4	6.4	9.3
		Line A	— 1. 2. 3. 4		
18	310.0	0.590	25.5	.....	.....
36	310.0	.....	26.0	.....	.....
37	310.0	.....	25.3	.....	.....
84	310.0	.....	25.8	.....	.....
101	310.0	.....	26.5	.....	.....
103	310.0	.....	26.1	.....	.....
104	310.0	.....	25.7	.....	.....
105	310.0	.....	26.0	.....	.....
109	310.0	.....	25.8	.....	.....
119	310.0	.....	25.1	.....	.....
119	310.0	.....	26.0	.....	.....
			Avg. = 25.8	2.7	5.3
		Total	Avg. = 25.7	5.5	8.1

The values of  $g_o$  for wires varying in diameter from 0.168 cm. to 0.928 cm. and for spacings from 90 to 600 cm. are constant within the limits of experimental error. The mean maximum value is:

$g_o = 29$  kv. per cm. at 25°C., and 76 cm. barometric pressure

Considerable variation should be expected in  $g_o$  values obtained on a long outdoor line, due to

1. Necessarily imperfect conductors, kinks, etc., in an outdoor line of this length.

2. Progressive change in the value of successive points on a given curve due to slight changes of wave shape, etc., as the voltages are increased, and the apparent shift of  $e_o$ .

The close agreement of  $g_o$  for wires is for the above reasons remarkable.

Discrepancies due to progressive change are not to be expected for standard line A to any great extent as the conductor spacing was always the same, and test conditions were kept as nearly constant as possible.

The above data shows that  $g_o$  may be considered constant for diameters of conductors and spacings within the practical range. This was further investigated over a greater range on the indoor line.

$$\frac{g_o \text{ cables}}{g_o \text{ wires}} = m_o$$

where  $m_o$  is a fraction which approaches unity as the irregularity of the surface is reduced.

The author has studied the irregularity factor,  $m_o$ , for conductors stranded in various ways and for single-phase and three-phase lines. For a given diameter the maximum value is obtained for a smooth tube. For the same diameters, a cable is usually good on only 0.87 per cent. or less of the voltage of a tube; in new cables 1 in. in diameter,  $m_o$  is approximately the same for 19, 37, and 61 strands and varies from 0.80 to 0.85; in new concentric cables it is generally near 0.80. In some other types of cables it is lower. The lowest value obtained was 0.70. Seven-strand cables are not desirable in large sizes, since the strands become mutilated. Rope-lay cables have the lowest values and should be avoided.

Types of cables with projecting irregularities should be avoided.

Although in the above investigation with 19, 37, and 61 strands there was no great difference in the loss, the measurements were slightly in favor of 37 strands. It seems inadvisable to use a stranding that would make the individual conductors too small compared to the cable diameter.

The disruptive critical voltage,

$$e_o = \delta m_o g_o r \log_e s/r \quad (35)$$

(See curve, Fig. 153.)

The loss equation may now be written

$$p = \frac{241}{\delta} (f + 25) \sqrt{r/s} (e - e_o)^2 10^{-5} \text{ kw./km.} \quad (34)$$

where  $p$  expresses the loss above the visual critical voltage  $e_v$ , and  $e_o$  is given in (35)

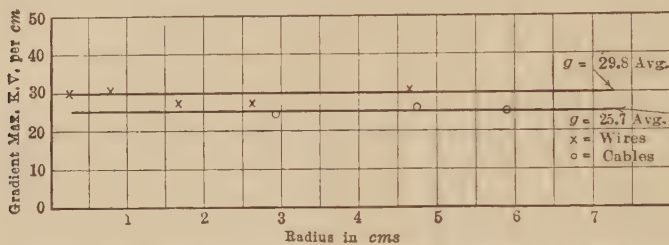


Fig. 153.— $g_o$  for wires and cables. (Data from Tables LVII and LVIII.)

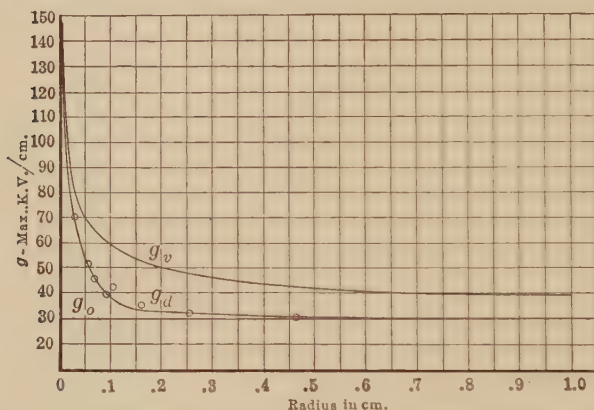


Fig. 154.—Comparison of  $g_v$ ,  $g_d$ , and  $g_o$ . ( $g_d$  values from Table LIX.)

Investigations on the indoor line over a range covering small conductors show that the disruptive gradient may be considered constant, for all practical purposes, when the conductor radius is greater than 0.20 cm. As the size of the conductor is decreased, the disruptive gradient increases very rapidly. If the disruptive gradient for any size of conductor is called  $g_d$ , we have found that this law may be expressed

$$g_d = g_o \delta \left( 1 + \frac{0.30}{\sqrt{\delta r}} \frac{1}{(1 + 230 r^2)} \right) \quad (36)$$

$$e_d = g_d r m_o \log_e \frac{s}{r} \quad (35a)$$

Thus, when  $r$  is large (above 0.2 cm.) practically  $g_d = g_o$ , and where  $r = o$ ,  $g_d = g_v$ .

Measured values of  $g_d$  for different conductors on the indoor line are given in Table LIX. Calculated and measured values are plotted in Fig. 154.

The corona loss equation over a greater range of conductor diameter and spacing may thus be written

TABLE LIX

Test No.	$r$ cm.	$g_d$ maximum measured	$g_d$ maximum calculated
12 B	0.032	67.5	70.7
13 B	0.032	70.3	70.7
14 B	0.032	71.0	70.7
18 B	0.032	71.0	70.7
15 B	0.032	71.0	70.7
16 B	0.032	71.0	70.7
19 B	0.032	69.6	70.7
17 B	0.032	71.2	70.7
20 B	0.032	69.5	70.7
21 B	0.032	69.3	70.7
		Avg. = 70.0	
27 B	0.057	51.7	51.3
26 B	0.057	51.3	51.3
25 B	0.057	51.7	51.3
24 B	0.057	51.3	51.3
		Avg. = 51.5	
30 B	0.071	45.4	45.4
33 B	0.0914	39.4	39.4
32 B	0.0914	39.4	39.4
42 B	0.105	42.2	37.6
41 B	0.105	42.2	37.6
37 B	0.105	42.5	37.6
		Avg. = 42.3	
45 B	0.164	36.5	33.0
44 B	0.164	33.6	33.0
		Avg. = 35.1	
49 B	0.256	30.8	31.1
48 B	0.256	32.1	31.1
47 B	0.256	33.2	31.1
		Avg. = 32.0	
56 B	0.464	31.8	30.2
55 B	0.464	31.8	30.2
54 B	0.464	31.5	30.2
		Avg. = 31.7	

$$p = 241(f + 25)\sqrt{\frac{r + \frac{6}{s} + 0.04}{s}} (e - e_d)^2 10^{-5} \text{ kw./km.} \quad (34a)$$

where  $e_d$  is obtained from equation (35a).

It may be interesting to note that equation (34) may be written in terms of the gradient, thus

$$p = A\sqrt{r/s} (f + 25) \left(\log \frac{s}{r}\right)^2 (r^2) (g - g_o)^2 \times 10^{-5}$$

Figure 155 shows measured curves plotted between  $g$  and  $p$  for a given wire at three different spacings. These curves all intersect the axis at  $g_o \text{ max.} = 30$ , at  $\delta = 1.0$ .

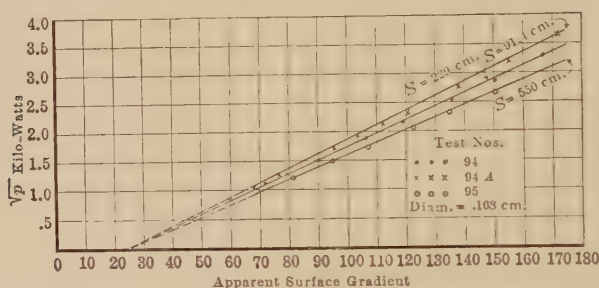


FIG. 155.—Relation between power loss and apparent surface gradient.

**Losses Near the Disruptive Critical Voltage— $e_o$ .**—If the conductors could be made perfectly smooth, no appreciable loss would occur below the visual critical voltage. Near the starting point of corona two effects occur, however, which cause a deviation of the loss from the quadratic law, equation (34), and which affect the loss in opposite directions:

(a) With perfect conductors, loss of power does not begin at the voltage  $e_o$ , at which the disruptive gradient is reached at the conductor surface, but only after the disruptive strength of air has been exceeded over a finite and appreciable distance  $a$  from the conductor, that is, at a higher voltage  $e_r$ . Since the convergency of the lines of dielectric force is great at the surface of small conductors, with such conductors, a considerable increase of the voltage is required to extend the disruptive gradient to some distance from the conductor, and  $e_r$  is considerably higher than  $e_o$ . With such conductors there would be no loss until  $e_r$  were reached. The loss would then suddenly take nearly the definite value calculated for this applied voltage from equation



(34). Even with polished conductors, in practice the decrease of loss below that given by equation 34 is appreciable with small conductors within the range between  $e_o$  and  $e_v$ , as seen in Fig. 136. With large conductors, however, the less convergency of the lines of dielectric force at the conductor surface requires a less voltage increase beyond  $e_o$  to extend the disruptive gradient to some distance from the conductor;  $e_o$  and  $e_v$  are, therefore, closer together, and this decrease of the loss below the theoretical value given by equation (34) is not appreciable.

(b) As the conductor surface can never be perfect, some loss of power occurs at and below the disruptive critical voltage at isolated points of the conductor, where irregularities

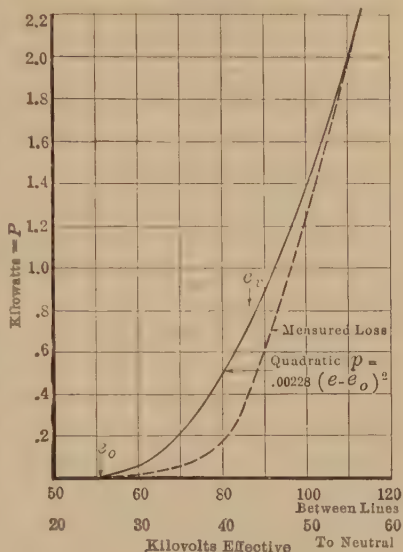


FIG. 156.—Corona loss for small conductors near the critical voltage.

No. 8 copper. Diameter, 0.328 cm. Length, 29.050 cm. Spacing, 122 cm. Temp. 15. Bar., 76.6. Line B.

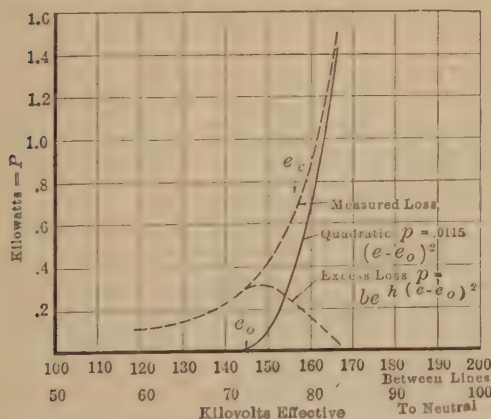


FIG. 157.—Corona loss for large conductors near the critical voltage. (Data same as Fig. 140.)

of the surface, scratches, spots of mud or dirt, etc., give a higher potential gradient than that corresponding to the curvature of the conductor surface. With small conductors, this loss is rarely appreciable, since the curvature of the conductor surface is of the same magnitude as that of its irregularities. It becomes appreciable,

however, for larger conductors, as seen in Fig. 157. This excess

of the loss beyond that given by the quadratic law equation essentially depends on the conductor surface, and is the larger the rougher or dirtier the surface. It is a maximum at the disruptive critical voltage  $e_o$ , and decreases above and below  $e_o$ , and is with fair accuracy represented by the probability curve

$$p = q\epsilon^{-h(e_o - e)^2} \quad (37)$$

where  $q$  is a coefficient depending on the number of spots, and  $h$  is a coefficient depending upon the size of spots.

Snow, sleet, and rain losses seem to be of the same nature, but frequently of far greater magnitude.

In equation (37),  $q$  and  $h$  naturally cover a wide range of values, depending upon the condition of the conductor surface. Since the losses near the corona starting point, which this equation involves, are extremely small and subject to change due to the slightest surface variations, it is difficult to conceive of a practical equation that would serve under all conditions. Experimental values near  $e_o$  are taken from Table XLIII and tabulated in Table LX, together with values calculated by the quadratic law. Corresponding experimental and calculated values are subtracted and also tabulated.

TABLE LX.—LINE A 1-2-3-4 FROM TABLE XLIII, TEST 36  
 $c^2 = 0.0117 e_o = 72.2$

Kilovolts between conductors $e'$	Kw. exp. $p_o$	Kw. $p =$ $0.0117(e - e_o)^2$	Excess loss $p_l = (p_o - p)$	$\log_e p_l$	$(e_o - e)^2$
120.4	0.11	.....	0.11	2.40	146.5
130.2	0.15	.....	0.15	2.71	49.0
139.2	0.22	.....	0.22	3.09	6.2
150.0	0.40	0.10	0.30	3.40	8.5
159.0	0.79	0.63	0.16	2.77	54.7
165.8	1.42	1.34	0.08	2.10	11.7

Figure 157 is plotted to a large scale to show the excess loss near  $e_o$ . As this is for large conductors,  $e_o$  and  $e_v$  are near together, and the effect of (b) predominates. In order to see if equation (37) holds, write

$$\log_e p_l = \log q - h(e_o - e)^2$$

Then the curve between  $\log p_l$  and  $(e_o - e)^2$  should be a straight line. This is shown in Fig. 158.

Values of  $q$  and  $h$  for Line A are of the order shown in Table LXI below.

TABLE LXI

Test No.	$q$ per cm. total conductor	$h$
30	$3.19 \times 10^{-6}$	0.0220
105	$2.47 \times 10^{-6}$	0.0208
103	$2.74 \times 10^{-6}$	0.0304

Figure 156 is plotted from values for a small smooth conductor. Here  $e_o$  and  $e_v$  are far apart and, as the curvature of the conductor surface is of the same magnitude as its irregularities, they do not greatly influence the loss. The (a) effect here predominates—that is, the loss near  $e_o$  is lower than that shown by the quadratic law.<sup>1</sup>

The loss between  $e_o$  and  $e_v$  is unstable as it depends upon surface conditions. In all cases the quadratic law is closely followed above  $e_v$ , and on large practical sizes of conductors with sufficient accuracy over the whole range.

In long lines where the irregularity factor varies at different points or where  $e_o$  varies due to other causes, the total loss would be the sum of losses on the different sections, thus

$$P = K l_1(e - e_{o1})^2 + l_2(e - e_{o2})^2 + l_3(e - e_{o3})^2$$

where  $l_1, l_2$ , etc., are the lengths of the sections and  $e_{o1}, e_{o2}$ , etc., are the corresponding disruptive voltages ( $e_o$ ).

It is obvious that loss in any section would not start until the applied voltage became equal to the  $e_o$  voltage for that section.

**Temperature and Barometric Pressure.**—Values of the disruptive critical voltage  $e_o$  covering a considerable temperature range are tabulated in Table LXII. Correction is made to a barometric pressure of 76 cm. on the assumption that  $e'_o$  varies directly with the pressure. In Fig. 159,  $1/e'_o$  is plotted with temperature. The straight line through these points cuts the temperature axis at  $-273^\circ\text{C}$ . or absolute zero. Temperature

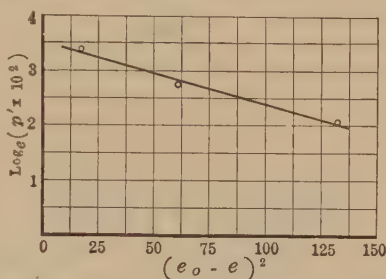


FIG. 158.—Determination of equation (37).

<sup>1</sup> This condition is likely to obtain to a greater extent at high altitudes as  $e_o$  and  $e_v$  are farther apart.

TABLE LXII.—TEMPERATURE AND DISRUPTIVE CRITICAL VOLTAGE  $e_0$ .  
(Standard Line A 1-2-3-4)

Test No.	Temperature		Bar. cm.	$e'_0$ kv. bet. lines	$e'_0$ corr. to 76 cm.	$1/e'_0$	Weather
	Wet	Dry					
18	16.0	18.5	75.5	138.5	140.0	0.00715	Bright sun
15	20.0	22.0	75.2	140.0	142.0	0.00705	Cloudy sun
37	10.0	13.0	75.7	141.0	142.0	0.00705	Bright sun
36	10.0	12.0	75.0	144.2	146.5	0.00683	Cloudy
109	-3.0	-2.0	73.9	148.8	150.8	0.00663	Hazy sun
84	1.0	3.0	75.2	149.0	151.0	0.00662	Cloudy
101	-1.0	-1.0	74.7	153.8	156.8	0.00638	Cloudy
103	-4.9	-4.5	75.7	155.3	156.7	0.00638	Sun
104	-9.5	-9.5	76.2	157.0	157.0	0.00637	Sun
119	-6.5	-6.0	76.5	156.6	156.1	0.00642	Sun
105	-13.0	-13.0	76.2	161.0	161.0	0.00622	Sun

was always measured in the shade. The points that do not fall well on the curve are the summer sunny day points. This is what would be expected, as the conductors were at a higher temperature than the recorded air temperature.

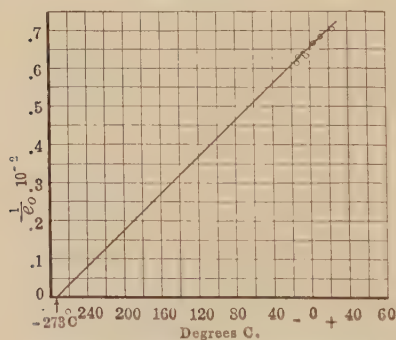


Fig. 159.—Effect of temperature on  $e_0$ .  
(Data from Table LXII.)

Figure 159 shows that the disruptive critical voltage or the disruptive gradient varies inversely as the air density. The data range, however, is not great.

The density of air at 25°C. and 76 cm. barometric pressure is taken as the standard.

#### Humidity, Smoke, Wind.

**Humidity.**—Line A was kept as a standard throughout the tests. A careful study of the disruptive critical voltage and  $e^2$  shows no appreciable effect of either humidity or “vapor products:”<sup>1</sup> (see Table LXIII). Visual tests, made on two short parallel wires indoors over a great humidity range, also bear this out.

It is quite probable that humidity has some slight effect on the loss after corona has once formed due to the change of the

<sup>1</sup> Mershon, *Trans. A.I.E.E.*, p. 845, 1908.

TABLE LXIII.—STANDARD LINE A.<sup>2</sup> CONDUCTORS 1-2-3-4

Test No.	Temperature		Relative humidity	Vapor product	$g_0$ reduced to 25 deg. C., 76 cm. bar.
	Wet	Dry			
15	20.0	22.0	0.84	0.55	18.8
18	16.0	18.5	0.75	0.35	18.5
36	10.0	12.0	0.78	0.25	18.8
37	10.0	13.0	0.67	0.21	18.3
84	1.0	3.0	0.69	0.11	18.7
101	-1.0	-1.0	1.00	0.17	19.2
103	-4.9	-4.9	1.00	0.13	18.9
104	-9.5	-9.5	1.00	0.08	18.6
105	-13.0	-13.0	1.00	0.06	18.8
109	-2.0	-2.0	1.00	0.12	18.7

<sup>2</sup>Line A was kept at constant test conditions for use as a standard in the study of varying atmospheric conditions, etc.

gas into vapor and the agglomeration of the water particles by the ions. This is noticed in the spark-over between needle points at very high voltage. In this case there is a very heavy brush discharge before spark-over. The sparking voltage increases with increasing humidity, due to the fog formed, when there is not a mixture of two gases, air and water vapor, as in the case where humidity is concerned, but actual water particles are in the air. The effect of humidity on the spark discharge observed by the author is discussed in Chap. V. Greater loss should be expected in corona measurements during fog, due to charge and discharge of the water particles. This causes loss at lower voltages and has the effect of decreasing the critical point.

While humidity has no effect on the starting point of corona, an effect might be expected on the loss after the discharge had already started. The reason that this is inappreciable is because the corona discharge from wires covers very little space.

*Smoke.*—It was difficult to get measurements to show the effect of smoke, as the prevailing winds were over the fields toward the city. At one time, however, during a change in the wind, thick smoke was blown over the line from smoke stacks of a factory, and the loss was increased. This, however, will probably not be a serious consideration in practice.

*Wind.*—Losses measured during very heavy winds show no variation from losses measured during calm weather. That the



losses do increase with increasing air velocity has been shown in laboratory apparatus. There is, however, no appreciable effect due to the comparatively low air velocity in practice.

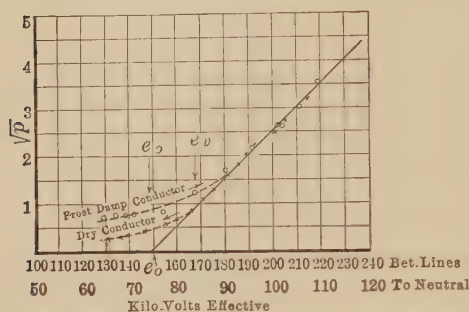


FIG. 160.—Corona loss with frosty and dry conductors.

(Conductor length, 109,500 cm. Spacing, 310 cm. Diameter, 1.18 cm. 3/0, 7-strand cable. Line A. Temp.,  $-2^{\circ}$  C. Bar., 74 cm.)

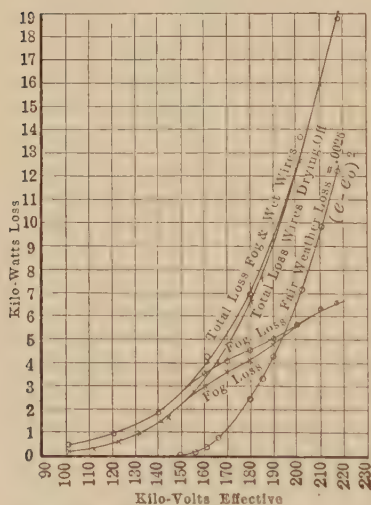


FIG. 161.—Corona loss during fog; conductors wet.

(Conductor length, 109,500 cm. Diameter, 1.18 cm. Spacing, 310 cm. 3/0, 7-strand cable. Line A. Temp., 2. Bar., 75.5.)

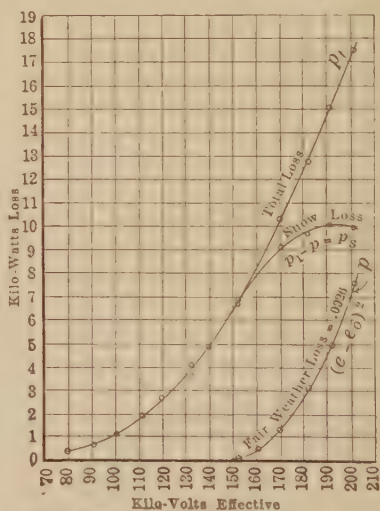


FIG. 162.—Corona loss during snow storm.

(Conductor length, 109,500 cm. Diameter, 1.18 cm. Spacing, 310 cm. 3/0, 7-strand cable. Line A. Temp., 0. Bar., 74.2.)

### Moisture, Frost, Fog, Sleet, Rain, and Snow.—

During some of the first tests, it was noted that the losses were sometimes greater on the “going-up curve” than on the “coming-down curve,” especially in the early mornings after heavy dew. The losses became less after the line had been operated for a while at high voltage. Figure 160 shows this

well for a conductor with a coating of frost. This excess loss was thought, at first, to be due to leakage through moisture on the

insulators. Insulators were put up without line wires, but measurements showed a very small insulation loss even during storms. It was then concluded to be due to moisture on the conductors themselves. Visual tests made on short lengths of wet

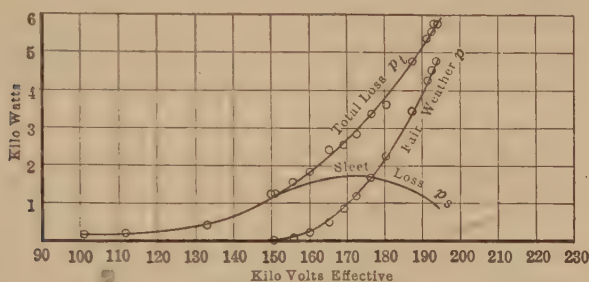


FIG. 163.—Corona loss during sleet storm.

(Conductor length, 109,500 cm. Diameter, 1.18 cm. Spacing, 310 cm. 3/0, 7-strand cable. Line A. Temp.,  $-1.0$ . Bar., 75.4.)

and dry cables showed this in a very striking manner. Two parallel dry cables were brought up to the critical point. Water was then thrown on the cables. What had been a glow on the surface of the dry cables now became, at the wet spots, a discharge extending as much as 5 to 8 cm. from the cable surface. This discharge reminded one of an illuminated atomizer. Illustrations (Figs. 67 and 68) show this but a greater part of the effect is lost in reproduction. The wires became quite dry and down to normal discharge after running at high voltage for a very few minutes.

The curves (Fig. 161), taken during the fog also show the combined effect of condensed moisture on the cables and free water particles in the air. The moisture particles on the conductor become charges and are repelled. The particles in the air also become charged and discharged, thus increasing the loss very greatly above that for dry conductors.

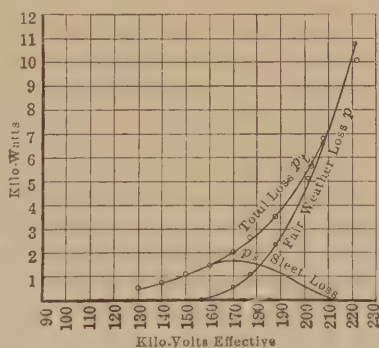


FIG. 164.—Corona loss with sleet on the wires.

(Conductor length, 109,500 cm. Diameter, 1.18 cm. Spacing, 310 cm. 3/0, 7-strand cable. Line A. Temp. 10.0. Bar., 76.)

The losses during snow and rain storms are much greater than fair weather losses at the same temperature and barometric pressure. In Fig. 162, the actual measured loss is plotted and also a corresponding calculated fair-weather loss. The difference between the two curves shows the excess loss due to snow. The effect of snow is greater than that of any other storm condition. This is because the particles are larger and a greater number strike the line, or come near the line.

The sleet curves are of special interest. Sleet had already started to form on the conductors, and was still falling when the tests were started. Figure 163 shows the loss curves. After the curves were taken, the line was kept at 200,000 volts for over an hour with no apparent diminution of sleet. This seems to show that sleet will form on high-voltage transmission lines.

The day after these tests were made was bright and clear and the conductors were still coated with sleet. A set of readings was taken, and it is interesting to note that the excess loss here is as great as when sleet was falling (see Fig. 164).

The excess loss for sleet, rain, or snow storms (over the fair-weather loss) seems, with increasing voltage, to approach a maximum and then to decrease again (the latter at a value very far above the disruptive critical voltage), and the curves of loss seem to have the general shape of the probability curve, as is to be expected, theoretically.

The above readings show the importance of taking weather conditions into account in the design of high-voltage transmission lines.

**Corona Loss Measurements with the Cathode Ray Oscillograph.**—An extensive corona loss investigation was carried out using the low-voltage, hot-filament, cathode-ray oscillograph<sup>1</sup> (see page 39, Chap. III; and page 99, Chap. IV).

The general arrangement for corona measurements is shown in Fig. 165. The measurements were usually made between a single wire and a plane. Precautions were taken to eliminate the end effect by making the measurements on about 10 ft. of wire in the central part of the plane. Precautions were also taken to guard against stray fields and to prevent phase angle displacement errors.

<sup>1</sup> PEEK, F. W., JR., "Law of Corona and the Dielectric Strength of Air IV," *Trans. A.I.E.E.*, p. 1009.

LLOYD and STARR, "Corona Loss Measurements by Means of the Cathode Ray Oscillograph," *Trans. A.I.E.E.*, p. 997, 1927.

With the above arrangement, the field across one pair of plates is proportional to the voltage while that across the other pair is proportional to the current. When voltage is applied across a capacity load, such as a conductor and ground plane, below corona, an ellipse is described, as shown in Fig. 166(a), the abscissas being proportional to the instantaneous voltages and the ordinates to the instantaneous current. These figures are

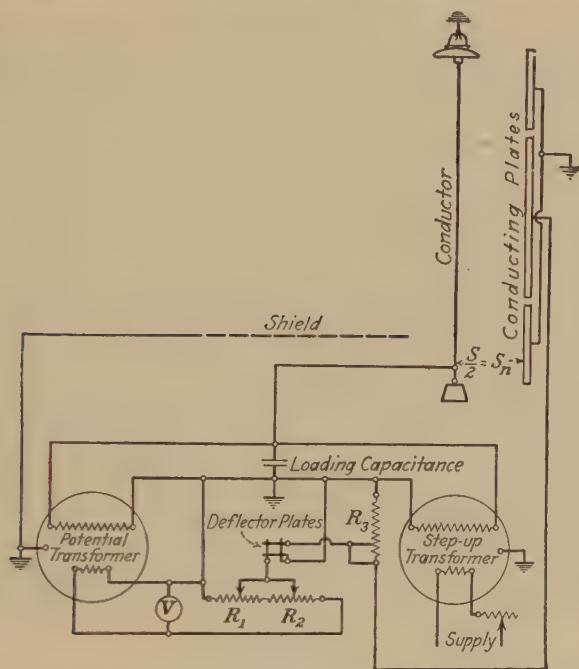


FIG. 165.—Arrangement of vertical ground plate and conductor for study of corona by means of cathode-ray oscillograph.

recorded photographically (see page 100, Chap. IV). The voltage deflections to the left are positive, while those to the right are negative. Positive currents cause deflections above the horizontal axis and negative currents below the axis. If the voltage wave is known, the voltage and current waves can be plotted, as shown in Fig. 85, page 100. As soon as the voltage of the conductor is raised above the corona starting value, the corona current component adds to the wattless capacity current and the ellipse becomes distorted, as shown in Fig. 166(b). The cyclogram then represents a power loss. This loss



is easily obtained by measurements of the instantaneous voltage and current and by simple calculations as follows:<sup>1</sup>

Each figure is divided into an integral number of equal time sections and the product of the mean ordinate by the mean abscissa is obtained for each section. The average of all such products is then multiplied by the circuit calibration constants, volts, and amperes per unit deflection of the cathode beam.

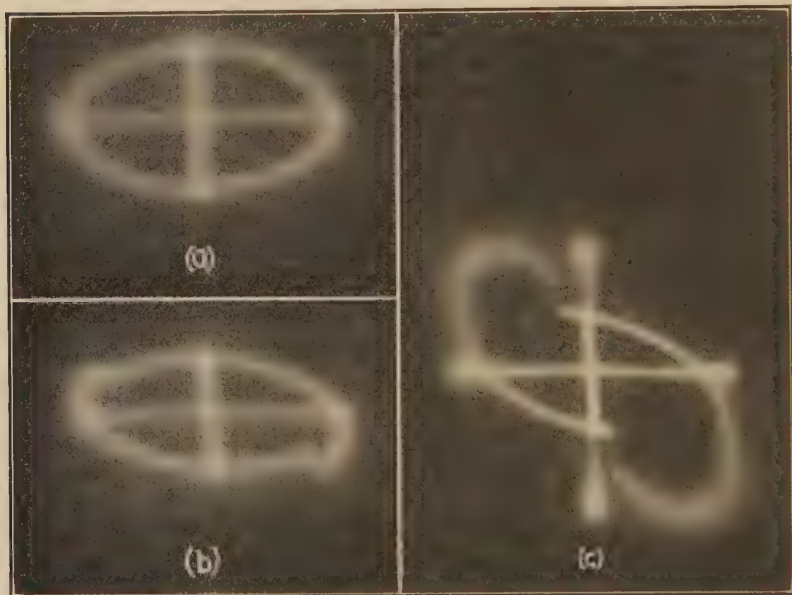


FIG. 166.—Corona current cyclograms.

- (a)—Below corona starting voltage.
- (b)—Just above corona starting voltage.
- (c)—Considerably above corona starting voltage.

The result is expressed in watts. This is equivalent to transcribing the figures to rectangular coordinates and then integrating the power wave in the usual manner. Power of the order of 0.1 watts can be measured with an accuracy of about 1.0 per cent.

Figures 167, 168, 169, and 170 show some of the corona loss curves obtained in this investigation. These data checked the earlier work<sup>1</sup> in that the losses above the  $e_0$  values follow the quadratic law.

<sup>1</sup> PEEK, F. W., JR., "Law of Corona and Dielectric Strength of Air I," *Trans. A.I.E.E.*, 1911.

LLOYD and STARR, "Corona Loss Measurements by Means of the Cathode Ray Oscillograph," *Trans. A.I.E.E.*, p. 997, 1927.



A short test was also made on an artificial corona set-up. In this, series condensers were each paralleled by a spark gap set to breakdown at the proper voltage, so as to simulate, roughly, the action of corona in its successive breakdown of the layers of air about a conductor. Some of the corona cyclograms secured in this test are shown in Fig. 171. It is apparent that they are very

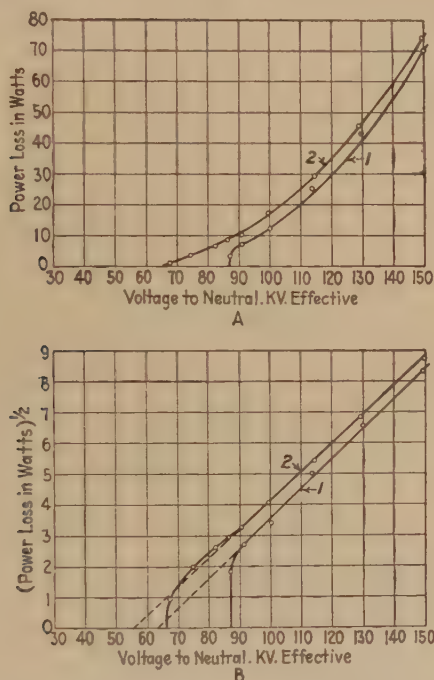


FIG. 167.—Corona loss measured by cathode-ray oscillograph.

Conductor: 0.928 cm. diameter.

Surface conditions: (1) smooth  
(2) mutilated.

Spacing: 161 cm. to neutral.

Length: 305 cm.

Frequency: 60 cycles.

similar to those obtained on actual conductors, except that there is not the shift in the figure due to the variable capacity effect present in real corona.

Corona loss can be studied from a somewhat different angle by replacing the resistance  $R_3$  (Fig. 165) by a capacitance or by a parallel combination of capacitance and high resistance. The ordinates of the cyclograms obtained are then proportional to

the instantaneous charges induced on the ground plate by the voltage on the conductor. Figure 172 shows a cyclogram obtained in this manner. The area of the cyclogram represents

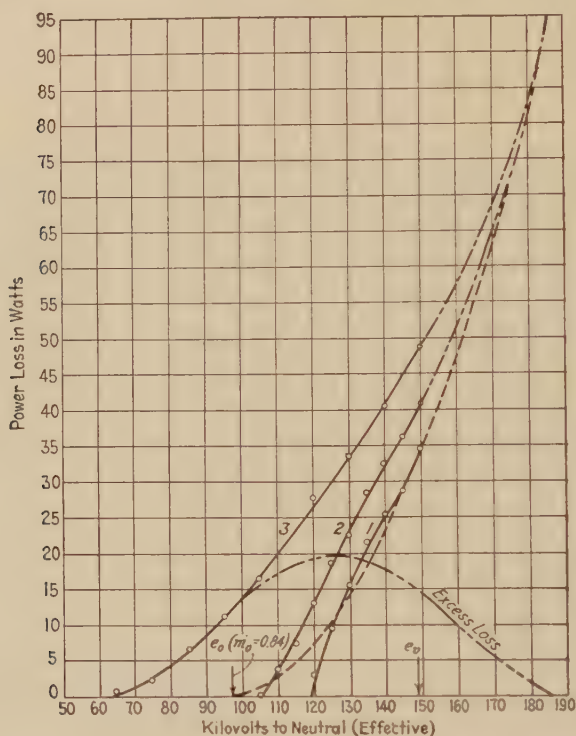


FIG. 168.—Corona loss measured by cathode-ray oscillograph.

Conductor: A. C. S. R. Cable  
 Aluminum—30 strands,  
 336,400 c.m.  
 Steel—7 strands  
 Diameter—0.741 inch.

Length: 10 ft.  
 Spacing to neutral: 63.5 inches.  
 Surface conditions: (1) smooth  
 (2) rough  
 (3) badly mutilated.

Frequency: 60 cycles.

the power loss per cycle for the particular conductor and conditions. This method of measurement has been used extensively by Dr. Ryan in his study of corona loss.<sup>1</sup>

<sup>1</sup> RYAN, H. J., *Trans. A.I.E.E.*, 1914.

RYAN and HENLINE, *Trans. A.I.E.E.*, 1924.

**Consideration of Space Charge Movement in Corona Power Loss.**—The mechanism of corona has been described (See Chap. IV, page 100) wherein the charge of the ionized space of the first half-cycle, in effect, adds to the charge on the conductor of the

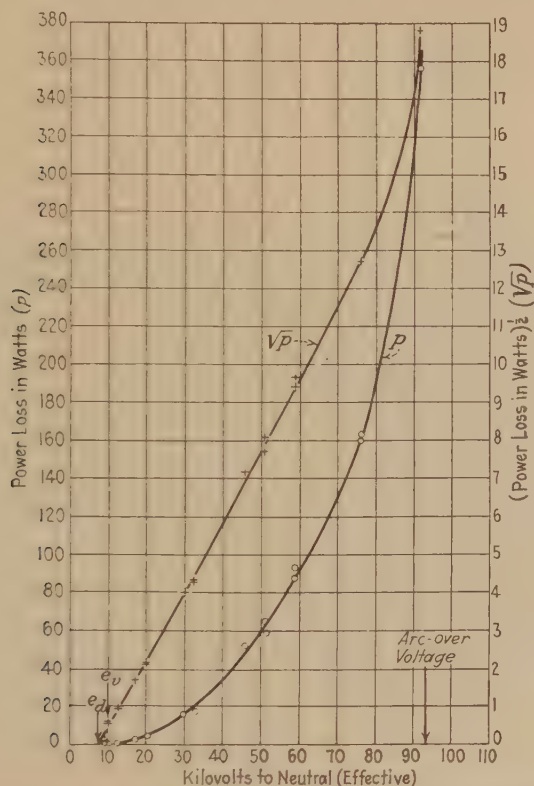


FIG. 169.—Corona loss measured by cathode-ray oscillograph.

Conductor: 0.015 in. diam. smooth.

Spacing: 7.5 in. to neutral.

Length: 10.0 ft.

Frequency: 60 cycles.

next half-cycle so that breakdown occurs when the sum of these two charges is equal to  $q_v$ , or causes a stress,  $g_v$ .

The space charge cylinder moves out from the conductor with increasing voltage, and is charged through the corona arcs until the wave reaches maximum. The arcs then die out or corona stops. Part of the energy in the "space charge" field is stored electrostatically and is returned to the circuit, and part is not

returned but is dissipated in heat, light and conduction. When the conductors are far apart, the main part of the loss occurs in the space between the conductor and corona cylinder. Where the conductors are close together, or the voltage is approaching the spark-over voltage, a conduction loss is also caused by ions

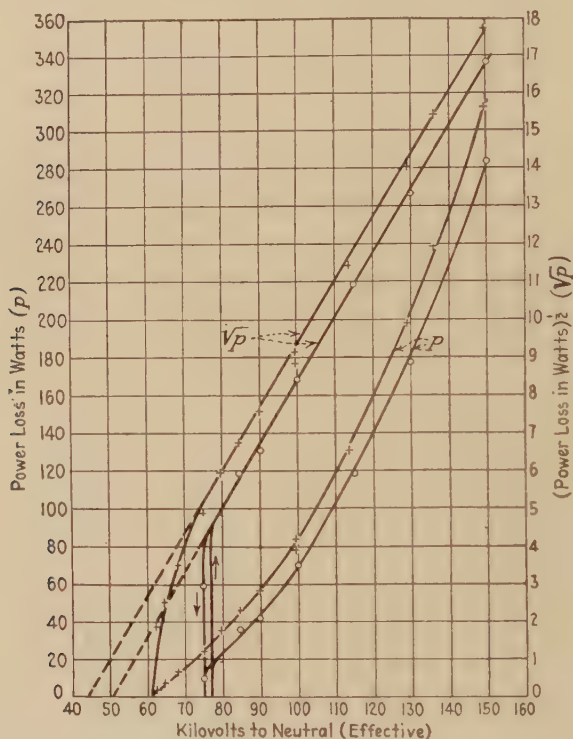


FIG. 170.—Corona loss measured by cathode-ray oscillograph.

Conductor: 0.365 in. diameter.

Surface conditions: ° smooth

+ rough

Spacing to neutral: 21.5

Length: 10 ft.

Frequency: 60 cycles.

migrating to the opposite conductor. The measurements show that over a very wide range of conditions the loss follows the quadratic law

$$p = k_1(e - e_0)^2$$

An examination of the mechanism makes this appear the rational form for the loss to take. This seems so for the following

reasons: The space charge is proportional to  $(e - e_0)C$ . Energy is required to move this charge through the field or through the voltage from the conductor to the corona cylinder. The voltage between the conductor and the space charge or corona cylinder is proportional to  $(e - e_0)$  and, in fact, appears to equal  $(e - e_0)$  for the higher frequencies and very large spacings. The energy may be considered as being lost in the resistance of the corona arcs charging and discharging the corona cylinder. The loss is thus

$$w = (e - e_0)(e - e_0)kC = (e - e_0)^2 kC$$



FIG. 171.—Artificial corona cyclograms.

- (a)—Just above corona starting voltage.
- (b)—Considerably above corona starting voltage.
- (c)—Over twice corona starting voltage—corona starting “below zero.”

or the power

$$p = 4fCk(e - e_0)^2$$

The above relation checks the measured values for large spacings at 60 cycles and for all spacings at 420 cycles. When the frequency is low or when the spacing is small, ions must pass from conductor to conductor. This is equivalent to a leakage loss or loss in a resistance intermittently placed from conductor to conductor. Then

$$p = k_2(f + a)C(e - e_0)^2$$

wherein the factors  $a$  and  $k$  are an integral part of the equation



and were originally determined empirically in the quadratic law. The part of the energy in the space charge that is returned to the circuit at the proper part of the wave is not lost but gives the extra capacity effect of corona.

There is no loss at  $e_0$  because breakdown does not take place until the voltage  $e_v$  is reached. There is then a sudden break over a finite distance from the conductor and the loss falls on the quadratic curve with  $e_0$  as the disruptive critical voltage. The stress between the conductor and the corona cylinder is not reduced to zero when corona starts but has a value approximately equal to  $g_0$  or  $g_d$  at the conductor and decreases outward to the

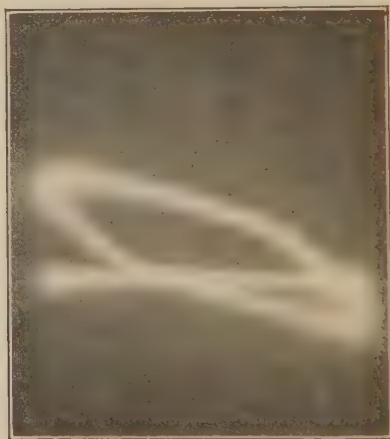


FIG. 172.—Corona loss cyclogram indicating coulomb-voltage relation per cycle

corona cylinder along approximately the same curve that obtained just before corona started. Beyond the corona cylinder, the average stress must be higher or the curve flatter to maintain the voltage proportional to  $e_0$  across the portion that is not ionized.

It might be expected at first glance that the disruptive critical voltage should be  $e_v$  rather than  $e_0$ , since loss does not start on polished conductors until  $e_v$  is reached. A more critical examination, however, shows that following the initial break controlled by  $g_v$ , the strength of air becomes  $g_0$ . Thus, although  $g_v$  controls the start of the loss, after the initial break occurs and corona extends out, the controlling gradient is  $g_0$ . This follows up to the maximum of the voltage wave when corona stops.  $g_v$  is required to cause the next start, etc.

It is interesting that when the applied voltage is zero, all of the energy is on the space charge and is

$$(e - e_v)^2 \frac{CC_2}{2C_1}$$

**Very High Frequency.**—Corona losses at very high frequency are difficult to measure. The curve in Fig. 173 is interesting. The drawn curve is calculated from formula 34(a); the points are measured values. Power was supplied from an Alexanderson 100,000-cycle alternator. The power was measured by adjusting reactance and capacity until unity power factor was obtained. The watts input was then the product of volts and amperes as measured by hot wire meters.

This good check seems to show that the formula applies over a large range, but complete conclusions cannot be drawn from this small amount of data.

Recent corona loss measurements at 420 cycles, made with the cathode-ray oscillograph, are shown plotted in Fig. 174. The ordinates used are the square root of the power and the straight line relation again indicates how well the quadratic law applies.

**Three-phase Corona.**—For equal voltage between lines, the voltage gradient at the conductor is 15.5 per cent. greater for equilateral three-phase lines than for single-phase lines with the same conductor and spacing. This means that corona starts at 15.5 per cent. lower line to line voltage three phase than single phase or that corona starts at the same *line to neutral voltage*, for both three-phase and single-phase lines. The *loss per conductor* at a given *voltage to neutral* is equal on practical single-phase and three-phase lines. This is confirmed by actual measurements made by the author (see page 374).

**Harmonics and Line-charging Current as Affected by Corona in Practice.**—An investigation was made to study the effects of corona in producing voltage and current harmonics in transmission systems.

When an alternating voltage higher than the critical corona voltage is applied to a conductor, the loss starts at a given point

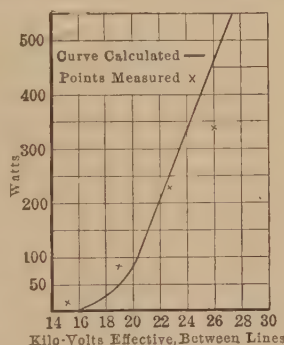


FIG. 173.—Corona loss at high frequency.

(Two parallel wires. Spacing, 67 cm. Radius of wire, 0.127 cm.  $f = 100,000$  ~. Total length, 200 cm.) Tests by Alexanderson.

during each half cycle as the voltage increases, continues over part of the half cycle, and finally ends at a given point. A varying amount of corona current and loss thus occurs during each voltage wave (see Fig. 85, page 100). It follows that if a sine-wave voltage high enough to cause corona loss is applied to conductors, the current cannot follow a sine wave but must be distorted or contain harmonics. The phenomenon is, in fact,

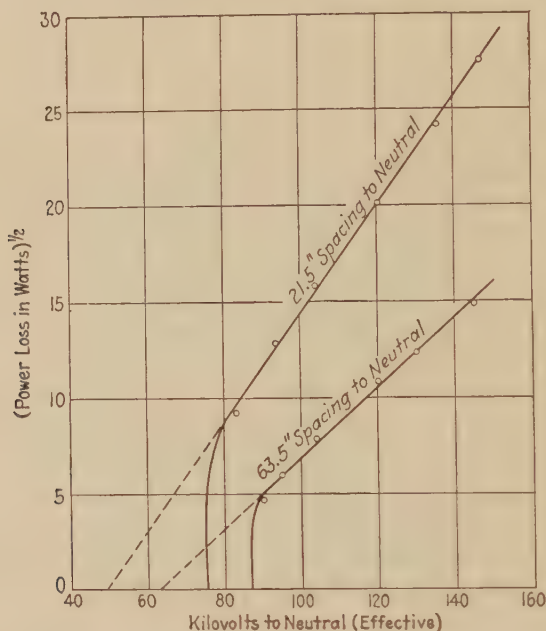


FIG. 174.—Corona loss at 420 cycles measured by cathode-ray oscillograph. (Expressed as  $P^{1/2}$  to show quadratic law relation.)

Conductor: 0.365 in. cm. diam., polished.

Length: 10 ft.

very similar to that in the exciting current wave of a transformer where distortion occurs chiefly due to changing permeability during each half cycle.

When corona loss occurs on three-phase lines with grounded neutral, three single-phase paths are afforded for the triple-frequency component of the current through the lines, the capacity to ground, the ground and the neutral ground connection, as shown in Fig. 175. If a transformer with a grounded neutral is used at the receiving end, part of the current may also be supplied through the transformer. The triple-frequency

currents cannot flow in the lines if the neutral is not grounded. This follows because the triple frequency components are  $3 \times 120$  degrees = 360 degrees apart or in phase. Fundamentally, the sum of the currents flowing to the neutral point must be zero. Since the currents are in phase, the triple component can satisfy this condition only when it is zero; it can flow over the lines only when single-phase paths are afforded through the grounded neutral. Since, with a sine-wave voltage, the corona current inherently contains a third harmonic (see Fig. 85), the voltage between line and neutral must be distorted if this component is suppressed. Higher odd harmonics are also caused by corona. With symmetrically arranged conductors, however, only the third and odd multiples of the third can appear on the lines.

Tests were made on short three-phase lines of very fine wire so that the corona loss would be excessive and exaggerate con-

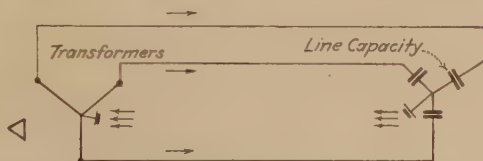


FIG. 175.—Three single phase paths for corona triple frequency current.

ditions.<sup>1</sup> The transformers were of such size that the corona loss was an appreciable load. A sine-wave voltage was used. There was a large triple-frequency current in the neutral.

Figure 176 gives a set of curves showing the corona characteristics of a three-phase line with delta Y-connected, grounded neutral transformers at the generating end and open-circuited at the receiving end. All of the measurements, with the exception of the line and neutral currents, were made on the low side but are corrected for losses and referred to the high side. The high side or capacity current starts at zero and increases in a straight line until the corona point is reached. The current then increases much more rapidly than the voltage. This increase in current is caused by a loss component and an added reactive component. The two components are plotted. It would seem that the apparent capacity of the line increases very rapidly with increasing voltage above the corona point. To account for the reactive component from a purely 60-cycle

<sup>1</sup> PEEK, "Voltage Harmonics Caused by Corona," *Trans. A.I.E.E.*, June, 1921.





## CHAPTER VII

### CORONA AND SPARK-OVER IN OIL AND LIQUID INSULATIONS

The most common liquid insulation is transformer oil obtained by fractional distillation of petroleum. This oil has various characteristics, in regard to flashing point, freezing point, viscosity, etc., depending upon the specific use to which it is to be put. The average characteristics of transformer oil are as follows:

	Medium (Transil—6)	Light (Transil—10c)
Flashing temperature....	180°–190° C.	133° C.
Burning temperature....	205°–215° C.	148° C.
Freezing point.....	–10°––15°	–40° C.
Specific gravity.....	(at 13.5° C.) 0.865–0.870	(at 15° C.) 0.87
Viscosity (Saybolt test)..	(at 40° C.) 100–110 sec.	(at 37.8° C.) 57 sec.
Acid, alkali, sulphur, moisture.....	None	None

Various other oils are insulators, as gasoline and cylinder oil; animal oils, as fish oil; vegetable oils, as linseed oil, nut oil, china wood oil, etc. All of these, when pure, have the same order of dielectric strength.

The so-called compounds made by dissolving solid gums in oil to increase viscosity are generally unreliable, unless used dry as varnish. Under the dielectric field the dielectrics of different permittivities tend to separate, and there is considerable loss. As in air there is very little loss in pure oil until local rupture, that is, brush discharge or corona, occurs.

The dielectric strengths of oils are usually compared by noting the spark-over voltage between two parallel brass discs 1.0 in. in diameter, and 0.1-in. separation. The spark-over voltage for good oils in the above standard gap should be between 50 and 70 kv. maximum, and hence, if the voltage wave is a sine, from 30 to

50 kv. effective.<sup>1</sup> No insulating oil should be used whose strength is below 22 kv.

**Different Electrodes.**—In Fig. 177 are plotted spark-over curves for different electrodes in good transformer oil. The characteristics are very much the same as for air, excepting the apparent strength is very much higher.

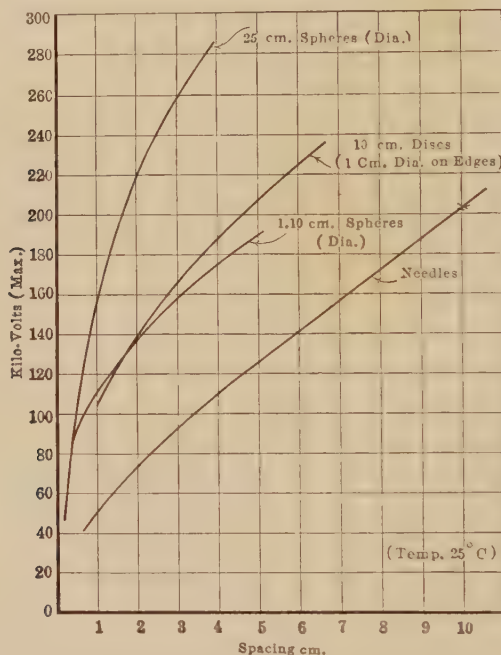


FIG. 177.—Spark-over of various shaped electrodes in oil at 60 ~.

Spark-over values for oil up to very high voltage and for various conditions will be found in the Appendix on pages 378, 393, 394, and 395. (See also curve on page 226.)

**Variation in Spark-over Voltage.**—If a number of successive spark-over tests are made in a large tank of oil, it will be found that there is considerable variation between the tests. This is illustrated in Fig. 178 for a large and a small gap. Note that the percentage difference is greater for the small gap. For the large gap, the difference may be 10 per cent. plus or minus from the average.

<sup>1</sup> The breakdown voltage of oil like that of air depends upon the maximum point of the wave.

About the same variation is found if the tests are made in a small receptacle and the oil is changed after each spark-over.

This variation is not appreciable in practice where barriers are used.

**Oil Under Pressure.**—When oil is placed under high pressure, the dielectric strength increases to some extent. This may be due to the increased strength of the occluded gases under pressure

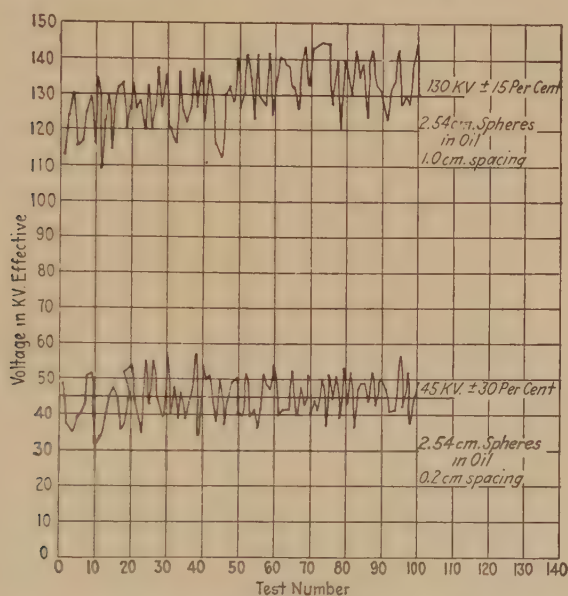


FIG. 178.—Curves showing variation of dielectric strength of oil during one hundred successive tests.

**Effect of Moisture.**—The slightest trace of moisture in oil greatly reduces its dielectric strength. The effect of moisture is shown in Fig. 179(a) for a disc gap. Water is held in suspension in oil in minute drops. When voltage is applied, these drops are attracted by the dielectric field. Thus they are attracted to the denser portions of the field and may form larger drops by collision. When attracted to and after touching a metal part, and, thus, having the same potential, they are immediately repelled. If the field is uniform, the drops form in conducting chains along the lines of force. It can be seen that the effect of moisture should vary greatly with the shape of the electrode, and with some shapes the moisture may even be

removed from the space between the electrodes by the action of the field, in which case its presence would not be detected by low-voltage breakdowns. In fact, for needle points and most electrodes at large spacing, the breakdown voltage for wet and dry oil is practically the same. Some investigators have claimed to have found an actual rise in the dielectric strength when moisture is added to dry oil under certain conditions.<sup>1</sup> Whether the water particles arrange themselves to redistribute the electrostatic stresses more uniformly in the oil, and thus increase the strength, is difficult to say. In transformers, moisture will generally be attracted to points under greatest stress. The most effective way of removing moisture is by filtration through blotting paper. Dirt in oil may have an effect very similar to moisture and the small conducting particles be made to bridge between electrodes by the dielectric field. Solid barriers are

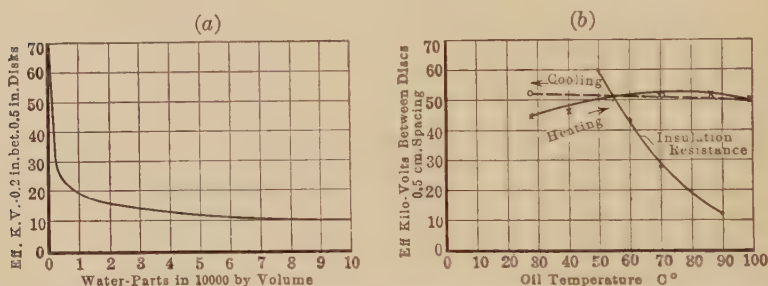


FIG. 179.—(a) Effect of water in oil. (Breakdown approximately proportional to gap spacing for short spacings.) (b) Effect of temperature on dielectric strength and insulation resistance. Tests at 60. ~

effective in preventing the complete lining up of moisture particles between electrodes. While they generally do not increase the puncture voltage for dry oil, they very greatly increase reliability in apparatus (see page 255 and Appendix).

**Temperature.**—Temperature over the operating range has very little influence on the strength of oil. The strength increases at the freezing point. The curve is shown in Fig. 179(b). The insulation resistance is also shown. The increase in strength with temperature is often only apparent and due partly to the decreasing insulation resistance which allows more current to flow through the oil, which tends to even up the stress, but mostly to the drying out of moisture particles by the high temperature. The increase at freezing should be expected, as an actual improve-

<sup>1</sup> MINER, C. F., *Trans. A.I.E.E.*, p. 248, 1927.

ment in dielectric properties results. For a perfectly dry oil the strength often decreases with increasing temperature or density, as in the case of air. Some tests have, however, indicated an increase in strength with temperature.

The specific resistance of transil oil (10 c) is approximately:

Temperature, Centigrade	Ohms, cm. cube.
60	$28 \times 10^{11}$
80	$9 \times 10^{11}$
100	$4 \times 10^{11}$
120	$2 \times 10^{11}$

The permittivity is approximately 2.6 times its specific gravity and thus decreases with increasing temperature.

Temperature plays an important rôle in the disintegration of oil. When the latter is heated and exposed to air or oxygen, a chemical reaction slowly takes place. The oil oxidizes to form a finely divided dark solid known as "sludge." An acid is created also. This change is accelerated by heating, being more than proportional to the rise of temperature. The effect varies with different oils but in most cases sludging becomes highly active above 100°C. It is particularly detrimental to cooling in transformers, as the solid deposits impair heat transfers by settling on the surfaces and in the oil passages.

**Spark-over and Corona in Oil.**—The theory of electrical breakdown of oil insulation has yet to be completely understood. The conduction between electrodes at the time of breakdown must take place through a movement of ions or electrons through the oil. It seems quite impossible that these changes could originate from the electrodes due to heat or electrostatic forces. Accordingly, their origin must be looked for in the liquid itself. This, therefore, involves a breaking up into ions of particles of the oil or its contained gas, moisture, or other impurities. This process may take place essentially through collision ionization, so common in pure gaseous conduction, or disruption by heating, or both. It has been suggested that the conduction in oil is of an electrolytic nature.

Some ascribe the breakdown of liquid and solid insulations to the non-homogeneity of the dielectrics, this tending to cause either concentration of electrostatic stresses or heating. This theory assumes, of course, that all dielectrics are non-homogeneous to some extent. Others are of the opinion that impurities,



such as fibers, moisture, etc., are the essential factors in oil failure.

The fact that the dielectric strength of oil increases with increased pressure, which will be alluded to later, lends strong evidence to the theory that the occluded gas may be the principal factor in the breakdown process. Also the oil puncture between flat plates takes place at higher voltages with the plates vertical than when they are horizontal, thereby tending to substantiate the occluded gas effect. In this gas theory it must be assumed that ions are included in the absorbed gases to initiate the ionization process, as a disruption of the oil particles themselves solely by the electric field would require excessive gradients. Gas bubbles usually rise to the surface profusely under voltage stress even before complete breakdown occurs, indicating a change of the oil particles from a liquid to a gaseous state. It is probably when this latter state reaches sufficient proportions to provide this more easily ionized medium in the path between electrodes

TABLE LXIV.—DIELECTRIC STRENGTH OF No. 6 TRANSIL OIL—SPARK-OVER BETWEEN SPHERES AT 60 ~

Spacing, cm.	Radius of spheres, cm.										Needles
	0.159		0.555		1.27		3.12		6.25		
	Kv. max.	Gra- dient max. kv./cm.	Kv. max.	Gra- dient max. kv./cm.	Kv. max.	Gra- dient max. kv./cm.	Kv. max.	Gra- dient max. kv./cm.	Kv. max.	Gra- dient max. kv./cm.	Kv. max.
0.129	44.6	449	48.0	304	47.1	364					
0.198	50.5	360									
0.264	59.2	365	73.9	333	73.5	310	74.3	288	74.8	289	
0.322	65.0	360									
0.378	71.1	364	90.0	295							
0.508	81.0	368			99.0	222	105.0	220	107.0	214	
0.650											41.6
0.766	89.9	353	106.0	225	117.0	187	128.0	182	132.0	180	
1.010	97.6	358	112.0	192			146.0	166	159.0	166	
1.270	104.0	361	116.0	176	157.0	158	171.0	158	177.0	147	57.0
1.780	111.0	384	131.0	171	165.0	143	203.0	137	214.0	130	
2.540	124.0	416	149.0	174	185.0	130	240.0	122	245.0	110	84.0
3.810	145.0	470	172.0	184	206.0	131	266.0	103	280.0	90	108.0
5.080	168.0	542	191.0	192	231.0	133					124.0
7.620											166.0
10.150											203.0

Oil between discs 0.5 cm. apart tested 58.5 kv. max. 25 deg. C.

TABLE LXV.—SPARK-OVER BETWEEN PARALLEL PLATES IN NO. 6 TRANSIL  
OIL AT 60 ~

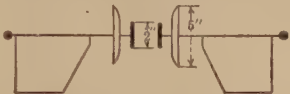
$e$ kv. max.	$X$ spacing cm.	$\vartheta_s \approx \frac{e}{x}$ kv./cm. (max.)	Remarks
34.6	0.254	136.3	
52.3	0.508	102.8	
71.0	0.762	93.0	
106.0	1.015	104.8	Distance between small and large discs = 0.476 cm.
114.0	1.270	89.6	
126.5	1.525	82.8	
125.2	1.270	98.2	
137.5	1.525	90.0	
158.0	1.778	85.0	
167.7	2.03	82.2	Same as above, except distance between small and large discs = 1.58 cm.
187.3	2.29	81.8	
196.5	2.54	77.2	
214.5	2.79	76.6	
225.0	3.05	74.0	
242.0	3.30	73.2	
113.2	1.27	88.8	4-in. flat discs, 0.5-cm. radius edge.
155.5	2.54	61.0	
212.0	5.08	41.7	
269.0	7.62	35.0	

TABLE LXVI.—CORONA IN OIL, WIRE AND PLATE  
(Distance of wire from plate = 16.5 cm. at 60 ~)

Kv. eff.	Radius wire, cm.	$\vartheta_v$ kv./cm. eff.	$\vartheta_v$ kv./cm. max.
50	0.025	278	393
60	0.050	185	262
80	0.0635	201	284
100	0.1520	122	173
55	0.00508	615	870

that complete failure occurs and an arc develops. Any heating that would enter, whether it is the principal factor or not, would surely assist materially in the breakdown process.

Corona in oil is not as steady or definite as in air. It appears to start quite suddenly and extend much farther out from the electrode than corona in air. It is much more difficult to detect

TABLE LXVII.—SPARK-OVER VOLTAGES FOR No. 6 TRANSIL OIL CONCENTRIC CYLINDERS

$R$ cm.	$r$ cm.	Kv. eff.	Kv. max.	$g_s$ max. kv./cm.	$\frac{1}{\sqrt{r}}$	$\frac{R}{r}$	Remarks
3.81	0.032	45.3	64.0	420.0	5.61	120.00	Tests made in long cylinders with belled ends. Oil between standard discs 0.5 cm. apart tested 58 kv. (max.) 25 deg. C.
3.81	0.238	60.0	84.8	127.7	2.05	16.00	
3.81	0.317	60.5	85.5	108.1	1.77	12.00	
3.81	0.635	69.5	98.3	86.3	1.26	6.00	
3.81	0.794	75.0	106.1	85.5	1.12	4.80	
3.81	0.952	73.0	103.2	78.1	1.02	4.00	
3.81	1.111	76.7	108.5	79.4	0.95		
3.81	1.270	76.0	107.5	77.0	0.89	3.00	
3.81	1.587	73.7	104.3	75.1	0.79	2.40	
3.81	1.905	66.3	93.7	70.7	0.72	2.05	
3.81	2.540	45.5	64.3	62.4	0.63	1.57	
6.67	5.560	29.2	41.3	40.6			Tests made on short cylinders where field is somewhat distorted.
6.67	5.080	43.7	61.8	44.8			
6.67	3.970	70.1	99.2	48.1			
6.67	3.240	84.4	119.5	51.0			
6.67	2.230	105.8	149.7	61.2			
6.67	1.955	105.0	148.5	61.9			
6.67	1.615	103.5	146.5	64.0			
6.67	1.270	101.3	143.2	67.5			
6.67	0.953	98.3	139.0	75.0			
6.67	0.635	94.0	133.0	89.2			
6.67	0.477	91.5	129.5	102.8			
6.67	0.318	85.3	120.7	121.0			
6.67	0.159	65.2	92.2	155.5			
6.67	0.079	62.2	88.0	251.4			
11.42	3.930	144.0	203.5	48.3			
11.42	2.280	163.0	230.4	63.0			
11.42	1.910	158.0	223.2	64.5			
11.42	1.270	160.0	226.0	81.5			
11.42	0.880	148.0	209.0	93.0			
11.42	0.520	90.0	127.3	79.5			

the starting point and, unless the conductors are very small or far apart ( $s/r$  large), corona does not appear before spark-over. For instance, in the Table LXVII when the outer cylinder is 3.81 cm. radius and the inner 0.0127 cm. radius ( $R/r = 300$ ), the corona and spark-over voltages are practically the same (see

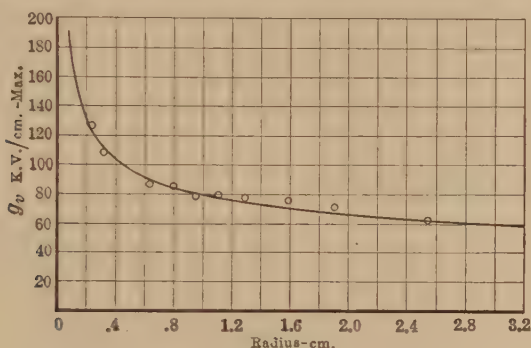


FIG. 180(a).—Strength of oil at 60  $\sim$ .  
(Concentric cylinders— $g_v$  at surface of inner cylinder.)

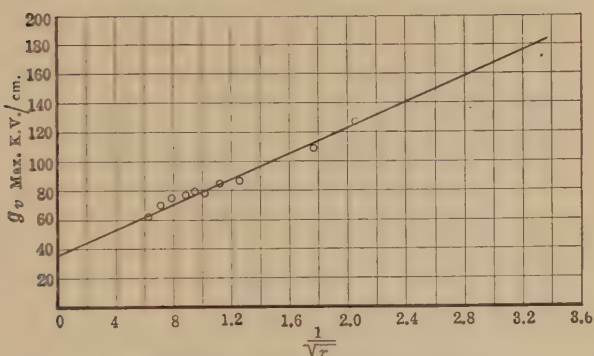


FIG. 180(b).—Strength of oil at 60  $\sim$ .  
(Method of reducing values given in Fig. 180a to equation.)

condition for spark-over and corona, Chap. III). The absence of corona, or rather the simultaneous appearance of corona and spark-over, unless the wires are very small or far apart, seems to mean that the mechanism of breakdown in oil is similar to that in air. Thus, as the voltage is increased, corona rupture occurs; this increases  $r$  to the condition for spark-over.

$$\frac{R}{(r + \text{distance broken down})} = \frac{R}{r_1} < \epsilon$$

and spark follows. The spark-over voltages and corona voltages

up to fairly high ratios  $R/r$  are, therefore, the same and may be used in determining the strength of oil.

The strength of oil for different sizes of wire from Table LXVII is plotted in Fig. 180a. The curve is similar to that for corona in air. Figure 180b shows that a straight line relation holds approximately between  $\frac{1}{\sqrt{r}}$  and  $g_v$ . Values are not used when  $R/r > 3.5$ . Thus, as in the case of air<sup>1</sup>

$$g'_v = g'_o \left( 1 + \frac{\infty}{\sqrt{r}} \right)$$

$$g_v = 36 \left( 1 + \frac{1.2}{\sqrt{r}} \right) \text{ kv./cm. max.}$$

$$g_v = 25.5 \left( 1 + \frac{1.2}{\sqrt{r}} \right) \text{ kv./cm. effective sine wave}$$

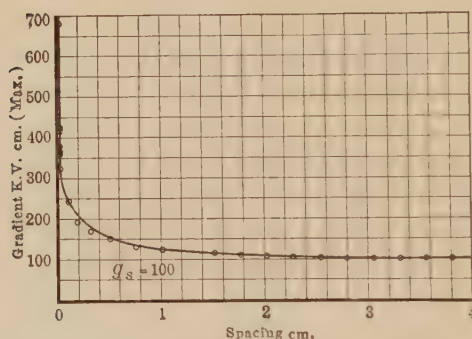


FIG. 181.—Showing increase of strength of oil at small spacings at 60 ~. (Spheres,  $R = 3.33$  cm.)

The ionizing distance is  $1.2\sqrt{r}$  or almost four times that of air.  $g_o$  and  $a$  vary to a considerable extent in oil. Oil should have low strength in bulk, but high apparent strength when subdivided or confined to make use of the large ionizing distance necessary to rupture.

Spark-over voltages and gradients are given for spheres at various spacings in Table LXIV. The characteristics of the curves between gradient and spacing are the same as those for air (see Fig. 42) as shown in Fig. 181. When the spacing is so small that it interferes with the ionizing distance, the apparent strength of oil increases. At spacings above this, the gradient

<sup>1</sup> PEEK, F. W., JR., "High Voltage Engineering," *Jour. Frank. Inst.*, December, 1913.



is constant until the separation is so great that corona forms before spark-over.

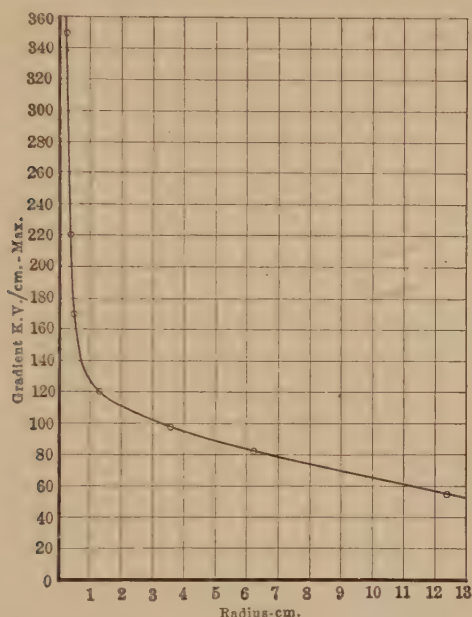


FIG. 182.—Strength of oil between spheres at 60 ~.  
(Data from constant part of the curve.)

TABLE LXVIII.—SPHERES IN OIL  
Gradient at constant part of the curve. Tests at 60 ~.  
Data from Table LXIV

Radius, cm.	Gradient, kv./cm. max.	$\frac{1}{\sqrt{R}}$	Radius, cm.	Gradient, kv./cm. max.	$\frac{1}{\sqrt{R}}$
0.159	348	2.51	1.27	120	0.89
0.237	260	2.05	3.12	98	0.56
0.355	222	1.68	6.25	82	0.40
0.555	169	1.35	12.50	56	0.28

The rupturing gradient at the *constant* part of the curve for various spheres is given in Table LXVIII, and is shown in Fig. 182. This may be written approximately

$$g_s = 28.3 \left( 1 + \frac{4}{\sqrt{R}} \right) \text{kv./cm. max.}$$

The ionizing distance is approximately  $2\sqrt{R}$ .

The spark-over voltages for concentric cylinders, where  $R/r <$  about 5, and for spheres above  $2\sqrt{R}$  spacing on the constant part of the curve, may be approximated by substituting  $g$  in the voltage formula

$$e = g_v r \log_e \frac{R}{r} \text{ cylinders} \quad (\text{use } g_v, \text{ p. 159})$$

$$e = g \frac{X}{f} \text{ spheres} \quad (\text{use } g_s \text{ above})$$

In oil, the apparent strength can be greatly improved by limiting the ionizing distance by barriers, etc. This can be seen in Tables LXIV and LXV, where  $e/X$  is given for parallel planes, and  $g_v$  for spheres. For the small spacings, the apparent rupturing gradient is very high, just as in the case of air. Strengths as

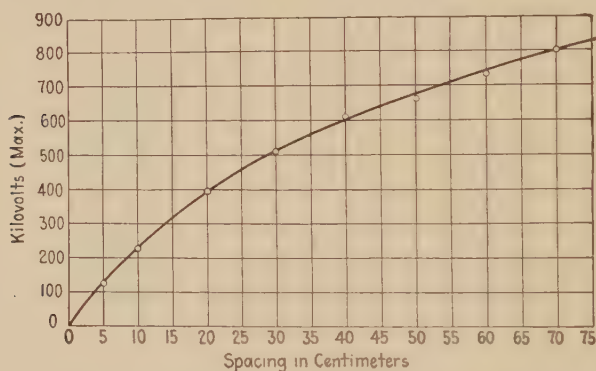


FIG. 183.—60-cycle breakdown voltage of transil oil (10-c) between points.

high as 700 kv. per centimeter have been reached. Insulation barriers give an added effect by preventing moisture particles from lining up.

Care must be taken, however, that the barriers are not so placed as to increase the stress on the oil by the high permittivity of the solid insulation.

Figure 183 shows a spark-over curve of a needle gap in oil, extending up to rather large spacings.

**Transient Voltages.**—Transient voltages of short duration greatly in excess of the low-frequency rupturing voltages may be applied to insulations without rupture. In other words, the rupture of insulation requires not only a sufficiently high voltage but also a definite minimum amount of energy. This means, also, that a definite but very small time elapses between the

application of voltage and breakdown. This is sometimes called the "dielectric spark lag" and has already been discussed for air in Chap. V.<sup>1</sup> At low frequency a given definite voltage is required to cause rupture during the comparatively unlimited time of application. This voltage is constant until the application is limited to a definite minimum time, when a higher voltage is required to accomplish the same results. Such transient voltages of short duration, and impulses of steep wave front, must not be confused with continuously applied high frequency where breakdown will generally take place at lower voltages, due to loss, etc.

In Table LXIX the relative breakdown voltages of gaps in oil, at 60 cycles, and for impulse voltages of steep wave front are given. An impulse voltage much higher than the 60-cycle voltage is required to break down a given gap. If similar air and oil gaps are set to rupture at the same low frequency voltage, a much higher transient voltage will be required to rupture the oil gap than the air gap, indicating greater time. An air gap may thus protect an oil gap, but not *vice versa* (see page 142 and Appendix).

TABLE LXIX.—COMPARISON OF 60-CYCLE AND IMPULSE SPARK-OVER IN OIL AND IN AIR

Oil				Air			
Gap	Spacing, cm.	Kv. 60 cy., max.	Kv. im- pulse, max.	Gap	Spacing, cm.	Kv. 60 cy., max.	Kv. im- pulse, max.
Stand. disc....	0.5	56.6	170.0	2/0 needles	5.1 17.5	50.2 108.0	67.8 198.0
2/0 needles...	1.0	50.2	103.3				
	2.0	68.8	157.0				
	3.0	89.2	233.3				
	4.0	108.0	321.0				
	0.25	37.2	117.3				
2.54-cm. spheres.	0.51	62.8	199.4				
	0.77	87.5	279.0				
	1.02	111.2	337.0				
6.25-cm. spheres.	0.25	47.5	162.5				
	0.51	68.3	244.5				
	0.70	88.3	267.0				
	1.02	115.8	284.0				

<sup>1</sup> PEEK, "The Effect of Transient Voltages on Dielectrics," *Trans. A.I.E.E.*, p. 1857, 1915.

The above voltages are measured by sphere gaps at low frequency and for impulse. The difference between the 60 cycles and impulse voltages increases as the steepness of the impulse increases. Oil is an excellent insulation in combination with barriers. On solid insulations the effect of transient voltages is cumulative. A partial break occurs which is enlarged by each succeeding impulse, until finally complete failure follows. With oil, such "cracks" are closed up by new oil immediately.

At continuously applied high frequency oil, breaks down at lower voltages than at 60 cycles. The following comparison made by the author is of interest:

TRANSIL OIL—BETWEEN FLAT TERMINALS—SQUARE EDGE—2.5-CM. DIAMETER—0.25-CM. SPACE—BREAKDOWN VOLTAGE GRADIENTS

60 cycles	High frequency alternator 90,000 cycles	Single impulse, sine <sup>1</sup> shape, corresponding to 200,000 cycles
Kv./mm. (max.)	Kv./mm. (max.)	Kv./mm. (max.)
17	6.7	39

**D.C. Strength of Oil.**<sup>1</sup>—The direct current strength of oil generally corresponds to the maximum ( $\sqrt{2} \times$  effective) 60  $\sim$  value.

<sup>1</sup> PEEK, "The Effect of High Continuous Voltages on Air, Oil, and Solid Insulation," *Trans. A.I.E.E.*, p. 783, 1916.

## CHAPTER VIII

### SOLID INSULATIONS

**General.**—Some of the principal solid insulations are paper, varnished cambric, oiled and varnished pressboard, built up press board, treated wood, mica, micanite, soft and hard rubber, synthetic resins, glass, and porcelain.

With gaseous and liquid insulations, as air and pure oil, there is very little loss up to the breakdown gradient. A gradient just under the breakdown gradient may be applied and held and the loss is so small that no appreciable heating results. Thus, the loss in air and oil is essentially a phenomenon above the electric elastic limit. This loss generally exists in some locally broken down part of the insulation, as the corona on the surface of a wire. The break does not extend through the whole insulation, and when the stress is removed, new air takes the place of the broken down air and all evidence of overstress is removed; in other words, in air and oil a local breakdown is "self healing."

Almost all insulations are partially conducting or have a very high resistance which is spoken of as insulation resistance. The actual resistance of the insulation itself, which is very high, apparently has no direct connection with the dielectric strength which is measured by the gradient or flux density or stress required to electrically strain the dielectric above the "electrical elastic limit" so that actual rupture or breakdown occurs. For instance, in a condenser made of two metal plates with a solid dielectric between them, when alternating-current potential is applied, energy is stored in the dielectric by electric displacement at increasing potential and delivered back to the circuit at decreasing potential, as long as the potential does not stress the insulation above the elastic limit. If the dielectric were perfect, a wattmeter in the circuit would indicate no loss. In all practical insulations, the wattmeter does read a loss due to the  $I^2R$  loss in the insulation and the dielectric loss, sometimes called "dielectric hysteresis."<sup>1</sup> If the voltage is sufficiently increased to exceed

<sup>1</sup> In what follows, the total loss will be called the dielectric loss (see pp. 37, 38).



the elastic limit, actual rupture or breakdown occurs; along this discharge path the insulation is destroyed. Air has a very high insulation resistance but not a very high dielectric strength. When the insulation resistance, however, of a given solid insulation becomes very low, as caused by moisture, etc., it is an indication of large loss and low breakdown voltage. Thus, the term "insulation resistance" generally takes into account the resistance of the occluded moisture.

**Insulation Resistance.**—The actual resistance of the insulating material itself is generally very high. Practically all solid and liquid insulations absorb moisture to a greater or less extent. The capillary tubes and microscopic interstices, etc., in the structure become filled with moisture and gases. In the non-homogeneous structure this makes a complicated arrangement of

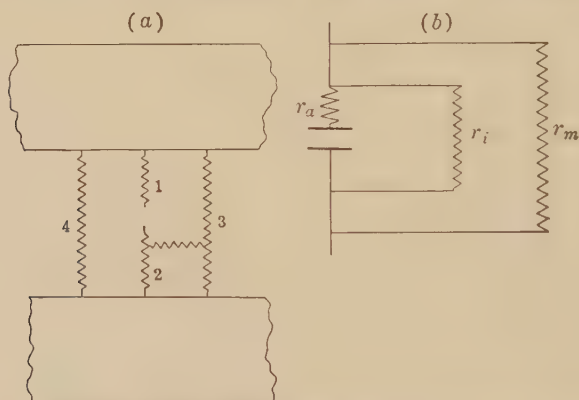


FIG. 184.—Diagrammatic representation of resistance arrangement in imperfect insulations.

capacities and resistances in series and in multiple. A simplified diagrammatic illustration of the distribution is shown in Fig. 184.

Let 184(a) represent a magnified section of insulation between two terminals, and 184(b) a diagrammatic representation. The resistance of the insulation itself, which is very high, may be represented by  $r_i$ . Let 1 be a partially conducting fiber which extends only partway through the insulation and is, thus, in series with a capacity. It may be represented by  $r_a$ . Let 3 and 4 be partially conducting fibers which extend all the way across and represented by  $r_m$ . There may also be leakage resistance over the surface.

Direct current is used to measure insulation resistance, as the charging current for alternating current is very large and masks the resistance current. Watt measurements are necessary, as well as volts and amperes, to determine the effective alternating-current resistance. The alternating-current and direct-current resistance should, however, be quite different. When direct current is used, sufficient time must elapse after the application of voltage to allow for absorption (see Chap. II, page 37).

With direct current, the only path for the current is through  $r_i$  and  $r_m$  in multiple which is, therefore, the resistance measured. The resistance varies with the applied potential, decreasing with increasing potential. The conducting particles are caused to line up, cohere, occluded gases break-down, etc., as the potential is increased.

When alternating-current voltage is applied to insulation, the capacity current must pass through  $r_a$ ; in shunt with this is the circuit through  $r_i$  and  $r_m$ . The loss in  $r_a$  must increase with increasing frequency, while the loss through  $r_i$  and  $r_m$  must remain constant at a given voltage, independent of the frequency. The greater loss will generally occur in  $r_a$ . The direct-current insulation resistance cannot be used in approximating the  $I^2r$  alternating-current loss. If the alternating-current loss is measured, as well as the voltage and current, the effective resistance may be calculated. This resistance loss, however, must be greater than that due to  $r_a$  as other losses are included.

In Table LXX some direct-current resistances are given for different materials. Note the effect of moisture absorbed from the air even for varnished materials.

With air and oil an appreciable loss begins only when a definite gradient, sufficiently large to cause local rupture as brush or corona, somewhere results; loss occurs after the elastic limit has been exceeded. The dielectric loss in solid dielectrics is essentially a loss below the elastic limit. In solid dielectrics, a stress may be applied lower than the elastic limit which, after a short time—on account of the heating and, hence, weakening of the insulation—will cause rupture.

The dielectric strength of most solid insulations is, thus, quite complicated because of the non-homogeneous structure tied together with high-resistance paths. While in short time tests the effect of these paths may be inappreciable, in long time tests the pyroelectric effect will cause the resistance to decrease at

TABLE LXX.—INSULATION RESISTANCE  
Resistance Megohms per Cm. Cube  
(Data obtained by Evershed, J.I.E.E., Dec. 15, 1913)

Material	D.c. volts			
	50	100	200	500
Cotton, dry.....	350.0	275.0	200.0	140
Cotton, not dried.....	2.8	2.5	2.2	.....
Micanite, exposed to air.....	220.0	175.0	160.0	140
Micanite, dried.....	.....	.....	300,000	200,000
Cylinder oil, trace of moisture.....	.....	22,000	22,000	22,000
Cylinder oil, dry.....	.....	36,000	36,000	36,000
Varnished cloth, 12 hr. after baking.	.....	35,000	35,000	35,000
Varnished cloth, 9 days after baking.	17,000	14,000	11,000	9,000

local points. For some types of solid insulation, this actually may be the controlling factor.

**Rupturing Gradients.**—Apply voltage lower than the puncture voltage between concentric cylinders with dry insulation between

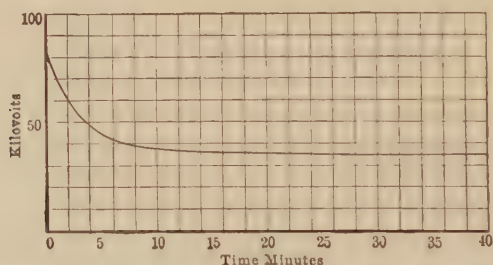


FIG. 185.—Insulation puncture voltage *vs.* time.

(Oiled pressboard, 2.5 mm. thick. The curve does not cut the kv. axes as it appears to on account of the time scale.)

surfaces, and gradually increase to the rupturing voltage within a short time so that there can be no appreciable rise in temperature. The mechanism of rupture will be quite different for oil or air, glass or porcelain, and cambric. For oil and air, corona results near the surface of the inner cylinder, the breakdown is local and

disappears when the stress is removed; or, if the stress is further increased, spark-over finally results. For glass or porcelain, as soon as overstress is reached locally, a crack results at the surface of the inner cylinder and complete breakdown follows. With cambric there is local rupture and local charring of the insulation which forms carbon "needles." The break is progressively increased; this continues until the breakdown is complete. A wet thread or gas bubble, as (1) in Fig. 184(a), may, in effect, act as a needle and thus cause breakdown. The breakdown gradients of solid insulations are thus variable and not as definite as with air and oil.

The puncture tests on solid insulations vary greatly between different samples of the same material, shape, and area of the electrodes, time of application of voltage, etc. Insulations should be thoroughly dried before tests are made.

In comparing solid insulations, it is generally best to make some arbitrary time tests to include the effect of dielectric loss and, thus, heating on the breakdown voltage. The effect of loss is cumulative; the insulation becomes warm and, while the loss increases with the temperature, the dielectric strength generally decreases with increasing temperature. The ultimate strength naturally, then, depends on the rate at which this heat is conducted away. This is illustrated in Fig. 185. With the electrode used, if the voltage is "rapidly applied" before heating occurs, 80 kv. are required to cause rupture.<sup>1</sup> If 50 kv. are applied, rupture does not occur until 4 min. have elapsed, while 30 kv. may be applied indefinitely without rupture if the room temperature is not increased. The curve does not cut the voltage axes as appears in the cut, on account of the time scale, but is an asymptote to it. The effect of temperature is also illustrated in Table LXXI, where, in one case, the electrode is of brass giving good heat conduction, and, in the other case, of wood coated with tin foil giving poor heat conduction. As the applied voltage approaches the rapidly applied rupturing voltage, there is not sufficient time for the insulation to heat to a great extent and the effect is about the same for either brass or the coated wood

<sup>1</sup> "Rapidly applied" voltage as used above means voltage applied within a fairly short time, a few seconds, and not impulse voltage or voltage of very steep wave front. "Instantaneous" is commonly used to designate this test; this term is confusing. The test itself is not wholly satisfactory as it is indefinite. It offers, however, a means of making a preliminary comparison of insulations.

electrode. The effect of heating is also shown by direct-current tests, page 257.

The effect of applying a high voltage, allowing different periods of rest for cooling, and then applying voltage until rupture, is

TABLE LXXI.—EFFECT OF HEAT CONDUCTING PROPERTIES OF  
TERMINALS ON TIME OF BREAKDOWN

Two Thicknesses of No. 12 Oiled Cloth  
(From Rayner, Journal I.E.E., Feb. 8, 1912)

Volts	Time of breakdown	
	Brass terminals	Wood terminals <sup>2</sup>
9,000	570.0 sec.	50.0 sec.
10,000	48.0 sec.	19.0 sec.
11,000	16.5 sec.	10.0 sec.
12,000	10.2 sec.	6.2 sec.
14,000	5.2 sec.	4.5 sec.

<sup>2</sup> Coated with tin foil.

shown in Table LXXII. The injurious effects of applying high voltage for different lengths of time is shown in Table LXXIII. This is probably due to the effect of heat and injury to the surface by corona.

TABLE LXXII.—RECOVERY IN VARYING PERIODS OF REST AFTER APPLI-  
CATION OF 9000 VOLTS FOR 1 MINUTE<sup>1</sup>

Two Thicknesses of No. 12 Oiled Cloth  
(From Raynor, Journal I.E.E., Feb. 8, 1912)

Period of rest	Time to break at 11,000 volts	Period of rest	Time to break at 11,000 volts
0.....	2.6 sec.	0	2.5 sec.
1 min.....	9.5 sec.	5 sec.	4.4 sec.
2 min.....	11.9 sec.	15 sec.	9.0 sec.
Fresh material....	12.0 sec.	60 sec.	9.8 sec.
.....	.....	Fresh material	20.5 sec.

<sup>1</sup> Time to break at 9000 volts, 1-1½ to 2 min.

The action of corona or breakdown of the air at the surface of the insulation is shown in Table LXXIV.



The arbitrary practical tests for *comparing* insulations are the rapidly applied (instantaneous) test, the one-minute test, and the endurance test. Rapidly applied breakdown voltage is found by applying a fairly low voltage and rapidly increasing

TABLE LXXIII  
(From Raynor, Journal I.E.E., Feb. 8, 1912)

Time of treatment at 5000 volts	Time of breakdown (left to cool over night)	
	At 6500 volts	At 7000 volts
0.....	22.0 min.	8.5 min.
1 hr.....	6.5 min.	8.3 sec.
2 hr.....	3.0 sec.	.....

TABLE LXXIV.—EFFECT OF AIR GAP (CORONA)  
Two Thicknesses of No. 12 Oiled Cloth  
10,000 Volts  
(Raynor, Journal I.E.E., Feb. 8, 1912)

Air gap, mm.	Time to puncture, seconds
0.00	42.0
0.30	34.0
0.50	27.5
0.75	24.0
1.05	120 (irregular)

until breakdown occurs. Voltage should be increased at about 5 kv. per second.

The minute test is made by applying 40 per cent. of the rapidly applied voltage and increasing this voltage 10 per cent. at 1-min. periods until puncture occurs. (Total time about 5 min.)

The endurance test is made by applying 40 per cent. of the minute test voltage and increasing the voltage 10 per cent. every hour or half hour until puncture occurs. These tests may be made at any given temperature. The electrode should be of a given size and weight. Ten-centimeter diameter electrodes, *slightly* rounded at the edges, will be found convenient. Table LXXV gives an example of such tests.

TABLE LXXV  
Muslin with Three Coats Varnish—Total Thickness 2 mm.  
Rapidly Applied (Instantaneous) Breakdown and Resistance

Temp., deg. cent.	Resistance in megohms for samples				
	1	2	3	4	5
20	73,400	73,400	97,900	97,900	73,400
75	650	390	310	270	170
100	100	90	73	70	50

Breakdowns in kilovolts. Tests made in oven at 100° C.

100	40.6	42	44	43	36.5
-----	------	----	----	----	------

Average breakdown 40.6 kilovolts

One-minute Test

Apply 40 Per Cent. of Rapidly Applied Breakdown Voltage for 1 Minute,  
with 10 Per Cent. Increase in Voltage Each Minute

Temp., deg. cent.	Resistance in megohms				
	6	7	8	9	10
20	73,400	73,400	73,400	97,900	97,900
75	320	333	451	274	330
100	50	60	70	40	60

Time under stress	Potential applied	Temperature for samples					
		6	7	8	9	10	Air
Start.....		100	100	101	103	100	100
1 min.....	16,000	101	101	103	104	102	100
2 min.....	17,500	102	102	104	105	103	100
3 min.....	19,000	105	104	106	108	105	100
4 min.....	20,500	111	108	108	111	107	100
5 min.....	22,000	121	112	111	117	108	100
5 min. 5 sec....	23,500					115 punctured	
5 min. 46 sec....	23,500	146 punctured					
6 min.....	23,500		118	114	129		100
6 min. 10 sec....	25,000				135 punctured		
6 min. 35 sec....	25,000			118 punctured			
7 min.....			135				100
7 min. 58 sec....	26,500		140 punctured				

## Endurance Test

Apply 40 Per Cent. of 1-minute Period Endurance Voltage, for 30-minute Periods Endurance Test, with 10 Per Cent. Raise in Voltage Each Period

Temp., deg. cent.	Resistance in megohms				
	11	12	13	14	15
22	74,300	74,400	74,400	99,100	49500
75	390	420	230	290	110
100	90	70	30	60	30

Time under stress	Potential applied	Temperature					
		11	12	13	14	15	Air
Start.....		99	100	100	101	99	100
0.5 hr.....	10,000	103	107	133	108	115	100
34 min.....	11,000			182	punctured		
54 min.....	11,000					198	punctured
1 hr.....	11,000	104	108		112		100
1.5 hr.....	12,000	106	111		114		100
2 hr.....	13,000	106	118		122		100
2 hr. 23 min.....	14,000				215	punctured	
2 hr. 25 min.....	14,000		203	punctured			
2.5 hr.....	14,000	136					
3 hr.....	15,000	143					
3 hr. 2 min.....	16,000	145	punctured				

A considerable amount of data is given here for the 1-min. time test. It must be remembered that in design only a fraction of the maximum gradient corresponding to this voltage is permissible for continuous operation, the particular percentage depending upon the design, the insulation, the rapidity at which heat may be radiated, or conducted away, etc. It is generally 10 to 15 per cent. on main insulation; it is often as low as 5 per cent., sometimes as high as 30 per cent.

**Strength vs. Thickness.**—Insulation tests are generally made for convenience on sheets between flat terminals. The gradient at the edges, even when these are rounded, is generally higher than the average gradient  $e/x$ . This edge effect is different with different thicknesses of insulation. The puncture voltage per centimeter thickness is always greater for thin sheets of insulation than for thick ones. This is partly due to the edge effect which

cannot be corrected for and becomes relatively greater as the thickness of insulation is increased. (At small spacings  $e/x$  is very nearly the true gradient; at large spacings  $e/x$  is not the true maximum gradient.)<sup>1</sup> It is also greatly due, in the time tests, to the better heat distribution and dissipation in the thin sheets and partly due to the fact that energy is necessary for disruption, so that when the rupturing distance is limited, as in the case of thin sheets, the apparent strenght increases.

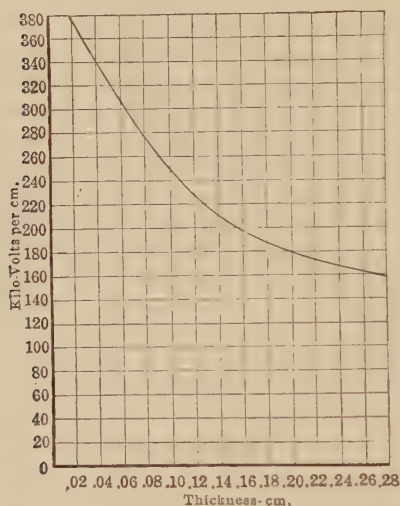


FIG. 186.—Insulation strength vs. thickness.

Figure 186 shows apparent variation in strength with thickness. Between parallel plates the apparent strength is approximately:

$$g_s = g \left( 1 + \frac{a}{\sqrt{t}} \right)$$

where  $g$  and  $a$  are constants and  $t$  is thickness.

The above theoretical expression is very similar in form to the breakdown relation for air (see page 58, Chap. IV). An equation derived from actual experimental data on insulation breakdown<sup>2</sup> is of the form  $KV = AT^n$ . Here,  $KV$  is the breakdown voltage in kilovolts,  $A$  the strength

per unit thickness,  $T$  the thickness, and  $n$  a numerical factor generally less than unity, and depending on the testing methods, the dielectric, and the insulation history; that is, the previous drying, treating, etc., it has undergone.

With a perfectly uniform field, the factor  $n$  would be unity. Due to the edge effect with the usual flat straight-edged electrodes, it is generally less than unity. The larger the electrodes, the higher the value of  $n$ . Figure 187 shows four curves illustrating this effect of electrode size. With a given electrode and dielectric,  $n$  can be raised by shielding the edge of the electrode with a ring of such a material as albarene stone.

<sup>1</sup> Special flat terminals are sometimes used with "shielded" edges so that  $e/x$  is the true gradient.

<sup>2</sup> CLARK and MONTINGER, *G. E. Review* p. 286, 1925.

The usual range of variation of  $n$  for insulations in general is from 0.5 to 1.0. The average  $n$  is about  $\frac{2}{3}$ , which is also the value for oil between pointed electrodes.

When shielded edges are used, it is generally best to make insulation tests under oil unless it is desired to make a study of the effect of corona on the insulation. With pointed electrodes, the instantaneous puncture voltage of a given insulation will be less

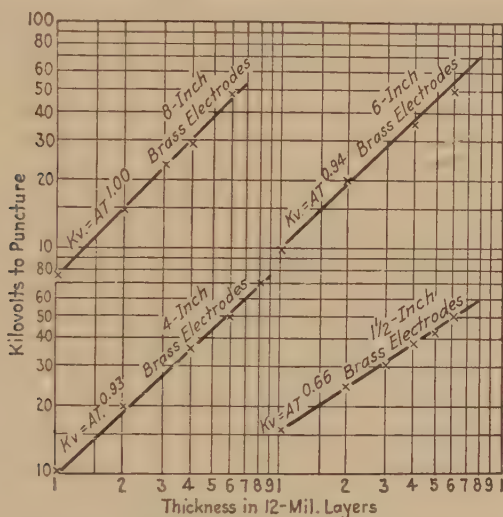


FIG. 187.—Effect of electrode size on the strength-thickness relation. Straight-edge brass electrodes with black varnished cloth (0.012 in.) tested in oil at room temperature using 60-cycle alternating current and minute test procedure. All points are averages of 10 tests. • All curves run simultaneously.

in oil than in air. This is not because the oil weakens the insulation but because corona forms on the point in air and spreads over the surface, giving the effect of a flat plate electrode.

**Dielectric Strength of Cables.**—Some tests of the dielectric strength of cables or concentric cylinders in solid insulation indicate that the breakdown gradient may follow the same general law as for air and oil, thus

$$g_v = g_o \left( 1 + \frac{a}{\sqrt{r}} \right) \text{ kv. per centimeter.}$$

A certain set of results for cables gave the constants as follows:

$$g_v = 100 \left( 1 + \frac{1.1}{\sqrt{r}} \right) \text{ kv. per centimeter}$$



This means that at breakdown the gradient is 100 kv. per centimeter at a distance of  $1.1\sqrt{r}$  cm. from the conductor surface where the gradient is  $g_v$ .<sup>1</sup>

**Solid and Laminated Insulation.**—The structure of most insulations is not homogeneous. If a given insulation is tested with terminals of varying area, it is found that the average puncture voltage becomes lower as the area is increased, and thus the chance of it covering a weak spot is increased. As would be expected, this approximately follows the probability law as shown in Fig. 188.

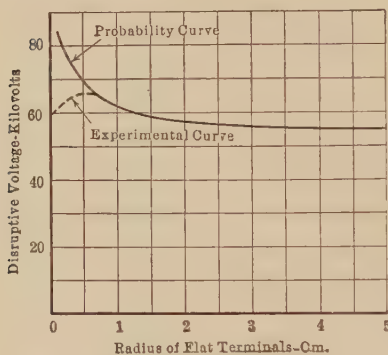


FIG. 188.—Insulation strength vs. area of terminal.

10	15
18	20
10	12

FIG. 189.—Variation in dielectric strength at different parts of a piece of insulation.

The reason that the experimental curve bends down is that the gradient is fairly constant until the terminal becomes small when the gradient increases, due to flux concentration with the smaller terminal. If the curves were plotted with actual gradients instead of voltages, the experimental curve would follow more closely the probability curve. The experimental gradient curve would, however, for the smaller sizes, bend up faster than the probability curve, due to greater apparent strength for smaller terminals, as for small spheres in the case of air. The curve between  $e/x$  and diameter for flat terminals of the larger sizes when the concentration at the edges is about constant should follow the probability curve.

For example, suppose Fig. 189 represents a piece of solid insulation 0.025 mm. thick and sufficiently large to contain every condition of "weak spot." Divide this into six equal squares

<sup>1</sup> PEEK, F. W., JR., "Discussion," *Trans. A.I.E.E.*, p. 611, 1922.

each of area  $a$ . The strength is marked on the various areas. Assume that an electrode is used giving no edge effect. With electrode of area  $a$  six tests are required to go over the whole piece. With electrodes of area  $2a$  three tests are required, with area  $3a$  two tests, and  $6a$  one test. The following results may be obtained:

Area electrode	No. of punctures	Total area covered	Volts per mm.		
			Maximum	Minimum	Average
$a$ .....	6	$6a$	20	10	14
$2a$ .....	3	$6a$	18	10	13
$3a$ .....	2	$6a$	12	10	11
$6a$ .....	1	$6a$	10	10	10

The results are somewhat similar to the lower points of the curve in Fig. 188.

On account of these characteristics alone, an insulation built up of laminations is much better than a solid insulation, as the weak spots in the laminations are not likely to line up. It is also much easier to make better and more uniform insulation in thin sheets.

Tests are useless for comparing insulation strengths unless made upon some standard basis. Great caution is necessary in the use of tabulated values of insulation strength in design. On account of the variable quality of solid insulation, tests must be continually made to see that the product does not change. Vacuum treatment is necessary before use to remove moisture. Even when all of the test conditions are known, experience is necessary to judge the proper factor of safety. Aside from this, stress concentrations due to the shapes and spacings of the conductors must always be considered and allowed for. It is generally not possible to do this with mathematical exactitude, but approximation must be made with all factors in mind. Care must be taken that the solid insulation is below the rupturing gradient at any local point. If such a point is broken down locally, the flux becomes still further concentrated. The puncture voltage will decrease with frequency, even over the commercial range, due to increasing loss with increasing frequency.

**Impulse Voltages and High Frequency.**—It takes energy and, therefore, time to rupture insulation. For a given potential a given number of cycles of very high-frequency voltages, where

heating does not result, are, therefore, much less injurious than the same number of cycles at low frequency. This also applies to impulse voltages of steep wave front. Continuously applied high frequency is, however, generally very injurious for two distinct reasons:

(1) On account of the very great loss at continuously applied high frequency the insulation may be literally burned up in a very short time even at low voltages. This condition does not result in practice from surges, etc., on low frequency lines, but in high-frequency generators, transformers, etc. In such apparatus it is important to use very smooth electrodes to prevent local concentration of stress and charring of insulation. This is especially so where contact is made with the air. If a local brush starts, on account of the great loss, it becomes very hot and extends out a considerable distance.

(2) In certain apparatus containing inductance and capacity, very high local potential differences may be produced by resonance and cause rupture by overpotential. The high frequency thus does not cause the rupture directly but makes it possible by causing overpotential. Local concentration of stress may also result in non-homogeneous insulation, as across the condenser and resistance combinations in Fig. 184.

The term "high frequency" is generally used in such a way that no distinction is made between sinusoidal high frequency from an alternator, undamped oscillations, damped oscillations, impulses of steep wave front, etc. Naturally, the effect of continuously applied undamped oscillations is quite different from a single high-voltage impulse of extremely short duration. As the effects are attributed to the same cause—high frequency—apparent discrepancies must result (see comparative tests, Table LXXVI, page 250).

If the time of application is limited below a definite value, higher voltages are necessary to produce the same results in the limited time. Impulse voltages of steep wave front many times in excess of the rupturing voltage may be applied to insulations without rupture if the application is very short—measured in microseconds. They may be caused in practice by lightning, switching, etc. If such voltages are sufficiently high, complete rupture may result at once. In any case, if these voltages are higher than the 60-cycle puncture voltages, the insulation will be damaged. As an example, an impulse voltage equal to three

times the 60-cycle puncture voltage may be applied to a line insulator. During the very small time between the application of the voltage and the arc-over through the air, the insulator is under great stress. It may be that up to the ninth application of such a voltage there is no evidence of any injury, while on the tenth application failure results. Each stroke has contributed toward puncture. It is probable that each application adds to or extends local cracks.<sup>1</sup>

Figure 190 shows the overvoltage necessary for puncture of solid insulation with limited time of application, the overvoltage

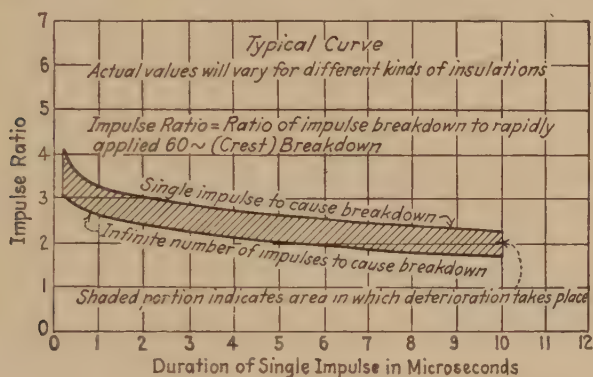


FIG. 190.—Impulse ratio and cumulative effect of impulses on solid insulation.

factor being expressed by impulse ratio. It is seen that voltages in excess of about 80 per cent. of the single-stroke breakdown value will cause deterioration and eventual failure if a sufficient number of impulses are applied.

**Variation of Dielectric Strength with Frequency.**—The loss in a given insulation increases approximately as the frequency or the loss per cycle is constant. It follows, as stated above, that the heating may be very great at the higher frequencies when the voltages are continuously applied. Since the dielectric strength decreases with the temperature, it must also decrease with increasing frequency. It is important, therefore, to consider the relative dielectric strengths at frequencies of the order of those used in practical operation.

For the 1-min. test, the breakdown voltage at 25 cycles is about 10 per cent. higher than the breakdown voltage at 60 cycles; at 120 cycles it is 10 per cent. lower than at 60 cycles, while at 500 cycles it is from 25 to 30 per cent. lower.

<sup>1</sup>See appendix.



It is sometimes necessary to make induced voltage tests on transformers at a frequency higher than the operating frequency, but not exceeding the above range. In such cases it is generally desirable to reduce the time of test rather than the voltage. If the time is reduced so that the same number of cycles occur, or inversely as the frequency, the test is somewhat more severe than for the full time at operating frequency.

**Cumulative Effect of Overvoltages of Steep Wave Front.—**

Voltages greatly in excess of the rapidly applied 60-cycle puncture voltage may be applied to insulation without rupture if the time of application is sufficiently short. All such overvoltages injure the insulation, probably by mechanical tearing, and the effect is cumulative. A sufficient number will cause breakdown. For example: A piece of oiled pressboard 3.2 mm. thick has a rapidly applied breakdown at 60 cycles of 100 kv. maximum. If sinusoidal impulses reaching their maximum in 2.5 microseconds are applied, the number of impulses to cause break-down is as follows:

Kv. maximum of impulse applied	Number to cause breakdown
100	$\infty$
140	100
150	16
155	2
165	1

If the impulses are of still shorter duration, a greater number are required to cause breakdown at a given voltage. Insulations, and line insulators, are often injured and gradually destroyed in this way by lightning.

**Strength vs. Time of Application.**—It was stated above that the strength varies with the time of application (see Figs. 185 and 190). The range of time shown in this curve is from a few seconds (instantaneous) to an indefinitely long time. Over the greater part of the plotted curve, heating is a factor and the great decrease is principally due to heating. Where the time of application is much less than instantaneous value, and heating can have no appreciable effect, the strength still increases very rapidly as the time of application is decreased. Some values from an actually measured curve are:

(14 layers impregnated paper between concentric cylinders)

$$R = 0.67 \text{ cm.}$$

$$r = 0.365 \text{ cm.}$$



Time, sec.	Kilovolts to puncture (maximum)
$\infty$	32.6
60.0	37.5
1.0	49.3
0.1	61.0
0.01	85.0
0.001	113.0
0.0001	196.0

$$g = 13.0 \left( 1 + \frac{0.5}{\sqrt[4]{T}} \right) \text{ kv./mm. max.}$$

The equation of the strength-time curve over the complete range obtained from an examination of a number of curves is of the form

$$g = g_s \left( 1 + \frac{a}{\sqrt[4]{T}} \right)$$

when  $T$  is the time of application in seconds, and  $g_s$  is the gradient in kv. per millimeter for indefinite time. The equation generally applies well over a range from infinite time to 0.01 sec. For shorter periods many insulations shatter and fail at voltages lower than the equation indicates.

Both  $a$  and  $g_s$  vary with the thickness of the insulation, temperature, etc.

In order that the strength may be high for indefinite time, the loss should be low.

**Permittivity of Insulating Material.**—In design, a knowledge of the permittivity (or dielectric constant) of insulating materials is as important as the dielectric strength. In general the permittivity of an insulating medium increases with its density. With gases and liquids the permittivity increases with a rise in pressure and decreases with a rise in temperature. The amount of this variation depends upon the insulating medium. It is negligible with air over the practical range of atmospheric conditions. With solid insulations, the permittivity of a given material increases practically in proportion to its specific gravity. The interpretation of this variation with solids is often confusing due to the porosity effect which enters. The study of dielectrics has also revealed that an increased permittivity in general means a decreased resistivity.<sup>1</sup> It is believed that these two characteristics of an insulating material are both affected by molecular polarity and density. The various properties of some of the common insulations are given in Table LXXVI.

<sup>1</sup> F. M. Clark, *Journal Frank. Inst.*, P. 17, July 1929

TABLE LXXVI.—DIELECTRIC STRENGTH OF SOLID INSULATIONS  
 Variation of Dielectric Strength with Thickness and Number of  
 Layers. (One-minute Tests—60-cycle—10-cm. Terminals in Oil. Values  
 Effective Sine Wave)

## PRESSBOARD

No. of layers	Thickness per layer, mm.	Total thick- ness, mm.	Kv./mm.—temperature 25 deg. C.		
			Varnished, kv./mm.	Oiled transil, kv./mm.	Linseed oil, kv./mm.
1	0.178	0.178	25.3	.....	25.3
1	0.254	0.254	26.3	39.3	23.6
1	0.508	0.508	21.0	.....	23.0
1	0.787	0.787	19.1	33.5	22.0
1	1.575	1.575	15.5	29.2	19.0
1	2.390	2.390	11.1	23.0	15.1
1	3.170	3.170	9.5	21.1	14.2
2	0.178	0.356	22.5	.....	21.0
2	0.254	0.508	17.7	33.5	19.7
2	0.508	1.016	12.8	.....	17.2
2	0.787	1.574	13.7	22.9	16.0
2	1.575	3.150	10.6	19.7	15.3
2	2.390	4.790	7.54	16.1	12.1
2	3.170	6.340	6.3	14.7	11.0
4	0.178	0.712	26.7	.....	16.6
4	0.254	1.016	22.6	29.8	15.3
4	0.508	2.032	16.8	.....	15.8
4	0.787	3.148	16.5	20.6	19.7
4	1.575	6.300	11.6	13.65	12.7
4	2.390	9.560	9.4	11.5	.....
4	3.170	12.680	6.6	.....	.....
6	0.178	1.068	25.5	.....	15.0
6	0.254	1.524	20.6	27.5	13.1
6	0.508	3.048	15.4	.....	14.4
6	0.787	4.702	14.9	20.0	17.8
6	1.575	9.450	.....	11.3	.....

TREATED WOOD  
 Temperature 25 deg. C.

	Across grain	kv./mm.		With grain	kv./mm.
1	12	6.42	1	30	2.47
1	15	4.53	1	60	1.57
1	20	3.85	1	90	1.27
1	25	3.02	1	120	1.12

PAPER  
(Untreated)

No. of layers	Thickness per layer, mm.	Total thickness, mm.	25° C., kv./mm.	100° C., kv./mm.
1	0.064	0.064	9.3	9.3
1	0.127	0.127	8.7	7.9
1	0.254	0.254	7.9	7.3
4	0.064	0.258	8.7	8.3
4	0.127	0.508	7.5	6.7
4	0.254	1.016	6.6	6.2
8	0.064	0.516	8.7	8.1
8	0.127	1.016	7.4	6.6
8	0.254	2.032	6.3	6.0

VARNISHED CLOTH

1	0.305	0.30	26.2	23.6
2	0.305	0.61	20.5	19.7
3	0.305	0.91	18.5	17.0
4	0.305	1.22	16.8	14.9
5	0.305	1.52	15.5	13.1
6	0.305	1.83	14.6	11.5
7	0.305	2.13	14.0	10.3
8	0.305	2.44	13.3	9.2
9	0.305	2.74	12.8	8.3
10	0.305	3.05	12.3	7.5

HARD RUBBER

No. of layers	Thickness per layer, mm.	Total thickness, mm.	Puncture voltage	
			25° C., kv./mm.	100° C., kv./mm.
1	0.0193	.....	59.7	.....
1	0.0223	.....	55.6	.....
1	0.0312	.....	48.7	.....
1	2.0	2.0	17.3	.....
1	3.0	3.0	14.2	.....
1	4.0	4.0	12.7	.....
1	5.0	5.0	11.8	.....
1	6.0	6.0	11.2	.....

## MICA

1	0.0508	0.0508	96.5	.....
1	0.1016	0.1016	88.7	.....
1	0.1524	0.1524	75.5	.....
1	0.2032	0.2032	62.6	.....
1	0.5080	0.5080	26.1	.....

## GLASS

Total thickness  
6.0

Kv./mm.  
10

The kv./mm. strength of glass decreases rapidly with increasing thickness.

## PORCELAIN

Total thickness, mm.	Kv./mm.
0.5	16.0
1.0	14.5
2.0	12.2
5.0	11.0
10.0	9.6
15.0	9.2

## VARIATION OF INSULATION STRENGTH WITH TIME OF APPLIED VOLTAGE

Material	Thickness, mm.	Time to puncture, min	25° C. kv./mm.	100° C. kv./mm.
Oil impregnated paper, 30 layers, 60-cy., 10- cm. diameter discs, round edges.	1.90	"Inst."	39.4	32.0
		1	33.1	27.3
		2	31.0	25.7
		4	29.2	24.5
		6	28.2	23.6
		10	26.8	22.7
		20	25.5	21.6
		40	23.6	20.5
		60	22.7	19.7
		80	22.1	19.3
		100	21.6	19.0

Note that for a given thickness the strengths of materials do not vary as greatly as might be expected.

Material	Thickness, mm.	Time to puncture, min.	Puncture voltage, 25° C.		
			1 layer, 0.30 mm. kv./mm.	5 layers, 1.50 mm. kv./mm.	10 layers, 3.0 mm. kv./mm.
Varnished cloth, 0.30 mm., 60-cy., 10-cm. diameter in air, round edges	0.30	"Inst."	52.5	36.1	27.2
		0.1	37.7	27.5	22.3
		0.2	34.5	25.8	19.7
		0.5	32.8	22.9	16.4
		1.0	32.5	21.0	14.3
		2.0	32.1	20.3	13.0
		3.0	31.8	19.9	12.6
		5.0	31.5	19.8	12.5
		10.0	31.1	19.7	12.3
		20.0	30.2	19.6	9.9

## PERMITTIVITY OF INSULATING MATERIALS

	Permittivity	Specific gravity
Asphalt.....	2-½	
Bakelite.....	4-½	
Cambric (varnished).....	4-½ to 5-½	1.15
Fiber (horn) dry.....	2-½	0.7 to 1
Fiber (horn) oil.....	4-½ to 5	0.9 to 1.5
Glass (crown).....	6	3 to 3.5
Glass (heavy flint).....	10	4.5
Gutta percha.....	3-½ to 4	
Lead stearate.....	5.2	
Lead palmitate.....	5.2	
Lead oleate.....	5	
Mica.....	5 to 7	
Oil (linseed).....	3-½	0.95
Oil (transil).....	2 to 2-½	0.8 to 0.9
Paper (dry).....	2.6	1.00
Paper (paraffined) .....	3 ½	
Paper (oiled).....	4	1.25
Paraffine .....	2 to 2.3	0.9



PERMITTIVITY OF INSULATING MATERIALS.—*Continued*

	Permittivity	Specific gravity
Pressboard (dry).....	3	1.25
Pressboard (oiled).....	4 to 6	1.40
Porcelain.....	4-½ to 5	2.4
Rubber (hard).....	3	
Rubber (vulcanized).....	2-½	
Shellac.....	3	
Sulphur.....	4	
Wood (treated).....	3 to 3-½	0.8 to 0.9

## COMPARATIVE INSULATION STRENGTH FOR HIGH FREQUENCY, IMPULSE, OSCILLATION AND 60-CYCLE VOLTAGES

Temperature 30 deg. C.

60 Cycles		High frequency (alternator), 90,000 cycles		Damped oscillation, train freq. 120 sec., 200,000 cycles		Single impulse, sine shape, cor- responding to half cycle of 200,000 cycle	Thickness, mm.	Layers
Inst.	1 min.	Inst.	1 min.	Inst.	1 min.			
kv./mm. (max.)		kv./mm. (max.)		kv./mm. (max.)		kv./mm. (max.)		

*Transil Oil* between Flat Terminals—Square Edge. 2.5-cm. Diameter, 0.25-cm. Space

17		6.7		30		39		
<i>Oiled Pressboard.</i> 10-cm. Diameter—Square-edge Discs in Oil								
35.5	31.0	9.5	7.3	37.0	29.0	72.0	2.5	1
39.5	37.0	6.1	4.1	42.0	24.0	.....	5.0	2
.....	.....	2.5	1.76	.....	.....	.....	15.0	3

*Varnished Cambric*

53.0	46.5	19.5	17.6	.....	.....	108.0	0.6	2
42.0	31.0	13.5	10.0	55.0	56.0	78.0	1.5	5
37.0	28.0	10.0	7.3	49.0	41.0	70.0	2.5	8
33.0	27.5	.....	.....	41.0	30.5	60.0	3.6	12

**Energy Loss in Solid Insulation.**—In general, energy loss in solid insulation:

1. Increases with increasing voltage.
2. Increases with increasing temperature.
3. Increases with increasing frequency.
4. Increases with increasing moisture content.
5. Increases with increasing impurities, as occluded air, etc.

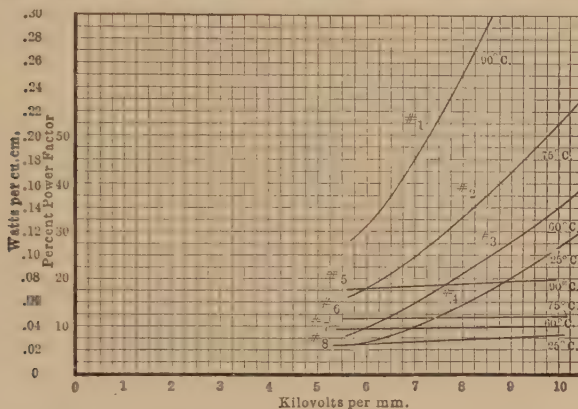


FIG. 191.—Insulation loss and power factor at 60 °.

(Oiled pressboard 5.0 mm. thick between parallel plates with rounded edges in oil. Curves 1, 2, 3, 4, watts per cubic centimeter. Curves 5, 6, 7, 8, power factor.)

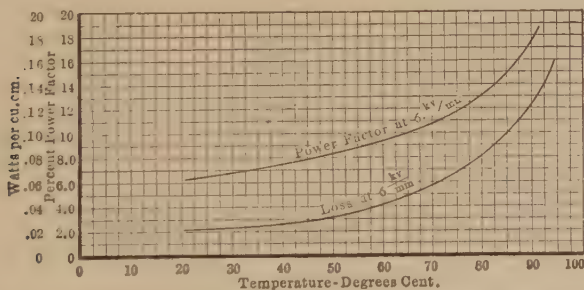


FIG. 192.—Insulation loss and power factor vs. temperature at 60 °.  
(Data, Fig. 191.)

For good uniform insulation free from foreign material, moisture, etc., the loss at constant temperature and frequency varies approximately as the square of the applied voltage. The author has found that approximately for good insulations

$$p = afe^2 = bfg^2 \times 10^{-6} \text{ watts per cubic centimeter.}$$

where  $f$  = frequency in cycles per second

$g$  = gradient kilovolt per millimeter effective

$b$  = constant varies with different insulations. It is 8 to 10 for varnished cambric in a uniform field, and thickness in order of 5 mm. (25° C.).

With occluded air or water, where the  $I^2r$  loss becomes large in comparison with the hysteresis loss, the rate of increase is greater. Due to combinations of resistance and capacity, it may then take the form<sup>1</sup>  $p = bfg^2 + (cf^2g^2 + ag^2)$ . Figure 191 shows characteristic curves between energy loss, power factor, and voltage of insulation in good condition.

The loss increases very rapidly with temperature. The temperature curves are shown in Fig. 192. Loss in different insulations is given in Table LXXVII.

TABLE LXXVII.—INSULATION LOSSES  
(Effective Sine Wave 60 Cycles)

Total thickness, mm.	Insulation	No. of layers	Temp., deg. C.	Volts per mm.	Watts per cu. cm.
4.0	Varnished cloth	15	25	4,000	0.005
				6,000	0.015
				8,000	0.035
				10,000	0.060
				12,000	0.090
4.0	Varnished cloth	15	90	4,000	0.025
				6,000	0.075
				8,000	0.150
				10,000	0.240
				12,000	0.350
2.5	Oil-treated paper	30	25	10,000	0.040
				14,000	0.070
2.5	Oil-treated paper	30	60	10,000	0.043
				14,000	0.080
2.5	Oil-treated paper	30	90	10,000	0.050
				14,000	0.100
2.5	Oil-treated paper	30	120	10,000	0.067
				14,000	0.138

These losses may be lower or very much higher, depending upon the condition of the insulation.

The increase of loss with frequency is shown in Table LXXVIII. The rate of increase of the loss with the frequency will vary greatly if the insulation contains moisture. If the moisture is

<sup>1</sup> See Fig. 184.

TABLE LXXVIII.—HIGH FREQUENCY LOSS IN DIFFERENT INSULATIONS  
(Alexanderson, Proc. Inst. Radio Engrs., June, 1914)

Volts per mm.	Frequency kilocycle	Material (thickness 5 mm.)							
		Glass		Mica		Varnished cambric		Asbestos	
		Loss watts, cu. cm.	P. F. avg.	Loss watts, cu. cm.	P. F. avg.	Loss watts, cu. cm.	P. F. avg.	Loss watts, cu. cm.	P. F. avg.
500	20	0.02	.....	0.02	.....	.....	.....	0.7	.....
500	40	0.05	1.4	0.04	1.8	0.08	.....	1.3	.....
500	60	0.08	.....	0.05	.....	0.12	3.3	2.0	.....
500	80	0.11	.....	0.08	.....	0.18	.....	.....	32.0
1000	20	0.08	.....	0.07	.....	.....	.....	3.0	.....
1000	40	0.20	1.4	0.12	1.8	0.28	.....	5.3	.....
1000	60	0.32	.....	0.24	.....	0.45	3.3	7.6	32.0
1000	80	0.40	.....	0.35	.....	0.65	.....	.....	.....

arranged in such a way as to approximate a condenser and resistance in series, as in Fig. 184, the loss may, over a limited range, increase approximately as the square of the frequency. If the insulation is in good condition, the loss may increase approximately directly as the frequency.

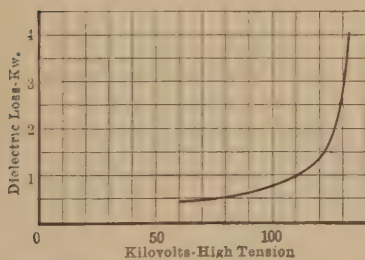


FIG. 193 (a).—Dielectric loss vs. voltage in a 2750 kv-a, 120 kv, 60 ~ transformer.

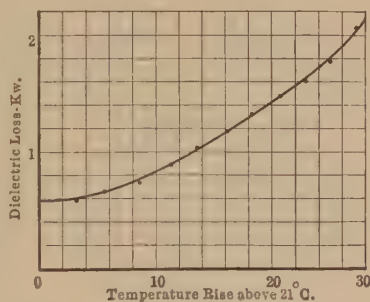


FIG. 193 (b).—Dielectric loss vs. temperature in a 3750 kv-a, 120 kv, 60 ~ transformer at 100 kv.

The best method of comparing different insulations is by measurement of losses.

Figures 193(a) and 193(b) show characteristic transformer dielectric loss curves taken several years ago at various voltages and temperatures. Although the transformers used were of rather old design with comparatively high losses, the curves, in

general, show the relation of loss to voltage and temperature in actual apparatus.

**Operating Temperatures of Insulations.**—The maximum operating temperature of insulations is indefinite. For low-voltage apparatus, temperatures not high enough to cause direct electrical failure may cause mechanical failure in short periods by drying out the insulation, cracking, etc. The maximum safe temperature, at which the life is not greatly shortened mechanically by cracking, drying out, etc., varies with different insulations, but is approximately as follows:

Fibrous materials, cloth, varnish, etc.....	100° C.
Asbestos, mica and similar materials, in combination with binders' varnish, etc.....	150° C.
Mica, asbestos—alone.....	very high.

These values are given without consideration of the electrical effects. Often the electrical properties will limit the tempera-

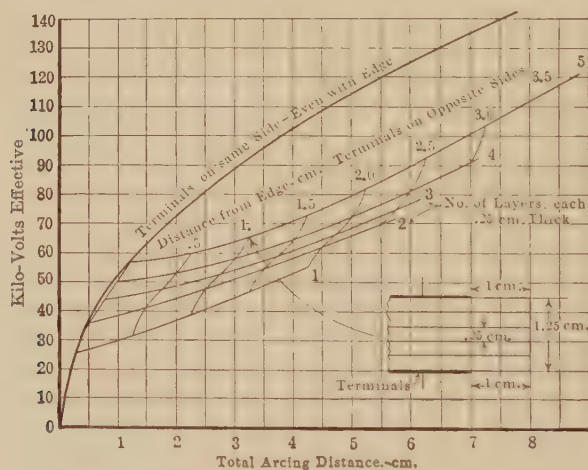


FIG. 194.—Surface arc-over in oil. (Hendricks.)

tures below these values. Heat conductivity must be considered in design, as well as the effect of sludging when insulations are in oil.

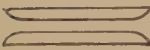

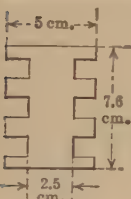

**Surface Leakage.**—Strictly speaking, on clean dielectric surfaces, appreciable leakage does not occur. What is generally termed "surface leakage" is a rupture of one dielectric at the surface of another dielectric by overflux concentration due to difference in permittivities, etc. For instance, on a porcelain insulator in air, the flux may be sufficiently concentrated at



portions of the surface to cause the air to rupture. The *appearance* is that of leakage over the porcelain surface. Surface leakage then is quite indefinite, and, for a given leakage distance, depends upon the position and shape of the electrodes, relative capacities of the materials, etc. (see Fig. 194). The effects of actual leakage and apparent leakage in air may be seen in Table LXXIX. In (1) the spark-over is given with the surface out. In (4) the decrease must be due to actual leakage as there is no flux concentration. In (2) and (3) flux concentration is balanced against increased surface.

**Solid Insulation Barriers in Oil.**—Properly placed barriers of solid insulation in oil greatly increase the strength of the oil spaces

TABLE LXXIX.—SURFACE ARC-OVER IN AIR

			Effective	
			kv.	kv./cm.
			128.0	16.8
			94.0	12.4
			87.0	11.4
			109.0	14.3
			89.0	11.7
			122.0	16.0
			62.0	8.0

NOTE.—Maximum possible kv. arc-over 128. Data shows that although corrugations increase stress, actual gain is made by their use by reduction of true leakage.

by limiting the thickness of the oil, preventing moisture chains lining up, etc. This should always be considered in design. In placing barriers, however, the arrangement should be such that the stress on the oil is not increased by the higher permittivity of the solid insulation (see Case 1, page 312 for illustration of this principle). Data for a simple arrangement are given in Table LXXX. It will be noted that, in most cases, the strength is not greatly increased on account of difference of permittivity of oil and solid insulation. The reliability is much greater, however.

TABLE LXXX.—PRESSBOARD BARRIERS IN OIL

	Kv. effective
Gap 0.24 cm.	
Oil only.....	23.0
1—0.08-cm. sheet of pressboard midway between electrodes.....	24.7
1—0.08-cm. sheet of pressboard against one electrode.....	22.7
<hr/>	
Gap 0.40 cm.	Kv. effective
Oil only.....	35.3
2—0.08-cm. sheets of pressboard against one electrode.....	36.5
<hr/>	
Gap 0.56 cm.	Kv. effective
Oil only.....	53.9
3—0.08-cm. sheets of pressboard against one electrode.....	44.0
<hr/>	
Gap 1.16 cm.	Kv. effective
Oil only.....	96.0
1—0.08-cm. sheet of pressboard 0.1 cm. from each terminal.....	95.3
1—0.08-cm. sheet of pressboard 0.33 cm. from each terminal.....	102.0
2—0.08-cm. sheet of pressboard at midpoint.....	88.5
1—0.08-cm. sheet of pressboard on each terminal.....	94.5

Strength of pressboard—0.08 cm., 15 kv.; 0.16 cm., 28 kv.

Terminals 6 cm. in diameter, rounded with a 3-cm. radius at the edges.

**Impregnation.**—Solid insulations built up from paper or cloth are subjected to a vacuum-drying process and then impregnation with oil, paraffin, or similar compound. The results are dielectrics of greater strengths and permittivities. If the impregnation is improperly done, for instance, so as to leave oiled and unoled spots, the dielectric strength may be less than the dry

paper alone. This is due to the difference in permittivities of the dry and oiled spots, which causes a concentration of stress on the electrically weak dry spots.

Such impregnated insulations are used extensively in transformers, high-voltage bushings, cables, etc. In general, these insulations are provided for immersion in oil immediately after impregnation so as to allow no exposure to air or moisture. It is largely due to this drying, impregnation, and oil immersion process carefully done, that it is now possible to design internally contained apparatus in practical sizes that will withstand very high voltages. The most recent instance of this has been the development of the oil-filled paper-insulated underground cable, installations of which are successfully operating at three-phase voltages of 132,000 volts.

**Mechanical.**—It is of great importance to arrange designs in such a way that local cracking or tearing is not caused by high localized mechanical stresses. This is especially so with porcelain, as in the line insulators. Expansion of a metal pin, localized mechanical stress due to sharp corners, expansion of improper cement, etc., will cause gradual cracking of the porcelain. The so-called deterioration of line insulators is often caused in this way.

**Direct Current.**—As the breakdown depends upon the maximum point of the voltage wave, the direct-current puncture voltage in air and oil is ( $\sqrt{2}$ ) or 1.41 times the sine wave alternating puncture voltage. In air and oil there is very little loss with alternating current until the puncture voltage is reached. With solid insulation, losses occur with alternating current as soon as voltage is applied. In the time tests, the insulation is thus considerably weakened by heating. This applies especially to thick insulation. This causes decreasing breakdown voltages in the time tests as the frequency is increased. In certain insulations, the loss is very small for direct current. The gain for direct current in solid insulation in the time tests is thus greater than the 41 per cent. given above (see Appendix).

**Occluded Air.**—Where careful work is not done, air films may be occluded in solid insulations. Such films are likely to break down and cause local heating, chemical action, and, finally, breakdown of the solid insulation. When such films are unavoidable, the stress should be limited below the breakdown of air. The strength of such film is the same as between metal electrodes (see data Appendix, page 382).

## CHAPTER IX

### LIGHTNING

**Nature of Lightning.**—Although the exact mechanism of charging a thunder cloud and the formation of the lightning stroke is not known, it can be explained in a general way.

From the results of field tests, in which the charges on falling raindrops were measured and from laboratory studies of the effect of air currents on water drops, G. C. Simpson<sup>1</sup> has developed a theory of thunder-cloud formation that is accepted by many. This theory involves water drops being broken up by air currents, the drops becoming positively charged and the air negatively charged. During thunder storms, there are always large falling drops and upward air currents. Drops large enough to fall against such currents are very unstable and easily broken. Simpson suggests that the rising air currents carry the negative charges to the clouds above. The broken positive drops rise while small, but fall as they increase in size. When this process brings the different portions of a cloud up to sufficient potentials, discharges in the form of lightning strokes take place between them. These strokes may be between clouds as well as within the same cloud and, in addition but less frequently, from cloud to earth. In this way, the upper regions of the cloud become negatively charged while the lower ones assume positive charges. Recent data seem to indicate, however, that most storm clouds are so charged that their upper portions are positive while their lower are negative, just contrary to the polarities dictated by Simpson's theory.<sup>2,3</sup> Simpson has recently advanced a further theory<sup>4</sup> wherein he differentiates between the physical shape of a positive and negative stroke. In addition he states that the negative discharges are less frequent but much more intense than the positive ones. The distinct difference between the corona

<sup>1</sup> SIMPSON, G. C., *Phil. Trans. Roy. Soc.*, A—209, 1909.

<sup>2</sup> SCHONLAND, B. F. J., *Proc. Roy. Soc.*, 118, p. 233, 1928.

<sup>3</sup> WILSON, C. T. R., *Phil. Trans. Roy. Soc.*, A—221, 1920, *Journal Frank. Inst.*, Vol. 208, p. 1, July, 1929.

<sup>4</sup> SIMPSON, G. C., *Proc. Roy. Soc.*, A—111, 1926.

discharge from a positive and a negative needle point was discussed in Chap. III. At higher voltages this dissimilarity persists and becomes quite marked at laboratory voltages of a million volts from ground.<sup>1</sup> From this, it would seem that a similar difference should exist in the physical nature of the discharges from the positive and negative poles of a cloud, as pointed out by Simpson. However, any attempt to differentiate between the polarity of strokes from their visible appearance alone would probably be very difficult in most cases due to the fact that a good deal of the discharge path and its branches are hidden from view.

**General Consideration of Lightning Theories.**—The lightning discharge is really the electrical breakdown of a large natural condenser with the clouds, or clouds and earth as the plates, and the air as insulation. Although the charging takes place slowly in some such manner as described above, the discharge takes place very rapidly. The energy is moderate, but because of the rapidity of discharge, the power or rate at which the energy is dissipated may be millions of horse power. The electrical energy is dissipated as heat, light, sound and chemical energy.

It is certain that a thunder cloud is formed by the separation of charges within it, but just how this occurs has not been definitely proven. When the field gradient at a certain point in a cloud becomes great enough, due either to an increased concentration of charge there, or to a charged portion approaching closer to an oppositely charged region, or to ground, local breakdown starts. This breakdown could be initiated by stray ions in the atmosphere and would be assisted by any heating and photoelectric effect that might enter. The ionization process would be cumulative, and the breakdown streamer would grow as long as the rate of charge loss by recombination through the streamer channel and leakage was less than the rate of supply due to the local generation process or the movement of fresh charges from the outside.

Just how far the streamer would grow and how much its conductivity would increase, would depend almost entirely on the amount of charge available. The process is similar to that occurring in the laboratory set-up used in studying the glow-spark-arc transition stages in an air gap breakdown. In this experiment the series-balancing impedance may be so adjusted as to regulate the flow of current in the breakdown and in that way govern its

<sup>1</sup> LUSIGNAN, J. T., *Trans. A. I. E. E.* p. 246, 1929.



voltage-current characteristics. With a low-current supply it may be held to the low-conductivity glow stage. When the current is allowed to increase, the discharge will gradually move into the low-voltage arc stage of high conductivity and assume a negative volt-ampere characteristic.

In the same way the initiating breakdown process in the thunder cloud may not progress any farther than the high-voltage glow stage before the available charge has all been dissipated. However should the breakdown reach some sort of a corona-like stage of low-voltage characteristics, the field will be transferred farther back into the charged regions due to the partial short-circuiting of the field by the low-voltage streamer. In that way, access is made to further charged positions of the cloud. In like manner, the other end of the streamer grows toward the opposite pole of the cloud, or to ground. If the accumulated and generated charge in the cloud is sufficient to supply the losses until the growing breakdown process has completely bridged the gap between opposite poles of the cloud or between one pole and ground, then the complete sudden collapse of the electrostatic field will take place. For this reason the preliminary stages of breakdown may take many seconds while the final complete breakdown coincident with the collapse of the field and the sudden release of bound charges, may be a matter of a few microseconds.

The inability of a portion of a cloud to continue to supply charge to the breakdown process at that point may result in the breakdown ceasing at the glow or possibly corona stage. This may account for the photographs of faint streamers and so-called "heat lightning" often obtained.

In the progress of a lightning stroke, more than one streamer may proceed from the head of the channel as it advances. Should the conductivity of one increase more than the others due to its encountering a greater source of charge or improved ionization facilities, then it will alter the electrostatic field by tending to short-circuit it along its path. This will rob the other branches of the voltage gradients necessary for their maintenance and they will cease. This would account for the short preliminary streamers photographed as branching out from the main lightning discharge channel. This same effect is found in the laboratory photographs of "impulse corona" on spheres as discussed on page 149, Chap. V.

As stated above, the time of the building-up stage of a stroke may be very long. In its final stage, considerable ionization and charge movements have taken place so that in effect the outer sheet of the cloud may be assumed to simulate a conducting surface. Thus, although separate charges on water drops are the initial charge storage, by the time the full stroke has developed, the outside surface of the cloud near the stroke may be considered equivalent to a metallic sheet. (In the same way, a number of highly charged shot separated by small insulating spaces on a smooth insulating surface would have the effect of a conducting plane. Gradual breakdown by local ionization would serve to connect the shot and make complete discharge possible.) Very high-local voltage gradients may take place in the cloud with more or less uniform and moderate average gradients between clouds, or from cloud and earth. In effect, this may be compared with the laboratory set-up of two parallel planes with a short point attached to the center of one or both planes. When voltage is applied, spark-over will occur at an average gradient of the order of 100 to 150 kv. per foot. Although very high-local gradients exist at the electrodes, the average gradient is important in engineering because it determines the induced voltage.

**Lightning Studies.**—Lightning energy may appear on conducting objects by a direct hit or by induction. A transmission line offers an ideal collector of lightning energy for study. The discussion that follows is the result of a study to determine the nature and characteristics of lightning and its effects on transmission lines, insulators, resistors, apparatus, etc. The general method followed has been to study lightning in the field and then go to the laboratory and attempt to reproduce the effects on models with a lightning generator. The work has progressed so far that it is now possible to express lightning characteristics in numerical values. A lightning generator of very high voltage has made possible the investigation of full-size apparatus, insulators, wood poles, etc. Wave shapes and voltages measured on transmission lines have been reproduced in the laboratory.

The results of the study of the effects of transient and lightning voltage on spark-over together with a description of the lightning generator will be found in Chap. V and the practical application will be found in Chap. XI.

**The Voltage and Energy of Lightning.**—By measuring voltages induced on transmission lines, it is possible to determine the potential and polarity of the lightning flash itself. Induced lightning voltages of over 500,000 volts were measured by the author on lines in Colorado in 1907 and 1908 and during the past few years voltages up to 2,800,000 volts have been detected on lines by surge voltage recorders. In many cases, the values have

been checked from records of simultaneous insulator flash-overs on the lines.

In the laboratory, models were made to scale representing a cloud and an insulated line for certain observed conditions. By means of the lightning generator, it was found that when a flash occurred from a given model cloud, 1 per cent. of its voltage was induced on the model line; but it was known by observation that the voltage induced on an actual line, under similar conditions, was of the order of 1,000,000. If this were 1 per cent. of the voltage of the actual lightning, the voltage of the flash must have been 100,000,000 volts. This gives an average gradient of 100 kv. per foot (330 kv. per meter) which is close to needle gap



FIG. 195.—Natural lightning stroke of 200,000,000 volts.

values of 150 kv. per foot (496 per meter)<sup>1</sup> and seems to be of the right order, although some variation may result. It is possible that higher instantaneous gradients may result near the path of the discharge. This value of 100 kv. per foot agrees with the gradients measured by others.<sup>2</sup>

The energy at 100,000,000 volts is of the order of 4 kw.-hr., but may be much higher, while the current is of the order of

<sup>1</sup> PEEK, F. W., JR., "Lightning," *Jour. Frank. Inst.*, February, 1925.

<sup>2</sup> NORINDER, H., *Elec. World*, Feb. 2, 1924.

100,000 amp. This value of current has been checked to some extent. For instance, in one case when a radio antenna was struck, a steel spring at one end of the antenna was just melted. Current time curves were then made on this spring by short circuiting a large generator through it. In another case, the current measured in a transmission tower struck by lightning was about 150,000 amp.

Figure 195 shows a 200,000,000-volt lightning stroke 2000 ft. long measured at Pittsfield, Mass.

The energy of lightning strokes must vary widely. The above value of 4 kw.-hr. is the energy stored in the field between a 1000-ft. square cloud and earth at 100,000,000 volts, the cloud height being 1000 ft. For potentials of 200,000,000 volts, energies of the order of 10 kw.-hr. seem reasonable. (A breakdown gradient of 100,000 volts per foot is assumed in the above estimates.) Going to the extreme, assume that it is possible for a 5000-ft. square, 5000-ft. high cloud to discharge to earth. The energy in the field in this case would be approximately 500 kw.-hr. This seems to be a rather high figure when the comparatively mild destructive effects of lightning are considered.

**How Induced Lightning Voltages Occur and Their Value.**—In Fig. 196 is shown the electrostatic field beneath a negatively charged thunder cloud. A short well-insulated wire situated along an equipotential surface takes the potential of the space in which it is located and becomes (+) on the side nearest the cloud and (−) on the side farthest from the cloud (Fig. 196(a)). When the cloud discharges, two charges on the wire go together and the potential of the wire becomes zero. It is sometimes possible for a spark to occur between insulated wires differently located in space, even though the cloud does not discharge. What is usually known as electrostatic induction, however, occurs as follows:<sup>1</sup>

Assume the line wire in Fig. 196(b) to be poorly insulated or grounded, or to extend beyond the cloud as in 196(c). The negative charge leaks away. The wire, under the cloud, becomes positively charged, its potential remaining zero prior to lightning discharge. When the cloud discharges, the bound positive charge on the wire is released, which causes it to take a potential above ground with a sign opposite to that of the cloud. If the cloud

<sup>1</sup> PEEK, F. W., JR., "Progress in Lightning Research in the Field and in the Laboratory," *Trans. A.I.E.E.*, 1929.



discharge is instantaneous, the line at every point momentarily assumes a potential above ground equal to the line height times the voltage gradient there. The gradient depends upon the position of the cloud with respect to the wire. Figure 197 shows a typical distribution of stress under a thunder cloud just

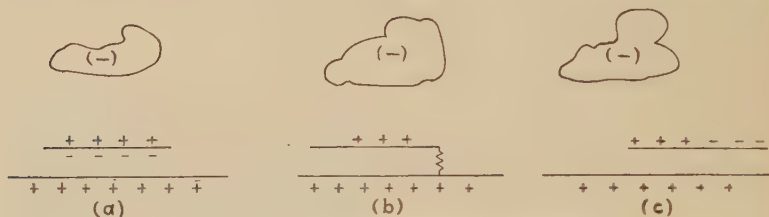


FIG. 196.—Voltages induced by lightning.

prior to discharge to earth. The maximum gradient that a line probably can experience is seen by Fig. 197 to be approximately 100 kv. per foot (or 330 kv. per meter) which would occur

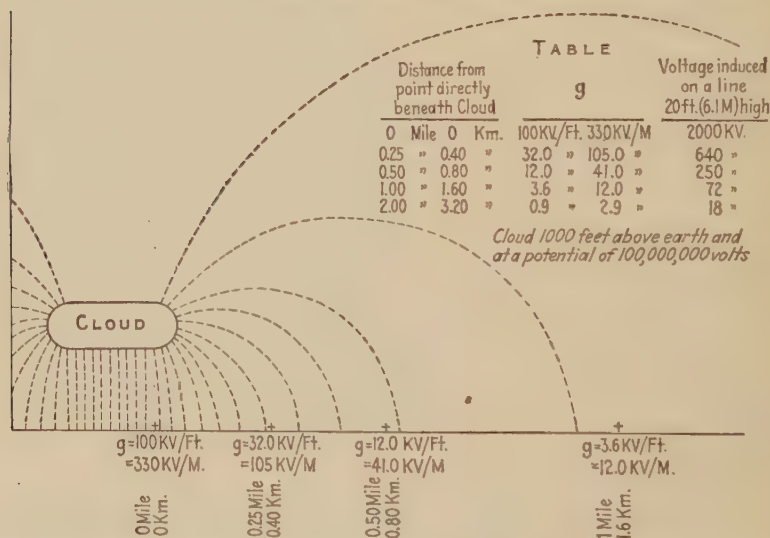


FIG. 197.—Electrostatic field and potentials in space caused by charged cloud.

directly beneath a cloud close to the discharge path. The value of induced voltage depends on the rate of cloud discharge and the original length and distribution of bound charge. In general, it may be expressed by the equation  $V = \alpha gh$ , where  $g$  = maximum gradient (100 kv. per foot)  $h$  = height of line, and  $\alpha$  =



reduction factor ( $=$  or  $< 1$ ) depending on rate of cloud discharge and distribution of bound charge. This factor will be discussed more fully later (see page 267). The reason that the line takes the voltage of the equipotential surface in space that would result from the cloud field of the line were waves present is readily understood. The line becomes charged due to its position in space. The resulting field about the line, while the charge is bound, is due to the linear field of the cloud plus the field on the line due to  $gh$ . When the cloud discharges, the linear field disappears and the line must rapidly rise to voltage  $gh$  due to the charge.  $V = gh$  applies only when the discharge of the cloud is very rapid or when the line is shorter than the cloud. This follows because  $V = Q/c$ . If the bound charge  $Q$  has time to spread out over the line while it is being released by the discharge of the cloud,  $c$  becomes large and  $V$  small. The rate of travel of the released charge is approximately 1000 ft. per microsecond.

**Traveling Waves.** *Origin of Traveling Waves.*—The distribution of bound charge along the line varies from point to point, corresponding to the intensity of the electrostatic field of the cloud. When the cloud discharges, the bound charge is released at the same rate at which the cloud discharges and causes traveling waves of potential and current to be propagated in both directions.

It is evident from symmetry considerations that the two sets of waves traveling away from the center of disturbance are exactly similar for a symmetrical bound charge, although this can be shown to be a mathematical consequence. Both the initial distribution of bound charge and the functional rate of cloud discharge probably vary over a wide range. General mathematical expressions involving infinite series and definite integrals have been derived for the traveling waves due to bound charges of any distribution and for cloud discharge rates following any law.<sup>1</sup> The practical application of such a mathematical analysis is extremely limited, however, because the integrations can be performed for only a few very simple functions, and the infinite series converge so slowly as to require the use of a mechanical process of summation.

A graphical method for determining the wave shapes corresponding to any arbitrary distribution of bound charge and rate of cloud discharge has been developed.<sup>1</sup> This method is based

<sup>1</sup> BEWLEY, L. V., *Trans. A.I.E.E.*, 1929.

upon the justifiable assumption that line distortion and attenuation may be neglected during the formation process. Referring to Fig. 198, suppose that the initial bound charge is rectangular in shape and is released according to an exponential law of cloud discharge. This exponential curve may be replaced, for practical purposes, by a superimposed stepped curve, shown in the figure, so that the bound charge may be considered as being released by a series of jumps. When the time increments between steps are taken sufficiently small, the stepped curve approaches coincidence with the actual exponential curve. Each of these steps

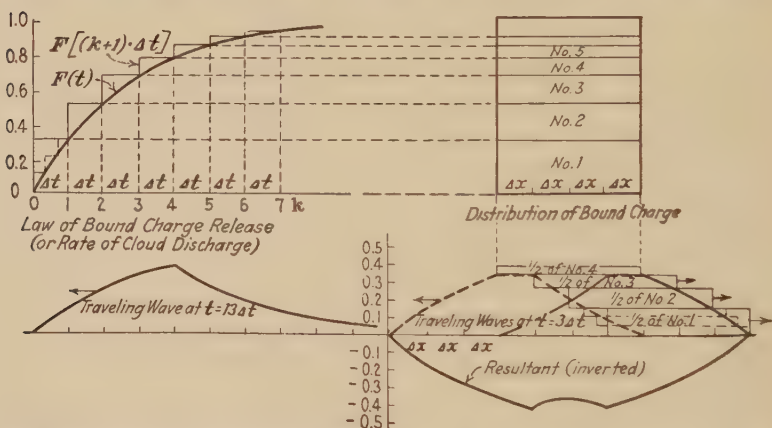


FIG. 198.—Graphical method of determining shape of traveling wave with assumed bound-charge distribution and cloud-discharge rate.

corresponds, then, to the instantaneous release of a definite part of the bound charge and gives rise to two exactly similar pairs of rectangular traveling potential and current waves proceeding in opposite directions from the center of disturbance. Thus, during the first time increment, one-half of block 1 has formed and moved out on the line a distance equal to the product of the time increment and velocity of propagation. Successive blocks are formed as progressive displacements in time and space, and their aggregate at any instant gives the space distribution at that instant. It will be noticed that the complete traveling waves cannot be superimposed in their relative space positions for periods of time less than it takes the cloud to discharge, because these waves are not fully developed until the end of the cloud discharge.

Figure 199 illustrates the formation of traveling waves from an initial peaked bound charge distributed over 2000 ft. of the line. The cloud is assumed to discharge exponentially in approximately 1 microsecond. In this case, the maximum crest occurs at the center of disturbance, or axis of symmetry, but is only about 20 per cent. greater than the crests of the traveling waves which are assumed to have suffered no attenuation. In general, as indicated before, the maximum crests during discharge and the crests of the traveling waves depend upon the initial distribution of bound charge and the rate of cloud discharge. This depend-

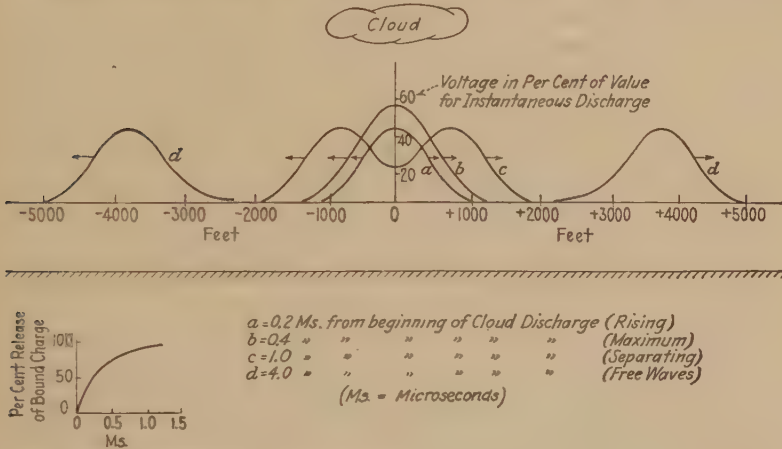


FIG. 199.—Formation of traveling waves from peaked bound charge (2000 ft. long) released in 1 microsecond.

ence is shown in Figs. 200 (a) and (b) for the case of rectangular distributions of bound charge and exponential discharge rates. In Fig. 200(a),  $\alpha$  is the reduction factor in the expression  $V = \alpha gh$  (see page 264) for determining the maximum crest voltage of the bound charge which occurs prior to separation of the charge into traveling waves.  $\alpha$  in Fig. 200(b) is the reduction factor as applied to the same expression for the crest value of the traveling wave.

In Fig. 201 have been plotted the actual calculated induced voltages on a typical transmission line for cloud lengths of 1000 and 2000 ft. and time intervals of discharge up to 10 microseconds. These curves clearly indicate that high induced voltages are not possible with slow rates of cloud discharge. The curve data of Fig. 201 have been based on a maximum field

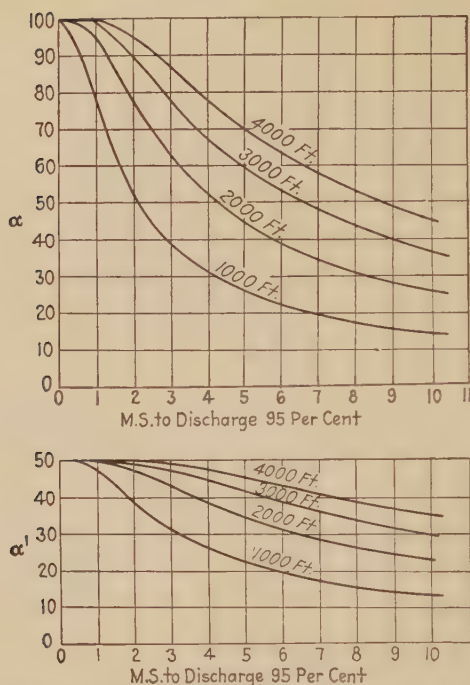


FIG. 200.—Reduction factors indicating effect of bound-charge distribution and cloud-discharge rate on induced voltages. (a) Reduction factor,  $\alpha$ , for maximum crest; (b) reduction factor,  $\alpha'$ , for crest of traveling wave.

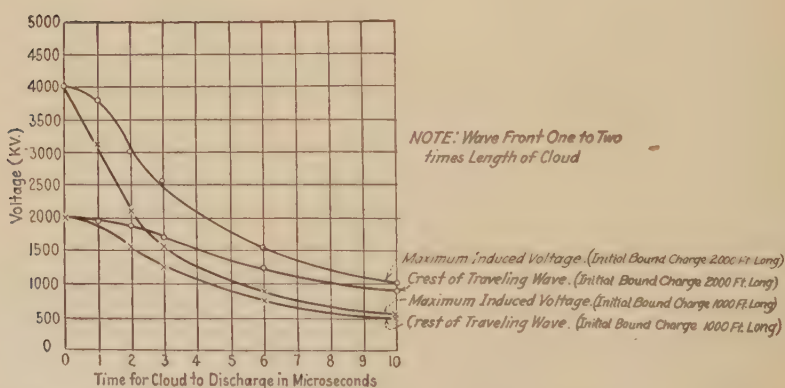


FIG. 201.—Maximum induced voltages on a typical transmission line for various bound charges and cloud discharge rates—line 40 ft. high.



gradient of 100 kv. per foot. At other portions of the cloud's electrostatic field where the gradient would be less, the above voltages would be correspondingly decreased.

*Traveling Waves on a Line.*—A wave in moving along a line suffers a change due to distortion and attenuation. Distortion involves a change in shape due to the different rates of propagation of the various harmonic components of the wave. Attenuation causes a general decrease in magnitude of the wave due to the diminishing amplitude of the harmonics incurred through corona and ohmic losses.

When a traveling wave strikes a transition point at which there is an abrupt change in circuit constants, as an open- or short-circuited terminal, a transformer bank, or a junction with another line, a part of the wave is reflected back on to the line, and a part may proceed on to other parts of the circuit. The incident, reflected and transmitted waves, may be expressed mathematically.<sup>1</sup> In fact, a general expression may be derived, as follows, which applies for all wave shapes striking transition points: Fig. 202(a) shows two lines joined by a concentrated impedance network consisting of a resistance  $R_o$ , an inductance  $L_o$ , and a capacitance  $C_o$  in parallel. There are seven immediate special cases of this connection, by employing in different combinations the limiting values  $R_o = 0$ ,  $R_o = \infty$ ,  $L_o = 0$ ,  $L_o = \infty$ ,  $C_o = 0$ , and  $C_o = \infty$ . In the analysis of the behavior of traveling waves at a transition point, the surge impedance of a connected line as  $Z_2$  enters the equations for the reflected and transmitted waves in exactly the same way as an equal resistance to ground  $R_2 = Z_2$ . Thus, Fig. 202(b) is the analytical equivalent to Fig. 202(a) except that  $e''$  is then merely the potential at point (y) instead of a traveling transmitted wave originating at that point. There are again seven special cases immediately obtainable by applying limiting values to the constants. Now let  $R_2 = 0$  and break  $R_o$  up into the two resistances  $R'_o$  and  $R''_o$  in parallel, so that Fig. 202(c) results. Here again it is conversely permissible to replace one of the resistances to ground, say  $R''_o$ , by the equivalent surge impedance of a line,  $Z''_o = R''_o$ , so that the conditions are then as shown in Fig. 202(d) and of this, there are also seven special cases. By these considerations, the equations which apply to Fig. 202(a) are directly reducible to a total of twenty-three subcombinations. For the more simple cases,

<sup>1</sup> BEWLEY, L. V., *Trans. A.I.E.E.*, 1929.



however, it sometimes is easier to derive the results from the differential equations than to reduce the general equation, due to the number of indeterminates involved, or to the necessity of transferring functions of imaginary quantities to functions of real quantities, etc.

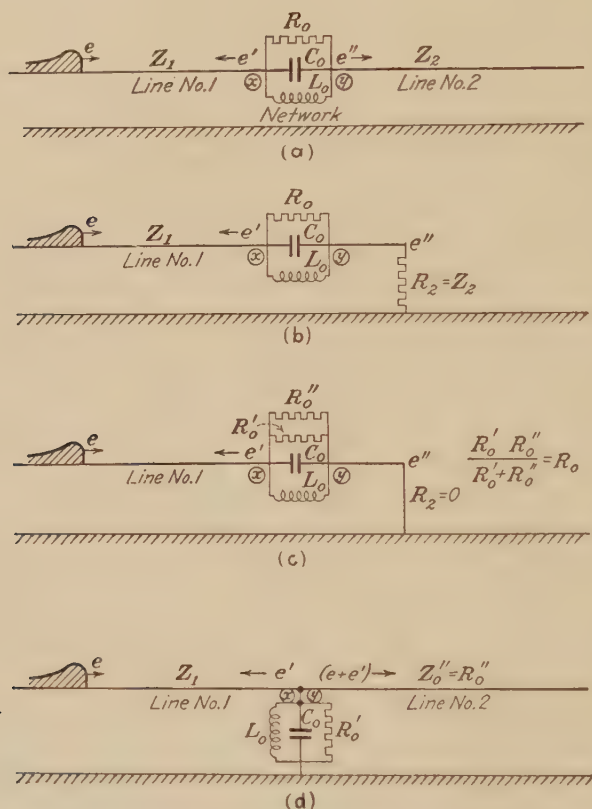


FIG. 202.—Diagrams of various equivalent networks.

Referring to Fig. 202(a), let the potential due to the incoming incident wave at point ( $x$ ) be given as time function by

$$e = E (\epsilon^{-at} - \epsilon^{-bt})$$

where the constants  $a$ ,  $b$ , and  $E$  are usually sufficient to define the crest, front, and tail of a characteristic traveling wave due to lightning. (Typical wave shapes expressed by this equation

are shown in Fig. 203.) The reflected wave at the point  $x$  is then given by

$$e' = \frac{Z_2 - Z_1}{Z_2 + Z_1} E \left\{ \frac{a^2 - 2\lambda a + w_o^2}{a^2 - 2\beta a + w_o^2} \epsilon^{-at} - \frac{b^2 - 2\lambda b + w_o^2}{b^2 - 2\beta b + w_o^2} \epsilon^{-bt} \right. \\ \left. + \frac{2(\beta - \lambda)}{w} \epsilon^{-\beta t} \left[ \sqrt{\frac{a^2}{a^2 - 2\beta a + w_o^2}} \sin(wt - \phi_1) - \sqrt{\frac{b^2}{b^2 - 2\beta b + w_o^2}} \sin(wt - \phi_2) \right] \right\}$$

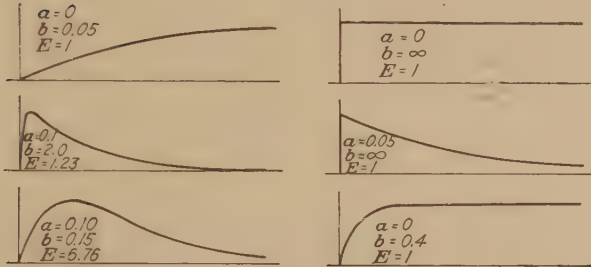


FIG. 203.—Typical wave shapes as may be expressed by equation:  
 $e = E(\epsilon^{-at} - \epsilon^{-bt})$

where

$$\lambda = \frac{Z_2 - Z_1 + R_o}{2R_o C_o (Z_2 - Z_1)} \quad w_o^2 = 1/L_o C_o \\ \beta = \frac{Z_2 + Z_1 + R_o}{2R_o C_o (Z_2 + Z_1)} \quad w^2 = w_o^2 - \beta^2 \\ \phi_1 = \tan^{-1} \left( \frac{w}{a - \beta} \right) \quad \phi_2 = \tan^{-1} \left( \frac{w}{b - \beta} \right)$$

The transmitted wave is

$$e'' = \frac{2Z_2}{Z_2 - Z_1} E \left\{ \frac{a^2 - 2\gamma a + w_o^2}{a^2 - 2\beta a + w_o^2} \epsilon^{-at} - \frac{b^2 - 2\gamma b + w_o^2}{b^2 - 2\beta b + w_o^2} \epsilon^{-bt} \right. \\ \left. + \frac{2(\beta - \gamma)}{w} \epsilon^{-\beta t} \left[ \sqrt{\frac{a^2}{a^2 - 2\beta a + w_o^2}} \sin(wt - \phi_1) - \sqrt{\frac{b^2}{b^2 - 2\beta b + w_o^2}} \sin(wt - \phi_2) \right] \right\}$$

where,

$$\gamma = \frac{1}{2R_o C_o}$$

Thus  $e''$  and  $e'$  are of the same general form. Indeed, except for the outside coefficients  $(Z_2 - Z_1)$  and  $2Z_2$ , the two equations are mutually convertible by an exchange of  $\lambda$  and  $\gamma$ .

Figure 204 shows typical cases of calculated waves at various kinds of transition points. Figure 204(a) is that of the incident and reflected waves at the open end of a line. In this case, the current stops and the total energy becomes electrostatic so that the voltage must double. In Fig. 204(b), where the end of the line is closed by a resistance equal to the surge impedance of the line, there is no reflection. In the short-circuited line of Fig. 204(c), there is a negative voltage reflection causing the resultant

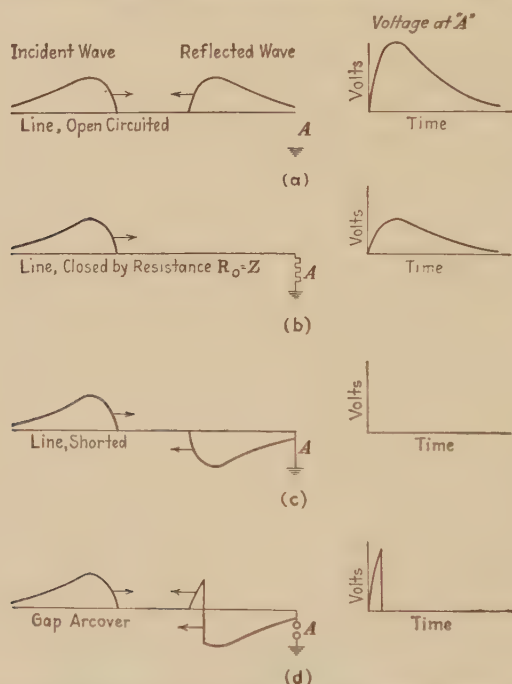


FIG. 204.—Traveling waves (calculated) at typical transition points.

end voltage to be zero. In Fig. 204(d), the effect on the reflected wave is shown when a gap spark-over near the crest of the wave short circuits the line.

Figures 204(e) and 204(f) show the calculated waves involved when a surge strikes the line end network given. This circuit may be considered as equivalent to a spark gap shunting a transformer (of capacitance  $C_o$ ) having a choke coil (of inductance  $L_o$ ) in series. In Fig. 204(e) are given the various voltage waves when no gap spark-over takes place, for both square and sloping incident waves. In Fig. 204(f), the same waves are given for

the case when gap spark-over occurs on the front of the incident wave.

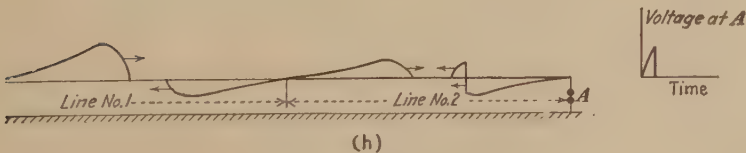
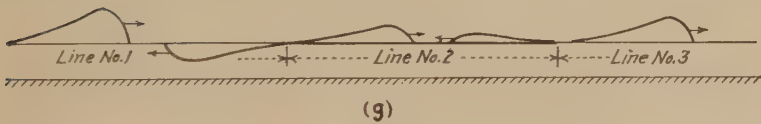
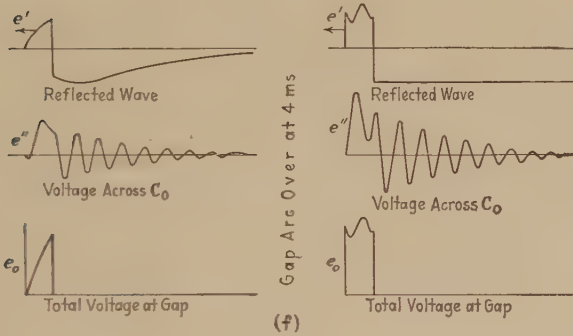
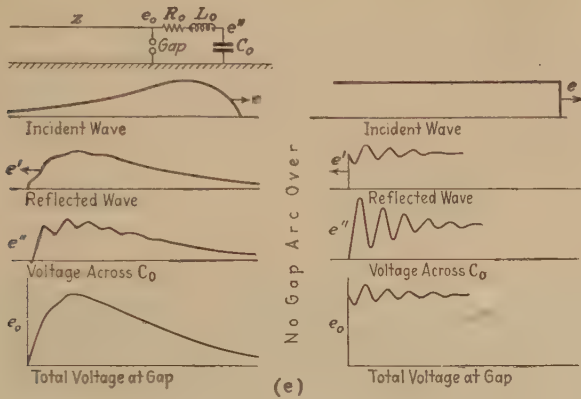


FIG. 204.—(Continued.)

In Fig. 204(g), the decrease in voltage of a traveling wave passing through a section of line of lower surge impedance is

shown. This section may be one having added ground wires, or an underground cable. Figure 204(h) gives a similar case except that a gap spark-over occurs at the end of the section of decreased surge impedance.

*Oscillograph Records of Lightning, Lightning Waves, and Impulses Lightning Waves.*—By coupling the recording circuit of a cathode-ray oscillograph to a transmission line by means of an electrostatic potentiometer, and providing an extremely rapid self actuating circuit, oscillograms of lightning waves have been obtained.<sup>1</sup> One wave recorded in this manner on a 220-kv.

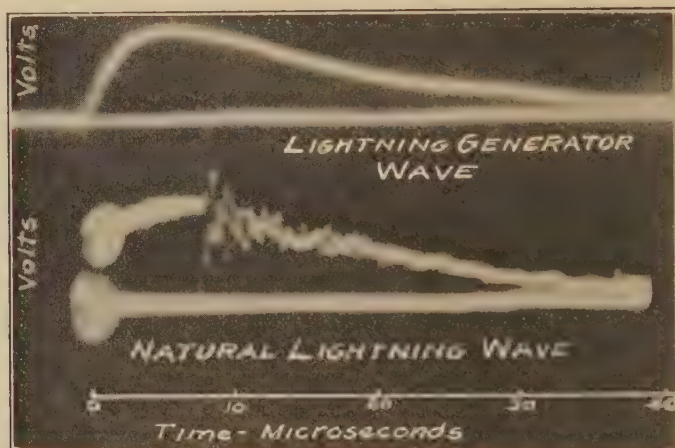


FIG. 205.—Comparison of natural lightning wave on transmission line as recorded by cathode-ray oscillograph, and artificial lightning wave recorded in same manner.

line is shown in Fig. 205. The front of this wave reaches its maximum value in 5 microseconds, decreases to half value in 20 microseconds, and reaches zero in 40 microseconds. The oscillating ripple is apparently due to a local flashover and is not really part of the original wave. A reproduction of this surge by the laboratory lightning generator (see page 144) is also shown in Fig. 205.

*Cloud Discharge Waves.*—Using the same method of recording but with the oscillograph coupled to a short antenna grounded through very high resistance, instead of a transmission line, records indicating rates of cloud discharge were secured. This

<sup>1</sup> PEEK, F. W., JR., "Progress in Lightning Research in the Field and in the Laboratory," *A.I.E.E.*, 1929.



followed because a charge cannot move along a short line. Accordingly, the potential of the antenna must rise at a rate and to a magnitude dependent upon the collapse of the cloud field. The time for the antenna voltage wave to reach maximum is thus a measure of the time required for the cloud to discharge while the voltage divided by the height of the antenna is a measure of the gradient. Oscillograms obtained in this manner indicated, in some cases, times of cloud discharges of the order of 1 to 2 microseconds. In this case, the leakage resistances attached to the antenna were of 2,000,000 ohms.<sup>1</sup>

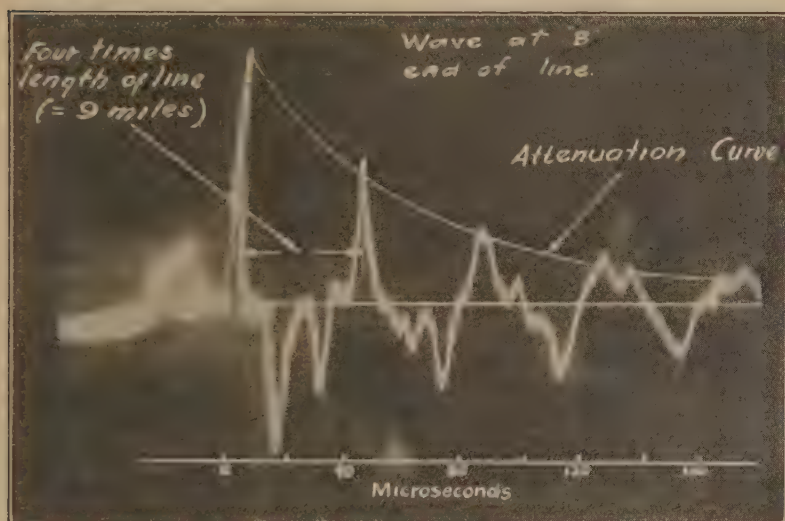


FIG. 206.—Cathode ray oscillogram of voltage wave, showing attenuation suffered in successive reflections from opposite ends of line.

*Artificial Traveling Waves.*—Impulse waves from the laboratory lightning generator were imposed upon a transmission line, and oscillographic studies made of the attenuations and reflections incurred under various conditions.<sup>2</sup> In one case, a short wave was sent over the line and the voltage record obtained at the open-circuited far end. Figure 206 shows the oscillogram secured, which indicates the attenuation incurred by the wave in its successive reflections back and forth over the line. Figure

<sup>1</sup> PEEK, F. W., JR., "Progress in Lightning Research in the Field and in the Laboratory," *A.I.E.E.*, 1929.

<sup>2</sup> PEEK, F. W., JR., "Lightning," paper presented before World Eng. Congress, Tokyo, Japan, 1929.

207(a) shows one of the typical short chopped waves starting from its point of origin. In traveling the length of the line it was attenuated to 71 per cent. of its initial value. On reaching the open end of the line it was reflected to double voltage or to 142 per cent. of its initial value as shown in Fig. 207(b). If a gap is set at the far end with a lightning spark-over voltage of 96 per cent. of the initial wave, the wave is reflected to 96 per cent. of its initial value as shown in Fig. 207(c). If a gap is set at the far end with a lightning spark-over voltage of 67 per cent. of the initial wave, the wave is reflected to 67 per cent. of its initial value as shown in Fig. 207(d).

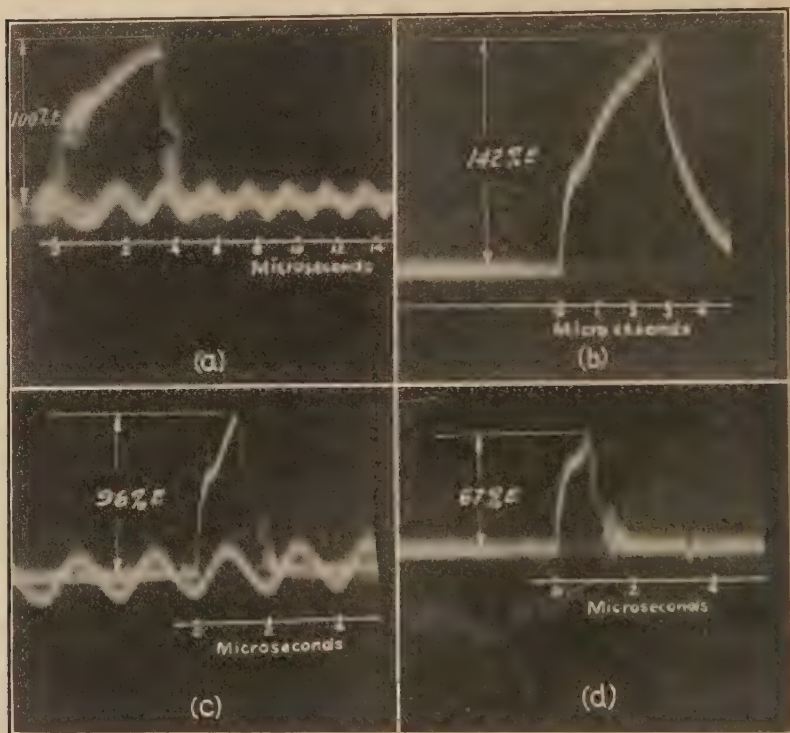


FIG. 207.—Cathode ray oscillograms of waves on transmission lines: (a) Initial wave at sending end; (b) initial wave reflected to double voltage at open far end, after attenuation to 71 per cent.; (c) wave at far end chopped by gap set at 96 per cent. of sending voltage; (d) wave at far end chopped by gap set at 67 per cent. of sending voltage.

per cent. of the initial wave, then the voltage at the far end cannot rise above this value but is chopped at the 96 per cent. value as indicated in Fig. 207(c). Figure 207(d) shows the voltage wave chopped by a gap set at 67 per cent. of the initial voltage.

That an ordinary moderate size transformer at the end of a line does not behave far differently from an open circuit is shown in Fig. 208. Here the difference in the reflected voltages at an

open circuit (Fig. 208(a)) and at a transformer (Fig. 208(b)) is seen to be only 2 per cent.

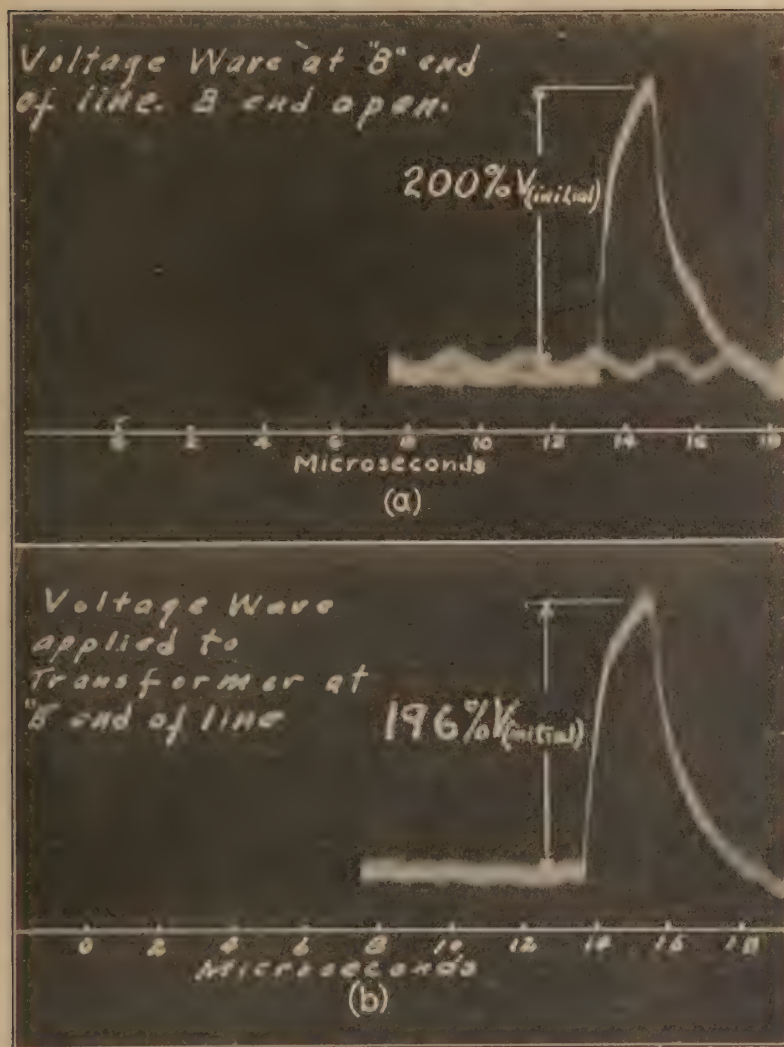


FIG. 208.—Cathode-ray oscillograms showing similar voltage waves striking (a) an open end, and (b) a transformer.

When a wave strikes an inductance in series with the line, part is reflected back over the line and part passes through. The latter part may cause very high voltages and oscillations if the

end is open or if it is closed by a transformer. The oscillations correspond to the natural period of the series inductance and the transformer capacitance. Figure 209(a) shows a wave that has struck an inductance after being chopped by an insulator spark-over to ground. Figure 209(b) is the voltage across a transformer caused by that part of the previous wave which passed through

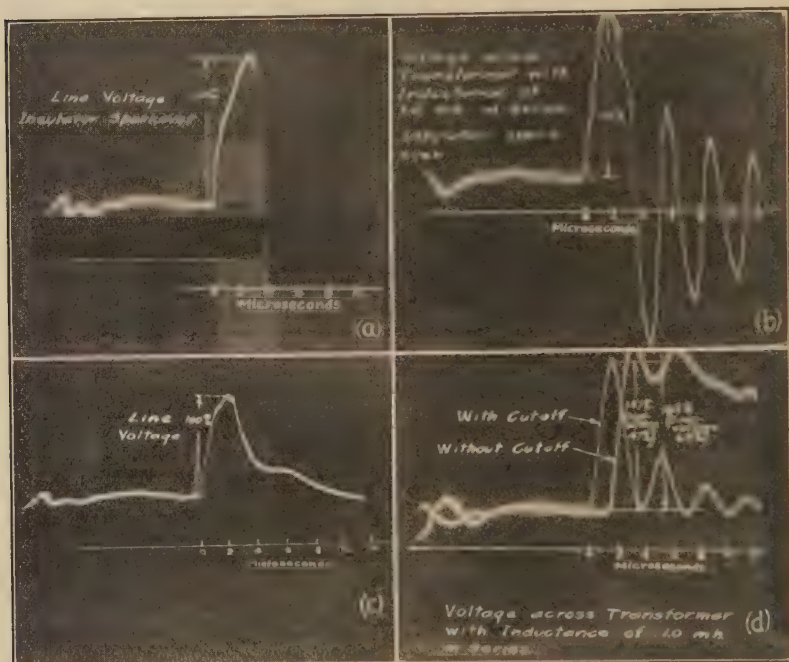


FIG. 209.—Cathode-ray oscillograms showing effect of series inductance on traveling waves: (a) Wave chopped by insulator on striking inductance; (b) part of wave in (a) passing through inductance and causing oscillations at transformer; (c) wave chopped upon striking inductance by gap with series resistance; (d) voltage rise and oscillations across transformer caused by part of wave passing through inductance (wave with and without being chopped).

the series inductance. An oscillation and an increase in voltage has resulted. Figure 209(c) shows a full wave striking an inductance. Figure 209(d) like Fig. 209(b) shows the voltage across a transformer caused by that part of the initial wave which passed through the series inductance. In Fig. 209(d), however, two cases are shown. In one case, the oscillations take place about axes lying above the zero axis as the tail of the original wave was sustained. In the other, the wave, on reaching the inductance, was cut off or chopped by a gap having a series resis-



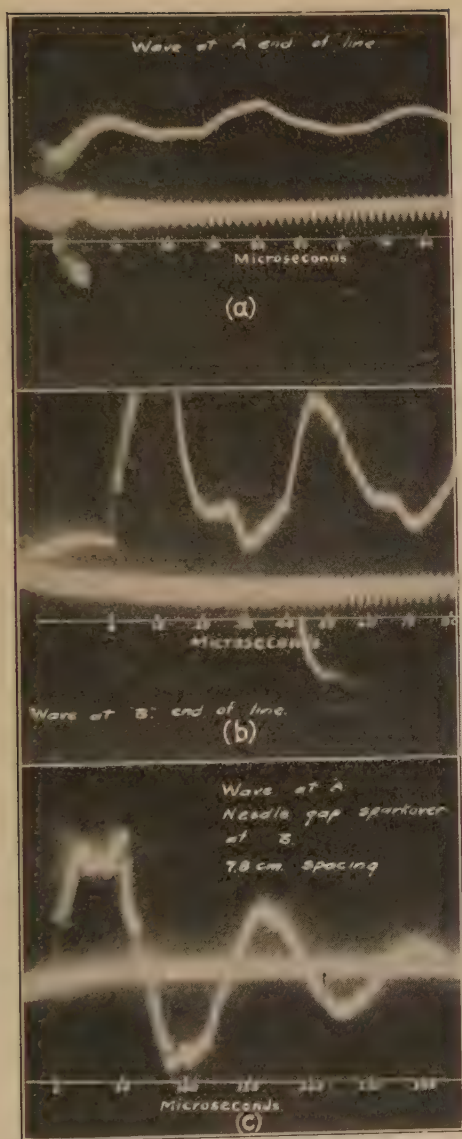


FIG. 210.—Cathode-ray oscillograms showing oscillations due to wave longer than line: (a) Voltage at sending end; (b) voltage at receiving end, open; (c) voltage at sending end with needle gap spark-over at far end.



tance and the oscillation was quickly damped. In both cases, a rise in voltage occurred after the wave passed through the inductance. From this it is apparent that a series inductance or "choke coil" not only affords no lightning protection but may introduce a hazard, a fact that was realized some time ago.<sup>1</sup> Resistances of proper values placed in parallel with series inductances will prevent the latter from introducing dangerous over-voltages and oscillations when struck by incoming surges. For this reason, reactors used for power limiting purposes should be shunted with resistances of proper values to guard against all possible transients. (Compare Figs. 204 and 209.)

Figure 210(a) is the voltage oscillogram at the sending end of a wave longer than the line. Figure 210(b) shows the voltage record of the same wave taken at the far end, which is open circuited. In Fig. 210(c) is given the voltage record at the sending end of the same line with a needle gap spark-over occurring at the far end. In this case, the sending end was shunted by a condenser. This causes an oscillation of lower frequency. (See Figs. 254, 255 and 256 for the effect of traveling waves on transformers.)

**Surge Voltage Recorder Investigation of Lightning.**—By means of surge voltage recorders or klydonographs (see page 106, Chap. IV) located along transmission lines, it has been possible to determine the magnitude and polarity of induced lightning voltages and the subsequent traveling waves set up by them. The low voltage applied to the instruments themselves is obtained from a capacity potentiometer attached to the line, usually a shielded string of suspension insulator units.

Considerable data have been gathered during the last few years on high-voltage lines in this way which has contributed to our understanding of lightning surges.<sup>2</sup> In general, these field data have seemed to indicate that the higher-voltage surges have been caused by negative lightning flashes, although records have been secured indicating a few positive strokes of equally high intensities. Some of the voltages measured were as high as 2,800,000 volts. The records showed the lightning flashes themselves to be unidirectional or else highly damped.

<sup>1</sup> "Effect of Transient Voltages on Dielectrics III," F. W. Peek, Jr., *Trans. A.I.E.E.*, 1923.

<sup>2</sup> Paper by W. W. Lewis, and companion papers on surge measurements, *Trans. A.I.E.E.*, p. 1111, 1928.

With instruments connected at frequent intervals along the lines investigated, it was possible to obtain the magnitude of each voltage surge as it progressed and, in that way, the rate of attenuation. As previously outlined, ohmic and corona losses are the principal cause of the dissipation of the energy of traveling waves. Consequently, attenuation would be pronounced at very high lightning voltages where corona losses would be excessive. Also, with surges of steep wave fronts, the skin effect would be enough to increase the ohmic losses considerably. Electromagnetic radiation losses are probably appreciable at steep waves, especially at points of reflection.

As pointed out previously, Fig. 206 shows attenuation of a laboratory wave on a line.

In the above lightning study on actual lines,<sup>1</sup> a very rapid attenuation was indicated for very high voltages which seemed to be approximated by the following equations due to Messrs. C. M. Foust and F. B. Menger:

$$e = \frac{e_o}{kle_o + 1}$$

$$A = -ke^2$$

in which

$e_o$  = the initial voltage at the point where the surge originated

$k$  = a proportionality factor which is found empirically

$l$  = the distance in miles from the origin of the surge

$e$  = voltage at any distance  $l$

$A$  = the attenuation in kilovolts per mile

The factor  $k$  for all the surges investigated has been found to be about 0.00016.

These equations are used as follows:

1. Assume the initial potential to be 2000 kv. Then at a distance 10 miles from the origin

$$e = \frac{2000}{(0.00016 \times 10 \times 2000) + 1} = 477 \text{ kv.}$$

The attenuation at the point of origin of the surge is

$$A = -0.00016 \times 2000^2$$

$$= -640 \text{ kv. per mi.}$$

2. If the initial surge was only 1000 kv. in magnitude, then the attenuation would be

$$\begin{aligned} A &= -0.00016 \times 1000^2 \\ &= -160 \text{ kv. per mi.} \end{aligned}$$

**General Character of Lightning Waves.**—When the maximum voltage of the lightning impulse causing an insulator spark-over is measured by a sphere gap or surge-voltage recorder, and the 60-cycle spark-over voltage of the insulator is known, then the effective duration of the wave can be estimated. For example, the lightning spark-over of insulator strings measured on the 220-kv. lines of the Pennsylvania Power and Light Company were found to average about 2000 kv. The 60-cycle crest spark-over voltage was 1000 kv. for these insulators. This indicates an average impulse ratio of 2.0. The usual impulse ratios of spark-overs caused by natural lightning vary between 1.8 and 2. In a few cases impulse ratios as high as 2.7 were obtained. Laboratory studies have shown that, for these values of impulse ratios, the effective duration varies from 1 to 20 microseconds, where the effective duration is the time that the voltage is above half voltage or approximately the time above the 60-cycle spark-over voltage, since lightning waves have been found to have impulse ratios of the order of 2.0.

The above does not mean that the lightning waves are always the same as the laboratory waves. In fact, many lightning flashovers of insulators probably occur on the rising front of a moderately steep wave giving the effective duration mentioned above. This is illustrated in Fig. 128(b). However, the effect is the same. Lightning waves must vary over a wide range. In fact oscillograms of natural lightning on lines frequently show waves with fronts varying from less than one microsecond to more than eight microseconds. Where the voltages are high enough to cause insulator flashovers, however, the waves must be steep or, in effect, of short duration. This follows because induced voltages cannot be high unless the cloud is discharged quite rapidly. Direct strokes must apply the voltage very rapidly.

Spark-over values by actual lightning and by laboratory waves are shown in Fig. 123. These waves are of the same general order of the wave shown in the oscillogram of lightning in Fig. 205. This wave was actually reproduced in the laboratory and used to test transformers, insulators, etc.

**The Ground Wire.**—When a grounded conductor is placed near and parallel to a transmission line, the capacitance of the line to ground is increased. This reduces the potential to ground

of the bound charge left on the line upon cloud discharge. If the ground wire is placed above the transmission line, the lightning induced voltage is further reduced due to the shielding effect introduced, that is, the ground wire permits less of the electrostatic lines of the cloud field to terminate on the line wires. This reduces the initial bound charge on the wires. The ratio of the induced line voltage with a ground wire and without one is generally termed the "protective ratio." The most important reason for placing the ground wire on top is for protection against direct strokes. To cause the voltage reduction, the ground wire must be kept at zero potential by connections to ground at comparatively short intervals. Otherwise, it acts exactly as the line wires since all of the conductors are charged in the same way.

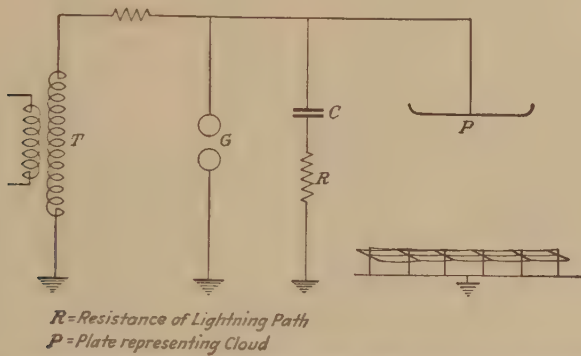


FIG. 211.—Lightning generator connections used in studying induced voltages on laboratory transmission lines.

Most calculations of the protection afforded by ground wires from induced voltages have been made from a purely static standpoint. A complete solution requires consideration of all factors involved, namely, the distribution of bound charge, rate of cloud discharge, grounding conditions, etc. Careful consideration is necessary in all cases involving infrequent and irregular grounds. The action of corona in increasing the effective size of the conductor and the loss is also important.

Laboratory tests were made with the lightning generator (see page 144 Chap. V) using model lines under model clouds, and measuring the induced voltages with and without ground wires in various arrangements. Figure 211 shows a diagram of the usual circuit connections. Figure 212 illustrates a typical model



set up for test, in this case to study the induced voltages on a line with varying heights of towers at a river crossing. The fact that the induced voltage depends upon the height of the line is readily shown by tests on such models. Some typical laboratory results obtained are given in Table LXXXI. These values have been checked by field tests on short full-sized lines.

In Fig. 213 is given a diagrammatic method (by E. W. Boehne) of determining the protective ratio of any practical ground wire arrangement. The three charts shown are derived from labora-



FIG. 212.—Typical laboratory cloud and transmission-line model for studying induced lightning voltages.

tory data secured with the model lines alluded to above. A typical example is worked out on page 287 from Fig. 213, to show the use of the charts. The protective ratios as derived from these charts for given ground wire arrangements have been checked very closely by actual field data.<sup>1,2</sup>

By increasing the capacity to ground of a line, the ground wire thereby lowers the surge impedance. This effect decreases the voltage of traveling waves, as shown in Fig. 204(g) and is made

<sup>1</sup> HEMSTREET, J. G., *Trans. A.I.E.E.*, p. 835, 1927.

<sup>2</sup> SPORN, PHILIP, *Trans. A.I.E.E.*, 1925, 1929.



use of particularly in protecting stations from incoming lightning waves on lines (see page 351).

The tests on models show that it is important to "ground" the ground wire at every pole. When good grounds cannot be made the ground wire is not so effective. The tests further show that the effect is the same whether or not the neutral of the system is grounded or what the nature of the discharge is. It is believed desirable to have the ground wire either of non-magnetic material, or of a conductor with the outer surface of non-magnetic material. In general, as Fig. 213 shows, the nearer the ground wire is to the line conductor the more effective it is for induced voltages. With the same spacing to the conductor, the effectiveness increases with the height of the line. It is desir-

TABLE LXXXI.—EFFECT OF GROUND WIRES ON LIGHTNING-INDUCED VOLTAGES  
(From Tests on Models)

Arrangement	Protective ratio	Arrangement	Protective ratio
.	1-52 per cent.	.	1-33 per cent.
0 0 0	2-44	0 0	2-38
1 2 3	3-52	0 0 0	3-44
.	1-40	0 0	
0 0 0	2-34	.	1-40
.	3-40	0 0	2-48
.	1-34	0 0 0	3-36
0 0 0	2-28	0 0	
.	3-34	.	
.	1-28	.	1-32
0 0 0 0	2-25	0 0	2-34
.	3-28	0 0 0	3-40
1 . 1		0 0	
0 0	1-42	.	1-25
2 2	2-49	0 0	2-30
0 0	3-56	0 0 0	3-37
3 3		0 0	
0 0			

(0) indicates conductor—(.) indicates ground wire

$$\text{Protective ratio (in per cent)} = \frac{\text{voltage with ground wire}}{\text{voltage without ground wire}} \times 100$$

Average values for various relative conductor and ground wire distances that have been used in practice.

able to place the ground wire above the line conductors to protect against direct strokes as well as to increase the "shielding" effect.

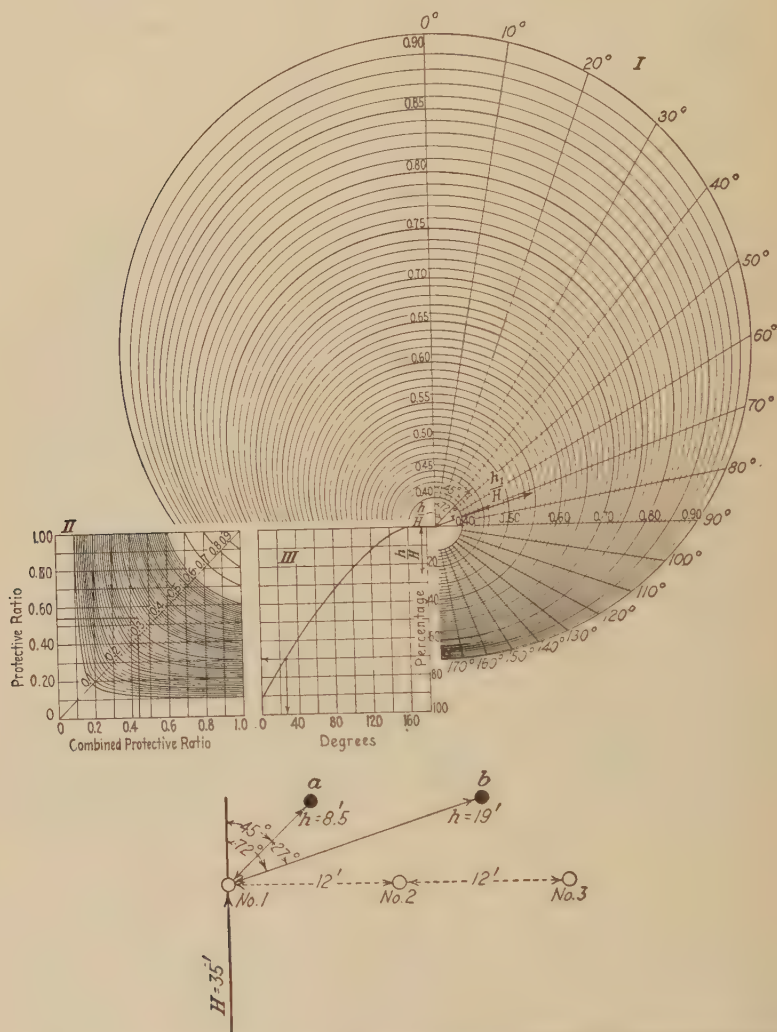


FIG. 213.—Ground-wire Chart. Diagrammatic method of determining protective ratio of ground wires.

The size of the ground wire should be approximately the size of the conductors. The effect of using several ground wires is shown in Table LXXXI. In addition to decreasing the induced

voltage, the ground wire reduces the energy induced on the line to about one-half, increases the corona losses of surges, and very greatly reduces the energy of direct hits by introducing a path to ground. In some cases it may be desirable to use two sets of ground wires, one near the conductors to limit induced voltages, and the other at a considerable distance above, to receive direct strokes, and conduct them to the grounded towers without involving the line conductors.

#### Example of Use of Ground-Wire Chart

Given: Conductors No. 1, No. 2, No. 3 at effective height  $H = 35'$  (where  $H$  = height of conductors at towers minus one-half the sag of the wires between towers). Ground wires  $a$  and  $b$ , at distances  $h = 8.5'$  and  $h_1 = 19'$ , respectively, and forming angles with conductor No. 1 of 45 degrees and 72 degrees, respectively, from the vertical.

Problem: To determine the protective ratio of ground wires  $a$  and  $b$  on conductor No. 1.

Solution:

(a)  $\frac{h}{H} = \frac{8.5}{35} = 24.2$  per cent. is scaled on Chart III and laid off on Chart I at an angle of 45 degrees. This gives a protective ratio of 0.44 for  $a$  on conductor No. 1.

Similarly,  $\frac{h_1}{H} = \frac{19}{35} = 54.2$  per cent. and gives a protective ratio of 0.54 for  $b$  on conductor No. 1.

(b) Chart II shows the combined effect of  $a$  and  $b$  to be 0.32 to which must be added an angular correction factor.

(c) Curve III at 27 degrees gives the value 0.70 which is multiplied by the difference between the value found in (b) and the smaller value in (a), or

$(0.44 - 0.32) \times 0.70 = 0.08$  which is the correction factor due to angle of 27 degrees.  
 $0.32 + 0.08 = 0.40$ , the protective ratio of  $a$  and  $b$  on conductor No. 1.

With no ground wires the estimated lightning voltage under worst conditions (see page 264) which can appear on conductor No. 1 is  $35 \times 100 = 3500$  kv. With  $a$  and  $b$  in the position shown, the voltage now becomes  $35 \times 100 \times 0.40 = 1400$  kv.

**Direct Lightning Strokes.** *Where Lightning Strikes and the Chances of Being Struck.*—Research on models in the laboratory shows that the lightning from a cloud overhead does not always

strike the highest object or rod unless its height is 2.5 per cent. of the cloud height.<sup>1</sup> The division of hits is about equal between rod and ground when the rod is 1.1 per cent. of cloud height. This all assumes the cloud as being directly overhead (see Fig. 214). The chance of the rod being hit is less when the cloud is not directly overhead. Lightning either strikes a rod or some distance away. Roughly, there is a protected area around the rod where no ground hits occur with a radius usually equal to about four or less times the height of the rod, over a wide range of conditions. The ratio of this radius to the rod height has

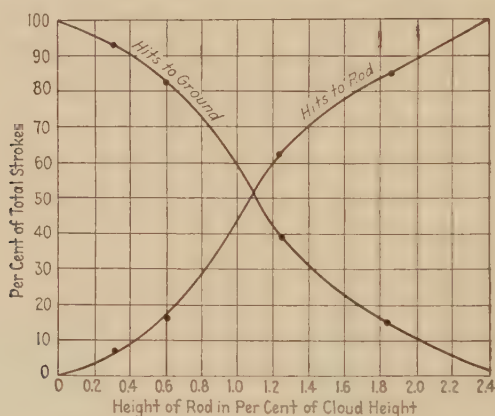


FIG. 214.—Division of laboratory lightning hits between rod and ground with different rod heights.

been termed the protective ratio. For a flat surface, with projections, it is better to speak of a protected space or volume which is that enclosed by a cone with its apex at the top of the rod and the radius of its base equal to the protective radius, as previously defined. Where the height of the rod or tower affording the protection is appreciable compared to the cloud height, the surface of the cone should be that as generated by the arc of a circle rather than a straight line. The radius of the circle would be equal to the lowest probable cloud height, and its center would be so located as to have the arc pass through the rod tip and be tangent to the mean ground level. The use of a straight-surfaced cone of protection is usually justified with low rods (less than 200 ft. in height). As will be discussed later, a building or other object to be protected must not extend above

<sup>1</sup> PEEK, F. W., JR., "Lightning," *Jour. Frank. Inst.*, February, 1925.

this cone. The protective radius has been determined by placing the rod or rods on a paper target and recording the hits by the marks on the paper. This study has been made with the cloud directly over the rod and with the cloud some distance away from the rod; clouds of different forms varying from points to spheres and flat plates have been used; the voltages used were (+) and (-) direct current, and impulses, and 60 cycles alternating current, always with the same general result, given in Fig. 215.<sup>2</sup> There is, however, one important factor that affects the protective ratio—that is, cloud height compared

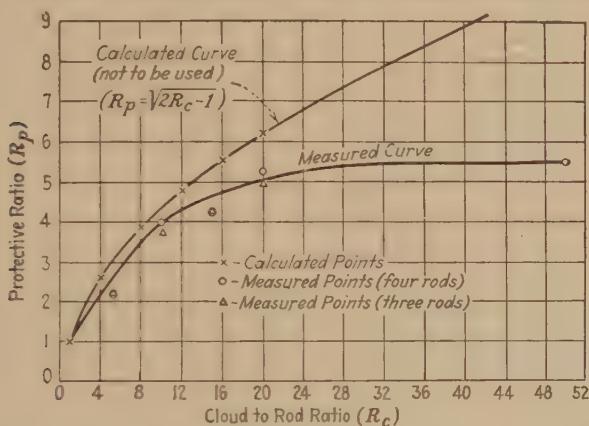


FIG. 215.—Curves showing relation between  $R_p$  (ratio of protected radius to rod height, or protective ratio), and  $R_c$  (ratio of cloud height to rod height). Calculated curve not to be used. See also Fig. 267, page 397.

to rod height. When the cloud is high compared to the rod, the protective ratio may be four or more. As the cloud height is decreased, the protective ratio becomes less. Its minimum value is one when the rod and the cloud are the same height. The value of four is generally reached when the cloud is ten times the height of the rod. The direct-current tests were made up to about 350 kv. above ground. An interesting fact about the direct-current test is that the rod is most effective when the cloud is negative. This seems to be due to the fact that corona from a positive point is of much greater length and intensity than that from a negative point (see page 103, Chap. IV). Consequently, a positive point or rod under a negative cloud would have much greater directive effect in guiding down-

<sup>2</sup> PEEK, F. W., JR., "Lightning," *Trans. A.I.E.E.*, p. 1131, 1926.



ward strokes to it, and, therefore, have greater protective value than if the cloud were positive. For a (+) cloud, the protective ratio of four is reached for a higher value of cloud rod ratio than ten, in fact, about twenty.

Tests were also made with wires under the cloud. Either the wire is hit or the ground some distance away. For a single wire, the ground is never hit nearer the plane of projection of the wire than about four times its height above ground.

A similar test was made on parallel ground wires. It was found that the ground between the wires was never hit when the separation of the wires was not greater than about four times their height. Both these ratios would apply for a cloud rod ratio of ten. The variation of the protective ratio with cloud height is given in Fig. 215 for rods. The laboratory tests also show that a ground wire over a transmission line is struck 98 per cent. of the time, while the conductors are struck the other 2 per cent. This is an important factor in favor of the ground wire.

Tests similar to the single-rod tests were made with three or four rods symmetrically arranged about a circle or with four rods on the axes of an ellipse. It was found that the area inside of the circles or ellipses was protected from direct hits if the heights of the rods were such that their protective circles overlapped, the radii of these circles being determined from Fig. 215. All projections within the area must lie below the surface of the so-called protective cones described above, the dimensions of these cones being fixed by the heights and locations of the rods.

Another interesting test showed that a hit can never occur within a circular tank when the height of the tank is greater than one-tenth its diameter.

*Protection of Buildings, Oil Tanks, Magazines, Etc.*—The principles already discussed can be applied to the protection of buildings, oil tanks, magazines, etc. While complete protection is usually impracticable from the standpoint of cost or other reasons, the hazard can generally be greatly reduced or almost removed by protective means. In some cases, the protection to be provided must take care of both direct strokes and induced sparks, while, in others, but one of these factors enters. Although the most severe lightning effects are caused by direct strokes, it is necessary, in order that the stroke may take place at a given spot, that the cloud be directly overhead at the

instant it is charged to sufficient voltage for discharge to earth. Consequently voltages by direct strokes are much less likely to take place than induced voltages, as the latter merely require the collapse of electrostatic fields which may occur with any storm within a radius of several miles, and with intercloud discharges as well as those to earth.

*Protection from Direct Strokes.*—In cases of tall buildings, chimneys, steeples, etc., in exposed areas where it is impractical to prevent direct hits, means for receiving these strokes are usually provided in the form of lightning rods placed on these structures. These rods must then have ample connections to ground for carrying the large current of a stroke, without any dangerous local heating or sparking in their circuits. The conductor or conductors from rod to ground should at least have a conductivity equivalent to a No. 00 solid copper wire (0.365 in. in diameter).<sup>1</sup>

In order to secure as complete protection as practicable from direct strokes for oil tanks, magazines, etc., high rods or towers around the structures or horizontal overhead conductors must be provided. As a rule, rods are preferable to overhead conductors, for unless the latter are very high and of large conductivity, there is the danger of secondary flashes to the structure below.

Considerable laboratory work has been carried out with models built to scale, particularly in connection with oil tank protection.<sup>2</sup> From this it was determined that a rod will protect all structures lying beneath a cone whose apex is the point of the rod and whose radius is equal to the protective radius of the rod, as discussed previously on page 289 (also, see Fig. 215). Figure 216 shows this principle as applied to an oil tank. In this way, any structure or group of structures can be protected from direct hits by rods or towers so arranged that their protective cones cover every portion not to be struck. The heights of the rods to be used vary with the cloud heights anticipated, as outlined previously (see Fig. 215), and they may be increased to give any added factor of safety desired. The above assumes all objects concerned to be on more or less level ground, as extra

<sup>1</sup> "Code For Protection Against Lightning"—Miscellaneous Publication of Bureau of Standards, No. 92.

<sup>2</sup> PEEK, F. W., JR., "Lightning, A Study of Lightning Rods and Cages with Special Reference to the Protection of Oil Tanks," *Trans. A.I.E.E.*, p. 1131, 1926.

precautions and consideration obviously must be given to oil tanks and the like situated on steep slopes. In such cases, the simplest rule to follow is to have the rods of such heights and locations that storm clouds coming in from any direction will always be considerably closer to some rod than any portion of the object to be protected.

In order to avoid sideflashes it is desirable that all rods be placed at a distance equal to their height from the objects being protected. Also their number and location should be such that all possible direc-

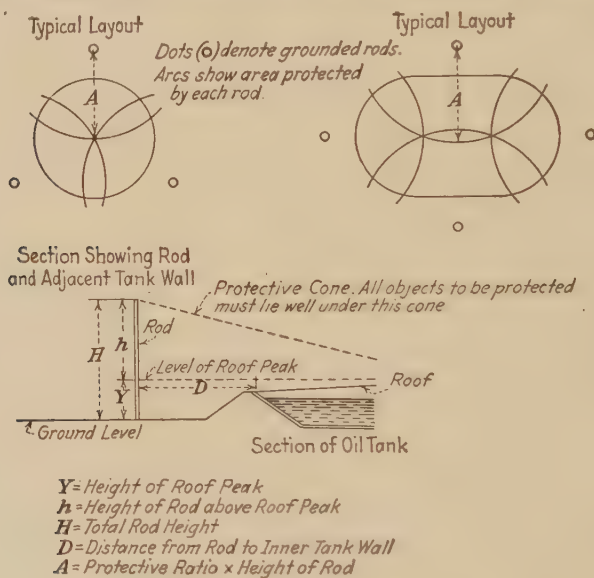


FIG. 216.—Method of protecting oil tanks from direct lightning strokes.

tions of storm approach are guarded. For example, this would require three equally spaced rods for a circular tank or building, and four for a square or rectangular structure.

**Protection from Induced Voltages.**—Electrostatically induced sparks may occur without cloud discharge between isolated conducting parts either metallic or liquid. Induced sparks are, however, usually caused on the collapse of a field with cloud discharge, in which case the bound charges so released (see page 263) encounter high-impedance paths to ground and set up local sparking.

Electromagnetic induction could create sparks as a result of heavy currents caused by direct strokes near-by, although such instances would probably be rare.

The danger from induced sparks only arises with the presence of explosive gas mixtures, readily ignitable materials, etc. If these cannot be avoided, the obvious remedy is to seek to shield the structure or container to as great an extent as practicable in order to reduce the movement of charges within to a minimum. Complete metal tanks, or structures entirely covered with metal, will provide complete solutions of the problem, but care should be taken in these cases that there be no poor electrical contacts between plates, and that no pipes or leads be brought in from the outside without making good contacts with the metal covering.

In lieu of a complete metal structure, some protection will be afforded by a metal cage. The danger from induced voltages will be reduced, the smaller the mesh of the cage and the more completely it covers the structure. Table LXXXII gives the results of laboratory lightning tests with models to ascertain the degree of protection given by cages.<sup>1</sup> These tests indicated that

TABLE LXXXII.—REDUCTION OF INDUCED VOLTAGES ON MODEL TANKS BY MEANS OF OVERHEAD NETS OR CAGES

Size of mesh used, in.	Clearance to tank, in.	Position of mesh	Induced voltage on tank	Actual induced voltage in percentage of voltage induced on unprotected tank
Cage or net 21 in. square				
.....	.....	No protection	41.4	100
$\frac{1}{4}$	1.0	Over top and around sides	0(+)	0(+)
2	1.0	Over top and around sides	3.2	8
2	1.0	Around sides only	20.7	50
2	1.0	Over top only	6.1	14.8
2	1.0	Over top only	5.5	13.3
2	2.0	Over top only	5.1	12.3
2	4.0	Over top only	5.9	14.3
2	8.0	Over top only	7.4	17.9
Net, 36 in. square over top only				
2	1.0	.....	2.4	5.8

Diameter of tank, 17 in.

Cloud height, 44.5 in.

Height of tank, 6 in.

Cloud voltage, 372 kv.

<sup>1</sup> SCHAEFFER, E. R., *Trans. A.I.E.E.*, p. 174, 1928.



sparking is possible even with cages of comparatively small mesh. Particular care should be taken with structures so protected that all metal parts be well connected electrically. Sparks may occur between puddles on roofs or on roofs made of partly conducting material.

*Summary.*—The safest arrangement for providing protection would be a completely covered metal structure, the metal being of ample thickness and well connected, so as to take care of direct strokes to it. A more practical arrangement would probably be a combination of rods or towers for receiving the direct hits and a thin metal roof and sides to eliminate induced voltages. Wire or mesh on or above the roof as an alternative to a complete metal covering would reduce the induced voltages somewhat, dependent on the size of mesh used.

**Explanation of Some Peculiar Effects.**—Figure 217 illustrates one instance in practice where actual lightning strokes have checked laboratory protective tests made with models. In this particular case, though at first sight the results seemed contradictory, it was later determined that all points struck were outside of the protecting areas of the higher buildings near-by.

The following experiment seems to explain some peculiar effects noted in practice. If a high wooden rod and a shorter metal rod are placed close together under a storm center, the metal rod is always struck. The wooden rod has no effect. If the wooden rod is dampened so that it becomes a conductor of high resistance, it is struck in preference to the metal rod. There is an immediate side flash, however, from the wood to the shorter metal rod. When the wood is made decidedly conducting, it acts like a metal rod and the discharge follows down its surface. The explanation is quite simple: The high resistance wood was conducting enough to carry the small charging current and thus determine the direction of the stroke. As soon as it was hit, however, its resistance was too high to carry the lightning current; it thus side-flashed to the rod. This explains why it is dangerous to stand under a tree; why chimneys are struck with disastrous side flashes; why wooden flag poles are struck and splintered. It also shows why a lightning rod up to the chimney top does not increase the hazard of being struck and, in case of a direct hit, carries the current and prevents destruction.

Other peculiar occurrences are explained: Assume a tall, dry, wooden church steeple and a clump of trees lower than the



teeple. A tree is struck and, about half way down, the tree is very badly shattered and blown apart. An examination shows that the lightning flash missed the high church steeple and appears to have struck underneath the branches of the tree.

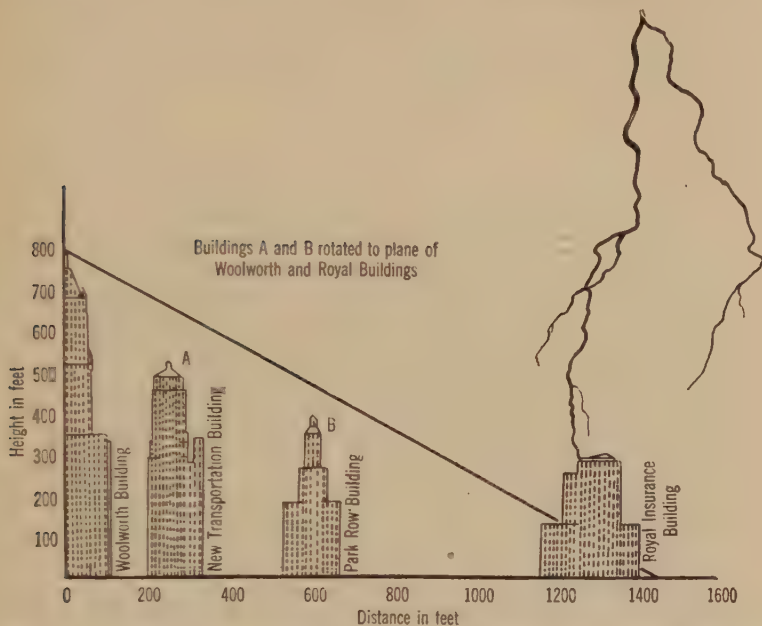


FIG. 217.—Example of actual protection from direct hits afforded buildings by other nearby buildings.

A simple explanation is as follows: The church steeple was too dry to influence the field. The tree was conducting enough to determine the path of the discharge and the top, sappy branches were able to conduct it. The trunk of the tree was too dry to carry the current and caused the tree to split. Such results were shown on a model.

## CHAPTER X

### PRACTICAL CORONA CALCULATIONS FOR TRANSMISSION LINES

**Summary of Various Factors Affecting Corona.**—If potential is applied between the conductors of a transmission line and gradu-



FIG. 218.—Corona at 230 kv. Line A. 3/0 cable. 310 cm. (122 in.) spacing.

ally increased, a point is reached when wattmeters placed in the circuit begin to read. The watt loss is low at first but increases with increasing voltages. At the point where the meters begin

to read, a hissing noise is heard, and if it is quite dark, localized streamers and glow points can be noticed at spots on the conductors. These first streamers are caused by dirt and irregularities. The watt increase, is still gradual. Slowly raising the voltage, the true visual critical corona point is finally reached. The effect is striking; corona suddenly jumps out, as it were, all along the line (see Fig. 218). The line immediately becomes

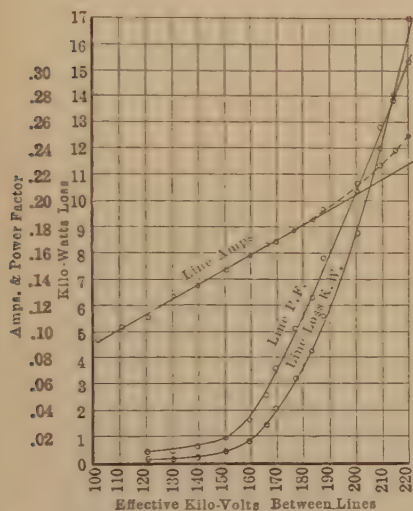


FIG. 219.—Characteristic corona loss, current, and power factor curves.

(Line A. Conductor length, 109,500 cm. (total). Spacing, 310 cm. Diameter, 1.18 cm. (3/0 cable). Temp., 12°C. Bar., 75.)

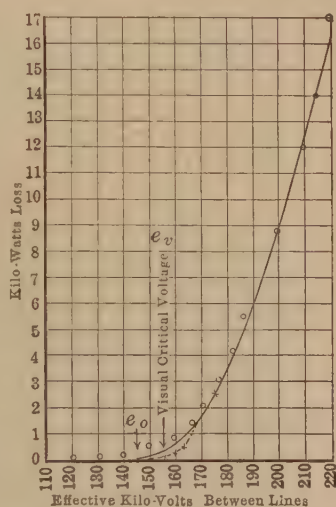


FIG. 220.—Loss near the critical voltage of new and old cables.

(Data Fig. 219. Line calculated. x, new cable. o, weathered cable.)

very noisy and the loss increases very rapidly with increasing voltage. The intensity of the light also increases with increasing voltage. If one is close to the conductors, an odor of ozone and nitrous oxide, the result of chemical action on the air, is noticed. There is, thus, heat, chemical action, light, and sound in the process of corona formation. These, naturally, all mean energy loss.

It becomes of great importance in the design of high-voltage transmission lines to know the various factors which affect the corona formation, and to have simple working formulæ for pre-determining the corona characteristics, so that the corona loss will not be excessive.

Loss begins at some critical voltage, which depends upon the size and spacing of the line conductors, altitudes, etc., and increases very rapidly above this voltage. Figures 219 and 220 show typical corona loss curves during fair weather.

An extensive investigation (see Chap. VI) on an experimental transmission line (see Fig. 221) has shown that the corona loss in fair weather is expressed by the equation:

$$p = a(f + c)(e - e_0)^2$$



FIG. 221.—Experimental transmission line.

where  $p$  = loss in kilowatts per kilometer length of single-line conductor

$e$  = effective value of the voltage between the line conductors and neutral in kilovolts<sup>1</sup>

$f$  = frequency

$c$  = a constant = 25

and  $a$  is given by the equation

$$a = \frac{A}{\delta} \sqrt{r/s}$$

where  $r$  = radius of conductor in centimeters

$s$  = the distance between conductor and return conductor in centimeters

<sup>1</sup> Hence, in single-phase circuits,  $e$  is one-half the voltage between conductors. In three-phase circuits,  $e$  is  $1/\sqrt{3}$  times the voltage between conductors.

$\delta$  = density of the air, referred to the density at 25° C. and 76 cm. barometer as unity

$A$  = a constant = 241

$e_o$  = the effective disruptive critical voltage to neutral, and is given by the equation

$$e_o = m_o g_o \delta r \log_e s/r \text{ kv. to neutral}^1$$

where  $g_o$  is the disruptive gradient of air in kilovolts per centimeter at 25°C. and 76 cm. barometer, and is constant for all practical transmission line sizes of conductor frequencies, etc. For very small conductors  $g_d$  is used (see pages 187, 192, 193).

$g_o$  = 21.1 kv. per centimeter (effective)

$m_o$  is a constant depending upon the surface condition of the conductions, and is

$m_o$  = 1 for perfectly smooth polished wire

$m_o$  = 0.98 to 0.93 for roughened or weathered wires, and decreases to

$m_o$  = 0.87 to 0.83 for seven-strand cables (where the radius is taken as the outer radius of the cable)

An investigation by the author has shown that for new cables up to 2.5 cm. (1 in.) in diameter the irregularity factor is approximately the same for 19-, 37-, and 61-strand cables (concentric lay). Under the above condition

$$m_o = 0.80 \text{ to } 0.87$$

depending upon the surface condition of the cable. It probably improves somewhat with use, as the abrasions become oxidized away. For new cables it is generally near 0.80.

With special types of cables values as low as 0.70 were obtained.

Seven-strand cables in the large sizes are undesirable since the large wires become mutilated and the irregularity factor becomes low.

Although in the above investigation with 19, 37, and 61 strands there was no great difference in the loss, the measurements were slightly in favor of 37 strands. It seems inadvisable to use a stranding that would make the individual conductor too small compared to the cable diameter.

<sup>1</sup> Hence, in single-phase circuits,  $e$  is one-half the voltage between conductors. In the three-phase circuits,  $e$  is  $1/\sqrt{3}$  times the voltage between conductors.



Luminosity of the air surrounding the line conductors does not begin at the *disruptive critical voltage*  $e_o$  but at a higher voltage  $e_v$ , the *visual critical voltage*. The *visual critical voltage*  $e_v$  is much higher for small conductors than the *disruptive critical voltage*  $e_o$ ; it is also higher for large conductors, but to a less extent. For very small conductors  $e_d$  replaces  $e_o$  (see page 192).

On perfectly smooth conductors no appreciable loss of power should occur below the visual voltage,  $e_v$ . Some loss does occur, however, due to irregularities of the wire surface, dirt, etc., as indicated by visible brush discharges, and local corona streamers (see page 195).

As the loss between  $e_r$  and  $e_o$  depends upon dirt, roughened condition of the wire surface, etc., it is unstable and variable and changes as the surface of the conductors changes. For the larger sizes of stranded transmission conductors in practice, the surface is generally such that the loss approximately follows the quadratic law, even between  $e_o$  and  $e_v$ . This is shown by the circles in Fig. 220 which are measured points on a weathered conductor. The crosses indicate how the points come on a new conductor. For a small conductor, the difference between the calculated and measured losses on the section of the curve between  $e_o$  and  $e_v$  is still greater. Above  $e_r$  the curves coincide and follow the quadratic law. In practice it is rarely admissible to operate above the  $e_o$  voltage.<sup>1</sup> Cases are known in which conductors have deteriorated by the action of nitric acid formed by excessive brush discharge.

It is interesting to note that the loss below  $e_r$  actually follows the probability curve

$$p_1 = qe^{-h(e_0-e)^2}$$

(see page 196).

The corona loss is:

(a) A loss proportional to the frequency  $f$  plus a small constant loss.

(b) Proportional to the square of the excess voltage above the disruptive critical voltage  $e_o$ .

(c) Proportional to the conductor radius  $r$  and  $\log s/r$ . The critical voltage thus increases very rapidly with increasing  $r$  and to a less extent with spacing.

<sup>1</sup> Operation at  $e_o$  voltage at high altitudes gives relatively greater margin and less loss than at sea level as there is greater difference between  $e_r$  and  $e_o$ .

The *disruptive critical voltage*  $e_0$  is the voltage at which the disruptive voltage gradient of the air is reached at the conductor surface. Hence it is:

(a) Proportional to the conductor radius  $r$  and  $\log_e s/r$ . The critical voltage thus increases very rapidly with increasing  $r$  and to a much less extent with increasing  $s$ .

(b) Proportional to the air density or becomes very low at high altitudes.

(c) Dependent somewhat on the conditions of the conductor surface, as represented by  $m$ .

The effects at various atmospheric conditions and storms on the critical voltage and loss will now be considered.

(a) *Humidity* has no effect on the critical voltage.

(b) *Smoke* lowers the critical voltage and increases the loss.

(c) *Heavy winds* have no effect on the loss or critical voltage at ordinary commercial frequencies.

(d) *Fog* lowers the critical voltage and increases the loss.

(e) *Sleet* on the wires, or falling sleet, lowers the critical voltage and increases the loss. High voltages do not eliminate sleet formation.

(f) *Rain storms* lower the critical voltage and increase the loss.

(g) *Snow storms* lower the critical voltage and increase the loss.

(h) At high altitudes the loss is very much greater on a given conductor, at a given voltage, than it is at sea level. For a given voltage larger conductors must be used at high altitudes.

Figure 222 shows a typical loss curve during storm and a corresponding fair weather curve.

*The above are all discussed in detail in Chap. VI.*

**Practical Corona Formulæ and Their Application.**—The formulæ required for the determination of the corona characteristics of transmission lines are

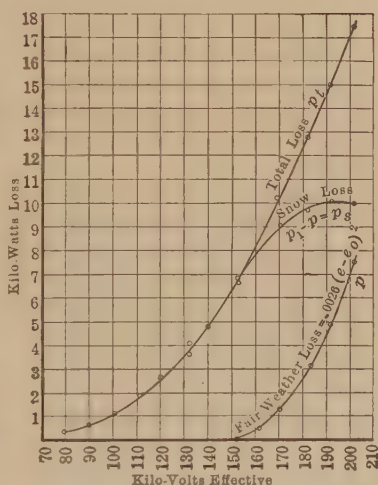


FIG. 222.—Comparison of fair weather and storm loss.

## METRIC UNITS

*Disruptive Critical Voltage*

$$e_o = 21.1 m_o r \delta \log_e s/r \text{ kv. to neutral} \quad (35)$$

*Power Loss*

$$p = \frac{241}{\delta} (f + 25) \sqrt{r/s} (e - e_o)^2 10^{-5} \text{ kw. per km. of single conductor} \quad (34)$$

Where the conductors are small use formulæ (34a), (35a), and (36), Chap. VI.

*Visual Critical Voltage*

$$e_v = 21.1 m_v \delta r \left( 1 + \frac{0.301}{\sqrt{\delta r}} \right) \log_e s/r \text{ kv. to neutral} \quad (20)$$

$$\delta = \frac{3.92b}{273 + t}$$

where

- $e$  = effective kilovolts to neutral applied to the line<sup>1</sup>
- $\delta$  = air density factor  
= 1 at 25°C., 76 cm. barometer
- $b$  = barometric pressure in centimeters
- $t$  = temperature in degrees Centigrade
- $r$  = radius of conductor, centimeters
- $s$  = spacing between conductor centers in centimeters
- $f$  = frequency cycles per second

For approximating storm loss consider  $e_o = 0.8$  of fair weather value in formula (35).

*Irregularity Factors*

- $m_o = 1$  for polished wires
- = 0.98 — 0.93 for roughened or weathered wires
- = 0.87 — 0.83 for seven-strand cables
- $m_v = m_o$  for polished wire = 1
- $m_v = 0.72$  for local corona all along cable
- $m_v = 0.82$  for decided corona all along cable

## ENGLISH UNITS

*Disruptive Critical Voltage*

$$e_o = 123 m_o r \delta \log_{10} s/r \text{ kv. to neutral} \quad (35')$$

*Power Loss*

$$p = \frac{390}{\delta} (f + 25) \sqrt{r/s} (e - e_o)^2 10^{-5} \text{ kw. of single conductor per mile} \quad (34')$$

<sup>1</sup>  $e$  = volts between line times  $1/\sqrt{3}$  for three-phase lines and volts between line times  $1/2$  for single-phase or two-phase lines.

Where the conductors are small use formulae (34a), (35a) and 36, Chap. VI.

### Visual Critical Voltage

$$e_v = 123m_v\delta r \left( 1 + \frac{0.189}{\sqrt{\delta r}} \right) \log_{10} s/r \text{ kv. to neutral} \quad (20')$$

$$\delta = \frac{17.9b}{459 + t}$$

where

$e$  = effective kilovolts to neutral applied to the line<sup>1</sup>

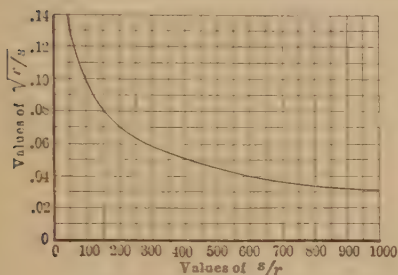


FIG. 223.

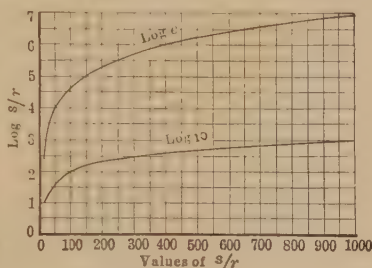


FIG. 224.

$\delta$  = air density factor

= 1 at 77°F. and 29.9 in. barometer

$b$  = barometric pressure in inches

$t$  = temperature in degrees Fahrenheit

$r$  = radius of conductor, inches

$s$  = distance between conductor centers in inches

$f$  = frequency, cycles per second

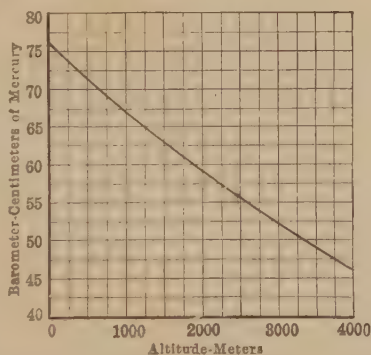
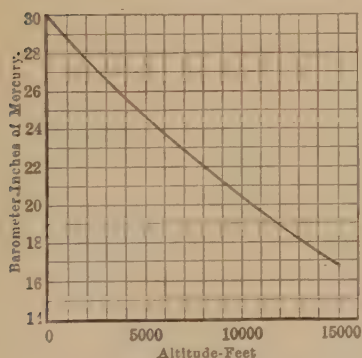


FIG. 225.—Approximate barometric readings at different altitudes.

<sup>1</sup> $e$  = volts between line times  $1/\sqrt{3}$  for three-phase lines and volts between line times  $1/2$  for single-phase or two-phase lines.

Figures 223 and 224 give values of  $\sqrt{r/s}$  and  $\log s/r$ , respectively. In Fig. 225 is plotted atmospheric pressure against altitude.

In order to illustrate the use of the formulæ, the following practical example is taken:

### EXAMPLE

Given:

Three-phase line.....	60 cycles
Length.....	100 miles
Spacing.....	120 in.
Conductor.....	1/0 cable—diam. 0.374 in.
Max. temperature.....	100°F.
Elevation.....	1000 ft.
Barometer (from Fig. 172).....	28.85 in.

Then  $s/r = \frac{120}{0.187} = 642$

$\log_{10} s/r = 2.81$  (from Fig. 171 or tables)

$\sqrt{r/s} = 0.0394$  (from Fig. 170 or calculated)

$\delta = \frac{17.9b}{459 + t} = \frac{17.9 \times 28.85}{459 + 100} = 0.925$

$m_o = 0.87$

$e_o = 123m_o\delta \log_{10} s/r = 123 \times 0.87 \times 0.187 \times 0.925 \times 2.81 \text{ (35')}$   
 $= 52.0 \text{ kv. to neutral}$

$p = \frac{390}{\delta} (f + 25) \sqrt{r/s} (e - e_o)^2 10^{-5} \text{ (34')}$   
 $= 0.014(e - 52.0)^2 \text{ kw. per mile of single conductor}$

Since there are three conductors:

$p = 0.042(e - 52.0)^2 \text{ kw. per mile of three-phase line}$

The conductor (100°F., 1000 ft. elevation) would glow at

$e_v = 123m_v\delta r \left(1 + \frac{0.189}{\sqrt{\delta r}}\right) \log_{10} s/r = 62.6 \text{ kv. to neutral (20')}$

or  $62.6 \times 1.73 = 108.3 \text{ kv. between lines}$

More decidedly at

$71.3 \times 1.73 = 123.4 \text{ kv. between lines}$

The visual corona cannot be observed except on a very dark cloudy night.



To show the effect of altitude, the characteristics of the same line are calculated for 10,000 ft. elevation and tabulated in Table LXXXIII. At this altitude

$$p = 0.0599(e - 36.8)^2 \text{ kw. per mile of three-phase line}$$

$$e_o = 36.8 \text{ kv. to neutral.}$$

$$(m_v = 0.72) 81.5 \text{ kv. local.}$$

Visual corona between lines

$$(m_v = 0.82) 92.7 \text{ kv. decided}$$

TABLE LXXXIII.—CORONA LOSS AT DIFFERENT OPERATING VOLTAGES

Kv. bet. lines	Kv. to neutral $e$	Kw. per mile and total in 100 miles							
		1000 ft. elevation				10,000 ft. elevation			
		Fair weather		Storms		Fair weather		Storms	
		$p$ per mile, 3 cond.	100 miles	$p$ per mile, 3 cond.	100 miles	$p$ per mile, 3 cond.	100 miles	$p$ per mile, 3 cond.	100 miles
50	28.9								
60	34.7							1.7	170
70	40.5					0.8	80	8.0	800
80	46.3			0.9	90	5.4	540	17.0	1,700
90	52.0	0.0	0	4.6	460	14.0	1,400	30.0	3,000
100	57.8	1.4	140	11.0	1,100	26.0	2,600	48.0	4,800
110	63.6	5.7	570	20.0	2,000	43.0	4,300	70.0	7,000
120	69.4	13.0	1,300	33.0	3,300	63.0	6,300	96.0	9,600
130	75.1	22.0	2,200	47.0	4,700	88.0	8,800	125.0	12,500
140	80.9	35.0	3,500	65.0	6,500	116.0	11,600	158.0	15,800
150	86.7	51.0	5,100	86.0	8,600	149.0	14,900	196.0	19,600

For approximating the storm loss consider

$$e_o = 0.80 \text{ per cent. of its value in fair weather.}$$

Then

$$p = 0.042(e - 0.8 \times 52.0)^2 = 0.042(e - 41.6)^2$$

This will give an idea of the maximum storm loss; it assumes a storm over the whole line at the same time, a condition that is most unlikely to occur. The storm loss will also generally be less due to lower temperatures.

The loss on a transmission line will vary from day to day depending upon the temperature and weather conditions. The above losses are calculated for summer temperature. For winter, the losses would be much lower.

**Methods of Increasing Size of Conductors.**—The corona starting voltage is increased by increasing the diameter of the con-

ductor. Thus, with the same amount of copper, a hollow tube would give a higher corona voltage.

For the same conductivity, an aluminum conductor has about a 25 per cent. greater diameter than a copper conductor and thus, approximately, 25 per cent. higher corona voltage.

In order to increase still further the advantage of aluminum at the larger sizes and maintain ample strength, a steel-core aluminum cable has been adopted. To secure this same increased diameter effect with copper, the manufacturers of copper cables have, in general, now adopted the use of a hollow, stranded conductor, the center core being either a twisted I-beam, a spiral, or a flexible tube.

The critical voltage may also be decreased by grouping together conductors of the same potential, but this generally is not practical on transmission lines.

**Conductors not Spaced in Equilateral Triangle.**—In three-phase problems, it has been assumed that the conductors are arranged in an equilateral triangle. When the conductors are not spaced in an equilateral triangle but, as is often the case in practice, symmetrically in a plane, corona will start at a lower voltage on the center conductor, where the stress is greatest, than on the outside conductor.

The actual critical voltage for the center conductor will be approximately 4 per cent. lower, and for the two outer conductors 6 per cent. higher, than the value for the same  $s$  in the equilateral triangle arrangement.

If a triangle is used where there is considerable difference between  $s_1$ ,  $s_2$ , and  $s_3$ , an exact calculation of the stress should be made. Such a calculation is quite complicated (see example Case 12, page 343).

**Voltage Change along Line.**—For long lines, the voltage and, therefore, the corona loss will vary at different parts of the line (see page 197). This may be allowed for in a long line by calculating the loss per mile at a number of points. If a curve is plotted with these points as ordinates and length of line as abscissa, the average ordinate may be taken as the loss per mile. The area of the curve is the total loss. A line operating very near the corona voltage may have no loss at load, but when the load is taken off there may be considerable loss due to the rise in voltage. This may sometimes be advantageous in preventing a very large rise in voltage when the load is lost. Grounding one

conductor will also cause considerable loss on a line operating near the corona voltage by increasing the stress on the air at the conductor surface.

**Agreement of Calculated Losses and Measured Losses on Commercial Transmission Lines.**—It is generally difficult to make an exact comparison, as, in most cases where losses have been measured on practical lines, all of the necessary data, such as

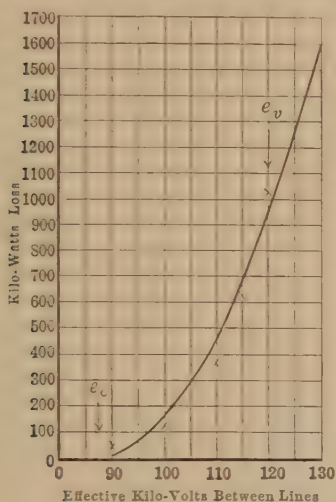


FIG. 226.

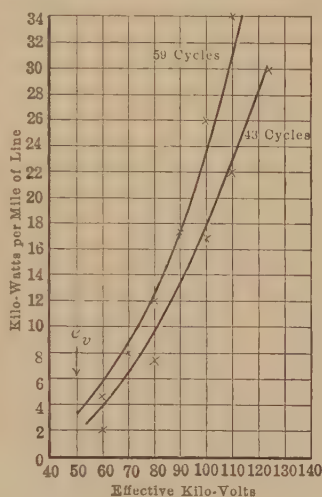


FIG. 227.

Comparison of calculated and measured losses.

FIG. 226.—Leadville. Three phase. (Test made by Faccioli.) 1/0 weathered cable. Spacing (flat) 124" (314 cm.). Diameter, 0.95 cm. Length of line, 63.5 miles (one conductor). Temp., 11°C. Bar., 60 cm. Frequency, 60—. Curve calculated. x measured.

FIG. 227.—Outdoor experimental line. (Tests by A. B. Hendricks, Pittsfield, 1906.) Wire conductor. Diameter, 0.064" (radius 0.081 cm.). Spacing 48" (132 cm.). Length, about 800 ft.  $\delta = 0.97$ .

temperature along line, barometric pressure, voltage rise at the end of line, etc., have not been recorded. A range of voltage extending considerably above  $e_v$  is necessary to determine the curve. It is not generally possible to place such high voltages on practical lines.

The several examples given are those in which it has been possible to obtain sufficient data to make a comparison. In Fig. 226 the drawn curve is calculated from the formulæ for the temperature, barometric conditions, etc., under which measurements were made. The crosses represent the measured values. This agreement between measured and calculated losses is very inter-

esting, as it is for a long three-phase line at very high altitude.<sup>1</sup> (Note that the greater part of the curve is below  $e_v$ .) In Fig. 227 are similar comparisons on a single-phase line at different frequencies. These measurements were made before corona was a factor in practical transmission. An exact agreement could not be expected, as the wave shape was not known and was probably not a true sine wave. Another rather interesting comparison is made in a publication describing the system of the Au Sable Electric Co.<sup>2</sup> The line of No. 0 copper cable is 125 miles long. With 140 kv. at the generating end, the voltage at the far end is 165 kv. Thus the loss per mile is greater at the far end than at the generating end. The average calculated loss per mile is 15 kw. The actual average loss by preliminary rough measurements was 15 to 20 kw. per mile. The above examples are given to illustrate how well the formulæ may be applied in the predetermination of the corona loss of commercial transmission lines.<sup>3</sup>

**Safe and Economical Voltages.**—It will generally be found that it is not safe or economical to operate a line above the fair weather  $e_o$  voltage (determined for average barometer and 77°F.). The  $e_o$  voltage gives a loss during storms of about 4.75 kw. per mile in the problem considered, but it is not likely that the storm will extend over the whole line at one time. Storm during cold weather will cause much less loss than the above. It thus is generally more economical to pay for the storm loss during small parts of the year rather than to try to eliminate it by an excessive conductor.

It is undesirable to operate the conductors above the glow point as there is likely to be considerable chemical action on the conductor surface.

Excessive corona loss may introduce undesirable harmonics in voltage and current (see Figs. 88 and 89). It is not probable, however, that there will be serious harmonics or chemical action with economical loss.

**High-voltage Conductor Sizes as Determined by Corona.**—Figures 228 and 229 give curves showing the corona starting voltages for typical copper and aluminum cables. The curves indicate the approximate voltages at which corona starts in fair

<sup>1</sup> Some of the first measurements on practical lines were made by Scott and Mershon, at high altitudes in Colorado. See *A.I.E.E.*, 1898.

<sup>2</sup> *N. E. L. A.*, June, 1912.

<sup>3</sup> PEEK, F. W., JR., "Comparison of Calculated and Measured Corona Loss," *Trans. A.I.E.E.*, p. 169, 1915.



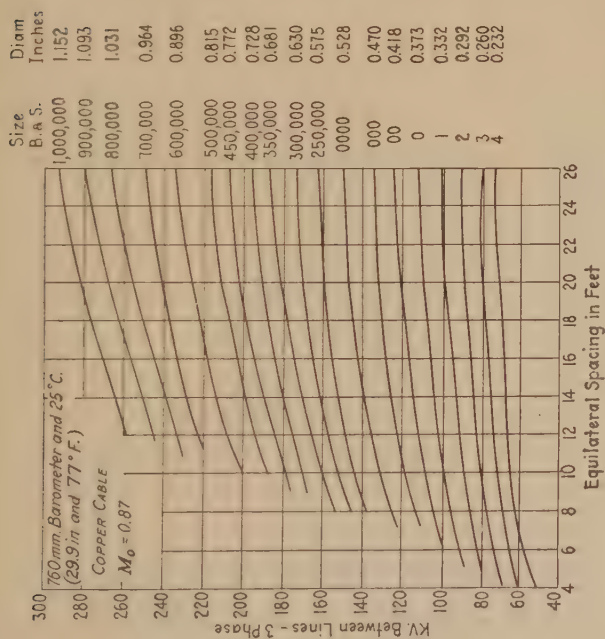


Fig. 228.—Corona starting voltages on standard concentric stranded *copper* cables, as affected by conductor diameters and spacings.

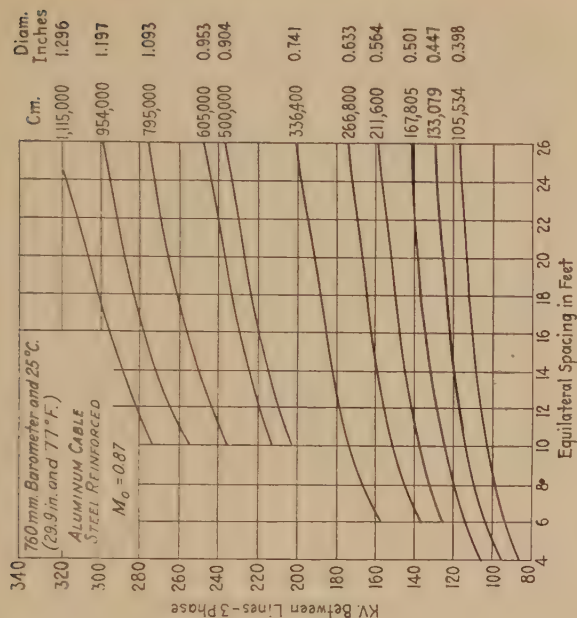
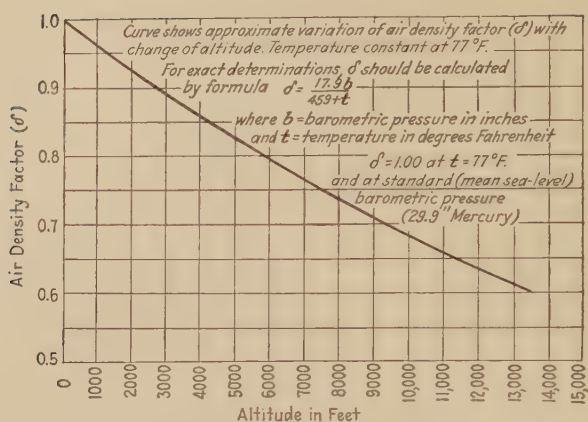
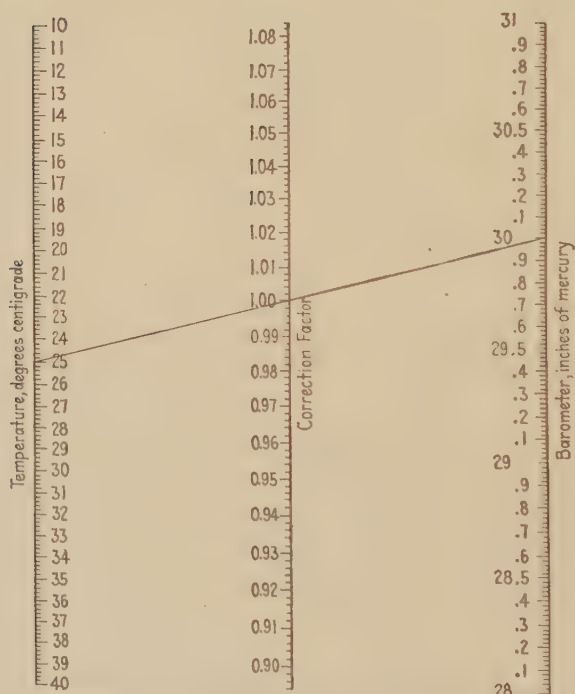


Fig. 229.—Corona starting voltages on standard concentric stranded *aluminum* cables, as affected by conductor diameters and spacings.



FIG. 230.—Air density factor ( $\delta$ ) as affected by altitude.

A straight line connecting the given temperature with the given barometric pressure intersects the center scale at a value equal to that of the air density factor ( $\delta'$ ) at that temperature and pressure

FIG. 231.—Alignment chart for determining air density factor ( $\delta$ ).

weather, sea-level conditions ( $\delta = 1$ ), and assuming an irregularity factor ( $m_o$ ) of 0.87. For correction for altitude only, the factor to be applied may be obtained from Fig. 230. At other temperatures and pressures, the air density factor ( $\delta$ ) should be taken from the alignment chart (Fig. 231).

#### EXAMPLE

For 3 0 copper cable, 10-ft. spacing, the limiting three-phase voltage for an altitude of 1200 ft. is

$$118,000 \times \delta = 118,000 \times 0.95 = 112,000 \text{ volts}$$

The loss at this voltage for both stormy and fair weather should be very small.

At 130,000 volts, the fair weather loss for this cable is 5 kw. per mile and the storm loss is 25 kw. per mile.

At 160,000 volts, the fair weather loss is 36 kw. per mile and the storm loss is 75 kw. per mile.

## CHAPTER XI

### PRACTICAL CONSIDERATION IN THE DESIGN OF APPARATUS WHERE SOLID, LIQUID, AND GASEOUS INSULATIONS ENTER IN COMBINATION

As important as the quality of the dielectric is the configuration of it and of the electrodes. It is also of importance in combining dielectrics of different permittivities to see that one does not weaken the other by causing unequal division of stress. It is possible to cause breakdown in apparatus by the addition of good insulation, dielectrically stronger than the original insulation. The theory of this was partly discussed in Chap. II, page 31.

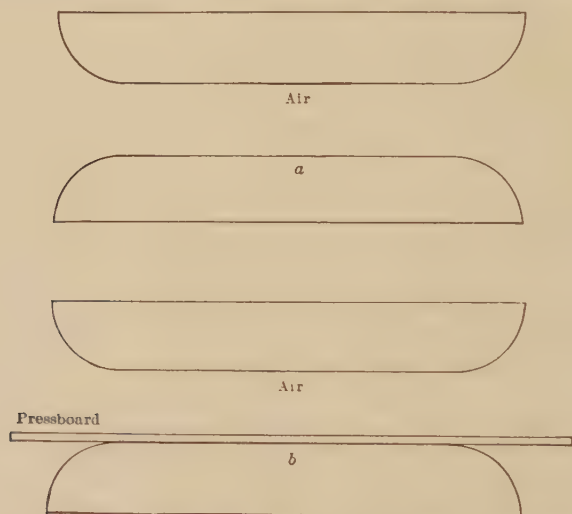


FIG. 232.—Causing breakdown by the addition of insulation.

**Case 1. Breakdown Caused by the Addition of Stronger Insulation of Higher Permittivity.**—As an example take two parallel plates rounded at the edges and placed 2 cm. apart in air, as in Fig. 232(a).

(1) Apply 60 kv. (maximum) between the plates. The gradient then is  $60/2 = 30$  kv. per centimeter maximum (neglect-

ing flux concentration at edges). As an average gradient of 31 kv. per centimeter maximum is required to rupture air there is no breakdown.

(2) Remove the voltage and insert between the plates a sheet of pressboard 0.2 cm. thick, as in Fig. 232(b). The constants of pressboard are

$$k = 4 \text{ rupturing gradient} = 175 \text{ kv. per centimeter maximum}$$

$$l_p = 0.2 \text{ cm.}$$

For air

$$k = 1 \text{ rupturing gradient} = 31 \text{ kv. per centimeter maximum}$$

Apply now the same voltage as before. The addition of the pressboard of higher permittivity has increased the capacity of the combination and, therefore, the total flux and the flux density in the air. The gradient has also been increased. The combination may be considered as two condensers in series.

Where  $c_1$  = capacity of air condenser,  $c_2$  = capacity of pressboard condenser;  $e_1$  = voltage across the air condenser,  $e_2$  = voltage across the pressboard condenser; the total flux is

$$\psi = c_1 e_1 = c_2 e_2$$

$$\psi = \frac{k_1 A}{l_1} e_1 = \frac{k_2 A}{l_2} e_2$$

$$\text{therefore, } \frac{k_1}{l_1} e_1 = \frac{k_2}{l_2} e_2$$

$$e = e_2 + e_1$$

$$\frac{k_1}{l_1} e_1 = \frac{k_2}{l_2} (e - e_1)$$

$$e_1 \left( \frac{k_1}{l_1} + \frac{k_2}{l_2} \right) = \frac{k_2 e}{l_2}$$

$$e_1 = \frac{\frac{k_2 e}{l_2}}{\frac{k_1}{l_1} + \frac{k_2}{l_2}} = \frac{l_1 k_2 e}{k_1 l_2 + k_2 l_1} = 58.4$$

$$e_2 = 60 - 58.4 = 1.6$$

$$g_1 = \frac{e_1}{l_1} = \frac{k_2 e}{k_1 l_2 + k_2 l_1}$$

$$\text{Then } g_1 = \frac{4 \times 60}{1 \times 0.2 + 4 \times 1.8} = 32.5 \text{ kv./cm. max.}$$

The air breaks down as  $g_1$  is higher than the critical gradient, causing breakdown of air. As the broken down air is conducting, most of the applied voltage is placed on the pressboard.

Thus, after the air ruptures, the gradient on the pressboard is:

$$g'_2 = \frac{60}{0.2} = 300 \text{ kv./cm. max.}$$

This is much greater than the rupturing gradient of pressboard and causes it to break down. The 2.0-cm. space, therefore, which is safe with air alone, is broken down by the addition of stronger insulating material of higher permittivity. The stresses on this combination could have been calculated directly from (16a), Chap. II.

Another and convenient way of looking at this is as follows:

$$\text{Flux} = \frac{\text{volts}}{\text{flux resistance or elastance}}$$

$S$  is termed the elastance and is the reciprocal of permittance. The reciprocal of the permittivity is termed the elastivity. For the given electrode arrangement,  $S$  is proportional to the elastivity and the length, as long as lines of force are practically straight lines. Let the relative elastivities be

$$\text{Air} = 1.0$$

$$\text{Pressboard} = 0.25$$

Let the absolute elastivity of the air be  $\sigma_a$ , and introduce for the sake of abbreviation  $a = \sigma_a A$ , where  $A$  is the area.

Then the elastances for the different circuits in the test are

(a) Air (2 cm.)	$S_1 = a \times 2 \times 1 = 2a$
(b) Pressboard (0.2 cm.)	$S_p = a \times 0.2 \times 0.25 = 0.05a$
(c) Air (1.8 cm.)	$S_a = a \times 1.8 \times 1 = 1.8a$
(d) 1.8 cm. air + 0.2 cm. pressboard	$S = S_p + S_a = 1.85a$

Thus when there is only air in the gap

$$\psi_1 = \frac{60}{2a} = \frac{30}{a}$$

When 0.2 cm. of air is removed and the same thickness of pressboard added, the total elastance is less and the flux increases or

$$\psi_2 = \frac{60}{1.85a} = \frac{32.5}{a}$$

The drop across the air is

$$\psi_2 \times S_a = \frac{32.5}{a} \times 1.85a = 58.4 \text{ kv.}$$

The drop across the pressboard is

$$\psi_2 \times S_p = \frac{32.5}{a} \times 0.05a = 1.6 \text{ kv.}$$



58.4 kv. is sufficient to cause 1.8 cm. of air to break down. When the air breaks down the full 60 kv. appears across the pressboard which, in turn, breaks down.

The case discussed above is an exaggerated example of conditions often met in practice. In many power stations little bluish needle-like discharges, called static, may be noticed around generator coils, bushings, etc. This static is simply overstressed or broken down air but, unlike Case 1, the solid dielectric is sufficiently thick so that very little extra stress is put upon it by the broken down air. Damage may be caused in the course of time, however, by local heating, chemical deterioration, etc.

**Case 2. Static or Corona on Generator Coils.**—Consider the terminal coil of a 13,200-volt generator, insulated by 0.25 cm. of built-up mica ( $k = 4$ ), and 0.45 cm. of varnished cambric ( $k = 5$ ). In the slot is an armor of 0.1-cm. horn fiber ( $k = 2.5$ ). In series with these is more or less air; assume 0.05 cm. for the purpose of this calculation. A section of the coil assembled in the machine is shown in Fig. 233.

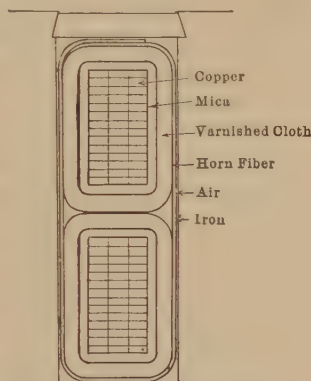


FIG. 233.—Corona on generator coils.

The stress on the air may be approximately found by assuming the conductors as one flat plate of a condenser, and the frame as the other.

Then	Kilovolts between lines	13.20 eff.
	Kilovolts to neutral	7.63 eff.
	Kilovolts to neutral	10.7 max.

$$\begin{aligned}
 g_{air} &= \frac{e}{k_4 \left( \frac{x_1}{k_1} + \frac{x_2}{k_2} + \frac{x_3}{k_3} + \frac{x_4}{k_4} \right)} & (16a) \\
 &= \frac{10.7}{1 \left( \frac{0.25}{4} + \frac{0.45}{5} + \frac{0.1}{2.5} + \frac{0.05}{1} \right)} \\
 &= \frac{10.7}{0.242} = 44 \text{ kv./cm. max.}
 \end{aligned}$$

Since the average disruptive strength of air is 31 kv. per centimeter, it will break down, forming corona. Experience has shown that in time the corona eats away the insulation by

mechanical bombardment, local heating, and chemical action, and ultimately a short circuit results.

Assume that the machine is operated at 8000 volts. The air is then stressed to 26.7 kv. per centimeter and corona does not form. Should one phase become grounded, however, the voltage of the other two above ground would become 8.0 kilovolts instead of 4.62 kilovolts, the gradient on the air would rise to 46.3 kv. per centimeter and corona would result. Assume now that there are no grounds, but that the machine, which shows no corona at 8.0 kilovolts at sea level, is shipped to Denver. The altitude of Denver is approximately 5000 ft. The corresponding barometer is 24.5 in. (Fig. 225), and hence the relative air density at 25°C. is 0.82. At this density the disruptive strength of air is  $0.82 \times 30 = 25.5$  kv. per centimeter. The air around the coils near the terminals having a gradient of 26.7 kv. per centimeter would glow.

Corona on machine coils may be prevented by tightly covering the surface of the coil with a conductor, as tinfoil, and connecting the foil to the iron frame of the machine; this, in effect, short circuits the air space. Naturally, the foil should be slit in such a way as to prevent it from becoming a short-circuited turn by transformer action. The end of the foil should also be shielded to prevent overstress.

**Case 3. Overstressed Air in Entrance Bushings.**—Assume that a  $\frac{3}{4}$ -in. conductor, supplying power at 33 kv., enters a building through a  $3\frac{1}{2}$ -in. porcelain bushing having a 1-in. hole (see diagram Fig. 234). The voltage between the rod and the ground ring is 19 kv. The stress on the air at the surface of the rod is

$$\begin{aligned} r_1 &= 0.375 \text{ in.} & k_1 &= 1 \\ r_2 &= 0.5 \text{ in.} & k_2 &= 4 \\ R &= 1.75 \text{ in.} \end{aligned}$$

$$\begin{aligned} g_{\text{air}} &= \frac{e}{xk_x \left( \frac{\log_e \frac{r_2}{r_1}}{k_1} + \frac{\log_e \frac{R}{r_2}}{k_2} \right)} & (17) \\ &= \frac{19 \times 1.41}{(0.375 \times 1) \left( \frac{\log_e 1.33}{1} + \frac{\log_e 3.5}{4} \right)} \\ &= 120 \text{ kv./in.} \\ \text{or} & \quad 47.5 \text{ kv./cm. max.} \end{aligned}$$

To cause corona on a rod of this size a gradient

$$\begin{aligned} g_v &= 31 \left( 1 + \frac{0.3}{\sqrt{r}} \right) \\ &= 31 \left( 1 + \frac{0.3}{\sqrt{0.375 \times 2.54}} \right) \\ &= 40.5 \text{ kv./cm. max.} \end{aligned}$$

is necessary. Hence, in the case considered, there will be corona, and chemical action on the rod which will become coated with a green surface of copper nitrate. The obvious cure for this is to coat the inside of the porcelain shell with a conductor and connect it to the rod.

Corona or static is often noticed where insulated cables come through a wall or bushing. For instance, three rubber covered cables may come through three bushings in a wall. If the voltage is high enough, a glow will appear around the rubber

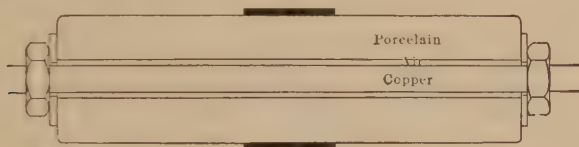


FIG. 234.—Corona in bushing.

in the air space inside the bushing. Ozone attacks rubber very rapidly. Such cables may soon be broken down by this simple cause. Such breakdowns are often ascribed to high frequency. The remedy is to short circuit the air space. In doing this by metal tubes slit lengthwise, to prevent eddy loss in the metal, care must be taken to bell the ends of the tube, otherwise the air will be stressed where the metal tube ends. The belled part may be filled with solid insulation.

**Case 4. Graded Cable.**—Assume that three insulations are available, all of exactly the same dielectric strength, but of permittivities as follows:

Insulation *A*,  $k = 5.4$

Insulation *B*,  $k = 3.6$

Insulation *C*,  $k = 2.0$

Rupturing gradient,  $g = 100$  kv. per centimeter

Assume that it is desired to insulate a 1.0-cm. wire using 1.75 cm. of insulation with an outside lead cover. The best way of

applying the insulation is so that each part is stressed in proportion to its respective strength. This ideal cable is impossible, but the more nearly this condition is realized the higher the voltage that may be applied to the cable without rupture.

(a) Using insulation *A* alone the breakdown voltage is

$$e = gr \log_e R/r = 75 \text{ kv.}$$

This is the same for either *B* or *C* alone.

(b) Using insulation *A* next to the wire, then *B*, then *C*, with thickness 0.25 cm., 0.6 cm., and 0.9 cm., respectively, as in Fig. 178(b), the rupturing voltage is

$$e = 133 \text{ kv.}$$

(c) Using the insulations in the reverse order as in Fig. 178(c), the rupturing voltage is

$$e = 63 \text{ kv.}$$

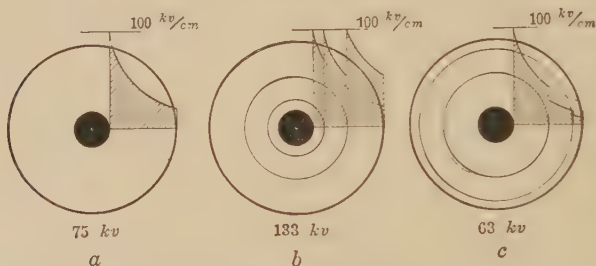


FIG. 235.—Graded cable.

(a) Not graded. (b) Insulations properly arranged. (c) Insulations improperly arranged. Noted breakdown voltage in each case.

Note that the area in Fig. 235(a), (b), and (c) represents the voltage, and, therefore, the rupturing voltage if the maximum  $g$  is the rupturing gradient. This example is given to show how important it is to properly arrange insulations. In general, the insulation of the highest permittivity should be placed where the field is densest. This applies not only to cables but all electrical apparatus. In spite of the fact that all of the above insulations had the same dielectric strength and the same total thickness, the rupturing voltages with the different arrangement were 133 kv., 75 kv., and 63 kv., respectively (use equation (17)).

**Case 5. Bushing.**—Other cases where the principle of putting insulation of high permittivity at points of dense field is shown are illustrated in Figs. 18 and 236. The solid insulation of the bushing in Fig. 18, page 35, because its contour follows the

lines of force, does not increase the stress on the air near it. It is, for that reason, much better than an insulator which has the insulation arranged in such a way that the stress on the air is increased in the denser part of the field. By inserting the high permittivity insulation in the dense fields at the rod, however, and cutting it away in the middle, a better arrangement is obtained (Fig. 236). In the zone between flux lines *a* and *b*, there is now the insulation of high permittivity and air of low permittivity in series in the same way as in the graded cable and with the same effect. In tests, the insulation of the type of Fig. 236 arced over at 18 per cent. higher voltage than that of Fig. 18 (of same overall dimensions) though its air path was 6.5 per cent. shorter.<sup>1</sup>

In practice, it is generally necessary to add corrugations to increase the leakage path on account of dirt settling on the surface, etc. The ideal design is not always the best in practice.

#### Case 6. Transformer Bushings.—

One of the most common bushings is the oil filled type. In the design of such a bushing two general problems present themselves: The internal stress on the oil, which determines the puncture voltage; the external stress on the air, which determines the arc-over voltage.

In the design of a bushing, however, the whole dielectric circuit must be considered at the same time.

If the surface of the shell follows a line of force, the internal field does not cut the shell and cause flux concentration at points on the shell; the voltage per unit length of surface, however, is not constant with this condition unless the lines of force are approximately straight parallel lines. A bushing, when parallel

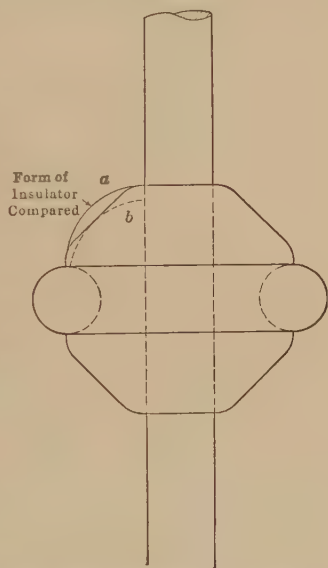


FIG. 236.—Bushing. Rod and torus.<sup>2</sup>

<sup>1</sup> FORTESCUE, *Trans. A.I.E.E.*, p. 907, 1913.

WEED, "Discussion," *Trans. A.I.E.E.*, p. 939, 1913.

<sup>2</sup> Figures 18 and 236 cannot represent practical leads as the rod and torus field is changed by the plane of the transformer case.



planes are approximated, theoretically, need not be over 2 in. high for a 100-kv. arc-over. This imposes a large diameter compared to length, and large well-rounded metal caps, etc. Such a bushing would arc-over with slightly dirty surfaces, moisture on surfaces, etc., at very low voltage. A practical bushing must generally be fairly long and corrugated (see Table LXXIX, page 255).

Where the surface follows a curved line of force, the internal field still does not cut the surface and cause the so-called leakage by local flux concentration, but the gradient is not constant along this line of force. Local breakdowns precede spark-over.

If the bushing surface does not follow a line of force, the lines from the outside pass through the shell to the inside. In this case, the shell should be so shaped that the stress is divided parallel to the surface and also perpendicular to the surface.

In an improperly designed bushing of this sort, breakdown might occur at places along the surface, and at other points out from the surface. For instance, as an extreme case, it might be imagined that the surface of a bushing followed an equipotential surface. There would then be no stress in the direction of the surface, but breakdown would occur by the stress perpendicular to the surfaces, as corona. Conversely, a condition might obtain which would cause greatest stress along the surface as when a line of force is followed. As the surface, due to dirt, etc., is generally weaker than the air, it is in most cases better not to have maximum stress along it (see Table LXXIX). In any case, the stress should be uniform, measured in either direction. Where the shells follow a line of force, the field is more readily approximated by experiment, or by calculation, than where the lines of force cut the shell, when flux refraction, etc., must be considered. The direction of the flux may be controlled by the arrangement of metal parts. The bushing problem is a space problem.

In practice, it is generally necessary to add petticoats. These should be placed so as to produce the minimum disturbance in the field with minimum stress along their surfaces.

Another type of bushing is the condenser bushing, built with the object of stressing all of the solid insulating material approximately equally. It consists of a number of cylindrical condensers of equal thickness, but of unequal lengths, arranged in such a way as to make the several capacities equal (Fig. 237). If this

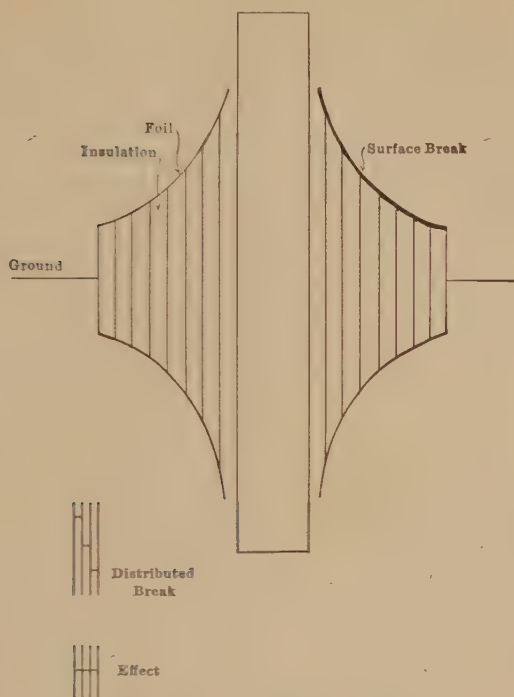


FIG. 237.—Condenser bushing.

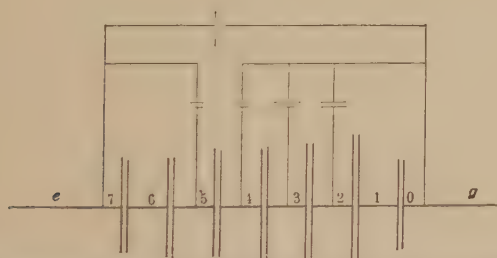
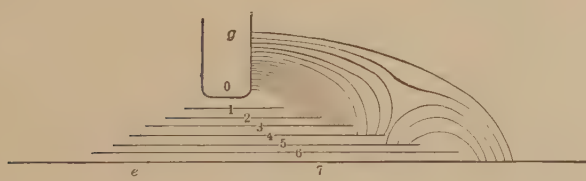


FIG. 238.—Diagrammatic representation of flux, and capacities in condenser bushing.

were exactly the case, the voltages across the equal thicknesses of insulation and equal distances along with the surface would be equal. This condition is possible but not generally reached on account of the capacity of the condensers to ground, to the central rod, and to each other (Fig. 238); to secure equal division of voltage here (Fig. 237) it would be necessary to connect the condenser plates to proper sources of potential. The condition

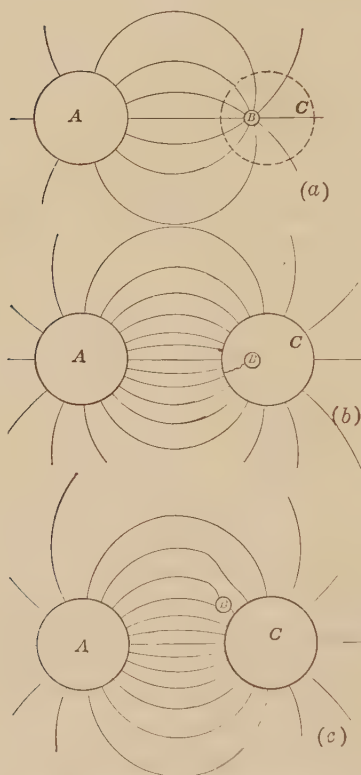


FIG. 239.—Simple illustration of flux control.

may be approached, however, to such a degree that a good practical bushing is the result when the insulating has been carefully done. A smaller diameter is obtained, but a greater length is required due to arcing distance in the air (*i.e.*, to avoid arcs of the nature of the heavy line, Fig. 237). The present practical form is a long thin bushing. (One disadvantage claimed is shown in the small sketch accompanying Fig. 237.) Little flaws in various parts of the lead are lined up by the metal parts and put directly in series. The separation of the insulation by metal is, from another standpoint, an advantage. A progressing corona streamer is stopped on reaching the metal surface at any layer. Concentration of flux at the edges of the metal cylinder must also be taken care of. The condenser bushing is often arranged with a metal cap for flux control.

**Case 7. Dielectric Field Control by Metal Guard Rings, Shields, Etc.**—It is sometimes practical to accomplish more with metal than by added insulation. In a case where the field is not uniform, but very much more dense at one point than at another, the flux may be made more uniform by relieving the dense portion and distributing over the less dense portion by a proper

arrangement of metal parts connected to a source of potential of the proper value. This is not always practical, as the necessary complicated potential connections often weaken the apparatus and make it much more liable to breakdown.

As a simple example: Fig. 239 represents two spheres of unequal size in air, one at potential  $e$  the other at potential  $-e$ , or a voltage  $2e$  between them. All the flux from  $A$  ends on  $B$ . The flux density at  $B$  is then much greater than at  $A$  and the air around  $B$  is very much more stressed than the air at the surface of  $A$ . The equipotential surface  $C$  may be covered with thin metal and no change takes place in the flux at  $A$  or  $B$ . If, however,  $C$  is connected by a wire to  $B$  the flux around  $B$  disappears

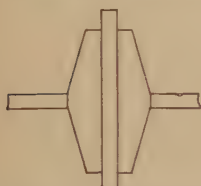


FIG. 240.—Entrance bushing.

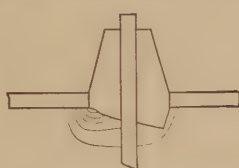


FIG. 241.—Making bushing shown in Fig. 240 operative by flux control after lower part had broken off.

and there is no stress on the dielectric at the surface of  $B$ . The total flux increases because of the greater capacity between  $A$  and  $C$ . The stress at  $A$ , due to increased flux density, increases, but it is still much less than the stress formerly at  $B$ , and a greater potential is required for spark-over. In other words, the insulation is more uniformly stressed and, therefore, working at greater efficiency. If, instead of surrounding  $B$  or completely shielding it, the sphere  $C$  be placed as in (c) and connected to  $B$  by a wire, the stress is relieved at  $B$  and increased at  $A$ . The distribution at  $B$  is again more uniform.

An actual example where this principle was made use of in an emergency by the author is illustrated in Figs. 240 and 241. While making the early corona tests (see Chap. VI, page 169), 200 kv. was carried through the roof of a shed by porcelain bushings. During a heavy wind storm, the roof was blown off and one bushing cracked as indicated by the jagged line. When the roof was replaced and an attempt made to put the bushing again into operation, it was found that bad arcing took place to the damp wood at 130 kv. As no extra bushings were immediately obtainable, and it was necessary to finish the experiments, the

expedient of field control was made use of. By hanging a metal torus made of a coil of wire on the rod, the work of about 15 min., the bushing was made operative up to 200 kv. This was not as good as a new bushing, not the best sort of bushing, but

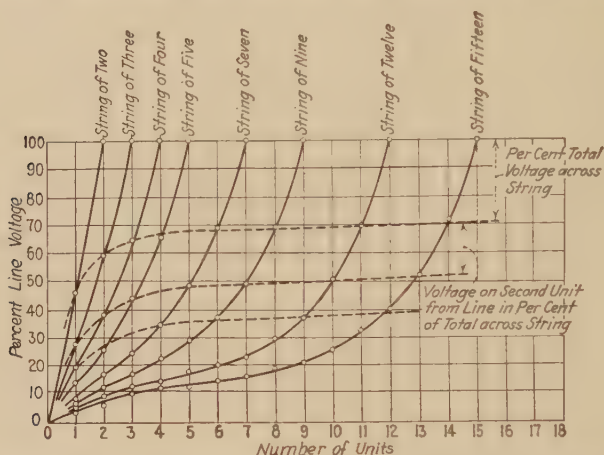


FIG. 242.—Typical voltage distribution curves on strings of suspension insulators.

it was a means of making a defective bushing operative, and prevented a shutdown of a month or more.

The effect of this shield is shown diagrammatically in Fig. 241. By moving the ring up and down the rod, a point of minimum flux density on the cracked surface of the porcelain is found. It

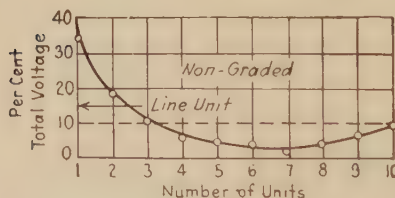


FIG. 243.—Voltage distribution on string of ten suspension insulators.

better distributed the flux and reduced the maximum flux density below the rupturing value.

**Case 8. High-voltage Suspension Insulators.**—When insulators in series are subjected to a voltage insufficient to produce appreciable corona

or surface leakage, such as in normal line operation, the potential across the insulator units is not evenly distributed, the highest percentage being across the line unit. Figure 242 shows voltage distribution curves for typical strings, while Fig. 243 gives the percentage of applied voltage across each unit in a string of ten. Uniform distribution would put 10 per cent. across each unit as indicated by the dotted line.



The reason for the unequal voltage stresses across the unit is due to the irregular capacity distribution as shown diagrammatically in Fig. 244. Figure 245 shows a corrected distribution by varying the internal capacities of the units themselves along the string in proportion to the currents.

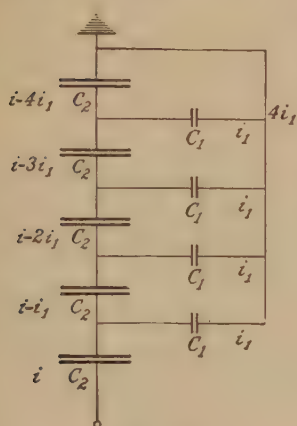


FIG. 244.

FIG. 244.—Cause of uneven voltage distribution on insulator strings. The capacities to ground ( $C_1$ ) cause an uneven current distribution through the insulator capacities ( $C_2$ ).

FIG. 245.—Voltage distribution on string of ten insulators graded with metal caps (see Fig. 246).

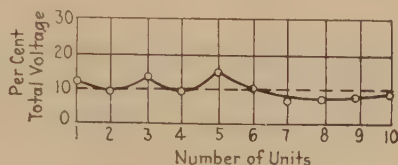


FIG. 245.

possible but impractical method is to use units of different designs and variable capacities in the same string.

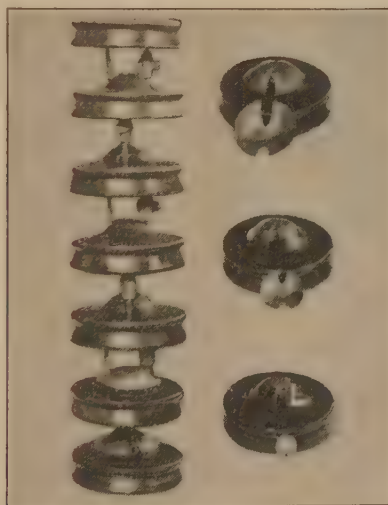


FIG. 246.—Suspension insulator string graded with caps or plates.

The most practical method of securing uniform voltage distribution is by means of a large metal shield at the line end. Figure

247 shows the effect of this in balancing the capacities to ground and Fig. 248 gives the curves of stress distribution over a twelve-unit string. Figure 249 shows a string with one of the early

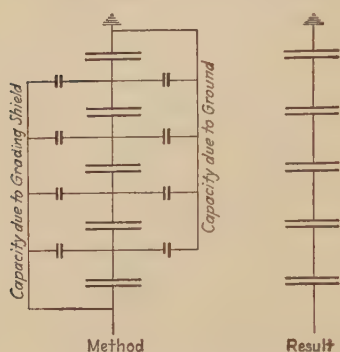


FIG. 247.—Effect of insulator-string shield in eliminating effect of capacity to ground.

forms of shields.

The shield eliminates corona on the string and directs the arc away from it. It does not increase the 60-cycle flashover voltage because, as the voltage nears this breakdown value on a non-shielded string, the corona and leakage currents increase sufficiently to automatically shield and grade the string without any extra metal attachments.

A lightning impulse wave applied to an insulator string involves such a brief time that the corona and surface discharges cannot distribute properly the voltage stresses over the units, as takes place with slower voltage applications. Consequently, the shield must be depended upon to provide the grading in this

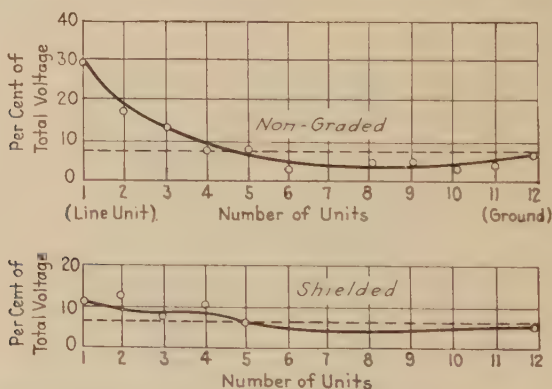


FIG. 248.—Effect of grading shield on voltage distribution of twelve-unit insulator string.

case and prevent abnormal voltages and early breakdown on the line units. In this way, the shield raises the lightning spark-over voltage.

In addition to the actual increase in lightning voltage discussed above, there is also an apparent increase which is probably of

more importance. In laboratory flashover tests when the energy of the lightning generator is limited, it is necessary to apply a higher voltage to a shielded string to cause spark-over. This apparent increase in voltage may be of the order of 25 per cent. The extra voltage must be applied because of the energy dissipated by the barrel of corona between the edges of the rings (see

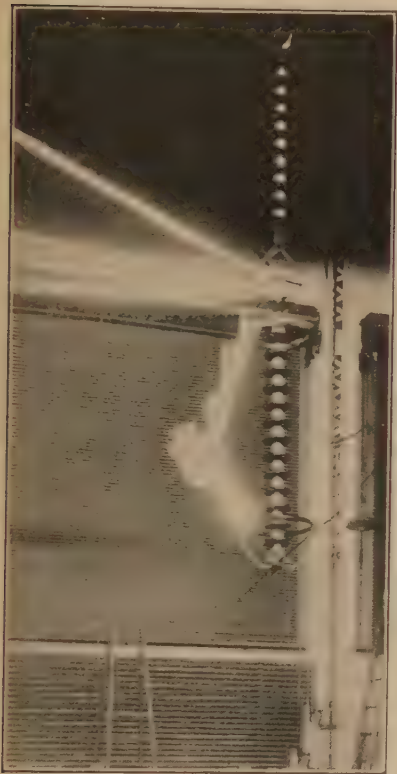


FIG. 249.—Insulator string shielded with early form of grading shield.



FIG. 250.—Dissipation of lightning energy by corona on insulator shields.

Fig. 250). The above order of gain has been observed when the energy available approximated that in an average span. This should be an approximate measure of the gain with the same shields in practice, since there is one string for each line per span. This energy dissipating effect by corona has been made use of by purposely designing grading rings of flat strap material in place of smooth surfaced pipes. Figure 251 shows such a

grading shield of recent design, applied to a standard suspension string. A lightning spark-over is occurring between rings.

Probably the most valuable function of the insulator shield is in preventing cascading of the string and consequent damage to the units by the arc. That shields prevent deterioration of the

units through improved distribution of voltage stresses is forcibly brought out in tests. In these it has been found that after a few lightning spark-overs, insulator units fail in the nonshielded strings, while there are no failures in the shielded strings.

The steeper the front of the impulse wave, the more difficult it is to prevent cascading. Consequently, the shields designed must be larger and more closely spaced. A shielding arrangement, so devised as to meet the worst conditions of lightning impulse in practice, may be such as to lower slightly the normal 60-cycle flashover of a string. This is no handicap, because the operating 60-cycle voltage never reaches flashover proportions, and lightning surges having an impulse ratio of



FIG. 251.—Suspension insulator showing equipped with recent type of grading shield designed to secure maximum dissipation of lightning energy by corona.

unity, and thus corresponding to 60-cycle waves, have never been observed in practice (see Chap. IX). The dry 60-cycle shielded spark-over voltage might be somewhat increased by using very large shield surfaces free from sharp ends and points. There can be no gain in practice in this way, however, because the large surfaces would be reduced to equivalent points under 60-cycle conditions when wet by the first raindrop. Laboratory tests have shown that lightning spark-over voltages are not affected by rain.



In brief, the various functions of the grading shield in the order of their importance are:

1. To prevent cascading of the string and damage to the insulator units.
2. To secure improved voltage distribution and thus lessen deterioration of the units under both normal operating voltage and applied impulse surges.
3. To increase the lightning spark-over voltage of the string.
4. To eliminate corona and surface discharges on the insulator units.

**Case 9. Insulation of Transformers.**—Figure 252 shows typical insulation designs for concentric and interleaved types

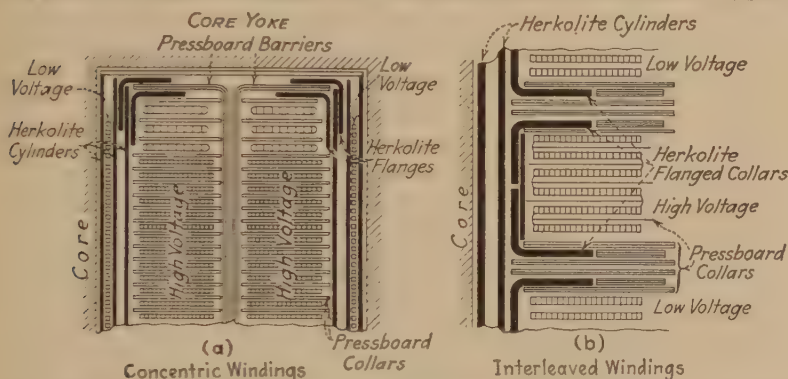


FIG. 252.—Cross-section diagrams of windings and insulation in moderate voltage power transformer.

of transformers. The principal forms of solid insulation used are specially treated paper cylinders and flanged collars, and pressboard barriers and collars. The need for the greatest dielectric strength and consequently the greatest design care enters in the insulation between the high-voltage and low-voltage windings, and between high-voltage winding and ground. In determining the relative amount of solid insulation and oil to resist puncture, a sufficient proportion of oil is used so that its maximum normal test stress will be well below its breakdown gradient. In addition, enough solid insulation is inserted to withstand a certain overvoltage, even though the entire oil path fails.

In order to minimize the danger of failure by creepage over insulation surfaces, all possible creepage paths are lengthened by extensions made to the collars, cylinders, and barriers. For the same purpose, flanged collars are provided at the ends of the



cylinders insulating the high-voltage winding as shown in Fig. 252. As a rule, the shortest creepage path over the solid insulation between two points is usually made from ten to twenty times the length of the direct puncture path through the solid insulation and oil.

**Case 10. Transient Considerations in Transformer Design.**—Apparatus must be designed to meet not only normal but also abnormal conditions to a reasonable extent. In the usual transformer, the voltage distribution is not uniform for all forms of applied waves, but varies with steepness and duration of the impulse, or frequency of the transient. High frequencies and steep impulses may cause excessive voltages at any part of the winding. The ideal transformer would be one in which the voltage distribution would be the same for all frequencies and wave shapes. It has been possible to secure these results with the so-called shielded or non-resonating design, which is an entirely new type.<sup>1,2,3</sup>

Figure 253 shows the advantages of this design. Here are plotted the results of tests on an actual transformer, shielded and non-shielded. In the shielded transformer the impulse and high-frequency voltage distribution is seen to be practically the same as the 60-cycle distribution. With the unshielded type, however, the envelope of impulse and high-frequency distribution in Fig. 253 shows extremely high-voltage concentrations in the windings. A comparison of the two shows that the shield reduces local transient voltages as much as 80 to 1. In the non-shielded transformer, lightning failure may occur anywhere in the winding, depending upon the wave shape. With the shielded winding free from localized stresses under all waves, breakdown is as definite as the flashover of an insulator string.

The reason for the varying distribution of voltage in a non-shielded transformer is briefly as follows: The initial lightning impulse distribution is determined by the distribution of the capacities in the windings due to the fact that the inductance at the first instant acts like an open circuit. This initial condition causes most of the voltage to appear at the line end due to

<sup>1</sup> PALUEFF, K. K., "Effect of Transient Voltages on Power Transformer Design," *Trans. A.I.E.E.*, 1929.

<sup>2</sup> PEEK, F. W., JR., "Lightning, Progress in Lightning Research in the Field and in the Laboratory," *Trans. A.I.E.E.*, 1929.

<sup>3</sup> BRAND and PALUEFF, "Lightning Studies of Transformers by Cathode Ray Oscillograph," *Trans. A.I.E.E.*, 1929.

the capacities to ground, an action similar to the distribution over an unshielded insulator string (see Fig. 247). This is true in both core and shell type transformers. The 60-cycle

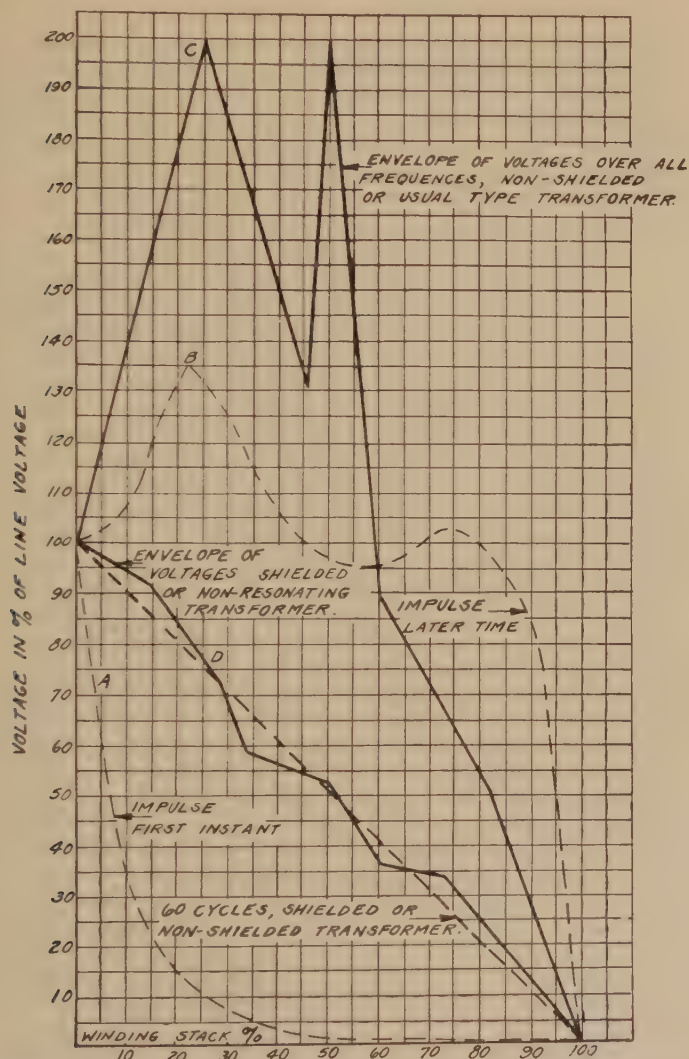


FIG. 253.—Voltage distribution in windings of shielded and non-shielded transformers at all frequencies.

or long duration voltage distribution depends on the inductance. If the voltage distribution, as determined by these two factors, is not the same, an oscillation results and lasts until a final distri-

bution corresponding to that of the inductance exists. With the shielded winding, however, the capacity and inductance distributions are made to correspond. The action of the capacity of the shield is instantaneous in making each part of the winding take its final share of the voltage. Since the instantaneous distribution is thus made to correspond to the final distribution, there are no oscillations.

Figure 254(a) shows an approximate equivalent diagram for the usual transformer. Figure 254(b) shows a shield added. Figure 254(c) shows the effect whereby a number of equal capacities to ground are connected to the winding at equal intervals.

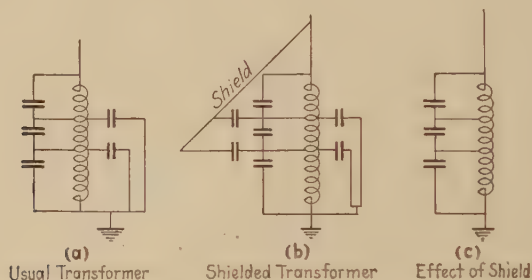


FIG. 254.—Diagrams showing equivalent transformer circuits.

A cathode-ray oscillographic study was made of the voltage distributions throughout transformer windings.<sup>1</sup> The oscillograms in Fig. 255(a) show a wave with a 15 microsecond front applied to the line end of the transformer. The double wave on this and some of the other records is the result of two measurements being made on the same film. Figure 255(b) shows that 83 per cent. of the voltage of the wave of Fig. 255(b) applied on the line appeared at the middle of the transformer. In Fig. 255(c) and Fig. 255(d) are given the results with a 25 microsecond wave. Figure 256 shows the voltage at various parts of the winding of an ordinary non-shielded transformer for a wave having a 5 microsecond front chopped by a line insulator and corresponding to surges measured in practice. The distribution in percentage of the voltage applied at the line end is as follows: 100 per cent. voltage at 97.2 per cent. of winding from ground; 82 per cent. voltage 83.3 per cent. from ground; 95.5 per cent.

<sup>1</sup> BRAND and PALUEFF, "Lightning Studies of Transformers by the Cathode Ray Oscillograph," *Trans. A.I.E.E.*, 1929.

voltage 75 per cent. from ground; 62.3 per cent. voltage 50 per cent. from ground; 51 per cent. voltage 33.3 per cent. from ground; 79 per cent. voltage 25 per cent. from ground; 79 per

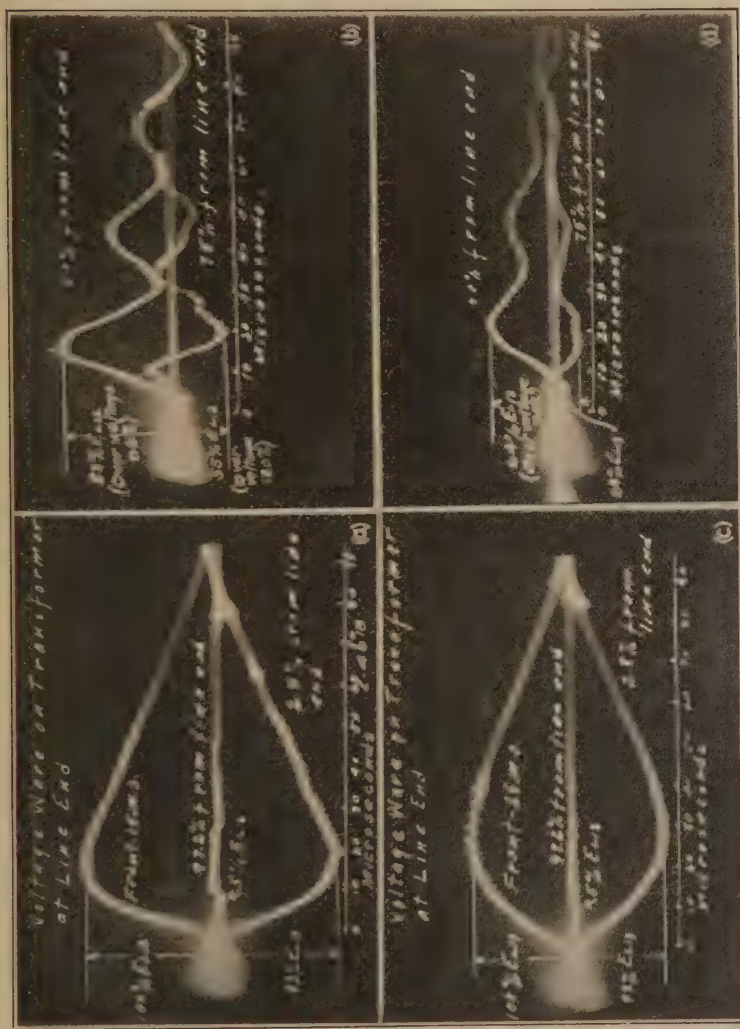


Fig. 255.—Cathode-ray oscillograms showing impulse voltage distributions in an ordinary transformer. (Long waves with 15 and 25 microsecond fronts—note high-internal voltages.)

cent. voltage, 16.6 per cent. from ground; 12.9 per cent. voltage 2.8 per cent. from ground. The difference in the shapes of the waves at various parts of the winding from the applied wave is evidence of oscillations. One record (Fig. 257) is sufficient to



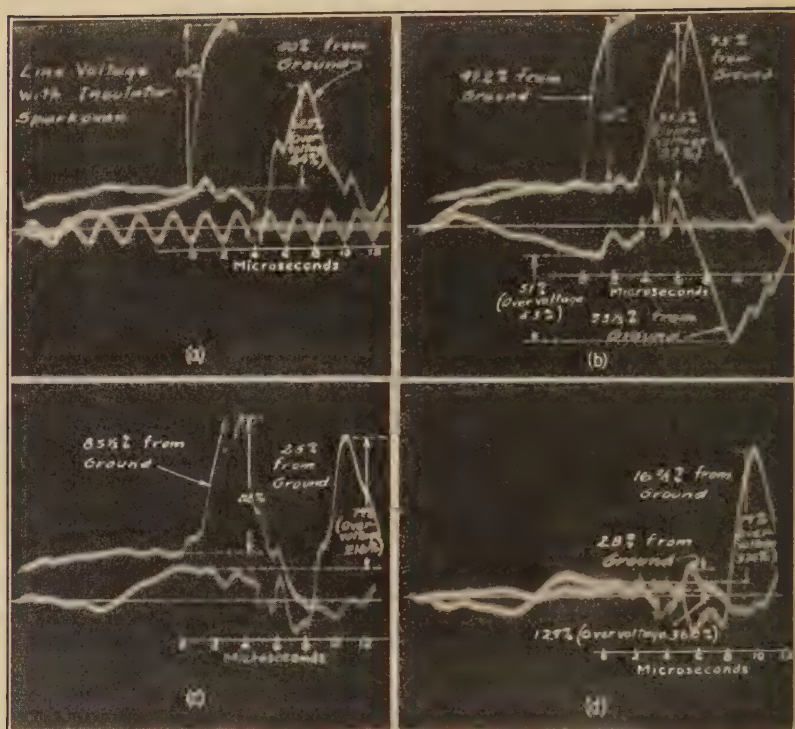


FIG. 256.—Cathode-ray oscillograms showing impulse voltage distributions in an ordinary transformer. (Chopped wave—note high-internal voltages.)

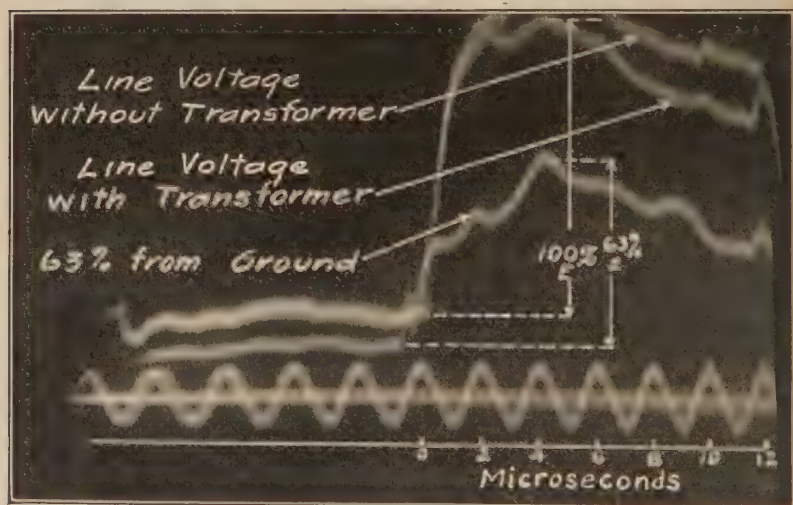


FIG. 257.—Cathode-ray oscillograms showing impulse voltage distribution in a "shielded" or "non-resonating" transformer. (Note that each part of winding takes its share of voltage and there is no resonance.)



show the result when the transformer is shielded. The applied waves are shown with and without the transformer as well as a wave taken at a point in the winding 63 per cent. from ground. The voltage at the 63 per cent. point is 63 per cent. of the applied voltage and the wave is exactly the same as the applied. This shows equal distribution and no oscillation. In addition to reducing the stresses in a transformer as much as 80 to 1, the shield is also of value in the 60-cycle testing routine, as it then provides the transformer with stresses equivalent to those of a lightning test, since the voltage distribution is the same. This is not true in the ordinary transformer where the 60 cycle test means little.

Although the transient crest voltages on lines due to switching are generally less than half those created by lightning, the internal oscillation voltages in non-shielded transformers caused by switching surges may be as much as twice those due to equal lightning voltages. Therefore, the two effects are approximately the same.

**Case 11. Dielectric Field.**—Draw the dielectric lines of force and equipotential surfaces between two parallel cylinders so that one-twelfth of the flux is included between any two adjacent lines of force, and one-twentieth of the voltage is between any two adjacent equipotential circles.

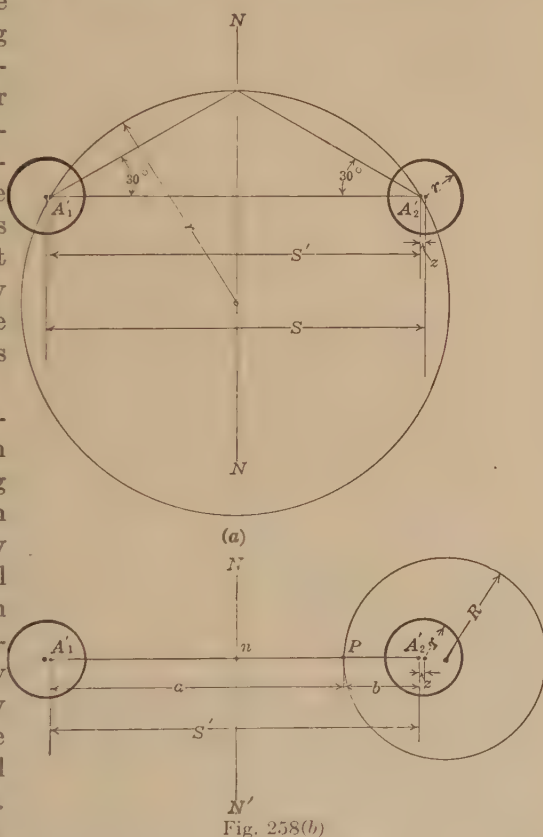


FIG. 258.—Method of drawing lines of force and equipotential surfaces.

Let  $S = 10$  cm. between conductor centers

$r = 1$  cm. = conductor radius

From Chap. II, page 22,

$$z = \frac{S - \sqrt{S^2 - 4r^2}}{2} = \frac{10 - \sqrt{100 - 4}}{2} = 0.10$$

The distance between focal points of the lines of force is

$$S' = S - 2z = 10 - 0.20 = 9.80$$

It is desired to include one-twelfth of the total flux between lines of force. Draw radial lines from the flux centers  $1\frac{1}{2} \times 180 = 30$  degrees apart (see Chap. II, pages 15 and 20). The point of intersection of a radial line with  $N. N.$  (Fig. 258(a)) is a point on the line of force. The line of force is, hence, a circle with center

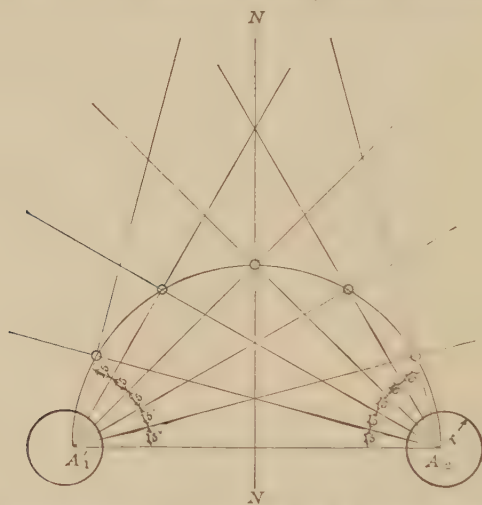


FIG. 259.—Graphical method of drawing lines of force between two cylinders. on  $N. N.$ , and passing through the point of intersection of the radial line  $N. N.$ ,  $A'1$ , and  $A'2$ . The lines of force are therefore determined. The centers, etc., might have been calculated from equation (8), page 20. The line of force is also determined graphically by drawing the diagonal line through the intersection of radial lines, as shown in Fig. 259.

The equipotential surfaces in this case may be found graphically in a similar way by drawing diagonals through the intersections of the circles of the component fields. Other resultant fields may be drawn from corresponding plane diagrams if the component fields are given for the same strength, or same potential differences between the equipotential surfaces. Any number

of fields may be so combined, two at a time. It is often possible to approximate, for practical purposes, the field of a complicated structure by so combining the simple fields of the component electrodes.

The equipotential surfaces are circles with centers on the line  $A'_1, A'_2$  (see equation (7), page 18). The distance of the center of the circles from  $A'_2$  is  $\frac{b^2}{a-b}$ , and the radius is  $\frac{ab}{a-b}$ , where  $a$  and  $b$  must be so chosen that the permittances between circles are equal.

For any point  $p$  on the line  $A'_1A'_2$  (Fig. 258), the potential to the neutral plane due to  $A'_2$  is

$$e_{2np} = \frac{-\psi}{2\pi Kk} \log \epsilon \frac{2b}{S'}$$

Due to  $A'_1$ , it is

$$e_{1np} = \frac{\psi}{2\pi Kk} \log \epsilon \frac{2a}{S'} = \frac{\psi}{2\pi Kk} \log \epsilon \frac{2(S' - b)}{S'}$$

The total voltage from any point  $p$  to the neutral is

$$e_{np} = e_{1np} + e_{2np} = \frac{\psi}{2\pi Kk} \left( \log \epsilon \frac{2(S' - b)}{S'} - \log \epsilon \frac{2b}{S'} \right)$$

$$e_{np} = \frac{\psi}{2\pi Kk} \log \epsilon \frac{(S' - b)}{b}$$

It is desired to divide the field up into  $n$  equal voltages between the conductor surface and the neutral plane. The potential from the conductor to neutral is  $e_n$  and is known

Due to  $A'_2$

$$e_{A2n} = \frac{-\psi}{2\pi Kk} \log \epsilon \frac{2(r - z)}{S'}$$

Due to  $A'_1$

$$e_{A1n} = \frac{\psi}{2\pi Kk} \log \epsilon \frac{2(S' - (r - z))}{S'}$$

$$e_n = \frac{\psi}{2\pi Kk} \log \epsilon \frac{S' - (r - z)}{r - z}$$

$$\therefore \psi = 2\pi Kk \frac{e_n}{\log \epsilon \frac{S' - (r - z)}{r - z}}$$

Let  $\beta$  be the fraction of the voltage  $e_n$  it is desired to place between the neutral plane and any point  $p$  on the surface under consideration, then (Fig. 258(b))

$$e_{np} = e_n \beta$$

$$\beta = \frac{1}{\log \epsilon \frac{S' - (r - z)}{r - z}} \log \epsilon \frac{(S' - b)}{b}$$

$$\log \epsilon \frac{(S' - b)}{b} = \beta \log \epsilon \frac{S' - (r - z)}{(r - z)} = \beta F$$

In this problem

$$\log \epsilon \frac{S' - (r - z)}{r - z} = \text{constant} = F$$

$$F = \log \epsilon \frac{9.8 - (1 - 0.1)}{(1 - 0.1)} = \log \epsilon \frac{8.92}{0.92} = 2.290$$

$$\log \epsilon \frac{S' - b}{b} = \beta F$$

$$\frac{S' - b}{b} = \text{anti-log} \epsilon \beta F$$

$$b = \frac{S'}{(\text{anti-log} \epsilon \beta F + 1)}$$

$b$  is thus determined.

If it is desired to find  $b$  for the first circle from the conductor  $\beta = 0.9$ .

$$b_1 = \frac{9.80}{7.7 + 1} = \frac{9.80}{8.7} = 1.13$$

For the next circle

$$\beta = 0.8$$

$$b_2 = \frac{9.80}{6.23 + 1} = 1.36$$

Other values are found and tabulated in Table LXXXIV.  $a$  and  $R$  are thus found. The circles may now be drawn with radii  $R$ , centers on  $A'_1 A'_2$ , and intersecting  $A'_1 A'_2$   $b$  cm. from  $A'_2$ .

TABLE LXXXIV.—EQUIPOTENTIAL SURFACES

$\beta$	$b$	$a = S' - b$	$R = \frac{ab}{a-b}$	$a - b$	$ab$
1.0	$b$	0.900	8.90	1.00	8.00
0.9	$b^1$	1.110	8.69	1.27	7.58
0.8	$b_2$	1.353	8.45	1.62	7.09
0.7	$b_3$	1.648	8.15	2.07	6.50
0.6	$b_4$	1.98	7.82	2.65	5.84
0.5	$b_5$	2.38	7.42	3.50	5.04
0.4	$b_6$	2.81	7.09	4.65	4.28
0.3	$b_7$	3.29	6.51	6.65	3.22
0.2	$b_8$	3.80	6.00	10.35	2.20
0.1	$b_9$	4.34	5.46	21.15	1.12
0.0	$b_{10}$	4.90	4.90	$\infty$	0.00

$$F = 2.290 = \text{constant} \quad z = 0.1 \quad S' = S - 2z = 9.8$$

The gradient at any point and, therefore, the equipotential surfaces may be found as follows:

The flux density at any point is

$$D = \frac{S'\psi}{2\pi x_1 x_2} \quad (\text{Pages 21 and 24.})$$

$$\psi = C_n e_n = \frac{2\pi k K e_n}{\log \left[ \frac{S}{2r} + \sqrt{\left( \frac{S}{2r} \right)^2 - 1} \right]}$$

$$D = \frac{2S'\pi k K e_n}{2\pi x_1 x_2 \log \left[ \frac{S}{2r} + \sqrt{\left( \frac{S}{2r} \right)^2 - 1} \right]}$$

$$g = \frac{D}{kK} = \frac{1}{x_1 x_2} \left[ \frac{S' e_n}{\log \left[ \frac{S}{2r} + \sqrt{\left( \frac{S}{2r} \right)^2 - 1} \right]} \right]$$

or for a given voltage, spacing and size of conductor, the term to the right is constant, and it follows:

$$g = \frac{1}{x_1 x_2} \text{ times a constant} = \frac{1}{x_1 x_2} M$$

is the gradient at any point  $x_1$  cm. from  $A'_1$  and  $x_2$  cm. from  $A'_2$ . Putting  $x_1$  in terms of  $x_2$  and the angle  $\alpha$  between  $x_2$  and the line  $A'_1 A'_2$

$$g = \frac{1}{x_2 \sqrt{x_2^2 + S'^2 - 2S'x_2 \cos \alpha}} M$$



(1) Find the maximum gradient at the conductor surface for 100 kv. between conductors. This may be found directly from equation (12a), pages 25 and 30, and is 26.7 kv. per centimeter.

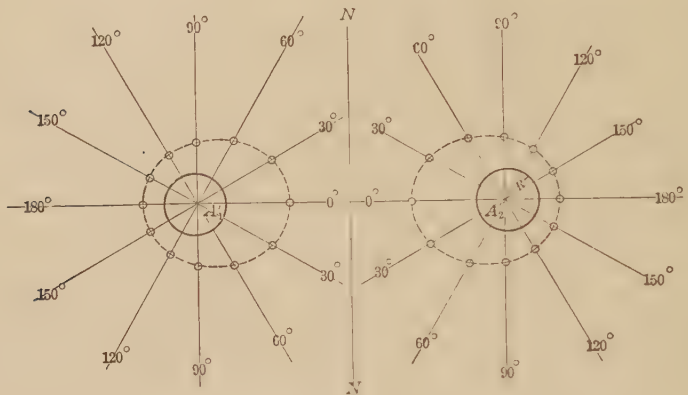


FIG. 260.—Method of plotting equigradient curves.

(2) Find the gradient at six equidistant points on the conductor surface for 100 kv. between conductors (see Table LXXXV).

TABLE LXXXV.—EQUIGRADIENT SURFACES

$\alpha$		0°	30°	60°	90°	120°	150°	180°
$g = 21.4$	$x_2 =$	1.16	1.13	1.07	1.00	0.97	0.94	0.93
$g = 16.1$	$x_2 =$	1.64	1.60	1.44	1.32	1.27	1.23	1.20
$g = 10.7$	$x_2 =$	2.91	2.85	2.25	2.00	1.85	1.75	1.74
$g = 8.9$	$x_2 =$	4.90	3.40	2.71	2.37	2.19	2.06	2.02
$g = 8.0$	$x_2 =$	<sup>1</sup>	4.0	3.08	2.59	2.38	2.26	2.20
$g = 5.34$	$x_2 =$	$4.9 \pm 4\sqrt{-1}$ <sup>1</sup>	8.20	4.70	3.81	3.27	3.17	3.10
$g = 2.67$	$x_2 =$	<sup>1</sup>	<sup>1</sup>	8.63	6.73	5.83	5.40	5.29

<sup>1</sup> Such a gradient does not exist on this line and hence  $x_2$  is imaginary. (See plot Fig. 8, page 16.)

Gradient at Equidistant Points on the Conductor Surface

Angle bet. horizontal $A'_1A'_2$ and line through point and conductor center	0°	30°	60°	90°	120°	150°	180°
$g$ .....	26.7	26.0	23.7	21.6	19.4	18.2	17.8

(3) Calculate the equipotential curves for gradients of 21.4, 16.1, 10.7, 8.9, 8.0, 5.34, and 2.67 kv. per centimeter at 100 kv. between conductors. This may be done from the above equation by putting  $g$  equal to the required gradient, and finding  $x_2$  for given values of  $\alpha$ . The results are tabulated in Table LXXXV and method of plotting is shown in Fig. 260.

A complete plot of Case 9 is shown in Fig. 8, page 16. Note that in such a diagram, the permittance or elastance of each of the small cells bounded by sections of lines of force and equipotential surfaces is equal.

*Determination of Potential of a Point in Space.*

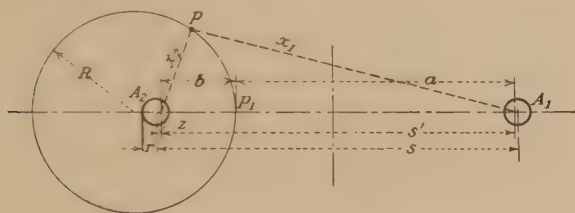


FIG. 261

Let  $P$  be any point in space

$r$  be the radius of the conductor

$S$  be the spacing between conductor centers (between conductor and image when necessary)

$z$  be the distance between conductor center and the focal point of the lines of force

$x_1$  be the distance between  $P$  and the focal point in conductor  $A_1$

$x_2$  be the distance between  $P$  and the focal point in conductor  $A_2$

$R$  be the radius of the equipotential surface (circle) passing through  $P$  and  $P_1$

Then

$$\frac{x_1}{a} = \frac{x_2}{b} \quad (\text{page 18})$$

Since

$$a = S' - b$$

$$bx_1 = S'x_2 - bx_2$$

and

$$b = \frac{x_2 S'}{x_1 + x_2} \quad (1)$$

Since

$$z = \frac{[S - (S^2 - 4r^2)^{1/2}]}{2} \quad (\text{page 22}) \quad (2)$$

$$S' = S - zz = S - S + (S^2 - 4r^2)^{1/2} = (S^2 - 4r^2)^{1/2} \quad (3)$$

and therefore

$$b = \frac{x_2(S^2 - 4r^2)^{1/2}}{(x_1 + x_2)} \quad (4)$$

The voltage from  $P_1$  (or  $P$ ) to neutral is

$$e_{np} = \psi \ln \left( \frac{S' - b}{b} \right) \frac{1}{2\pi Kk} \quad (\text{page 337})$$

and since

$$\psi = 2\pi Kk e_n / \ln \left( \frac{S' - (r - z)}{r - z} \right) \quad (\text{page 337})$$

$$e_{np} = e_n \left[ \frac{\ln \left( \frac{S' - b}{b} \right)}{\ln \left( \frac{S' - (r - z)}{r - z} \right)} \right] \quad (5)$$

where  $e_n$  is the known voltage from conductor to neutral.

Substituting in (5) the values obtained in equations (2), (3), and (4), we get

$$e_{np} = e_n \left| \frac{\ln \left[ \frac{(S^2 - 4r^2)^{1/2} - \frac{x_2(S^2 - 4r^2)^{1/2}}{x_1 + x_2}}{\frac{x_2(S^2 - 4r^2)^{1/2}}{x_1 + x_2}} \right]}{\ln \left[ \frac{(S^2 - 4r^2)^{1/2} - \left\{ r - \left( \frac{S - (S^2 - 4r^2)^{1/2}}{2} \right) \right\}}{r - \left( \frac{S - (S^2 - 4r^2)^{1/2}}{2} \right)} \right]} \right|$$

$$= e_n \left[ \frac{\ln \left( \frac{x_1}{x_2} \right)}{\ln \left[ \frac{(S^2 - 4r^2)^{1/2} + S - 2r}{(S^2 - 4r^2)^{1/2} - S + 2r} \right]} \right] \quad (6)$$

NOTE.—The quantities  $e_{np}$  and  $e_n$  are in the same units. Also the quantities  $x_1$ ,  $x_2$ ,  $S$ , and  $r$  are in the same units.

From (6) we can obtain

$$e_{np} = e_n \frac{\ln \left( \frac{x_1}{x_2} \right)}{\ln \left[ \frac{S}{2r} + \left\{ \left( \frac{S}{2r} \right)^2 - 1 \right\}^{1/2} \right]} \quad (7)$$

or

$$e_{np} = e_n \frac{\ln\left(\frac{x_1}{x_2}\right)}{\cosh^{-1} \frac{S}{2r}} \quad (8)$$

Assume Cartesian axes through the center of conductor  $A_2$ , the  $X$  axis containing the center of conductor  $A_1$ . Let the coordinates of  $P$  be  $x, y$ . Then

$$x_2^2 = (x - z)^2 + y^2$$

and

$$x_2 = [(x - z)^2 + y^2]^{\frac{1}{2}} \quad (9)$$

Substituting (2) in (9), we get

$$x_2 = \left[ \left( x + \frac{(S^2 - 4r^2)^{\frac{1}{2}}}{2} - \frac{S}{2} \right)^2 + y^2 \right]^{\frac{1}{2}} \quad (10)$$

Also

$$x_1^2 = (S - x - z)^2 + y^2$$

And

$$x_1 = \left[ \left( \frac{S}{2} + \frac{(S^2 - 4r^2)^{\frac{1}{2}}}{2} - x \right)^2 + y^2 \right]^{\frac{1}{2}} \quad (11)$$

NOTE.—The quantities  $x, y, x_1, x_2, S$ , and  $r$  are in the same units.

**Case 12. Dielectric Fields in Three Dimensions.**—The field of a conductor arrangement which must be considered in three dimensions, as a rod and torus, rod through a plane, etc., is generally represented on a plane figure in such a way that if the figure were revolved about its axis, the solid would be formed surrounded by its three-dimensional field. The small cells of the plane figure bounded by sections of lines of force and equipotential surfaces would form cells in the solid of equal permittance.

In the case of figures, as those for parallel wires, a wire in a cylinder, and parallel planes, it is possible to represent the field by considering only two dimensions. The height and thickness of the cells on the plane give constant permittance, or average

height  
thickness = constant. The third dimension is then the length of the wire and need not be considered in drawing these cells.

In the case of the three-dimensional field, the cells on the plane must be of such a height and thickness that the solid cells have constant permittance, or where the cell is small

$$\frac{hr}{t} = \text{constant}$$

This can readily be seen from Fig. 262.

It is a general law that the cells must be so arranged that the stored energy may be a maximum or the permittance a maximum. In cases where the field need only be considered in two dimensions, it is thus possible, without

great difficulty, to draw a field by a series of approximations in which the cells have a constant  $\frac{h}{t}$  or add up to

maximum permittance. The lines of force must be normal to the electrodes and to the equipotential surfaces at the point of contact. This is also possible for a three-dimensional field, but extremely difficult because the cells must be drawn in such a way that the solid cells have constant permittance.

The best way in which to determine a field that cannot be readily calculated is experimentally. If the electrodes are immersed in an electrolyte in a large tank made of insulat-

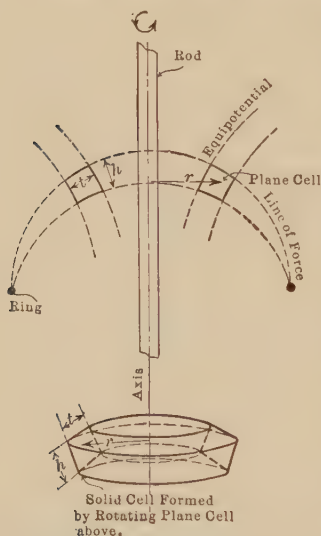


FIG. 262.—Dielectric field in three dimensions.

ing material, and a small current passed between them, equipotential surfaces may be measured at equal voltage intervals on a plane through the axis of revolution by means of a galvanometer.<sup>1</sup> These surfaces correspond to the dielectric-equipotential surfaces. The lines of force may be drawn at right angles to these, so as to divide the field into solid cells of equal capacity (see above). It is difficult in practice to get results by this method when the problem includes several permittivities.

Theoretically, it would be possible to use a solid material to represent, for instance, the porcelain shell of an insulator, and

<sup>1</sup> Fortescue has described this method. See *Trans. A.I.E.E.*, p. 907, 1913. Much more exact results may be obtained than those shown in this paper.

RICE, C. W., *Trans. A.I.E.E.*, p. 905, 1917.



the electrolyte to represent the air. The resistivities of the two materials should then have the same ratio as the elastivities of porcelain and air. It is difficult to find a solid material with a resistivity in the order of that of an electrolyte.

As a less exact experimental method, the lines of force may be obtained by mica filings and the problem then solved by approximations. These methods may be developed into very useful ones for a study of flux control, etc.

**Case 13. Effect of Ground on the Permittance and Gradient for Parallel Wires.**—Such problems are solved by taking the “images” symmetrically below the ground, as in Fig. 263.

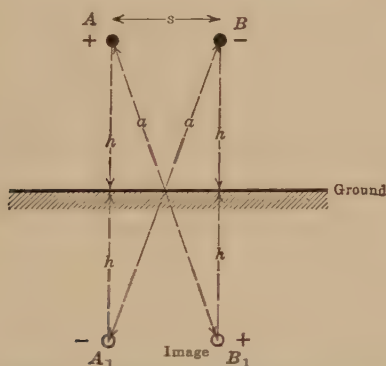


FIG. 263.—Effect of ground on capacity between parallel wires.

Voltages between  $AB$  due to  $A, B, A_1, B_1$  are

$$\begin{aligned} e_A &= + \left( \frac{\psi}{2\pi kK} \right) \log_e \frac{S}{r} \\ e_B &= - \left( \frac{\psi}{2\pi kK} \right) \log_e \frac{r}{S} \\ e_{A_1} &= - \left( \frac{\psi}{2\pi kK} \right) \log_e \frac{a}{2h} \\ e_{B_1} &= + \left( \frac{\psi}{2\pi kK} \right) \log_e \frac{2h}{a} \end{aligned} \quad \left( \begin{array}{l} S \cong S' \text{ where the wires} \\ \text{are far apart} \end{array} \right)$$

The total voltage is

$$\begin{aligned} e &= e_A + e_B + e_{A_1} + e_{B_1} = \frac{\psi}{\pi kK} \left( \log_e \frac{S}{r} + \log_e \frac{2h}{a} \right) = \frac{\psi}{\pi kK} \log_e \frac{S}{r} \frac{2h}{a} \\ C &= \frac{\psi}{e} = \frac{\pi kK}{\log_e \frac{S}{r} \frac{2h}{a}} \text{ (Bet. lines)} \end{aligned}$$

Where the wires are far apart the gradient is

$$g = \frac{e}{2 r \log_e \frac{S}{r} \frac{2h}{a}}$$

The problem for a number of wires may be solved in the same way. The fluxes from the different wires may then not be the same and the solution is more difficult as a number of simultaneous equations must be written and solved.

**Case 14. Three-phase Dielectric Field with Symmetrical and Unsymmetrical Spacings.**—The fluxes between conductors on a three-phase line vary sinusoidally with the voltages. The instantaneous values of voltages may be added algebraically as above. The effective or maximum values are found by geometrical addition.

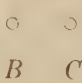
To illustrate: find the fluxes for three three-phase conductors in an equilateral triangle, and also for flat spacing. In order to greatly simplify the problem, the effects of ground or images will be neglected, and the conductors considered far apart.

Then due to fluxes from

$$\begin{array}{c} A \quad | \quad B \quad | \quad C \\ (a) \ E_{AB} = \frac{1}{2\pi kK} (\psi_A \log_e \frac{AB}{r} + \psi_B \log_e \frac{r}{BA} + \psi_C \log_e \frac{CB}{CA}) = e \sin \theta \\ (b) \ E_{BC} = \frac{1}{2\pi kK} (\psi_A \log_e \frac{AC}{AB} + \psi_B \log_e \frac{BC}{r} + \psi_C \log_e \frac{r}{CB}) = \\ e \sin (\theta - 120) \end{array}$$

Only two of the three equations which may be written as above are independent, since the sum of the voltages must be zero. The other independent equation is

$$(c) \quad \psi_A + \psi_B + \psi_C = 0$$

Conductors Spaced in a Triangle  (equilateral triangle).

Substituting spacing  $S$  in (a) and (b) and solving for  $\psi_A$ ,  $\psi_B$ , and  $\psi_C$

$$\psi_B = - \frac{2\pi k K e}{3 \log_e \frac{S}{r}} (1.5 \sin \theta + 0.866 \cos \theta)$$

Let  $e(1.5 \sin \theta + 0.866 \cos \theta) = e_a (\sin \theta - \alpha)$   
 put  $\theta = 90$  and  $\theta = 0$  and solve for  $e_a$  and  $\alpha$

$$\psi_B = \frac{2\pi k K e}{\sqrt{3} \log_e \frac{S}{r}} \sin (\theta - 150) = \frac{1.16(\pi k K) e}{\log_e \frac{S}{r}} \sin (\theta - 150)$$

$$\psi_A = \frac{2\pi k K e}{\sqrt{3} \log_e \frac{S}{r}} \sin (\theta - 30) = \frac{1.16(\pi k K) e}{\log_e \frac{S}{r}} \sin (\theta - 30)$$

$\psi_C$  may be found in the same way, or for this particular case,  $\psi_A$ ,  $\psi_B$ , and  $\psi_C$  are equal by symmetry.

For single phase

$$\psi = \frac{2\pi k K e}{2 \log_e \frac{S}{r}}$$

Therefore, when the wires are far apart, and with the same voltage between lines, the three-phase stress is  $\frac{2}{\sqrt{3}}$  times the single-phase stress.

*Flat Spacing*  $\begin{matrix} A & B & C \\ \circ & \circ & \circ \end{matrix}$ .—Putting  $S$ ,  $S$ , and  $2S$  in  $a$  and  $b$  and solving as before

$$\begin{aligned} \psi_B &= \frac{2\pi k K e}{\sqrt{3} \log_e \frac{S}{r} - 0.58 \log 2} \sin (\theta - 150) \\ &= \frac{2\pi k K e}{\sqrt{3} \log_e \frac{S}{r} - 0.4} \sin (\theta - 150) \end{aligned}$$

The flux and, therefore, the stress when the wires are far apart, is greatest on the middle wire. For  $\frac{S}{r} = 500$  it is 4 per cent. greater than on the wires with the same  $S$  and triangular spacing as above.  $\psi_A$ , and  $\psi_C$  are 6 per cent. lower than for the triangular

spacing. The gradients vary in the same way. Corona, therefore, starts on the center wire at a 4 per cent. lower voltage, and on the outer wires at a 6 per cent. higher voltage than for triangular spacings.

**Case 15. Occluded Air in Insulation.**—It is interesting to estimate the effect of occluded air in solid insulation. Assume that in the process of manufacture air bubbles have formed in a sheet of rubber insulation. The sheet is 1 cm. thick. The bubbles are thin compared to the rubber, and long in the direction of the length of the sheet. It is estimated that the largest ones are 0.01 cm. thick, and 0.1 cm. long and wide. The electrodes which the rubber insulates may be assumed as being practically parallel planes. The working voltage is 40 kv., or the stress is 40 kv. per centimeter effective in the rubber. As the air bubbles are not thick enough to greatly disturb the field, the same flux passes through the air as through the rubber. The permittivity of the rubber is 3. The stress on the air is, therefore,  $3 \times 40 = 120$  kv. per centimeter effective. Air breaks down at 21.2 kv. per centimeter effective at atmospheric pressure. It seems probable that these bubbles will break down, even after allowance is made for the extra strength of thin films, and a possible pressure higher than atmospheric. See Appendix. It is probable that the solid insulation would soon break down on account of heat and chemical action.

**Case 16. General.**—(a) Estimate the visual corona voltage when wires are wet. Compare with the visual corona voltage when wires are dry.

Calculate  $g_v$  from the formula on page 77, Chap. IV. Insert the value in formula (20). Maximum  $e_r$  to neutral is thus found. If the voltage used is a sine wave, reduce to effective kilovolts by dividing by  $\sqrt{2}$ . For a three-phase line the voltage between wires may be found by multiplying by  $\sqrt{3}$ ; for a single-phase line, by multiplying by 2. Compare with dry visual critical voltage calculated from equation (20); page 53.

(b) At what voltage will the above wires spark-over wet and dry single phase; three phase?

Estimate dry spark-over voltage from equation given on page 113, Chap. V. Estimate wet arc-over voltage by assuming needle-gap spark-over.

(c) Calculate the dry arc-over curve for a 10-cm. sphere (grounded) at  $\delta = 0.90$ , and spacings from 1.5 to 10 cm.

Use equation (13b), Chap. V. Estimate a wet spark-over curve as outlined for spheres on page 139, Chap. V.

(d) What is the voltage required to puncture 0.5 cm. of paper insulation when the time of application is limited to  $\frac{1}{100}$  sec.? In 100 sec.?

Use equation on page 238, Chap. VIII, of the form

$$g_s = g \left( 1 + \frac{a}{\sqrt[4]{T}} \right)$$

$$e_s = g_s \times \text{thickness}$$

(e) Estimate the loss per cubic centimeter at 1000 cycles in a piece of varnished cambric, at 5.0 kv. per millimeter, 25° C. Use equation page 251, Chap. VIII.

(f) What is the breakdown gradient of a piece of porcelain 2 cm. thick?

$$g = 7.5 \left( 1 + \frac{0.94}{\sqrt{t}} \right)$$

where  $t$  = thickness in millimeter

$g$  = gradient in kv. per millimeter (effective)

(See Chap. VIII, page 238.)

**Case 17. Lightning-proof Transmission Line and Coordination of Transformer Insulation and Line Insulation.**—It is interesting to consider whether a lightning proof transmission line is possible or practicable. It has been shown (see Chap. IX), that the lightning voltage is independent of the operating voltage and depends upon the height of the line; that the ground wire greatly reduces the lightning voltages; and that the lightning flashover voltage of insulation and the breakdown voltage of apparatus are known.<sup>1</sup> A consideration of these factors shows that a line of moderate height, protected with ground wires and properly insulated could usually be made lightning proof against induced voltages at a reasonable cost. In order to make a line safer from direct strokes, the necessity of ground wires above the line is almost obvious because, no matter what the insulation, the limit will be the sparking distance from line to ground. With ground wires, the stroke would usually take place to the wires and then along the wires to the tower, preventing insulation arc-over. Where the line is badly exposed to direct strokes,

<sup>1</sup> PEEK, F. W., JR., "Lightning, Progress in Lightning Research in the Field and in the Laboratory," *Trans. A.I.E.E.*, 1929.



however, special precaution should be taken in the design of the tower so that side flashes are not likely to take place to the conductor. An ideal arrangement would be to have the usual ground wires as near the conductors as practicable in order to limit induced voltages, and to provide an additional wire above these to receive direct strokes. This latter wire should be high enough above the ground wires to prevent any side flashes to them. Special precautions as to length of span, ground resistance, distance from conductor to ground wire, lightning rods, extra ground wires, and frequently distributed discharge devices (permitting lightning to discharge to ground but preventing the power current from following) may be necessary to assure immunity against direct strokes in badly exposed sections. A low tower is advantageous from the standpoint of direct hits because it is less likely to be struck. Induced voltages are the most probable cause of dangerous surges on moderately insulated lines, and direct strokes on highly insulated lines.

The limit of the voltage in any line is the lightning flashover voltage of the insulator. It is very important, therefore, when designing a system so to proportion the insulation that the transformer lightning breakdown voltage is higher than the lightning breakdown voltage of the line insulators in the vicinity of the station. It is obviously not good engineering to make the transformer the weakest link in the insulation chain. The insulators on the rest of the line may be as strong as desired.

The grading shield is as important to the insulator string as the ground wire is to the line. It not only reduces the maximum stress but increases the lightning spark-over voltage and causes the arc to clear the string. It also increases the energy dissipation which has the effect of increasing the spark-over voltage. The horn and similar arcing devices cannot cause the arc to clear without a serious reduction of the flashover voltage.

In addition to the above factors, the location of the line is very important. The ideal line would thus be as low in height as practicable, be protected by one or more ground wires, and be well insulated, with insulators protected by grading shields. The transformer insulation should be stronger than the bushing which in turn should be stronger than the line insulators in the immediate vicinity. By immediate vicinity it is meant that the coordinated insulation should start within 75 ft. of the apparatus and preferably extend out about  $1\frac{1}{2}$  mile. As a precaution,

extra ground wires may be added on the coordinated sections to provide against local disturbances. With extra ground wires, the lightning voltages can be reduced in proportion to the insulator strength.

As an example of a transmission line designed with the above precautionary measures in mind, consider a typical 220-kv. installation. The conductors should be arranged in the regular horizontal configuration and as low as possible, probably 40 ft. above ground. At this height, the induced lightning voltage would be  $40 \times 100 \text{ kv.} = 4,000,000$  volts (see page 263, Chap. IX) for an instantaneous cloud discharge. Under the worst conditions the time of cloud discharge would probably never be less than a microsecond so that the maximum induced voltage would probably never equal the instantaneous value of 4,000,000 volts. With one or more ground wires provided, the induced voltage would be reduced to less than one-half (see page 264, Chap. IX), or less than 2,000,000 volts. From Fig. 123, page 151, it is seen that this is less than the spark-over voltage of 14 units for typical lightning surges. Accordingly, suspension strings of 14 units would probably prove satisfactory for the usual case where direct strokes are not numerous. For greater safety, one or more units might be added to the string and the spark-over voltage raised to any value desired. Arcing rings should be provided for the protection of the insulator units. This will cause a further increase in the lightning spark-over voltage. The latter is not affected by rain, so that the curve of Fig. 123 applies under all climatic conditions. The above considerations do not include the rapid attenuation factor present with high lightning voltages (see page 281) so that the above estimates are optimistic from that standpoint.

At portions of the line, particularly exposed to direct lightning strokes, special ground wire arrangements should be made—that is, their height and number should be such as to insure their receiving all hits directed towards the lines. Their resistances to ground at each tower should be particularly low, also, being held down to several ohms if possible. Lightning rods either at the towers or alongside of the line might also be added, if they seem warranted. (See directions for installing rods to take direct strokes, Chap. IX, pages 287–294.)

Near the stations, the line insulation should be reduced below the flashover voltage of the transformer bushings, as previously

outlined. In most cases, it is probably well to add extra ground wires in this section to lower the surge impedance and, in that way, reduce the voltage in proportion to the reduction in insulation and, also, take the above precautions for direct hits if the locality is particularly exposed.

*Summary.*—The requisites for securing maximum lightning protection on a transmission line are briefly as follows:

1. The line right-of-way should be so located as to avoid lightning storm paths as much as possible.

2. All line conductors should be strung as near the ground as possible.

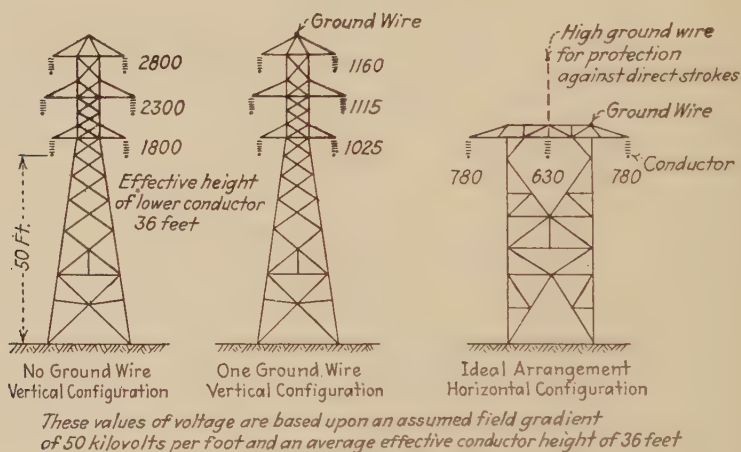


FIG. 264.—Comparison of induced lightning voltages on towers of different designs.

3. One or more overhead ground wires should be provided with as low resistance to ground as possible.

4. All insulator strings should be equipped with grading shields.

5. The line insulation near a station should be decreased, if necessary, so as to have a flashover voltage lower than that of the transformer bushings. Extra ground wires should be provided in this reduced insulation section.

6. In sections particularly exposed to lightning, extra protection from direct strokes should be provided in the form of additional, higher, and better grounded ground wires and, possibly, lightning rods, or special discharge devices frequently

distributed along the line to permit the lightning but not the power current to discharge to ground. Progress is being made in the development of such discharge devices, the nature of which will make it economically possible to arrange one on every insulator string of important lines, or on sections badly exposed to lightning storm paths.

In designing towers, the members must be so arranged that the sparkover voltage from line to tower at any point, allowing for conductor swinging, must be greater than the flashover voltage of the insulator string. The lightning sparkover voltage between metal parts should be obtained from the needle gap curve, Fig. 122, page 150, for corresponding distances. Corresponding lightning sparkover voltages for insulator strings are found on Fig. 123, page 151.

In Fig. 264 are given several designs of transmission towers and the lightning induced voltages which may appear on their conductors. It is readily apparent that the ideal arrangement shown in the figure, which is designed along the above recommendations, should suffer far less lightning trouble than the others. The proper design procedure in any case should be governed by economic as well as engineering considerations.

**Case 17. Wood Poles.**—The insulating value of a wood pole to lightning voltages has been measured up to 5,000,000 volts. The measurements show that the strength of wood poles of such varying degrees of wetness and dryness that might occur in practice, range from 100 to 300 kv. per foot. 180 kv. per foot is a good average value. Thus a pole 35 ft. high with a 5-ft. crossarm would have a lightning spark-over voltage of  $40 \times 180 = 7200$  kv. The insulator would add very little to a pole of this length. When the length of wood in series with the insulator is not over 10 ft., however, from 75 to 100 per cent. of the insulator flashover voltage may be considered as added to that of the

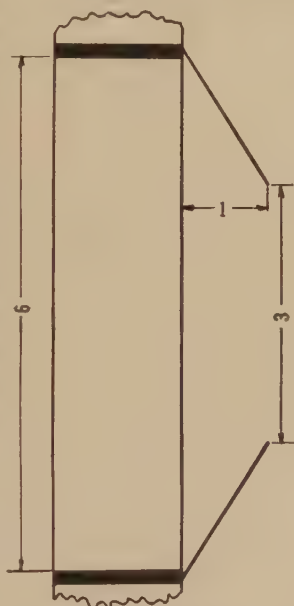


FIG. 265.—Proportions for wood-pole protective gap.

(Note discussion in text below.)



wood to comprise the total pole insulation. A practical example of this is a pole made conducting by a lightning rod to prevent splitting, with the insulation depending upon the insulator and crossarm. In a case of this kind, part of the insulation of

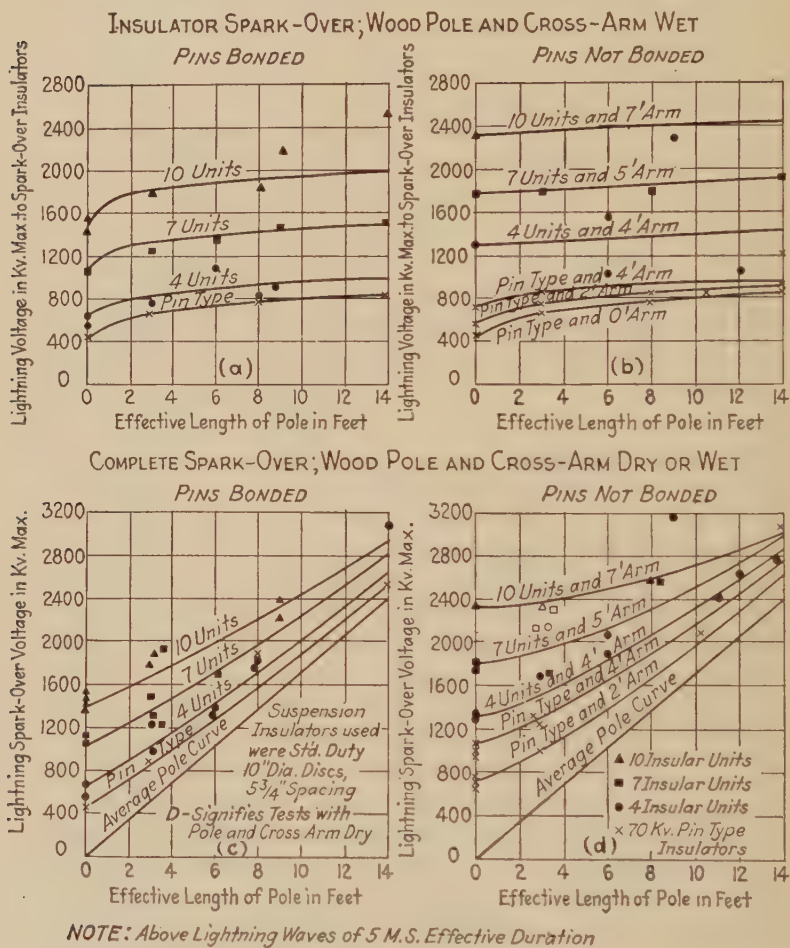


FIG. 266.— Lightning spark-over voltage for various wood-pole constructions.

the pole could be utilized and protection from splitting afforded at the same time by placing a gap in series with the lightning rod. The 6-3-1 ratio shown in Fig. 265 was found satisfactory under ideal conditions. However, for purposes of safety a 6-2-1 ratio should be used.



Whether a pole is wet or dry makes very little difference on the lightning voltage necessary to cause complete flashover to ground. When a pole is quite wet, however, incipient sparks will take place over the insulator alone. These sparks, tending to go to ground from two or more conductors, may thus cause phase-to-phase arc-overs at voltages lower than the spark-over voltage of the pole to ground. Figure 266 illustrates this. For example, Fig. 266(c) shows that the complete spark-over of a 10-unit insulator string and a 10-ft. effective pole length, (represented by the distance from a cross-arm to a ground guy wire connection) is practically 2400 kv. In Fig. 266(a) it is seen that the lightning spark-over of the ten insulators alone (i.e. with 10 ft. of wood pole still in series with the insulators but with incipient sparks over the insulators only) under the same conditions requires but 1900 kv. Accordingly, the latter lightning voltage might be sufficient for a phase-to-phase power short-circuit. To reduce this hazard the distance between conductors should be as great as practicable, the pins should not be bonded, and metal cross arms should be avoided.

While wood poles without rods or ground wires may have very high lightning spark-over voltages, there is always a danger of long outages due to split and burned poles that could not be tolerated on important lines. The porcelain insulator is more reliable. By use of gaps as illustrated above, however, part of the insulating value of the wood may be used to advantage on certain secondary lines.

**Case 18. Determination of Lightning Wave Characteristic from Insulator Sparkover.**—Assume that a 14-unit insulator string is flashed over on a line and that a surge voltage recorder at that point indicates a crest voltage value of 2,000,000 volts. Referring to Fig. 123, Page 151, it is seen that the lightning sparkover of 14 units at 2,000,000 volts requires that the lightning wave have an effective length of 5 micro-seconds. Accordingly, to simulate this sparkover in the laboratory, an impulse wave must be used whose duration above half crest voltage *up to the sparkover point* is 5 micro-seconds. The effect is the same whether the wave shape selected results in sparkover on the front or on the tail, as long as the crest value is 2,000,000 volts and the total wave duration above half voltage is 5 micro-seconds. Under these conditions, sparkover will occur on approximately 50 per cent. of the applied waves. (See Pages 142, 154, 155, and 281.)

# DATA APPENDIX

## 1. MEASURED CORONA LOSS

### Indoor Line—60-cycle

The current and watts given are measured values due to corona, divided by the total conductor length in kilometers. Corrections have been made for transformer and leads. The voltage is given to neutral. As these measurements were made on a single-phase lines, the voltages between wires were twice the value given. To obtain kilovolts per kilometer of conductor multiply amperes per kilometer by volts between lines.

CORONA LOSS—INDOOR LINE—60-CYCLE

Test 10B			Test 11B		
Eff. kv. to neutral, $e_n$	Amp. per km.	Loss kw./km., $p$	Eff. kv. to neutral, $e_n$	Amp. per km.	Loss kw./km., $p$
10.52	.....	0.07	13.7	.....	0.33
12.52	.....	0.51	16.7	.....	0.92
14.80	.....	1.40	18.1	.....	1.11
17.10	.....	3.20	19.9	0.070	1.64
18.20	.....	4.02	24.7	0.100	3.95
19.60	.....	6.83	29.3	0.150	6.90
22.30	0.225	9.44	33.2	0.189	10.40
24.90	0.310	15.03	36.3	0.223	14.20
27.20	0.395	20.63	39.7	0.268	18.75
29.70	.....	.....	44.0	0.325	26.73
28.00	0.404	22.40	47.3	0.380	34.20
25.90	0.342	16.80	50.2	.....	.....
23.60	0.263	11.80	45.2	0.350	29.20
20.80	.....	7.16	41.5	0.293	22.20
18.40	.....	4.14	37.4	0.238	15.69
16.10	.....	1.98	31.0	0.163	8.08
			27.0	0.128	5.29
			22.3	0.082	2.53

Spacing, 15.25 cm.

Radius, 0.032 cm.

Total cond. length, 0.0838 km.

$\delta = 1.02$ .

Spacing, 30.5 cm.

Radius, 0.032 cm.

Total cond. length, 0.0838 km.

$\delta = 1.02$ .

Test 13B			Test 15B		
Eff. kv. to neutral, $e_n$	Amp. per km.	Loss kw./km., $p$	Eff. kv. to neutral, $e_n$	Amp. per km.	Loss kw./km., $p$
19.5	0.051	0.96	17.3	.....	0.35
24.3	0.071	1.78	23.7	0.059	1.17
29.6	0.099	3.23	30.2	0.078	2.34
34.0	0.133	4.95	36.1	0.109	3.92
38.0	0.146	6.49	42.2	.....	5.76
43.0	.....	9.13	49.8	0.166	9.26
46.7	0.196	12.51	56.7	0.200	13.21
52.4	0.224	16.35	62.5	0.223	16.70
57.5	.....	21.00	66.5	0.246	20.00
62.5	0.285	26.25	71.4	.....	24.35
68.3	0.327	34.40	78.6	0.310	30.95
73.1	0.359	40.60	84.4	0.322	37.20
79.1	0.385	50.50	89.4	0.345	41.90
84.0	.....	59.50	95.4	.....	50.50
90.0	0.430	72.00	99.3	0.395	58.60
93.6	0.460	83.10	91.0	0.369	45.60
102.0	0.510	93.40	81.6	0.310	34.10
			67.9	.....	21.55
			52.1	0.177	10.46
			39.1	0.126	4.44
			27.0	0.068	1.74

Spacing, 61 cm.

Radius, 0.032 cm.

Total cond. length, 0.0838 km.

 $\delta = 1.03$ .

Spacing, 91.5 cm.

Radius, 0.032 cm.

Total cond. length, 0.0838 km.

 $\delta = 1.012$ .

Test 20B			Test 21B		
Eff. kv. to neutral, $e_n$	Amp. per km.	Loss kw./km., $p$	Eff. kv. to neutral, $e_n$	Amp. per km.	Loss kw./km., $p$
17.8	.....	0.21	19.8	.....	0.81
24.6	.....	1.29	24.5	.....	1.15
30.1	.....	2.17	27.2	.....	2.02
36.2	0.110	3.71	30.7	.....	2.19
42.0	0.128	5.16	34.8	.....	3.42
47.0	0.159	6.94	39.8	0.129	3.86
53.2	0.190	9.80	44.8	0.156	5.04
62.0	0.233	14.60	50.4	0.177	6.47
67.6	0.258	19.23	55.1	0.212	8.45
73.4	0.273	21.12	60.6	0.234	10.80
78.1	.....	26.70	64.6	0.246	12.40
85.2	0.346	33.10	70.0	0.266	15.10
93.2	0.385	42.70	77.9	0.310	19.30
100.2	.....	51.70	87.6	.....	26.60
87.0	0.350	35.60	94.3	.....	32.60
76.1	0.298	25.00	101.5	.....	41.00
65.2	0.250	15.95			
49.4	0.178	7.44			
40.1	0.114	4.55			

Spacing, 122 cm.

Radius, 0.032 cm.

Total cond. length, 0.0421 km.

 $\delta = 1.018$ .

Spacing, 183 cm.

Radius, 0.032 cm.

Total cond. length, 0.0342 km.

 $\delta = 1.012$ .

Test 22B			Test 24B		
Eff. kv. to neutral, $e_n$	Amp. per km.	Loss kw./km., $p$	Eff. kv. to neutral, $e_n$	Amp. per km.	Loss kw./km., $p$
20.7	.....	0.72	20.1	.....	0.24
24.5	.....	1.01	25.3	.....	0.98
27.2	.....	1.21	32.0	.....	1.84
30.9	.....	1.98	36.0	0.103	3.18
34.6	0.100	2.34	41.0	0.120	4.52
40.1	0.121	3.57	45.7	0.138	6.11
45.2	0.149	4.53	50.3	.....	8.30
50.3	0.171	5.71	57.0	0.185	11.57
55.1	.....	7.43	62.2	0.210	15.10
60.2	0.215	9.13	67.3	0.240	19.15
64.6	0.230	11.05	72.4	0.266	23.20
69.5	.....	11.99	77.5	0.290	27.50
78.5	.....	16.37	82.3	.....	32.10
87.5	0.345	23.00	87.8	.....	37.90
94.2	0.380	26.00	92.5	.....	43.80
103.2	0.417	34.50	97.3	.....	50.80
			100.5	.....	55.60
			79.0	.....	28.70
			65.0	.....	17.10
			52.7	.....	9.90

Spacing, 274.5 cm.

Radius, 0.032 cm.

Total cond. length, 0.0342 km.

 $\delta = 1.012$ .

Spacing, 91.5 cm.

Radius, 0.057 cm.

Total cond. length, 0.0818 km.

 $\delta = 1.0009$ .



Test 26B			Test 28B		
Eff. kv. to neutral, $e_n$	Amp. per km.	Loss kw./km., $p$	Eff. kv. to neutral, $e_n$	Amp. per km.	Loss kw./km., $p$
20.0	.....	0.37	10.6	.....	.....
23.2	0.053	0.98	14.2	.....	.....
29.0	.....	2.24	16.1	.....	0.18
32.8	.....	3.36	18.4	.....	0.43
37.1	0.124	5.14	20.2	.....	0.98
41.1	0.141	6.60	22.2	0.061	1.34
46.7	0.173	9.90	24.0	0.069	1.83
51.3	0.202	12.32	25.0	0.072	2.20
57.1	0.232	18.30	27.0	0.087	2.93
61.1	0.262	22.30	30.2	0.120	5.00
66.2	0.290	28.40	34.0	0.157	7.88
72.0	0.332	36.60	36.7	0.178	10.30
75.7	0.334	40.80	36.7	0.181	10.10
80.7	.....	50.50	40.7	0.212	14.80
85.0	0.413	56.50	44.5	0.265	20.30
88.7	0.431	64.00	47.1	0.298	24.80
91.0	0.464	71.40	51.7	0.369	35.20
96.5	0.515	83.40	49.6	0.342	30.80
101.0	0.562	104.00	43.0	0.251	18.20
82.8	0.396	54.50			
74.7	0.333	39.00			
69.7	.....	33.00			
60.0	0.255	22.70			

Spacing, 0.61 cm.

Radius, 0.057 cm.

Total cond. length, 0.08186 km.

 $\epsilon = 1.002$ .

Spacing, 30.5 cm.

Radius, 0.057 cm.

Total cond. length, 0.0818 km.

 $\epsilon = 0.993$ .

Test 30B			Test 32B		
Eff. kv. to neutral, $e_n$	Amp. per km.	Loss kw./km., $p$	Eff. kv. to neutral, $e_n$	Amp. per km.	Loss kw./km., $p$
21.7	.....	0.18	22.5	.....	0.21
25.6	.....	0.92	27.2	0.049	0.31
31.5	.....	2.45	32.5	0.062	1.41
36.2	.....	4.30	37.2	0.086	2.70
40.5	0.138	5.80	41.1	0.100	3.68
45.7	0.156	8.60	45.6	0.123	5.03
49.7	0.180	11.70	50.3	0.146	7.35
54.2	0.204	15.30	55.0	0.178	10.18
59.5	0.238	19.50	60.0	0.194	13.50
64.0	0.269	24.60	65.7	0.222	17.40
68.2	0.290	29.70	72.0	0.257	23.20
73.0	0.322	36.30	77.2	0.278	27.60
78.5	0.352	45.20	82.5	0.298	31.40
83.5	0.384	54.00	89.2	.....	40.00
88.2	0.441	63.00	92.2	.....	44.00
95.0	0.486	76.00	85.2	.....	35.80
96.5	0.500	81.20	70.0	.....	20.80
100.0	0.530	92.00	61.7	.....	14.32
103.0	0.600	114.30			
90.2	0.459	60.20			
79.5	0.356	45.30			
75.2	0.319	38.60			
65.5	.....	26.20			
51.7	.....	13.40			

Spacing, 61 cm.

Radius, 0.071 cm.

Total cond. length, 0.0815 km.

 $\delta = 0.98$ .

Spacing, 91.5 cm.

Radius, 0.914 cm.

Total cond. length, 0.0815 km.

 $\delta = 1.002$ .

Test 33B			Test 41B		
Eff. kv. to neutral, $e_n$	Amp. per km.	Loss kw./km., $p$	Eff. kv. to neutral, $e_n$	Amp. per km.	Loss kw./km., $p$
24.7	.....	0.31	28.3	.....	.....
29.8	.....	1.53	35.5	0.071	2.72
32.6	.....	2.45	41.0	0.108	4.90
35.6	.....	3.50	48.6	0.184	10.40
39.3	.....	4.96	53.7	0.208	13.25
43.7	.....	6.37	59.0	0.234	17.50
47.5	.....	9.57	63.8	0.265	23.40
51.5	.....	12.9	69.4	0.306	30.02
56.3	.....	15.5	73.6	0.353	35.70
60.2	.....	20.8	71.9	0.325	34.10
65.5	.....	34.8	60.1	0.244	19.85
67.0	.....	29.6	54.2	0.210	13.65
54.4	.....	15.3	59.9	0.250	19.35
			57.0	0.224	16.30
			47.0	0.161	8.87

Spacing, 61 cm.

Radius, 0.0914 cm.

Total cond. length, 0.0815 km.

 $\delta = 1.006$ .

Spacing, 61 cm.

Radius, 0.105 cm.

Total cond. length, 0.0423 km.

 $\delta = 1.001$ .

Test 45B			Test 47B		
Eff. kv. to neutral, $e_n$	Amp. per km.	Loss kw./km., $p$	Eff. kv. to neutral, $e_n$	Amp. per km.	Loss kw./km., $p$
22.3	.....	0.06	45.0	0.080	0.37
25.8	.....	0.12	50.0	0.100	0.74
29.7	.....	0.34	54.5	0.104	1.90
35.7	.....	1.41	60.5	.....	5.76
39.5	.....	2.70	65.7	0.152	9.13
44.2	.....	4.78	70.5	0.174	12.60
50.2	.....	8.10	75.5	0.205	16.30
54.0	.....	10.70	79.0	0.230	18.75
59.5	.....	14.70	87.0	.....	26.80
64.5	.....	19.50	91.7	.....	31.40
69.0	.....	24.80	96.5	.....	38.20
74.0	.....	30.10	93.5	0.321	34.10
79.7	.....	37.20	90.0	.....	29.80
82.7	.....	43.40	82.0	.....	21.70
88.7	.....	56.20	75.8	.....	16.20
98.0	.....	59.00	58.0	.....	4.22
99.7	.....	80.50	42.6	.....	0.49
103.0	.....	84.50	40.0	.....	0.24
86.7	.....	52.20			
75.5	.....	32.70			

Spacing, 61 cm.

Radius, 0.164 cm.

Total cond. length, 0.0185 km.

 $\delta = 0.996$ .

Spacing, 91.5 cm.

Radius, 0.256 cm.

Total cond. length, 0.0815 km.

 $\delta = 0.996$ .

Test 48B			Test 49B		
Eff. kv. to neutral, $e_n$	Amp. per km.	Loss kw./km., $p$	Eff. kv. to neutral, $e_n$	Amp. per km.	Loss kw./km., $p$
44.1	.....	0.61	40.5	.....	1.16
47.2	.....	1.11	44.5	.....	3.13
51.7	.....	3.87	43.0	.....	2.27
54.5	.....	5.90	46.8	.....	5.70
60.8	.....	10.60	50.6	.....	12.30
67.2	.....	17.15	55.6	.....	19.25
71.5	.....	20.70	58.8	.....	.....
75.5	.....	26.70	53.8	.....	16.05
81.7	.....	33.30	49.6	.....	9.70
76.6	.....	27.10	45.7	.....	5.27
78.5	.....	29.40	43.2	.....	2.82
74.0	.....	23.90	39.3	.....	1.23
69.5	.....	18.30			
68.0	.....	16.55			
58.2	.....	8.10			
52.7	.....	4.10			

Spacing, 61 cm.

Radius, 0.256 cm.

Total cond. length, 0.0815 km.

 $\delta = 1.00$ .

Spacing, 30.5 cm.

Radius, 0.256 cm.

Total cond. length, 0.0815 km.

 $\delta = 0.996$ .



Test 51B			Test 54B		
Eff. kv. to neutral, $e_n$	Amp. per km.	Loss kw./km., $p$	Eff. kv. to neutral, $e_n$	Amp. per km.	Loss kw./km., $p$
62.5	0.159	9.15	25.5	0.051	.....
68.0	0.190	14.55	31.8	.....	.....
72.0	0.220	20.10	37.7	.....	0.06
78.0	0.261	28.45	42.7	.....	0.30
87.3	0.318	40.20	47.1	.....	0.30
91.5	.....	49.70	57.0	.....	0.49
82.0	.....	34.60	63.2	.....	1.03
72.8	.....	22.10	69.7	.....	1.81
56.0	.....	5.65	76.5	0.152	5.08
61.5	.....	10.20	78.7	0.164	6.48
67.2	.....	15.75	84.5	0.184	12.22
70.2	.....	19.30	89.3	0.210	17.20
			95.0	0.238	23.90
			99.1	0.263	28.40
			102.2	.....	31.90
			97.2	.....	26.00
			92.0	.....	20.90
			87.0	.....	16.50
			76.7	.....	5.82
			82.0	.....	9.10
			72.1	.....	2.67

Spacing, 61 cm.

Radius, 0.333 cm.

Total cond. length, 0.0817 km.

 $\delta = 0.999$ .

All of the above tests were taken at a temperature of about 25 deg. C.

Spacing, 91.5 cm.

Radius, 0.464 cm.

Total cond. length, 0.0825 km.

 $\delta = 0.982$ .**Outdoor Line—60-cycle**

Columns 1, 2, and 3 are actual measured values and include transformer and lead losses. Column 4, the actual corona loss, for the length of line used in the test is obtained from Column 3 by subtracting transformer and lead losses.

These tests were made on comparatively long single-phase lines out of doors, and the conductor surfaces, etc., were not in as good condition as in the case of the indoor line. Transformer losses for several temperatures are given. The voltage values are effective between lines.

Test No. 146, Line A <sup>1</sup>				Test No. 18, Line A			
Kv. bet. lines	Amp.	Kw.	Kw. line loss, p	Kv. bet. lines	Amp.	Kw.	Kw. line loss, p
63.5	0.056	0.07	0.01	80.0	0.040	0.12	0.01
80.5	0.077	0.12	0.02	90.0	0.100	0.16	0.02
90.1	0.092	0.15	0.02	101.1	0.107	0.20	0.04
107.5	0.113	0.30	0.12	112.0	0.113	0.25	0.05
115.2	0.121	0.35	0.14	121.6	0.123	0.30	0.06
126.2	0.135	0.63	0.37	129.5	0.131	0.35	0.07
134.2	0.146	0.85	0.55	140.0	0.146	0.49	0.16
142.5	0.154	1.29	0.95	150.0	0.160	0.76	0.38
150.0	0.164	1.95	1.45	160.0	0.172	1.60	1.17
158.0	0.173	2.69	2.25	152.0	0.162	0.90	0.51
166.1	0.185	4.00	3.48	164.2	0.174	2.00	1.55
165.0	0.183	3.51	3.02	172.0	0.187	3.40	2.90
173.7	0.196	5.00	4.45	183.2	0.205	5.60	5.02
163.4	0.184	2.70	2.23	188.2	0.210	6.92	6.30
170.4	0.193	4.20	3.67	196.4	0.223	9.02	8.42
181.0	0.198	6.06	5.42	202.2	0.237	11.06	10.36
203.0	0.251	12.84	12.04	206.0	0.242	12.90	12.09
199.2	0.243	11.50	10.73	187.2	0.211	6.95	6.34
193.4	0.227	9.10	8.49	196.4	0.225	9.60	8.90
176.4	0.197	4.74	4.17	Total conductor length, 109,500 cm.			
165.6	0.184	2.70	2.21	Spacing, 310 cm.			
162.8	0.180	2.38	1.81	No. 3/0 7-strand hard-drawn copper-			
154.4	0.169	1.28	0.85	weathered cable, diam. 1.18 cm.			
166.0	0.176	2.94	2.45	Temperature, wet, 16 deg. C.			
184.4	0.198	6.49	5.87	dry, 18.5.			
172.0	0.193	3.85	3.31	Barometer, 75.5 cm.			
160.0	0.177	2.03	1.57	Bright sun, wind.			
146.2	0.162	0.80	0.42	Test No. 146, Line A			
138.0	0.150	0.52	0.19	Total conductor length, 109,500 cm.			
127.6	0.137	0.40	0.12	Spacing, 310 cm.			
122.5	0.129	0.33	0.08	No. 3/0 7-strand cable, dia. 1.18 cm.			
111.2	0.117	0.25	0.04	Temperature, wet, 24 deg. C.			
101.0	0.105	0.20	0.03	dry, 30 deg. C.			
				Barometer, 75.7 cm.			
				Hazy.			

<sup>1</sup>This curve was taken after the line had been standing idle over a month in the summer. The "going up" points show an excess loss due to dust and dirt on the conductor. This disappears at high voltage and does not show in the "coming down" readings.

	Test No. 102			
	Kv. bet. lines	Amp.	Kw.	Kw. line loss, <i>p</i>
	201.0	0.232	6.05	6.65
	211.0	0.277	9.10	8.63
	189.0	0.210	3.54	3.19
	181.8	0.200	2.36	2.04
	170.8	0.189	1.10	0.80
	160.0	0.176	0.60	0.36
	149.0	0.162	0.36	0.16
	201.0	0.231	6.15	5.75
	149.0	0.162	0.39	0.19
	140.5	0.150	0.29	0.12
	135.5	0.145	0.25	0.10
	124.5	0.131	0.20	0.08
	113.5	0.118	0.16	0.08
	102.3	0.103	0.13	0.07
Total conductor length, 109,500 cm.				
Spacing, 310 cm.				
No. 3/0 7-strand H. D. copper- weathered cable, diam. 1.18 cm.				
Temperature, wet, 1 dry, 1				
Barometer, 7.47 cm.				
Cloudy.				

Test No. 84, Line A				Test No. 105, Line A			
Kv. bet. lines	Amp.	Kw.	Kw. line loss, p	Kv. bet. lines	Amp.	Kw.	Kw. line loss, p
120.0	0.138	0.24	0.15	79.8	0.080	0.03	0.01
129.0	0.150	0.30	0.19	90.7	0.093	0.04	0.01
160.0	0.175	0.78	0.61	101.5	0.106	0.06	0.02
181.0	0.202	3.65	3.40	109.5	0.114	0.08	0.03
189.0	0.212	4.65	4.36	120.5	0.127	0.10	0.04
203.0	0.237	7.84	7.48	130.0	0.139	0.14	0.06
213.0	0.252	11.20	10.78	141.5	0.154	0.19	0.09
205.0	0.239	8.70	8.18	147.0	0.165	0.21	0.08
Total conductor length, 108,500 cm.				153.6	0.168	0.25	0.12
Spacing, 310 cm.				159.0	0.178	0.30	0.16
No. 3/0 7-strand cable (H. D. copper-weathered), 1.18 cm.				169.8	0.199	0.51	0.35
Temperature, wet, 1 deg. C.				174.0	0.190	0.70	0.53
dry, 3 deg. C.				181.0	0.198	1.20	1.02
Barometer, 75.2 cm.				186.2	0.204	1.74	1.55
Cloudy.				192.6	0.212	2.70	2.49
				200.6	0.221	4.00	3.77
				208.6	0.237	5.60	5.34
				216.0	0.247	7.40	7.13
				221.0	0.259	9.00	8.70
				227.0	0.271	11.00	10.66
				234.0	0.288	13.60	13.25
				189.0	0.210	2.30	2.10
				195.0	0.217	3.10	2.88
				203.8	0.229	4.96	4.72
				212.0	0.242	6.70	6.44
				219.0	0.257	8.60	8.31
Total conductor length, 109,500 cm.							
Spacing, 310 cm.							
No. 3/0 7-strand H. D. copper-weathered cable, diam. 1.18 cm.							
Temperature, wet, 13 deg. C.							
dry, 13 deg. C.							
Barometer, 76.2 cm.							
Bright sun, no wind, snow on ground.							

Test No. 100, Line B				Test No. 73, Line B			
Kv. bet. lines	Amp.	Kw.	Kw. line loss, p	Kv. bet. lines	Amp.	Kw.	Kw. line loss, p
67.0	.....	0.02	0.02	43.0	0.016	.....	.....
77.0	0.025	0.03	0.02	60.0	0.022	.....	.....
88.0	0.028	0.05	0.02	69.7	0.026	0.08	0.06
98.9	0.035	0.07	0.03	80.6	0.030	0.10	0.07
109.5	0.040	0.12	0.07	90.5	0.034	0.15	0.11
119.5	0.043	0.22	0.14	101.5	0.038	0.30	0.26
128.0	0.050	0.42	0.32	91.0	0.034	0.09	0.05
137.0	0.054	0.90	0.78	90.5	0.034	0.10	0.06
144.0	0.060	1.94	1.80	70.3	0.026	0.06	0.04
161.2	0.078	4.50	4.31	101.6	0.038	0.17	0.12
153.0	0.070	3.04	2.88	101.6	0.038	0.17	0.12
173.8	0.090	6.60	6.47	109.5	0.041	0.40	0.36
185.0	0.103	8.72	8.36	105.5	0.040	0.14	0.09
200.0	0.106	11.90	11.59	115.0	0.040	0.14	0.09
185.0	0.103	8.76	8.50	115.0	0.0425	0.88	0.82
159.0	0.078	4.10	3.92	121.5	0.048	0.16	0.09
139.0	0.058	1.22	1.10	126.5	0.053	2.00	1.93
161.2	0.080	4.70	4.51	130.5	0.055	2.48	2.40
211.8	0.135	14.80	14.46	140.5	0.064	3.70	3.61
				144.5	0.073	4.26	4.16
Total conductor length, 29,050 cm.				70.5	.....	0.03	0.00
Spacing, 91.4 cm.				91.5	0.030	0.06	0.02
0.375-in. galv. steel cable, diam.				106.0	0.038	0.18	0.13
0.953 cm.				150.0	0.078	4.80	4.69
Temperature wet, 1 deg. C.							
dry, 1 deg. C.				156.4	0.083	5.80	5.68
Barometer, 74.7 cm.				161.0	0.089	6.72	6.67
Cloudy.				166.0	0.093	7.50	7.36
				Total conductor length, 29,050 cm.			
				Spacing, 91.4 cm.			
				0.23-in. galv. steel cable, diam.			
				0.585 cm.			
				Temperature wet, 1 deg. C.			
				dry, 3 deg. C.			
				Barometer, 75.2 cm.			
				Cloudy.			



Test No. 79, Line B				Test No. 80, Line B			
Kv. bet. lines	Amp.	Kw.	Kw. line loss, p	Kv. bet. lines	Amp.	Kw.	Kw. line loss, p
213.0	0.105	8.64	8.38	81.0	0.029	0.07	0.04
205.0	0.010	7.68	7.40	91.0	0.032	0.09	0.05
202.0	0.094	7.40	7.13	100.5	0.035	0.12	0.07
186.0	0.088	6.00	5.80	110.5	0.038	0.16	0.11
181.0	0.081	5.00	4.80	120.5	0.041	0.40	0.34
168.4	0.072	3.96	3.81	130.5	0.048	1.30	1.22
159.6	0.063	3.00	2.88	139.5	0.055	2.25	2.17
150.0	0.058	2.24	2.13	153.0	0.067	3.20	3.09
138.0	0.048	1.14	1.06	160.0	0.075	4.40	4.28
120.0	0.043	0.20	0.14	172.0	0.084	5.70	5.54
120.0	.....	0.26	0.20	181.0	0.094	7.00	6.82
110.0	0.071	0.19	0.14	192.0	0.103	8.50	8.28
99.0	0.068	0.13	0.09	199.0	0.109	9.40	9.15
				213.0	0.124	11.70	11.38
Total conductor length, 29,050 cm. Spacing, 244 cm. 0.23-in. galv. steel cable, diam. 0.585 cm. Temperature, wet, 1 deg. C. dry, 3 deg. C. Barometer, 72.5 cm. Cloudy.				Total conductor length, 29,050 cm. Spacing, 152 cm. 0.23-in. galv. steel cable, diam. 0.585 cm. Temperature, wet, 1 deg. C. dry, 3 deg. C. Barometer, 72.5 cm. Cloudy.			

## CORONA LOSS—OUTDOOR LINE—60-CYCLE

Test No. 125, Line B				Test No. 126, Line B			
Kv. bet. lines	Amp.	Kw.	Kw. line loss, <i>p</i>	Kv. bet. lines	Amp.	Kw.	Kw. line loss, <i>p</i>
80.0	0.025	0.06	0.05	100.0	0.031	0.12	0.09
88.0	0.031	0.13	0.11	110.0	0.037	0.22	0.17
101.0	0.037	0.32	0.29	119.0	0.041	0.44	0.36
110.0	0.041	0.74	0.68	131.0	0.050	1.36	1.22
120.0	0.050	1.67	1.59	142.0	0.056	2.38	2.16
128.0	0.056	2.56	2.44	151.0	0.065	3.23	2.92
140.0	0.067	4.00	3.80	160.0	0.074	4.20	3.78
150.0	0.08	5.42	5.12	171.0	0.082	5.45	4.93
159.6	0.09	6.86	6.46	181.0	0.09	6.56	5.89
168.4	0.101	8.30	7.80	194.0	0.102	8.20	7.34
181.0	0.112	10.36	9.68	202.0	0.111	9.26	8.30
190.0	0.122	12.24	11.44	212.0	0.117	10.84	9.74
201.0	0.134	14.68	13.61	222.0	0.128	12.44	11.18
213.0	0.148	17.28	16.14	231.0	0.135	13.80	12.38
206.0	0.144	15.76	14.72	225.0	0.129	12.88	11.58
196.6	0.128	13.60	12.70	217.0	0.124	11.64	10.45
186.2	0.117	11.44	10.69	205.0	0.112	9.70	8.70
175.0	0.103	9.20	8.59	196.6	0.104	8.56	7.68
165.6	0.096	7.76	7.27	186.6	0.096	7.32	6.56
153.4	0.083	5.92	5.57	176.0	0.086	6.12	5.51
143.0	0.074	4.56	4.33	165.0	0.078	4.96	4.49
134.0	0.064	3.34	3.18	156.4	0.069	3.96	3.59
123.0	0.053	2.00	1.90	142.4	0.056	2.46	2.24
114.0	0.044	1.00	0.94	134.0	0.051	1.60	1.45
104.0	0.038	0.38	0.34	125.0	0.044	0.82	0.71

Total conductor length, 29,050 cm.

Spacing, 91.4 cm.

No. 4 H. D. copper wire, diam. 0.518 cm.

Temperature, wet, 5.0 deg. C.  
dry, 4.6 deg. C.

Barometer, 75.9 cm.

Cloudy, slight breeze.

Total conductor length, 29,050 cm.

Spacing, 183 cm.

No. 4 H. D. copper wire, diam.  
0.518 cm.Temperature, wet, 5.0 deg. C.  
dry, 4.5 deg. C.

Barometer, 75.9 cm.

Cloudy, slight breeze.

Test No. 137, Line B				Test No. 138, Line B			
Kv. bet. lines	Amp.	Kw.	Kw. line loss, <i>p</i>	Kv. bet. lines	Amp.	Kw.	Kw. line loss, <i>p</i>
80.0	.....	0.05	0.02	79.2	.....	0.06	0.03
90.5	0.025	0.11	0.06	91.2	0.025	0.12	0.07
100.5	0.029	0.35	0.26	99.9	0.027	0.26	0.18
110.7	0.037	0.95	0.78	111.4	0.036	0.08	0.65
121.0	0.044	1.42	1.19	120.8	0.039	1.22	1.06
131.0	0.051	2.11	1.76	121.5	0.049	1.90	1.59
141.5	0.056	2.70	2.26	141.0	0.055	2.30	2.20
150.8	0.064	3.24	2.72	149.0	0.059	2.80	2.34
161.0	0.072	4.05	3.40	161.0	0.066	3.40	2.85
172.0	0.078	4.80	4.05	171.4	0.074	4.20	3.53
183.0	0.084	5.60	4.73	181.4	0.079	4.80	4.05
196.0	0.093	6.60	5.59	192.0	0.085	5.60	4.73
205.0	0.102	7.60	6.44	202.2	0.092	6.56	5.67
202.0	0.098	7.30	6.19	214.4	0.11	7.50	6.35
186.0	0.087	6.00	5.08	197.0	0.089	6.10	5.15
165.0	0.075	4.30	3.63	174.0	0.076	4.40	3.71
145.0	0.061	2.86	2.40	153.2	0.063	3.00	2.51
124.0	0.047	1.75	1.46	134.4	0.051	2.00	1.67
103.0	0.032	0.60	0.47				

Total conductor length, 29,050 cm.

Spacing, 366 cm.

No. 8 new H. D. copper wire, diam.  
0.328 cm.

Temperature, wet, 1.5 deg. C.  
dry, 1.5 deg. C.

Barometer, 76.6 cm.

Bright sun, slight breeze.

Total conductor length, 29,050 cm.

Spacing, 488 cm.

No. 8 new H. D. copper wire, diam.  
0.328 cm.

Temperature, wet, - 1.5 deg. C.  
dry, + 1.5 deg. C.

Barometer, 75.5 cm.

Bright sun, slight breeze.

Test No. 92, Line B				Test No. 95, Line B			
Kv. bet. lines	Amp.	Kw.	Kw. line loss, <i>p</i>	Kv. bet. lines	Amp.	Kv.	Kw. line loss, <i>p</i>
27.5	0.008	.....	.....	222.0	0.115	8.80	7.00
34.5	0.009	.....	.....	199.8	0.104	6.80	5.38
39.5	0.011	.....	.....	181.0	0.089	5.36	4.24
44.5	0.013	0.02	0.01	158.0	0.076	3.80	2.98
51.0	0.015	0.05	0.04	140.0	0.064	2.84	2.24
56.5	0.017	0.10	0.09	120.0	0.053	1.92	1.44
61.5	0.019	0.22	0.20	102.0	.....	1.21	0.96
66.5	0.023	0.37	0.31	91.5	0.034	0.93	0.75
71.0	0.024	0.49	0.40	79.5	0.028	0.63	0.51
76.0	0.028	0.60	0.49	68.7	0.021	0.63	0.52
83.0	0.032	0.81	0.66	60.0	0.017	0.18	0.16
90.5	0.037	1.07	0.88	50.0	0.014	.....	.....
101.0	0.041	1.43	1.17	Total conductor length, 29,050 cm.			
110.5	0.050	1.80	1.46	Spacing, 550 cm.			
120.5	0.055	2.30	1.88	0.066 in. galv. steel wire, diam.			
131.5	0.060	2.80	2.28	168 cm.			
144.5	0.068	3.50	2.84	Temperature, wet, 1.0 deg. C.			
158.0	0.081	4.40	3.57	dry, 3.0 deg. C.			
170.0	0.086	5.30	4.33	Barometer, 75.0 cm.			
181.0	0.094	6.18	5.15	Cloudy, no wind.			
190.0	0.099	6.70	5.43				
204.0	0.110	8.00	6.50				
215.0	0.117	9.00	7.30				
222.0	0.123	9.64	7.84				
Total conductor length, 29,050 cm.							
Spacing, 410 cm.							
0.066-in. galv. steel wire, diam. 168 cm.							
Temperature, wet, 0.5 deg. C.							
dry, 2.0 deg. C.							
Barometer, 75.0							
Cloudy, no wind.							

## TRANSFORMER LOSS

Kv.	Amperes	Kw.	Kv.	Amperes	Kw.
101.5	0.008		71.5	0.005	0.02
131.5	0.010	0.15	82.0	0.006	0.03
147.3	0.011	0.25	97.0	0.007	0.05
			112.0	0.008	0.06
163.8	0.013	0.42	132.8	0.009	0.09
181.5	0.014	0.54			
201.8	0.016	0.69	149.0	0.010	0.12
			178.4	0.013	0.18
	30° C.		201.0	0.014	0.22
			223.0	0.016	0.30
				3° C.	

COMPARISON OF THREE-PHASE AND SINGLE-PHASE CORONA LOSS  
Measurements and Calculations on Experimental and Commercial Lines

THREE-PHASE CORONA LOSS ON A 683,500 CM. ALUMINUM (STEEL CORE)  
CONCENTRIC STRANDED CABLE

Long Commercial Line

61 strands

2.44 cm. diameter

Individual strands 0.268 cm. diameter

(Indoor Line)

Temperature = 11.0° C.

Barometer = 720 mm.

$m_0 = 0.90$

Conductors in same

Elevation approximately 450 m.

horizontal plane—

(Air density)  $\delta = 0.994$

$f = 50$  cycles

Spacing = 5.80 m.

(factor)

Height (at towers) =

11.3 m.

Kv. (eff.) between lines	Kv. (eff.) to neutral	Three-phase corona loss in kw. per km.	
		Measurements	Calculation
274	158	10.9	11.0
269	156	8.0	8.0
256	148	3.4	2.6
242	140	1.7	0.1
230	133	0.1	0
216	125	0.6	0
201	116	0	0



At  $\delta = 1.00$   $e_0 = 139$  kv. to neutral

$p = 0.0262(e - 139)^2$  kw. per kilometer

Measurements on 31.4 kilometer section of commercial line of Southern California Edison Co.

WOOD, R. J. C., *Elec. World*, p. 277, Feb. 11, 1922.

———, *Elec. World*, p. 882, May 6, 1922.

———, *Jour., A.I.E.E.*, Vol. XLI, p. 471, 1922.

THREE-PHASE CORONA LOSS TEST ON A 163.5 KILOMETER COMMERCIAL LINE  
110,000 Circular Mil Copper Cable

7 strands

$r = 0.48$  cm.

Elevation (approx.) = 230 meters

Conductor in same vertical plane.

Temperature =  $5^\circ$  C.

Spacing = 3.66 m.

Barometer = 745 mm.

Height (lowest conductor) = 8 to 12 m.

Weather = Cloudy

Transformer connection:

$f = 30$  cycles

Line normally operated at 140 kv.

Delta-Wye.

Kilovolts (effective) between lines			3-phase corona loss in kw./km.	
Sending end	Receiving end	Average kv. (eff.)	Measured	Calculated
102.0	97.8	99.9	0	0
112.0	109.8	110.9	0.012	0.018
122.1	121.1	121.6	0.14	0.66
132.5	132.5	132.5	0.55	2.28
142.5	143.9	143.2	3.42	4.76
152.7	155.1	153.9	8.50	8.24
163.2	166.2	164.7	14.3	12.7
173.5	177.3	175.4	20.6	18.1
183.8	188.1	186.0	27.3	24.3
194.1	199.0	196.6	34.5	31.4
204.1	209.5	206.8	41.0	37.7
214.8	220.0	217.4	47.6	48.0
225.0	229.8	227.4	54.0	57.4

Calculated  $e_0 = 108.9$  kv. effective between lines

$e = 149.3$  kv.

Measurements on 30-cycle, 140,000-volt line of the Consumers Power Company. (LEWIS, W. W., *Trans. A.I.E.E.*, Vol. XL, p. 1079, 1921.)

COMPARISON OF THREE-PHASE AND SINGLE-PHASE CORONA LOSS ON A  
600,000 CIRCULAR MIL CONCENTRIC STRANDED CABLE

61 strands  
 $r = 1.13$  cm.

(Indoor Line)

New conductor,  $m_o = 0.81$      $\delta = 0.974$     Conductors in same horizontal  
 Fair weather,  $m_s = 1.00$     60 cycles    plane. Spacing = 3.90 m.  
 Height = 7.5 m.

Length of each conductor (approximately) = 30 m.

Three-phase corona loss				Single-phase corona loss			
Kv (eff) be- tween lines	Kv. (eff) to neutral	Kw./km. three phase	Kw./km. per con- ductor	Kv. (eff.) between lines	Kv. (eff.) to neutral	Kw./km. single- phase	Kw./km. per con- ductor
272	157	79.5	26.5	314	157	52.7	26.4
257	149	56.4	18.8	298	149	35.8	17.9
242	140	35.1	11.7	282	141	23.0	11.5
233	135	25.0	8.3	270	135	16.4	8.2
220	127	17.1	5.7	257	128	12.1	6.0
207	120	10.8	3.6	240	120	8.8	4.4
198	115	8.5	2.8	228	114	6.2	3.1
189	109	5.0	1.7	215	108	4.1	2.0

NOTE.—Excess loss at low voltages partly due to rough new conductors.

## 2. DIRECT-CURRENT TESTS

(Tests from Peek, A.I.E.E., June, 1916, unless otherwise noted)

## Spark-over and Corona in Air

**Sphere Gaps.**—The direct-current voltage required to spark-over a given spacing is the same as the maximum alternating current.

TABLE I.—A.C. AND D.C. SPARK-OVER VOLTAGES OF 20 NEEDLES IN AIR

Spacing, cm.	Kilovolts 60 cycle (max.)	Kilovolts d.c.
5.1	51.0	52.0
7.6	62.5	63.0
10.2	76.5	73.5
12.7	88.3	82.5
15.3	98.3	90.5

$\delta = 0.98$

Hum. = 34 per cent.

TABLE II.—D.C. AND A.C. VISUAL CORONA AND SPARK-OVER VOLTAGES  
(Concentric Cylinders—Normal Air Density  $\delta = 1$ )

R radius outer cylinder, cm.	r wire radius, cm.	R/r	Corona				Spark-over			
			60 cycle calc. kv. (max.)	D.c. + kv.	D.c. — kv.	A.c. $\rho_{max}$ kv./cm.	D.c. $\rho_v$ kv./cm.	60 cy. kv. max.	D.c. + kv.	D.c. — kv.
3.81	0.0038	1000.0	4.9	6.4	6.4	186.0	244.0	....	Vibrates be-	
3.81	0.0129	295.0	8.4	8.4	8.3	113.0	113.0	70.0	fore sparkover	
3.81	0.0573	66.5	17.2	17.2	17.2	71.5	71.5	40.0	52.8	61.0
3.81	0.130	29.3	25.2	25.2	25.2	56.9	56.9	25.5	48.8	54.5
3.81	0.239	16.0	33.5	31.8	33.8	51.0	51.3	33.9	47.5	52.8
3.81	0.635	6.0	48.9	49.0	49.0	42.9	43.0	48.1	49.5	53.2
3.81	1.110	3.4	54.7	54.8	54.8	40.5	40.6	54.5	54.5	55.5

TABLE III.—D.C. AND A.C. VISUAL CORONA VOLTAGES  
(Concentric Cylinders at Various Air Densities)

R radius outer cylinder cm.	r radius wire cm.	R/r	$\delta$	A.c. calc. 60 cy. kv. (max.)	D.c. + kv.	D.c. — kv.	A.c. calc. $\rho_v$ (max.)	D.c. $\rho_v$ + kv./cm.	D.c. $\rho_v$ — kv./cm.
2.90	0.239	12.1	1.00	30.0	30.0	30.0	50.5	50.5	50.5
2.90	0.239	12.1	0.915	28.0	27.8	27.8	47.0	46.8	46.8
2.90	0.239	12.1	0.857	26.3	....	26.2	44.2	....	44.0
2.90	0.239	12.1	0.824	25.7	25.5	....	43.3	42.9	....
2.90	0.239	12.1	0.797	25.1	....	25.1	42.2	....	42.2
2.90	0.239	12.1	0.720	23.1	23.1	....	38.8	38.8	....
2.90	0.239	12.1	0.680	22.1	....	22.1	37.1	37.1	....
2.90	0.239	12.1	0.550	19.1	19.2	19.3	32.1	32.2	32.4
2.90	0.239	12.1	0.435	15.7	15.7	16.0	26.4	26.4	26.9
2.90	0.239	12.1	0.357	13.5	13.5	....	22.7	22.7	....
2.90	0.239	12.1	0.260	10.7	10.9	11.6	18.0	18.4	19.5
2.90	0.239	12.1	0.082	4.8	4.4	4.6	8.07	7.4	7.75

TABLE IV.—COMPARISON OF RESULTS<sup>1</sup>  
Critical Surface Intensity: Kilovolts per Centimeter

Alternating current				Continuous current			
Diam. wire, cm.	White- head	Peek	White- head & Brown	White- head & Brown +	Farwell +	White- head & Brown —	Farwell —
0.074	81.2	80.7	80.3	76.0	75.7	80.8	76.9
0.090	76.6	76.0	76.0	71.9	71.6	76.1	72.0
0.107	72.9	72.3	72.5	68.9	68.3	72.4	69.8
0.125	69.9	69.2	69.6	66.2	65.5	69.3	67.2
0.166	64.8	64.1	64.8	61.9	61.1	64.2	62.9
0.231	59.9	59.1	60.1	57.6	56.6	59.1	58.7

<sup>1</sup>Whitehead, A.I.E.E., Feb., 1917. See also Whitehead, A.I.E.E., June, 1920.

TABLE V.—D.C. SPARK-OVER OF PIN TYPE PEDESTAL INSULATORS

Insulator number	60-cycle spark-over kv. max.	D.c. spark-over—kv.	
		Top +	Top —
1	191	154	230
2	226	230	.....
3	283	260	.....
4	212	200	229

#### D.c. Spark-over in Oil

TABLE VI.—D.C. AND A.C. SPARK-OVER TESTS ON 2/0 NEEDLES IN No. 8  
TRANSIL OIL AT 25 DEG. C.

Needle gap, cm.	60 cycle kv. (max.)	D.c. kv. (max.)
0.317	21.2	21.7
0.635	34.7	33.5
1.27	50.5	50.2
1.91	65.0	66.0
2.54	86.5	82.5

#### D.c. Strength of Solid Insulation

TABLE VII.—VARIATION OF 60 CYCLE PUNCTURE VOLTAGE WITH TIME OF APPLICATION ON VARNISHED CAMBRIC

Tests Between 2.5-in. Plates, 1¼-in. Radius Edge, in No. 6 Transil Oil

Temperature, deg. C.	Sheets	Thickness, mm.	kv. (max.)	Time, sec.
25	1	0.30 (12 mils)	24.8	2.3
			21.3	12.0
			19.5	17.3
			17.7	41.5
			15.9	198.0
			14.2	900.0
100	1	0.30	14.5	2.0
			13.2	7.0
			12.6	11.0
			12.0	25.0
			10.8	620.0
			9.9	1400.0
25	2	0.60	29.8	213.0
			26.7	700.0
			25.6	1418.0
25	3	0.90	53.0	8.0
			45.2	51.5
			42.5	80.0
			41.7	138.0
			38.9	370.0
			37.1	905.0
25	4	1.20	69.3	4.0
			65.0	13.0
			64.3	15.0
			55.8	39.0
			53.0	80.0
			50.8	155.0
			47.3	580.0



TABLE VIII.—VARIATION OF D.C. PUNCTURE VOLTAGE WITH TIME OF APPLICATION ON VARNISHED CAMBRIC

Tests Between 2.5-in. Plates,  $1\frac{1}{4}$ -in. Radius Edge, in No. 6 Transil Oil

Temperature, deg. C.	Sheet	Thickness, mm.	kv. (max.)	Time, sec.
25	1	0.30	28.8	8.3
			27.2	20.0
			25.5	54.0
			23.8	94.0
			22.1	363.0
			20.4	668.0
			18.8	5400.0
100	1	0.30	21.0	1.5
			20.3	2.0
			19.6	38.0
			18.6	72.0
			17.0	600.0
			15.9	470.0
			15.2	1920.0
25	2	0.60	52.5	26.0
			50.0	50.0
			47.0	230.0
25	3	0.90	80.3	68.0
			77.5	130.0
			77.2	350.0
			75.5	1400.0
25	4	1.20	127.2	7.0
			120.0	16.0
			115.2	45.0
			110.0	100.0
			107.5	185.0
			105.0	330.0
			104.6	730.0

TABLE IX.—A.C. AND D.C. PUNCTURE VOLTAGES OF VARNISHED CAMBRIC FOR VARIOUS THICKNESSES AND TIME OF APPLICATION

Time of application, seconds		$\infty$	100	50	10	2
Sheets	Thickness, mm.	Kilovolts to puncture (max.)				
1	0.30 a.c.	11.0	16.5	17.5	20.5	25.5
	0.30 d.c.	18.0	23.5	24.5	27.5	32.5
2	0.60 a.c.	20.0	31.0	33.0	39.0	47.0
	0.60 d.c.	43.0	49.5	51.0	55.5	62.5
3	0.90 a.c.	30.0	42.0	45.0	52.0	62.0
	0.90 d.c.	70.0	79.0	81.0	86.0	95.0
4	1.20 a.c.	37.0	52.0	55.0	64.0	78.0
	1.20 d.c.	96.0	111.0	114.0	123.0	137.0

## Gradient Kv. per Mm. (Max.)

1	0.30 a.c.	36.6	55.0	58.5	68.5	85.0
	0.30 d.c.	60.0	75.0	82.0	92.0	108.0
2	0.60 a.c.	33.3	51.5	55.0	65.0	78.0
	0.60 d.c.	72.0	82.0	85.0	92.0	104.0
3	0.90 a.c.	33.3	46.5	50.0	57.9	69.0
	0.90 d.c.	77.5	87.5	90.0	95.5	105.0
4	1.20 a.c.	30.9	43.3	45.8	53.2	65.0
	1.20 d.c.	80.0	92.5	95.0	102.0	106.0

## 3. STRENGTH OF AIR FILMS

CORONA TESTS ON AIR FILMS BETWEEN TWO GLASS PLATES  
(60 ~.—Glass Plate on Each Electrode)

Thickness, cm.		Per- mittivity	$\delta$	Corona starting voltage maxi- mum	Strength of air films kv./cm. max. reduced to $\delta = 1$		Temp. deg. C. $t$	Bar pressure $b$ cm.
Air space	Both glass plates				$E_a$	$g_a$		
0.0025	0.910			7.2	0.96	21,100	161.0	196.0
0.0053	0.910	7.2	0.96	17,400	137.0	139.0	285	73.6
0.0120	0.910	7.2	0.96	10,600	88.0	95.0	285	73.6
0.028	0.910	7.2	0.96	9,350	63.0	59.0	285	73.6
0.0562	0.910	7.2	0.96	9,050	53.0	50.6	285	73.6
0.122	0.910	7.2	0.96	10,700	44.5	44.5	285	73.6
0.275	0.910	7.2	0.96	14,300	36.8	39.3	285	73.6
0.455	0.910	7.2	0.96	19,100	35.6	36.8	285	73.6
0.0051	0.910	9.3	0.74	7,660	101.0	143.0	114	72.9
0.0122	0.910	9.3	0.74	7,050	96.5	95.0	114	72.9
0.0260	0.910	9.5	0.73	5,180	58.5	59.6	120	72.9
0.0560	0.900	9.4	0.73	5,890	53.0	50.6	116	72.5
0.120	0.900	9.4	0.73	6,670	42.4	44.4	117	
0.275	0.900	9.3	0.73	10,100	37.3	39.0	114	72.5
0.455	0.900	9.3	0.73	14,160	35.1	36.8	116	72.5

## Corona on Air Films Between Tape Insulated Conductors

0.635	0.645	3.2	0.95	26,900	34.0	35.1	25	72.8
0.630	0.645	3.5	0.75	33,400	36.2	35.1	107	72.8

 $g_a$  = strength of entrapped film. $g_s$  = strength of film between metal spheres.

See Dubsy, Dielectric Strength of Air Films Entrapped in Solid Insulation, A.I.E.E. Feb., 1914.

## SPARK-OVER OF GAPS AT SMALL SPACINGS AND VARIOUS AIR DENSITIES

Spark-over, volts (Max.)	$px$	$\delta x$
	0.010	0.000132
1050	0.015	0.000197
640	0.020	0.000264
400	0.030	0.000394
355	0.040	0.000526
350	0.050	0.000660
395	0.100	0.001320
550	0.300	0.003950
700	0.500	0.00660
850	0.700	0.00920
1030	0.965	0.01270
1700	1.930	0.02540
2200	2.900	0.03820
2700	3.860	0.05100
3750	5.800	0.07650
4680	7.740	0.1020
5600	9.660	0.1270
6530	11.600	0.1520
7370	13.520	0.1770
8210	15.450	0.2010

$x$  = spacing, cm.

$p$  = pressure, cm.

$\delta$  = relative air density.

Paschen's Law: To find spark-over voltage multiply pressure or density by spacing and find corresponding  $E_{max}$ .

#### 4. THE EFFECT OF TRANSIENT, IMPULSE, OR LIGHTNING VOLTAGES ON AIR, OIL, AND SOLID INSULATION

The following tests were made by means of the original impulse generator.<sup>1</sup> Unless otherwise noted, the impulses correspond to *single* half cycles of sine waves of the indicated frequency. The time of application is, therefore, generally not more than a few microseconds<sup>1</sup> (millionths of a second).

##### Wave Shape

TABLE I.—IMPULSE SPARK-OVER VOLTAGES OF NEEDLES AND SPHERES  
(Effect of Wave Shape)

Needle gap				Sphere gap (25 cm. spheres)			
Spacing, cm.	Continuously applied (60 ~) spark-over kv. (max.)	Impulse spark-over kv. (max.)	Imp. ratio	Spacing, cm.	Continuously applied (60 ~) spark-over kv. (max.)	Impulse spark-over kv. (max.)	Imp. ratio
Wave No. 1 (Sine Shape)							
2.30	26.5	36.5	1.34	1.15	35.5	35.5	1.00
3.50	38.0	60.0	1.58	2.00	59.0	60.0	1.02
4.50	45.0	77.2	1.71	2.60	75.0	77.2	1.03
5.10	49.1	91.0	1.86	3.00	87.0	90.0	1.05
5.40	51.2	102.0	1.99				
6.10	56.2	113.0	2.00				
6.70	59.0	119.0	2.02				

$R = 520$  ohms

$C = 0.0005 \times 10^{-6}$  farads

$L = 0.312 \times 10^{-3}$  henrys

Wave No. 4							
8.80	70.5	81.5	1.16	2.60	80.0	81.5	1.02
12.50	87.5	105.0	1.20	3.50	103.0	105.0	1.02
21.00	127.0	145.0	1.14	5.40	145.0	145.0	1.00
23.80	141.0	163.0	1.16	6.50	159.0	163.0	1.02
26.40	152.0	180.0	1.18				
30.50	171.0	207.0	1.21				

$R = 6800$

$C = 0.004 \times 10^{-6}$  farads

$L = 0.604 \times 10^{-3}$  henrys

Wave No. 1							
Time, microseconds.....	0.0	0.1	0.2	0.5	1.0	1.5	4.0
Per cent. max. kv.....	0	52	75	100	48	-10	0

Wave No. 4							
Time, microseconds.....	0.0	0.1	0.2	0.5	1.0	1.5	4.0
Per cent. max. kv.....	0	52	75	100	98	96	88

Wave No. 1 approximately half cycle sine wave.

$R$ ,  $L$  and  $C$  constants of impulse circuit.

<sup>1</sup> PEEK, "The Effect of Transient Voltages on Dielectrics," *Trans A.I.E.E.*, p. 1857, 1915.



## Time Lag—Frequency

TABLE II.—VARIATION OF SPARK-OVER VOLTAGES OF SPHERES AND NEEDLES FOR SINGLE HALF CYCLES OF SINE WAVES CORRESPONDING TO DIFFERENT FREQUENCIES

Needles				Spheres 25 cm.			
Spacing, cm.	60 ~ spark- over kv. (max.)	Impulse spark- over kv. (max.)	Impulse ratio	Spacing, cm.	60 ~ spark- over kv. (max.)	Impulse spark- over (max.)	Impulse ratio
55 Kilocycles							
3.50	38.0	38.0	1.00	1.25	38.0	38.0	1.00
5.10	49.4	49.4	1.00	1.65	49.4	49.4	1.00
7.00	59.2	59.2	1.00	2.00	59.2	59.2	1.00
8.50	69.0	69.0	1.00	2.35	69.0	69.0	1.00
9.60	75.0	76.0	1.01	2.60	76.0	76.0	1.00
10.60	79.0	84.0	1.06	2.90	83.5	84.0	1.00
11.30	83.0	91.0	1.09	3.10	90.5	91.0	1.00
12.50	88.5	97.0	1.10	3.40	97.5	97.0	1.00
13.70	94.5	106.0	1.12	3.70	104.0	106.0	1.02
$R = 700 \text{ ohms}$		$L = 3.17 \times 10^{-3} \text{ henrys}$		$C = 0.004 \times 10^{-6} \text{ farads}$			
100 Kilocycles							
2.70	31.8	35.4	1.10	....	....	....	....
6.50	58.0	65.0	1.13	....	....	....	....
9.0	71.5	89.0	1.26	....	....	....	....
11.4	83.5	110.0	1.32	....	....	....	....
13.6	93.0	127.0	1.36	....	....	....	....
....	....	....	....	....	....	....	....
$R = 2980 \text{ ohms}$		$L = 2.50 \times 10^{-3} \text{ henrys}$		$C = 0.001 \times 10^{-6} \text{ farads}$			
350 Kilocycles							
				12.5 cm. Spheres			
2.20	26.1	32.6	1.25	1.05	33.0	32.6	0.99
3.20	35.2	50.2	1.42	1.65	49.4	50.2	1.02
4.30	44.4	67.0	1.51	2.30	65.6	67.0	1.02
5.85	55.0	83.5	1.52	2.90	81.0	83.5	1.03
7.00	61.2	100.0	1.63	3.45	95.0	100.0	1.05
8.60	69.5	117.0	1.68	4.25	113.0	117.0	1.05
9.85	76.0	134.0	1.76	....	....	....	....
$R = 430 \text{ ohms}$		$L = 0.312 \times 10^{-3} \text{ henrys}$		$C = 0.001 \times 10^{-6} \text{ farads}$			
900 Kilocycles							
1.65	9.2	14.2	1.52	0.40	14.1	14.1	1.00
1.20	15.2	28.3	1.86	0.90	28.2	28.2	1.00
1.80	21.6	42.3	1.91	1.40	42.3	42.3	1.00
2.60	29.7	56.5	1.92	1.90	55.0	56.5	1.02
3.10	33.9	70.7	2.08	2.40	68.0	70.5	1.03
3.60	38.9	84.7	2.18	2.90	82.0	84.5	1.03
4.00	42.3	99.0	2.34	3.50	95.0	98.5	1.04
....	....	....	....	3.70	100.0	106.0	1.06
$R = 400 \text{ ohms}$		$L = 0.166 \times 10^{-3} \text{ henrys}$		$C = 0.00025 \times 10^{-6} \text{ farads}$			

The above waves are single half cycles of sine waves of the frequency indicated.

## Corona

TABLE III.—TRANSIENT CORONA  
(Single Half Sine Wave)

Concentric Cylinders in Air

Bar = 76 cm.

 $t = 25$  deg. C. $\delta = 1$ Outer Cyl. rad.  $R = 8.8$  cm.

Wire radius $r$ cm.	60 ~ tests			Impulse tests			
	Calc. corona kv. (max.)	Test corona kv. (max.)	Test spark- over kv. (max.)	Corona		Spark- over kv. (max.) 1 in 10	Single half sine wave frequency kilocycles
				A kv. (max.)	B kv. (max.)		
0.0318	.....	13.4	135.0	13.8	15.6	100.0	100
				14.7	16.0	.....	500
				15.1	16.1	.....	900
0.0573	20.5	20.0	110.0	21.2	23.7	100.0	100
				22.0	24.0	.....	500
				22.6	24.0	.....	900
0.130	31.4	31.3	49.6	32.3	33.2	103.0	100
				33.5	34.0	.....	500
				34.2	34.8	.....	900
0.95	86.0	85.0	86.0	85.0	86.0	108.0	100
				87.0	87.5	.....	500
				87.5	88.0	.....	900
1.425	100.0	98.0	98.0	99.0	99.0	110.0	100
				99.0	99.5	.....	500
				100.0	101.0	.....	900

Bar = 76 cm.

 $t = 25$  deg. C. $\delta = 1$  $R = 3.81$  cm.

0.0129	5.7	....	....	8.5	.....	32.0	100
				9.2	.....	68.0	500
				9.5	.....	.....	900
0.0318	12.3	12.0	49.0	13.4	14.7	33.0	100
				13.5	14.7	67.5	500
				14.5	15.0	.....	900
0.0573	17.2	....	40.0	17.4	18.2	35.0	100
				20.0	20.5	66.0	500
				24.0	24.7	.....	900
0.239	33.5	....	33.9	33.4	37.1	44.7	100
				37.0	38.9	63.7	500
					37.0	103.0	900
0.318	38.0	37.9	37.9	38.5	39.0	45.0	100
				39.5	40.0	64.0	500
				41.6	42.0	98.0	900
0.635	49.0	48.1	48.1	49.0	49.7	50.0	100
				50.0	50.5	62.0	500
				51.6	52.0	81.0	900
1.27	55.0	55.0	54.5	55.0	55.0	55.0	100
				56.0	56.0	57.0	500
				56.0	56.0	59.3	900

Comparison of 60 ~ and transient corona for different sizes of wire in center of a cylinder. The voltage at which transient corona first appeared is given in col. A. Corona appeared on every application for voltages given in col. B. The difference is probably for positive and negative wire.

## Air Density

TABLE IV.—EFFECT OF AIR DENSITY ON TRANSIENT CORONA AND SPARK-OVER

Concentric Cylinders<sup>1</sup>

Outer cylinder radius, $R = 3.08$ . Inner cylinder, $r = 0.0573$ cm.									
Corona					Spark-over				
Meas. 60 ~ kv. max.	Cal. 60 ~ kv. max.	Impulse kv. max.	Impulse ratio	$\delta$	60 ~ kv. max.	Impulse kv. max.	Impulse ratio	$\delta$	Single half sine freq. kilo- cycles
2.8	2.75	3.5	1.27	0.064	....	10.7	....	0.064	100
4.8	4.80	5.5	1.15	0.160	7.0	13.0	1.86	0.160	100
6.0	5.95	6.65	1.13	0.248	9.3	15.5	1.67	0.248	100
7.6	7.57	8.4	1.10	0.330	11.0	17.5	1.59	0.330	100
11.6	11.60	12.7	1.09	0.630	16.6	27.3	1.65	0.630	100
14.4	14.40	15.5	1.07	0.847	20.2	30.2	1.50	0.847	100
16.2	16.20	17.2	1.06	1.00	22.5	31.9	1.42	1.000	100
2.6	2.58	4.0	1.55	0.051	....	28.5	....	0.040	900
4.8	4.86	6.5	1.34	0.166	5.0	31.0	6.2	0.085	900
7.6	7.60	10.1	1.32	0.333	7.5	37.0	4.94	0.173	900
9.5	9.50	12.1	1.28	0.465	13.3	47.0	3.54	0.440	900
13.5	13.30	16.3	1.23	0.765	15.8	53.0	3.35	0.590	900
16.2	16.20	20.0	1.23	1.00	18.8	60.0	3.19	0.765	900
....	.....	....	....	.....	22.5	67.5	3.00	1.00	900
Outer Cylinder Radius, $R = 3.08$ cm. Inner Cylinder, $r = 0.635$ cm.									
7.3	7.7	8.5	1.16	0.127	7.3	8.5	1.16	0.127	100
13.0	13.0	14.9	1.14	0.253	13.0	14.9	1.14	0.253	100
15.0	15.3	16.6	1.11	0.309	15.0	16.6	1.11	0.309	100
17.0	16.8	18.3	1.08	0.350	17.0	18.3	1.08	0.350	100
24.0	23.8	24.5	1.02	0.535	24.0	24.5	1.02	0.535	100
29.0	29.0	28.9	1.00	0.702	29.0	28.9	1.00	0.702	100
34.5	35.5	34.5	1.00	0.863	34.5	34.5	1.00	0.863	100
39.0	40.3	40.5	1.03	1.002	39.0	40.5	1.03	1.002	100
Outer Cylinder Radius, $R = 3.08$ cm. Inner Cylinder, $r = 0.635$ cm.									
3.5	3.9	8.6	2.46	0.049	3.5	20.3	5.80	0.049	900
9.0	9.8	11.9	1.31	0.165	9.0	25.0	2.78	0.165	900
14.0	14.1	17.3	1.23	0.280	14.0	30.5	2.18	0.280	900
21.2	21.2	22.5	1.07	0.462	21.3	37.6	1.77	0.462	900
26.2	26.3	28.0	1.06	0.604	26.0	43.5	1.67	0.604	900
32.0	32.2	35.6	1.01	0.773	32.0	48.5	1.52	0.773	900
39.0	40.3	40.2	1.00	1.00	39.0	52.5	1.34	1.00	900

<sup>1</sup> Tests above made in a metal lined glass tube.

## Polarity

TABLE V.—POSITIVE AND NEGATIVE SPARK-OVER  
(Dissimilar Electrodes)

Wire in Cylinder			$R = 3.81$ cm.
Radius, cm.	Voltage kv.		Per cent. difference
	wire		
	+	-	
1.27	57.0	57.0	0
0.187	51.0	58.5	15
0.0318	49.8	60.6	22

## Point and plate

Spacing cm. for a given applied voltage when point is	
+	-
5.15	3.05

Approx.—500 kilocycle wave.

## Air Films

TABLE VI.—TRANSIENT SPARK-OVER VOLTAGES AT SMALL SPACINGS  
(Between 6.25 cm. Diameter Spheres.  $\delta = 1$ )

Spacing, cm.	60 ~		100 kc. impulse			900 kc. impulse		
	Spark-over		Volts kv.	Gradi- ent kv. per cm.	Impulse ratio	Volts kv.	Gradi- ent kv. per cm.	Impulse ratio
	Volts max. kv.	Gradi- ent max. kv. per cm.						
0.0025	0.50	196	0.78	305.0	1.57	0.81	325.0	1.64
0.0051	0.73	143	1.23	242.0	1.69	1.10	216.0	1.51
0.0076	0.90	118	1.70	212.0	1.80	1.78	235.0	1.98
0.0102	1.07	105	2.11	207.0	1.98	2.18	215.0	2.04
0.0127	1.17	92	2.44	192.0	2.08	2.55	200.0	2.18
0.025	1.52	60	4.50	178.0	2.95	5.00	198.0	3.04
0.051	2.62	52	6.15	122.0	2.35	8.50	168.0	3.25
0.102	4.62	46	8.75	87.0	1.90	12.80	126.0	2.77
0.25	9.77	40	14.90	61.0	1.52	21.50	84.1	2.20
0.51	17.50	36	22.50	46.0	1.28	28.50	56.0	1.63
1.27	39.20	35	42.00	37.0	1.06	47.00	37.0	1.20
1.90	57.50	35	57.50	35.0	1.00	62.50	36.0	1.09
2.54	88.50	35	88.50	35.0	1.00	90.00	35.0	1.02

Accuracy of impulse voltages best above 5 kv.

## Insulators

TABLE VII.—EFFECT OF POLARITY ON INSULATOR SPARK-OVERS  
200 kc.

60 ~ spark-over kv., max.	Impulse spark-over kv. varying polarity, max.		Impulse spark-over kv. predetermined polarity, max.	
	Pin type insulators (max. gradient on cap)		Cap +	Cap -
98	1 spark-over in 10 impulses.	108	108	
	10 spark-overs in 10 impulses.	130	...	134

TABLE VIII.—EFFECT OF DIFFERENT WAVE SHAPES ON TIME LAG OF  
IMPULSE SPARK-OVERS OF INSULATOR (5 $\frac{3}{4}$ -IN. SPACING - 10-IN.  
DIAMETER CAP AND PIN SUSPENSION INSULATORS)

Number of insulator units	Complete wave front (micro-seconds)	Length wave tail to 50 per cent. crest value (micro-seconds)	Average time lag (micro-seconds)	Spark-over (kv. crest)	60-cycle spark-over (kv. crest)	Impulse ratio
3	1	60	5	329	297	1.11
3	1	60	1.5	368	297	1.24
2	1	60	4	233	214	1.08
3	0.5	60	5	399	297	1.35
3	0.5	60	2	441	297	1.49
2	0.5	60	4.5	277	214	1.29
3	0.25	20	4.7	416	297	1.40
2	0.25	20	4.6	298	214	1.39
3	0.25	5	4.4	457	297	1.54
2	0.25	5	4.3	316	214	1.48



TABLE IX.—EFFECT OF SERIES RESISTANCE  
Effect of Resistance on Impulses Spark-over of Sphere Gap

Applied impulse, voltage to spark- over	Series resistance	12.5 sphere gap cm. setting kv. max.	60-cycle voltage to cause spark-over kv. max.
106	0	3.95	106.0
106	2,500	3.60	98.5
106	5,000	3.30	92
106	10,000	2.80	80.0
106	20,000	2.30	66.0
106	30,000	2.05	59.1

IMPULSE SPARK-OVER VOLTAGE INSULATOR IN SERIES WITH RESISTANCE

Series resistance, ohms	60-cycle spark-over kv. max.	Impulse spark-over kv. max.
0	119.0	127.0
5,000	119.0	190.0
10,000	119.0	235.0
20,000	119.0	320.0
30,000	119.0	420.0
50,000	119.0	600.0

TABLE X.—DISRUPTIVE STRENGTH OF WATER  
 Impulse Disruptive Strength of Water  
 2.54-cm. spheres

Gap, centimeters	Impulse kv. max. water	Impulse kv. max. air	Ratio
0.1	49.5	3.5	14.1
0.2	86.0	7.0	12.3
0.3	105.5	11.0	9.6
0.5	126.0	17.5	7.2
0.7	137.0	24.0	5.7
1.0	149.0	33.0	4.5
1.3	159.0	42.0	3.8
1.5	165.0	46.0	3.6

Resistance 20,000.

60-DEG. POINTS OF  $\frac{1}{8}$ -IN. RODS

1.00	56.5	25.0	2.05
2.00	72.0	35.3	2.15
3.00	92.0	41.0	2.25
4.00	113.0	46.5	2.42
5.00	134.0	51.5	2.61
6.00	156.0	56.5	2.76

Resistance 40,000 ohms.

Tests made inside 6 in. (15 cm.) diameter glass sphere. Resistance measured at 1.0 cm. setting of gap.

TABLE XI.—SPARK-OVER VOLTAGE OF INSULATOR AT DIFFERENT AIR PRESSURES DURING RAIN

(See Fig. 104)

Rain Tests (0.2 in. per Minute at 45 deg.)

Room bar. cm.	Vacuum cm. (in the cask)	Pressure cm. (in the cask)	Temp. C. (in the cask)	$\delta$ (in the cask)	Kilovolts spark-over (effective)
60-cycle Spark-over					
75.6	41.2	34.4	18.0	0.46	28
75.6	36.0	39.6	18.0	0.53	31
75.6	31.1	45.5	18.0	0.61	35
75.6	25.0	50.6	18.0	0.68	39
75.6	15.6	59.0	18.0	0.79	45
75.6	7.8	67.8	18.0	0.91	50
75.6	0.0	75.6	18.0	1.02	57

Impulse Spark-over 200 Kilo Cycles—Single Wave (Effective Kv.)

75.6	41.2	34.4	18.0	0.46	62
75.6	36.0	39.6	18.0	0.53	68
75.6	31.1	45.5	18.0	0.61	72
75.6	25.0	50.6	18.0	0.68	77
75.6	15.6	59.0	18.0	0.79	84
75.6	7.8	67.8	18.0	0.91	92
75.6	0.0	75.6	18.0	1.02	98

PEEK, F. W., JR., "The Effect of Altitude on the Spark-over Voltage of Bushings, Leads, and Insulators." *Trans. A.I.E.E.*, December, 1914.

*G. E. Rev.*, June, 1916. Tests made in a large wooden cask.

## Oil

TABLE XII.—IMPULSE AND 60 ~ BREAK-DOWN VOLTAGES IN OIL

Spacing, cm.	60 ~ kv. max.	Impulse kv. max.	Impulse ratio oil	Impulse ratio same spacing in air	<i>f</i>
Between Disks 2.5 cm. Diameter					
0.5	56.6	170	3.00	....	Approx. 230 kc.
Between Needles					
1.0	50.0	103	2.00	....	Approx. 230 kc.
2.0	69.0	157	2.20	1.20	
3.0	89.0	233	2.60	1.21	
4.0	108.0	321	3.00	1.25	
2.54 Spheres—Small Spacings Spacing less than $4\sqrt{R}$					
0.25	70.0	160	2.30	....	Approx. 230 kc.
0.50	100.0	245	2.45	....	
0.70	115.0	270	2.35	....	
1.00	140.0	285	2.05	....	

TABLE XII (Continued).—IMPULSE AND 60 ~ BREAK-DOWN VOLTAGES IN OIL

## Between 2/0 Needles

Needle spacing, cm.	60 ~ spark- over kv. (max.)	Impulse, kv.	Impulse ratio	<i>f</i>
0.32	28.0	36.5	1.30	100 kc.
0.64	40.0	70.0	1.75	(single
1.27	63.0	128.5	2.04	half sine
1.70	74.0	175.0	2.37	wave)
2.00	81.0			
3.00	104.0			
0.20	20.0	36.0	1.80	500 kc.
0.32	28.0	64.0	2.30	(single
0.42	31.5	92.0	2.92	half sine
0.56	37.0	121.5	3.29	(wave)

TABLE XIII.—COMPARATIVE STRENGTH OF OIL FOR HIGH FREQUENCY, IMPULSE, OSCILLATORY, AND 60 CYCLE VOLTAGES  
(Transil Oil Between Flat Disk Terminals, Square Edges. 2.5 cm. Diameter; 0.25 cm. Space)

## Break-down Gradients

60 cycle kv. per cm. max.	Single impulse sine shape corresponding to 200 kilocycles, kv. per cm. max.	Damped oscillations train frequency 120 per second. Fre- quency 200 kilocycles, kv. per cm. max.	High-frequency al- ternator 90 kilo- cycles, kv. per cm. max.
170	390	300	67

## Solid Insulations

TABLE XIV.—COMPARATIVE INSULATION STRENGTH FOR HIGH FREQUENCY IMPULSE, OSCILLATORY AND 60 CYCLE VOLTAGES  
Temperature 30 deg. C.

60 cycles		High frequency (alternator) 90,000 cycles		Damped oscilla- tion. Train freq. 120 sec. 200,000 cycles		Single im- pulse sine shape, cor- responding to half cycle of 200,000 cy.	Imp. ratio	Thick- ness, cm.	Lay- ers
kv. per cm. (max.)		kv. per cm. (max.)		kv. per cm. (max.)		kv. per cm. (max.)			
Rapidly applied	1 min.	Rapidly applied	1 min.	Rapidly applied	1 min.				

Transil Oil Between Flat Terminals—Square Edge  
2.5 cm. Diameter—0.25 cm. Space

170	...	67	.....	300	...	390	2.10	0.25	1
-----	-----	----	-------	-----	-----	-----	------	------	---

## Oiled Pressboard

## 10 cm. Diameter Square Edge Disks in Oil

355	310	95	72.0	370	290	720	2.3	0.25	1
395	370	61	41.0	420	240	....	....	0.50	2
		25	17.6	...	...	....	....	1.50	3

## Varnished Cloth

## 10 cm. Diameter Square Edge Disks in Oil

530	465	195	176.0	...	...	1080	2.26	0.06	2
420	310	135	100.0	550	560	780	2.50	0.15	5
420	310	100	73.0	490	410	700	2.25	0.25	8
330	275	...	.....	410	305	600	2.20	0.36	12

"Rapidly applied" voltage brought to puncture value in a few seconds.



## 5. STRENGTH OF OIL AT LARGE SPACINGS

## BETWEEN POINTS

Spacing, centimeters	Spark-over, kilovolts maximum
5	127
10	226
20	395
30	510
40	610
50	662
60	735
70	805

## FLAT DISCS WITH ROUNDED EDGE

Diameter, 25 cm.	Radius of edges, 2.5. cm.
5	310
10	460
15	650
20	780
25	900

If the space between the discs is divided into ducts by press-board barriers, the total breakdown voltage will be increased. Incipient sparks will, however, start at the voltages in the table. It is assumed that the barriers do not occupy more than 25 per cent. of the space.

The above tests were made on dry oil at 60 cycles.

## CORONA AND SPARK-OVER AT VERY HIGH VOLTAGES

TABLE I.—VISUAL CORONA ON PARALLEL BRASS TUBES

60 cycles<sup>1</sup>( $\delta = 1.0$ )

Inches	Spacing, centimeters	Visual kilovolt efficiency	
		Calculated	Observed
Diameter 3.5 in. (8.9 cm.)			
75.5	192	790	730
111.5	283	876	895
147.5	375	915	915
183.5	466	990	990
Diameter 1.75 in. (4.45 cm.)			
73.7	188	490	490
109.7	279	538	560
145.7	370	568	600
181.7	463	604	675
Diameter 1.0 in. (2.54 cm.)			
73	185	340	370
109	277	364	380
181	460	402	415

<sup>1</sup> PEEK, "Tests at 1,000,000 Volts," *Elec. World*, Dec. 31, 1921.PEEK, "The Insulation of High Voltage Transmission Lines," *G. E. Rev.*, February, 1922.

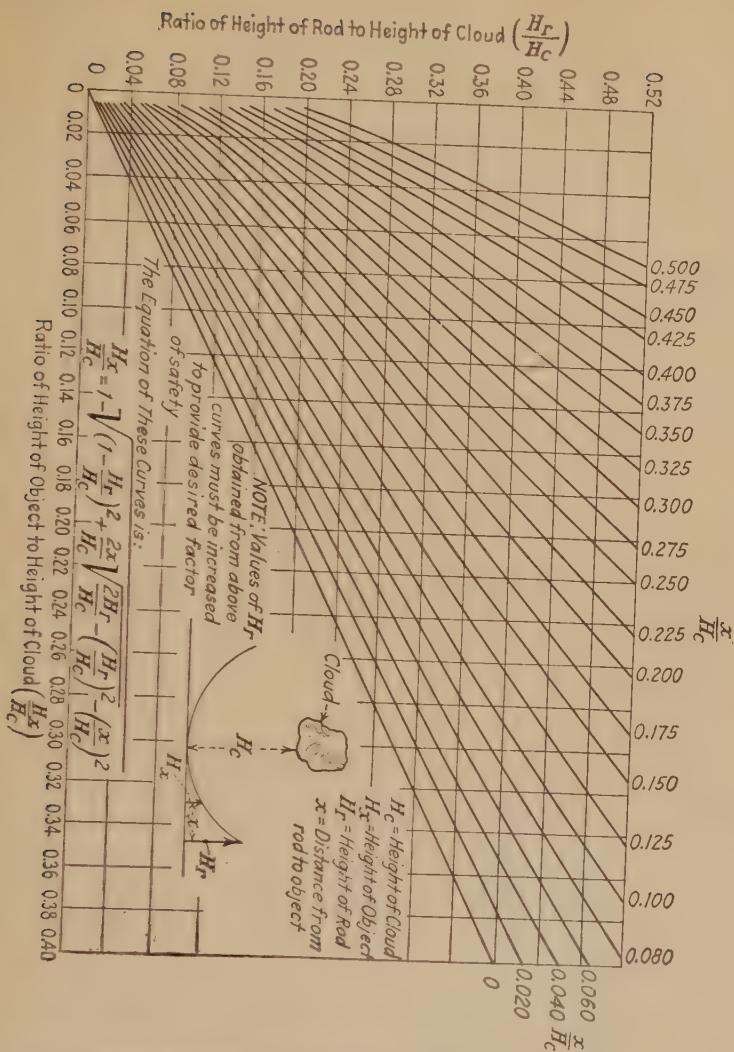


FIG. 267.—Curves showing minimum theoretical limit of height of lightning rod ( $H_r$ ) for protecting given object of height  $H_x$ , under thunder-cloud of height  $H_c$ . Actual height of lightning rod should be increased in proportion to factor of safety desired.



# INDEX

## A

	PAGE
Air, at very low pressures.....	44, 132
breakdown stages of.....	46
compressed, breakdown of.....	132
density, effect of.....	62, 125, 126
occluded in solid insulation.....	348
(See Corona).	
Alpha particle.....	41
Altitude, effect of, on corona loss.....	197
voltage.....	61, 62
on flashover of bushings and insulators.....	158, 316
on sphere gap sparkover.....	125
variation of air density with.....	61, 310
Arc, characteristics.....	47
Atoms.....	40
Attenuation of traveling waves.....	275, 281

## B

Barriers in oil.....	appendix, 161, 217, 255, 395
Beta particle.....	41
Bohr atom.....	40
Bushing, condenser type.....	320
effect of altitude on sparkover of.....	158
oil-filled type.....	319
overstressed air in.....	316
rod and torus.....	319
transformer.....	319

## C

Cable, dielectric strength of.....	239
graded.....	34, 317
oil filled.....	257
Capacity (see Permittance).	
Cathode ray oscillograph, description of.....	39
measurements with.....	99, 274, 332
Cathode rays.....	39
Choke coils.....	280
Cloud, thunder, formation of.....	258



	PAGE
Compressed air, dielectric strength of.....	132
Conduction through gases.....	42
Conductors, transmission	
corona on ( <i>see</i> Corona loss, Corona visual voltage, Etc.).	
lightning on.....	265, 274, 281
size, determination of.....	308
stranding, effect of.....	191, 299
surface irregularities, on.....	191, 299
typical forms of.....	306
Corona, attenuation of lightning waves.....	275, 281
calculations for practical transmission lines.....	296
condition for spark or.....	28, 109, 114
in entrance bushings.....	316
in entrapped air films.....	appendix, 71, 348
on generator coils.....	315
in oil.....	219
Corona current, effect on capacity current of line.....	211
harmonics caused by.....	211
oscillograms of.....	99
Corona loss, a.c. and d.c. ....	183
disruptive critical voltage.....	188
effect of frequency.....	179, 211
humidity.....	198
moisture, frost, fog, sleet, snow and rain, 196, 198	200
smoke and wind.....	199
temperature and pressure.....	197
harmonics due to.....	211, 308
law of.....	179, 188, 192, 194
loss near the disruptive critical voltage.....	194
practical calculations.....	301
probability law.....	196, 202
quadratic law.....	179
for small conductors.....	187, 192, 193
three-phase.....	211
Corona on transmission lines ( <i>see</i> Transmission lines).	
Corona, visual, a. c. and d. c. ....	appendix, 48, 54, 59, 84
calculation for concentric cylinders.....	58, 64, 66, 73
of gradient of.....	50, 58, 64, 73, 77, 81
of voltage of.....	52, 69
wet.....	76, 348
on conductors of same potential close together.....	82
derivation of law of.....	59, 63, 73
diameter of.....	84
effect of air density on.....	52, 61
cable surface on.....	53, 81, 191
conductor material on.....	53, 56, 78
surface on.....	53, 191
current in conductor on.....	53, 78
diameter of conductor.....	49, 54, 56, 58

	PAGE
Corona, visual, effect of dirt on.....	76
frequency on.....	75
humidity on.....	53, 78
initial ionization on.....	53, 78
oil on surface on.....	53, 76
pressure on.....	61, 67
small spacing on.....	52, 67
spacing on.....	49, 54-56
temperature on.....	61, 62
water on.....	53, 76
wave shape on.....	53, 76
law of, for concentric cylinders.....	58, 64, 66, 73
for parallel wires.....	52, 53, 64, 66, 73
with lightning and impulse.....	76
mechanical vibrations with.....	98
peculiar effects in breakdown by.....	167
photographic study of.....	84
positive and negative.....	67, 94, 103
rectifying effect of.....	103
stroboscopic study of.....	84
three-phase.....	211, 236
Cosmic rays.....	42
Cyclograms.....	99, 202
Cylinders, concentric, flux density.....	13
gradient.....	14, 29
permittance or capacity.....	13, 29
sparkover and corona in oil with.....	223
visual corona ( <i>see</i> Visual corona).....	48 <i>et seq.</i>
parallel ( <i>see</i> Wires).	

## D

Dielectric, addition of fluxes.....	14
circuit,.....	314
displacement.....	10
flux control.....	36, 223
density between concentric cylinders.....	14
between parallel planes.....	11
for parallel wires.....	14, 24
sum of at a point.....	17, 21
refraction.....	31
formulae for different electrodes.....	30
hysteresis.....	37
spark lag in air.....	142
oil.....	226
solids.....	241, 244
Dielectric field, analogy with Hooke's Law.....	6, 10
magnetic field.....	2
between concentric cylinders.....	13, 34

	PAGE
Dielectric field, between parallel planes.....	11
wires.....	14
control.....	322
energy stored in.....	9, 10
transfer in transmission.....	9, 10
equation of equipotential surfaces between parallel wires.....	17
for spheres.....	26
lines of force between parallel wires.....	21
from spheres.....	26
experimental determination of.....	2, 343
image of.....	345
methods of construction.....	335
resultant.....	15
superposition of.....	15
in three dimensions.....	343
three phase.....	346
of thunder cloud.....	264
Dielectrics, combination of dielectrics of different permittivities.....	31
in multiple.....	35
in series.....	32
gaseous.....	38, 109, 169
liquid.....	215
non-homogeneous.....	38
solid.....	229
Direct current, corona loss.....	183
sparkover.....	appendix, 166
Direct lightning strokes ( <i>see</i> Lightning).	
Dirt, effect of on insulator sparkover.....	165

## E

Elastance.....	12, 314
Elastivity.....	12, 314
Electron theory.....	39
Equipotential surfaces, construction of.....	335
equation of, for parallel wires.....	17
spheres.....	26
in three dimensions.....	343
Experimental study of, corona loss.....	169
dielectric fields.....	2, 107, 343
lightning.....	261, 280, 282, 287
solid insulations.....	229
sparkover.....	109
strength of oil.....	215
visual corona.....	54

## F

Flux ( <i>see</i> Dielectric flux).	
Frequency, effect on corona loss.....	179, 211

	PAGE
Frequency, effect on solid insulation.....	243, 250
visual corona.....	75
(See High frequency).	

## G

Gamma rays.....	41
Gap, method of measuring high voltages.....	116
small, breakdown of.....	67, 132
sphere.....	118
Gradient, at any point.....	22, 24, 339, 341
at different points around a conductor.....	339, 341
between concentric cylinders.....	14, 30
between large spheres.....	27
between parallel planes.....	13
wires.....	24, 27
cloud, thunder.....	258
equigradient surfaces.....	337, 340
law of visual corona (see Visual corona).....	48 et seq.
lightning.....	262
Green's theorem.....	21
Ground wires, use of.....	282, 349
Guard rings.....	322, 324

## H

Harmonics due to corona.....	211, 308
High frequency, effect of, in design.....	241, 330
on corona loss.....	211
on oil.....	228, 250
on solid insulation.....	241, 250, 252
loss in solid insulation.....	252
Hysteresis, dielectric.....	37, 38, 229, 252
Humidity, effect on corona loss.....	198
voltage.....	78
insulator sparkover.....	163
needle gap sparkover.....	117

## I

Images.....	345
Impulse generator.....	144
Impulse ratio.....	143
Impulse voltage, caused by lightning.....	262, 265
effect of, on air.....	142
on insulators.....	148
on solid insulations.....	241, 250
on sparkover in oil.....	226
measurement of.....	148
oscillograms on lines of.....	274

	PAGE
Insulation, breakdown caused by the addition of.....	312
how measured.....	12
Insulation, coordination of, on transmission lines.....	349
Insulation, solid, area of electrode.....	240
barriers in oil.....	217, 255
breakdown caused by addition of.....	312
common.....	215
comparison of strengths for impulses, oscillations, high frequency and low frequency.....	241, 250
cumulative effect of overvoltages of short duration	241
d.c. strength.....	appendix, 257
effect of d.c. on.....	257
impulse voltages and high frequency on	241, 250, 252
energy loss in.....	251
high frequency loss in.....	252
hysteresis.....	229
impregnation of.....	256
laminated.....	240
law of energy loss in.....	251, 252
strength vs. thickness.....	237, 349
vs. time.....	244
mechanical.....	257
methods of testing.....	233, <i>et seq.</i>
occluded air in.....	71, 257, 348
operating temperatures of.....	254
permittivity of.....	249
resistance.....	38, 230
strength under high frequency.....	250
impulses.....	241, 250
oscillations.....	250
vs. thickness.....	237
vs. time.....	244
tables of properties of.....	246, 249
Insulation, wood pole.....	353
Insulations, air.....	48, 109, 169
compressed air.....	44, 67, 132
gaseous.....	48, 109, 169
liquid.....	153
oil.....	153
solid.....	229
Insulators, effect of altitude on sparkover of.....	158
humidity on sparkover of.....	163
rain on sparkover of.....	163
suspension, arcing devices for.....	324
shielding of.....	324
sparkover of.....	138, 148
Ionization, as affecting corona voltage.....	78
by collision or impact.....	43



	PAGE
Ionization, general consideration of.....	46
definition of.....	43
by photo-electric effect.....	45, 134
by thermal effect.....	45
Ionizing potentials of gases.....	44
Irregularity factor, $m_0$ .....	53, 191, 299
Isotopes.....	41

## K

Klydonograph ( <i>see also</i> Surge voltage recorder).....	106
---	-----

## L

Lichtenberg figures.....	105
Lightning.....	258
choke coils, effect on.....	280
direct strokes, protection from.....	287, 397
field studies.....	274, 295
generator.....	144
ground wire, considerations with.....	282
induced voltages, origin of.....	263
protection of oil tanks, etc. from.....	292
transmission lines from.....	282, 349
laboratory studies.....	275, 282, 287
nature of.....	258
oscillograms of discharge rate of.....	274
of waves caused by.....	274
peculiar effects associated with.....	294
proof transformers.....	330
transmission line.....	349
protection of buildings, oil tanks, etc. from.....	290, 397
transformers from.....	330, 349
rods, for protection from direct strokes.....	287, 397
sparkover of gaps.....	150
strength of insulators.....	151, 281
insulation.....	243
traveling waves caused by.....	265, 281
voltage and energy of.....	262
wave attenuation.....	275, 281
waves.....	269, 274
Light, ultra-violet ( <i>see</i> Ultra-violet light).	
Lines of force, construction of.....	335
equation of, between parallel wires.....	19
for spheres.....	26
three-dimensional field.....	343
perpendicular to equipotential surface.....	21
thunder cloud.....	264
Liquid insulation ( <i>see</i> Oil).	

## M

Magnetic field, analogy with dielectric field.....	2, 3
experimental plot of.....	2, 3
$m_o$ , values of.....	191, 299

## N

Needle gap.....	117
effect of humidity on.....	117
sparkover curve in air.....	117, 118
in oil.....	216, 226
voltage in rain.....	138
Non-resonating transformer.....	330

## O

Oil, barriers in.....	161, 217, 255
corona and sparkover in.....	215, 219
d.c. strength.....	appendix, 228
effect of moisture in.....	217
temperature on.....	218
formulae for strength of.....	224, 226
high frequency in.....	228
law of sparkover and corona.....	224, 226
needle gap sparkover in.....	216, 226
permittivity of.....	219, 249
physical characteristics of transil oil.....	215
pressure, under.....	217
sparkover for different electrodes in.....	216, 226
variation in.....	216
specific resistance in.....	219
surface leakage in.....	254
temperature, effect of.....	218
transient voltages in.....	226, 250
Oscillations, effect of, on solid insulations.....	241, 250
on sphere gap voltages.....	140
measurements of.....	138, 153
precautions against, in testing.....	134

## P

Permittance or capacity, between concentric cylinders.....	14, 30
spheres.....	25
between eccentric spheres.....	31
between parallel planes.....	11
wires.....	23, 30
comparison of single phase and three phase..	346
effect of ground on, for parallel wires.....	345
formulae for different electrodes.....	30
in series.....	12

	PAGE
Permittivity.....	12
of oil.....	219
of solid insulations.....	249
Photo-electric effect.....	45
Planes, parallel, flux density.....	11, 12
gradient.....	12
permittance or capacity of.....	11
sparkover in oil.....	155, 157
Polarity effect in sparkover.....	166
Potential at a point.....	17, 341
Potential difference between two points.....	17, 341
Potential, ionizing, of gases.....	44
Potentials, addition of.....	17
Pressure ( <i>see</i> Air density).	
high ( <i>see</i> Air, compressed).	
Probability law of corona.....	196
Problems breakdown caused by addition of stronger insulation.....	312
bushing.....	318
condenser bushing.....	319
dielectric field, construction of.....	335
control.....	322
experimental determination of.....	344
in three dimensions.....	343
effect of ground on dielectric field between parallel wires.....	345
entrance bushings.....	316
general problems on the calculation of sparkover of parallel wires, insulation loss, strength, etc.....	348
graded cable.....	317
high frequency.....	330
lightning-proof transmission line design.....	349
static, on generator coils.....	315
three-phase dielectric field for flat and triangular spacings..	346
transformer design.....	329, 330
wood pole.....	353
Protection, lightning ( <i>see</i> Lightning).	
Protective ratio, of ground wires.....	285, 286
of lightning rods.....	289

## R

Radioactive materials.....	41
Rain, effect of, on corona loss.....	200
on insulator sparkover.....	163
on sphere gap sparkover.....	138
Rectification by corona.....	103
Resistance, use of in measuring circuits.....	134, 136
Rods, lightning ( <i>see</i> Lightning).	

## S

	PAGE
Shielded winding transformer.....	330
Sludging, in oil.....	219
Smoke, effect of, on corona.....	199
on sparkover.....	165
Snow, effect of, on corona loss.....	200
Solid insulation ( <i>see</i> Insulation, solid).	
Spark lag.....	142
Sparkover, condition for spark or corona.....	28, 109, 114
d.c.....	appendix, 140
effect of altitude on, for bushings and insulators.....	158, 217
for spheres.....	126
humidity on.....	117, 163
water and rain on.....	138, 163
gaps for measuring high voltage.....	117, 118, 148
impulse ( <i>see</i> Impulse voltages).	
influence of water and oil on.....	116, 138
lightning and transient.....	appendix, 142, 148
for needle gap.....	117
in oil.....	215, 219
for parallel wires.....	109
polarity effect on.....	166
rain and water on insulators.....	appendix, 163
at small spacings.....	appendix, 71, 124, 132
for spheres.....	118
three-phase.....	166
time lag in.....	142
Specific resistance, of oil.....	219
solid insulation.....	230
Spheres, air films between.....	67
concentric permittance, dielectric field.....	26
corona or sparkover for.....	68
density correction for air films.....	appendix, 71
effect of ground on sparkover voltages.....	137
water and rain on arc-over voltages.....	138
experimental determination of effect of altitude.....	125
law of disruption.....	73
sparkover in air.....	73
in oil.....	224, 226
as a means of measuring high voltage.....	118, 148
precautions against oscillations.....	134
rupturing gradients for different sizes.....	72
sparkover, calculation of.....	121, 124
correction for altitude.....	125
curves.....	119 <i>et seq.</i>
at small spacings.....	71
at high frequency, oscillations and impulses.....	138
strength of oil around.....	225

	PAGE
Spheres, two large equal spheres, field between gradient, permit- tance, etc.....	26
small equal spheres .....	27
Steep wave front.....	142, 148, 226, 244, 250
Surface irregularity factor ( $m_s$ ).....	191, 299
Surface leakage, air.....	255, 320
oil.....	254
Surge voltage recorder.....	106, 280
Symbols, table of.....	xiii

## T

Temperature, effect of, on corona voltage.....	62
in ionization and spark formation.....	45
on sparkover.....	125
Terminal ( <i>see</i> Bushing).	
Testing, method of testing solid insulations.....	233, <i>et seq.</i>
sparkover, precautions in.....	134, 136
Thermal ionization.....	45
Third harmonic.....	211, 308
Three-phase dielectric fields between conductors with flat and triangular spacings.....	346
corona.....	211
sparkover.....	166
Time lag in sparkover.....	142
Transformer, bushing.....	319
condenser bushing.....	320
design, care in.....	329, 330
non-resonating.....	330
oil-filled bushing.....	319
Transformer voltage rise due to high frequency testing.....	330
sparkover.....	135
Transmission lines, agreement of calculated and measured, corona losses.....	307
corona limit of voltage on, with working tables	308
corona on.....	169, 296
lightning-proof.....	349
practical example of corona loss calculation.....	304
formulae and their application.....	301
method of increasing size of conductors	305
safe and economical voltages.....	308
sparkover voltage of.....	113, 150, 151
three-phase, comparison of permittance with single-phase.....	346
with triangular and flat spacing	346, 347
voltage change along lines.....	306
wood pole.....	353
Traveling waves, nature of.....	265, 281
oscillograms of.....	274



## U

	PAGE
Ultra-violet light, effect on corona voltage.....	78
sparkover.....	134
photo-electric effect of.....	45
Units, table of.....	xi

## V

Visual corona (*see* Corona).

## W

Wave front, effect of.....	142
Weather, effect of, on corona loss.....	196-198, 200
Wires, calculation of sparkover on, wet and dry.....	109, 348
visual corona on, wet and dry.....	76, 348
corona loss on.....	169, 296, 348
effect of ground on permittance or capacity and gradient.....	345
equation of equipotential surfaces.....	17
lines of force.....	19
experimental plot of field between.....	2, 3, 344
flux density.....	14
gradient.....	24, 30
ground.....	282, 349
law of sparkover and corona in oil.....	224, 226
lines of force.....	15
method of drawing dielectric field for.....	335
permittance or capacity.....	23, 30
sparkover.....	109
wet.....	116
visual corona ( <i>see</i> Visual corona).....	48 <i>et seq.</i>
Woodpoles, lightning strength of.....	353

## X

X-rays.....	41, 45, 134
-------------	-------------





621.3194 P37A



a39001



007328019b

66-1  
74605  
68



